JOURNAL OF THE MYANMAR ACADEMY OF ARTS AND SCIENCE

Chemistry

Vol. XVIII, No.1B, July, 2020

Myanmar Academy of Arts and Science

Journal of the Myanmar Academy of Arts and Science

Vol. XVIII, No.1B

Contents

Chemistry

Edition

2020, July, 1000 Copies

Published by

Dr Aung Min (00322) Chairman, Journal Publication Committee,
Myanmar Academy of Arts and Science

ISSN 2520-0186
LCCN 2003-323143

Printed by

U Win Aung (00171), Manager,
Universities Press, Yangon, Myanmar

EXTRACTION OF GOLD FROM IRON PYRITE ORE BY ACID LEACHING AND BIOLEACHING

Khin Cho Lin[1], San Nwe Zin[2], Daw Hla Ngwe[3]

Abstract

In this study, acid leaching and bioleaching of iron pyrite ore collected from Sakhangyi gold mining site, Moehti Moemi mining area, Yamethin Township, Mandalay Region were conducted. In acid leaching of iron pyrite ore from Sakhangyi (SKG) gold mining site, aqua regia and di- isobutyl ketone have been used as extraction solvents. In bioleaching process, a bioleaching bacterium, *Acidithiobacillus ferrooxidans* was used. *A. ferrooxidans* was cultured on selected 9 K medium. Leaching of iron pyrite ore sample was done under different leaching parameters (time, pH, ore size and temperature). The leachant has been characterized by atomic absorption spectroscopy. According to acid leaching of iron pyrite ore, Au content of iron pyrite ore was 1.2 ppm, after extracting with DIBK (AAS). The optimum conditions for bioleaching process using *A. ferrooxidans* were found to be 1.5 of pH, 90 ^{o}C, 250 µm ore size after 6 days bioleaching time to get the highest gold content (6.25 ppm).

Keywords: Acid leaching, bioleaching, *Acidithiobacillus ferrooxidans*, gold, Atomic absorption spectroscopy

Introduction

Microbial processes have been developing to assist in the commercial recovery of gold from refractory ores. Iron and sulphur oxidizing acidophilic bacteria are able to oxidized certain sulfide ores containing encapsulated particles of elemental gold. Bio-oxidation of gold ores may be a less costly, less polluting alternative to other oxidation pretreatments such as roasting and pressure oxidation (Sen, 2015). Recently, bio-oxidation of gold ores has been implemented as a commercial process, and is under study worldwide for further application to refractory gold ores. Sulphide-oxidizing bacteria degrade the sulfide matrix surrounding gold, but do not leach the gold itself (Olson, 1994).

Bioleaching, the conversion of an insoluble metal into a soluble form by biological oxidation. Metals for which this technique is mainly employed for recovery includes, copper, cobalt, nickel, iron, sulphur, zinc and uranium. For recovery of gold and silver the activity of leaching bacteria is applied only to remove interfering metal sulphide from ores bearing the precious metals prior to cyanidation treatment. The application of bacterial leaching to metal recovery from mineral ores has progressed steadily in the last 20 years (Rohwerder *et al*., 2003). Bioleaching has improved the efficiency of the mineral procession industry by lowering of the overall capital and procession costs and by diminishing environmental concerns associated with the pollution derived from emission of smelting operations (Quatrini and Holmes, 2005).

Metal sulphides are oxidized by certain bacteria, forming soluble metal sulphates and sulphuric acid. Iron pyrite and arseno pyrite ores are prominent minerals in refractory gold ores and are readily bio-oxidized. The most commonly studied pyrite oxidizing bacteria are thermophilic *Acidithiobacillus ferrooxidans*, that oxidizes ferrous iron or reduced sulphur

[1] 4PhD Candidate, Department of Chemistry, University of Yangon
[2] Dr, Associate Professor, Department of Chemistry, Bago University
[3] Dr, Professor and Head, (Retd.), Department of Chemistry, University of Yangon

compounds. Moderately thermophilic pyrite oxidizing bacteria are found in mine spoils containing pyrite material that are undergoing weathering (Olson, 1994). It thrives in the pH range of 1.5 to 6, temperature in the range of 28-95 °C (Natal'ya and Muravyov, 2010). The present study, two methods of leaching: acid leaching and bioleaching were used for extraction of gold (Ahmad *et al*., 2015). In acid leaching based on aqua regia was used for sample digestion and di-isobutyl ketone (DIBK) was used as extraction solvent (Raju, 2005).

Materials and Methods

Collection and Preparation of Samples

Soil and ore samples, for this study, were selectively chosen and collected from Sakhangyi (SKG) gold mining site, Moehti Moemi, Yamethin township approximately 150 kilometers southeast of Mandalay at latitude 20° 21′ 35″ (N) and longitude 96° 24′ 47″(E). The collected soil sample is dried in air, ground and sieved through 200 mesh size and pH of the soil sample was determined. The iron pyrite ore sample was grounded, powdered (200-250 μm), and prepared by cone and quartering (Figure 1). Removal of silica from this iron pyrite ore sample was carried out by using hydrofluoric acid (Zahan *et al*., 2017).

(a) (b) (c) (d)

Figure 1 Cone and quartering method for iron pyrite ore
(a) Gathered material into a cone and flatten
(b) Divided into quarters
(c) Opposite quarters taken for mixing and forming
(d) The reduced sample

Isolation of and Identification *A. ferrooxidans*

A. ferrooxidans was cultured on selected 9 K medium, which mixed with solution A and solution B (Silverman and Ludgren, 1959). Solution A was prepared by adding 0.3 g of $(NH_4)_2SO_4$, 0.01 g of KCl, 0.05 g of K_2HPO_4, 0.05 g of $(MgSO_4)$ $7H_2O$ and 0.001 g of $Ca(NO_3)_2$ to 100 mL of distilled water. Solution B was prepared by dissolving 2.2 g of $FeSO_4$ in 50 mL of distilled water. This two solutions were mixed and adjusted (pH 1.5) with 10 N sulphuric acid and sterilized in autoclave (Silverman and Ludgren, 1959). Soil sample containing 9 K medium was placed on a rotary shaker with 200 rpm for 8 days. After 8 days, bacteria were taken with a sterilized inoculation loop from conical flask (9 K medium) and streaked in glucose yeast beef (GYB) medium plate by streak plate method. Then, it was incubated in an incubator at 37 ^oC for 7 days. After 7 days, single colonies of *A. ferrooxidans* species were grown on glucose yeast beef plate. Next, single colonies of *A. ferrooxidans* species were transferred to nutrient agar medium for culturing the pure colonies (Figure 2) (Silverman and Ludgren, 1959). The bacteria were identified by morphological examinations, gram staining and twelve biochemical tests

(Cruickshank, 1968**).** The selected bacteria were also characterized by phenotypic and genotypic identification (Grigorii *et al*., 2003).

Figure 2 Culture medium of isolated *A. ferrooxidans*

Extraction of Gold by Acid Leaching of Iron Pyrite Ore

Iron pyrite ore sample (10 g) was transferred into a porcelain crucible and roasted for 1 h in a muffle furnace at 650 °C. The roasted samples were transferred into a glass beaker (400 mL) and freshly prepared aqua regia (3:1) was added to stabilize $AuCl_3$ complex, during evaporation on a hot plate for at least 1 h. This solution was cooled, filtered and followed by discarding the residue. 18 mL of Sorenson's salt solution (250 mL distilled water and 560 g $Na_2HPO_4.\ 2H_2O$), 5 mL of 1 % Aiquot 336 (methyl trioctyl ammonium chloride) and 5 mL of D.I.B.K (di-isobutyl ketone) were added to this clear solution. This solution was allowed to separate and upper layer of D.I.B.K phase adsorbed the gold. This phase was collected for determination of gold by AAS (Raju, 2005).

Extraction of Gold by Bioleaching of Iron Pyrite Ore

(1) Effect of leaching time

9 K basal medium (50 mL each) was placed in each of six conical flasks and pH was adjusted to 1.5 with 10 N H_2SO_4 and sterilized at 121°C for 20 min. One loop each of the 7 days old cultured (*A. ferrooxidans*) and 5 g of iron pyrite ore (250 µm) were added into each of six conical flasks. Then, the conical flasks were shaken on a shaker at 200 rpm and 30 °C for 2, 4, 6, 8, 10 and 12 days. Liquid samples (20 mL each) were withdrawn and gold contents were measured by atomic absorption spectroscopy.

(2) Effect of pH

9 K basal medium was prepared accordingly with initial pH values of 1, 1.5, 2.0, 2.5, 3.0 and 3.5 with 10 N H_2SO_4 and sterilized 121 °C for 20 min. One loop each of the 7 days old cultured (*A. ferrooxidans*) and 5 g of iron pyrite ore (250 µm) were added into each of six conical flasks. Then, the conical flasks were shaken on a shaker at 200 rpm, 30 °C for 6 days. Liquid samples (20 mL each) were withdrawn centrifuged and gold contents were measured by atomic absorption spectroscopy.

(3) Effect of ore size

9 K basal medium (50 mL) was placed in each of three conical flasks and pH 1.5 was adjusted with 10 N H_2SO_4 and sterilized 121 °C for 20 min. One loop each of the 7 days old cultured (*A. ferrooxidans*) and 5 g of iron pyrite ore (150 µm, 250 µm, 350 µm) were added into each of three conical flasks. Then, the conical flasks were shaken on a shaker at 200 rpm, 30 °C for 6 days. Liquid samples (20 mL each) were withdrawn centrifuged and gold contents were measured by atomic absorption spectroscopy.

(4) Effect of leaching temperature

9 K basal medium (50 mL) was placed in each of four conical flasks and pH 1.5 was adjusted with 10 N H_2SO_4 and sterilized 121 °C for 20 min. One loop each of the 7 days old cultured (*A. ferrooxidans*) and 5 g of iron pyrite ore (250 µm) were added into each of the four conical flasks. Then, the conical flasks were shaken on a shaker at 200 rpm (30 °C, 60 °C, 90 °C, 120 °C) for 6 days. Liquid samples (20 mL each) were withdrawn, centrifuged and gold contents were measured by atomic absorption spectroscopy.

Determination of Gold Content at Optimum Conditions

The experimental procedure was carried out by using 9 K medium (50 mL) with initial pH 1.5 in a 50 mL of conical flask and sterilized at 121 °C for 20 min. One loop each of the 7 days old cultured (*A. ferrooxidans*) and 5 g of iron pyrite ore (250 µm) were added into a conical flask. Then, the conical flask was shaken on a shaker with 200 rpm all 90 °C for 6 days. Liquid sample (20 mL each) was withdrawn and gold content was measured by atomic absorption spectroscopy.

Results and Discussion

In this study**,** the soil and ore samples were collected from Sakhangyi (SKG) gold mining site, Moehti Moemi, Yamethin Township, Mandalay Region (Figure 3). The SKG soil sample was found to be moderately acidic (pH 5.7). *A. ferrooxidans* was isolated from this soil using 9 K basal salt medium. It was also identified by phenotypic and genotypic characterization (16S rDNA amplification by PCR) (Khin Cho Lin *et al*., 2018). According to phenotypic identification, *A. ferrooxidans* was gram negative, single rode shape and motile. According to genotypic identification, amplification conditions were optimized using genomic DNA from pure culture of isolated bacteria. The extraction of genomic DNA can be done for molecular characterization and detection of sequencing for identification of *A. ferrooxidan.* 16S rDNA amplification by PCR gave a few bands after gel electrophoresis. Each each band is corresponded in size to the expected product of 118 bp.

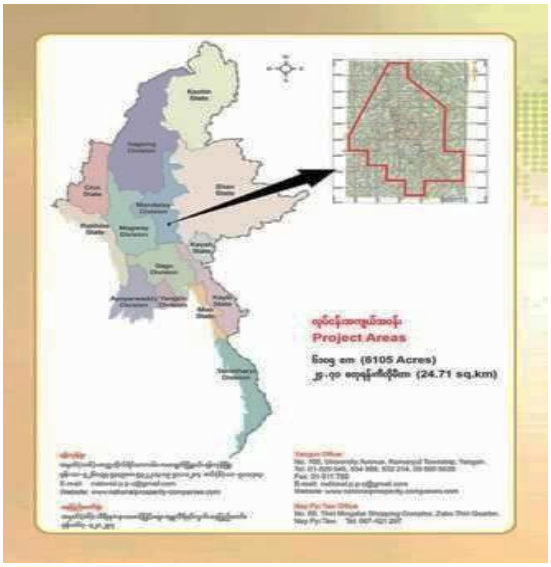

Figure 3 Location of Moehti Moemi Gold Mine in Yamethin Township, Mandalay Region

Gold Extracted from Iron Pyrite Ore by Acid Leaching Method

From the results of extraction of gold from iron pyrite ore by acid leaching method, the gold content 1.2 ppm was detected by AAS method. The amount of gold content obtained from acid leaching was significantly lower than that obtain from bioleaching. This is due to the low grade iron pyrite ore. Acid leaching is the suitable extraction method for high grade ores while bioleaching is the most effective method for low grade ore.

Gold Extracted from Iron Pyrite Ore by Bioleaching Method

In this method, various parameters such as effect of leaching time, effect of pH, effect of ore size and effect of temperature on the gold extraction were studied.

(1) Effect of leaching time

The amount of gold by bioleaching process was conducted with by varying leaching time. The highest gold content was 3.25 ppm after 6 days of leaching time. Therefore, leaching efficiency by the microorganism is dependent on the growth rate of organism. The more increase the leaching time, the less growth of microorganism and decrease the gold content (Table 1 and Figure 4) were observed.

Table 1 Effect of Leaching Time on Gold Content Extracted from Iron Pyrite Ore with *A. ferrooxidans* (AAS)

No.	Leaching time (day)	Au Content (ppm)
1	2	0.02
2	4	0.02
3	6	3.25
4	8	0.02
5	10	0.01
6	12	0.01

pH = 1.5, amount of Iron Pyrite Ore = 5 g, temperature = 30 ^{o}C, ore size = 250 µm

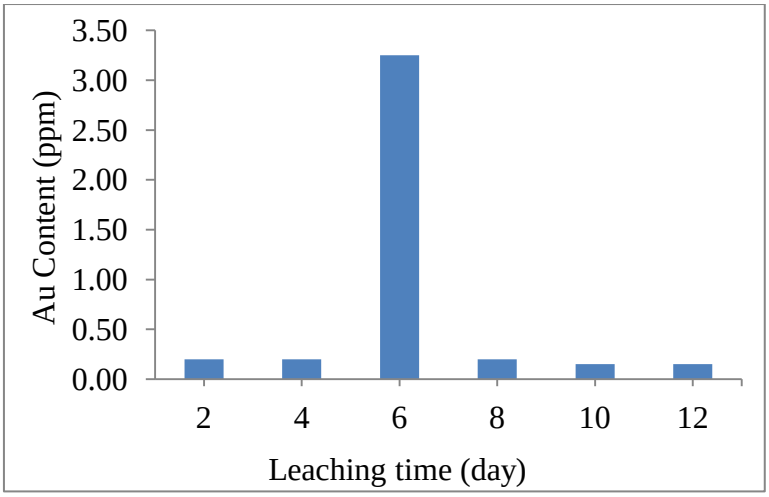

Figure 4 Effect of leaching time on gold content extracted from iron pyrite ore with *A. ferrooxidans* (AAS)

(2) Effect of pH

The experiment was carried out within the pH range of 1 to 3.5. At pH 1.5 the maximum content of gold was 0.02 ppm (Table 2 and Figure 5). Therefore, the control of acidity is important in leaching, because an acid environment must be maintained to keep ferric iron and other metals in solution.

Table 2 Effect of pH on Gold Content Leached from Iron Pyrite Ore with *A. ferrooxidans* (AAS)

No.	pH	Au Content (ppm)
1	1.0	0.01
2	1.5	0.02
3	2.0	0.01
4	2.5	0.01
5	3.0	0.01
6	3.5	0.01

amount of Iron Pyrite Ore = 5 g, temperature = 30 °C, ore size = 250 µm, leaching time = 6 days

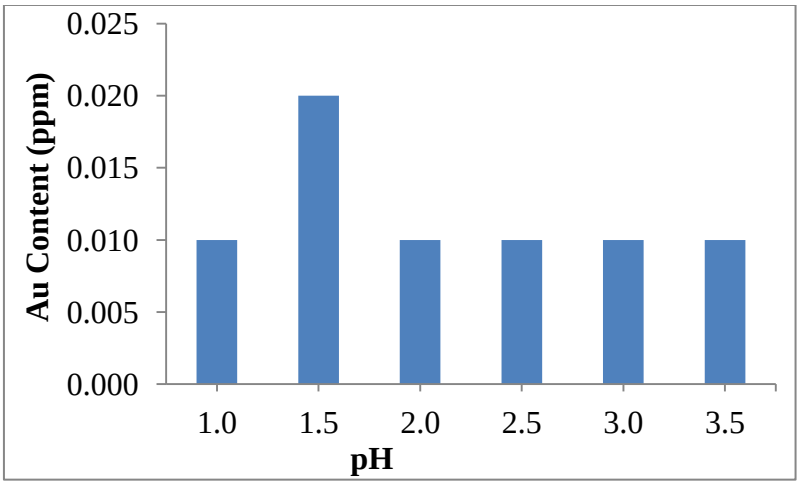

Figure 5 Effect of pH on gold content leached from iron pyrite ore with *A. ferrooxidans* (AAS)

(3) Effect of ore size

The effect of particle size of iron pyrite ore powder on bioleaching process is shown in Table 3 and Figure 6. The nature of substrate is a key role in bacterial leaching process. In this study different particle sizes of 150 µm, 250 µm and 350 µm were used for bioleaching. It was observed that powdered iron pyrite ore with 250 µm gave the highest leaching of gold (0.02 ppm). The rate of leaching of metals is essentially limited by the accessible surface of the minerals and can be enhanced by grinding the minerals of the pieces of ore to small grains.

Table 3 Effect of Ore Size on Gold Content Leached from Iron Pyrite Ore with *A. ferrooxidans* (AAS)

No.	Ore size (µm)	Au Content (ppm) (AAS)
1	150	0.01
2	250	0.02
3	350	0.01

amount of Iron Pyrite Ore = 5 g, temperature = 30 °C, leaching time = 6 days, pH = 1.5

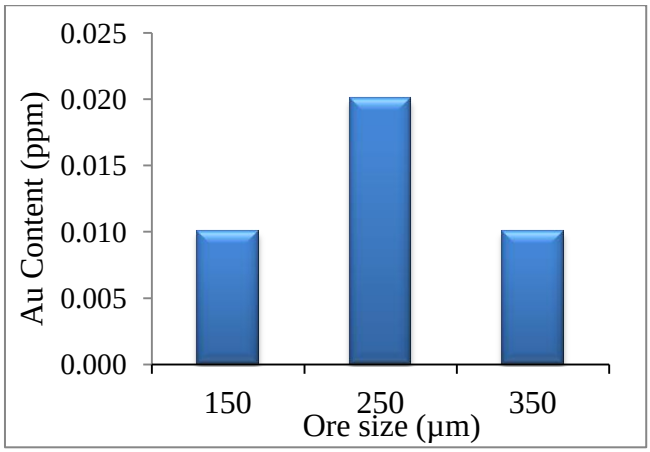

Figure 6 Effect of ore size on gold content leached from iron pyrite ore with *A. ferrooxidans* (AAS)

(4) Effect of Temperature

The effect of incubation temperature on leaching of iron pyrite ore powder is shown in Table 4 and Figure 7. In this study different incubation temperatures (30 °C, 60 °C, 90 °C, 120 °C) were used for bioleaching. It was observed that the highest amount of gold content was 0.02 ppm at 90 °C. It may be due to that although *A. ferrooxidans* is thermophilic it could not survive at high temperature > 90 °C. So, metal leaching property of the bacteria may decrease.

Table 4 Effect of Temperature on Gold Content Leached from Iron Pyrite Ore with *A. ferrooxidans* (AAS)

No.	Temperature (°C)	Au content (ppm) (AAS)
1	30	0.01
2	60	0.01
3	90	0.02
4	120	0.01

amount of Iron Pyrite Ore = 5 g, leaching time = 6 days, pH = 1.5, ore size = 250 µm

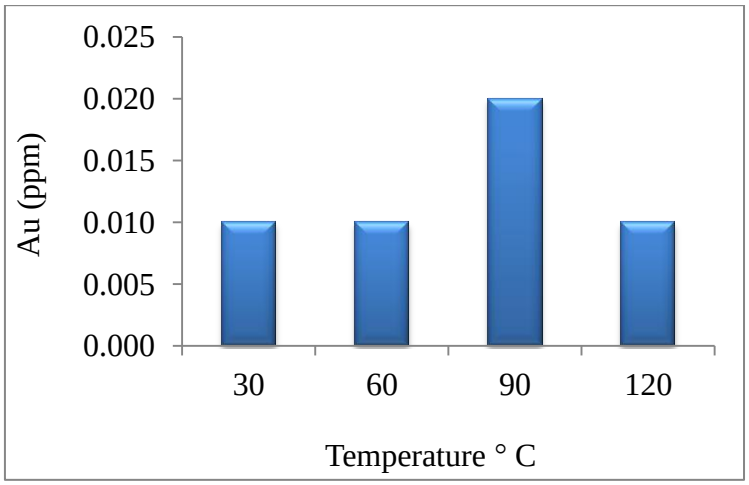

Figure 7 Effect of temperature on gold content leached from iron pyrite ore with *A. ferrooxidans* (AAS)

In gold extraction from iron pyrite ore by bioleaching method, the optimum conditions were found to be pH 1.5, leaching time 6 days, ore size 250 µm and temperature 90 °C giving 6.25 ppm of gold content.

Conclusion

In this study, acid leaching and bioleaching of iron pyrite ore collected from Sakhangyi (SKG) gold mining site, Moehti Moemi, Yamethin township have been revealed. In acid leaching process, aqua regia was used for sample digestion and extraction with D.I.B.K. The amount of gold content extracted by acid leaching was 1.2 ppm. In bioleaching process, *Acidithiobacillus ferrooxidans* was cultured on selected 9 K basal medium and used for leaching of iron pyrite ore powder. Most soluble content of gold was observed to be 3.25 ppm after 6 days of bioleaching. The optimum conditions for bioleaching process using *A. ferrooxidans* were found to be 1.5 of pH, 90 °C, 250 µm ore size after 6 days bioleaching time to get the highest gold content (6.25 ppm).

Acknowledgements

The authors would like to express their profound gratitude to the Department of Higher Education (Yangon Office), Ministry of Education, Yangon, Myanmar, for provision of opportunity to do this research and Myanmar Academy of Arts and Science for allowing to present this paper.

References

Ahmad, H. Z., Kham, A. and Raza, A. (2015). " Extraction of Metals from Electronic Waste". *Global Journal of Technology and Optimization,* vol.1, pp. 5-8.

Cruickshank, R. (1968). *Medical Microbiology*. Edinburgh: 11th ed., E. and S. Livingstone Ltd., pp. 125-128.

Grigorii, L., Tat'yana, P. and Tamara, F. (2003). "Phylogenetic Heterogenetity of the Species *Acidithiobacillus ferrooxidans". International Journal of Systematic and Evolutionary Microbiology*, vol. 53, pp. 113-119.

Khin Cho Lin, San Nwe Zin and Daw Hla Ngwe. (2019). "Isolation and Genotypic Identification of *Acidithiobacillus ferrooxidans*". *J. Myanmar Academy of Arts and Science*, vol. XVII, No. 1A, pp. 591-602.

Natal'ya, V. and Muravyov, M. (2010). "Two-stage Bacterial-chemical Oxidation of Refractory Gold-bearing Sulphide Concentrates". *Hydrometallurgy*, vol. 101 (1-2), pp. 28-34.

Olson, J. G. (1994). "Microbial Oxidation of Gold Ores and Gold Bioleaching". *FEMS Microbial Letters*, vol. 119**,** pp**.** 1-6.

Quatrini, R. and Holmes, D. S. (2005). "Genomic Insights into the Iron Uptake Mechanisms of the Biomining Microorganism *A. ferrooxidans*". *Journal of Industrial Microbiol Biotechnol*, vol. 32, pp. 606-614.

Raju, S. V. P. (2005). "Comparison of Different Extraction Methods to Determine Gold in Geological Samples". *Journal of Scientific and Industrial Research*, vol. 65, pp. 65-67.

Rohwerder, T., Gehrke, T. and Kinzler, K. (2003). "Bioleaching Review Part A". *Applied Microbiology and Biotechnology*, vol. 63(3), pp. 239-248.

Sen, C. (2015). "Bioleaching of Gold: An Alternative Green Mining Technology for 21st Century". *Microbiology World*, vol. 2 (3), pp. 13-14.

Silverman, M. P. and Lundgren, D. G. (1985). "Study on the Chemolithotrophic Iron Bacterium *Thiobacillus ferrooxidans*: An Improved Medium and a Harvestion Procedure for Securing High Cell Yields". *J. Bacteriol*, vol. 77, pp. 642-674.

Zahan, S., Tanmi, T. and Rahman, S. (2017). "Extraction of High Purity SiO_2 from Raw Quartz". *Imperial Journal of Interdiscilpinary Research (IJIR)*, vol. 2, pp. 2001-2004.

PHYTOCHEMICAL CONSTITUENTS AND SOME BIOLOGICAL ACTIVITIES OF THE STEMS OF *ALLAMANDA CATHARTICA* L. (SHWEWA-PAN)

Yin Yin Tun[1] , Khine Zar Wynn Lae[2], Nwet Nwet Win[3], Daw Hla Ngwe[4]

Abstract

The aim of this research is to isolate bioactive compound of the stems of *Allamanda cathartica* L. (Shwewa-pan) and to investigate some biological activities. According to the phytochemical tests, alkaloids, flavonoids, terpenoids, steroids, glycosides, organic acids, phenolic compounds, saponins, tannins and carbohydrates were found to be present in the stems. The ethanol and watery extracts of total phenolic content (31.98 ± 0.94 mg GAE/g, 18.91 ± 0.53 mg GAE/g), total flavonoid contents (226.67 ± 8.50 mg QE/g, 100.67 ± 9.29 mg QE/g), total steroid contents (278.81 ± 7.70 mg CE/g , 154.72 ± 13.31 mg CE/g) and total tannin contents (317.5 ± 0.00 mg TAE/g, 25.83 ± 14.4 mg TAE/g) were observed respectively. By thin layer and silica gel column chromatographic methods, one compound, 2, 5, 7 - trihydroxy - 3 - (4 - hydroxyphenyl) - 4H - chromen - 4 - one (0.22 %, m.pt 151 °C), was isolated from ethyl acetate extract of the stems and identified by ^{1}H NMR, ^{13}C NMR, HMQC, HMBC and EI MS spectroscopies. The antioxidant activity of ethanol extract (IC_{50} =10.97 µg/mL) determined by DPPH radical scavenging activity assay was higher than that of watery extract (IC_{50} = 68.37 µg/mL). All of the extracts have mild antimicrobial activity (inhibition zone diameters = 12~18 mm) against all of the microorganisms. According to the results of brine shrimp cytotoxicity bioassay, both ethanol and watery extracts have cytotoxic effect. It was found that EtOAc, PE and EtOH extract exhibited the inhibition of tumor formation. Both ethanol and watery extracts did not show antiproliferative activity, however, 2, 5, 7 - trihydroxy - 3 - (4 -hydroxyphenyl) - 4H - chromen - 4 - one showed activity against A 549 (IC_{50} = 41.7 µg/mL), MCF 7 (IC_{50} = 47.9 µg/mL) and Hela (IC_{50} = 8.91 µg/mL) human cancer cell lines.

Keywords : *Allamanda cathartica* L., antioxidant activity, antimicrobial activity, cytotoxicity, antitumor activity, antiproliferative activity, 2, 5, 7-trihydroxy-3 - (4 hydroxyphenyl) - 4H - chromen - 4 - one

Introduction

Plants based drugs have been used worldwide in traditional medicines for the treatment of various diseases. Shwewa-pan scientifically known as *A.cathartica* is of the plant family Apocynaceae. Genus is *Allamanda* and species is *cathartica.* Myanmar name is Shwewa-pan and also called Shwe-pan-nwe. Other common names are Golden trumpet, Yellow bell, Buttercup flower and Angle's trumpet (Chandrasekhar *et al*., 2012). Allamanda species are apparently native to northern Brazil Guyana, Surinam and probably French Guiana. It is a genus of climbing shrubs. The distribution of this species is global but is mainly presented in subtropical to tropical (Uduak and Esther, 2015). In Myanmar it is cultivated as ornamental garden plants. *A.cathartica* has long been used in traditional medicine for treating malaria and jaundice. The leaf extract was found to promote wound healing. The flower is also used as a laxative. The chemical constituents are allamandin, allamandicin, allamdin, plumericin, isoplumericin, plumieride, ursolic acid, beta-amyrin, beta-sitosterol, fluvoplumeirin, lupeol, quercetin, kaempferol, glabridin and naringenin (Fah, 2013).

[1] Dr, Assistant Lecturer, Department of Chemistry, Bago University
[2] Dr, Lecturer, Department of Chemistry, University of Yangon
[3] Dr, Associate Professor, Department of Chemistry, University of Yangon
[4] Dr, Professor and Head (Retd.,), Department of Chemistry, University of Yangon

A. cathartica (Shwewa-pan) has been chosen for this research because it has various biological activities and bioactive chemical constituents, and also due to the lack of scientific report on the locally grown *A. cathartica*. In this research work, screening of phytochemical constituents and investigation of antioxidant, antimicrobial and antitumor activities of the stems of *A.cathartica* (Shwewa-pan) were carried out on the respective various crude extracts.

Materials and Methods

Plant materials

The stems of *A. cathartica* were collected from Bago University Campus, Bago Township, Bago Region, during October, 2015. Some pharmacological activities such as antioxidant activity, antimicrobial activity, cytotoxicity, antitumor activity and antiproliferative activity of various crude extracts of the stems were determined in.

Phytochemical Screening

Preliminary phytochemical tests such as alkaloids, flavonoids, terpenoids, steroids, glycosides, organic acids, starch, phenolic compounds, saponins, tannins, carbohydrates, cyanogenic glycosides, reducing sugars and α- amino acids tests were carried out according to the appropriate reported methods (Sofowora, 2000).

Determination of Nutritional Values

The nutritional values such as moisture, ash, fiber, protein, fat and carbohydrate contents were determined by the respective AOAC method. (AOAC, 2000)

Preparation of Various Crude Extracts

(i) Preparation of pet-ether extracts

100 g of each dried powdered sample was extracted with 250 mL of pet-ether (60-80 °C) by using Soxhlet extractor. The filtrates were concentrated by removal of the solvent to give the respective pet-ether crude extract.

(ii) Preparation of ethyl acetate extracts

50 g of each dried powdered sample was extracted with 150 mL of ethyl acetate in similar manner mentioned in above procedure to yield the respective ethyl acetate extract.

(iii) Preparation of 95 % ethanol extracts

The marc from ethyl acetate extracts were refluxed with 150 mL of 95 % ethanol for 6 hours and filter under suction. Evaporation of the solvent was done under reduced pressure to get 95 % ethanol extract.

(iv) Preparation of watery extracts

Watery extract of each dried powdered sample was prepared by boiling 100 g of sample with 250 mL of distilled water for 6 hours and filtered. The filtrates were concentrated by removal of the water to give watery extract.

Determination of Total Phenol content by Folin-Ciocalteu reagent (FCR) method

The total phenolic content (TPC) in each sample was estimated by Folin-Ciocalteu method according to the procedure described by Song *et al.,* (2010). Each extract solution (1000 µg/mL) was mixed with 5 mL of F-C reagent (1:10) and incubated for about 5 min. To each test tube, 4 mL of 1 M sodium carbonate was added and the test tubes were kept at room temperature for 15 min and UV absorbance of reaction mixture was read at λ_{max} 765 nm. The blank solution was prepared as the above procedure by using distilled water instead of sample solution. Total phenol content was estimated as milligram gallic acid equivalent per gram (mg GAE/g) of extract.

Determination of Total Flavonoid Content by Aluminium chloride method

The total flavonoid content (TFC) in each sample was estimated by Aluminium Chloride method according to the procedure described by Song *et al.,* (2010). Each extract solution (1000 µg/mL) was mixed with 1.5 mL of methanol, 0.2 mL of 1 % $AlCl_3$ solution and 2.8 mL of distilled water. The absorbance of reaction mixture was at λ_{max} 415 nm. The blank solution was prepared as the above procedure by using distilled water instead of sample solution. Total flavonoid content was estimated as milligram quercetin equivalent per gram (mg QE/g) of extract.

Determination of Total Steroid Content by Zak's method

The total steroid content (TSC) in each sample was estimated by Zak's method according to the procedure described by Zak *et al.*, (1981). Each extract solution (1000 µg/mL) was prepared by ferric chloride diluting agent. The test sample solution (5 mL) was added 4.0 mL of concentrated sulphuric acid to each tube. After 30 minutes incubation, intensity of the colour was read at 450 nm. The blank solution was prepared as the above procedure by using ferric chloride diluting agent instead of sample solution. Total steroid content was estimated as milligram cholesterol equivalent per gram (mg CE/g) of extract.

Determination of Total Condensed Tannin by Broadhurst's method

The total condensed tannin contents were determined by method of Broadhurst and Jones (1978) with slight modification, using tannic acid as a reference compound. A volume of 0.4 mL of extract is added to 3 mL of a solution of vanillin and 1.5 mL of concentrated hydrochloric acid. After 15 min of incubation the absorbance was read at 500 nm. The blank solution was prepared as the above procedure by using methanol instead of sample solution. The condensed tannin was expressed as milligram of tannic acid equivalent per gram of extract.

Isolation and Identification of Phytochemical Constituent from EtOAc Extract of Stems of *A. cathartica* by Column Chromatography

Dried powdered stems sample (1000 g) were percolated in 1000 mL of 70 % EtOH for one week and filtered. This procedure was repeated for three times. Then the filtrate was concentrated by using a vacuum rotatory evaporator to get EtOH extract (23 g). Then the EtOH extract was defatted by using pet-ether and the defatted EtOH extract was successively partitioned between EtOAc and water. The EtOAc layer was concentrated under reduced

pressure using vacuum rotatory evaporator. Ethyl acetate crude extract (23 g) from the stems of *A. cathartica* was subjected to column chromatographic separation using silica gel (63-210 µm mesh). Gradient elution was performed successively with PE: EtOAc system in the ratios of 5:1, 3:1, 1:1, 1:2, 1:5 v/v followed by EtOAc only and MeOH only. Successive fractions obtained were combined on the basis of their behavior on TLC. Finally, seven main fractions F-I to F-VII was obtained.

After the solvents have been evaporated, fraction F-I (f_{1-2}), F-II (f_{3-4}). F-IV (f_{8-27}), F-V (f_{28-29}), F-VI (f_{30-31}) and F-VII (f_{32-33}) were obtained. The fraction F-III was evaporated and washed with pet-ether, giving yellow powder of the Compound A in 121.1 mg (0.22 % of yield).

The isolated compound was then identified by using joint application of its physicochemical properties and modern spectroscopic techniques such as UV, FT IR, NMR and Mass spectroscopies, and compared with the reported data. The NMR and Mass spectra of the isolated compound were measured at Division of Natural Product Chemistry, Institute of Natural Medicine, and University of Toyama, Japan.

Screening of Antioxidant Activity of Ethanol and Watery Extracts of the Stems of *A. cathartica*

In this experiment, DPPH (2 mg) was thoroughly dissolved in EtOH (100 mL). This solution was freshly prepared in the brown coloured reagent bottle and stored in the fridge for no longer than 24 h. Each tested samples (2 mg) and 10 mL of EtOH were thoroughly mixed by shaker. The mixture solution was filtered and the stock solution was obtained. By adding with EtOH, the sample solutions in different concentrations of 200, 100, 50, 25, 12.5 and 6.25 µg/mL were prepared from the stock solution. The effect on DPPH radical was determined by using the method of Marinova and Batchvarov (2011). The control solution was prepared by mixing 1.5 mL of 50 µM DPPH solution and 1.5 mL of EtOH using shaker. The test sample solution was also prepared by mixing thoroughly 1.5 mL of 50 µM DPPH solutions and 1.5 mL of each sample solution. The mixture solutions were allowed to stand at room temperature for 30 min. Then, the absorbance of each solution was measured at 517 nm by using UV-1650 spectrophotometer. Absorbance measurements were done in triplicate for each concentration and then mean values so obtained were used to calculate percent inhibition of oxidation. The capability to scavenge the DPPH radical was calculated by using the following equation:

$$\% \text{ RSA} = \frac{A_c - (A - A_b)}{A_c \times 100}$$

Where, %RSA = Radical Scavenging Activity
A_c = absorbance of the control (DPPH only) solution
A_b = absorbance of the blank (EtOH + Test sample solution) solution
A = absorbance of the test sample solution

Screening of Antimicrobial Activity of Various Crude Extracts of the Stems of *A. cathartica* by Agar Disc Diffusion Method

The screening of antimicrobial activity of various crude extracts such as PE, EtOAc, EtOH, watery extracts of the stems of *A. cathartica* were carried out by agar disc diffusion method at Fermentation Laboratory, Pharmaceutical Research Department, Ministry of Industry,

Yangon, Myanmar. Six microorganisms namely *Bacillus subtilis, Staphylococcus aureus, Pseudomonas aeruginosa, Bacillus pumilus, Candida albicans* and *Escherichia coli* were used for this test (Perez *et al*., 1990).

Determination of Cytotoxicity

The cytotoxicity of crude ethanol and watery extracts of the sample was investigated by using brine shrimp lethality bioassay according to the procedure described by Dockery and Tomkins, 2000. The brine shrimp (*Artemia salina*) was used in this study for cytotoxicity bioassay (Ali *et al*., 2016). Brine shrimp cysts (0.5 g) were added to the 1.5 L of artificial sea water bottle. This experiment was carried out at the Department of Chemistry, Yangon University, Myanmar. The suspension was aerated by bubbling air into the funnel and kept for 24 h at room temperature. After aeration had been removed, the suspension was kept for 1 h undisturbed, whereby the remaining unhatched eggs dropped. In order to get a higher density of larvae, one side of the separating funnel was covered with aluminium foil and the other illuminated with a lamp, whereby the phototropic larvae were gathering at the illuminated side and could be collected by pipette. The shrimp larvae were transferred to an agar well filled with 9 ml of salt water and the dead larvae counted (number N). A solution of crude extract (1, 10, 100, 1000 ppm) (1 mL) was added and the plate kept at room temperature in the dark. After 24 h, the dead larvae were counted in each well under the microscope (number A). The still living larvae were killed by addition of ca. 0.5 mL methanol so that subsequently the total number of the animals could be determined (number G).The control solution was prepared as the above procedure by using distilled water instead of sample solution. The mortality rate M was calculated in %. Each test row was accompanied by a brine solution (number B). The mortality rate M was calculated by using the following formula:

$$M = \left[\frac{(A - B - N)}{(G - N)} \right] \times 100$$

M = percent of the dead larvae after 24 h

A = number of the dead larvae after 24 h

B = average number of the dead larvae in the brine solution after 24 h

N = number of the dead larvae before starting of the test.

G = total number of brine shrimps

Screening of Antitumor Activity of the Various Crude Extracts from the Stems of *A. cathartica*

The antitumor activity of ethanol, ethyl acetate and petroleum ether extracts from the stems of *A. cathartica* was examined by Potato Crown Gall (PCG) or Potato Disc Assay (PDA) method (Coker *et al.,* 2003) at the Fermentation Laboratory, Pharmaceutical Research Department, Ministry of Industry, Yangon, Myanmar.

Fresh disease-free potatoes were purchased from a local market. Tubers of moderate size were surface sterilized by immersion in 0.1 % sodium hypochlorite for 20 min. Ends were removed and the potatoes were soaked an additional 10 min. A core of the tissue was extracted from each and discarded. The remainder of the cylinder was cut into 1.0 cm thick discs with a

surface sterilized scalpel. The discs were then transferred to agar plates (1.5 g of agar dissolved in 100 mL deionized distilled water, autoclaved for 20 min at 121 ºC, 20 mL poured into each Petri dish). Each plate contained four potato discs and 4 plates, were used for each of the sample solution.

Sample (0.05, 0.10, 0.15 g) was individually dissolved in DMSO (1 mL) and filtered through Millipore filters (0.22 μm) into sterile tube. This solution (0.5 mL) was added to sterile distilled water (1.5 mL), and broth culture of *A. tumefaciens* in PBS (2 mL) was added. Controls were made in this way; DMSO (0.5 mL) and sterile distilled water (1.5 mL) were added to the tube containing 2 mL of broth culture of *A. tumefaciens.* By using a sterile disposal pipette, 1 drop (0.05 mL) each from these tubes was used to inoculate each potato disc by spreading it over the disc surface. After inoculation, Petri dishes were sealed by film and incubated at 27~30 ºC for 3 days. Observation was made on appearance of tumors on potato discs after 3 days under stero-microscope followed by staining with Lugol's iodine (10 % KI and 5 % I_2) after 30 min and compared with control. The antitumor activity was examined by observation of tumor produced or not on the potato discs. The results are shown in Table 4.

Determination of Antiproliferative Activity

Antiproliferative activity of ethanol and watery extracts were investigated in *in vitro* by using cancer cell lines at Division of Natural Product Chemistry, Institute of Natural Medicine, and University of Toyama, Japan. The cell lines used were Hela (human cervix cancer), A 549 (human ung cancer) and MCF 7 (human breast cancer). K562 α-Minimum essential medium with L-glutamine and phenol red (α -MEM, Wako) were used for cell cultures. All media were supplemented with 10 % fetal bovine serum (FBS, sigma) and 1 % antibiotic antimycotic solution (Sigma). For MCF 7 cell, 1 % 0.1 M non-essential amino acid (NEAA, Gibco) and 1 % 1 mM sodium pyruvate (Gibco) were also supplemented. The *in vitro* antiproliferative activity of the crude extracts was determined by the procedure described by Win *et al.* (2015). Briefly, each cell line was seeded in 96-well plates (2×10^3 per well) and incubated in the respective medium at 37 °C under 5 % CO_2 and 95 % air for 24 h. After the cells were washed with PBS (Nissui Pharmaceuticals), serial dilutions of the tested samples were added. After 72 h incubation, the cells were washed with PBS and 100 μL of medium containing 10 % WST-8 cell counting kit (Dojindo; Kumamoto, Japan) solution was added to the wells. After 2 h incubation, the absorbance at 450 nm was measured. The concentrations of the crude extracts were 200, 100, 10 μg/ mL and 10, 1, 0.1 mM for positive control were prepared by serial dilution. Cell viability was calculated from the mean values of the data from three wells using the equation below and antiproliferative activity was expressed as the IC_{50} (50 % inhibitory concentration) value. 5-fluorouracil (5FU) was used as positive control.

$$(\%)\ \text{Cell viability} = 100 \times \frac{\left\{\text{Abs}_{(\text{test samples})} - \text{Abs}_{(\text{blank})}\right\}}{\left\{\text{Abs}_{(\text{control})} - \text{Abs}_{(\text{blank})}\right\}}$$

Results and Discussion

Types of Phytochemicals Present in the Stems of *A. cathartica*

In order to find out the types of phytochemical constituents present in the stems of *A. cathartica*, the phytochemical tests were preliminary carried out according to the reported procedure. From the data findings, it was observed that various secondary metabolites such as alkaloids, flavonoids, terpenoids, steroids, glycosides, organic acids, starch, phenolic compounds, saponins and tannins together with starch and carbohydrates were present, however cyanogenic glycosides, reducing sugars and α- amino acids were not detected in the samples. According to these results, it can be seen that the roots samples might contain potent bioactive secondary metabolites.

Some Nutritional Values of the Stems of *A. cathartica*

The nutritional values were determined by AOAC method resulting 6.91 % of proteins, 2.04 % of moisture, 2.71 % of ash, 62.42 % of fiber and 10.33 % of fat and 5.7 % of carbohydrate in the stems of *A. cathartica.* According to these results, the root samples were found to be high in fiber content. Fiber is a type of carbohydrate that the body cannot digest. Though most carbohydrates are broken down into sugar molecules, fiber cannot be broken down into sugar molecules, and instead it passes through the body undigested. Fiber helps to regulate the body's use of sugars, helping to keep hunger and blood sugar in check.

Total Phenol Contents (TPCs) of the Crude Extracts of the Stems of *A. cathartica*

The total phenol content of the ethanol and watery extracts of the stems were determined with spectrophotometric method by using Folin-Ciocalteu reagent. The total phenol content of the ethanol extract was 31.98 ± 0.94 mg GAE/g those of watery extract was 18.91± 0.53 mg GAE/g. The results are shown in Table 1.

Total Flavonoid Contents (TFCs) of the Crude Extracts of the Stems of *A. cathartica*

The total flavonoid content of the ethanol and watery extracts of the stems were determined with spectrophotometric method by aluminium chloride reagent. The total flavonoid contents of ethanol and watery extracts of the stems were found to be 226.67 ± 8.50 mg QE/g and 100.67 ± 9.29 mg QE/g respectively. The results are shown in Table 1.

Total Steroid Contents (TSCs) of the Crude Extracts of the Stems of *A. cathartica*

The total steroid content of the ethanol and watery extracts of the stems were determined by Zak's method were found to be 278.81 ± 7.70 mg CE/g and 154.72 ± 13.31 mg CE/g of crude extracts, respectively. The results are shown in Table 1.

The Total Condensed Tannin Contents (TCTCs) of the Crude Extracts of the Stems of *A.cathartica*

The total condensed tannin in the ethanol and watery extracts estimated by Broadhurst's method were found to be the same content of 317.5 ± 0.00 mg TAE/g and 25.83 ± 14.4 mg TAE/g, respectively. The results are shown in Table 1.

Table 1 Total Phenol Contents (TPCs), Total Flavonoid Contents (TFCs), Total Steroid Contents (TSCs) and Total Condensed Tannin Contents (TCTCs) of Crude Extracts

Types of compounds	EtOH extracts	Watery extracts
TPCs (mg GAE ± SD)/g of extract	31.98 ± 0.94	18.91 ± 0.53
TFCs (mg QE ± SD)/g of extract	226.67 ± 8.50	100.67 ± 9.29
TSCs (mg CE ± SD)/g of extract	278.81 ± 7.70	154.72 ± 13.31
TCTs (mg TAE ± SD)/g of extract	317.5 ± 0.00	25.83 ± 14.40

Identification of the Compounds Isolated from the EtOAc Extract from the Stems of *A. cathartica*

From the silica gel column chromatographic separation of EtOAc extract of the stems, one compound was isolated; compound A as white crystal in 1.51 % of yield based on EtOAc extract. Melting point of compound A was found to be 151°C and its R_f value was observed to be 0.6 (n-hexane: EtOAc, 3:1 v/v). Compound A is soluble in chloroform, methanol and ethyl acetate but insoluble in pet-ether, ethanol and acetone. It was isolated as a flavonoid compound containing phenolic -OH group.

Compound A was then structurally identified by using 1D and 2D NMR and EI-MS spectroscopies. The integration of ^{1}H NMR (500 MHz, $CDCl_3$) spectrum (Figure 1) indicated the presence of only six protons in the compound A. The two doublet signals with coupling constant of 10 Hz appeared at δ_H 8.00 ppm and the two doublet signals with coupling constant of 10 Hz appeared at δ_H 6.89 ppm showed that there were four methine groups. The singlet signals appeared at δ_H 6.15 ppm and 6.39 ppm indicated the presence of two methine groups.

According to the ^{13}C NMR (125 MHz, $CDCl_3$) spectrum (Figure 2) of the isolated compound A, it was found that there were fifteen carbons including six methine carbons at the chemical shifts of δ_C 130.04, 130.04, 115.96, 115.96, 98.72 and 94.05 ppm, eight quartenary carbons at δ_C 164.4, 161.25, 159.71, 156.71, 147.32, 136.19, 122.21 and 103.58 ppm and one carbonyl group at δ_C 176.42 ppm.

The C and H ($^{1}J_{C\text{-}H}$) one bond correlation of A is described in HMQC spectrum (Figure 3) and Table 2.

According to mass spectrum (Figure 4), the molecular weight of the isolated compound A was found to be m/z 286. From NMR spectral data, it could be assumed that there were 15 carbons, 6 protons, one carbonyl group and hydroxyl group (more than one). If this compound contains two hydroxyl groups, the partial molecular formula is $C_{15}H_8O_4$ with molecular weight of m/z 252. The remaining molecular weight of m/z was 34. Consequently, the isolated compound must contain another two oxygen atoms as two hydroxyl groups. The complete structural formula of this isolated compound must be assigned as $C_{15}H_{10}O_6$ with the molecular weight 286.

The correlation between the protons directly attached to the carbons, i.e., types of carbons (methyl, methine and quarternary carbons) was studied by HMQC spectrum (Figure 3). Furthermore, the long range proton-carbon correlation was also examined by using 2 D HMBC spectrum (Figures 5, 6, 7 and 8).

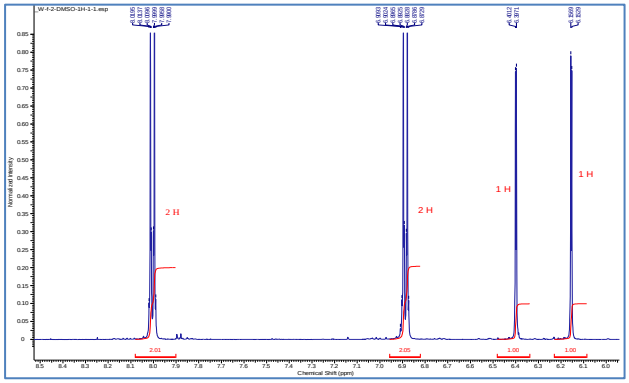

Figure 1 ^{1}H NMR spectrum (500 MHz, $CDCl_3$) of the isolated compound

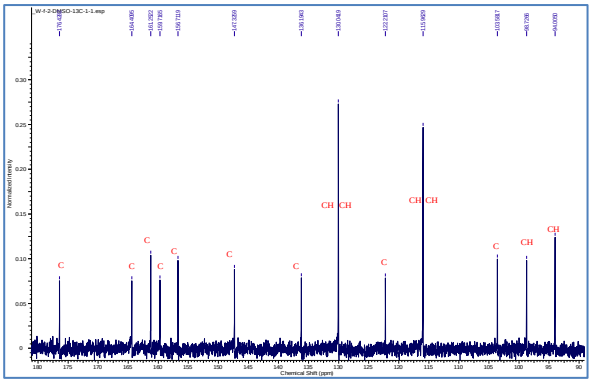

Figure 2 ^{13}C NMR spectrum (125 MHz, $CDCl_3$) of the isolated compound

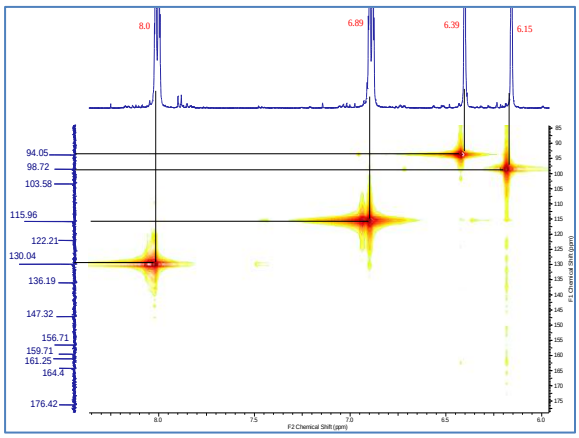

Figure 3 HMQC spectrum (500 MHz, $CDCl_3$) of the isolated compound A

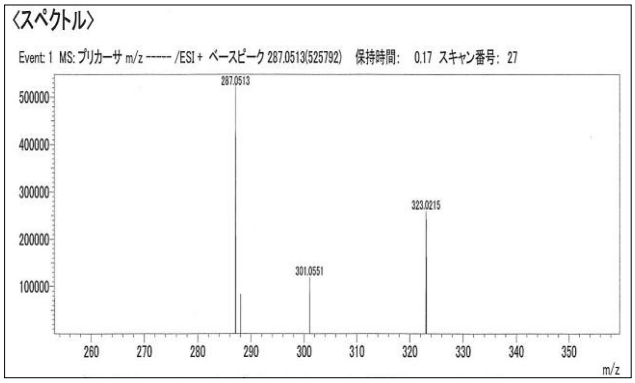

Figure 4 Mass spectrum of the isolated compound YYT-2

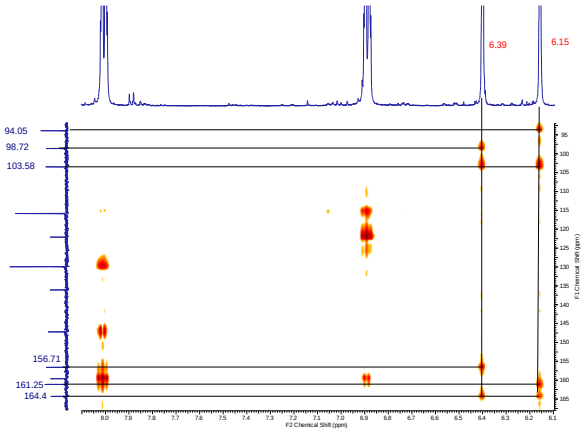

Figure 5 MBC spectrum of the isolated compound A

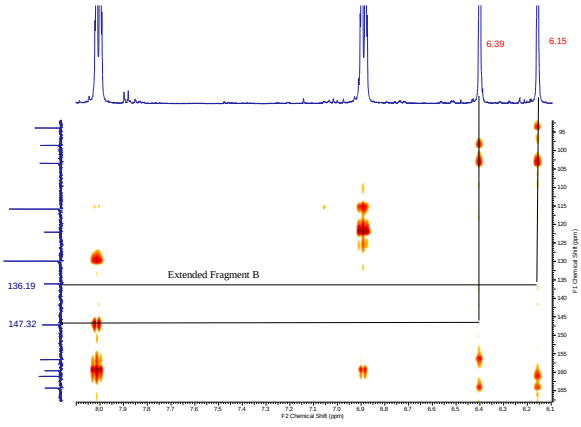

Figure 6 HMBC spectrum of the isolated compound A

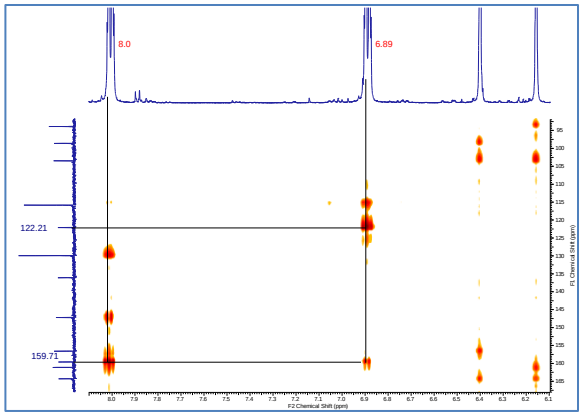

Figure 7 HMBC spectrum of the isolated compound A

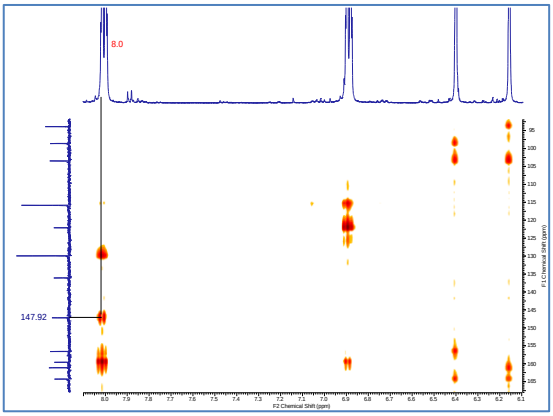

Figure 8 HMBC spectrum of the isolated compound A

Table 2 ^{1}H and ^{13}C NMR (500 MHz, $CDCl_3$ and 125 MHz, $CDCl_3$) and HMQC Assignment of Isolated Compound A

δ_C, type	δ_H, (*J* in Hz)
176.42, C=O	-
164.4, C-OH	-
161.25, C	-
159.71. C-OH	-
156.71, C-OH	-
147.32, C	-
136.19, C-OH	-
130.04, CH	8.00, d (10)
130.04, CH	8.00, d (10)
122.21	-
115.96, CH	6.89, d (10)
115.96, CH	6.89, d (10)
103.58	-
98.72, CH	6.15, s
94.05, CH	6.39, s

Finally, the structure of the isolated compound A was assigned as 2, 5, 7 - trihydroxy - 3 - (4 - hydroxyphenyl) - 4H - chromen - 4 – one.

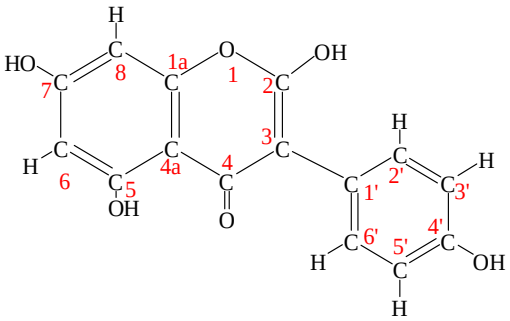

2, 5, 7 - trihydroxy - 3 - (4 - hydroxyphenyl) - 4H - chromen - 4 – one

Antioxidant Activity of the Stems of *A. cathartica*

The antioxidant activity was measured in terms of hydrogen donating or radical scavenging ability of the EtOH and watery extracts of the samples by using the stable radical DPPH. The radical scavenging activity of standard gallic acid is shown in Table 3 and Figure 9. The results are shown in Table 4, Figure 10 and 11. From these observations, the radical scavenging activity of EtOH extracts (IC_{50} = 10.97 μg/mL) was found to be greater than watery extracts (IC_{50} = 68.37 μg/mL).

Table 3 Radical Scavenging Activity of Standard Gallic Acid

Sample	% RSA ± SD at Different Concentration (μg/mL)					IC_{50} (μg/mL)
	0.625	1.25	2.5	5	10	
Gallic Acid	25.20 ± 1.40	53.58 ± 0.88	65.53 ± 1.13	74.82 ± 0.59	94.59 ± 0.48	1.17

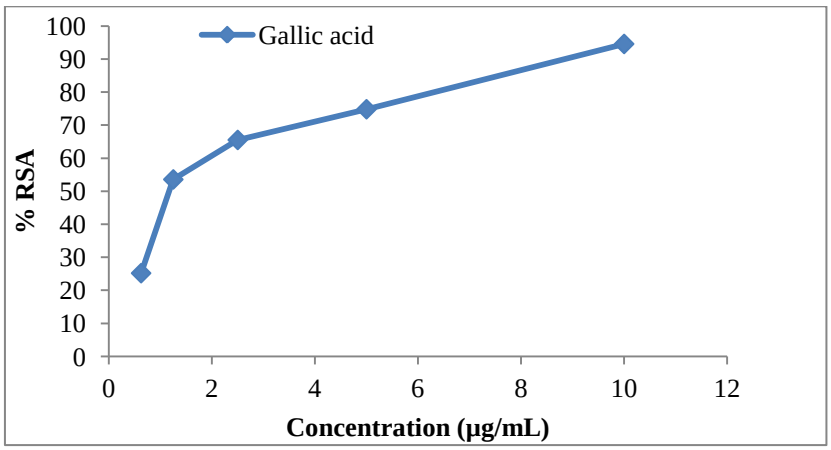

Figure 9 A plot of % DPPH free radical scavenging activity *vs* different concentrations of standard gallic acid

Table 4 % Radical Scavenging Activity and IC_{50} Values of Crude Extracts of the Stems of *A. cathartica* by DPPH Radical Scavenging Assay

Extracts	% RSA ± SD at Different Concentration (μg/mL)						IC_{50} (μg/mL)
	6.25	12.5	25	50	100	200	
Ethanol (Stems)	22.39 ± 0.00	51.49 ± 0.00	58.96 ± 0.02	79.10 ± 0.00	81.34 ± 0.00	95.52 ± 0.00	10.97
Watery (Stems)	4.25 ± 0.63	12.53 ± 1.42	23.04 ± 3.32	39.15 ± 0.16	68.68 ± 1.58	98.66 ± 0.95	68.37

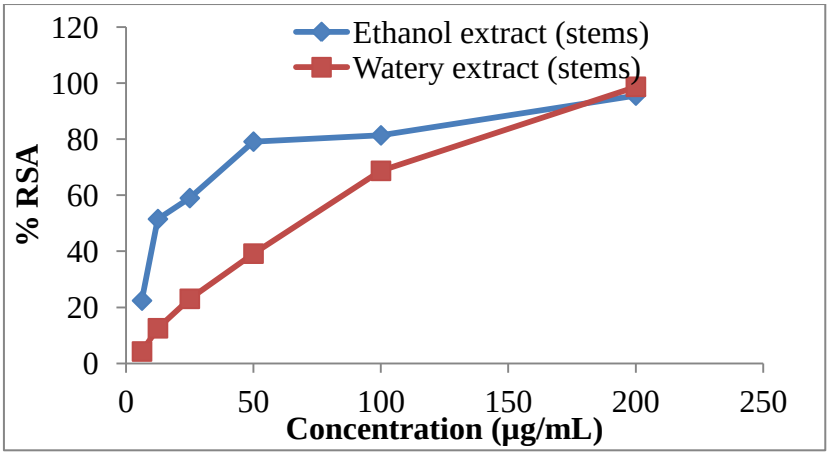

Figure 10 A plot of % DPPH free radical scavenging activity *vs* different concentrations of crude extracts of the stems of *A. cathartica*

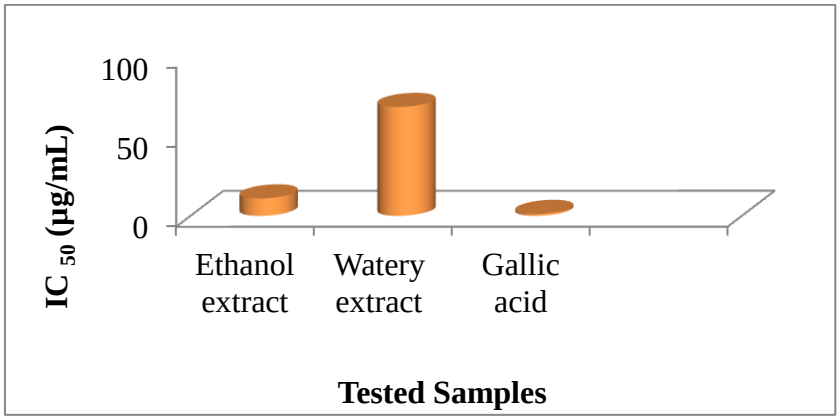

Figure 11 A bar graph of IC_{50} values of stems of *A. cathartica* (DPPH free radical scavenging assay)

Antimicrobial Activity of Crude Extracts of the Stems of *A. cathartica*

Four crude extracts such as PE, EtOAc, EtOH and water extracts from the stems of *A. cathartica* were subjected to screening of antimicrobial activity against six different pathogenic microbes such as *Bacillus subtilis, Staphylococcus aureus, Pseudomonas aeruginosa, Bacillus pumilus, Candida albicans and Escherichia coli* using agar well diffusion method. This method is based on zone diameter including the well diameter, in millimeter (mm). The larger the zone diameter, the higher the activity is. According to the results, PE, EtOH and EtOAc extracts of stems showed mild antimicrobial activities against all tested microorganisms whereas watery extract of the stems did not show antimicrobial activity against *P. aeruginosa* and *E. coli*. The resulted data are shown in Table 5.

Table 5 Inhibition Zone Diameters of Various Extracts of the Stems of *A. cathartica* against Six Microorganisms by Agar Well Diffusion Method

No.	Microorganisms	Inhibition Zone Diameters (nm) of Different Crude Extracts			
		PE	EtOAc	EtOH	Watery
1	*Bacillus subtilis*	13 (+)	14 (+)	16 (++)	13 (+)
2	*Staphylococcus aureus*	13 (+)	15 (++)	14 (+)	14 (+)
3	*Pseudomonas aeruginosa*	18 (++)	18 (++)	15 (++)	-
4	*Bacillus pumilus*	12 (+)	13 (+)	14 (+)	15 (++)
5	*Candida albicans*	12 (+)	14 (+)	15 (++)	15 (++)
6	*Escherichia coli*	14 (+)	14 (+)	14 (+)	-

Agar well – 10 mm, 10 mm ~ 14 mm (+), 15 mm ~ 19 mm (++), 20 mm and above (+++)

Cytotoxicity of the Ethanol and Watery extracts of the Stems of *A. cathartica*

The cytotoxicity of water and ethanol extracts from the sample was evaluated by brine shrimp cytotoxicity bioassay. This bioassay is general toxicity screening for bioactive phytoconstituents and their derivatives. A model animal that has been used for this purpose is the brine shrimp, *Artemia salina* (Tawaha, 2006). The cytotoxicity of crude extracts was expressed in term of mean ± SEM (standard error mean) and LD_{50} (50% Lethality Dose) and the results are shown in Table 6. In this experiment, standard potassium dichromate ($K_2Cr_2O_7$) and caffeine were chosen because $K_2Cr_2O_7$ is well-known toxic in this assay (Salinas and Fernendez, 2006) and caffeine is a natural product. According to the results of brine shrimp cytotoxicity bioassay, all of the tested samples have cytotoxic effect.

Table 6 Cytotoxicity of Ethanol and Watery Crude Extracts of the Stems Samples

Crude extracts	Dead % by using different concentrations (μg/mL) of samples				LD_{50} (μg/mL)
	1	10	100	1000	
EtOH	40.00 ±17.32	90.30 ± 0.53	100±0.00	100 ± 0.00	2.79
Watery	48.83 ±14.95	80.65 ± 6.01	82.35 ±10.04	84.83 ± 5.29	1.34
*Caffeine	0 ± 0	0 ± 0	9.582 ±0.917	12.73 ±4.103	>1000
*$K_2Cr_2O_7$	48.63 ±19.19	73.13 ±4.076	74.67 ±11.8	100 ± 0	1.5

*****standard

Antitumor Activity of the Stems of *A. cathartica*

Antitumor activity in this study was investigated by potato crown gall (PCG) assay as it is a valuable tool that indicated antitumor activity of the tested samples by their inhibition of the crown gall formation that was induced in wounded potato tissues by *Agrobacterium tumefaciens*.

Table 7 Tumor Inhibition by the Crude Extracts from the Stems of *A. cathartica*

Test Samples	Extracts/Compound	Concentrations of Samples (g/mL/disc)	Tumor Inhibition Activity
Control	-	0.00	-
Stem	PE	0.05	+
	PE	0.10	+
	PE	0.15	+
	EtOAc	0.05	+
	EtOAc	0.10	+
	EtOAc	0.15	+
	EtOH	0.05	+
	EtOH	0.10	+
	EtOH	0.15	+

(+) antiumor activity present, (-)antiumor activity absent

It could be clearly seen from the Table 7 that, all of the samples inhibited tumor growth in a concentration dependent manner. Significant tumor inhibition was observed at the concentrations of 0.05, 0.10 and 0.15 g/mL/disc.

Since, tumor inhibition significantly occurred by the extracts of the stems of *A. cathartica* on potato discs, it could be concluded that *A. cathartica* might be used as a potential source of antitumor agent.

Antiproliferative Activity of the Stems of *A. cathartica*

Antiproliferative activity was studied in vitro using human cancer cell lines. Screening of antiproliferative activities of ethanol and watery extracts from the stems of *A. cathartica* was done by using three human cancer cell lines such as A 549 (human lung cancer), MCF7 (human breast cancer) and Hela (human cervix cancer). Antiproliferative activity was expressed as the IC_{50} (50 % inhibitory concentration) value. 5-Fluorouracil was used as positive control. The antiproliferative activity of crude extracts is summarized in Table 8. Ethanol and watery extracts of stems did not show antiproliferative activity. Compound A was found to possess antiproliferative activity against lung cancer (A 549) (IC_{50} = 41.7 µg/mL), breast cancer cell (MCF 7) (IC_{50} = 47.9 µg/mL) and cervix cancer cell (Hela) (IC_{50} = 8.91 µg/mL).

Table 8 Antiproliferative Activities of the Crude Extracts and the Isolated Compound A of *A. cathartica*

Samples	IC_{50} (µg/mL) of Various Samples against Tested Cell Lines		
	A 549	MCF 7	Hela
EtOH extract	>100	>100	>100
Watery extract	>100	>100	>100
Compound A	41.7	47.9	8.91
*5FU	10.2	11.5	6.93

A 549 = Lung cancer cell lines; MCF = Breast cancer cell lines; Hela = Cervix cancer cell lines; *5FU = 5 Fluorouracil

Conclusion

From the overall assessment concerning with the investigation of phytochemicals and biological activities on the stems of *A. cathartica*, the following inferences could be deduced. One organic compound, 2, 5, 7 - trihydroxy - 3 - (4 - hydroxyphenyl) - 4H - chromen - 4 – one (0.22 %, mpt. 151 °C) was isolated from ethyl acetate crude extract of the stems by using silica gel column chromatographic separation technique. The ethanol extract possessed greater antioxidant activity than that of the watery extract. According to the antimicrobial activities, PE, EtOH and EtOAc extracts of stems showed mild antimicrobial activities against all tested microorganisms whereas watery extract of the stems did not show antimicrobial activity against *P. aeruginosa* and *E. coli.* Furthermore EtOAc, PE and EtOH extracts of stems were also found to inhibit the formation of tumor. However, ethanol and watery extracts did not show antiproliferative activitiy, compound A showed antiproliferative activity against A 549 (41.7 µg/mL), MCF 7 (47.9 µg/mL) and Hela (8.91 µg/mL).

In conclusion, antimicrobial, antioxidant and antitumor activities of different extracts obtained from the stems of *A. cathartica* grown in Myanmar could be evaluated. In conclusion, the chemical constituents in ethanol extract of the stems were found to be rich comparing with other extracts. Among the chemical constituents, total condensed tannin contents were observed to be highest in ethanol extract. The second and third highest chemical constituents were found to be the steroid and flavonoid compounds. Flavonoid and tannin compounds can prevent the development of bacteria and can be converted to inactive substances. Among the nutritional constituents of both of the sample powder, the fiber content was observed in highest amount. Fiber is a type of carbohydrate that the body cannot digest. Though most carbohydrates are broken down into sugar molecules, fiber cannot be broken down into sugar molecules, and instead it passes through the body undigested. Fiber helps to regulate the body's use of sugars, helping to keep hunger and blood sugar in check. The ethanol extract of stems showed the distinct higher activities such as antioxidant activity than the watery extract. Therefore, the present study will contribute that the stems of *A. cathartica* can be used in the traditional medicinal formulation for the treatment of many diseases.

Acknowledgements

The authors would like to express their profound gratitude to the Department of Higher Education (Lower Myanmar), Ministry of Education, Yangon, Myanmar, for provision of opportunity to do this research and Myanmar Academy of Arts and Science for allowing to present this paper. Greatful thanks are also to Professor Dr Hiroyuki Morita, Institute of Natural Medicine, University of Toyama for his help and suggestions throughout course of antiproliferative activity and for NMR and MS spectroscopic measurements.

References

Ali, N., Zada, A., Ali, M. and Hussain, Z. (2016). "Isolation and Identification of *Agrobacterium tumefaciens* from the Galls of Peach Tree". *Journal of Rural Development and Agriculture*, vol. 1 (1), pp. 39-48.

A.O.A.C. (2000). *Official and Tentative Methods of Analysis.* Association of Official Analytical Chemists, USA: 17th Ed., Gaithersburg, Maryland, AOAC International, pp. 63-67.

Broadhurst, R. B. and Jones, W. T. (1978). "Analysis of Condensed Tannins using Acidified Vanillin". *J. Sci. Food Agr.*, vol. 29, pp. 788-794.

Chandrasekhar, N., Siddartha, V. and Venkateswarlu, B. (2012). "Evaluation of Antimicrobial Activity of Flower Extracts of *Allamanda cathartica* L.". *International Journal of Pharma World Research*., vol. 3, (2), pp. 1-20.

Coker, P.S., Radcke, J., Guy, C. and Camper, N. D. (2003). "Potato Tumor Induction Assay: A Multiple Mode of Action Drug Assay". *Phytomedicine,* vol. 10, pp. 133-138.

Dockery, M. and Tomkins, S. (2000). *Brine Shrimp Ecology*. London : 1st Ed., The British Ecology Society, pp. 92-93.

Fah, W. K. (2013). *Tissue Culture Studies, Secondary Metabolites and Pigment Extraction from Allamanda cathartica L.*. MSc Thesis, University of Malaya, Kuala Lumpur, pp. 13-14.

Marinova, G. and Batchvarov, V. (2011). "Evaluation of the Methods for Determination of the Free Radical Scavenging Activity by DPPH". *J.Agric. Sci*., vol. 17, 11-24.

Perez, C., Paul, M. and Bazerque, P. (1990). "Antibiotic Assay by Agar Well Diffusion Method.". *Alta BioMed Group Experiences,*vol. 15, pp. 113-115.

Salinas, M. M. G. and Fernandez, S. S. (2006). "A Modified Microplate Cytotoxicity Assay with Brine Shrimp Larvae (*Artemia salina*)". *Pharmacology*, vol. 3, 633–638.

Sofowora, E. A. (2000). "Phytochemical Screening of Nigerian Medicinal Plants". *J. Intergrative Med*., vol. 41, pp. 234-24.

Song, F. L., Gan, R. Y., Zhang, Y., Xiao, Q., Kuang, L. and Li, H. B. (2010). "Total Phenolic Contents and Antioxidant Capacities of Selected Chinese Medicinal Plants". *Int. J. Mol. Sci.,* vol. 11, pp- 2367-2372.

Tawaha, A. K. (2006). "Cytotoxicity Evaluation of Jordanian Wild Plants Using Brine Shrimp Lethality Test". *J. Appl. Sci.*, vol. 8 (1), 12-17.

Uduak, A. E. and Esther, S. U. (2015). "Comparative Phytochemical Screening and Nutritional Potentials of the Stems, Leaves and Flowers of *Allamanda cathartica* (Apocynaceae)". *International Journal of Science and Technology*., vol. 4 (6), pp. 284-253.

Win N. N., Ito, T., Aimaiti, S., Imagawa, H., Ngwe, H., Abe, I. and Morita, H. (2015). "Kaempulchraols A–H, Diterpenoids from the rhizomes of *Kaempferia pulchra* collected in Myanmar". *J. Nat. Prod.*, vol. 78, pp. 1113–1118.

Zak, B., Dickenman, R. C., White, E. G., Burnett, H. and Cherney, P.J. (1981). "Rapid Estimation of Free and Total Cholesterol". *Life Sciences,* vol. 24 (18),pp. 16.

PURIFICATION, IMMOBILIZATION AND BIOCHEMICAL CHARACTERIZATION OF FUNGAL LACCASE FROM MUSHROOM, *TRAMETES VERSICOLOR*

Khaing Khaing Myint[1], Ohn Ohn Soe[2], Daw Hla Ngwe[3]

Abstract

In this research, laccase isolated from fungal source of mushroom, *Trametes versicolor*, white rot fungi in solid state fermentation. Laccase was purified by ammonium sulphate fractionation (20 % and 70 %) and dialysis followed by Sephadex G-100 gel filtration chromatography. In each purification step protein content was determined by Biuret method using Bovine Serum Albumin as standard at 560 nm and laccase activity was determined by gauaicol assay method at 450 nm. The extracellular laccase from *T. vesicolor* was purified to 12.72 fold. The purity of laccase was confirmed by SDS-PAGE as single band. The molecular weight of purified laccase was found to be 60.26 kDa. The immobilization of laccase was carried out by gel entrapment technique using sodium alginate- gelatin- agar mixed gel. The highest laccase activities were found at pH 5 for free laccase at 40 ^{o}C and pH 6 for the immobilized laccase. The optimal temperatures of free laccase and the immobilized laccase were 40 ^{o}C and 45 ^{o}C, respectively, showing the improvement in thermal stability of immobilized laccase. The reaction order of both free and immobilized laccase catalyzed reactions was first order reaction.

Keywords: Laccase, *Trametes versicolor*, guaiacol, immobilization, gel entrapment technique

Introduction

Laccase (benzenediol: oxygen oxidoreductase, EC 1.10.3.2) belongs to a group of polyphenol oxidases containing copper atoms in the catalytic centre and usually called multicopper oxidases (Baldrian, 2005). They are extracellular, multicopper enzymes that use molecular oxygen to oxidize various aromatic and non-aromatic compounds by a radical-catalysed reaction mechanism (Thurston, 1994). Laccases can oxidize *o*-and *p*-diphenols, aminophenols, methoxy-substituted phenols, benzenethiols, polyphenols, polyamines, hydroxyindols, some aryl diamines and a considerable range of other compounds but do not oxidize tyrosine. Its rather low specificity makes laccase a promising tool in transforming many toxic substituted phenols or even non-phenolic compounds such as polycyclic aromatic hydrocarbons. Due to its high efficiency, low cost, and good availability, it has been widely used in various applications including environmental bioremediation (Ashrafi *et al*., 2013; Zhang *et al*., 2012), the food industry (Dhillon *et al*., 2012) and textile engineering (Basto *et al*., 2007).

However, free enzymes have the weakness of non-recyclability, and reusability in industrial applications. These problems can be well solved by enzyme immobilization. Among the various immobilization techniques such as adsorption, crosslinking, entrapment and so on, the entrapment method may be a good choice for enzyme immobilization, as the process of entrapment is mild and causes relatively little damage to the enzyme native structure (Dura ´n *et al*., 2002).

[1] 4 PhD Candidate, Department of Chemistry, University of Yangon
[2] Dr, Associate Professor, Department of Chemistry, University of Yangon
[3] Dr, Professor and Head (Retired), Department of Chemistry, University of Yangon

Laccases are widely distributed in nature and also been detected in plants (lacquer, mango, mung bean, peach, pin etc.), bacteria (*Bacillus subtilis*, *Escherichia coli*, *Pseudomonas syringae*) and especially in fungi (Majeau *et al*., 2010; Lu *et al*., 2017). Among them, white-rot fungi is the major laccase producer, and *Trametes versicolor* is an important representative of white-rot fungi.

Submerged and solid-state modes of fermentation are used intensely for the production of laccase. Submerged fermentation involves the nurturing of microorganisms in high oxygen concentrated liquid nutrient medium. Solid state fermentation is suitable for the production of enzymes by using natural substrates such as agricultural residues because they mimic the conditions under which the fungi grow naturally (Brijwani *et al*., 2010; Couto and Sanromán *et al.,* 2005; Pandey *et al.,* 1999). The lignin, cellulose and hemicelluloses are rich in sugar and promote fungal growth in fermenter and make the process more economical (Couto and Toca-Herrera, 2007).

This study is aimed to isolate laccases from white-rot fungi, *Trametes versicolor* using banana skin under solid state fermentation and to compare the kinetic properties of free laccase and laccase immobilized by alginate-gelatin-agar mixed gel.

Materials and Methods

Chemicals

Potassium hydroxide, guaiacol, sodium acetate buffer, phosphate-citrate buffer, Bovine Serum Albumin(BSA), culture medium, Tween-80, ammonium sulphate, Sephadex G- 100, sodium dodecylsulphate polyacrylamide gel, Coomassie brilliant blue, and a standard high molecular weight protein markers, sodium alginate, gelatin, agar, calcium chloride were used.

Apparatus

Conical flasks, digital pH meter, a constant temperature water bath, UV visible spectrophotometer, glass column (2.0 × 40 cm), an incubator, a shaker, a centrifuge, voltage current stabilizer, air compressor, digital balance, slab gel mould and electrophoresis apparatus, 5 mL syringe were used.

Sample Collection

The mushroom samples were collected in sterile plastic bags from the timber industry compound, Insein Township, Yangon Region, Myanmar.

Isolation and Purification of Laccase Enzyme Solution by Solid State Fermentation

Chopped banana skin (1.0 cm × 1.0 cm) (70 g) was autoclaved at 120 °C for 20 min and then soaked in 200 mL of 83.17 mM potassium hydroxide solution for 1 h to neutralize the organic acid. The samples were dried at room temperature for one day after washing thoroughly with distilled water.

The composition of culture medium consisted of 3 g of peptone, 10 g of glucose, 0.6 g of potassium dihydrogen phosphate, 0.001 g zinc sulphate, 0.4 g dipotassium hydrogen phosphate, 0.0005 g of iron(II) sulphate, 0.05 g manganese(II) sulphate and 0.5 g magnesium sulphate in

1 L of distilled water . An inducer , copper (II) sulphate pentahydrate (0.0001 g) and one drop of Tween - 80 were added to the culture medium.

Laccase was extracellularly excreted by *Trametes versicolor* during solid state fermentation. Three loops of fungal strain, 5 mL of culture medium and 30 g of the pretreated banana skin were inoculated in a 500 mL conical flask. This flask was incubated at 30 °C for 18 days. Fungal growth and enzyme activity were assayed periodically. To optimize the time for fungal growth, the fermented matter (2 g) of the specified period (3, 6, 9, 12, 15, 18 days) was obtained by adding 10 mL of distilled water to it. The flasks were mixed for 30 min at room temperature using a shaker (180 rpm). Solids were removed first by filtering and then by centrifuging at 2000 rpm for 20 min. The cell free supernatant obtained was used as crude enzyme extract for purification. (Khaing Khaing Myint *et al.,* 2018).

Purification of Laccase

After 12 days of fermentation, the fermented matter of *Trametes versicolor* was dissolved in acetate buffer (pH 5) with 1:10 ratio and shaken on the shaker for 20 min. It was filtered to remove mycelia, followed by centrifugation at 2000 rpm for 30 min. The supernatant thus obtained was subjected to the total protein precipitation with ammonium sulphate in the range of 20–70 % saturation to obtain partially purified enzyme extract. It was concentrated and dialysed overnight against sodium acetate buffer at pH 5. Gel filtration chromatography was performed using Sephadex G-100 column (2.0 × 40 cm). The dialyzed sample was then applied to Sephadex G- 100 for further purification. Active fractions with high laccase activity and high protein content were pooled together and the resulting solution was subjected to sodium dodecylsulphate polyacrylamide gel electrophoresis. To determine the purity of the purified laccase and its molecular weight, sodium dodecyl sulfate-polyacrylamide gel electrophoresis was performed and protein was visualized by staining the gel with Coomassie brilliant blue. The molecular mass of laccase was determined by comparing with standard high molecular weight protein markers.

Immobilization of Purified Laccase

The purified laccase was immobilized with alginate-gelatin-agar mixed gel by gel entrapment method. A mixture of 3g of sodium alginate and 3 g of gelatin were mixed with 10 mL of distilled water and stirred for 30min and then added 0.5 g of agar. A mixed gel solution obtained was added to 1 mL of purified enzyme solution. It was taken up with 5mL syringe and injected drop-wise into 250 mL of 1 % $CaCl_2$ solution.

Determination of Laccase Activity

Activity of the free and immobilized laccase was determined by Guaiacol assay method according to Desai *et al*. (2011). Guaiacol (2 mM) in sodium acetate buffer (10 mM pH 5.0) was used as substrate. The assay mixture contained 3 mL acetate buffer, 1 mL guaiacol and 1 mL enzyme solution. For blank solution, 1 mL of distilled water was used instead of enzyme solution. The oxidation of guaiacol was monitored spectrophotometrically after incubation of the mixture at 30 ºC for 15 min by measuring the increase of absorbance at 450 nm. The laccase activity was calculated using the extinction coefficient of guaiacol (12,100 M^{-1} cm^{-1}) at 450 nm. One unit of enzyme was defined as amount of enzyme required to oxidize 1 micromole of guaiacol per minute.

Determination of Protein Content

Protein content of the free and immobilized enzyme was determined by Biuret method using Bovine Serum Albumin (BSA) as standard at 560 nm. The calibration curve of BSA was constructed to determine the concentration of protein in the enzymes (Khaing Khaing Myint *et al.,* 2018).

Characterization of Laccase

Effect of pH

The optimum pH of laccase- catalyzed reaction for the free and immobilized laccase enzymes were investigated by spectrophotometric method. For the study on the effect of pH, the reaction mixtures contained 1 mL each of guaiacol (2 mM) as substrate, 1 mL each of enzyme solution and 3 mL each of buffers of different pH values (acetate buffer pH 3, pH 4, pH 5, phosphate-citrate buffer pH 6 and pH 7). The mixtures were incubated at 40 ºC for 15 min and the absorbance values were recorded at 450 nm. For immobilized laccase, number of beads equivalent to 1 mL of enzyme was used instead of enzyme solution.

Effect of Temperature

The free and immobilized laccase activities were determined at the range of temperature 25-60 ^{o}C with difference of 5 degrees between each temperature values while other conditions were kept constant.

Kinetic pararmeters

The reaction rate was determined with different concentrations of guaiacol in the range of 0.4 mM to 3.6 mM while other conditions were kept constant. The kinetic constant K_m and V_{max} were calculated for the free and immobilized laccase using guaiacol as substrate.

Results and Discussion

Purification of the Isolated Laccase

In this study, laccase was extracted from *Trametes versicolor* by solid state fermentation and the extract was purified by using ammonium sulphate precipitation method followed by Sephadex G -100 gel filtration chromatography. Figure 1 shows the variation of absorbance of protein at 280 nm and the variation of activity of laccase with fraction number. The fraction numbers from 23 to 43 were pooled.

Total Activity, Total Protein and Specific Activity of Crude Laccase Enzyme Obtained in each Purification Step

Figure 1 shows the chromatogram of variation of absorbance of protein at 280 nm and activity of laccase with fraction number. The fraction numbers from 23 to 43 with high protein content and high laccase activity were pooled.

The crude extract having specific activity of 0.22 μmol min^{-1} mg^{-1} was subjected to ammonium sulphate precipitation followed by gel filtration and resulted in specific activity of 2.80 μmol min^{-1} ml^{-1} mg^{-1} at the final purification step. So 12.72 fold purification was achieved (Table 1).

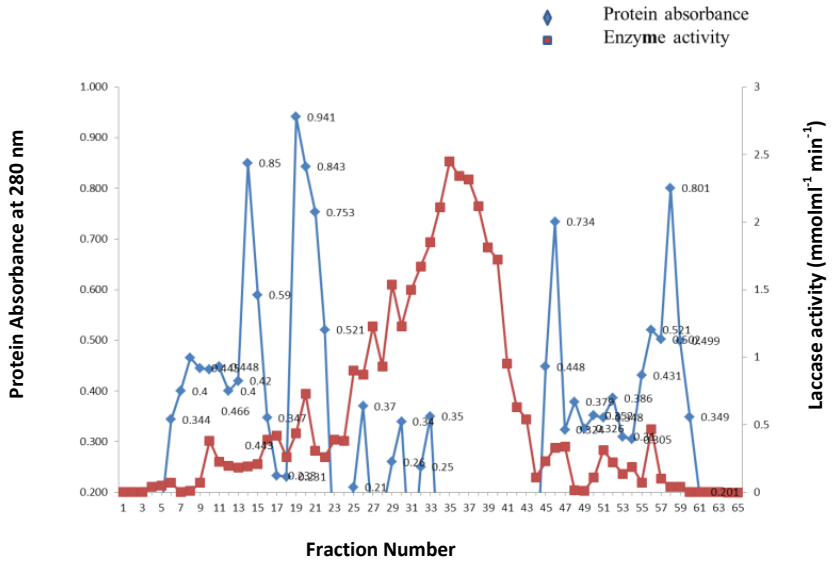

Figure 1 Chromatogram of laccase extract on Sephadex G-100 gel chromatography

Table 1 Total Activity, Total Protein and Specific Activity of Laccase Enzyme Obtained in each Purification Step

Purification steps	Total activity (µmol min^{-1})	Total protein (mg)	Specific activity (µmol min^{-1} mg^{-1})	Purification (fold)
Crude enzyme solution	6720	30000	0.22	1
After 20 % $(NH_4)_2SO_4$ precipitation	2590	5000	0.52	2.36
After 70 % $(NH_4)_2SO_4$ precipitation	3770	1600	2.36	10.72
After dialysis	999	400	2.50	11.36
Gel filtration	22.4	8	2.80	12.72

Determination of Molecular Weight of the Purified Laccase

The purified laccase was homogenous showing a single-protein band on SDS-PAGE. Thus, activity staining of purified enzyme showed that only one extracellular laccase was secreted. The molecular weight of purified laccase was further confirmed by comparing its electrophoretic mobility with those of protein standards of known molecular weights.

Figure 2 shows the zymogram of sodium dodecylsulphate polyacrylamide gel electrophoresis, lane (a) for a standard high molecular weight protein markers and lanes (b) and (c) for the purified laccases. The molecular weight of purified laccase was observed to be 60.26 kDa from the plot of relative molecular mass versus log molecular weight of standard proteins (Table 2 and Figure 3).

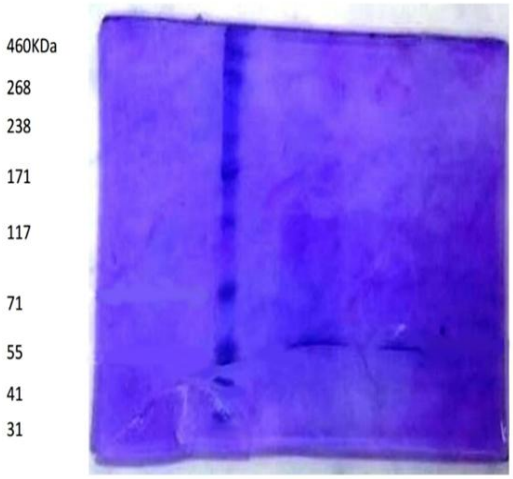

(a) (b) (c)

Figure 2 Photograph of sodium dodecylsulphate polyacrylamide gel electrophoresis: Lane (a) Standard high molecular weight marker proteins Lanes (b) purified laccase and (c) purified laccase

Table 2 Relationship between Molecular Weight of Standard High Protein Markers (HMW) and Relative Mobility (R_f) Values Obtained from SDS – PAGE

No	HMW marker protein	Molecular weight (Da)	Log molecular weight	R_f
1	Standard I (kinase)	460000	5.6628	0.08
2	Standard II	268000	5.4281	0.14
3	Standard III	238000	5.3766	0.28
4	Standard IV (phosphorylase B)	171000	5.2330	0.36
5	StandardV (galactosidase)	117000	5.0682	0.48
6	Standard VI (bovine serum albumin)	71000	4.8513	0.65
7	Standard VII (glutamic dehydrogenase)	55000	4.7404	0.82
8	Standard VIII(turkey albumin)	41000	4.6128	0.86
9	Standard IX (carbonic anhydrase)	31000	4.4914	0.95

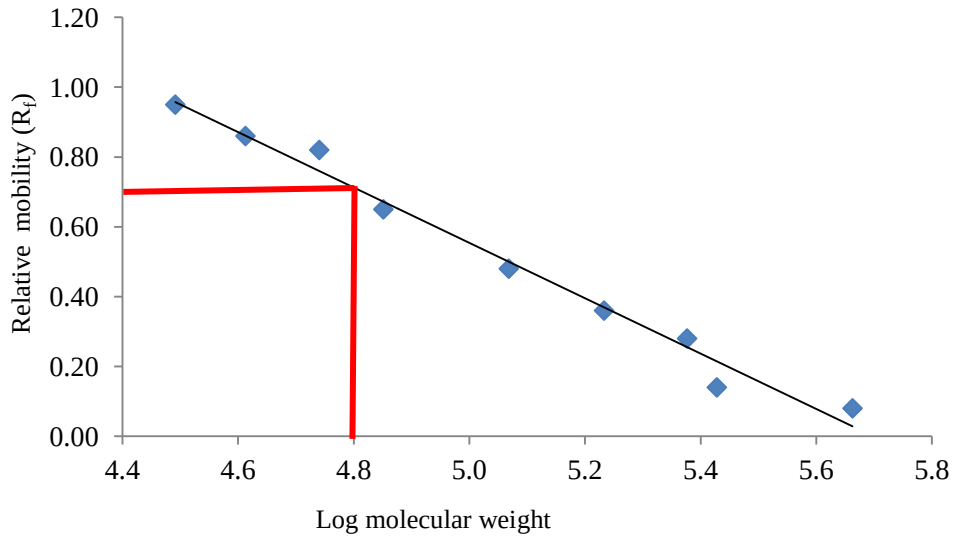

Figure 3 A plot of log molecular weight of standard protein markers as a function of R_f values

Optimum pH of the Free and Immobilized Laccase

The effect of pH on the activity of the free and immobilized laccase was studied in the pH range from 3 to 7 in which pH 3 to 5 using acetate buffer and pH 6 to 7 using citrate -phosphate buffer. Table 3 and **Figure 4** show that the optimum pH value was 5 for free laccase and 6 for the immobilized laccase The free laccase showed the highest activity at pH 5 with guaiacol as substrate, which is consistent with other reports (Palmieri *et al*., 1997; Heinzkill *et al*., 1998). However, after immobilization by physical adsorption, the optimal pH was shifted from pH 5 to pH 6. Ghorbani *et al*. (2018) reported that the optimum pH of the laccase immobilized on porous zinc oxide nanoparticles was 6. In comparison with the free laccase, the immobilized laccase exhibited higher activity than the free laccase between pH 3 to 7. Thus the laccase immobilization by gel entrapment could increase the pH resistance of high catalytic activity and this property is crucial in practical applications, e.g., in the treatment of textile industrial waste effluent.

Table 3 Relationship between Activities of the Free and Immobilized Laccase and pH of Solutions at 40 ^{o}C

No.	pH	Buffer	Laccase activity (μmol mL^{-1} min^{-1})	
			Free laccase	Immobilized laccase
1	3	Acetate	1.074	2.694
2	4	Acetate	1.260	3.471
3	5	Acetate	5.619	4.320
4	6	Citrate - Phosphate	4.269	5.895
5	7	Citrate - Phosphate	1.810	2.520

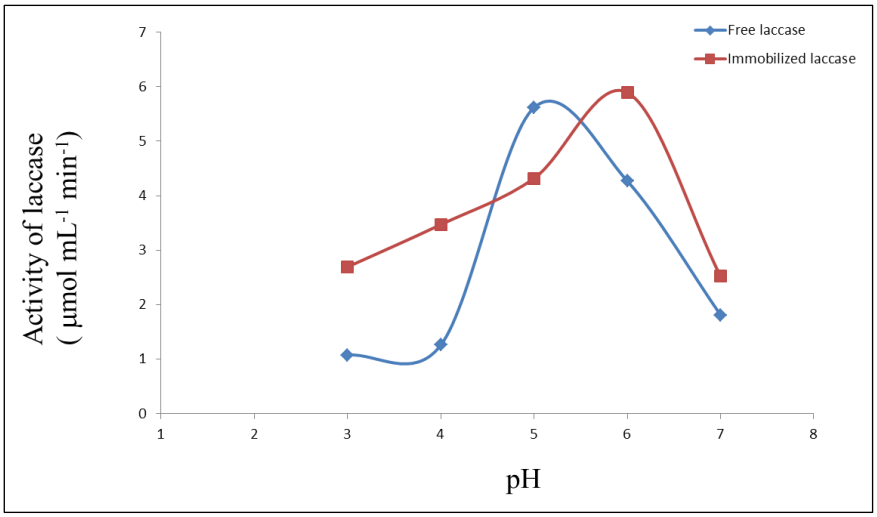

Figure 4 Plot of laccase activity as a function of pH of the solution

Optimum Temperature of the Free and Immobilized Laccase

The effect of temperature on the activity of the free and immobilized laccases was also studied in the temperature range of 25–60 °C (Table 4 and Figure 5). The activities of either free or immobilized laccase increased with increasing temperature until optima and thereafter decreased with further increase of temperature. The optimum temperature of free laccase was 40 ^{o}C. Optimum temperature of laccase from *Trametes versicolor* was reported as 45 ^{o}C (Stoilova *et al.,* 2010). The optimum temperature of immobilized laccases was found to be higher than that of free laccase and shifted from 40 °C to 45 °C.The shift of the optimum temperature indicates an increase in the thermal stability of the immobilized laccases.

Table 4 Relationship between Activities of Laccase and Temperature at pH 5

No	Temperature (^{o}C)	Laccase activity (µmol mL^{-1} min^{-1})	
		Free laccase	Immobilized laccase
1	25	4.358	5.147
2	30	5.279	5.976
3	35	5.509	6.144
4	40	6.152	7.174
5	45	5.399	7.688
6	50	4.127	7.234
7	55	3.644	5.901
8	60	2.550	4.940

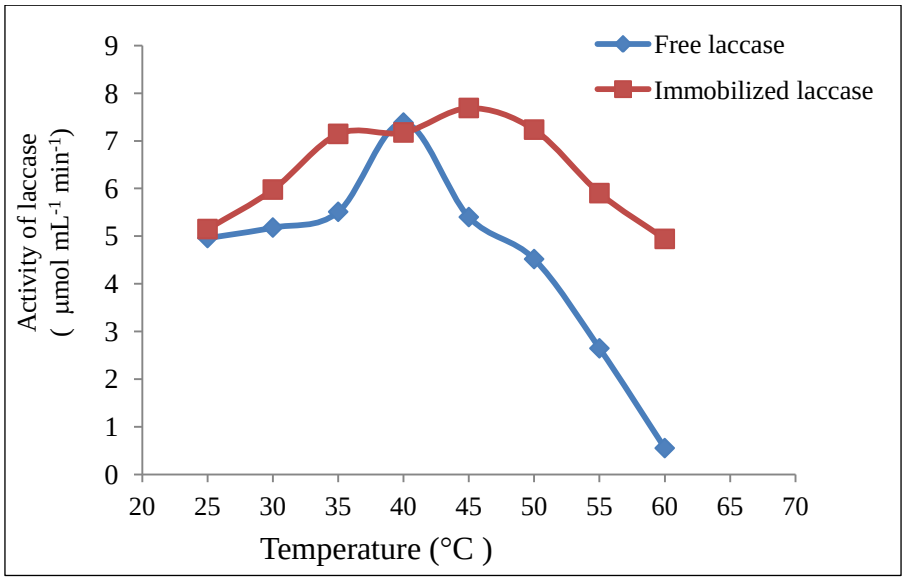

Figure 5 Plot of laccase activity as a function of temperature at pH 5

Kinetic Parameters

Relationship between velocities of free and immobilized laccase catalyzed reaction and guaiacol substrate concentration is shown in Table 5 and Figure 6 (Michaelis-Menten plot). At relatively low guaiacol concentration, initial velocities of both free and immobilized laccase increased almost linearly with increase in concentration of guaiacol. At higher guaiacol concentration, the initial velocities increased by smaller and smaller extent in response to increase in concentration of guaiacol. Michaelis-Menten equation, $v = \frac{V_{max}[S]}{K_m} + [S]$ explains kinetics, but because it is nonlinear, is a little hard to deal with real practical data. From Michaelis-Menten plot K_m values were found to be 0.55 mM and 0.70 mM for guaiacol substrate and V_{max} values were 13.81 µM min^{-1} and 17.47 µM min^{-1}, respectively, for the free and immobilized laccase- catalyzed reactions.

Lineweaver-Burk plot or double reciprocal ($\frac{1}{v}$ vs $\frac{1}{[S]}$ plot) transformation distorts the error in the measurements. As shown in Figure 7 , the noisiest data are too heavily weighted when linear regression is used to determine the best straight line. From this Lineweaver-Burk plot K_m values were found to be 0.68 mM and 1.00 mM for guaiacol substrate and V_{max} values were 16.86 µM min^{-1} and 22.49 µM min^{-1}, respectively, for free and immobilized laccase- catalyzed reactions.

Eadie-Hofstee plot (v vs $\frac{v}{[S]}$ plot) not only yields K_m and V_{max} magnifies departures from linearity which may not be apparent in a double reciprocal plot. From Eadie-Hofstee plot (Figure 8) of free and immobilized laccase- catalyzed reactions K_m values were found to be 0.65 mM and 0.98 mM for guaiacol substrate and V_{max} values were 16.64 µM min^{-1} and 23.22 µM min^{-1}, respectively.

Table 5 Relationship between Velocities of the Free and Immobilized Laccase Catalyzed Reactions and Guaiacol Substrate Concentration

[S] mM	-[S] mM	1/[S] mM^{-1}	V ($\mu M min^{-1}$)		1/V ($\mu M^{-1} min$)		V/[S] (x 10^{3} min^{-1})		[S]/V (x 10^{-3} min)	
			Free	Immo	Free	Immo	Free	Immo	Free	Immo
0.4	- 0.4	2.500	6.198	6.551	0.161	0.153	15.495	16.3774	0.065	0.061
0.8	- 0.8	1.250	9.217	10.099	0.108	0.099	11.521	12.6240	0.087	0.079
1.2	- 1.2	0.833	11.096	12.562	0.090	0.080	9.247	10.4683	0.108	0.096
1.6	- 1.6	0.625	11.840	14.876	0.084	0.067	7.400	9.2975	0.135	0.108
2.0	- 2.0	0.500	12.837	16.143	0.078	0.062	6.419	8.0716	0.156	0.124
2.4	- 2.4	0.417	13.030	16.694	0.077	0.060	5.429	6.9559	0.184	0.144
2.8	- 2.8	0.357	13.570	17.025	0.074	0.059	4.846	6.0803	0.206	0.164
3.2	- 3.2	0.313	13.580	17.355	0.074	0.058	4.244	5.4236	0.236	0.184
3.6	-3.6	0.278	13.810	17.466	0.072	0.057	3.836	4.8515	0.261	0.206

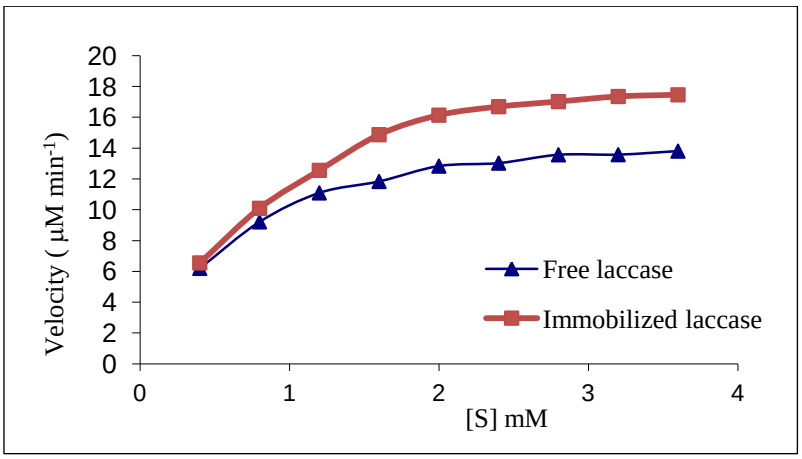

Figure 6 Plot of velocity as a function of guaiacol substrate concentration for the free and immobilized laccase- catalyzed reactions

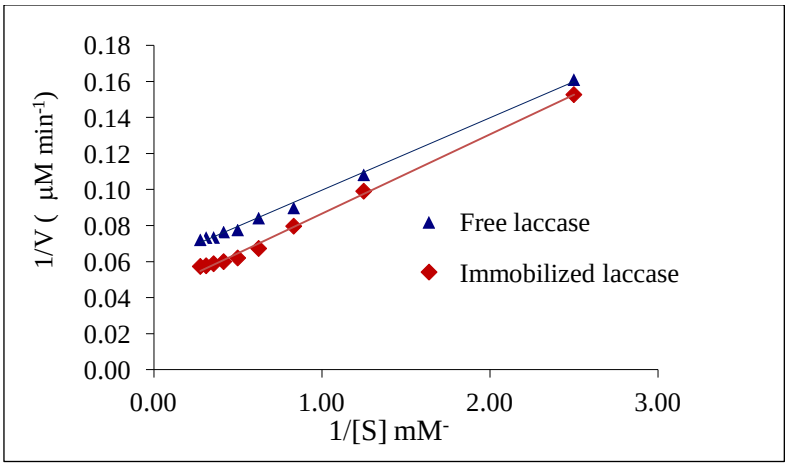

Figure 7 Lineweaver- Burk plot of 1/V vs 1/[S] used for evaluation of K_m and V_{max} for free and immobilized laccase-catalyzed reactions

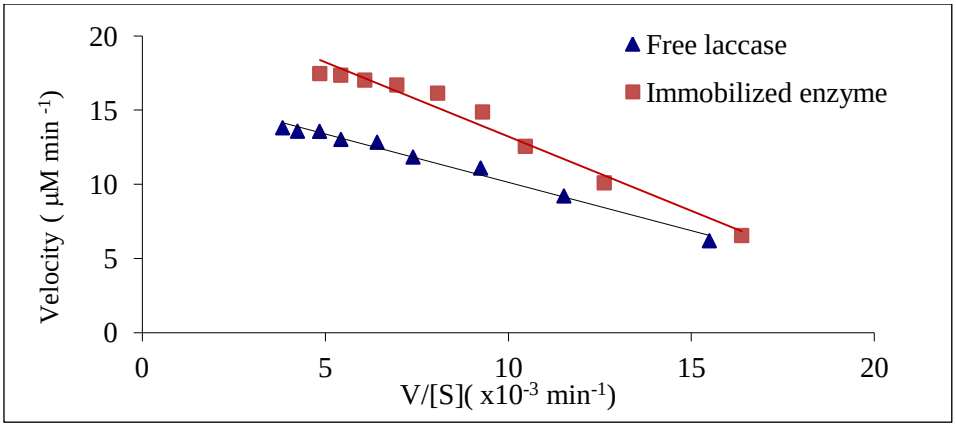

Figure 8 Eadie -Hofstee plot of V vs V/[S] used for evaluation of K_m and V_{max} for the free and immobilized laccase-catalyzed reactions

Figure 9 shows Hanes-Wilkinson plot ([S]/V vs [S] plot) of free and immobilized laccase-catalyzed reactions. From this plot, K_m values were found to be 0.60 mM and 0.91 mM for guaiacol substrate and V_{max} values were 16.25 μM min^{-1} and 22.43 μM min^{-1}, respectively, for the free and immobilized laccase-catalyzed reactions.

Figures 10 and 11 are the Eisenthal- Cornish Bowden plost or direct linear plots. [S] values are plotted on the negative X-axis and observed v values on the Y-axis. From Eisenthal-Cornish Bowden plot of free and immobilized laccase-catalyzed reactions K_m values were found to be 0.61 mM and 0.91 mM for guaiacol substrate and V_{max} values were 16.10 μM min^{-1} and 21.00 μM min^{-1}, respectively.

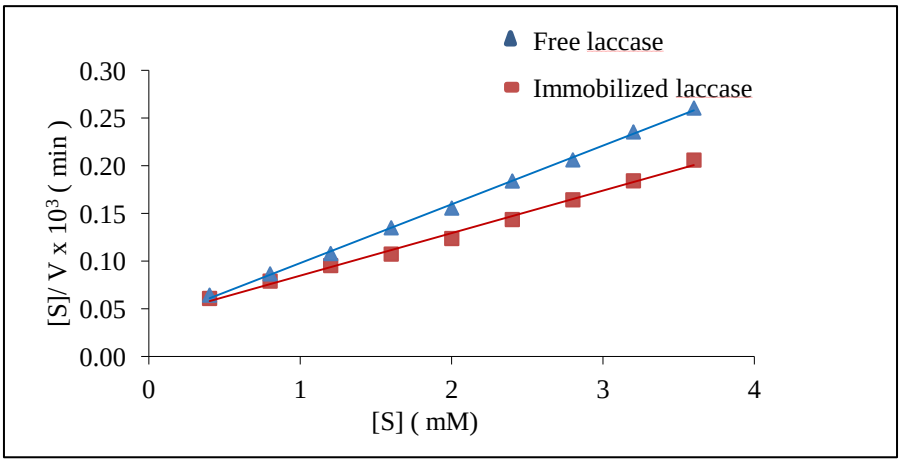

Figure 9 Hanes-Wilkinson plot of [S]/V vs [S] used for evaluation of K_m and V_{max} for the free and immobilized laccase-catalyzed reactions

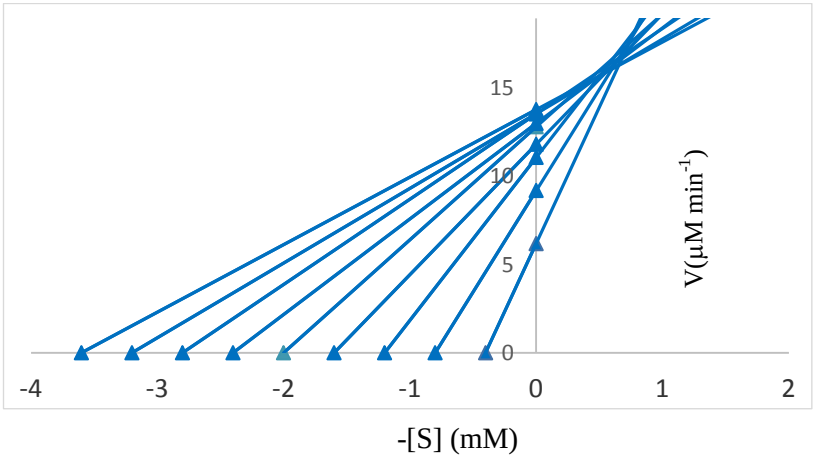

Figure 10 Eisenthal-Cornish-Bowden or direct linear plot of V vs - [S] used for evaluation of K_m and V_{max} for the free laccase-catalyzed reaction

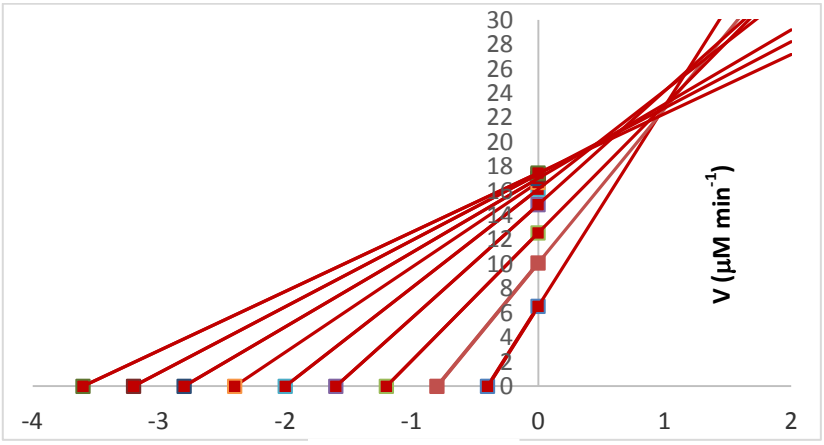

Figure 11 Eisenthal-Cornish-Bowden or direct linear plot of V vs - [S] used for evaluation of K_m and V_{max} for the immobilized laccase-catalyzed reaction

Table 6 shows the K_m and V_{max} values of free and immobilized laccase-catayzed reactions by different methods. K_m and V_{max} values obtained by different methods were found to be agreed with each other. K_m and V_{max} are significant coefficients in guiding scientific research and engineering design. The more firmly the enzyme binds to its substrate, the smaller will be the value of K_m. The results show good affinity of the enzyme for guaiacol substrate.

Table 6 Comparison of K_m and V_{max} Values of Free and Immobilized Laccase-Catayzed Reactions by Different Methods

No	Methods	K_m (mM)		V_{max} (μM min^{-1})	
		Free laccase	Immobilized laccase	Free laccase	Immobilized laccase
1	Michaelis –Menten	0.55	0.70	13.81	17.47
2	Lineweaver- Burk	0.68	1.00	16.86	22.97
3	Eadie -Hofstee	0.65	0.98	16.64	23.22
4	Hanes-Wilkinson	0.60	0.91	16.25	22.43
5	Eisenthal-Cornish-Bowden	0.61	0.91	16.10	21.00

When the Michaelis–Menten equation is written in the form of a straight line, the Hill equation (Martin, 1993),

$$\log \frac{V}{V_{max} - V} = n \log[S] - \log K_m$$

is obtained. The equation states that, when [S] is low compared to K_m, the reaction velocity increases as the n^{th} power of [S].

In the present work, n value was determined from the plot of $\log \frac{V}{V_{max} - V}$ vs. log [S] using the linear regression method (Table 7 and Figure 12) .The reaction order (n) for laccase was calculated to be 0.94 for free laccase and 0.90 for immobilized laccase proving that the reaction order is first order.

Table 7 Relationship between $\log \frac{V}{V_{max} - V}$ and log [S] for the Determination of Reaction Order of Laccase –Catalyzed Reaction

No	[S] (mM)	log [S]	V(mMmin^{-1})		$\log \frac{V}{V_{max} - V}$	
			Free	Immo	Free	Immo
1	0.4	-0.398	6.198	0.581	-0.235	-0.399
2	0.8	-0.097	9.217	1.206	0.081	-0.105
3	1.2	0.079	11.096	1.926	0.285	0.082
4	1.6	0.204	11.840	2.360	0.373	0.211
5	2.0	0.301	12.837	3.193	0.504	0.374
6	2.4	0.380	13.030	3.404	0.532	0.384
7	2.8	0.447	13.570	4.128	0.616	0.436
8	3.2	0.505	13.580	4.143	0.617	0.463
9	3.6	0.556	13.810	4.532	0.656	0.502

V_{max} = 16.86 μM min^{-1} (Free laccase)

= 22.97 μM min^{-1} (Immobilized laccase)

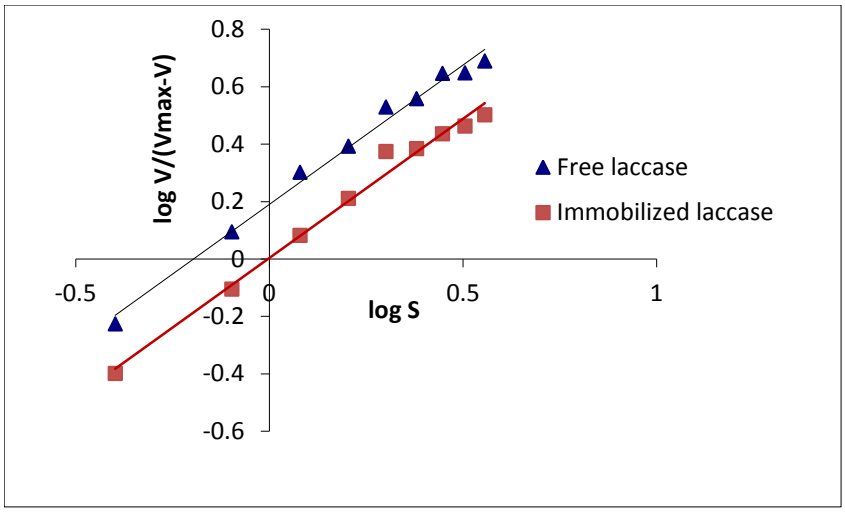

Figure 12 Plot of $\log \frac{V}{V_{max} - V}$ as a function of log [S] used for evaluation of reaction order for the free and immobilized laccase-catalyzed reactions

Conclusion

This study revealed that interesting novel laccase producers can be discovered from the environments especially mushroom. Banana skin , the main waste of banana plant, can be used as support-substrate for production of laccase at low cost by *Trametes vesicolor* under solid state condition. Purification of laccase by ammonium sulphate precipitation, dialysis and Sephadex G- 100 gel filtration chromatography revealed that the specific activity of crude and purified laccase were 0.22 μmol $min^{-1}mg^{-1}$ and 2.80 μmol $min^{-1}mg^{-1}$ respectively. Laccase was purified by 12.72 fold over crude extract. The molecular weight of Laccase from *T. vesicolor* is 60.26 kDa by gel electrophoresis using SDS-PAGE. The optimum pH of free laccase was 5 and after immobilization it was shifted to 6. The optimum temperature of free laccase was 40 ^{o}C and that of immobilized laccase was 45 ^{o}C. From Lineweaver-Burk method, Michaelis-Menten constant K_m of the free laccase was 0.68 mM and that of immobilized laccase was 1.00 mM and maximum velocity V_{max} of free laccase-catalyzed reaction was 16.86μM min^{-1} and it increased to 22.97 μM min^{-1} in the immobilized laccase-catalyzed reaction.

Acknowledgements

The authors would like to express their profound gratitude to the Department of Higher Education, Ministry of Education, Myanmar for provision of opportunity to do this research and to the Myanmar Academy of Arts and Science for allowing to present this research paper.

References

Ashrafi, S.D., Rezaei, S., Forootanfar, H., Mahvi, A. H. and Faramarzi, M. A. (2013). "The Enzymatic Decolorization and Detoxification of Synthetic Dyes by the Laccase from a Soil-isolated Ascomycete, Paraconiothyrium variabile". *Int. Biodeterior. Biodegrad.*, vol. 85, pp. 173–181.

Baldrian, P. (2005). **"**Fungal Laccases – Occurrence and Properties**".** *FEMS Microbiol Rev.*, vol.30, pp.215-242.

Basto, C., Tzanov, T. and Cavaco-Paulo, A. (2007). "Combined ultrasound-laccase assisted bleaching of Cotton". *Ultrason. Sonochem.* , vol.14, pp.350-354.

Brijwani, K., Oberoi, H. S. and Vadlani, P. V. (2010). "Production of a Cellulolytic Enzyme System in Mixed-culture Solid-state Fermentation of Soybean Hulls Supplemented with Wheat Bran". *Process Biochemistry*, vol. 45(1), pp. 120-128.

Couto, S. R. and Sanromán, M. A. (2005). "Application of Solid-state Fermentation to Ligninolytic Enzyme Production". *Biochemical Engineering Journal*, vol. 22 (3), pp. 211-219.

Couto, S. R., and Toca-Herrera, J. L. (2007). "Laccase Production at Reactor Scale by Filamentous Fungi". *Biotechnology Advances*, vol. 25 (6), pp. 558-569.

Desai,S.S., Tennali, G. B., Channur, N., Anup, A. C., Deshpande, D. and Murtuza, B. P. A. (2011). "Isolation of Laccase Producing Fungi and Partial Characterization of Laccase". *Biotechnol. Bioinf. Bioeng.*, vol.1(4), pp.543-549.

Dhillon, G.S., Kaur, S., Brar, K. and Verma, M. (2012). "Flocculation and Haze Removal from Crude Beer using in-house Produced Laccase from Trametes versicolor Cultured on Brewer's Spent Grain". *J. Agric. Food Chem.*, vol.60, pp.7895–7904.

Dura´ n, N., Rosa, M. A., Annibale, A. D. and Gianfreda, L. (2002). **"**Applications of Laccases and Tyrosinases (Phenoloxidases) Immobilized on Different Supports: A Review**".** *Enzyme. Microb. Technol.* , vol. 31, pp. 907–931.

Ghorbani, Gh.**,** Ebrahimi, M. and Farhadyar, N. (2018). "The Immobilization of Laccase Enzyme from *Trametes versicolor* on the Surface of Porous Zinc Oxide Nanoparticles and Studying Features of the Immobilized Enzyme ". *Int. J. Bio-Inorg. Hybr. Nanomater*., vol. 7(1),pp. 21-28.

Heinzkill, M., Bech, L., Halkier, T., Schneider, P. and Anke,T. (1998). "Characterization of Laccases from Wood – rotting Fungi (Family Coprinaceae)". *Applied Environmental Microbiology,* vol.64 , pp.1601 –1606.

Khaing Khaing Myint, Ohn Ohn Soe, and Daw Hla Ngwe. (2018). "Isolation and Characterization of Fungal Laccase from Trametes Versicolor" . *J. Myanmar Academy of Arts and Sciences*, Vol. XVII. No.1A, pp. 603-618

Lu, L., Zhao, M., Zhang, B.B., Yu, S.Y., Bain, X.J. and Wang, Y. (2007). "Purification and Characterization of Laccase from *Pycnoporus sanguineus* and Decolorization of an Anthraquinone Dye by the Enzyme". *Appl Microbiol Biotechnol.*, vol.74, pp.1232–1239.

Majeau, J. A., and Tyagi, R. D. (2010). "Laccases for Removal of Recalcitrant and Emerging Pollutants". *Bioresour. Technol*., vol. 101, pp. 2331–2350.

Palmieri, G., Giardina, P., Bianco C., Scaloni, A., Capasso, A. and Sannia, G. (1997). "A Novel White Laccase from *Pleurotus ostreatus". J. Biochem.,* vol. 272, pp. 31301-31307.

Pandey, A., Selvakumar, P., Soccol, C. R. and Nigam, P. (1999). "Solid State Fermentation for the Production of Industrial Enzymes". *Current Science*, vol. 77 (1), pp. 149-162.

Stoilova, I., Krastanov, A. and Stanov, V. (2010). "Properties of Crude Laccase from *Trametes versicolor* produced by Solid – State Fermentation". *Advan. in Biosci. and Biotech.*, vol.1, pp.208-215.

Thurston, C.F. (1994). "The Structure and Function of Fungal Laccase". *Microbiol.*, vol. 140, pp.19-26.

Zhang, Y., Zeng, Z. T., Zeng, G. M., Liu, X. M., Liu, Z. F., Chen, M., Liu, L. F., Li, J. B. and Xie, G.X. (2012) ."Effect of Triton x-100 on the Removal of Aqueous phenol by Laccase Analyzed with a Combined Approach of Experiments and Molecular Docking". *Colloid Surf*, vol.97, pp. 7–12.

Zhao, Lu, L., Zhang, M. B. B., Yu, S. Y., Bain, X. J. and Wang, Y. (2007). "Purification and Characterization of Laccase from *Pycnoporus sanguineus* and Decolorization of an Anthraquinone Dye by the Enzyme". *Appl Microbiol Biotechnol.*, vol.74, pp.1232–1239.

STUDY ON QUALITATIVE AND QUANTITATIVE PHYTOCHEMICAL CONSTITUENTS AND SOME BIOLOGICAL ACTIVITIES OF *CLITORIA TERNATEA* L.(AUNG – MAE –NYO) FLOWERS

Hnin Wuit Yee[1], Ni Ni Than[2]

Abstract

The purpose of the research is to study the qualitative and quantitative phytochemical constituents and some biological activities such as antimicrobial activity, antitumor activity and acute toxicity activity of *Clitoria ternatea* L. (Aung-mae-nyo) flowers. The qualitative phytochemical screening of *C. ternatea* was examined by test tube method which revealed the presence of various bioactive components like alkaloids, flavonoids, carbohydrates, glycosides, phenol, saponin, terpenoids, tannin, quinones, amino acid and sterols. From the results of quantitative phytochemical screening such as total phenol contents determined Folin's Ciocalteu's method were observed to be 43.22 mg of GAE/ g in water extract and 75.72 mg of GAE /g in ethanol extract. The total flavonoids content in water and ethanol extracts determined by aluminium chloride method were observed to be 33.75 mg QE/g and 58.44 mg QE/g. The values for the water and ethanol extracts of total carbohydrate content determined by Anthrone method were found to be 374.68 mg GE/g and 265.23 mg GE/g. The total tannin contents in water and ethanol extracts were presented as 3.23 g TAE/100 g and 7.45 g TAE/100 g. The antimicrobial activity of the ethanol and water extracts of *C. ternatea* flowers was investigated against six tested microbial strains: *B. subtilis, S. aureus, P. aeruginos, B. pumilus, C. albicans* and *E. coli* by agar well diffusion method. It can be observed that ethanol extract is more active on tested microbial strains than water extract. Antitumor activity was carried out with water and ethanol extracts by Potato Crown Gall (PCG) test. From this experiment, both extracts were found to prevent the tumor formation with the dose of 0.1 and 0.15 mg/disc. The ethanol and water extracts of sample were also studied on acute toxicity by the Organization for Economic Co-operation and Development (OECD) Guideline. The acute toxicity test on albino mice indicated no toxic effect in both extracts of sample.

Keywords: *Clitoria ternatea* L., qualitative and quantitative phytochemical constituents, extractable matter, antimicrobial, antitumor, antioxidant, acute toxicity

Introduction

In many parts of the world, traditional knowledge and biodiversity still play an important role in health care, culture, religion, food security, environment and sustainable development. In herbal medicine, the one or more active ingredients are derived from the aerial and non-aerial parts, juices, resins and oils of the plant either in crude state or as pharmaceutical formulation (Gupta *et al.,* 2010). Currently, many people in developed countries have begun to turn to alternative or complementary therapies, including medicinal herbs. The use of herbal remedies is more prevalent in patients with chronic diseases such as cancer, diabetes, asthma and end-stage renal disease (WHO, 1991).

Clitoria ternatea L. is an appealing perennial climber with conspicuous blue or white flower. It is commonly known as "Aparajita", "butterfly pea", "shankhapuspi" and belongs to the Fabaceae family. It is traditionally used to deal with diverse illness (Manjula *et al*., 2013). The plant is native to South-East Asia and allotted in tropical Asia including India, the Phillipines and Madagascar. In Myanmar, it is found in Kachin, Mandalay, Sagaing and Yangon. It is commonly known as pe-nauk-ni, aung-me-hpyu and aung-me-nyo (Robert and Gary, 2018).

The whole plant extract has potential medicinal values such as anti-helmintic, anti-inflammatory, antipyretic, antibacterial, analgesic, antidepressant, anxiolytic, sedative, anticonvulsant, anticancer and antioxidant activity. Especially, *C. ternatea* contains an

[1] Dr, Assistant Lecturer, Department of Chemistry, University of Yangon
[2] Dr, Professor and Head, Department of Chemistry, University of Yangon

antioxidant called flavonoids, anthocyanin, phenolic compounds which activate antioxidant activity helps decrease oxidative stress caused by disease causing and aging free radicals. And also, it contains proanthocyanidin which increases blood flow to the capillaries of the eyes, useful in treatment of glaucoma, blurred vision, retinal damage or tired eyes (Chakraborty *et al*., 2017). In several Indian studies, butterfly pea exhibited significant antimicrobial effects against *Staphylococcus aureus*. Moreover, *C. ternatea's* cyclotides has efficient anti-cancer and anti-tumor activity which can cause cancer cell death by disrupting cell membrane integrity (Divya *et al.*, 2018).

Materials and Methods

Collection of Plant Sample *Clitoria ternatea* L.

The flowers sample of *C. ternatea* (Figure 1) was collected from Tharkayta Township, Yangon Region. These samples were identified at Department of Botany, University of Yangon. The collected samples were cleaned and air-dried at room temperature. The dried sample was ground into powder using grinding machine (Figure 2). The dried powdered samples were used for chemical and biological experiment.

Figure 1 Photographs of *Clitoria ternatea* L. flowers

Fresh sample Dried sample Dried powder

Figure 2 Preparation of dried powder sample of *Clitoria ternatea* L. flowers

Preliminary Qualitative Phytochemical Investigation of *C. ternatea* Flowers

In order to find out the types of phytoorganic constituents such as alkaloids, flavonoids, carbohydrates, phenols, saponins, tannins, quinones, terpenoids, oxalate compounds, glycosides,

amino acids, sterols and resins in the sample, preliminary phytochemical tests were carried out according to the appropriate reported methods. The results are shown in Table 1.

Determination of Total Phenolic Contents in Crude Extracts of *C. ternatea* Flowers

The total phenolic content (TPC) assay was performed in accordance with modifications. A 1 mL of each sample solution was mixed with 5 mL of Folin- Ciocaltea Reagent in a test tube covered with aluminium foil. After 5 min, 5 mL of 10% Na_2CO_3 was added to each test tube. The sample was then incubated for 90 min at room temperature. The absorbance was measured at 765 nm spectrophotometrically (KWF UV-7504). A standard curve of Gallic acid solutions (range from 6.25 – 100 µg mL^{-1}) was used for calibration. The experiment was done in triplicate. Concentrations of Gallic acid equivalent (GAE) in the plant extracts were calculated from the linear regression equation explored from standard curve construction for Gallic acid (Table 2 and Figure 4). TPC in the water and ethanol extracts of plant sample were expressed as (mg GAE/g). The resultant data are presented in Table 3.

Determination of Total Flavonoids Contents in Crude Extracts of *C. ternatea* Flowers

The total flavonoids content was determined by the aluminium chloride calorimetric assay. 0.3 mL of plant extracts were mixed with 0.15 mL of $AlCl_3.6H_2O$ (0.3 M), 0.15 mL of $NaNO_2$ (0.5 M), and 3.4 mL of 30 % methanol in a test tube, after 5 min, 1mL of NaOH was added. Then the absorbance was measured at 415 nm and quercetin was used as a standard solution of flavonoids. The absorbance data and calibration curve are shown in Table 4 and Figure 5. The total flavonoid content was examined with the quercetin equivalents consistent with mg QE/g of dried fraction. The data are described in Table 5.

Determination of Total Carbohydrate Contents in Crude Extracts of *C. ternatea* Flowers

The 100 mg of the sample was into a boiling tube. Then the sample was hydrolyzed by putting in a boiling water bath for 3 h with 5 mL of 2.5 M HCl then cooled to room temperature. And then, it was neutralized with solid Na_2CO_3 until the effervescence ceases. The volume was made up to 100 mL and centrifuge at 10,000 rpm for 20 min. Then the 0.5 and 1 mL aliquots were taken for further analysis. The standard was prepared by 0, 0.2, 0.4, 0.6, 0.8 and 1.0 mL of the glucose. The absorbance data and calibration curve are shown in Table 6 and Figure 6. The volume was made up to 1.0 mL in all the tubes by adding distilled water. Then 4 mL of anthrone reagent was added (Dissolve 200 mg anthrone in 100 mL of ice-cold 95 % H_2SO_4, which prepare fresh before use). Then the mixture was heated for 8 min by using boiling water bath. Cooled rapidly and read the green color at 620 nm. The observed data are shown in Table 7.

Determination of Total Tannin Contents in Crude Extracts of *C. ternatea* Flowers

One hundred milligrams (100 mg) each of the powdered sample was weighed and put into 150 mL conical flask. 10 mL of distilled was added and shaken for 1 h in a mechanical shaker. This was filtered into a 50 mL conical flask and made up to the mark. The freshly prepared extract (1 mL) of sample was diluted to 10 mL with distilled water, and mixed with 0.5 mL of 0.1 M $FeCl_3$ in 0.1 M HCl and 0.5 mL of 0.008 M $K_3Fe(CN)_6$. The mixture was allowed to stand for 1 minute for color development, and absorbance was read at 720 nm. Tannin content was extrapolated from a standard curve (prepared with tannic acid at concentration of 0.0625, 0.125, 0.25, 0.5 and 1.0 mg/mL) and absorbance versus concentration of standard tannic acid (Table 8 and Figure 7). The tannin content was determined by the method of Van-Burden and Robinson, 1981. The tannin content of sample was calculated and data are described in Table 9.

Screening of Antimicrobial Activity of *C. ternatea* Flowers by Agar Well Diffusion Method

Antimicrobial activity of water and ethanol extracts of (Aung-Mae-Nyo) flowers were studied by agar well diffusion method at Pharmaceutical Research Department, Insein, Yangon Region. The agar well plate diffusion method was used to test the antibacterial action of the extracts on 24 h broth culture of the organisms used. At first, the extracts (1 g each for 6 species of bacteria) were introduced into sterilized Petri-dishes and dissolved in 1mL of respective solvents: H_2O and EtOH. And then, 1 mL each of the bacterial suspension of 24 h of nutrient agar was streaked evenly onto the surface of trypticase soy agar plates with sterile cotton swab. Immediately after hardening of the agar well were made with a 10 mm sterile cork borer from each seeded agar. After removing the agar, the wells were filled with the drug extracts (0.1 mL) to be tested. The plates were incubated at 37 °C for 18 - 24 h. The diameters of the inhibition zone were measured and recorded in mm. The results are shown in Table 10 and Figure 8.

Screening of Antitumor Activity of *C. ternatea* Flowers by Potato Crown Gall Test

Isolated *Agrobacterium tumefacien* has been maintained as solid slants under refrigeration. For inoculation into the potato discs, 48 hours broth cultures containing 5×10^7 - 5×10^9 cell/mL was used. Fresh, disease free potatoes were purchased from a local market. Tubers of moderate size were surface sterilized by immersion in 0.1 % sodium hypo chloride for 20 min. Ends were removed and the potatoes were soaked an additional 10 min. A core of the tissue was extracted from each end and discarded. The remainder of the cylinder was cut into 0.5 cm thick discs with a surface sterilized scalpel. The discs were then transferred to agar plates (1.5 g of agar dissolved in 100 mL sterile distilled water (DW), autoclaved for 20 min at 121°C, 20 mL poured into each petri-dish). Each plate contained four potato discs and 4 plates, were used for each sample dilution.

Each sample of 0.05, 0.1 and 0.15 mg was separately dissolved in DMSO (2 mL) and filtered through Millipore filters (0.22 µm) into sterile tube. This solution (0.5 mL) was added to sterile DW (1.5 mL), and broth culture of *A. tumefaciens* in PBS (2 mL) was added. Control was made in this way; DMSO (0.5 mL) and sterile DW (1.5 mL) were to the tube containing 2 mL of broth culture of *A. tumefaciens*. Using a sterile disposable pipette, 1 drop (0.05 mL) from these tubes was used to inoculate each potato disc, spreading it over the disc surface. After inoculation, Petri dishes were sealed by per film and incubated at 27 - 30 °C for 3 weeks. Tumors were observed on potato discs after 21 days under stereo-microscope followed by staining with Lugol's iodine (10 % KI and 5 % I_2) after 30 min and compared with control. The antitumor activity was examined by observation of tumor produced or not. The results are shown in Table 11 and Figure 9.

Acute Toxicity of *C. ternatea* Flowers Crude Extracts on Albino Mice Model

The acute toxicity of different doses of crude extracts was evaluated by the methods of OECD Guidelines for the Testing of Chemicals 423 (Diener *et al*., 1995). According to the test description, total number of 15 adult female albino mice, weighing (25-30 g) were selected and divided into five groups and each group contained three animals. They were maintained in accordance with the recommendation of the guide for the Care and Used of Laboratory Animals published by the US National Institutes of Health (NIH Publication N. 85-23, revised 1996) for studies involving experimental animals. They had free access to feed and clean drinking water during the three days' acclimatization period and throughout the experimental period. They were fasted for 18 h before giving the extracts. Groups (I) and (II) mice were orally administrated with ethanol extract of sample 300 mg/kg and 2000 mg/kg (b.wt) dose. Groups (III) and (IV) mice were giving orally with water extract of sample 300 mg/kg and 2000 mg/kg (b.wt) dose. Group

(V) mice performed as a control group. All groups of mice were kept in the three mice in the separated room at the room temperature and they were treated with cleaned water and normal animal food as shown in Figure 3. After administration of extract on each group of animals were observed first 6 hours continuously for motility and behavior changes. The motility during 14 days was noted (number of death or percent death) and the results obtained from acute toxicity effect are described in Table 12.

(a) (b)

Figure 3 Acute toxicity test on albino mice (DDY strain)
(a) Mice were put in standardized boxes, natural light and temperature, allowed free access to both water and animal feed
(b) Oral toxicity test on albino mice

Results and Discussion

Sample Collection and Preparation

The sample *C. ternatea* flowers was collected from Tharkayta Township, Yangon Region during December 2018 to February 2019 and identified by an authorized botanist, Department of Botany, University of Yangon. The fresh samples were cleaned by washing with water and air dried. The dried samples were kept in the sealed air tight container to prevent moisture changes and other contamination. These samples were used for chemical and biological investigation throughout the research work.

Qualitative Phytochemical Constituents of *C. ternatea* Flowers by Test Tube Method

Preliminary phytochemical screening of *C. ternatea* powder revealed the presence of several compounds. The main phytochemical constituents include alkaloids, flavonoids, carbohydrates, glycosides, phenol, saponin, terpenoids, oxalate compounds, tannin, quinones, amino acid and sterols. These compounds are described as potent biologically active compound found in used medicinal plant parts which are precursors for clinically useful drugs. However, resin was not detected at the assay conditions. The obtained data are shown in Table 1.

Table 1 Qualitative Phytochemical Results of *Clitoria ternatea* L.

No.	Test	Extract	Test reagent	Observation	Results
1	Alkaloids	1% HCl	Mayer's reagent	Pale yellow ppt	+
			Dragendorff's reagent	Orange ppt	+
			Wagner's reagent	Brown ppt	+
2	Flavonoids	EtOH	Dilute HCl and 20% NaOH	Intense yellow color	+
3	Carbohydrate	H_2O	Molisch's reagent and conc: H_2SO_4	Red ring	+
4	Phenol	EtOH	5% $FeCl_3$	Deep blue color	+
5	Saponins	H_2O	Distilled water	Frothing	+
6	Tannins	H_2O	Gelatin ,1% $FeCl_3$ and 1% HCl	Cherry red color	+
7	Quinones	EtOH	Conc: HCl	Yellow color	+
8	Terpenoids	H_2O	Chloroform and conc: H_2SO_4	Reddish brown ppt	+
9	Oxalate compounds	H_2O	Glacial acetic acid	Violet color	+
10	Glycosides	H_2O	Glacial acetic acid, 5% $FeCl_3$ and conc: H_2SO_4	Brown ring	+
11	α-amino acids	H_2O	Ninhydrin reagent	Purple color	+
12	Sterols	H_2O	Chloroform, acetic anhydride, conc: H_2SO_4	Intense pink color	+
13	Resins	H_2O	Distilled water	No turbidity	–

+ = Present, - = Absent

Total Phenol Contents of *C. ternatea* Flowers by Folin-Ciocalteu Method

In this study, the total phenolic content of *C. ternatea* was estimated by Folin-Ciocalteu method. Phenols react with an oxidizing agent phosphomolybdate in F-C reagent under alkaline conditions and result in the formation of blue colored complex, the molybdenum blue which is measured at 765 nm colorimetrically. Total phenolic content (TPC) was expressed as micro gram of Gallic acid equivalent (GAE) per milligram of crude extract (mg GAE/g). The total phenol content of ethanol extract (75.72 ± 0.20 mg GAE/ g) was found to be higher than water extract (43.22 ± 1.20 mg GAE/ g). The observed absorbance data of different concentrations of standard concentrations of standard gallic acid solution are summarized in Table 2 and standard calibration curve is shown in Figure 4. The resulting data are shown in Table 3.

Table 2 Absorbance of Different Concentrations of Standard Gallic Acid Solution

No.	Concentrations (µg/mL)	Absorbance (Mean value) at 765 nm
1	6.25	0.168
2	12.50	0.233
3	25.00	0.326
4	50.00	0.510
5	100.00	0.868

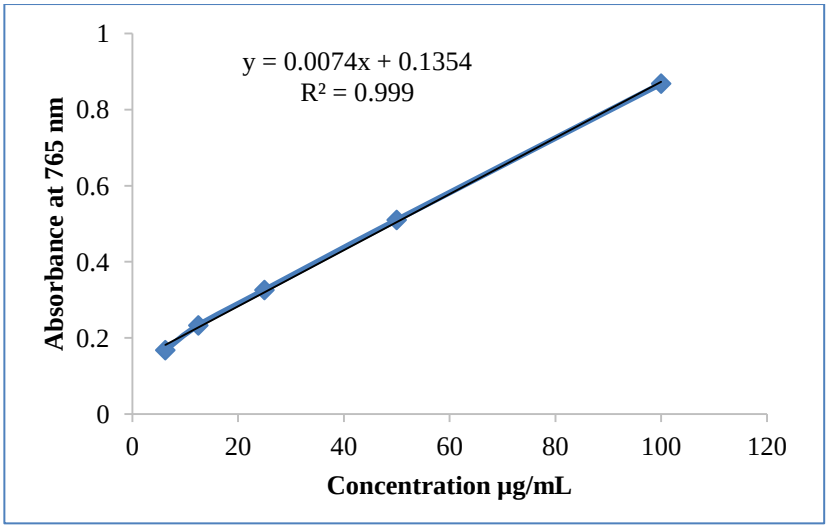

Figure 4 Calibration curve for the standard gallic acid solution

Table 3 Total Phenol Content (TPC) of Ethanol and Water Extracts of *C. ternatea*

No.	Extracts	TPC (mg GAE/g ± SD)
1	Ethanol	75.72 ± 0.20
2	Water	43.22 ± 1.20

Total Flavonoids Contents of *C. ternatea* Flowers by Aluminium Chloride Colorimetric Method

The total flavonoids contents in the examined different crude extract using the aluminium chloride colorimetric assay were expressed in terms of quercetin equivalent. The values obtained for the concentration of total flavonoid were expressed as mg of quercetin equivalent/g of dry mass. The total flavonoid content of water extract (33.75 ± 0.54 mg QE/g) was observed to be lower than ethanol extract (58.44 ± 1.12 mg QE/ g). The observed absorbance data of different concentrations of standard quercetin solution are summarized in Table 4 and standard calibration curve is shown in Figure 5. The resulting data are expressed in Table 5. In this case ethanol extract of sample have high content of flavonoid.

Table 4 Absorbance of Different Concentrations of the Standard Quercetin Solution

No.	Concentrations (µg/mL)	Absorbance (Mean value) at 415 nm
1	0.62	0.008
2	1.25	0.016
3	2.50	0.025
4	5.00	0.041
5	10.00	0.071
6	20.00	0.130

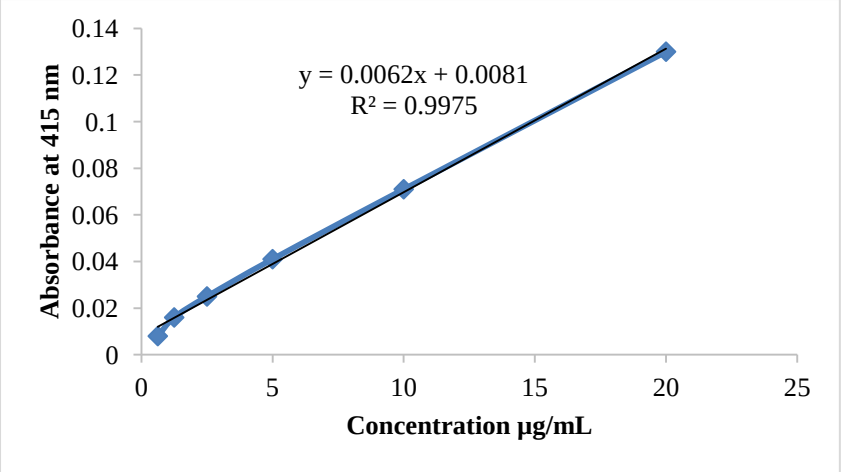

Figure 5 Calibration curve for the standard quercetin solution

Table 5 Total Flavonoids Content (TFC) of Ethanol and Water Extracts of *C. ternatea*

No.	Extracts	TFC (mg QE/g ± SD)
1	Ethanol	58.44 ± 1.12
2	Water	33.75 ± 0.54

Total Carbohydrate Contents of *C. ternatea* Flowers by Anthrone Method

The carbohydrate content in different plant extract using the Anthrone method was expressed in terms of glucose equivalent. The observed absorbance data of different concentrations of standard glucose solution are summarized in Table 6 and standard calibration curve is shown in Figure 6. The total carbohydrate content of water extract (374.68 ± 0.86 mg GE/g) was observed to be higher than ethanol extract (265.23 ± 1.14 mg QE/ g). The resulting data are shown in Table 7.

Table 6 Absorbance of Different Concentrations of the Standard Glucose Solution

No.	Concentrations (µg/mL)	Absorbance (Mean value) at 620 nm
1	3.13	0.143
2	6.25	0.227
3	12.50	0.341
4	25.00	0.531
5	50.00	0.898

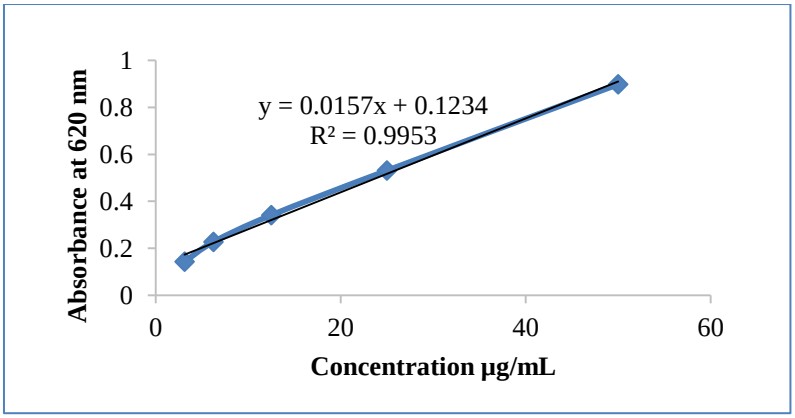

Figure 6 Calibration curve for standard glucose solution

Table 7 Total Carbohydrate Content (TCC) of Ethanol and Water Extracts of *C. ternatea*

No.	Extracts	TCC (mg GE/g ± SD)
1	Ethanol	265.23 ± 1.14
2	Water	374.68 ± 0.86

Total Tannin Contents of *C. ternatea* Flowers

Tannin is widely distributed in plant and occurs in solution in cell sap, often in distinct vacuoles. Tannins are readily soluble in water or alcohol given as stringent solution that is useful in medicine (Ibrahim *et al.*, 2004). In this research, tannins content for flowers of *Clitoria ternatea* L. were determined. For the analysis of tannin content, it is necessary to prepare a calibration curve from a series of standard tannic acid solutions at 720 nm. It was found that the plot of absorbance *vs* concentration of tannic acid is distributed in Figure 7 and the data are expressed in Table 8. After that the tannin contents were calculated by using standard comparison method. It can be obtained that tannin content is evidently high in the ethanol extract of sample (7.45 ± 0.32 g TAE/100 g) compared to the water extract of sample (3.23 ± 0.54 g TAE/100 g). The obtaining data are shown in Table 9.

Table 8 Absorbance of Different Concentrations of the Standard Tannic Acid Solution

No.	Concentrations (mg/mL)	Absorbance (Mean value) at 720 nm
1	0.062	0.087
2	0.012	0.143
3	0.250	0.289
4	0.500	0.535
5	1.000	0.986

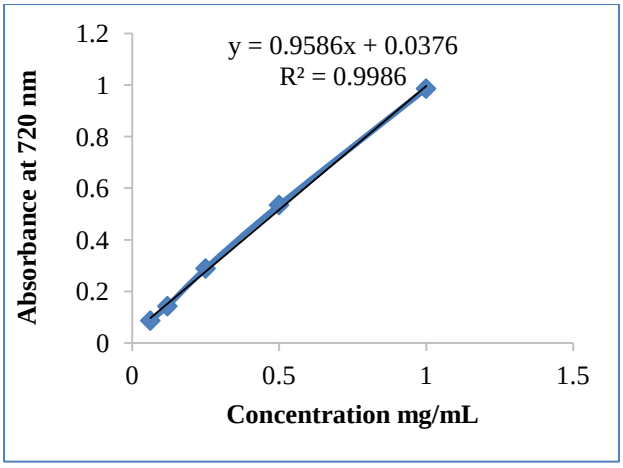

Figure 7 Calibration curve for standard tannic acid solution

Table 9 Total Tannin Content (TCC) of Ethanol and Water Extracts of *C. ternatea*

No.	Extracts	TTC (g TAE/100g ± SD)
1	Ethanol	7.45 ± 0.32
2	Water	3.23 ± 0.54

Antimicrobial Activity of Ethanol and Water Extracts of *C. ternatea* Flowers by Agar Well Diffusion Method

The ethanol and water extract of samples were tested on six species of microorganisms including *B. subtilis*, *S. aureus*, *P. aeruginosa*, *B. pumilus*, *C. albicans and E. coli*. The results are shown in Figure 8 and Table 10. According to the results, ethanol extract detected more effective in water extract. It can be found that stronger antibacterial effect for gram positive bacteria such as *B. subtilis*, *S. aureus* and *B. pumilus* than others and the inhibition zone diameters of tested samples against six microorganisms were found in the range of 19 to 26 mm in ethanol extract and 15 to 19 mm in water extract.

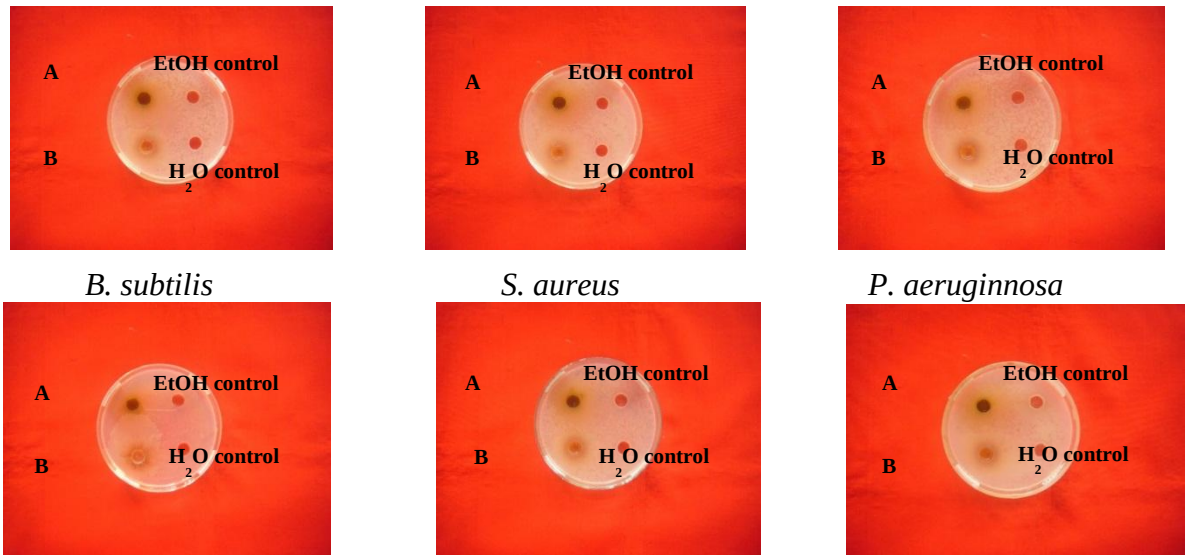

A = ethanol extract sample, B = water extract sample

Figure 8 Antimicrobial activity screening of ethanol and water extracts of *C. ternatea*

Table 10 Inhibition Zone Diameter (mm) of Crude Extracts of *C. ternatea* Flowers Against Tested Microorganisms

Sample	Extracts	Inhibition zone diameter (mm) against different microorganisms					
		B. subitilis	***S. aureus***	***P. aeruginosa***	***B. pumilus***	***C. albicans***	***E. coli***
C. ternatea	EtOH	26 (+++)	24 (+++)	19 (++)	23 (+++)	19 (++)	20 (+++)
	H_2O	19 (++)	17 (++)	15 (++)	17 (++)	15 (++)	16 (++)
Control	EtOH	–	–	–	–	–	–
	H_2O	–	–	–	–	–	–

Agar Well – 10 mm
10 mm ~ 14 mm (+) - low activity
15 mm ~ 19 mm (++) - medium activity
20 mm ~ above (+++) - high activity

Antitumor Activity of *C. ternatea* Flowers by Potato Crown Gall Test

The antitumor activity of ethanol and water extracts of *C. ternatea* Flowers were investigated by using PCG test with bacterium *A. tumefaciens*. For inoculation of potato disc, 48 h broth cultures containing 5×10^9 cells/mL were used. The tested samples were dissolved in DMSO, diluted and mixed with bacterial culture for inoculated on the cleaned and sterilized potato disc, and incubated for 7 days, at room temperature. After that the tumors were appeared on potato discs and checked by staining the knob with Lugol's solution. In the control, the formation of white knob on the blue background indicated the presence of tumor cells because there is no protein in tumor cells. The activities of test samples did not form any tumor on the potato discs and its surface remained blue. Tumors were counted with the aid of dissecting scope after staining with Lugol's solution.

From this experiment, it was found that both ethanol and water extracts of *C. ternatea* were good for preventing the tumor formation with the dose of 0.10 and 0.15 mg/disc in *vitro* potato disc assays. In addition, both ethanol and water extracts were not significantly inhibited the formation of tumor with the dose of 0.05 mg/disc. The quantitative criteria and results are expressed as (-) for high inhibition, (+) for less inhibition and (+++) for non-inhibition of tumor growth after visual comparison with the control (Table 11 and Figure 9).

Table 11 Antitumor Activity of Crude Extracts of *C. ternatea* Flowers by PCG Test

Sample	Extracts	Concentration (mg)/disc		
		0.05	**0.10**	**0.15**
Clitoria ternatea	Ethanol	+	-	-
	Water	+	-	-
Control	D/W	++		

Tumor Inhibition: (++) = non activity, (+) = less activity, (-) = high activity

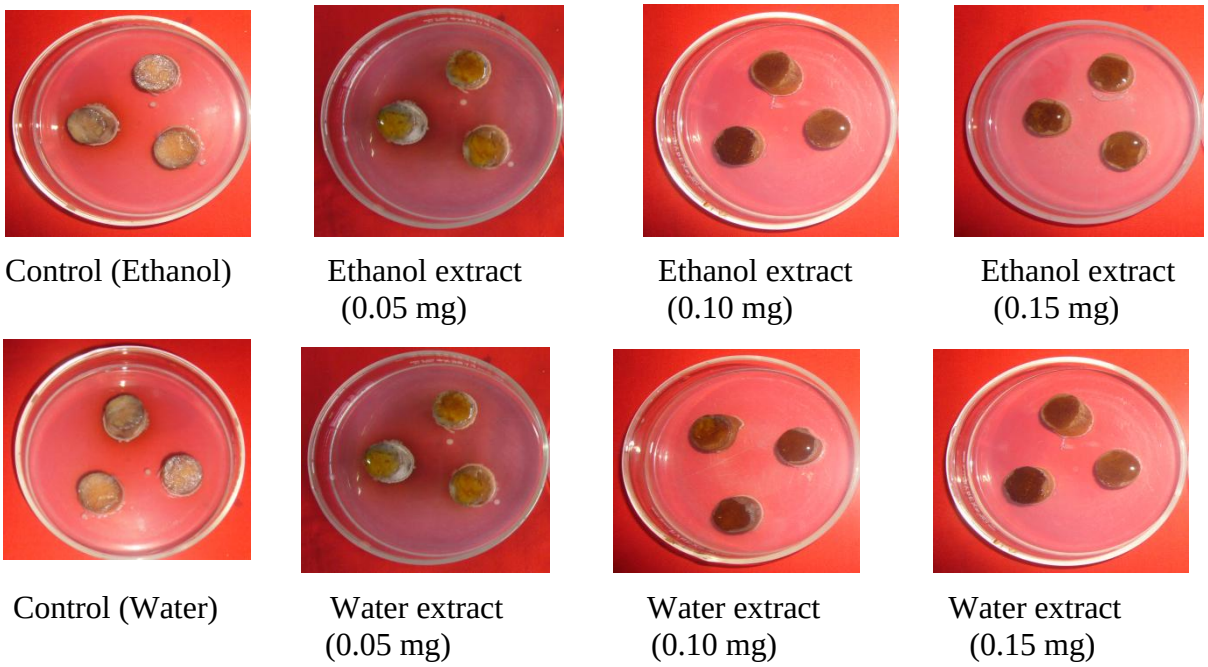

Figure 9 Antitumor screening of ethanol and water extracts of *C. ternatea* flowers incubated for 7 days

Acute Toxicity Study of Crude Extracts of (Aung-Mae-Nyo) Flowers

The acute toxicity screening of ethanol and water extract of *C. ternatea* flowers were prepared with the dose of 300 mg/kg and 2000 mg/kg body weight in each of albino mice. The conditions of mice groups were recorded after fourteen days' administration. The results shown no lethality of the mice was observed up to fourteen days. Each group of animals was also observed still alive and did not show any visible symptom of toxicity like restlessness, respiratory disorders, convulsion, aggressive activities, coma and death. Even with the dose up to 2000 mg/kg body weight administration, there is no lethality after 14 days. Therefore, ethanol and water extracts of *C. ternatea* flowers was free from acute toxic effect under condition. The results are distributed in Table 12.

Table 12 Acute Toxicity Effect of Crude Extracts of *C. ternatea* Flowers on Albino Mice Model after 14 Days Administration

No	Groups	Drug Administration	Dosage mg/kg (b. wt)	No. of death per tested mice	% of death
1.	I	Ethanol extract	300	0/3	0
2.	II	Ethanol extract	2000	0/3	0
3.	III	Water extract	300	0/3	0
4.	IV	Water extract	2000	0/3	0
5.	V (control)	Distilled water	-	0/3	0

Note: Each group contains 3 no: of mice
There is no acute toxicity in ethanol and water extracts of *C. ternatea* Flowers.

Conclusion

From the overall assessments of the research work, the following inferences could be deduced. In the qualitative phytochemical screening of *Clitoria ternatea* L. (Aung-Mae-Nyo) flowers, alkaloids, flavonoids, carbohydrates, glycosides, phenol, saponin, terpenoids, oxalate compounds, tannin, quinones, amino acid and sterols are present. But, a resin is not detected. From the results of quantitative phytochemical screening in ethanol and water extract, the total phenol content, total flavonoids and total tannin content (75.72 mg GAE/g, 58.44 mg QE/g and 7.45 g TAE/100g) in ethanol extract were evidently higher than (43.22 mg GAE/g, 33.75 mg QE/g and 3.23 g TAE/100g) in water extract. But, the total carbohydrate content of water extract (374.68 mg GE/g) was observed to be higher than ethanol extract sample (265.23 mg GE/g). In the studying on the antimicrobial activity of *C. ternatea* flowers, the ethanol extract showed more active on tested microbial strains than water extract. Among them, ethanol extract sample was more effective on gram positive bacteria such as *B. subtilis, S. aureus and B. pumilus* than the other. By the screening of antitumor activity, both extracts of *C. ternatea* flowers were found to prevent the tumor formation with the dose of 0.10 and 0.15 mg/disc. From acute toxicity test, it was observed that the ethanol and water extracts of sample were free from toxic effect even with the dose up to 2000 mg/kg body weight administration to the tested albino mice. Based on this scientific investigation, some biological activities of *C. ternatea* flowers can be well known and it is useful for people's health as natural medicine.

Acknowledgements

The authors would like to express their profound gratitude to the Department of Higher Education (Lower Myanmar), Ministry of Education, Yangon, Myanmar, for provision of opportunity to do this research and Myanmar Academy of Arts and Science for allowing to present this paper.

References

Chakraborty, S., Sahoo, S. Bhagat, A. and Dixit, S. (2017). "Studies on Antimicrobial Activity, Phytochemical Screening Tests, Biochemical Evaluation of *Clitoria ternatea* L. Plant Extract". *International Journal of Research Granthaalayah*, vol. 5(10), pp.1-12

Diener, W., Mischke, U. Kayser, D. and Schled, E. (1995). "The Biometric Evaluation of the OECD Modified Version of the Acute-Toxic-Class Method (Oral)". *Arch Toxicol*, vol. 66, pp. 455-470

Divya, A., Anbumalarmathi, J. and Aruna Sharmili, S. (2018). "Phytochemical Analysis, Antimicrobial and Antioxidant Activity of *Clitoria ternatea* Blue and White Flowered Leaves". *Advanced in Research*, vol. 14 (5), pp. 1-13

Gupta, G. K., Chahal, J. and Bhatia, M. (2010). "*Clitoria ternatea* (L.) Old and New Aspects". *Journal of Pharmacy Research*, vol. 3 (11), pp. 2610-2614

Ibrahim, D., Muhammad, I. Ashiru, S. Sani, I. She hu, K. Ailweo, A. A. and Aligue, R. U. (2004). "Qualitative and Quantitative Phytochemical Screening of *Mimosa pudica* Plant Extracted Touch Me Not". *American Journal of Biological Chemistry*, vol. 2(2), pp. 8-6

Manjula, P., Mohan, C. H. Sreekanth, D. Keerthi, B. and Prathibha, B. (2013). "Phytochemical Analysis of *Clitoria ternatea* L., A Valuable Medicinal Plant". *J. Indian bot. Soc.*, vol. 92 (3), pp. 173-178

Robert, A. D. and Gary, A. K. (2018). "The Medicinal Plants of Myanmar". *PhytoKeys*, vol. 102, pp. 128-129

WHO. (1991). *Guidelines for the Assessment of Herbal Medicines, Programmed on Traditional Medicine*. Geneva: 1st Ed., World Health Organization, pp. 91-94

SORPTION OF VANADIUM(V) FROM MINERALIZED CHLORIDE-SULFATE SOLUTION BY FIBROUS IONITES MATERIALS

Nway Shwan Oo[1], I. D.Troshkina[2]

Abstract

In present work, the possibility of recovery of vanadium(V) from mineralized chloride-sulfate solutions by fibrous ionites materials of the FIBAN brand was investigated. (FIBAN is the abbreviation word for fibrous ionites brand which were produced by the Institute of Physical Organic Chemistry, Academy of Sciences of Republic Belarus). Equilibrium and kinetic characteristics of sorption of vanadium(V) by the fibrous ion exchangers (anionites and cationites) FIBAN brand, FIBAN AK-22, FIBAN A-6 and FIBAN K-1, which contain functional groups: $-NH_2$, =NH, ≡N, $-COOH$,$-N^+\equiv$, =NH and $-SO_3^- H^+$ had been studied. It is established that the maximal sorption capacity of FIBAN AK-22 and FIBAN A-6 with regard to kinetic sorption rate of vanadium (V) is observed at pH=4. Sorption isotherms of vanadium by using FIBAN AK-22 is convex shape being described by Langmuir constant K_L= 190 ± 9mL/g (R^2 – 0.8) and FIBAN A-6 is linear shape by Henry constant K_H = 2.09 ± 0.20 L/g (R^2 – 0.95), respectively. Integral sorption kinetic curves were found under conditions of a limited solution volume, and the order of effective diffusion coefficients of vanadium by using anion exchangers FIBAN AK-22 and FIBAN A-6 which are constituted 10^{-15} and 10^{-14} m^2/s respectively. The average apparent activation energies during the sorption of vanadium (V) for anion exchanger FIBAN AK-22 was 6.2 ± 2.0 kJ /mol and for FIBAN A-6, 19.9 ± 4.7 kJ/mol. It may be indicated that the flow of the sorption rate of vanadium and sorption process took place in the external diffusion region. Additionally, the maximum sorption capacity of fibrous cation exchanger FIBAN K-1 for sorption of vanadium(V) in the form of oxo-vanadate VO_2^+ was observed at pH = 1. From this study, it was found that cation exchanger has higher sorption rate than anion exchangers.

Keywords: vanadium(V), chloride-sulfate solution, sorption, FIBAN, fibrous ion exchangers, anionites, cationites

Introduction

Vanadium is an important rare metal which has been widely used in ferrous and non-ferrous alloys to improve its hardness, tensile strength, and fatigue resistance (Wang *et al*., 2013) for various purposes and the chemical industry. Recently vanadium is also known as "**new green element**". The need for clean and renewable sources of energy is generating increased interest in vanadium due to the recent development of the vanadium flow battery, also known as vanadium red-ox battery (VRB), and its utilization in the storage of energy produced by green sources such as wind and solar (Hammond, 2013).

The recovery of rare element—vanadium—from waste solutions, which are formed when processing natural mineral and organic complex raw materials, is an alternative process of increasing their mining, which promotes the improvement of environmental situation in the industrial zone of enterprises. The vanadium concentration in worked out solutions can reach 200 mg/L and higher (Mizin *et al*., 2005).

Vanadium is a heavy metal. Compounds of pentavalent vanadium are most toxic, since they retard the synthesis of fatty acids and inhibit certain ferment systems. The limiting

[1] Dr, Lecturer, Department of Chemistry, Myeik University

[2] Dr, Professor, Department of Technology of Rare Elements and Nanomaterials, D. Mendeleev University of Chemical Technology of Russia (MUCTR)

admissible concentration of vanadium in water of household and cultural–domestic water use is 0.1 mg/L (Sanitary-Epidemiological Rules and Standards, 2010), while its content in waste waters entering biological sewage purification facilities is normalized at a level of 5 mg/L. It is reasonable to apply the sorption method for the recovery of metals from solutions with their low content. Vanadium is preferentially recovered applying strongly basic and complexing ionites. The separation of these metals from water solutions can be also performed by sorption with fibrous ionites, for example, vanadium with cellulose - based fibers (TsM, TsM-A2, and TsM-A3 brands). It is known that fibrous ionites possess better kinetic characteristics than traditional granulated sorbents (Soldatov *et al*., 1990).

This study is aimed to find the sorption characteristics of fibrous ionites of the FIBAN series with the recovery of vanadium(V) from mineralized solutions and compare the kinetic sorption rate of vanadium metal ions on anionites and cationites.

Materials and Methods

Fibrous ionites FIBAN series of following brands: AK-22 and A-6 (anionites), and K-1(cationites), which were developed at the Institute of Physical Organic Chemistry, Academy of Sciences of Republic Belarus. These ionites have been synthesized by polymer and a similar transformation of polyacrylonitrile fibers (Palant *et al*., 2007). They are characterized by a developed system of meso-pores and micro-pores. Structure and surface appearance of fibrous ion exchangers FIBAN micrograph showed the heterogeneity of their surface and the cylindrical shape of the filaments with a diameter substantially the same length. Figure 1 is representative for fibrous ion exchanger FIBAN A-6 image and its electron micrograph is shown in Figure 2.

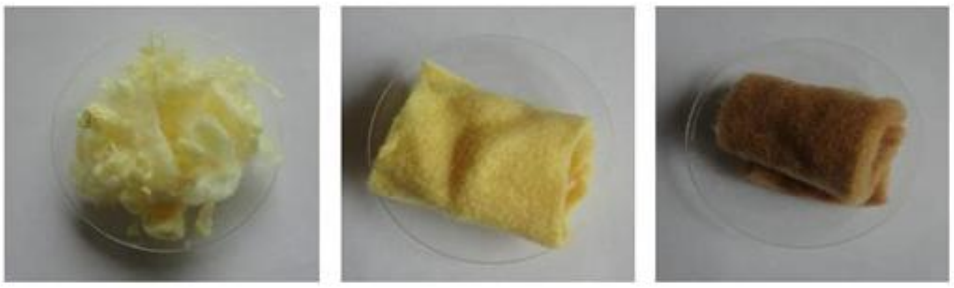

Figure 1 Fibrous ionites FIBAN series of brands anionites (AK-22), (A-6), and cationites (K-1)

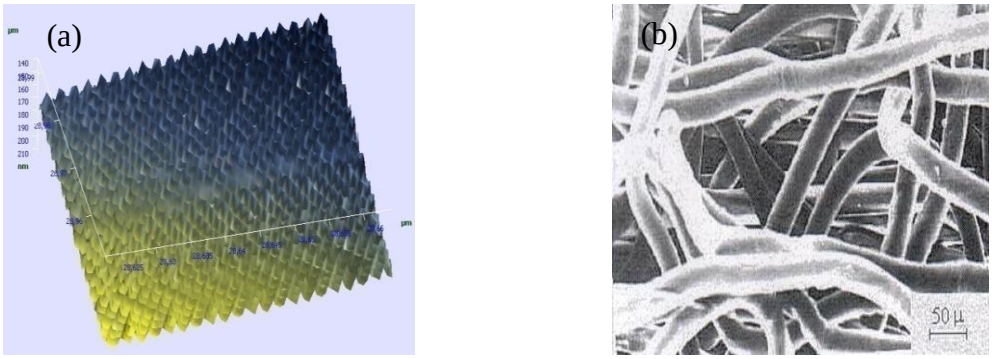

Figure 2 SEM micrographs of fibrous anionites (a) FIBAN AK- 22 (b)FIBAN A- 6 (Filament diameter 20-50 microns)

Electron micrographs of the starting monofilament polypropylene, and polypropylene grafted with 100 % monopolymer styrene (98 %) and divinylbenzene (2 %) and a schematic structure of a fibrous sorbents - sulfonic FIBAN K-1 are shown in Figure 3.

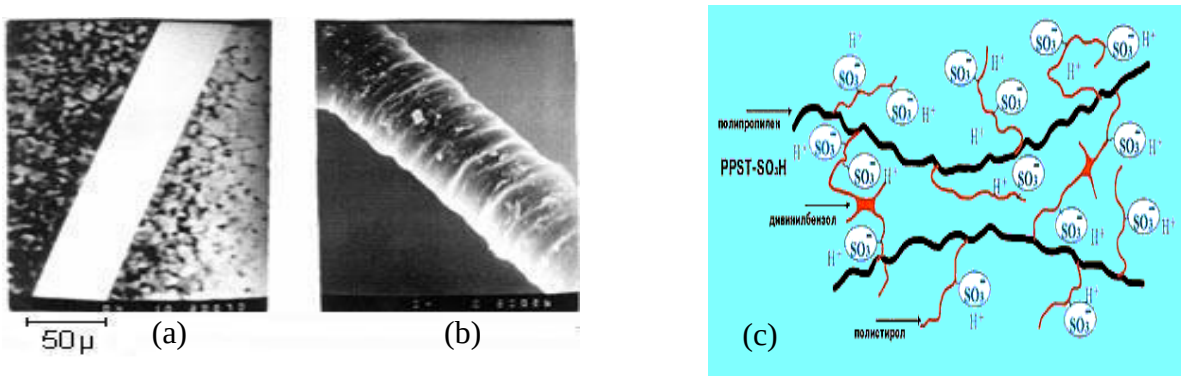

Figure 3 SEM micrographs of the filaments (a) FIBAN K-1 starting polypropylene and (b) polypropylene grafted with styrene and (c) divinyl benzene monopolymer and a diagram of the structure of fibrous sulfonic FIBAN K-1 (Soldatov *et al*., 2004)

Ionites of the FIBAN series of brands AK-22, A-6, and K-1, the main physicochemical characteristics of which are presented in Table 1.

Table 1 Characteristics of Fibrous Ionites FIBAN

Ionite	**FIBAN AK-22**	**FIBAN A-6**	**FIBAN K-1**
Functional group	$-NH_2$, =NH, ≡N, -COOH	$(C_3H_5O)(CH_3)_2N^+Cl^-$, $-N(CH_3)_2$	$-SO_3^-H^+$
Basic of polymer	polyacrylonitrile fiber		Polypropylene fiber with a graft copolymer of styrene and divinyl benzene
Form (staple fiber)	Needle punched nonwoven fabric	woven fabric	Needle punched nonwoven fabric
optimal capacity, mg-equiv/g	3.5 - (amino), 1.0 - (–COOH)	2.0 ($-N^+\equiv$), 0.8 ($-NR_2$)	3.0
Swelling, g_{water}/g ion exchanger	0.7	1.2	1.0
Working pH range	0 – 8	0 – 13	0 − 14

The investigation into the sorption characteristics of fibrous ionites of the FIBAN A-6 series, which contain groups of quaternary and secondary amines, and FIBAN AK-22 ionites with amino-carboxyl groups was performed as applied to the recovery of vanadium (V) from diluted mineralized solutions which contained 0.1g/L Vanadium (V), 1.0 g/L Cl^- and 30.0 g/L SO_4^{2-}. The selection of ions is conditioned by their broad spread in natural and manufacturing solutions. The ion state of vanadium (V) largely depends on its concentration and acidic medium. It is reported that there are twelve vanadium (V) species in solution. These can be categorized as

cationic species VO_2^+, neutral species $VO(OH)_3$ and anionic species.The anionic species are divided into decavanadate species ($V_{10}O_{26}(OH)_2^{4-}$, $V_{10}O_{27}(OH)^{5-}$ and $V_{10}O_{28}^{6-}$), mononuclear species ($VO_2(OH)_2^-$, $VO_3(OH)^{2-}$ and VO_4^{3-}) and other polyvanadate species ($V_2O_6(OH)^{3-}$, $V_2O_7^{4-}$, $V_3O_9^{3-}$ and $V_4O_{12}^{4-}$). In the ion exchange process, anion exchange resins are used for the adsorption of vanadium mostly in the form of anionic and poly-nuclear species, such as $V_{10}O_{28}^{6-}$, $HV_{10}O_{28}^{5-}$ and $H_2V_{10}O_{28}^{4-}$ (Zeng *et al*.2010).

In accordance with literature data in the pH range from 1 to 3, appropriate waste solutions of pH, ionic form of existence of vanadium ranges from a cation to anion. At a concentration of 200 mg/L and a pH of less than 1.5 in solution exists *oxo-cation* VO_2^+, and at higher pH exists *as decavanadates anion* $HV_{10}O_{28}^{5-}$ as shown in Figure.4. In connection with this, taking into account the acidity of waste solutions for the extraction of vanadium was used the anion ampholytes of different types.

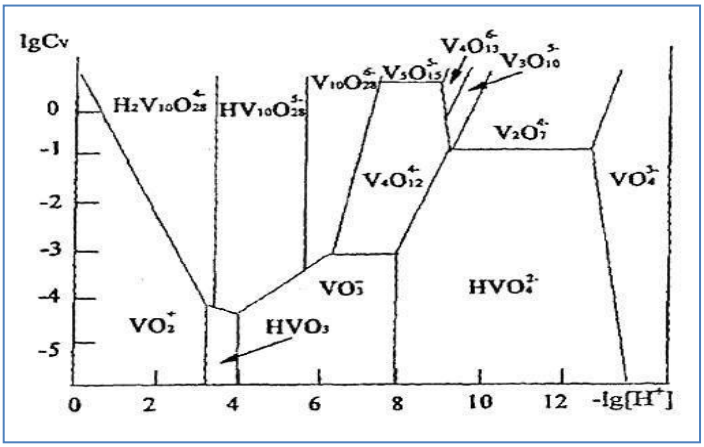

Figure 4 Dependence ion states of vanadium (V) on the pH of the aqueous solution (Mizin *et al*.,2005)

Effect of pH

The sorption of metals from solutions was investigated in static conditions with the ratio of fiber ionites (g) to solution volume (mL) equal to 1: 2000. After contacting the phases under intense stirring on a shaker and their separation, the concentration of metals in the solution (*C*) and the sorption capacity of ionites (SC) were determined by the balance relationship. The vanadium contents in solutions were determined by the photometric method.

Sorption Isotherm

Equilibrium sorption characteristics were studied under static conditions with the ratio of fiber ionites (g) to solution volume (mL) equal to 1: 2000 at pH 4. For determination of sorption isotherm for vanadium, the anionites FIBAN AK-22 and FIBAN A-6 were contacted with the solution for 48 h (including 4 hours at a stirring rate of 160 oscillations per minute) at room temperature. The experiment was carried out to complete saturation of the sorbent. After two days, the solution was analyzed for vanadium ion and was separated from the solution and contacted with a fresh portion of solution. The sorption is generally described by isothermal, that are functions relating the amount of sorbate on the ionites (sorbent). Langmuir and Henry models are used to describe the sorption process.

Kinetic Sorption Study

The same procedure was followed to investigate the effect of temperature on sorption process. The sorption kinetics of vanadium(V) with ionites FIBAN AK-22 and FIBAN A-6 were determined by the limited solution volume method using the installation of thermostated (temperature-controlled) cells at temperatures of 293, 313 and 333 K.

Results and Discussion

Effect of pH

Taking into account the complexity of behavior of vanadium in aqueous solutions, the influence of pH of solutions on the sorption of vanadium (V) with ionites FIBAN A-6 and FIBAN AK-22 was preliminarily studied. The dependence of SC on pH is presented in Figure. 5. It was shown that the largest sorption capacity for vanadium is attained at pH 4.

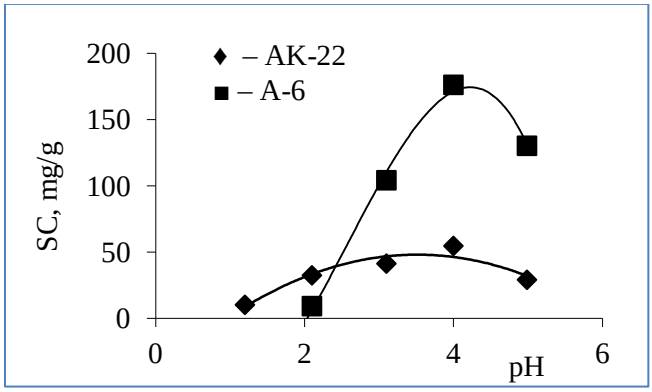

Figure 5 Dependence of capacity of the FIBAN series ionites on the solution pH

Vanadium was extracted and performed further investigations by using the FIBAN AK-22 and FIBAN A-6 ionite with the selected optimal acidity. At pH 4, vanadium is situated preferentially in the form of the anion as decavanadate-$HV_{10}O_{28}^{5-}$ ion which can be adsorbed by the FIBAN AK-22 and FIBAN A-6 anionites according to the following exchange reaction:

for sorption vanadium by FIBAN AK-22

$$5(R\text{-}NH_3)_2SO_4 + 2[HV_{10}O_{28}]^{5-} \longrightarrow 2(R\text{-}NH_3^+)_5\,[HV_{10}O_{28}]^{5-} + 5SO_4^{2-};$$

When decavanadate-ion interact with the functional groups of the anionites FIBAN A-6, the following reactions may occur:

with quaternary ammonium base groups

$$5(R_4N^+)_2SO_4 + 2[HV_{10}O_{28}]^{5-} \longrightarrow 2\,(R_4N^+)_5[HV_{10}O_{28}]^{5-} + 5SO_4^{2-},$$

with secondary amines groups

$$5[R\text{–}[N(CH_3)_2H]^+]_2SO_4^{2-} + 2[HV_{10}O_{28}]^{5-} \rightarrow 2[R\text{–}[N(CH_3)_2H]^+]_5[HV_{10}O_{28}]^{5-} + 5SO_4^{2-}$$

Investigation of equilibrium characteristics of ionites (FIBAN AK-22 and FIBAN A-6) for sorption of vanadium(V) from mineralized solution

The results of the experiment are shown in Figure. 6. The isotherm obtained for the resulting vanadium concentration was a convex shape, which coincide with Langmuir equation.

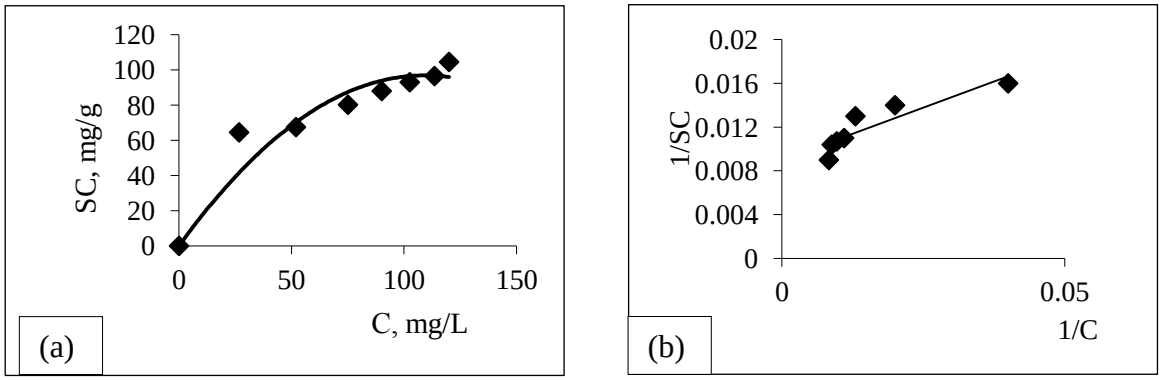

Figure 6 Langmuir isotherm of sorption for vanadium (V) from mineralized chloride-sulfate solution with anionite FIBAN AK-22.

Processing of data on the sorption equilibrium of vanadium with FIBAN AK-22 was carried out by the Langmuir equation in the coordinates "1/SC to 1/C, which describes the isotherm of this nature. Langmuir constant and maximum sorption capacity of the processing were calculated from linearized coordinates (Figure.6,b). The calculated Langmuir constant K_L and the maximum sorption capacity of the ion exchanger FIBAN AK-22 amounted to (190± 45) mL/g and 93.1 mg/g, respectively, with a correlation coefficient R^2 - 0,8.

Sorption isotherm of vanadium (V) with FIBANA-6 was studied by using the Henry equation (Frolov.,1982):

$SC = K_H \cdot C$,

where SC – sorption capacity of the ionites for vanadium, mg /g;

K_H – Henry's law constant, mL/mg;

C –equilibrium concentration of vanadium, mg /L.

In the studied concentration range of vanadium (up to an equilibrium concentration of 110 mg/L) obtained isotherm is linear shape (Figure.7) and can be described by the Henry equation with constant: (2.09 ± 0.20) L/g (R^2= 0.955). The resulting equilibrium data were indicated that the fibrous FIBAN AK-22 has considerably better capacitive characteristics as compared with the ion exchanger FIBAN A-6.

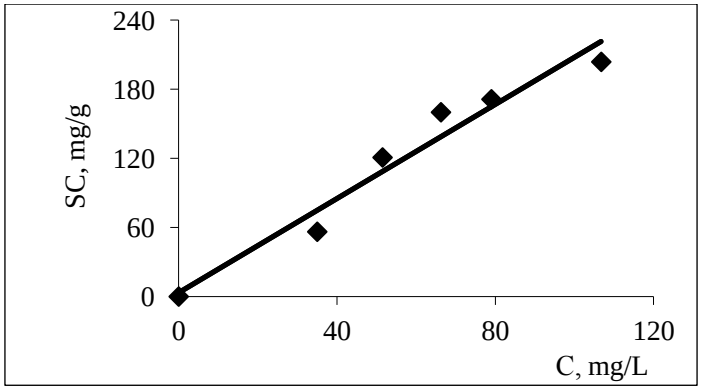

Figure 7 Henry isotherm of sorption for vanadium (V) from mineralized chloride -sulfate solution with anionite FIBAN A-6.

Investigation of Kinetic Characteristics of Ionites (FIBAN AK-22 and FIBAN A-6) for the Sorption of Vanadium(V) from Mineralized Solution

Integral kinetic curves of sorption of vanadium at different temperatures are shown in Figure. 8 (a, b). Integral characteristic kinetic curves of sorption of vanadium ion by FIBAN AK-22 and FIBAN A-6 in the coordinates (sorption capacity SC - time τ) and (saturation F - time τ) are shown in Figures 8 and 9, respectively, and data for their processing are presented in Table 2.

Effective diffusion coefficients of vanadium on the fibrous ionite FIBAN AK-22 and FIBAN A-6 are calculated allowing for the half-transformation time ($\tau_{0.5}$).

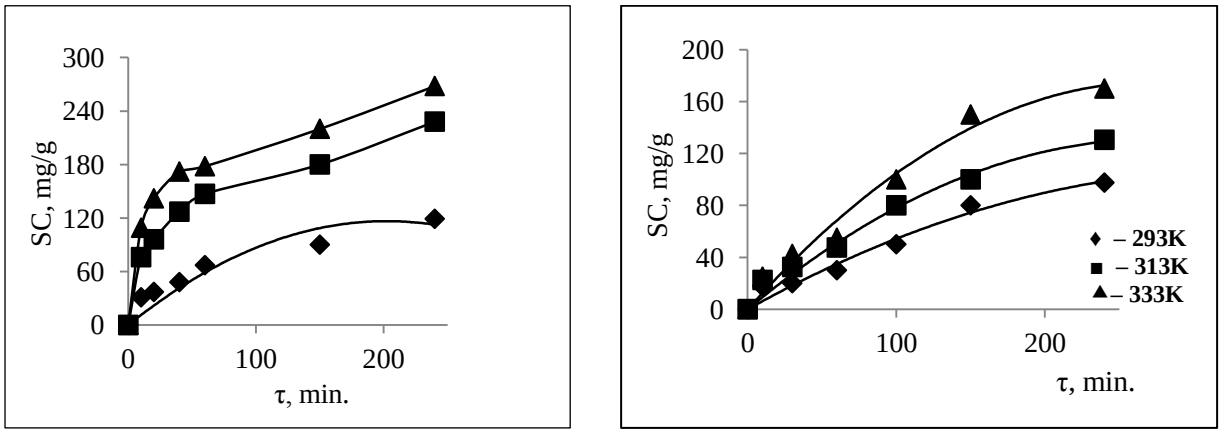

(a) (b)

Figure 8 Integral kinetic curves of sorption of vanadium from mineralized chloride - sulfate solution by using (a) anionites FIBAN AK-22 and (b) anionites FIBAN A-6.

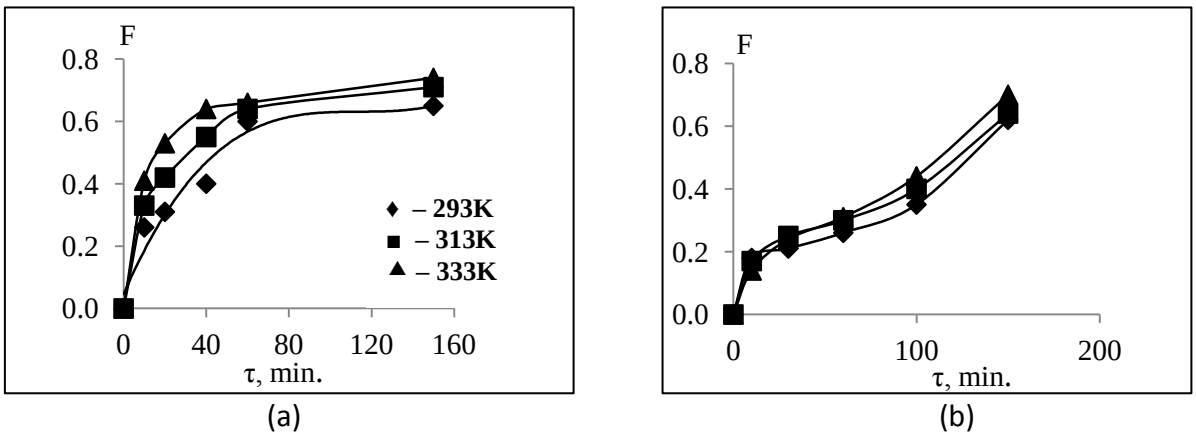

Figure 9 Time dependence of the saturation degree (F) of the (a) FIBAN AK-22 and (b) FIBAN A-6 anionites with vanadium

According to the integral kinetic curves of sorption of vanadium in the coordinates of the (degree of saturation (F) - time (τ)),half-transformation time, $\tau_{0.5}$ was graphically calculated (Table 2).

Effective diffusion coefficient of vanadium on the fibrous ionite were calculated, taking into account the half- transformation time. The calculation was performed using the formula (Kokotov, 1979):

$$D_{eff} = (0.065 \cdot R^2) / \tau_{0.5},$$

where D_{eff} – effective diffusion coefficients of vanadium on the fibrous ionite, (m^2/s), $\tau_{0.5}$– half-transformation time, (s) , and R – the fiber radius, (m) (its average magnitude is 30 microns meter.)

Table 2 Kinetic Characteristics of Vanadium (V) by FIBAN AK-22 and FIBAN A-6

Temperature (K)	**Half time sorption $\tau_{0.5}$ (s)**		**Effective diffusion coefficient (m^2/s)**	
	AK-22	**A-6**	**AK-22**	**A-6**
293	8100	3300	$3.2x10^{-15}$	$7.9x10^{-15}$
313	7800	2100	$3.3x10^{-15}$	$1.2x10^{-14}$
333	6000	1200	$4.3x10^{-15}$	$2.1x10^{-14}$

Table 2 shows that the order of effective diffusion coefficients of vanadium are in the range of $10^{-15} - 10^{-14}$ m^2/s. Using the calculated effective diffusion coefficients of vanadium ionites,the apparent activation energy of adsorption of vanadium by ionites FIBAN AK-22 and FIBAN A-6 are calculated by an equation similar to the Arrhenius equation (Kokotov, 1979):

$$D = D_0 \cdot e^{-E_{act.}/RT}$$

where $E_{act.}$ − the apparent activation energy (J/mol), D_o − constant (m^2/s), D – effective diffusion coefficient of vanadium ionites (m^2/s), R – universal gas constant (8.3144 J/mol), T – Temperature (K).

Table 3 Activation Energy During the Sorption of Vanadium with FIBAN AK-22 and FIBAN A-6

Interval Temperature (K)	Activation energy of sorption of vanadium $E_{act.}$ (kJ/mol)		Mean value of the apparent activation energy (kJ/mol)	
	AK-22	A-6	AK-22	A-6
293-313	1.2±0.5	15.9± 4.5		
293-333	6.0±1.8	19.8± 4.8	6.2±2.0	19.9± 4.7
313-333	11.5±3.3	24.2± 7.7		

As shown in Table 3, the average apparent activation energy of FIBAN AK-22 was calculated by an equation similar to the Arrhenius equation, is equal to (6.2 ± 2.0) kJ /mol, which may be indicated the flow of the sorption of vanadium by the external field. For FIBAN A-6, the average apparent activation energy was (19.9 ± 4.7) kJ/mol, which may be indicative of the flow of the sorption of vanadium by the external field (Rakov *et al*.,1993). According to the resulting data, the sorption rate of FIBAN A-6 is a mite higher than AK-22 by the above resulting data, elution characteristics for sorbent FIBAN AK-22. Proceedings integral kinetic curves and the data on the effective diffusion coefficient of vanadium(V) by using fibrous ion exchangers FIBAN AK-22 and FIBAN A-6 show that the low speed (rate) of the sorption of vanadium present in the acidic condition, mainly in the form of large-ion decavanadate $HV_{10}O_{28}^{5-}$. Delayed kinetics of sorption of vanadium fibrous ion exchanger can be apparently explained by lower mobility due to sufficiently large size decavanadate $HV_{10}O_{28}^{5-}$ adsorbed ion, which has a considerable charge, and rather large size and by the necessity of spatial orientation during the sorption.

Furthermore, sorption of vanadium(V) was investigated at acidic medium- oxo-cations VO_2^+ state, which is smaller than decavanadate $HV_{10}O_{28}^{5-}$ ion size. For this purpose, strong-fibrous cation exchanger FIBAN K-1 containing sulfonic groups was used as a sorbent for sorption of vanadium(V) by changing pH. Preliminary study of the effect of pH on the sorption of vanadium cation exchanger FIBAN K-1 is shown in (Figures 10 and 11). It can be seen the distribution ratio of vanadium(V), decreases with increasing the pH of the solution. The distribution coefficient of vanadium in ionities was calculated as the ratio of the equilibrium sorption capacity of the ion exchanger to the equilibrium concentration in the solution.

$$K_d = SC/C_{V,}$$

where, K_d – distribution ratio of vanadium (mL/g), SC – equilibrium sorption capacity (mg /g), C_V–the equilibrium concentration of vanadium in the solution in mg /L.

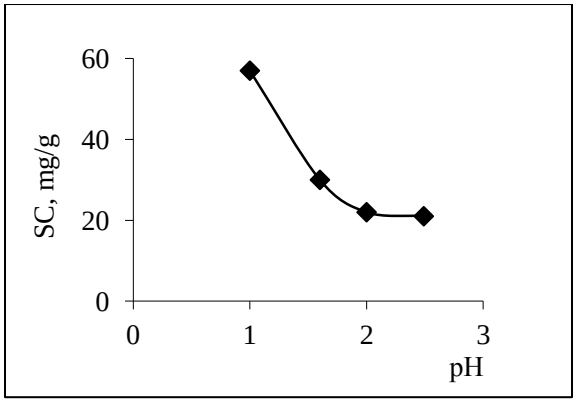

Figure 10 Dependence of the sorption capacity of cationites FIBAN K-1 on pH

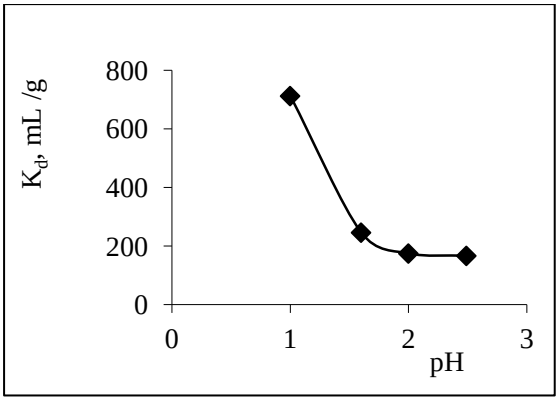

Figure 11 Dependence of distribution ratio of the cationites FIBAN K-1 on pH

The maximum distribution coefficient of vanadium in ionite FIBAN K-1 was observed at pH of 1 (Figure 11). Integral sorption kinetic curve of vanadium(V) by using cationites FIBAN K-1 at this pH in the coordinates of the "degree of saturation of the F – time τ" is shown in Figure 12.

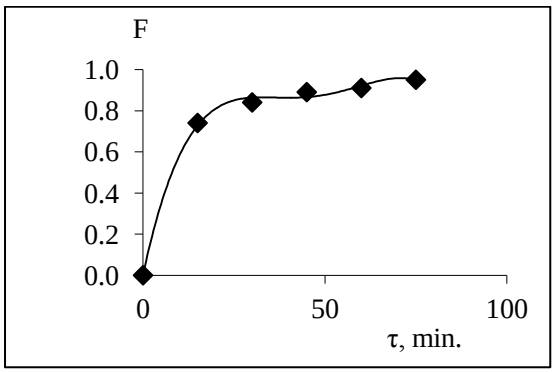

Figure 12 Integral kinetic curves of sorption of vanadium(V) by cationites FIBAN K-1 from the mineralized chloride-sulfate solutions (pH 1).

Integral kinetic sorption curves were obtained in conditions of limited volume of the solution. According to the integral kinetic curves of sorption of vanadium in the coordinates of the (degree of saturation (F) – time (τ)), half-transformation time, $\tau_{0.5}$ was graphically calculated. For FIBAN K-1, effective coefficient of vanadium diffusion (5.4×10^{-14} m^2/s) was calculated, taking into account the time of half-reaction in Table 4.

Table 4 Comparison of Effective Diffusion Coefficients of Vanadium(V) during the Sorption of Ion Exchangers FIBAN

Mark of the ion exchanger FIBAN	pH	Half-transformation time, $\tau_{0.5}$ (s)	The effective diffusion coefficient (m^2/s)
AK-22	4.0	8100	3.2×10^{-15}
K-1	1.0	480	5.4×10^{-14}

A comparison of the effective diffusion coefficients of vanadium on the fibrous ionites FIBAN AK-22 and FIBAN K-1, as well as the integral of the kinetic curves in the coordinates of the (degree of saturation of F – time τ), obtained by the sorption it these ion exchangers shows that a decrease in the size of the adsorbed ion vanadium(V) sorption rate increases significantly: the effective diffusion coefficient increases by more than an order of magnitude.

Conclusion

Recovery of vanadium(V) from mineralized chloride-sulfate solutions by fibrous materials of the FIBAN series (anionites and cationites), (FIBAN AK-22), (FIBAN A-6) and (FIBAN K-1) which contain functional groups: ($-NH_2$, =NH, ≡N, -COOH), ($-N^+\equiv$, =NH), and ($-SO_3^-$ H^+) respectively were studied. The maxium sorption rate for vanadium (V) of decavanadate $HV_{10}O_{28}^{5-}$ and oxo-vanadate VO_2^+ was observed in the pH range 1 – 4. Sorption isotherms of vanadium from mineralized solution by using ionites FIBAN AK-22 has a convex shape. Langmuir constant K_L is (190 ± 9) mL/g (R^2–0.8), the maximum sorption capacity – 93.1 mg /g. Sorption isotherm of ion exchanger FIBAN A-6 has a linear shape and is described by Henry constant K_H (2.09 ± 0.20) L/g (R^2 – 0.955). For methods of limiting the volume of solution, integral kinetic curves of sorption of vanadium(V) ion by using exchangers FIBAN were obtained. It was found that the sorption of vanadium(V) in the form of decavanadate ion from the chloride- sulfate solution (pH ≥ 2) by using nitrogen-containing fibrous ion exchangers (FIBAN AK-22 and FIBAN A-6) took place in the external diffusion region. The effective diffusion coefficients of vanadium on the fibrous ionite FIBAN AK-22 increases from 3.2 x 10^{-15} to 4.3 x 10^{-15} m^2/s, ion exchanger FIBAN A-6, 7.9 x 10^{-15} to 2.1 x 10^{-14} m^2/s over the temperature range 293 – 333 K. The activation energy of sorption of vanadium(V) by ion exchanger FIBAN AK-22 is (6.2 ± 2.1) kJ/mol, that of ion exchanger FIBAN A-6 (19.9 ± 4.7) kJ/mol. It is established that the diffusion of oxo-vanadate VO_2^+ in the strongly acidic condition by cationites FIBAN K-1 occurs at a higher sorption rate than the diffusion of decavanadate ions $HV_{10}O_{28}^{5-}$ by anionites FIBAN AK-22 and FIBAN A-6.

Acknowledgements

This work was financially supported by the Ministry of Education, Union Republic of Myanmar. Special mention to my supervisor Professor Dr Troshkina I. D from Department of Technology of Rare Elements and Nanomaterials, D. Mendeleev University of Chemical Technology of Russia (MUCTR), for her excellent discussion and advice of this work. I also wish to express my sincere of Dr Ni Ni Oo, Rector of Myeik Universiy, Dr Thi Thi Aye, Professor and Head, Department of Chemistry, Myeik University, and Prof. Dr Myint Myint May for their advice and encouragements and also for kindly allowing me to write as research article for this work.

References

Frolov, Yu.G. (1982). *Course of Colloid Chemistry*. Moscow: Khimiya. p.400.

Hammond, A.D. (2013). " Vanadium, the New Green Metal: Mineral Deposits in the Colorado Plateau". *J. Mining Enginering*.(December).pp.1-7.

Kokotov, Yu.A. and Pasechnik,V.A. (1979). *Equilibrium and Kinetics of Ion Exchange*. Leningrad: Khimiya.p.336.

Mizin, V.G., Rabinovich, E.M and Sirina,T.P. (2005). *Complex Processing of Vanadium Raw Materials*. Yekaterinburg: Ural Branch Russ. Acad.Sci. (UrO RAN). p.416.

Muzgin,V.N., Khamzina L.B., Zolotavin V.L and Bezrukov I.Ya. (1981). *Analytical Chemistry of Vanadium*. Moscow: Nauka.p.216.

Palant, A.A., Troshkina, I.D and Chekmarev, A.M. (2007). *Metallurgy of Rhenium*. Moscow: Nauka. p.298.

Rakov, E. G and Haustov.C. B. (1993). *Processes and The Productions of Radioactive and Rare Metals*. Moscow. Metallurgy. p.59.

Sanitary - Epidemiological Rules and Standards. (2010). SanPiN. 2.1.4.2580-10.

Soldatov,V.S., Polus, Z., Pawlowska, M and Maczka I. (2004)."A Srong Acid Nonwoven Filtering Medium for Deep Air Purification". *Fibres & Textiles in Eastern Europe*.vol.12, pp.56-61.

Soldatov,V.S and Sergeev,G.I. (1990)."Fibrous Ion Exchangers: Perspective Sorbents for Extraction of the Heavy Metals Ions from Aqueous Solutions". *J. All Russian Chemical Society*. vol.35, pp.101–106.

Wang, L., Yimin, Z., Tao, L., Jing, H and Yi, W. (2013). "Comparison of Ion Exchange and Solvent Extraction in Recovering Vanadium from Sulfuric Acid Leach Solutions of Stone Coal. " *J. Hydrometallurgy*. vol. 131, pp. 1-7.

Zeng, L., Li, Q.G., Xiao, L. S and Zhang, Q.X. (2010). "A Study of the Vanadium Species in an Acid Leach Solution of Stone Coal using Ion Exchange Resin." *J.Hydrometallurgy*, vol.105, pp.176-178.

BIOSORPTION OF COPPER AND NICKEL IONS BY NON-LIVING BIOMASS OF *ASPERGILLUS* SPECIES

Ohnmar Aye[1], Ye Myint Aung[2]

Abstract

Two different fungi were isolated from agricultural soil in Pathein Township. Both isolates were studied on the basis of morphological and microscopical characteristics. Pure cultures of fungal isolates were identified with the help of literature keys of Ando (2016). According to morphology and distinct characters, the two fungal strains were identified as *Aspergillus* sp. 1 and *Aspergillus* sp. 2. The two *Aspergillus* species were tested for their tolerance against heavy metals such as Cu^{2+} and Ni^{2+} ions at different concentration of 10 mM, 20 mM, 30 mM, 40 mM and 50 mM. It was observed that *Aspergillus* sp. 1 tolerance against Cu^{2+} ion and *Aspergillus* sp. 2 tolerance against Ni^{2+} ion. The ability of isolated fungal strains towards biosorption potential of metal ions from industrial wastewater sample were also studied. In this study, the adsorption efficiency of biomass was determined by using the functions of contact time and biomass dose. The biosorption capacity of *Aspergillus* sp. 1 reached 47.58 % removal of Cu^{2+} ion, while *Aspergillus* sp. 2 was expressed 39.04 % removal of Ni^{2+} ion. The finding revealed that fungi of two *Aspergillus* species showed higher metal-tolerant and biosorption capacity of copper and nickel ions from wastewater.

Keywords: metal-tolerant, biosorption, *Aspergillus* sp., contact time

Introduction

Heavy metal pollution is a serious environmental problem of global concern. Heavy metals are continuously released into the environment due to industrial and technological developments, and contamination of agricultural soil with heavy metals is a major problem at industrial and defense-related sites all over the world. The industrial effluents are generated from hundreds of small and large manufacturing and plating industries such as metallurgical, electroplating, metal finishing, tanneries, chemical manufacturing, mine drainage, and battery manufacturing, and contain considerable amounts of heavy metals at elevated concentrations. (Malik and Jaiswal, 2000).

Filamentous fungi and yeasts have been used in many wastewater treatments to bind metallic elements. Fungi are one of the industrial fermentation waste biomass which is really excellent metal sorbed. So, fungi including yeasts have received increased attention. Fungi gives good efficient and economical for sequestering heavy toxic metals from dilute aqueous solutions by biosorption because: it offers the advantage of having a high percentage of cell wall materials, it shows excellent metal binding properties, it is available in large quantities from the antibiotic and food industries, it provides an eco-friendly environment (Gadd, 1993).

Traditional methods used for the removal of heavy metals from the environment are in general expensive and potentially risk due to the possibility of the generation of hazardous by-products. For example, the use of conventional technologies, such as ion exchange, chemical precipitation, reverse osmosis, and evaporative recovery, for this purpose is often inefficient and very expensive. In recent years, the biosorption process has been studied extensively using microbial biomass as biosorbents for heavy metal removal (Gavrilesca, 2004).

[1] Dr, Lecturer, Department of Chemistry, Pathein University
[2] Dr, Professor and Head, Department of Chemistry, Pathein University

The main purpose of the present study was characterization of metal-tolerant fungi isolated from soil samples and selection of more resistant strains. The reason for the selection of the fungi is that the organisms that usually adapt the conditions of metals and in future these fungi could be used as biosorption tool.

Materials and Methods

Isolation of Soil Fungi by Serial Dilution Method

In serial dilution method, 0.1 g of dried soil sample was diluted with 10 mL sterile water. The final test tubes of dilution series were cultured on low carbon agar (LCA) medium and incubated for 5 to 7 days. After incubation, pure colonies were obtained by cultured in potato glucose agar (PGA) medium (Phay and Yamamura, 2005).

Media used for the isolation of soil fungi

(1) Low Carbon Agar (LCA) Medium (Ando, 2004)		**(2) Potato Glucose Agar (PGA) Medium (Ando, 2004)**	
Glucose	2.0 g	Potato	200 g
Sucrose	2.0 g	Glucose	20 g
K_2HPO_4	1.0 g	Agar	18 g
$MgSO_4.7H_2O$	0.5 g	Yeast Extract	1.0 g
KNO_3	1.0 g	DW	1.0 L
KCl	0.5 g	pH	6.5
Agar	18 g		
DW	1.0 L		
pH	6.5		

(After autoclaving chloramphenicol 0.03 g was added to both media)

Identification of Isolated Fungi

Fungal isolate were studied for its morphological features under light microscope at Botany Department, Pathein University. The cultures were identified on the basis of macroscopic (colonial morphology, colour, shape, diameter and colony appearance) and microscopic characteristics (septation in mycelium, shape and structure of conidia). The mycelia were observed at visual inspection. The microscopical characters including conidiophore, vesicle, conidia and hyphae were observed.

Determination of Metal-Tolerant Fungi by Spot Culture Method

A disk of mycelium was inoculated aseptically on potato glucose agar (PGA) plates supplemented individually with 10, 20, 30, 40 and 50 mM of heavy metal. The inoculated plates were incubated at 25 °C at least for 15 days. Three replicates for each of concentrations and control (medium without metal) were used. The effect of the heavy metal on the growth of the isolates was estimated by minimum inhibitory concentrations (MICs). MIC is defined as the lowest concentrations of metal that inhibit visible growth of the isolate (Hassen and Saidi, 1998).

Study on Biosorption of Toxic Heavy Metals from Industrial Wastewater

The biosorption process was generally applied for the toxic heavy metals (Cu^{2+} and Ni^{2+} ions) removal from industrial wastewater.

Industrial wastewater sample was collected from Shwe Lin Ban Industrial Zone, Shwe Phyi Thar Township, Yangon (Figure 1). The wastewater samples were taken at a distance of about 1 m from the point source of drainage and at a depth of 0.2 m below the surface of water with sterilized prewashed polyethylene container. The initial concentrations of Cu^{2+} and Ni^{2+} ions in the wastewater were analyzed by Atomic Absorption Spectrophotometer (AAS) from Ministry of Education, Department of Research and Innovation (DRI), Yangon.

In this study, the fungal species *Aspergillus* sp. 1 and *Aspergillus* sp. 2 were used as biosorbent for removal of metal ions from wastewater. The heavy metal removal was determined by the effect of biomass dose and contact time.

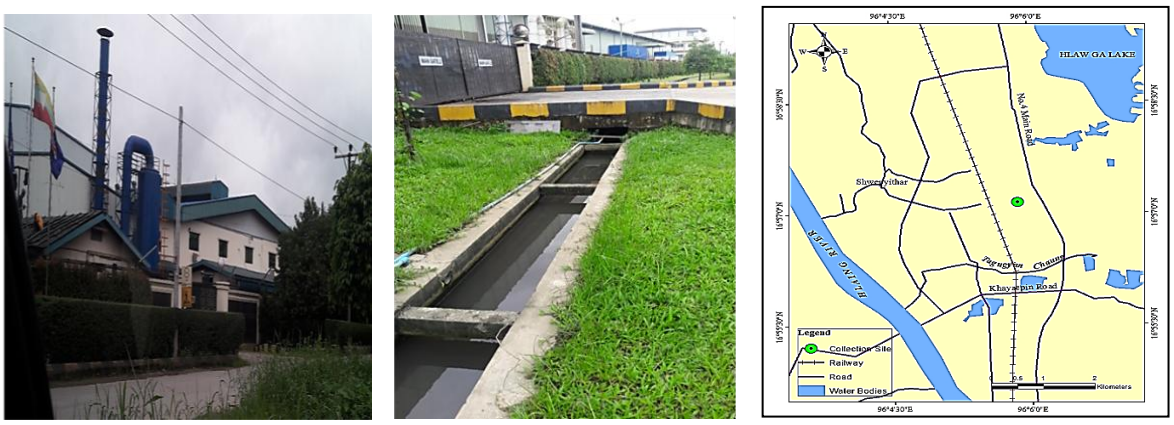

(a) (b) (c)

Figure 1 Wastewater sample collected sites

(a) Battery factory (b) Drainage of wastewater (c) Location map

Results and Discussion

Identification of Isolated Fungi

Morphological and microscopical descriptions of OMA-1

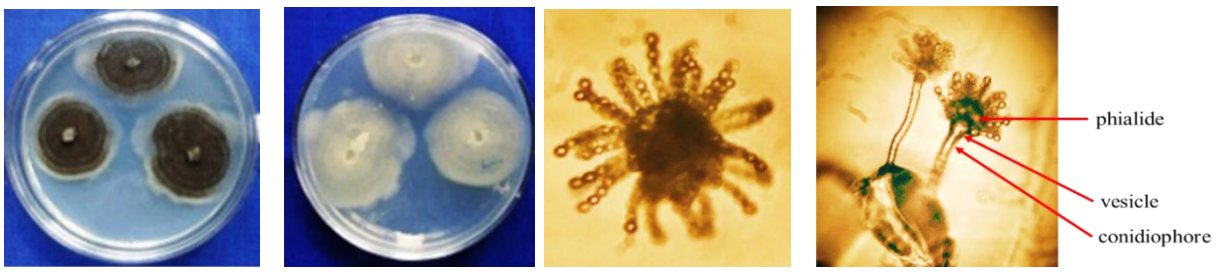

(a) (b) (c) (d)

Figure 2 Micromorphological characters of OMA-1

(a) Front view (b) Reverse view (c) Conidia (d) Microscopical description

The colonies are fast growing and mature within 3 days. The colonies are flat and powdery in texture. The front colour of the colony is black center and white edge. The reverse colour is whitish grey or creamy (Figure 2).

The hyphae are septate and hyaline. The conidiophores stipes are smooth-walled, hyaline and erect. The conidiophores terminate in a spherical to pyriform vesicle. The vesicle, phialide, metulae and conidia are the parts to form the conidial head. The conidia are globose to subglobose, one-celled, smooth-walled, dark brown to black are produced in long chains.

Morphological and microscopical description of OMA-2

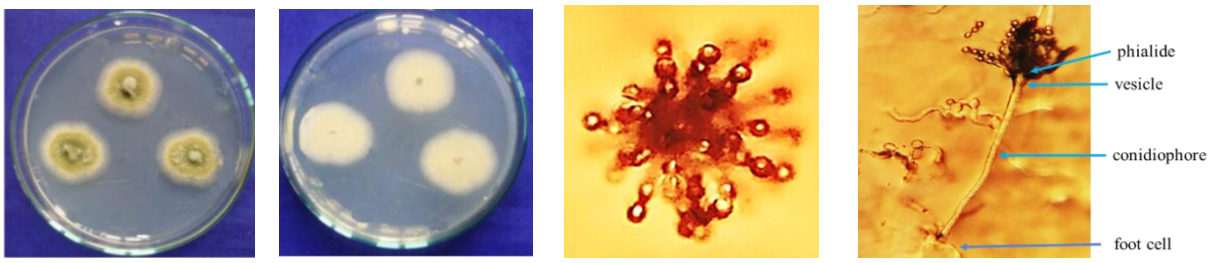

(a) (b) (c) (d)

Figure 3 Micromorphological characters of OMA-2
(a) Front view (b) Reverse view (c) Conidia (d) Microscopical description

The colonies are flat often with granular, yellow at first but quickly becoming bright to dark yellow-green with age. The reverse colour is whitish or creamy (Figure 3).

The hyphae are septate. The large cell of the hyphae are known as foot-cells. From each foot cell arises a vertical branch, is called conidiophore. Each conidiophore elongates and end in a dome-shaped head called the vesicle. The sterigmata or phialides are the tubular outgrowths, which are produced directly from the vesicle. The conidia are produced in long basipetal chains, and is enormous numbers. The conidia are spherical and unicellular structure. The conidia are brownish in colour (Figure 3).

Identification key of OMA-1 and OMA-2

The OMA-1and OMA-2 fungus were identified as *Aspergillus* sp.1 and *Aspergillus* sp.2 according to keys of Ando, (2016) as follows. The results are summarized in Table 1.

1. Conidial Ontogeny (i) Conidial production is chain
   (ii) Type of conidial production is Phialo type
   (iii)Type of conidial ontogeny is Enteroblastic chain
2. Conidiophores - Typical conidiophores with septa, simple and unbranched.
3. Conidiophores - Elongate along with conidial production
4. Arrangement of Conidiogenous cells - Independent (Parallel)
5. Development of Conidiogenous cells - Stable
6. Conidial production loci of Conidiogenous cells - Mono
7. Conidia (i) Shape - Simple, (ii) Spore - Amerospore
8. Hyphae - with septa regularly
9. Identified these fungus as *Aspergillus* sp.

Scientific Classification

Kingdom	:	Fungi
Phylum	:	Ascomycota
Class	:	Eurotiomycetes
Order	:	Eurotiales
Family	:	Trichocomaceae
Genus	:	*Aspergillus* sp.

Table 1 Morphological and Physical Characteristics of the Isolated Fungal Species

Characteristics	***Aspergillus* sp.1**	***Aspergillus* sp.2**
Colony diameter	53.5 mm	55.04 mm
Conidial colour	Black	Brown
Conidial shape	Globose	Globose
Conidiophore colour	Brown	Brown
Mycellial colour	Black center with white edge	Yellowish green
Colonial reverse	Whitish grey	Cream
No. of sterigmata	Present in two series	Present in one series

Screening of Metal-Tolerant Fungi by Spot Culture Method

In this study, heavy metal- tolerant fungi were screened and the minimum inhibitory concentration of Cu^{2+} and Ni^{2+} were determined (Figures 4 and 5). The growth pattern appears to suggest tolerance development or adaptation of the fungi to the presence of heavy metals. In the presence of heavy metal relative to the control, the growth rate of the fungi decreased with increased in metal ions concentration. At lower metal ions concentrations, the tested fungal isolates were very resistant and exhibited strong growth. Higher metal ion concentrations caused a reduction in growth and increased the length of the lag phase compared to the control. A reduction in the growth rate is a typical response of fungi to toxicants, whereas the lengthening of the lag phase is not always present.

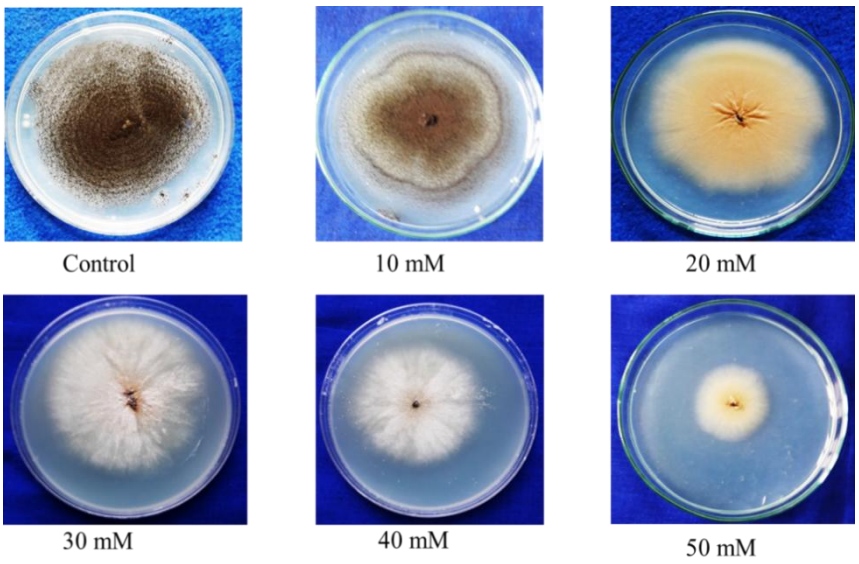

Figure 4 Growth of *Aspergillus* sp.1 after exposure to concentration of Cu^{2+} ion for 15 days

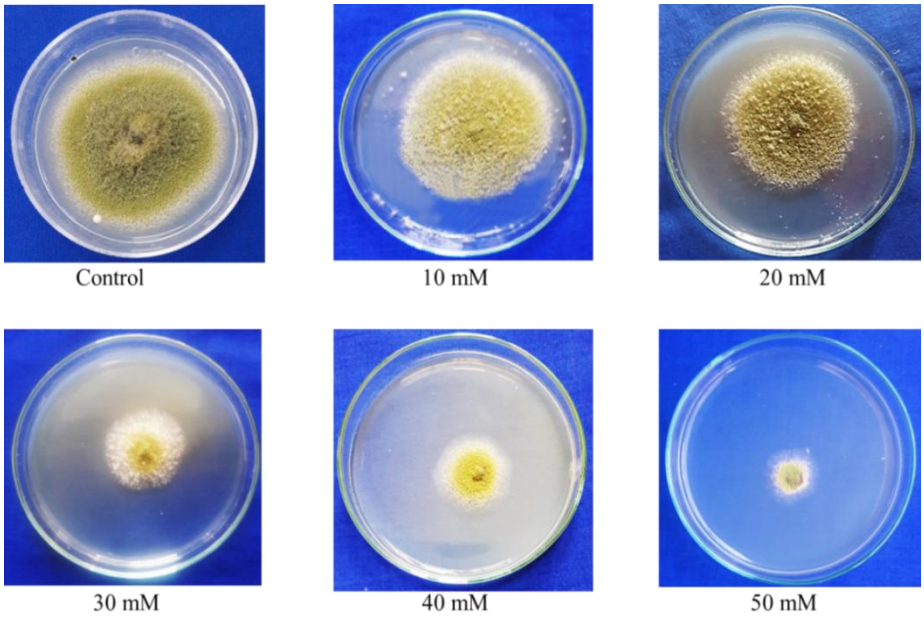

Figure 5 Growth of *Aspergillus* sp.2 after exposure to concentration of Ni^{2+} ion for 15 days

Study on Biosorption of Toxic Heavy Metals from Industrial Wastewater

Table 2 and Figure 6 showed the effect of biomass dose on percent removal of metal ions. It was obvious that removal percent increased with increased in dosage and significantly decreased at dosage 0.5 g. This may be due to the increase in surface area and number of available active site for adsorption of metal ions with saturation of cell surface.

The removal percent on effect of contact time are shown in Table 3 and Figure 7. It was found that percent removal increased gradually to the maximum adsorption and then decreased with increased in contact time. It may be explained by initial rapid uptake due to surface adsorption and subsequent slow uptake due to the specific sites are saturated with metal ions.

Table 2 Effect of Biomass Dosage on Removal of Cu^{2+} and Ni^{2+} Ions by Different Fungal Biosorbents

Contact time = 4 h
pH = 6.0

Dosage (g)	Removal (%)	
	Cu^{2+} (by *Aspergillus* sp. 1)	Ni^{2+} (by *Aspergillus* sp. 2)
0.1	42.74	32.49
0.2	43.27	34.50
0.3	46.77	35.01
0.4	47.58	39.04
0.5	43.80	36.02

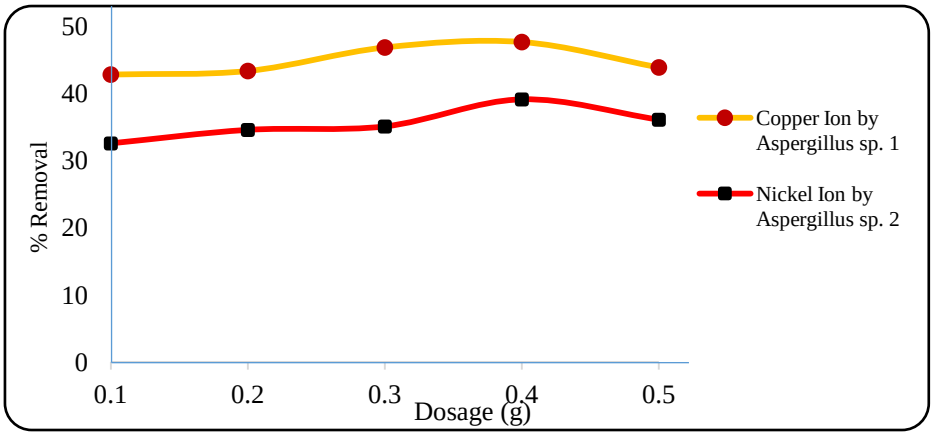

Figure 6 Effect of biomass dosage on removal of Cu^{2+} and Ni^{2+} ions by *Aspergillus* sp. 1 and *Aspergillus* sp. 2

Table 3 Effect of Contact Time on Cu^{2+} and Ni^{2+} Ions Removal by Different Fungal Biosorbents

Biomass dose = 0.4 g

pH = 6.0

Contact Time (h)	Removal (%)	
	Cu^{2+} (by *Aspergillus* sp. 1)	Ni^{2+} (by *Aspergillus* sp. 2)
2	48.11	28.96
4	48.38	31.23
6	49.46	32.24
8	49.19	31.48
10	48.92	30.73

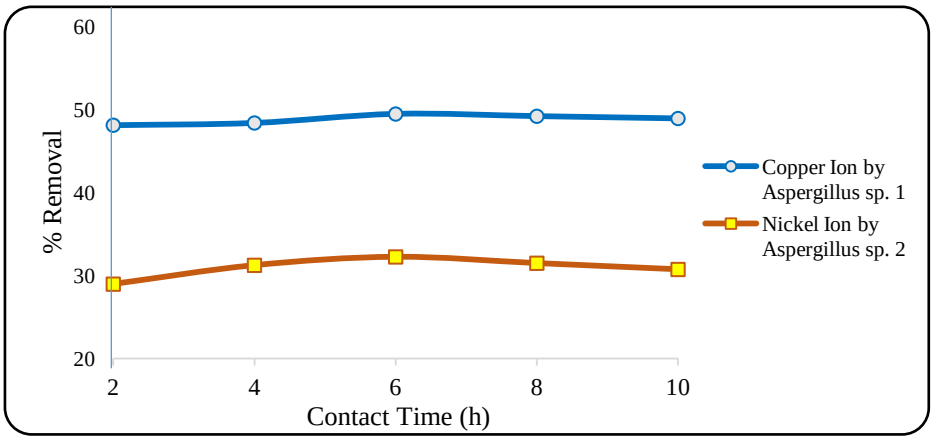

Figure 7 Effect of contact time on removal of Cu^{2+} and Ni^{2+} ions by *Aspergillus* sp. 1 and *Aspergillus* sp. 2

Adsorption Isotherm Assessment

Adsorption isotherm shows the distribution of solute between the liquid and solid phases and can be described by the standard Langmuir isotherms (Figures 8, 9 Tables 4, 5) and Freundlich models (Figures 10, 11 and Tables 6, 7).

Langmuir equation which is valid for monolayer sorption on to a surface with a finite number of identical sites and the linearized form of this model equation is given as

$$\frac{C_e}{q_e} = \frac{C_e}{q_{max}} + \frac{1}{(q_{max}\ b)}$$

Where C_e is the equilibrium concentration , q_{max} is the maximum amount of the metal ion per unit weight of the adsorbent to form a complete monolayer and b is a constant related to the affinity of the binding sites. q_{max} and b can be determined from the linear plot of C_e /q versus C_e.

The empirical Freundlich model also considers mono molecular layer coverage of solute by the adsorbent.

$$\log q = \log K + \frac{1}{n} \log C_f$$

where, K and n are the Freundlich constants characteristics of the system. The q_{max} value of these isotherm model reflects the metal affinity to the sites of biomass. That is the number of metal ions which form a complete monolayer on the surface of the biomass. The linearized Langmuir and Freundlich adsorption isotherm parameters are shown in Table 8 with the value of linear regression coefficients. The coefficients of determination (R^2) are 0.9973 and 0.9920 for Cu^{2+} and Ni^{2+} ions respectively. The values for linear regression (R^2) indicated that the adsorption nature is well fitted with both models.

Table 4 Langmuir Isotherm Data for the Biosorption of Cu^{2+} Ion by *Aspergillus* sp.1

C_e (mmol L^{-1})	q_e (mmol g^{-1})	C_e/q_e (g L^{-1})
8.18	9.05	0.91
8.24	4.39	1.87
8.27	2.87	2.88
8.33	2.08	3.99
8.38	1.61	5.18

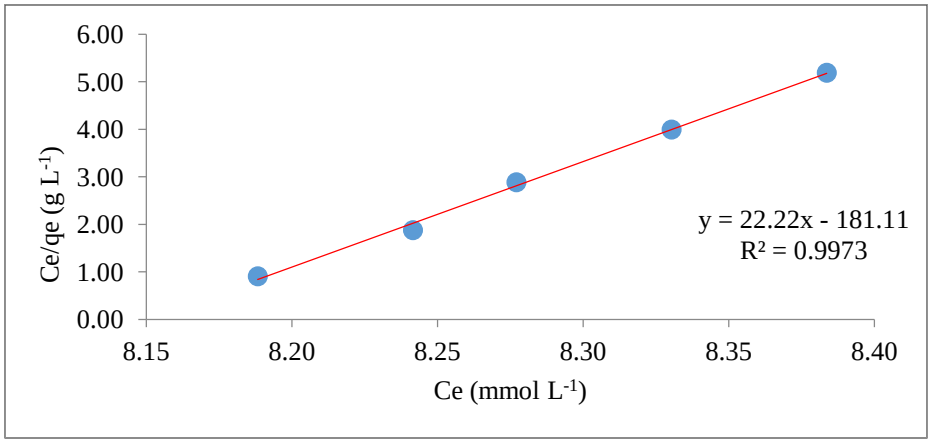

Figure 8 Langmuir adsorption isotherm of Cu^{2+} ion by *Aspergillus* sp.1

Table 5 Langmuir Isotherm Data for the Biosorption of Ni^{2+} Ion by *Aspergillus* sp.2

C_e (mmol L^{-1})	q_e (mmol g^{-1})	C_e/q_e (g L^{-1})
7.11	14.45	0.49
7.12	7.20	0.98
7.13	4.78	1.49
7.14	3.57	1.99
7.15	2.85	2.50

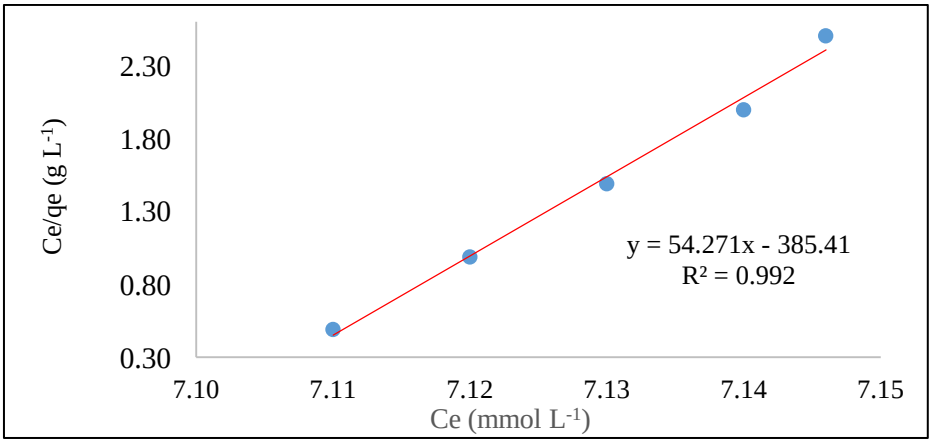

Figure 9 Langmuir adsorption isotherm of Ni^{2+} ion by *Aspergillus* sp.2

Table 6 Freundlich Isotherm Data for the Biosorption of Cu^{2+} Ion by *Aspergillus* sp.1

C_e (mmol L^{-1})	q_e (mmol g^{-1})	log C_e (mmol L^{-1})	log q_e (mmol L^{-1})
8.188	9.0586	0.913	- 0.039
8.241	4.596	0.916	- 0.038
8.277	2.871	0.917	- 0.037
8.330	2.087	0.920	- 0.035
8.383	1.616	0.923	- 0.034

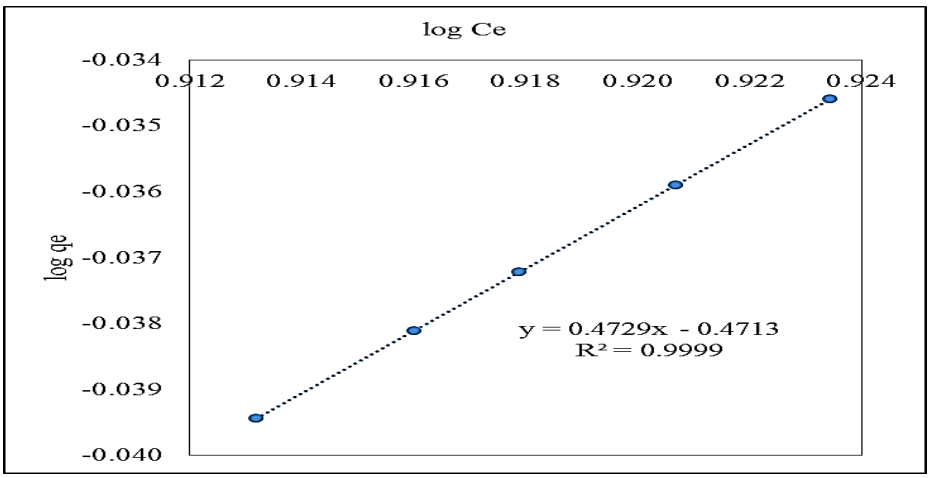

Figure 10 Freundlich adsorption isotherm of Cu^{2+} ion by *Aspergillus* sp.1

Table 7 Freundlich adsorption isotherm of Ni^{2+} ion by *Aspergillus* sp.2

C_e (mmol L^{-1})	q_e (mmol g^{-1})	log C_e (mmol L^{-1})	log q_e (mmol L^{-1})
7.1100	14.4500	0.8519	-0.0696
7.1200	7.2000	0.8525	-0.0693
7.1300	4.7833	0.8531	-0.0690
7.1400	3.5750	0.8537	-0.0687
7.1460	2.8540	0.8541	-0.0685

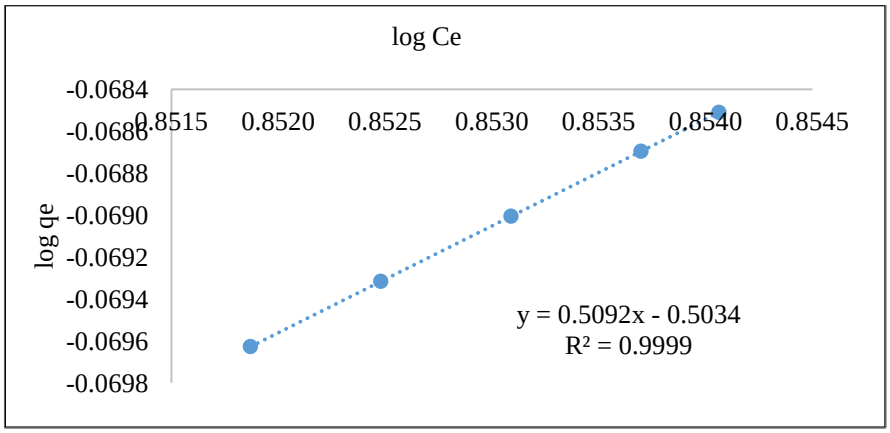

Figure 11 Freundlich adsorption isotherm of Ni^{2+} ion by *Aspergillus* sp.2

Table 8 Isotherm Parameters for the Biosorption of Metal Ions

Metal Ions	Biomass	Langmuir Model			Freundlich Model		
		q_{max} (mg g^{-1})	R^2	b (L mg^{-1})	K_f	R^2	N
Cu^{2+}	*Aspergillus* sp.1	2.8599	0.9973	0.0019	0.3378	0.9999	2.1146
Ni^{2+}	*Aspergillus* sp.2	1.0814	0.9920	0.0024	0.2876	0.9999	1.8002

Conclusion

Soil fungi were isolated from agriculture soil samples by using serial dilution method whereas LCA and PGA media were used. Morphological and microscopic characters of the isolated fungi were identified by using keys of Ando (2016). According to morphology and distinct characters, OMA-1 fungus was identified as *Aspergillus* sp. 1, OMA-2 fungus was identified as *Aspergillus* sp. 2.

Fungal isolates were tested for their tolerance against different concentrations of metal ions such as Cu^{2+} and Ni^{2+}. *Aspergillus* sp.1 was most tolerant to metal concentration of copper, and different isolates of *Aspergillus* sp.2 was tolerant to nickel ion at MIC 50 mM. This means that the levels of resistance are different among different isolates.

In the biosorption study of wastewater treatment, the industrial wastewater was collected and initial metal ion concentrations of copper and nickel in collected sample were analyzed. The

biosorption of heavy metals by using different biomass showed different results. According to results, ability of *Aspergillus* sp. 1 was found to adsorb the copper ion with excellent properties and maximum removal of 49.46 % at optimum dose 0.4 g and contact time 6 h. The adsorption capacity of *Aspergillus* sp. 2 was expressed as 32.24 % removal of nickel ion at 0.4 g of adsorbent dose and 6 h contact time.

The adsorption quantity was evaluated by Langmuir and Freundlich models. The plot of C_e/q_e Vs C_e in various biomass dose was found to be linear indicating the applicability of classical Langmuir adsorption isotherm. The coefficients of determination (R^2) are 0.997 and 0.992 for Cu^{2+} and Ni^{2+} ions respectively. The values for linear regression (R^2) indicated that the adsorption nature is well fitted with Langmuir model. The higher metal adsorption of 2.8599 mg g^{-1} was observed for Cu^{2+} ion whereas the lower uptake was 1.0814 mg g^{-1} for Ni^{2+} ion. For the Freundlich model, log q_e vs log C_e was plotted and K_f and n values are Freundlich constants related to the adsorption capacity and intensity of the sorbents, respectively. The sorption capacity parameter K_f was observed that 0.3378 for Cu^{2+} ion and 0.2876 for Ni^{2+} ion respectively. The results of this study revealed that the fungal cells of *Aspergillus* sp. 1 and *Aspergillus* sp. 2 have greater potential application for the removal of copper and nickel ions from industrial wastewater sample.

Acknowledgements

Special thanks are extended to Ministry of Education, Department of Higher Education for the permission of the research project. We feel a deep sense of gratitude to Dr Si Si Hla Bu, Rector, Pathein University for his invaluable encouragement. We would be grateful to Dr Nilar Myint and Dr Than Tun, Pro-rectors, Pathein University for their continuous suggestions. Thanks are also extended to Dr Than Than Oo, Professor, Department of Chemistry, for their guidance, encouragement and invaluable suggestions.

References

Ando, K. (2004). "*Isolation and Identification of Fungi*". Workshop, Biotechnology Development Centre, Pathein University

Ando, K. (2016). "*Identification of Mitosporic Fungi*". Biological Resource Center, National Institute of Technology and Evaluation (NITE), Japan

Gadd, G. M. (1993). "Interaction of Fungi with Toxic Metals". *New Phytol*, vol.124, pp. 25-60

Gadd, G. M., White, C. and Rome, L.D. (1988). "*Heavy Metal and Radionuclide by Fungi and Yeast*". In P.R Norris and D. P. Kelly (Editors) Biohydrometallurgy. Wilts. UK. pp.122

Gavrilesca, M. (2004). "Removal of Heavy Hetals form the Environment by Biosorption". *Eng. Life Sci*, vol. 4(3), pp. 219-232

Hassen, A. and Saidi, N. (1998). "Resistance of Environmental Bacteria to Heavy Metal". *Bioresour, Technol*, vol. 64, pp. 7-15

Malik, A. and Jaiswal, R. (2000). "Metal Resistance in *Pseudomonas* Strains Isolated from Soil Treated with Industrial Wastewater" .*World J. Microb. Biot*, vol.16, pp.177

Phay, N. and Yamamura, H. (2005). "Approach Method for Rare Microorganisms from Soil Sources". *J. Microbial*, vol.76, pp.23-236

Raja Rao. P. and Bhargavr, Ch. (2013). "Studies on biosorption of Heavy Metals using Pretreated Biomass of Fungal Species". *Int. J. of Chemistry and Chemical Engineering*, vol.3 (3), pp.171-180

POLYPYRROLE-SODIUM BENTONITE COMPOSITES AND ITS ELECTRICAL AND OPTICAL PROPERTIES

Aye Myat Maw[1], Mya Theingi[2], Khin Than Yee[3]

Abstract

The application of bentonite to polymer industry is growing year by year. Bentonite is hydrophilic in nature and polymer is hydrophobic character. This makes the chemically incompatible. Therefore, NaCl treated bentonite as filler was used in the presence of sodium dodecyl sulphate as surfactant and pyrrole monomer to prepare polypyrrole-sodium bentonite composites by in-situ chemical oxidative polymerization method. In the preparation of polypyrrole-sodium bentonite composites (PPy-SDS-NaB), the various amounts of bentonite (4%, 8% and 12% w/v) were used. The resultant composites were designed by PPy-SDS-NaB 1, PPy-SDS-NaB 2 and PPy-SDS-NaB 3, respectively, where, PPy-SDS-NaB means polypyrrole-sodium bentonite composites in the presence of sodium dodecyl sulphate and the numbers refer to the amount of bentonite compositions. The prepared composites were characterized by FT IR, XRD, SEM and TG-DTA techniques. Their electrical properties were analyzed in the frequency range of 1 to 10 MHz by LCR measurement. From the analysis of LCR measurement, it was observed that PPy-SDS-NaB 1 has more electrical conductivity than other two composites. The optical property of the prepared composites were also analyzed in the wavelength range of 200 to 600 nm by using UV-Vis spectrophotometer and the optical band gaps were calculated by Taucs relation. From the analysis of absorption spectra, it was found that the band gaps of prepared composites are in the semiconductor wide band gap ranges of 4.0 eV to 3.8 eV and that shows great promise in sensors as well as electronic applications.

Keywords: Polypyrrole, Sodium-Bentonite, In-situ Chemical Oxidative Polymerization, Sodium Dodecyl Sulphate, Electrical Conductivity, Optical Property

Introduction

Polymer composites can be defined as polymers that have been filled with natural or synthetic compounds to improve their properties. The polymer is called "matrix", if the filler is in the nanometer range, the composite is called "nanocomposite" (Hernandez-Hernandez *et al*., 2016). Nanocomposite polymer materials filled with organo-bentonite are growing development. The addition of an organo-bentonite to the polymer matrix leads to increase of the mechanical strength, thermal stability, gas permeability and water-repellent properties of the polymers (Yoleva *et al*., 2016). In the energy industry, the polymer nanocomposites positively affect the creation of forms of sustainable energy by offering new methods of energy extraction from benign and low cost resources. One example is the fuel cell membranes; other applications include solar panels, nuclear reactors and capacitors (Anadao, 2012).

Conductive polymers, also known as synthetic metals, have electric, magnetic and optical properties which can be compared to those of semiconductors. They are also called conjugated polymers because they present conjugated C=C links in their main chains, which allows for the creation of an electron flux under certain conductions. The conductivity of this kind of polymer depends on the polymer chain order at the moment of synthesizing the nanocomposite (Hernandez-Hernandez *et al*., 2016).

[1] PhD Candidate, Department of Chemistry, University of Yangon
[2] Dr, Lecturer, Department of Chemistry, University of Yangon
[3] Dr, Lecturer, Department of Chemistry, Myeik University

Conducting polymers such as Polyaniline (PAni), Polypyrrole (PPy), and Polythiophene (PTh), have found many industrial applications due to their unique characteristics, such as the dual function of ionic and electronic conductivity, large surface area and good mechanical properties (Utami *et al*., 2016). The standard conducting polymers (CPs; i.e., Polypyrrole (PPy), Polythiophene (PTh), Polyaniline (PANI)) can be polymerized both chemically and electrochemically. Among the conducting polymers, PPy is one of the most frequently studied polymers because of high electric conductivity, ion exchange property, environmental stability as regards oxygen and water, and ease of synthesis (Wang *et al*., 2001; Bouabdallah and Djelali, 2014). Therefore, it has been widely used in electrochemical applications (e.g., as an electrode material, in electrochemical energy storage, as a catalyst support in fuel cells, in supercapacitors and in solar cells (Utami *et al*., 2016)

The present work reports the preparation of polypyrrole-sodium bentonite composites in the presence of sodium dodecyl sulphate on the local bentonite in Myanmar. Three methods are widely used in the polymer/clay nanocomposite preparation. They are in-situ polymerization, solution dispersion and fusion intercalation methods. In this work, it is proposed to use in-situ chemical oxidative polymerization method because it is ease of synthesis (Anadao, 2012).

The objective of this work is to study electrical conductivity and optical property for polypyrrole-sodium bentonite composites based on polypyrrole and organobentonite. Bentonite clay was used as filler in conductive composites because it is naturally abundant in Myanmar, low cost, ion exchange properties and has high thermal resistance and shell-shaped crystalline structure with nanometric thickness.

Materials and Methods

Sample Collection

Pyrrole monomer was purchased from Aladdin Industrial Corporation, Shanghai and used without further purification. Ferric chloride was purchased from Super Shell Chemical store at 27^{th} street, Pabedan Township, Yangon and used as an oxidizing agent. Sodium chloride, supported by Physical Chemistry Laboratory, was used for the alkaline activation. Sodium dodecyl sulphate (SDS), $NaC_{12}H_{25}SO_4$ (Mw 288 g mol^{-1}) was used as surfactant for the organic modification. Purified bentonite clay was collected from Saga Inn village, Ta Da U Township. Distilled water was used as the solvent in all analyses.

Synthesis of the Activated Bentonite (NaB)

The pure bentonite was saturated with sodium ions by stirring for 10 hours in a 0.01 M sodium chloride solution. Then the filtered solid was washed with distilled water to remove the excess salt. Sodium-Bentonite (NaB) was dried at 100 °C, ground and sieved by 100 mesh (Motawie *et al*., 2014).

Synthesis of Polypyrrole and Polypyrrole-Bentonite Composites

First, 3.4 mL of pyrrole monomer was added to 25 mL of ethanol under constant stirring at 5-10 °C. Next, 25 mL of 0.1 M $FeCl_3.6H_2O$ solution was added to the monomer drop wise. The reaction mixture was stirred at 5-10 °C for 1 h. The resulting black precipitate was filtered

and washed with distilled water to remove unreacted monomer and excess ferric chloride. The black precipitate was dried at 60-70 °C in the incubator.

Polypyrole-bentonite composites were prepared by adding different amounts of sodium-bentonite clay (1 g, 2 g and 3 g) with sodium dodecyl sulphate to pyrrole monomer. First, bentonite clay was dispersed in 25 mL of water under constant stirring. Sodium dodecyl sulphate and Pyrrole monomer was added drop by drop to sodium-bentonite clay suspension by constant stirring at 5-10 °C and then an oxidizing agent was mixed with clay-monomer-surfactant solution dropwise under constant stirring and they were dispersed in an ultrasonic bath for half past hour. The purification step was performed as described above. The resulting composites were denoted as PPy-SDS-NaB X, where PPy-SDS-NaB means Polypyrrole-Sodium Bentonite composite and X refers to the mass of sodium-bentonite clay. For example, PPy-SDS-NaB 1 means that the used mass of sodium-bentonite is 1 g. So, the compsites were designated as PPy-SDS-NaB 1, PPy-SDS-NaB 2 and PPy-SDS-NaB 3, respectively.

Preparation of Pellets

The obtained black powders (PPy and PPy-SDS-NaB composites) were pressed into pellets with diameter 1.5 cm and thickness 0.16 cm using MAEKAWA Testing machine.

Characterization of the Prepared Samples

The structural characterization of polypyrrole-sodium bentonite composites was analysed using FT IR. The interaction of polymer-bentonite composites was investigated by XRD analysis. The morphological structure of the prepared composites was characterized by SEM. Thermal properties of the composites were analysed by TG-DTA. The frequency dependent electrical conductivity were also determined by LCR meter in the frequency range of 1-10 MHz and optical property were also studied in the wavelength range of 200 to 600 nm by UV-Vis spectrophotometer.

FT IR spectrum was recorded in the range of 4000-400 cm^{-1} by using 8400 SHIMADZU, Japan FT IR spectrophotometer.

X-ray diffraction (XRD) analysis was carried out using Rigaku X-ray Diffractometer, RINI 2000/PC software, Cat. No 9240 J 101, Japan. Copper tube with nickel filter was used. The diffraction pattern was recorded in terms of 2θ in the range of 10-70 °.

The scanning electron microscopy (SEM) images were obtained using JSM-5610 Model SEM, JEOL-Ltd., Japan.

Thermogravimetric analyses of samples were performed using TG-DTA apparatus, (Hi-TGA 2950 model). The temperature ranged between 0 °C and 600 °C under nitrogen gas (at a rate of 50 mL/min).

For the electrical conductivity measurements, the obtained samples were pressed in the form of pellet using MAEKAWA Testing machine. The dielectric permittivities such as D, K and tangent loss of composites were determined using LCR-B110G meter (DC 20-10 MHz) in the frequency ranged of 1-10 MHz at ambient temperature. Frequency dependent electrical conductivity was evaluated by using dielectric equation;

$$C = \frac{\varepsilon' \varepsilon_0 A}{d}$$

$$\tan \delta = 2 \pi f R C$$

$$\omega = 2\pi f$$

$$\sigma_{ac} = \omega \tan \delta \, \varepsilon' \, \varepsilon_0$$

where, C is capacitance (pF), ε' is dielectric constant, ε_0 is electrical permittivity in vacuum (8.85×10^{-14} F cm^{-1}), d is sample thickness (cm), ω is circular frequency (MHz), tan δ is dielectric loss tangent and σ_{ac} is electrical conductivity (μS cm^{-1})

For their optical property, the absorbance and transmittance o PPy, PPy-B and PPy-CP-B composites were measured by UV spectrometer. Their optical absorption spectra have been recorded in the wavelength range from 200 nm to 600 nm. Optical band gap of them has been evaluated by using Taucs relation.

$$\alpha = 2.303 \left(\frac{A}{t}\right) \qquad R = \left(\frac{n-1}{n+1}\right)^2 \qquad \sigma = \frac{\alpha n c}{4\pi}$$

where, α = molar absorption coefficient (cm^{-1}), A = absorbance, t = thickness of matter, R=reflectance, n = refractive index, c = velocity of light in the space and σ = optical conductivity.

Results and Discussion

Polyyrrole and polypyrrole-sodium bentonite composites were synthesized by the method described in materials and method section. The resultant polypyrrole and composites are black in color because they are fully oxidized. They were characterized by modern techniques (FT IR, XRD, SEM and TG-DTA). Moreover, their electrical and optical properties were investigated by LCR meter and UV-Vis spectrophotometer.

FT IR Analysis

Figure 1 shows the FT IR spectrum of polypyrrole. The assignment data is summarized in Table 1. In the spectrum of polypyrrole, the peak observed at 3232 cm^{-1} corresponds to N-H stretching vibration and the peak at 1529 cm^{-1} corresponds to N-H bending vibration. The peak at 1031 cm^{-1} can be attributed to C-H deformation of polypyrrole. The C-N stretching absorption band was detected at 1145 cm^{-1}. In the spectrum of bentonite, the bands observed at 3696 cm^{-1} and 1641 cm^{-1} can be attributed to O-H stretching and O-H bending vibrations. The peaks observed at 1045 cm^{-1} is due to Si-O bond stretching vibrations, while the band at around 918 cm^{-1} corresponds to Al-O stretching vibration. The peaks at 1033 cm^{-1} and 1383 cm^{-1} in all the spectra of all composites can be attributed to Si-O stretching vibration and C-H deformation in polypyrrole (Figure 2 and Table 2). The characteristics peaks of PPy and bentonite in the composites indicate the interaction of PPy in bentonite clay (Silverstein *et al*., 2003).

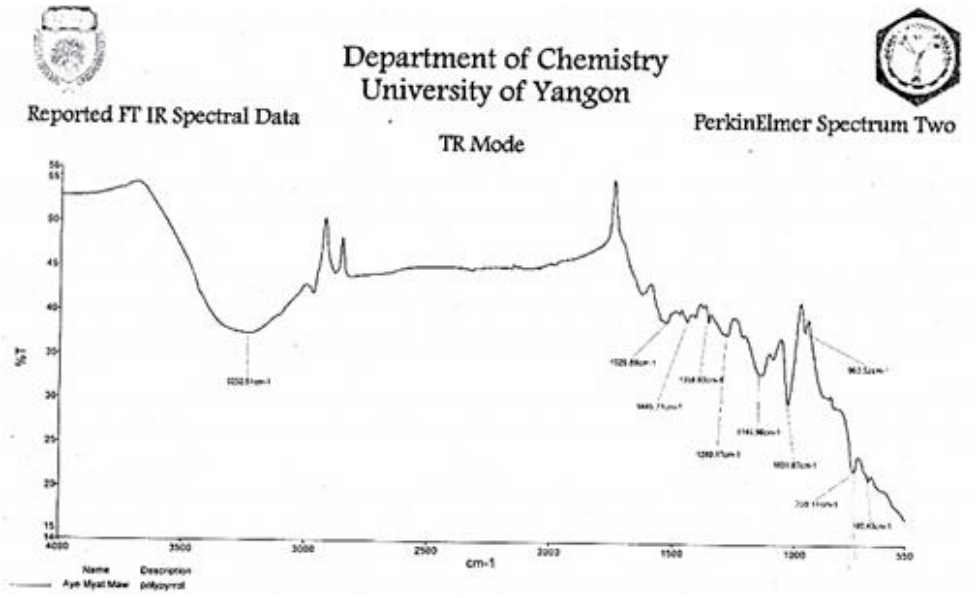

Figure 1 FT IR spectrum of the prepared polypyrrole

Table 1 FT IR Band Assignments of the Prepared Polypyrrole

Observed wave number (cm^{-1})	*Literature wave number (cm^{-1})	Band Assignment
3232	3460-3280	stretching vibration of polypyrrole
3107	3100-3000	H stretching in aromatic ring
2970 2881	2970-2850	stretching (asym) and (sym)
1529	2565-1475	bending
1445	1460-1440	ring stretching
1280 1145	1280-1180	stretching
1031	1050-1030	deformation in polypyrrole
963	980-960	bending
759	770-690	out of plane bending

***** Silverstein *et al.*, 2003

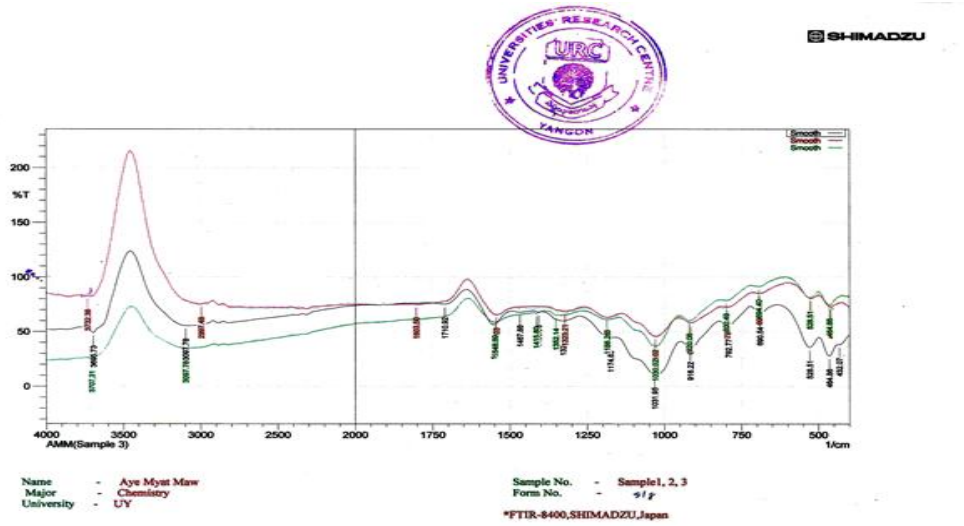

Figure 2 FT IR spectra of (a) PPy-SDS-NaB 1, (b) PPy-SDS-NaB 2 and PPy-SDS-NaB 3 composites

Table 2 FT IR Band Assignments of PPy-SDS-NaB Composites

Observed wavenumber (cm^{-1})			*** Literature wavenumber (cm^{-1})**	**Band Assignment**
PPy-SDS-NaB 1	**PPy-SDS-NaB 2**	**PPy-SDS-NaB 3**		
3732	3707	3695	3700-3200	O-H stretching (and) N-H strectching
2997	3097	3097	3100-3000	= C-H stretching in aromatic ring
1803	-	1710		
1545	1548	1552	1650-1550	O-H bending (and) N-H bending
-	1415	1467	1460-1440	C-C ring stretching in polypyrr0le
1323 1186	1352 1186	1329 1174	1450-1200	C-H deformation of polypyrrole
1030	1030	1031	1110-830	Si-O stretching
916	920	916	950-900	C-H bending (or) Al-OH bending
796	800	792	790-750	Si-O bending
692	694	690	721-681	Si-O-Si stretching
524	528	528	525	Al-O stretching
461	484	464	700-450	Mg-OH stretching

***** Silverstein *et al*., 2003

XRD Analysis

The interaction of PPy-SDS-NaB composites was investigated by XRD. Figure 3 (a-d) represents the XRD patterns of polypyrrole, and a series of PPy-SDS-NaB composites with different bentonite content, respectively. In Figure 3, the X-ray diffractions of all composites show sharp peaks at 2θ ~ 28°. The characteristics XRD peak of polypyrrole was found to be amorphous nature at 2θ value between 20° and 30°. The average crystallite sizes of polypyrrole-sodium bentonite composites from (011) and (110) peaks are evaluated using Debye Scherrer's equation and the data are shown in Table 3. From the data in Table 3, it was found that the crystallite size of the prepared PPy-SDS-NaB 1 composite has the smallest average crystallite size (48 nm) among the three composites.

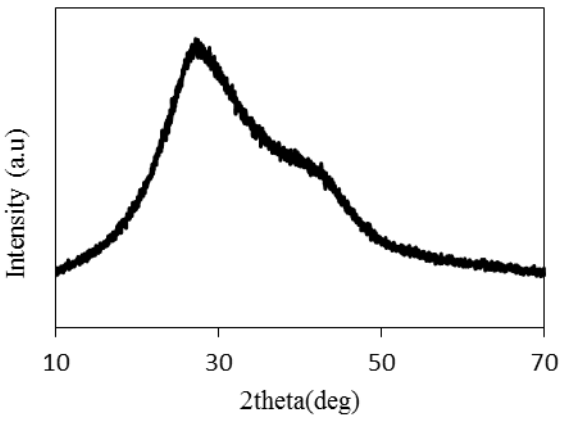

Figure 3(a) XRD diffraction pattern of PPy

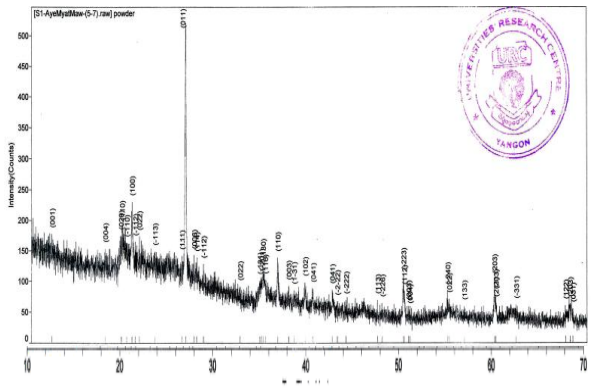

Figure 3(b) XRD diffraction pattern of PPy-SDS-NaB 1 composite

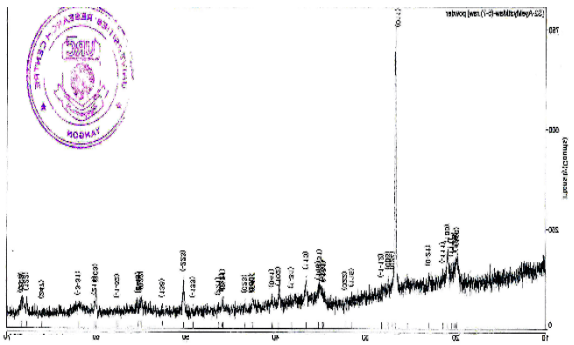

2theta(deg)

Figure 3(c) XRD diffraction pattern of PPy-SDS-NaB 2 composite

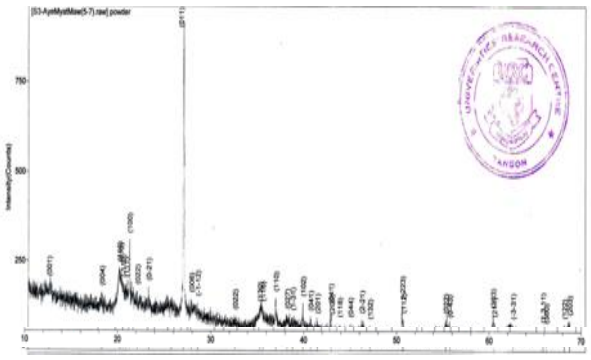

2theta(deg)

Figure 3(d) XRD diffraction pattern of PPy-SDS-NaB 3 composite

Table 3 Average Crystallite Sizes of PPy-SDS-NaB Composites

Sample	2θ	d (A°)	h k l	F W H M	Average Crystallite Sizes (nm)
PPy-SDS-NaB 1	26.633	3.3442	011	0.170	48
	36.538	2.4572	110	0.162	
PPy-SDS-NaB 2	26.680	3.3384	011	0.151	53.5
	36.563	2.4556	110	0.147	
PPy-SDS-NaB 3	26.649	3.3423	011	0.118	58
	36.559	2.4558	110	0.163	

SEM Analysis

Figure 4 (a-d) shows the morphological differences between the polypyrrole and PPy-SDS-NaB composites. The surface morphology of polypyrrole is in the globular structure as shown in Figure 4 (a). After polymerization, the composites show significant changes in morphology as shown in Figures 4 (b-d). The surface morphology of PPy-SDS-NaB composites are as agglomerates. They are not much difference in their morphology. It may be due to homogeneous distribution of bentonite and polypyrrole. The structures of composities exhibit more ordered and denser structure with an increasing amount of bentonite clay.

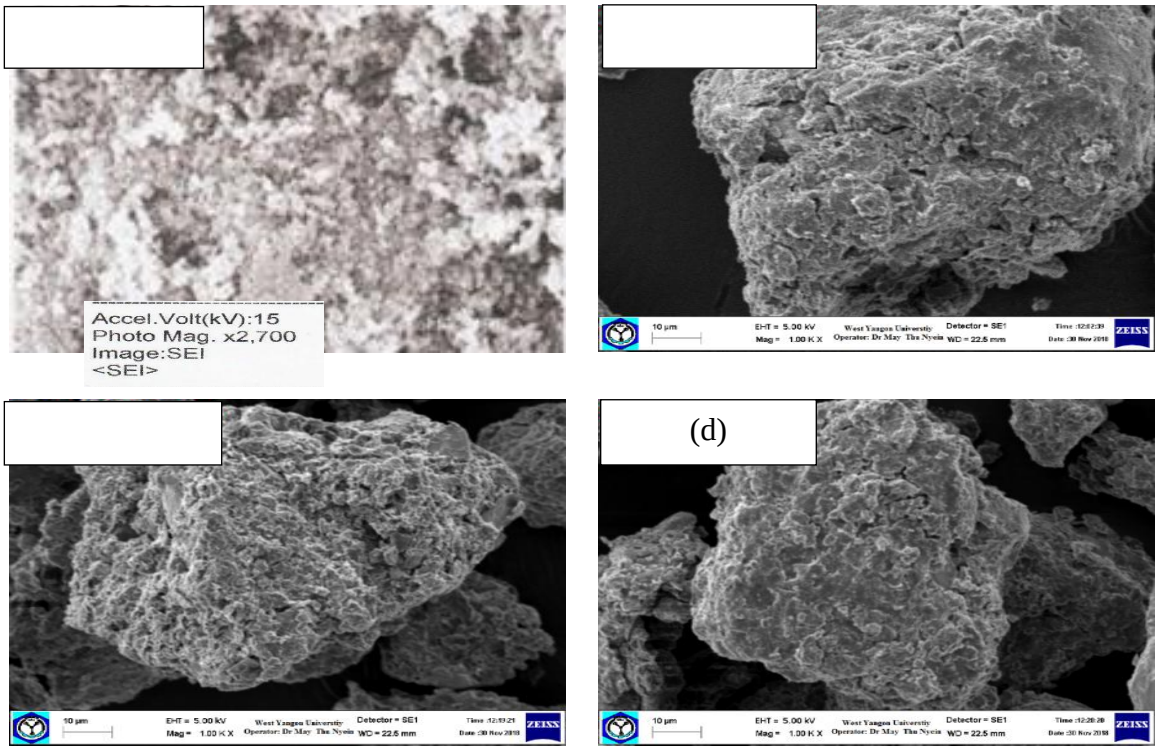

Figure 4 SEM micrographs of (a) polypyrrole, (b) PPy-SDS-NaB 1, (c) PPy-SDS-NaB 2, and (d) PPy-SDS-NaB 3 composites

Thermal Analysis

Thermogravimetric analysis (TGA) and differential thermal analysis (DTA) thermograms of prepared polypyrrole and prepared polypyrrole-bentonite composites are shown in Figure 5. Weight loss percent of PPy-SDS-NaB composites are listed in Table 4. TGA curve of prepared PPy indicates that there are two stages of decomposition in Figure 5 (a). Small exothermic peak observed at 40 °C with 10.08 % weight loss is due to the loss of volatile materials of PPy. Exothermic peaks observed at 272 °C and 589 °C with the 75.51 % weight loss is due to the thermal decomposition of polymer chain. It was observed that prepared PPy shows a poor thermal stability.

For PPy-SDS-NaB composites, three stages of weight loss are also observed. First weight loss in the temperature range between 38-100 °C is due to the dehydration of absorbed water and moisture. Second weight loss in the temperature range between 100-375°C may be due to the cleavage of CH_3-, CH_2- from surfactant molecule and the loss of volatile materials of polypyrrole and the final weight loss in the temperature range between 375-600 °C is due to dehydroxylation of bentonite samples. It can be seen that the incorporation of PPy with bentonite increases the thermal stability of PPy-SDS-NaB composites relative to that of PPy. This enhancement in thermal stability is due to the fact that the introduction of well-dispersed bentonite can prevent the heat to transmit quickly and then improve the thermal stability of composites. Therefore, polypyrrole-sodium bentonite composites exhibit higher thermal stability than pure polypyrrole. According to data in Table 6, it was found that more increase bentonite content in composites, higher thermal stability in them. When compare to other polymer composites (PPy-SDS-NaB 1 and PPy-SDS-NaB 2), PPy-SDS-NaB 3 has 18.33 % of weight loss.

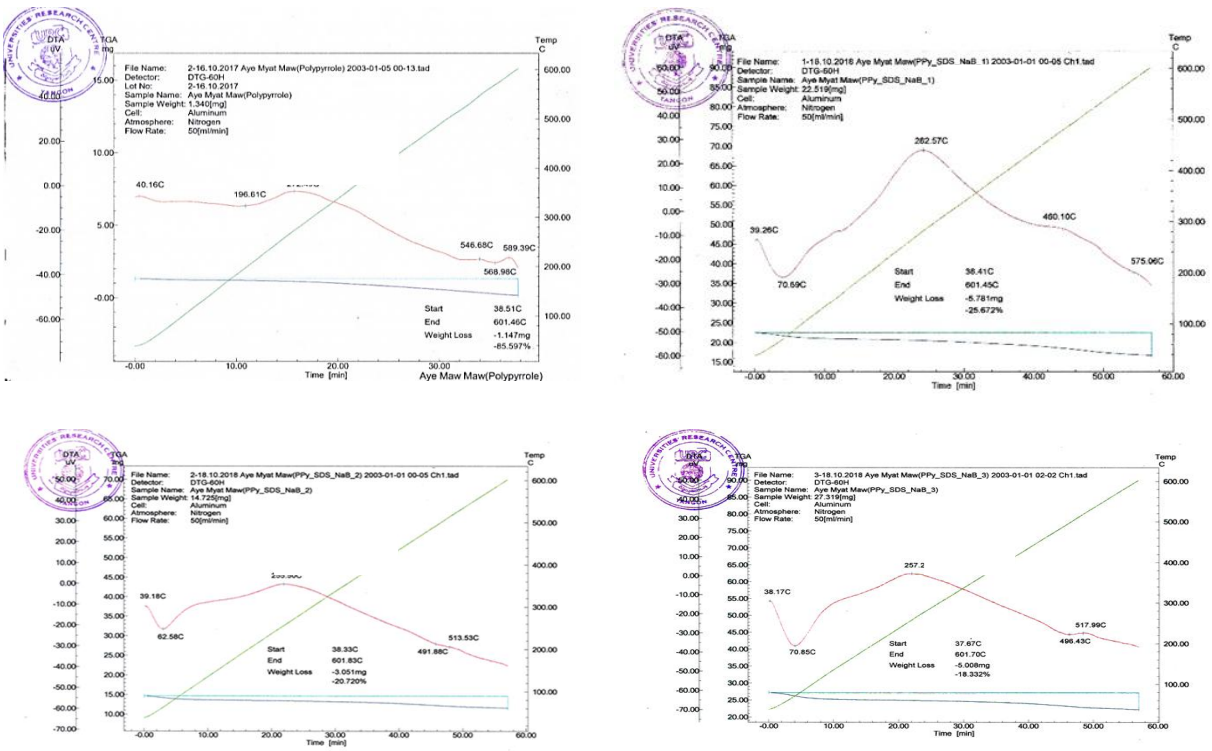

Figure 5 TG-DTA thermograms of (a) prepared polypyrrole (b) PPy-SDS-NaB 1 composite (c)PPy-SDS-NaB 2 composite, and (d) PPy-SDS-NaB 3 composite

Table 4 Total Weight Loss Percent of Pure Bentonite and Polypyrrole-Bentonite Composites from TG-DTA Analyses

Sample	Temperature range (°C)	Peak's temperature (°C)	Nature of Peak	Weight Loss (%)	Total Weight Loss (%)
(a) PPy	37 – 180	40	Exo	10.08	85.59
	380 -600	272 and 589	Exo	75.51	
(b) PPy-SDS-NaB 1	38 – 100	70	Endo	4.44	25.67
	100 -375	282	Exo	6.66	
	375 - 600	460	Exo	14.57	
(c) PPy-SDS-NaB 2	38 – 100	62	Endo	5.07	20.72
	100 -375	255	Exo	6.24	
	375 - 600	513	Exo	9.41	
(d) PPy-SDS-NaB 3	38 – 100	70	Endo	7.49	18.33
	100 -375	257	Exo	4.99	
	375 - 600	517	Exo	5.85	

Dielectric Properties

The frequency dependent dielectric permittivities such as ε′, ε″ and tangent loss (tan δ) and dielectric conductivity (σ_{ac}) of prepared PPy and PPy-SDS-NaB composities are presented in Figures 6 (a-d). As shown in Figures 6 (a, b) the dielectric permittivities decreases as the amount of bentonite in the composites increases. It is also seen that the relative permittivity decreases with increasing frequency. Both ε′ and ε″ exhibit typical dielectric behavior especially at high frequencies. This can be interpreted that the maximum interaction occurs at low frequency. The dielectric tangent loss (tan δ), which is related to the imaginary part of dielectric conductivity (ε″), decreases with increasing frequencies. PPy-SDS-NaB 1 has a higher dielectric conductivity than PPy-SDS-NaB 2 and PPy-SDS-NaB 3. It may be due to the effect of both surfactant and sodium treated bentonite. According to Figure 6 (a), dielectric conductivity for PPy-SDS-NaB 3 can be negligible. It may be interpreted that as the amount of sodium treated bentonite increases, dielectric conductivity cannot be affected. The change in dielectric permittivity with respect to bentonite clay percentage and high dielectric permittivity values can be attributed to the absorbed moisture in interlayer of bentonite clay.

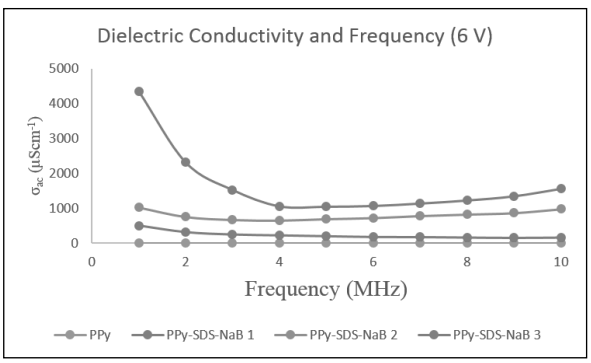

(a)

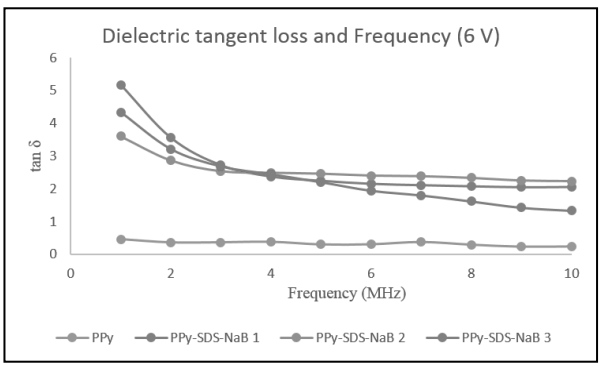

(b)

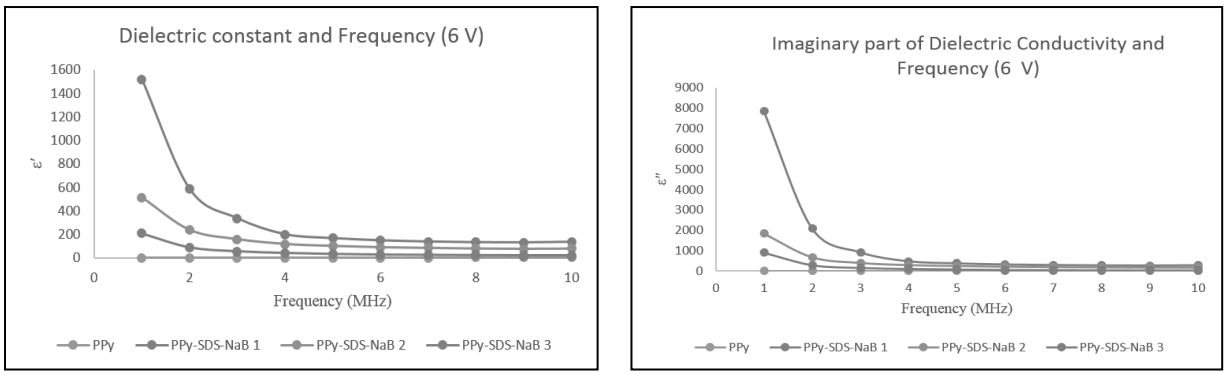

(c) **(d)**

Figure 6 Plots of relationship between frequency and (a) dielectric conductivity (b) dielectric tangent loss (c) dielectric constant and (d) imaginary part of dielectric conductivity of PPy and PPy-SDS-NaB composites at 6 V potential

Optical Properties

The optical properties of prepared PPy and PPy-SDS-NaB composities were studied by UV-vis spectrophotometer. The absorption coefficient (α) was calculated from the absorption spectra. The optical band gap values were evaluated using Taucs' realation. The electronic transition is presented in Figure 7. In general, the band gap values depend on the crystal structure of the composites and the arrangement and distribution way of atoms in the crystal lattice. From the curves shown in Figure 7, it was found to be the band gap values of 3.2 eV, 3.8 eV, 4 eV and 3.8 eV for PPy, PPy-SDS-NaB 1, PPy-SDS-NaB 2 and PPy-SDS-NaB 3 composites, respectively.

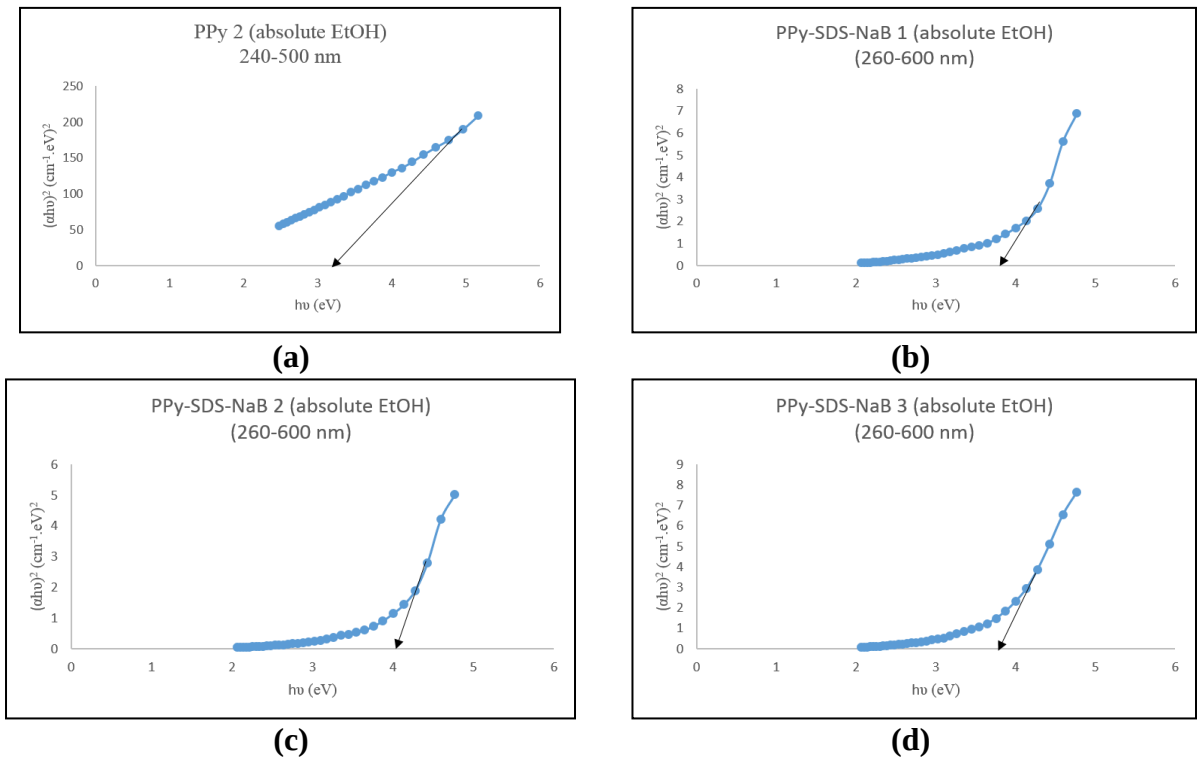

(a) **(b)**

(c) **(d)**

Figure 7 Tauc's plot of $(\alpha h\upsilon)^2$ against $(h\upsilon)$ for (a) polypyrrole (PPy) (b) PPy-SDS-NaB 1 composite (c) PPy-SDS-NaB 2 composite (d) PPy-SDS-NaB 3 composite

Conclusion

In this study, polypyrrole and PPy-SDS-NaB composites were performed by chemical oxidative polymerization in aqueous medium. The polymerization mechanism and chemical structures of composite materials are investigated by means of XRD and FT IR. XRD results confirmed the insertion of PPy between the interlayers of bentonite clays. The morphological study showed that polypyrrole polymerization occurred within bentonite interlayers. It is shown that the denser and more compact morphology of PPy-B composites with the increase in amount of bentonite clay. Intercalated composites are found to be more thermally stable than pure polypyrrole. The overall thermal stability trends are PPy-SDS-NaB 3 > PPy-SDS-NaB 2 > PPy-SDS-NaB 1 > PPy in the TG-DTA thermograms. FT IR analysis shows the incorporation of PPy in the clay structure. The prepared PPy-SDS-NaB 1 can be used as a promising material for the variety of electrical applications within these frequency range of 1-10 MHz at 6 V potential because it exhibits improved thermal properties, reduced flammability and better dielectric barrier properties than unfilled polymer. Therefore, cheap filler-like sodium treated bentonite can be effectively used as a good reinforcement for PPy matrix. From the analysis of absorption spectra, it was found that the optical band gaps of prepared composites with the various amounts of sodium bentonite are in the semiconductor wide band gap ranges of 4.0 eV to 3.8 eV. Thus it shows great promise in sensors as well as electrical applications.

Acknowledgements

The authors would like to express their profound gratitude to the Department of Higher Educaion (Lower Myanmar), Ministry of Education, Yangon, Myanmar, for provision of opportunity to do this research and Myanmar Academy of Arts and Science for allowing to present this paper.

References

Anadao, P. (2012). "Polymer/Clay Nanocomposites: Concepts, Researches, Applications and Trends for The Future". Brazil: Polytechnic school, University of Sao Paulo, pp. 1-16

Bouabdallah, A. B. and Djelali, N. E. (2014). "Synthesis of Polypyrrole's Support Adsorbed on Bentonite . Applications in Wastewater Treatment". *Rev. Roum. Chim*., vol. 59(8), pp. 627-637

Celik, M. and Onal, M. (2011). "Synthesis, Characterization and Properties of Conducting Polypyrrole/Na-montmorillonite Nanocomposites". *Journal of Thermoplastic Composite Materiala*, vol. 25(4), pp. 505-520

Hernandez-Hernandez, K. A., IIIescas, J., Diaz-Nava, M. C., Muro-Urista, c. R., Martinez-Gallegos, S. and Ortega-Aguilar, R. E. (2016). "Polymer-Clay Nanocomposites and Composites: Structures, Characteristics, and Their Applications in the Removal of Organic Compounds of Environmental Interest". *International Standard Serial Number (ISSN 2161-0444): Journal of Medicinal Chemistry,* vol. 6(3), pp. 110-118

Motawie, A. M., Madany, M. M., EI-Dakrory, A. Z., Osman, H. M., Ismail, E. A., Badr, M. M., EI-Komy, D. A. and AbuIyazied, D. E. (2014). " Physico-chemical Characteristics of Nano-organicbentonite prepared using Different Organo-modifiers". *Egyptian Journal of Petroleum*. 23, pp. 331-338

Silverstein, R. M., Webster, F. X. and Kiemle, D. J. (2003). *Spectrometric Identification of Organic Compounds*. New York :7th Edition, John Wiley and Sons, Inc.

Utami, R. S., Puspasari, I., Shyuan, L. K., Mohamed, A. B. and Alva, S. (2016). "Effect of Process Parameters on The Synthesis of Polypyrrole by The Taguchi Method". *International Standard Serial Number (ISSN 1394-2506): Malaysian Journal of Analytical Science*, 20(3), pp. 660-669

Wang, l. X. and Li, X. G. and Yang, Y. L. (2001). "Preparation, Properties and Applications of Polypyrroles". *Reactive and Functional Polymers*, vol. 47, pp. 125-139

Yoleva, A., Djambazov, S. and Michai, G. (2016). "Organic Modification of Bulgarian Bentonite By An Easy Low Cost Method". *Journal of Chemical Technology and Metallurgy*, vol. 51(3), pp. 275-280

PREPARATION AND CHARACTERIZATION OF $LiNi_{1-X}Co_XO_2$ ($0.2 \leq X \leq 0.5$) NANOCRYSTALLINE POWDER

Naw Mon Thae Oo[1], KhinThan Yee[2], Hnin Yu Wai[3]

Abstract

The main aim of the research work is to study the preparation and characterization of $LiNi_{1-x}Co_xO_2$ ($0.2 \leq x \leq 0.5$) nanocrystalline powder. $LiNi_{1-x}Co_xO_2$ ($0.2 \leq x \leq 0.5$) nanocrystalline powders for lithium ion batteries were prepared by a modified sol–gel method using lithium nitrate ($LiNO_3$), cobalt (II) nitrate ($Co(NO_3)_2.6H_2O$), nickel(II) nitrate ($Ni(NO_3)_2.6H_2O$) as starting materials, de-ionized water as solvent, citric acid ($C_6H_8O_7.H_2O$) as chelating agents and carboxy methyl cellulose as dispersant agent. The prepared $LiNi_{1-x}Co_xO_2$ ($0.2\leq x \leq 0.5$) nanocrystalline powder was characterized by TG- DTA, XRD, FT IR and SEM analyses.TG-DTA analysis of the synthesized $LiNi_{1-x}Co_xO_2$ ($0.2 \leq x \leq 0.5$) nanocrystalline powder was carried out to determine the appropriate calcination temperatures. The prepared $LiNi_{0.8}Co_{0.2}O_2$ powders were calcined at 600, 700, 800, 900 and 1000 °C. The resulting calcined powders were characterized by XRD technique. The lattice parameters and the average crystalline size of the samples calcined at different temperatures were calculated using Debye Scherrer equation. It was observed that the crystallite size increases with increasing calcination temperature which may be due to the growth of particle size but the sample calcined at 800 °C was selected as optimum temperature because the sample ($LiNi_{0.8}Co_{0.2}O_2$) has high crystallinity and small crystallite size at this temperature. From XRD spectrum, the observed value of average crystallite size of $LiNi_{0.8}Co_{0.2}O_2$ are 29.58 nm, 32.24 nm, 17.22 nm, 29.25nm and 47.62 nm at different temperatures. Therefore, the other three compounds such as $LiNi_{0.7}Co_{0.3}O_2$, $LiNi_{0.6}Co_{0.4}O_2$ and $LiNi_{0.5}Co_{0.5}O_2$ were also prepared by using the same methods. The prepared ($LiNi_{0.7}Co_{0.3}O_2$, $LiNi_{0.6}Co_{0.4}O_2$ and $LiNi_{0.5}Co_{0.5}O_2$) nanopowders calcined at 800°C were characterized by XRD. From XRD spectrum, the average crystalline size of prepared three compounds are 69.94 nm, 41.76 nm, and 43.43 nm at 800 °C. From FT IR analysis, it was only found stretching vibration of metal- oxygen chemical bonds. Surface feature study of the prepared nanocrystalline powders were observed from SEM. It was observed that agglomeration increase with high porosity and increasing Co doping levels.

Keywords: $LiNi_{1-x}Co_xO_2$nanopowders, sol-gel, calcination temperatures, crystallite size

Introduction

The lithium nickel–cobalt oxide (Li Ni_{1-x} Co_xO_2) used as cathode material was grown at appropriate temperature using sol-gel method. Lithium nickel cobalt oxide ($LiNiCoO_2$) has been widely studied as a cathode material for lithium ion secondary batteries since it has good capacity, high specific energy, good power rates, low self-discharge, and excellent cycle life (Lu *et al*., 2014).

Layered lithium transition-metal oxides (LTMOs) such as lithium cobalt and lithium nickel are the most advanced studied electrode materials. Many lithium intercalated transition metal oxides have been studied as the positive electrode material used in high energy density rechargeable batteries (Sathiy *et al*., 2011).

[1] PhD Candidate, Department of Chemistry, University of Yangon
[2] Dr, Lecturer, Department of Chemistry, University of Myeik
[3] Dr, Lecturer, Department of Chemistry, University of Yangon

The sol–gel method has been used to prepare $LiNi_{1-x}Co_xO_2$ at lower temperature and shorter time, and mostly, compound powders with uniform morphology, narrow particle size distribution, and high homogeneity.

In the present work, $LiNi_{1-x}Co_xO_2$, nanopowders for lithium ion batteries were prepared by a modified sol–gel method. The prepared $LiNi_{1-x}Co_xO_2$powders were calcined at different temperature. The characterization of the $LiNi_{1-x}Co_xO_2$powders ($0.2 \leq x \leq 0.5$) nanocrystalline powders were prepared at optimum temperature by sol-gel method. The prepared nanocrystalline powders were also characterized by XRD, SEM, FT IR and TG-DTA techniques.

Materials and Methods

Sample Collection

Lithium nitrate, cobalt nitrate, nickel nitrate, citric acid, carboxy methyl cellulosewas purchased from BDH Chemicals Ltd. Poole Englandandcitric acid used as achelating agent and carboxy methyl cellulose used as a dispersant agent. Distilled water was used as the solvent in all analyses.

Modern instruments techniques were used SEM (Scanning Electron Microscope), XRD (X- ray Diffractometer), TG-DTA (Thermogravimetry /Differential Thermal Analysis) and FT IR (Fourier Transform Infrared Spectroscopy).

Preparation of $LiNi_{1-x}Co_xO_2$ ($0.2 \leq x \leq 0.5$) Nanocrystalline Powder

$LiNi_{1-x}Co_xO_2$nanocrystallinepowder was prepared by sol-gel method using lithium nitrate, cobalt nitrate, nickel nitrate, citric acid, carboxy methyl cellulose and deionized water.

Firstly, (6.9 g) oflithium, (23.2g), (20.35 g), (17.44 g), (14.54 g) of nickel (II) and (5.8 g), (8.73 g), (11.64 g), (14.55 g) of cobalt (II) nitrate salts (1:0.8:0.2M), (1:0.7:0.3 M), (1:0.6:0.4 M), (1:0.5:0.5 M) was added 100 ml of deionized water. Next, 42 g of citric acid (the molar ratio of citric acid/ total metal ions = 1) was added 100 ml of deionized water. The individual solutions were mixed and after that with a small amount of carboxy methyl cellulose (the molar ratio of cellulose to total cations was 5×10^{-6}) was added into this solution. The mixture solution was heated at 65°C for 12 h under constant stirring to form the sol. The sol was then evaporated at 120°C in dry oven until the gel was formed. The gel solution was calcined at various temperatures (300°C, 600°C, 700°C, 800 °C, 900°C and 1000°C for 4 h). Finally, the samples were ground smoothly in an agitate motor. The resulting powders were characterized by SEM, XRD, FT IR and TG-DTA.

Characterization of the Prepared Samples

The chemical composition of$LiNi_{1-x}Co_xO_2$in mass percentage was determined by Flame spectroscopy and Wet analysis. The structural characterization of $LiNi_{1-x}Co_xO_2$ nanocrystalline powder was analysed using FT IR. The interaction of $LiNi_{1-x}Co_xO_2$ nanocrystalline powder was investigated by XRD analysis. Thermal properties of these powders were evaluated by TG-DTA. The morphological structure of the prepared these powder was characterized by SEM.X-ray diffraction (XRD) analysis was carried out using Rigaku X-ray Diffractometer, RINI 2000/PC software, Cat. No 9240 J 101, Japan. Copper tube with nickel filter was used. FT IR spectrum was recorded in the range of 4000-400 $cm^{-1}$by using 8400 SHIMADZU, Japan FT IR spectrophotometer. The scanning electron microscopy (SEM) images were obtained using JSM-

5610 Model SEM, JEOL-Ltd., Japan. Thermogravimetric analyses of samples were performed using TG-DTA apparatus, (Hi-TGA 2950 model).The temperature ranged between 0°C and 600 °C under nitrogen gas (at a rate of 50mL/min).

Results and Discussion

XRD Analysis

The XRD pattern of the prepared $LiNi_{0.8}Co_{0.2}O_2$ nanocrystalline powders calcined at different temperatures are shown in Figures 1- 4 and the average crystalline size, crystal system and lattice parameter are listed in Table 1. XRD pattern of the prepared $LiNi_{1-x}Co_xO_2$ ($0.2 \leq x \leq 0.5$) nanocrystalline powders calcined at 800 °C are shown in Figure 5 and summarized in Table 2. The prepared sample calcined at 800 ºC was selected as optimum temperature because it has high crystallinity and small crystallite size at that temperature. By XRD analysis to the four Co doped $LiNiO_2$ samples, it was found that the layer structure is not very clear in $LiNi_{0.8}Co_{0.2}O_2$ sample. But increasing Co doping level the layer structure formation are distinct. Among the different doping level of $LiNiO_2$ compounds it was found that $LiNi_{0.6}Co_{0.2}O_2$ has perfect layer structure and small crystallite size than other two compounds ($LiNi_{0.7}Co_{0.3}O_2$ and $LiNi_{0.5}Co_{0.5}O_2$). The crystalline size of $LiNi_{1-x}Co_xO_2$nanocrystalline powder was calculated by using Scherrer's equation (Ahmed *et al*., 2012).

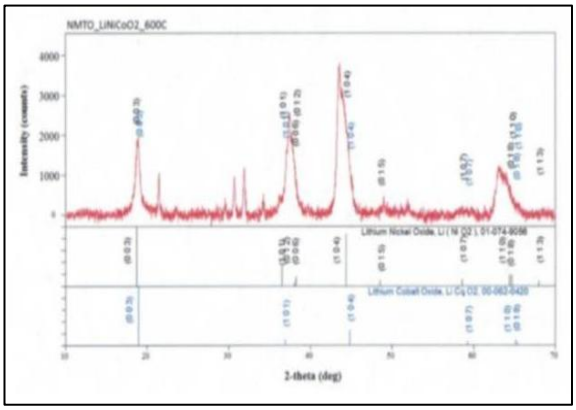

Figure 1 XRD diffractogram of prepared $LiNi_{0.8}Co_{0.2}O_2$ powder at 600 °C

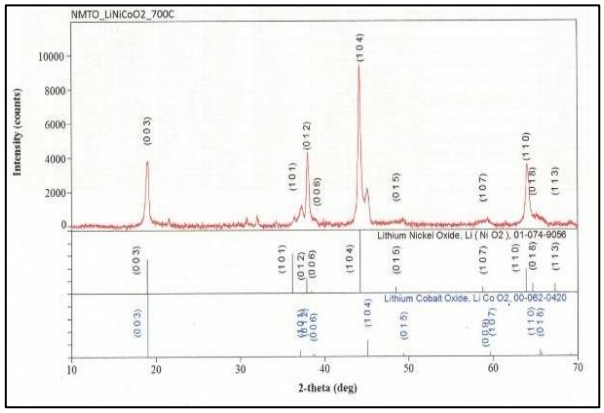

Figure 2 XRD diffractogram of prepared $LiNi_{0.8}Co_{0.2}O_2$ powder at 700 °C

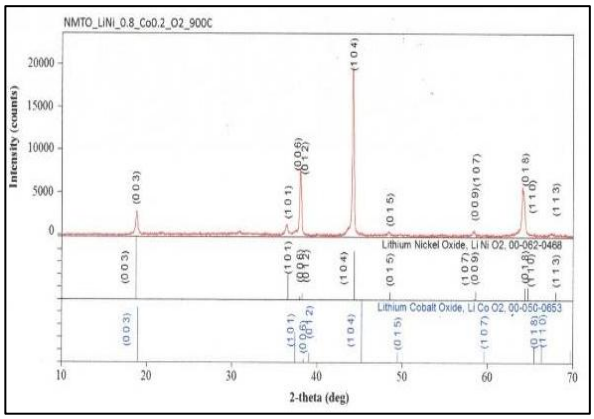

Figure 3 XRD diffractogram of prepared $LiNi_{0.8}Co_{0.2}O_2$ powder at 900 °C

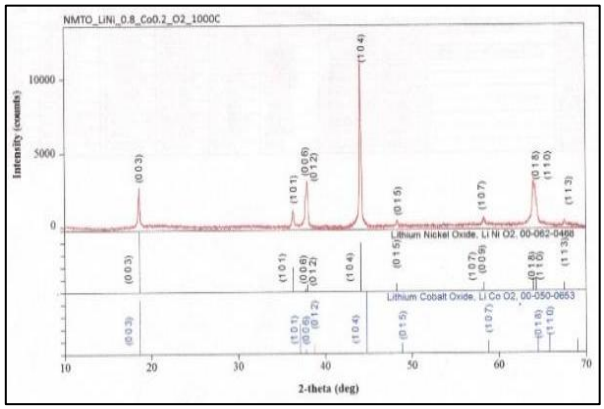

Figure 4 XRD diffractogram of prepared $LiNi_{0.8}Co_{0.2}O_2$ powder at 1000 °C

Table 1 Average Crystalline Size of the Prepared $LiNi_{1-x}Co_xO_2$ Powder at 800 °C for 4 h from XRD analysis

Temperature (°C)	Average crystalline size from		Lattice Parameters		Crystal System
	XRD data (nm)	by using Debye Scherrer equation (nm)	a /A°	c /A°	
600	21.5	29.58	2.8804	14.1890	Hexagonal
700	28.98	32.24	2.9101	14.0365	Hexagonal
900	33.74	29.25	2.8150	14.0493	Hexagonal
1000	54.73	47.62	2.8362	14.2793	Hexagonal

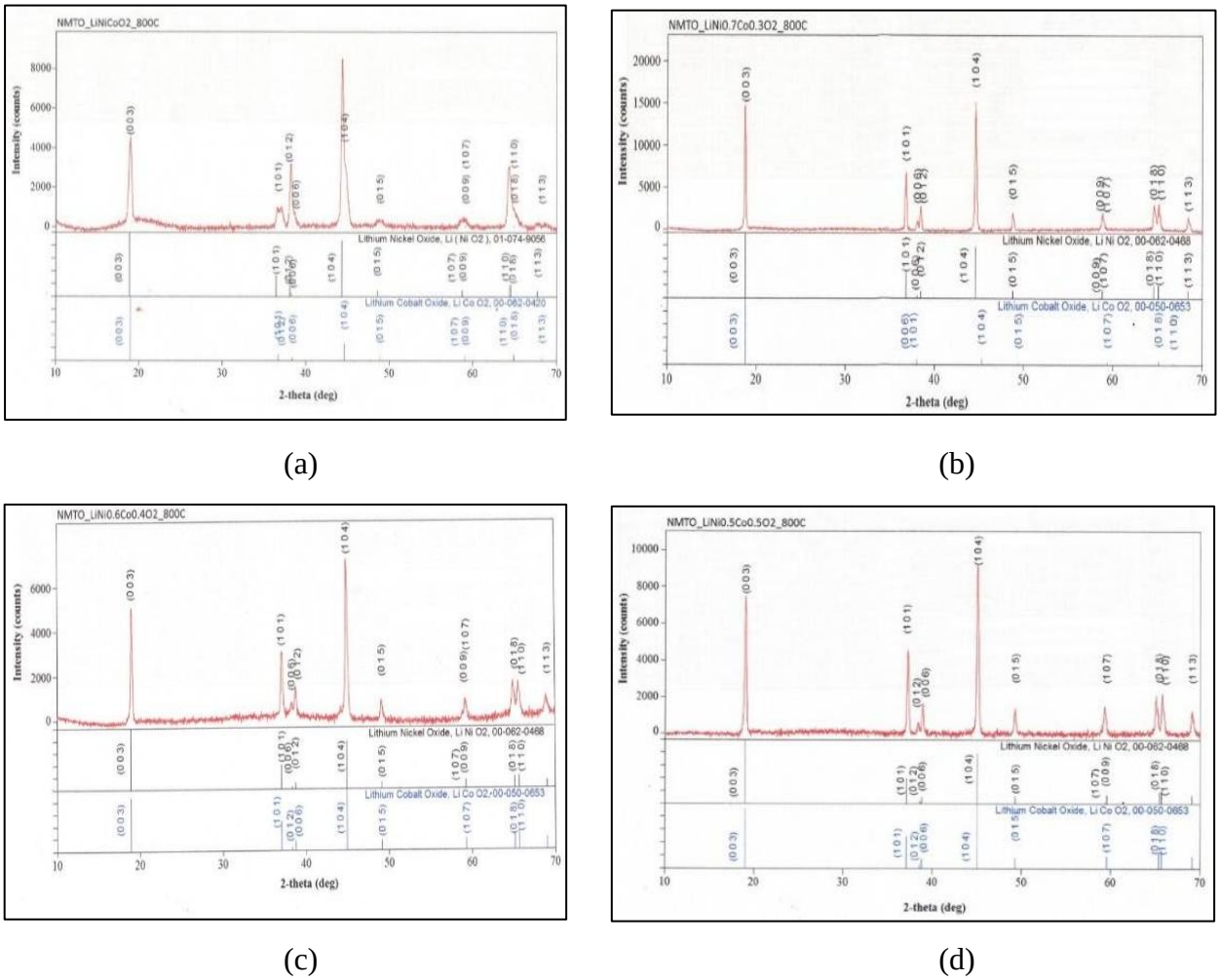

Figure 5 XRD diffraction patterns of (a) $LiNi_{0.8}Co_{0.2}O_2$ (b) $LiNi_{0.7}Co_{0.3}O_2$ (c) $LiNi_{0.6}Co_{0.4}O_2$ (d) $LiNi_{0.5}Co_{0.5}O_2$powder by sol-gel method calcined at 800 °C for 4 h

Table 2 Average Crystalline Size of Prepared $LiNi_{1-x}Co_xO_2$ Powder at 800 °C for 4 h from XRD analysis

Samples	Average crystalline size (nm)		Lattice Parameters		Crystal System
	XRD data	by using Debye Scherrer equation	a / A°	c /A°	
$LiNi_{0.8}Co_{0.2}O_2$	19.49	17.22	2.8925	14.1185	Hexagonal
$LiNi_{0.7}Co_{0.3}O_2$	75.5	69.94	2.7979	14.1885	Hexagonal
$LiNi_{0.6}Co_{0.4}O_2$	39.91	41.76	2.8412	14.0712	Hexagonal
$LiNi_{0.5}Co_{0.5}O_2$	42.58	43.43	2.8386	13.9974	Hexagonal

FT IR Analysis

FT IR data indicated the presence of functional groups in the $LiNi_{1-x}Co_xO_2$ powder. The FT IR spectra of the prepared $LiNi_{1-x}Co_xO_2$ powder calcined at 800 °C are shown in Figures 6 and 7, the spectral assignments shown in Table 3. In the spectrum of $LiNi_{1-x}Co_xO_2$ ($0.2 \leq x \leq 0.5$) nanocrystalline powder, the peak observed stretching vibration of metal oxygen bond (Silverstein *et al*., 2013).

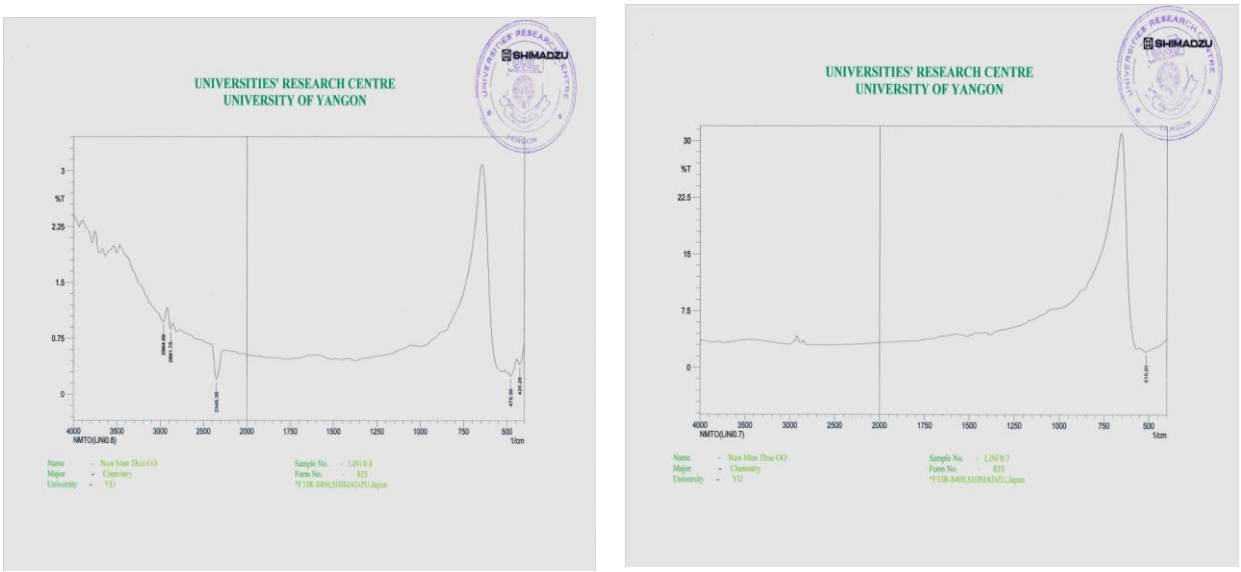

(a) (b)

Figure 6 FT IR spectra of (a) $LiNi_{0.8}Co_{0.2}O_2$ (b) $LiNi_{0.7}Co_{0.3}O_2$ nanocrystalline powder prepared by sol-gel method calcined at 800°C for 4 h

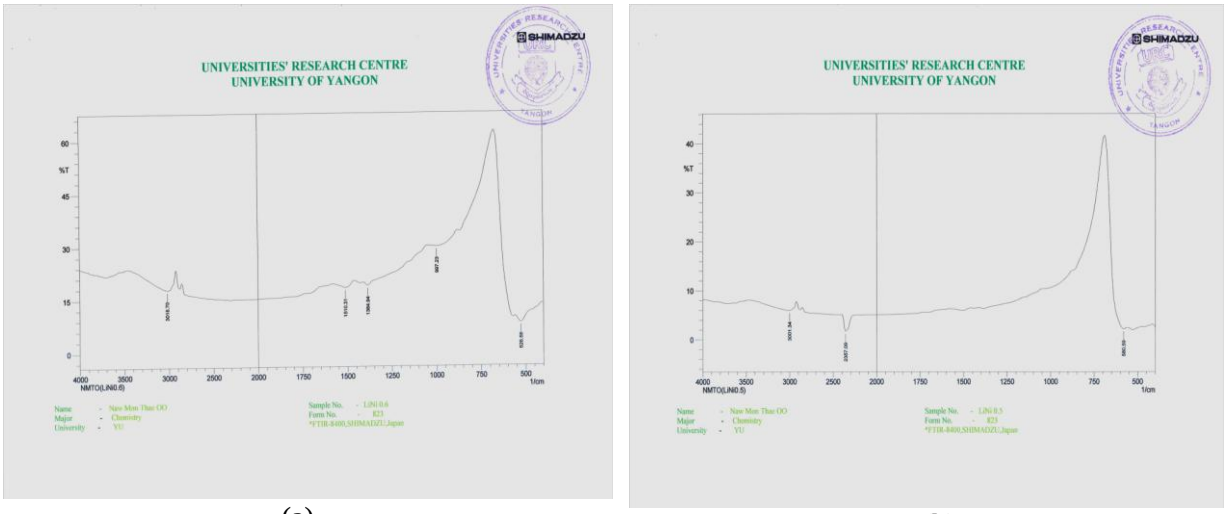

(a) (b)

Figure 7 FT IR spectra of (a) $LiNi_{0.6}Co_{0.4}O_2$ (b)$LiNi_{0.5}Co_{0.5}O_2$ nanocrystalline powder prepared by sol-gel method calcined at 800 °C for 4 h

Table 3 Band Assignments of FT IR Spectra of the Prepared $LiNi_{1-x}Co_xO_2$ Powder by Sol-gel Method Calcined at 800°C for 4 h

Observed wave number (cm^{-1})				***Literature Wave Number (cm^{-1})**	**Band Assignments**
$LiNi_{0.8}Co_{0.2}O_2$	$LiNi_{0.7}Co_{0.3}O_2$	$LiNi_{0.6}Co_{0.4}O_2$	$LiNi_{0.5}Co_{0.5}O_2$		
478	515	526	580	650-400	Stretching vibration of M-O bond

Silverstein *et al*., 2003

SEM Analysis

Particle morphology was studied by obtaining micrographs using JOEL-JSM-5610, Japan, Ion sputter-JEC-1600 (Sahoo *et al.,* 2010). The morphology of prepared $LiNi_{1-x}Co_xO_2$ Powder were investigated by SEM in Figure 8-9. SEM microphotograph of $LiNi_{1-x}Co_xO_2$ Powder calcined at 600 and 800 °C show the spherical agglomeration of porous nature and irregular shaped morphology. When the temperature was increased to 800°C well defined form of particles was observed. It was observed that agglomeration increase with increasing Co doping levels. The $LiNi_{0.5}Co_{0.5}O_2$ has higher porosity than other three compounds.

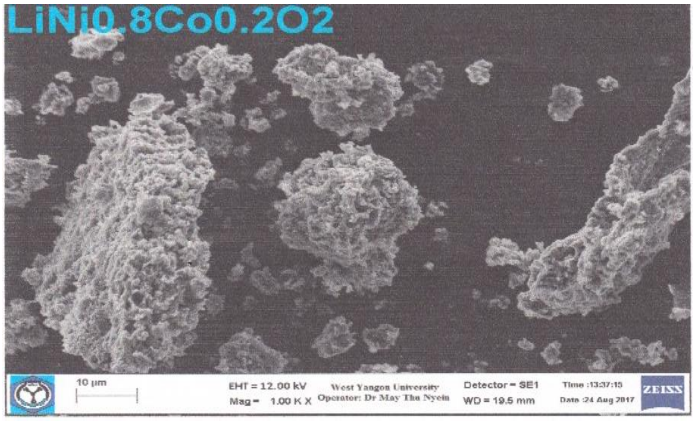

Figure 8 SEM microphotograph of the prepared $LiNi_{0.8}Co_{0.2}O_2$ powders at 600 °C

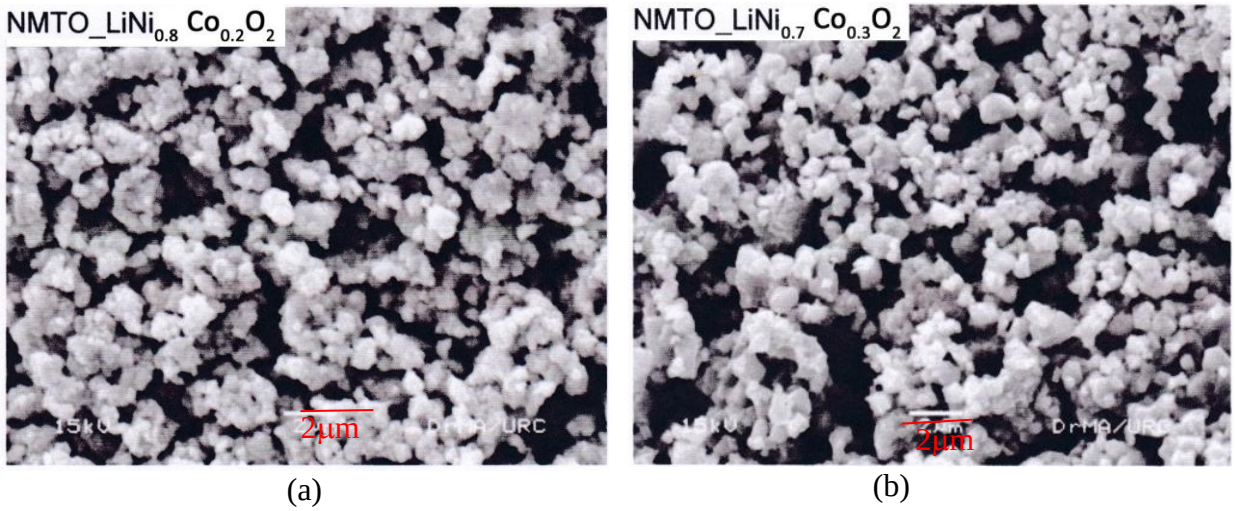

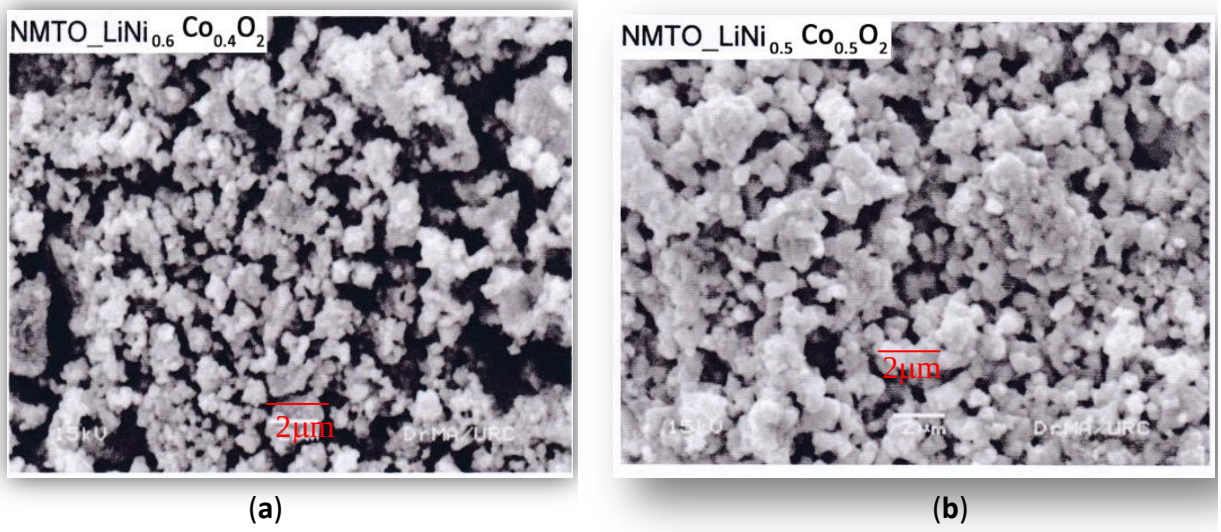

Figure 9 SEM microphotographs of the prepared (a) $LiNi_{0.8}Co_{0.2}O_2$ (b) $LiNi_{0.7}Co_{0.3}O_2$ (c) $LiNi_{0.6}Co_{0.4}O_2$(d) $LiNi_{0.5}Co_{0.5}O_2$ powder by sol-gel method calcined at 800 ˚C for 4h

Thermal Analysis

Thermogravimetric analysis (TGA) and differential thermal analysis (DTA) themogram of prepared $LiNi_{1-x}Co_xO_2$ powders heated at 300 °C, are shown in Figure 10. Total weight loss $LiNi_{1-x}Co_xO_2$are listed in Table 4. It was found the prepared sample calcined at 300 °C, the temperature range between38-110 °C, endothermic peak was observed. And The first weight loss is due to the removal of absorbed water and moisture. The temperature range between 110-410 °C, exothermic peak was observed. The second weight loss is due to the decomposition of nitrate and the burn out of organic species in the powder 410-600°C, endothermic and exothermic peak was observed. The final weight loss is due to the burning of carbon-residue in the temperature range between 410-600°C, endothermic peak was observed. Prepared $LiNi_{1-x}CoO_2$ nanocrystalline powder calcined at 800 °C are shown in Figure 11 and there are no prominent weight losses observed in TG curves and there are also no prominent heat absorbing or evolving processes found in DTA curves at this temperature are summarized in Table 5.

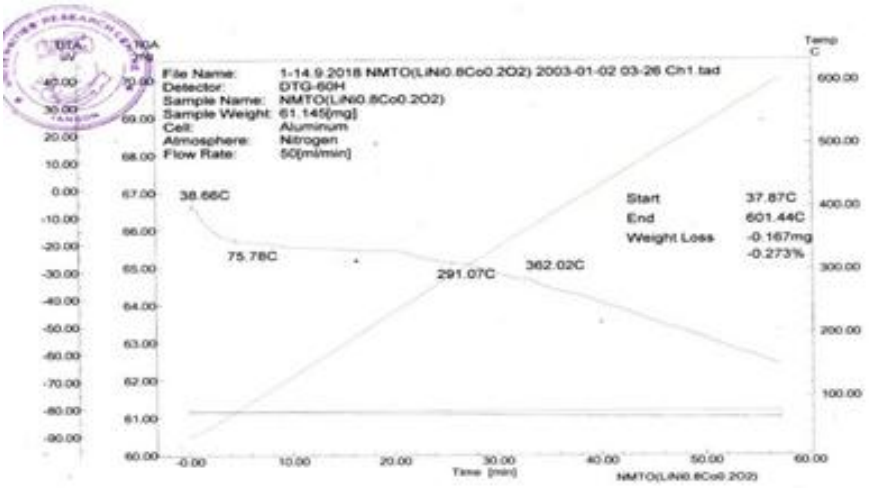

Figure 10 TG -DTA thermogram of the prepared $LiNi_{0.8}Co_{0.2}O_2$powderat 300 °C

Table 4 Thermal Analysis of $LiNi_{0.8}Co_{0.2}O_2$ Powders at 300 °C from TG-DTA Data

Temperature range (°C)	Weight loss (%)	Peak's Temperatures (°C)	Nature of peak	TG remark
38-110	5.06	74	Endothermic	The first weight loss Is due to the removal of absorbed water and moisture
110-410	6.49	401	Exothermic	The second weight loss is due to the decomposition of nitrate and the burn out of organic species in the powder
410-600	12.97	474 552	Exothermic Exothermic	The third weight loss is due to the burning of carbon-residue
Total weight loss 24.52				

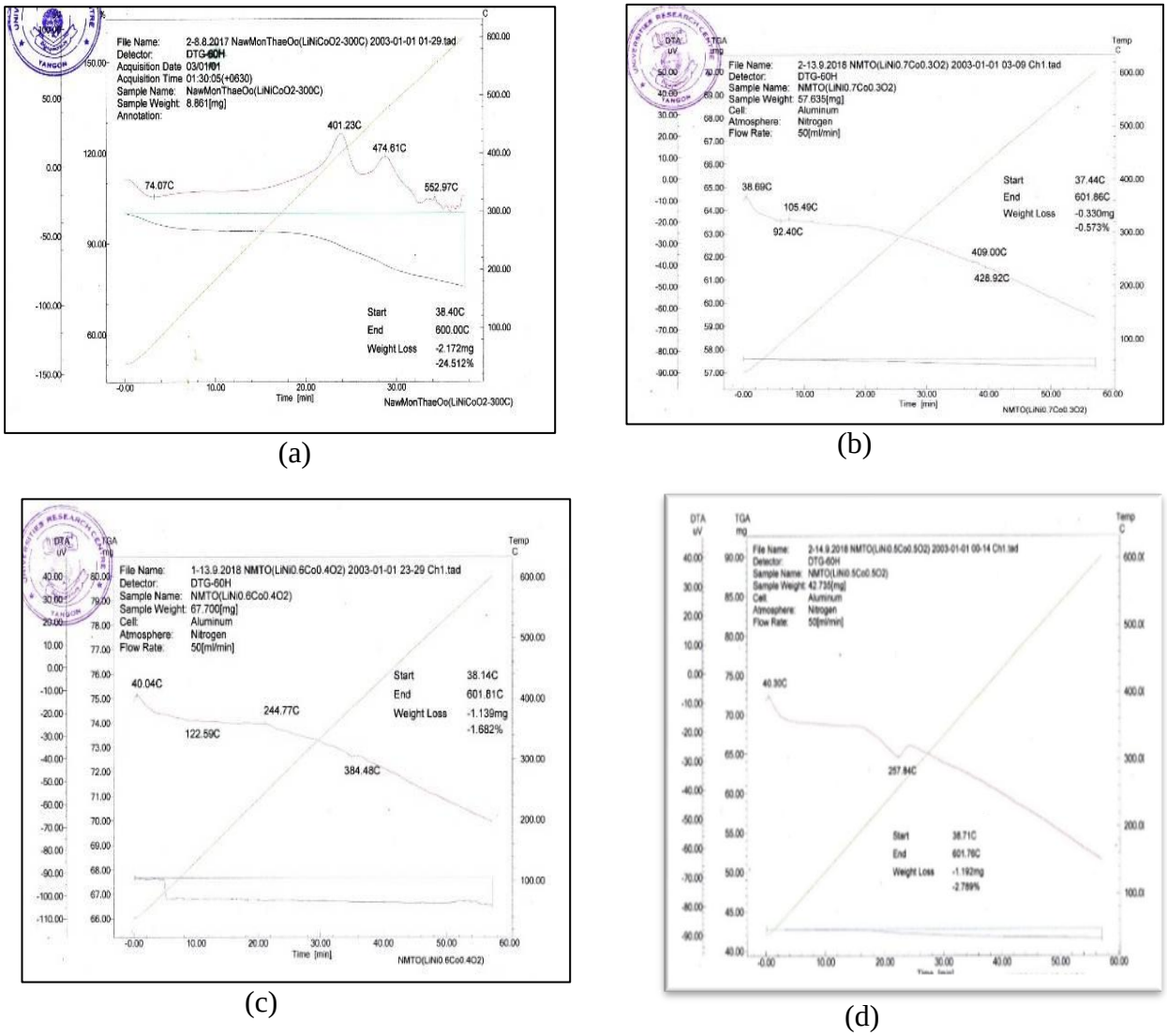

Figure 11 TG -DTA thermogram of the prepared (a) $LiNi_{0.8}Co_{0.2}O_2$ (b) $LiNi_{0.7}Co_{0.3}O_2$ (c) $LiNi_{0.6}Co_{0.4}O_2$ (d) $LiNi_{0.5}Co_{0.5}O_2$ powder by sol-gel method calcined at 800 °C for h

Table 5 Total Weight Loss Percent of $LiNi_{1-x}Co_xO_2$nanocrystalline powder from TG-DTA Analyses

Samples	Weight loss (%)	TG remark
$LiNi_{0.8}Co_{0.2}O_2$	0.273	Thermally stable within the temperature range between 38 and 600 °C
$LiNi_{0.7}Co_{0.3}O_2$	0.573	
$LiNi_{0.6}Co_{0.4}O_2$	1.682	
$LiNi_{0.5}Co_{0.5}O_2$	2.789	

Conclusion

$LiNi_{1-x}Co_xO_2$ nanocrystalline powder was prepared by using sol-gel method at different calcination temperatures. By using Scherrer's equation, the crystalline size of $LiNi_{1-x}Co_xO_2$ nanocrystalline powder was calculated to be 29.58 nm (600°C), 32.24 nm (700°C), 17.22 nm (800°C), 29.25 nm (900°C) and 47.62 nm (1000°C). The sample calcined at 800 ºC was selected as optimum temperature because it has high crystallinity and small crystallite size at that temperature. By XRD analysis, Co doped $LiNiO_2$ samples, it was found that layer structure is not very clear in $LiNi_{0.8}Co_{0.2}O_2$ sample. But increasing Co doping level the layer structure formation are distinct. Diffraction patterns of other three sample clearly show (0 0 6)/ (0 1 2) peaks and (0 1 8)/ (1 1 0) peaks splitting and it is the characteristic of a perfect layer structure. Average crystalline size of three prepared $LiNi_{0.7}Co_{0.3}O_2$, $LiNi_{0.6}Co_{0.4}O_2$ and $LiNi_{0.5}Co_{0.5}O_2$ samples are 69.94, 41.76 and 43.43 nm. According to TG-DTA performance on $LiNi_{0.8}Co_{0.2}O_2$ sample calcined at 300 °C, it was found that crystallization temperature is about 500 °C. Total weight loss percent is 24.52% observed in TG curves. Prepared $LiNi_{1-x}Co_xO_2$ sample calcined at 800°C, there are no prominent weight losses observed in TG curves and there are also no prominent heat absorbing or evolving processes found in DTA curves. From FT IR analysis, it was only found the stretching vibration of metal- oxygen chemical bonds and so it may conclude that the prepared four $LiNi_{1-x}Co_xO_2$ samples calcined at 800 °C have no impurity. Agglomeration of $LiNi_{0.5}Co_{0.5}O_2$is more than other three compounds. It was observed that agglomeration increase with increasing the Co doping levels. The $LiNi_{0.5}Co_{0.5}O_2$ has higher porosity than other three compounds and it may be concluded that the porosity decrease with increasing the Co doping levels.

Acknowledgements

The authors would like to express their profound gratitude to the Department of Higher Education (Lower Myanmar), Ministry of Education, Yangon, Myanmar, for provision of opportunity to do this research and Myanmar Academy of Arts and Science for allowing to present this paper.

References

Ahmed, M., Mohammad, R. F. and Reza, M. (2012). "Modified Scherrer Equation to Estimate More Accurately Nano-Crystalline Size Using XRD". *World Journal of Nano Science and Engineering*, vol.2, pp. 154-160.

Lu, C.H., Chang, H.H. and Lin, Y.K. (2004). "Preparation and Characterization of Nanosized Lithium Cobalt Oxide Powders Lithium-ion Batteries." *Ceram. Int.*, vol.30, 1641-1645.

Sahoo, S. K., Agrawal, K., Polke, B.G. and Raha, K.C. (2010). "Characterization of γ and α- Fe_2O_3Nanopowders Synthesized by Emulsion Precipitation Calcination Route and Rheological Behaviour of α- Fe_2O_3". *International Journal of Engineering, Science and Technology*, vol.2, pp118-126.

Sathiya, M., Hemalatha, K., Ramesha, Shukla, A.K. and Parkash, A.S. (2011). "Nitrates- melt synthesized $LiNi_{0.8}Co_{0.2}O_2$ and its Performance as Cathode in Li-ion Cells". *Journal of Material Science*, vol. 34, pp. 1693-1698.

Silverstein, R. M., Webster, F. X. and Kiemle, D. J. (2003). *Spectrometric Identification of Organic Compounds*. New York: 7th Edition, John Wiley and Sons, Inc.

INVESTIGATION OF PHYTOCHEMICAL CONSTITUENTS AND SOME BIOLOGICAL ACTIVITIES OF THE SPINE OF *ZANTHOXYLUM RHETSA* (ROXB.) DC. (KA-THIT-PHU)

Chan Myae Kyaw[1,2], Khine Zar Wynn Lae[3], Daw Hla Ngwe[4]

Abstract

In the present study, *Zanthoxylum rhetsa* (Roxb.) DC. (Ka-thit-phu) was chosen for the investigation of the phytochemical and some biochemical activities. The spines of *Z. rhetsa* were collected from Dawei Township, Tanintharyi Region. The preliminary phytochemical screening indicated the presence of alkaloids, α-aminoacids, carbohydrate, cardiac glycoside, flavonoids, glycosides, organic acids, phenolic compounds, polyphenol, saponin, steroids, tannins and terpenoids in the spines of *Z. rhetsa.* According to the physicochemical analyses, the dry powdered sample was found to contain 5.46 % of total ash, 1.45 % of water soluble ash, 0.19 % of acid insoluble ash, 8.54 % of moisture content, <100 of foaming index and swelling index of 5 mL/g of the sample. The EDXRF elemental analysis showed some elements such as Si, S, Ca, K, Fe, Mn and Cu present in the sample. The extractable matters (% w/w) were found to be 4.6, 3, 2.6, 2.2, 2.0, 1.0, 0.2 % (w/w) by extracting with different polarities of solvents such as water, methanol, ethanol, acetone, ethyl acetate, chloroform and petroleum ether, respectively. The ethanol extract was observed to have higher total phenol content (51.92 ± 0.54 mg GAE/g) and total flavonoid content (50.61 ± 2.29 mg QE/g) than the watery extract (41.56 ± 0.83 mg GAE/g of TPC and 36.97 ± 1.05 mg QE/g of TFC). Antimicrobial activities (12~20 mm) of seven different extracts of the sample were determined against some fungal and bacterial species by using agar well diffusion method. The antioxidant activities of ethanol extract (IC_{50} = 1.15 μg/mL) and watery extract (IC_{50} = 2.89 μg/mL) were determined by DPPH radical scavenging activity assay. The ethanol extract of the sample was observed to possess the higher α-amylase inhibition activity (IC_{50} = 113.01 μg/mL) and α-glucosidase inhibition activity (IC_{50} = 120.56 μg/mL) than the watery extract (IC_{50} =137.00 μg/mL and IC_{50} = 446.78 μg/mL) and therefore ethanol extract might possess higher antidiabetic potency than watery extract. The crude extracts such as PE, EtOAc, Acetone, MeOH, EtOH, $CHCl_3$ and watery extracts exhibited the inhibition of tumor formation at the dose of 0.3 g/disc up to 7 days determined on tumor produced bacteria by using PCG (Potato Crown Gall) test. *In vitro* antiproliferative activity of ethanol and watery extracts was evaluated against human cancer cell lines: Hela (cervical) (IC_{50} = 3.74 μg/mL and IC_{50} = > 200 μg/mL), MCF-7 (breast) (IC_{50} = 7.71 μg/mL and IC_{50} = > 200 μg/mL), A549 (lung) (IC_{50} = 4.77 μg/mL and IC_{50} = > 200 μg/mL) cancer cell lines by CCK-8 Assay (Cell Counting Kit-8).

Keywords : *Zanthoxylum rhetsa* (Roxb.) DC. (Ka-thit-phu), total phenol content, total flavonoid content, antioxidant activity,antitumor activity, antidiabetic activity, antiproliferative activity

Introduction

At present, natural products have been used for thousands of years for the benefit of mankind, as important sources of food, clothing, cosmetics, building materials, tools, medicines and crop protection agent. Researches in this field are becoming more numerous to the point of getting about half of pharmaceuticals are pesticides from natural sources (Newman and Cragg,

[1] Assistant Lecturer, Department of Chemistry, University of Yangon
[2] PhD Student, Department of Chemistry, University of Yangon
[3] Dr, Lecturer, Department of Chemistry, University of Yangon
[4] Dr, Professor and Head, (Retd.), Department of Chemistry, University of Yangon

2007). *Zanthoxylum rhetsa* (Roxb.) DC. is a plant in the family of Rutaceae. In Myanmar, *Z. rhetsa* named Ka-thit-phu is found in the Tanintharyi Region. The plant is also traditionally used as antidiabetes, antispasmodic, diuretic and anti-inflammatory agent and bears significant antinocipective and antidiarrheal activities. The fruits and stem bark of this plant are used traditionally as a stimulant, astringent, stomachic and digestive and prescribed for urinary infection, dyspepsia, heart troubles, tooth ache, asthma and bronchits. Most exotic past research has studied the properties of Z. *rhetsa* extracts from the bark and root, and it was found to reduce the free radicals that cause the death of cancer cells (Sreelekha, 2012). Antimicrobial activities were also reported against some fungal and bacterial species by Poorniam *et al.,* (2018). Oil extracted from seeds can be used for the effective in cholera and is useful as an antiseptic, disinfectant and anti-inflammatory agent (Nalin *et al*., 2018). The water extract of the spine of Z. *rhetsa* was used to treat pain relief and to increase lactation in nursing mothers (Lalitharani *et al.,* 2013). The bark extract of Z. *rhetsa* has great potential for use or a natural active ingredient in anti-ageing cosmetic preparations (Ramesh *et al.,* 2013).

However, there is still lack of reports from the research on locally cultivated *Z. rhetsa*. Hence in this study, the spine of *Z. rhetsa* is chosen for the investigation of some phytochemical composition and some biological activities from its ethanol and watery extracts.

Materials and Methods

The spine samples were collected from Dawei, Tanintharyi Region, Myanmar. The plant was identified and authenticated at the Department of Botany, University of Yangon. After collection, the washed spines were air-dried in shade for about two weeks and ground into the coarse powder with the help of a mechanical grinder. The powders of the samples were used to extract with solvents of various polarities by using ultrasonic effect and to analyze phytochemical composition.

Phytochemical Analysis

The selected spine powders were subjected to qualitative phytochemical tests for the classification of various bioactive constituents present (Harborne, 1973). Phytochemical screenings were carried out by using standard procedures to detect the presence of alkaloids, glycosides, carbohydrates, α-amino acids, phenolic compounds, flavonoids, steroids, terpenoids, saponins, tannins, starch, reducing sugars and organic acids. After addition of specific reagents to the test solution, the observation of colour change or precipitate formation was noted and recorded.

Some Physicochemical Analyses

In this study, the crude plant material was subjected to the evaluation of some physicochemical properties. The various parameters were evaluated such as total ash content, water soluble ash content, acid insoluble matter content, moisture content, foaming index and swelling index. In addition, the relative abundance of elements present in the spine sample was determined by EDXRF spectrometer at the University of Monywa, Monywa.

The crude extracts of the sample were prepared by extracting the sample with different solvents such as petroleum ether, ethyl acetate, ethanol, methanol and water by percolation method. All of these extracts were kept for the determination of total phenol contents, total flavonoid contents, antimicrobial activity, antioxidant activity, antitumor activity, antidiabetic activity and antiproliferative activity.

Determination of Total Phenol Contents

The total phenol contents (TPC) in ethanol and watery extracts were estimated by the Folin-Ciocalteu method according to the procedure described by Saxena *et al.* (2013) and gallic acid was used as a standard. The sample solution (50 ppm) was prepared by dissolving 0.005 g of extract in methanol making up to 100 mL solution. Firstly, 0.5 mL of the prepared sample was mixed with 0.5 mL methanol. Then, 0.5 mL of Folin-Ciocalteu reagent (FCR: H_2O, 1:10) was added to the mixture and incubated for 5 min. 4 mL of 1 M sodium carbonate solution was added to each tube and the tubes were kept at room temperature for 2 h and the UV absorbance of each reaction mixture was recorded at λ_{max} 765 nm. The control solution was prepared as the above procedure by using distilled water instead of sample solution. Total phenolic content was estimated as mg gallic acid equivalents per g of EtOH/water extract.

Determination of Total Flavonoid Contents

The total flavonoids contents of the ethanol and watery extracts were measured by employing the method involving aluminium trichloride ($AlCl_3$) reagent and quercetin was used as standard (Kalita *et al.,* 2011). In the determination of total flavonoid contents, quercetin was used to construct the calibration curve. Quercetin (0.01 g) was dissolved in methanol and then diluted to various concentrations of 6.25, 12.50, 25, 50 and 100 μg/mL. A calibration curve was made by measuring the absorbance of the above different solutions at 415 nm (λ_{max} of quercetin) with a Shimadzu UV-1800 spectrophotometer. Ethanol/watery extract solution in 50 ppm was prepared by dissolving 0.005 g of each extract in 100 mL of methanol solution. Each extract stock solution (0.5 mL), 1.5 mL methanol, 0.1 mL of aluminium chloride, 0.1 mL of potassium acetate solution and 2.8 mL of distilled water were added and mixed well. The blank solution was prepared in similar way by replacing aluminium chloride with distilled water. Their absorbance was measured at 415 nm.

Screening of Antimicrobial Activity

Antimicrobial activity of different crude extracts (PE, EA, EtOH, MeOH, $(CH_3)_2CO$, $CHCl_3$ and water) of the sample was screened *in vitro* by agar well diffusion method (Perez *et al*.,1990). Bacterial cultures used in the research involved three strains of gram positive bacteria (*Bacillus subtilis, Staphyloccous aureus* and *Bacillus pumilus*), two strains of gram negative bacteria (*Pseudomonas aeruginosa* and *Escherichia coli*) and one strain of fungi (*Candida albicans*). This experiment was carried out at Pharmaceutical Research Department, Insein Township, Yangon Region, Myanmar.

Determination of Antioxidant Activity

The antioxidant activity of EtOH and H_2O extracts were spectrophotometrically determined by DPPH radical scavenging assay method (Brand-Williams *et al.,* 1995). The

control solution was prepared by mixing 1.5 mL of 60 µM DPPH solution and 1.5 mL of 95 % ethanol with vortex mixer. The sample solution was also prepared by mixing thoroughly the 1.5 mL of 60 µM DPPH solution and 1.5 mL of test sample solution. The solutions were allowed to stand for 30 min at room temperature. After 30 min, absorbance was measured at 517 nm by using a spectrophotometer UV 1601 PC (P\N 206-6750), Shimadzu corporation. Absorbance measurements were done in triplicate for each solution and the mean values obtained were used to calculate % inhibition of oxidation by the following equation,

$$\% \text{ oxidative inhibition} = \frac{A_c - (A - A_b)}{A_c} \times 100\ \%$$

% oxidative inhibition = % oxidative inhibition of test sample

A_c = absorbance of the control (DPPH alone)

A_b = absorbance of the blank (EtOH + Test sample solution)

A = absorbance of test sample solution

Then, IC_{50} (50 % inhibitory concentration) values were also calculated by linear regressive excel program.

Screening of Antidiabetic Activity

The α-amylase inhibitory effects of ethanol and watery crude extracts with five different concentrations (6.25, 125, 250, 500, 1000 µg/mL) were determined by using α-amylase inhibition assay. The tested samples (1 mL) were pre-incubated with 1 mL of phosphate buffer and 2 mL of α-amylase at 37 ºC for 20 min and thereafter 0.4 mL (1 % w/v) starch solution was added. The mixture was further incubated at 37 ºC for 30 min. Then the reaction was stopped by adding 2 mL of DNS reagent and the contents were heated in a boiling water bath for 10 min. A blank was prepared without plant extracts and another without the analyse enzyme, replaced by equal quantities of buffer. The absorbance was measured at 540 nm. The reducing sugar released from starch was estimated as maltose equivalent from a standard graph. Acarbose was used as standard. The anti-diabetic activity was determined through the inhibition of α-amylase which was expressed as a percentage of inhibition and calculated by the following equations.

$$\% \text{ Inhibition} = [A_{control} - (A_{Sample} - A_{Blank}) / A_{control}] \times 100$$

where, % Inhibition = % α-amylase inhibition

$A_{control}$ = absorbance without sample solution

A_{sample} = absorbance of sample

A_{Blank} = absorbance of sample + distilled water solution

Then, the IC_{50} values were calculated by linear regressive excel program.

Determination of α-Glucosidase Inhibitory Activity

The α-glucosidase inhibitory effects of ethanol and watery crude extracts with five different concentrations (6.25, 125, 250, 500, 1000 µg/mL) was determined by using a modified assay of that described by McCue *et al*., (2005). The α-glucosidase was assayed using 0.4 mL of sample extracts and 1 mL of 0.1 M phosphate buffer (pH 0.9) containing 2 mL of α-glucosidase solution, which was then uncubated at 25 ºC for 10 min. After the pre-incubatuion period, 0.5 mL

of 0.005M *p*-nitrophenyl-α-D-glucopyranoside solution was added to each well at timed intervals. The reaction mixtures were incubated at 25 ºC for 5 min. After incubation, absorbance readings of the samples were recorded at 405 nm and compared with a control that had 0.4 mL of buffer solution in place of the extract. Acarbose was used as standard. The anti-diabetic activity was determined through the inhibition of α-glucosidase which was expressed as a percentage of inhibition and calculated by the following equations.

$$\% \text{ Inhibition} = [A_{control} - (A_{Sample} - A_{Blank}) / A_{control}] \times 100$$

where, % Inhibition = % α-glucosidase inhibition

$A_{control}$ = absorbance without sample solution

A_{sample} = absorbance of sample

A_{Blank} = absorbance of sample + distilled water solution

Then, the IC_{50} values were calculated by linear regressive excel program.

Screening of Antitumor Activity

The antitumour activity of methanol, ethanol and watery extracts of the sample was examined by Potato Discs Assay Method (Ali *et al*., 2016). This experiment was carried out at Pharmaceutical Research Department, Insein Township, Yangon Region, Myanmar. Tumor producing bacteria, *Agrobacterium tumefaciens*, isolated from *Sandoricum koetjape* Merr. (Thitto) leaves were used in this study. This bacterial strain has been maintained as solid slants under refrigeration. For inoculation on the potato discs, 48 h broth cultures containing 5×10^7~5×10^9 cell / mL were used. Fresh, disease free potato tubers were obtained from local markets and were transferred within 48 h to the laboratory.

Tubers of moderate sizes were surface-sterilized by immersion in 50 % sodium hypochlorite (Clorox) for 20 min. The ends were removed and soaked for 10 min more in Clorox. A core of the tissue was extracted from each tuber by using surface-sterilized (ethanol and flame) 2.5 cm wide cork borer and 2 cm pieces were removed from each end and discarded and the remainder of the cylinder was cut into 1.0 cm thick discs with a surface-sterilized cutter. The discs were then transferred to 1.5 % agar plates (1.5 g of Difco agar was dissolved in 100 mL of distilled water, autoclaved and 20 mL poured into each petri dish). Each plate contained three discs. This procedure was done in the clean bench in the sterile room. The sample (0.1, 0.15 and 0.2 g) was filtered through Millipore filters (0.22 µm) into a sterile tube. A 0.5 mL of this solution was added to 1.5 mL of sterile distilled water and 2 mL of broth culture of *A. tumefaciens* strain (48 h culture containing 5×10^7~ 5×10^9 cells/ mL) were added aseptically.

Controls were made in this way; 0.5 mL of DMSO and 1.5 mL of sterile distilled water were added to the tube containing 2 mL of broth culture of *A. tumefaciens* (from the same 48 h culture). Using a sterile disposable pipette, 1 drop (0.05 mL) from these tubes was used to inoculate each potato disc, spreading it over the disc, surface. The process of cutting the potatoes and incubation must be conducted within 30 min. The plates were sealed with tape to minimize moisture loss and incubated at room temperature and counted with microscope and compared with control. The antitumor activity was examined by observation if tumor is produced or not.

Determination of Antiproliferative Activity

Antiproliferative activity of ethanol and watery extracts were investigated in *vitro* by using cancer cell lines at Division of Natural Product Chemistry, Institute of Natural Medicine, University of Toyama, Japan. The cell lines used were Hela (human cervix cancer), A549 (human lung cancer) and MCF 7 (human breast cancer). K562 α-Minimum essential medium with L-glutamine and phenol red (α-MEM, Wako) were used for cell cultures. All media were supplemented with 10 % fetal bovine serum (FBS, sigma) and 1 % antiobiotic antimycotic solution (Sigma). For MCF 7 cell, 1 % 0.1 M non-essential amino acid (NEAA, Gibco) and 1 % 1 mM sodium pyruvate (Gibco) were also supplemented. The *in vitro* antiproliferative activity of the crude extracts was determined by the procedure described by Win *et al.* (2015). Briefly, each cell line was seeded in 96-well plates (2×10^3 per well) and incubated in the respective medium at 37 °C under 5 % CO_2 and 95 % air for 24 h. After the cells were washed with PBS (Nissui Pharmaceuticals), serial dilutions of the tested samples were added. After 72 h incubation, the cells were washed with PBS and 100 μL of medium containing 10 % WST-8 cell counting kit (Dojindo; Kumamoto, Japan) solution was added to the wells. After 2 h incubation, the absorbance was measured at 450 nm. The concentrations of the crude extracts were 200, 100, 10 μg/ mL and 10, 1, 0.1 mM for positive control were prepared by serial dilution. Cell viability was calculated from the mean values of the data from three wells using the equation below and antiproliferative activity was expressed as the IC_{50} (50 % inhibitory concentration) value. 5-fluorouracil (5FU) was used as positive control.

$$(\%)\ \text{Cell viability} = 100 \times \frac{\left\{\text{Abs}_{(\text{test samples})} - \text{Abs}_{(\text{blank})}\right\}}{\left\{\text{Abs}_{(\text{control})} - \text{Abs}_{(\text{blank})}\right\}}$$

Results and Discussion

Phytochemicals Present in the Spine of *Z. rhetsa*

The spine sample of *Z. rhetsa* collected from Dawei Township, Tanintharyi Region was found to contain some of the secondary metabolites such as steroids, glycosides, phenolic compounds and terpenoids (Table 1) according to preliminary phytochemical screening. According to the physicochemical determination of the sample, the spine sample was found to contain (5.46 %) of total ash, (1.45 %) of water soluble ash, (0.19 %) of acid insoluble ash, (8.54 %) of moisture content, (< 100) of foaming index and 5mL/g of swelling index in the sample (Table 2).

Some Physicochemical Properties of the Spine of *Z. rhetsa*

As shown in Table 3, it can be seen that organic compounds are predominant in the sample, and other elements such as Si, S, Ca are also present in reasonable composition but K and Fe were present in medium amount and Cu was present in very little amounts based on the relative abundance of elements.

The soluble matter contents of the spine powder of *Z. rhetsa* in solvents of different polarities were observed 4.6 % in water, 3.0 % in methanol, 2.6 % in ethanol, 2.2 % in acetone, 2.0 % in ethyl acetate, 1.0 % in chloroform and 0.2 % in Petroleum ether (Table 4). Therefore, it

indicated that the phytochemicals present in spine sample were mostly the polar organic compounds.

Table 1 Results of Phytochemical Screening of the Spine of *Z. rhetsa*

Test	Extract	Test reagents	Observation	Results
Alkaloids	1%HCl	Dragendorff's reagent	Orange ppt.	+
		Mayer's reagent	Cream colour ppt	+
α-Amino acids	H_2O	Ninhydrin	Purple spot	+
Carbohydrates	H_2O	10%α-naphthol, Conc. H_2SO_4	Red ring	+
Cardiac glycoside	Dry powder	Glacial acetic acid, 5% $FeCl_3$	Blue colour	+
Flavonoids	EtOH	Conc. HCl, Mg ribbon	Green colour	+
Glycosides	H_2O	10% lead acetate	White ppt	+
Organic acids	EtOH	Bromocresol green	Blue color	+
Phenolics compounds	EtOH	10% $FeCl_3$	Dark blue colour	+
Polyphenols	EtOH	1% $FeCl_3$, $K_3Fe(CN)_6$	Dark blue colour	+
Protein	NaOH	$CuSO_4$	No colour change	-
Reducing sugar	H_2SO_4	Benedict's solution	No colour change	-
Saponins	H_2O	Shaking	Frothing	+
Starch	H_2O	I_2 solution	No dark blue colour	-
Steroids	PE	Conc. H_2SO_4 & acetic anhydride	Green colour	+
Tannins	H_2O	1% gelatin solution	Green colour	+
Terpenoids	$CHCl_3$	Conc. H_2SO_4 & acetic anhydride	Pink colour	+

(+) = Presence, (−) = absence

Table 2 Approximate Physicochemical Determination of the Spine of *Z. rhetsa*

Parameter	Value
Total ash content (%)	5.46
Water soluble ash content (%)	1.45
Acid insoluble matter content (%)	0.19
Moisture content (%)	8.54
Foaming index	< 100
Swelling index (mL/g)	5

Table 3 Relative Abundance of Elements in the Spine of *Z. rhetsa* by EDXRF

Macro and Micronutrients	Relative abundance (%)
Si	0.131
S	0.061
Ca	0.052
K	0.044
Fe	0.027
Mn	0.002
Cu	0.002
CH	99.681

Table 4 Extractable Matter Contents in the Spine of *Z. rhetsa*

Solvents	Weight of extractable matter (% w/w)
Water	4.6
Methanol	3.0
Ethanol	2.6
Acetone	2.2
Ethylacetate	2.0
Chloroform	1.0
Petroleum Ether	0.2

Total Phenol and Total Flavonoid Contents in the Spine of *Z. rhetsa*

Total phenol and total flavonoid contents in the spine of *Z. rhetsa* are shown in Figure 1 and Table 5. Total phenol contents of the extracts were calculated from the regression equation of calibration curve (Y = 0.0638 x + 0.0169; R^2 = 0.9941) and expressed as mg gallic acid equivalents (GAE) per gram of sample in dry weight. To perform the calculation of the total flavonoid contents in the samples by using Kiranmai *et al.* (2011) method, a standard curve is needed which is obtained from a series of absorbance of different quercetin concentrations (Y= 0.0019x +0.0115; R^2 = 0.9955). It can be seen that the total phenol of the ethanol extract (51.92±0.54 mg GAE/g of extract) was slightly higher than that of watery extract (41.56 ± 0.83 mg GAE/g of extract. In the case of total flavonoid content, total flavonoid content of ethanol extract (50.61 ± 2.29 mg QE/g of extract) is significantly higher than that of water extract (36.97 ± 1.05 mg QE/g of extract). The ethanol extract showed higher total phenol content and total flavonoid content than watery extract, indicating that phenolic and flavonoids compounds were more soluble in organic solvent than water. Generally, extracts with a high amount of phenolic compounds might exhibit high antioxidant activity.

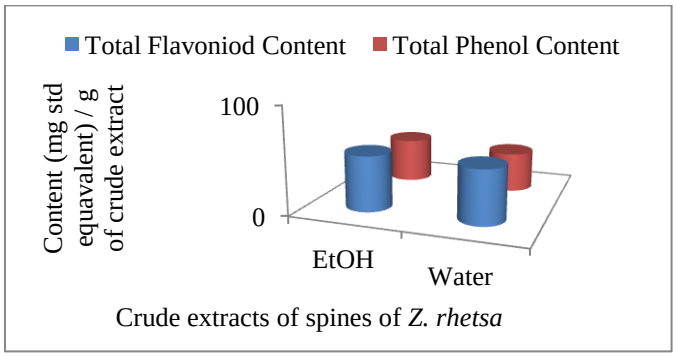

Figure 1 Total phenol and total flavonoid contents of *Z. rhetsa* Spine

Table 5 Total Phenol Content (TPC) and Total Flavonoid Content (TFC) of Crude Extracts

Types of compounds	EtOH extract	Water extract
TPC (mg GAE ± SD)/g of extract	51.92 ± 0.54	41.56 ± 0.83
TFC (mg QE ± SD)/g of extract	50.61 ± 2.29	36.97 ± 1.05

Antimicrobial Activity of the Spine of *Z. rhetsa*

The antimicrobial activity was assessed by agar well diffusion method which is equally suited to the screening of antibiotics or the products of plant evaluation and is highly effective for rapidly growing microorganisms and the activities of the test extracts are expressed by measuring the zones (mm) of inhibition. Generally, the more susceptible the organism, the bigger is the zone of inhibition. Antimicrobial activities of six different extracts (PE, EA, EtOH, MeOH, $(CH_3)_2CO$, $CHCl_3$, H_2O) of the sample were also determined against some fungal and bacterial species. The observed data are tabulated in Table 6. Generally, ethyl acetate and acetone extracts have higher activities (14~24 mm) on gram positive bacteria: *B. subtilis* and *B. pumilus*. Although acetone extract showed higher activity on *S. aureus* and *E. coli* (20 mm), ethyl acetate extract did not inhibit well. Ethyl acetate extract was found to possess higher antimicrobial activity against *P. aeruginosa* (23 mm), however, acetone extract (15 mm), exhibited low activity. Ethanol, methanol, chloroform and watery extracts were observed to exhibit medium antimicrobial activities against all tested microorganisms whereas pet-ether extract did not show any activity against all tested microorganisms.

Table 6 Inhibition Zone Diameters of some Crude Extracts against Six Microorganisms by Agar Well Diffusion Method

Organism	Inhibition Zone Diameters (mm) of Crude Extracts							
	PE	**EA**	**EtOH**	**MeOH**	**$CHCl_3$**	**Water**	**Acetone**	**Control**
Bacillius subtilis	-	24 (+++)	20 (+++)	15 (++)	15 (++)	14 (+)	20 (+++)	-
Staphylococcus aureus	-	14 (+)	17 (++)	15 (++)	18 (++)	13 (+)	20 (+++)	-
Pseudomonus aeruginosa	-	23 (+++)	14 (+)	13 (+)	12 (+)	13 (+)	15 (++)	-
Bacillus pumilus	-	21 (+++)	12 (+)	17 (++)	15 (++)	14 (+)	20 (+++)	-
Candida albicans	-	22 (+++)	15 (++)	15 (++)	15 (++)	13 (+)	18 (++)	-
E. coli	-	16 (++)	15 (++)	17 (++)	15 (++)	-	20 (+++)	-

Agar Well – 10 mm; control - solvent used; 10 mm ~ 14 mm (+) (low activity);
15 mm ~ 19 mm (++) (medium activity); above 20 (+++) (high activity)

Antioxidant Activity of the Spine of *Z. rhetsa*

Most of the medicinal plants possess phytochemicals and antioxidant activity. Flavonoids and tannins are phenolics which are a major group of compound in plants. These compounds act as primary antioxidant or free radical scavengers (Ayoola *et al*., 2008). The antioxidant activity of watery and ethanol extracts of the sample was studied by DPPH free radical scavenging assay (Marinova and Batchvarov, 2011). Gallic acid was used as standard. The DPPH (2, 2-diphenyl-1-picrylhydrazyl) assay is widely used to investigate the free radical scavenging activities of several natural compounds such as crude extracts of plants. DPPH radical is scavenged by antioxidant through the donation of electron forming the reduced DPPH. Sample's colour change from purple to pale yellow which can be quantified by its decrease of absorbance at wavelength 517 nm (Maw *et al*., 2011). The radical scavenging activity of crude extracts were expressed in term of % RSA and IC_{50} (50 % inhibition concentration). The results are shown in Table 7. From these observations, the larger DPPH radical scavenging activity was observed in ethanol extract, which inhibited 50 % of free radicals at the concentration of 1.15 μg/mL (IC_{50}) than the water extract which inhibited 50% of free radicals at the concentration of 2.89 μg/mL (IC_{50}). It can be inferred that the antioxidant potency of the ethanol extract was found to be stronger than that of the watery extract in antioxidant property.

Table 7 DPPH Free Radical Scavenging Activity (% RSA) and IC_{50} of Crude Extracts of the Spine Sample and Standard Gallic Acid

Samples	% RSA ± SD at Different Concentrations (μg/mL)						IC_{50} (μg/mL)
	0.3125	0.625	1.25	2.5	5	10	
EtOH extract	35.50 ± 1.39	39.63 ± 0.45	52.02 ± 5.58	62.34 ± 3.41	80.63 ± 0.45	88.99 ± 5.31	1.15
Watery extract	28.42 ± 2.51	31.66 ± 1.39	34.41 ± 6.33	47.59 ± 5.21	62.93 ± 4.43	76.30 ± 0.95	2.89
Standard Gallic Acid	43.69 ± 1.28	64.28 ± 1.97	71.45 ± 1.40	86.45 ± 2.22	86.99 ± 1.15	87.12 ± 1.97	0.41

In vitro Screening of Antidiabetic Activity

Diabetes is a clinical syndrome characterization by hyperglycemia due to absolute or relative deficiency of Insulin. Recent decades have experienced a sharp increase the incidence and prevalence of diabetes mellitus. One antidiabetic therapeutic approach is to reduce gastrointestinal glucose production and absorption through the inhibition of carbohydrate digesting enzyme such as α-amylase and α-glucosidase. Inhibition of amylase and glucosidase enzymes involved in digestion of carbohydrates can significantly decreases the past prandial increase of blood glucose after a mixed carbohydrate diet therefore can be an important strategy in management of blood glucose (Narkhede *et al*., 2011).

The ethanol extract of the spine of *Z. rhetsa* (IC_{50} = 113.01 μg/L) possessed the higher α-amylase inhibition activity than the watery extract (IC_{50} = 137.00 μg/L) and also ethanol extract of the spine sample (IC_{50} = 120.56 μg/L) possessed the higher α-glucosidase inhibition property than the watery extract (IC_{50} = 446.78 μg/L) (Table 8 and 9). Both the ethanol and watery extracts possessed lower antidiabetic activity than standard acarbose which showed α-amylase inhibition activity with IC_{50} =0.016 μg/mL and α-glucosidase inhibition activity with IC_{50} = 0.042 μg/mL.

Table 8 α-Amylase Inhibition and IC_{50} of Ethanol and Watery Extracts of Spine of Ka-thit-phu

Samples	% Inhibition in Different Concentrations (μg/mL)					IC_{50} (μg/mL)
	62.5	125	250	500	1000	
EtOH extract	33.85 ± 0.44	53.82 ± 0.78	71.90 ± 0.44	100 ± 0.44	122.8 ± 0.00	113.01
Water extract	31.64 ± 0.22	44.27 ± 0.66	59.19 ± 1.89	89.66 ± 1.22	115.86 ± 4.79	137.00

Table 9 α-Glucosidase Inhibition and IC_{50} of Ethanol and Water Extracts of Spine of Ka- thit-phu

Samples	% Inhibition in Different Concentrations (μg/mL)					IC_{50} (μg/mL)
	62.5	125	250	500	1000	
EtOH extract	30.42 ± 3.72	51.49 ± 0.29	80.33 ± 2.05	141.74 ± 1.02	164.44 ± 3.26	120.56
Water extract	35.67 ± 0.34	38.59 ± 1.02	42.47 ± 0.68	52.06 ± 1.88	102.06 ± 5.66	446.78

Antitumor Activity of the Spine of *Z. rhetsa*

The antitumor activity of various crude extracts (MeOH, EtOH, H_2O, Acetone, EtOAc, $CHCl_3$, PE) the spine sample was investigated by using PCG test with the isolated tumor forming bacterium *A. tumefaciens*. The 48 h broth cultures containing 5 x 10^9 cells/mL were used to inoculatethe potato disc. The tested samples were dissolved in DMSO to dilute and the diluted samples were mixed with the bacterial culture for inoculation. After preparing the inoculums, the bacterial suspension was inoculated on the cleaned and sterilized potato discs, and incubated at room temperature for 3 days. Then, the tumors appeared on potato discs and checked by staining the knob with Lugol's (I_2-KI) solution. In the control, the formation of white knob on the blue background indicated tumor formation. The active test samples did not form any tumor on the potato discs and its surface remained blue. This experiment revealed that all of the tested

samples exhibited the inhibition of tumor formation at the dose of 0.3 g/disc after 5 days and 7 days treatment (Table 10).

Table 10 Observation of Tumor Inhibition by Different Concentrations of Crude Extracts of the Spine Sample after 5 Days and 7 Days Treatment

Extracts	Observation of Tumor Formation by Different Concentrations of Crude Extracts		
	0.1 g/disc	**0.2 g/disc**	**0.3 g/disc**
MeOH	+	+	-
EtOH	+	+	-
H_2O	+	+	-
Acetone	+	+	-
EtOAc	+	+	-
$CHCl_3$	+	+	-
PE	+	+	-
Control	++		

(+) Tumor formation (-) No Tumor formation

Antiproliferative Activity of the Spine of *Z. rhetsa*

Cancer is a malignant tumor or malignant neoplasm, is a group of diseases involving abnormal cell growth with the potential to invade or spread to other parts of the body. Many traditional plant treatments for cancer are used throughout the world, and some of these plants have been scrutinized while a good number of them are yet to receive scientific scrutiny. Among them, the spine of *Z. rhetsa* was selected for this study since they are widely distributed in Myanmar. Antiproliferative activity is the activity relating to a substance used to prevent or retard the spread of cells, especially malignant cells, into surrounding tissues. Antiproliferative activity was studied in *vitro* using human cancer cell lines. Screening of antiproliferative activities of ethanol and watery extracts from the spine of *Z. rhetsa* was done by using three human cancer cell lines such as Hela (human cervix cancer) and MCF7 (human breast cancer). Antiproliferative activity was expressed as the IC_{50} (50 % inhibitory concentration) value. 5-Fluorouracil was used as positive control. The antiproliferative activity of crude extracts are summarized in Table 11. From the results, the IC_{50} values were found to be 3.74 μg/mL against cervix cancer, 7.71 μg/mL against breast cancer and 4.77 μg/mL against lung cancer by ethanol extract and >200 μg/mL against cervix cancer, >200 μg/mL against breast cancer and >200 μg/mL against lung cancer by watery extract, respectively. Since the lower the IC_{50} values, the higher the antiproliferative activity, ethanol extract was more potent than watery extract in antiproliferative activity on the selected cell lines.

Table 11 Antiproliferative Activity of Crude Extracts against Three Types of Cancer Cell Lines

Samples	IC_{50} (μg/mL) of Various Samples against tested cell lines		
	Hela	**MCF 7**	**A 549**
EtOH Extract	3.74	7.71	4.77
Watery Extract	>200	>200	> 200
5FU	14.14	16.04	16.04

Hela - human cervical cancer cell lines MCF 7 - human breast cell lines
A549 - human lung cancer cell lines 5FU* - Fluorouracil (drug for cancer)

Conclusion

From the overall assessment concerning with investigation of phytochemicals and some biological activities on the spine of *Z.rhetsa* (Roxb.) DC. (Ka-thit-phu), ethanol extract was observed to possess higher antimicrobial, antioxidant, antidiabetic and antiproliferative activities than watery extract, it might be due to its higher contents of total phenols and total flavonoids. According to the observations, since the ethanol and watery extract of Ka-thit-pu spine showed these activities, these extracts may be effectively used for the treatment of skin disease, wound infections, diarrhea and also as antioxidant for curing the oxidative stress related diseases, some forms of cancer and some age-related disorders. The quantitative and qualitative phytochemical analytical data are also expected to be applicable to some extent in the medicinal formulation by using the spine of *Z. rhetsa*.

Acknowledgements

The authors would like to express our gratitude to the Department of Higher Education, Ministry of Education, Myanmar, for their permission to do this research and also to the Myanmar Academy of Arts and Science for allowing to read this paper.

References

Ali, N., Zada, A., Ali, M. and Hussain, Z. (2016). " Isolation and identification of *Agrobactgerium tumefaciens* from the Galls of Peach Tree". *Journal of Rural Development and Agriculture,* vol. 1(1), pp. 39-48.

Ayoola, G. A., Coker, H. A. B., Adesegun, S. A., Bello, A. A. A., Obaweya, K., Ezennia, E. C., and Atangbayila, T. O. (2008). "Phytochemical Screening and Antioxidant Activities of Some Selected Medicinal Plants Used for Malaria Therapy in Southwestern Nigeria". *Tropical Journal of Pharmaceutical Research,* vol. 7, pp. 1019–1024.

Brand-Williams, W., Cuvelier, M. E. and Berse, C. (1995). "Use of a Free Radical Method to Evaluate Antioxidant Activity". *Lebensm.-Wiss. u.-Technol*., vol. 28 (1),pp. 25-30.

Harborne, J. B. (1973). *Phytochemical Methods : A Guide to Modern Techniques of Plant Analysis*. London: 2nd Ed., pp. 37-38.

Kalita, S., Kumar, G., Karthik, L. and Rao, K. V. B. (2011). "Phytochemical Composition and *In Vitro* Hemolytic Activity of *Lantana camara* L. (Verbenaceae) Leaves". *Pharmacology,* vol.1, pp. 59-67.

Kiranmai, M., Mahender, K. C. B., and Ibrahim, M. D. (2011). "Free Radical Scavenging Activity of Neem Tree (*Azadirachta indica* A. Juss Var., Meliaceae) Root Bark Extract". *Asian Journal of Pharmaceutical and Clinical Research,* vol.4 (4), pp. 134-136.

Lalitharani, S., Kalpanadevi, V. and Mohan, V.R, (2013). "Pharmacognostic Studies on the Spine of Zanthoxylum rhetsa (Roxb.) D.C". *Journal of Bioscience Discovery*, vol. 4(1), pp. 3-11.

Marinova, G. and Batchvarov, V. (2011). "Evaluation of the Methods for Determination of the Free Radical Scavenging Activity by DPPH", *Bulgarian Journal of Agricultural Science*. vol. 17, pp. 11–24.

Maw, S. S., Mon, M. M. and Oo, Z. K. (2011). "Study on Antioxidant Activities of Some Herbal Extracts". *World Academy of Science, Engineering and Technology*, vol. 51, pp. 450–452.

McCue, P., Kwon, Y. I. and Shetty, K. (2005). "Anti-amylase, anti-glucosidase and anti angiotensin I converting enzyme potential of selected foods", *J Food Biochem.* vol. 29, pp. 278–294.

Nalin, W., Chareeporn, A., Phanchana, S., Ian, H. F., Chayanin, P. and Donruedee, S. (2018). " Chemical Compositions and Biological Properties of Essential Oils from *Zanthoxylum rhetsa* (Roxb.) DC. And *Zanthoxylum Limonella* Alston". *Journal of Tradit Complement Altern Med. Sci*., vol. 15(2), pp.12-18.

Narkhede, M. B., Ajimire, P. V., Wagh, A. E., Manoj, M. and Shivashanmugam AT. (2011). " In *vitro* Antidiabetic Activity of *Caesalpina, Digyna* (R.) Methanol Root Extract" *Asian Journal of Plant Science and Research,* vol. 1 (2), pp. 101-106.

Newmon, D.J. and Cragg, G.M. (2007). " Natural Products as Sources of New Drugs over the Last 25 Years." *Journal of Natural Products*, vol. 70, pp. 461-477.

Perez, C., Paul, M. and Bazerque, P. (1990). "Antibiotic Assay by Agar Well Diffusion Method.". *Alta BioMed Group Experiences,* vol. 15, pp.113-115.

Poornima, K., Krishnakumar, K. and Veena, V. (2018). "Phytochemical and Antibacterial Assay of *Zanthoxylum rhetsa* (Roxb.) DC". *International Journal of Research in Biosciences*, vol. 7(2), pp.41-45.

Ramesh, K. S., Syahida, S.A., Faridash, A., Intan, S. I., Yaya, R. and Khozirah, S. (2013). "Photoprotective Properties of *Zanthoxylum rhetsa*: An in Vitro Analysis". *Journal of Chemical and Pharmaceutical Research,* vol. 5(12), pp. 1512-1520.

Saxena, M., Saxena, J., Nema, R., Singh, D. and Gupta, A. (2013). "Phytochemistry of Medicinal Plants". *Journal of Pharmacognosy and Phytochemistry*, vol. 1 (6), pp.168-172.

Sreelekha, M. (2012). "Studies on Secondary Plant Metabolites and their Biological Properties. PhD (Thesis), Department of Chemistry, University of Calicut, India, pp. 2-13.

Win, N. N., Ito T., Aimaiti, S., Kodama, T., Imagawa, H., Ngwe, H., Asakawa, Y., Abe, I. and Morita, H. (2015). "Kaempulchraols I-O: New Isopimarane Diterpenoids from *Kaempferia pulchra* Rhizomes Collected in Myanmar and their Antiproliferative Activity". *Tetrahedron*, vol. 71, pp. 4707-4713.

STUDY ON THE FABRICATION, EVALUATION OF MECHANICAL AND PHYSICAL PROPERTIES OF PARTICLEBOARD MADE FROM GIANT REED (*ARUNDO DONAX L.*) AND APPLICATION

Saw Win[1], Win Win Nu[2], Myint Sandar Win[3]

Abstract

Single-layer experimental particleboards were made from internode of giant reed culms with different particle sizes (4 mm, 2 mm, 1 mm, 500 μm, 250 μm) of particles bonded with urea-formaldehyde resin. Urea-formaldehyde resin (25 %) was mixed with 2 mL of 0.4 % ammonium sulphate hardener and 1 mL cashew nut shell liquid for each panel to improve strength and other properties. The panels were tested for mechanical properties including modulus of rupture (MOR), impact strength, hardness, tensile strength and physical properties such as density, moisture content (MC), water absorption (WA) and swelling thickness (ST) according to the procedures defined by British Standard and Indian Standard methods. The overall results showed that most panels fulfilled FAO (2013) standard for MOR, WA and ST. The surface fracture of PBS4 (500 μm) is more uniform and fibers are not pull out from the surface. This tend to be more enhanced the MOR, less WA and ST of particleboard. PBS4 (500 μm) had the highest MOR, the lowest WA and ST values. Particle size was found to have a profound effect on the board properties.

Keywords: Giant reed, urea-formaldehyde, cashew nut shell liquid, particle size, particleboard, mechanical properties and physical properties

Introduction

The demand for composite wood products, such as plywood, oriented strand board, hardboard, particleboard, medium-density fiberboard, and veneer board products has recently increased substantially throughout the world (Youngquist, 1999, Sellers, 2000). According to a report from Food and Agricultural Organization (FAO) of the United Nations, the worldwide demand of particleboard panels were 56.2 Mm^3 in 1998 (Youngquist and Hamilton, 2000). The feasibility of using fast-growing trees and agricultural residues as raw materials for particleboard production has been explored by a number of researchers. Particleboard can be considered as a common product of wood industry. Particleboard is widely used around the world in furniture manufacturing and house construction (Youngquist, 1999). The production of particleboard involved compression of wood particles with other lignocelluloses materials and adhesive at high pressure. The adhesive used to bind the wood particles made from natural or synthetic products (Bono *et al*., 2011).

In the last decade, European agricultural research has focused much attention on the research for new, non-food crops with regard to their industrial utilization. The grass *Arundo donax* L. (giant reed) (Poaceae) has been considered as one of the more-promising crops (Shatalov and Pereira, 2005). Giant reed is a perennial herbaceous species growing in grasslands and wetlands, and is an invasive, riparian plant and potential bioenergy crop (Lewandowski *et al*., 2003, Graziani and Steinmaus, 2009). Giant reed is thought to have originated from Asia, but

1. Dr, Associate Professor, Department of Engineering Chemistry, West Yangon Technological University
2. Dr, Associate Professor, Department of Botany, Myeik University
3. Dr, Professor (Head), Department of Engineering Chemistry, West Yangon Technological University

it is also considered as a native species in the countries surrounding the Mediterranean Sea (Lewandowski *et al*., 2003). In the Southeast of Spain, giant reed was used as a building material (walls, frameworks, roofs, fences) for livestock and housing and for erosion control until the beginning of the 20th century. Giant reed has consumed water from the river that is needed for agricultural use. Large clumps alter stream flow patterns, increase flood damage (Frandsen and Jackson, 1994, Moran and Goolsby, 2009), and displace populations of native plants and animals (Bell 1997, Herrera and Dudley 2003). Physical (burning), mechanical (mowing or mulching, and chemical control (Tracy and Deloach, 1999) are the methods commonly used to solve these problems, but they do not have sufficient impact. Giant reed has been grown at the bank of the stream, river, in grasslands and wetlands of almost regions except hilly regions in Myanmar. In this research giant reed culms were used to manufacture particleboard panels in order to give added value to the residue. Some physicochemical properties of giant reed are shown in Table 1.

Table 1 Physicochemical Properties of Internode of Giant Reed Culms (Stems)

Component	Shatalov Values* 2001	Ververis Values** 2004
Ash (%)	6.14	4.53
Lignin (%)	21.31	-
α-Cellulose (%)	32.93	36.27
Hemicelluloses (%)	28.48	-
Fiber (%)	33.90	-
Fiber Length (mm)	1.20	1.22
Fiber width (μm)	14.60	-
Fiber wall thickness (μm)	4.60	4.40
Fiber diameter (μm)	-	17.30

* Shatalov *et al.,* (2001)
**Ververis *et al.,* (2004)

At the present time, the majority of particleboard manufacturer employs formaldehyde-based adhesive such as phenol-formaldehyde (PF), urea-formaldehyde (UF), and melamine-urea-formaldehyde (MUF) as the main adhesives (Bono *et al*., 2011). Urea-formaldehyde (UF) is chemically known as urea-methanol, non-transparent thermosetting resin. UF is obtained by heating urea and formaldehyde in the presence of ammonia or pyridine as catalyst. UF was first synthesized in 1884 by Holzer. It is a great resin for bonding particle. UF is the commercial resin popularly used for wood-based panel product (Lee *et al*., 2011).

Cashew nut shell liquid is used to reduce urea-formaldehyde resin, formaldehyde and volatile organic compounds emission (Kim, 2009). It is also used to reduce biodegradability (fungicity and insect). Cashew nut shell liquid improves water resistance, corrosion and insulation resistance (Bisanda *et al*., 2003). Particleboard having the best physical properties such as water absorption and swelling thickness was made of ammonium sulphate hardener and small chips. (Mohsen, 2011). The presence of hardener enhances the cross linking between the resin and hardener thus increases the tensile strength (Sulaiman *et al*., 2008).

The objectives of this study are to use particles from giant reed culms, of different sizes, as a raw material for laboratory made particleboard panels and to test the properties of such boards to determine if they are comparable to particles made from other species.

Materials and Methods

Materials

Giant reed culms (*Arundo donax* L.), were collected from West Yangon Technological University Campus, Hlaing Tharyar Township in Yangon (Myanmar) and were dried for 2 months under ambient conditions, to 6.3 % moisture content, before use. The average culm height, diameter, and thick of wall 550 cm, 1 cm and 0.5 cm, respectively. After removing any remains of pulms and leaves, the culms were manually cut into slices (ca. 3 cm long) and crushed or blended in Henser Mixer about 10 minutes. The particles were then classified using a Horizontal Screen Shaker with sizes of 4 mm, 2 mm, 1 mm, 500 μm and 250 μm to remove oversize and undersize (dust) particles. A sample of the different sizes of the particles can be seen in Figure 1.

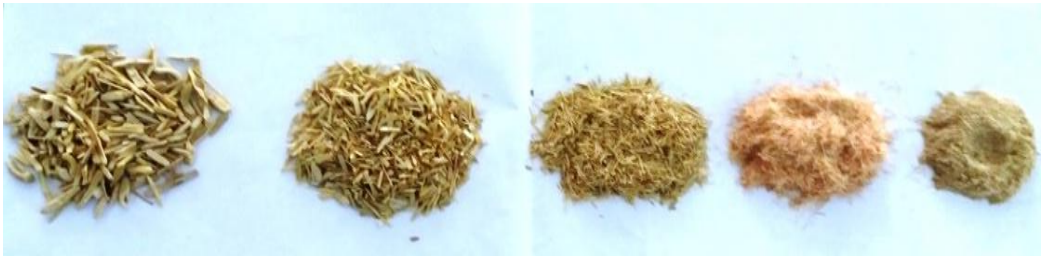

4 mm 2 mm 1 mm 500 μm 250 μm

Figure 1 Giant reed particles with different sizes

Particles were blended with urea-formaldehyde (UF) resin with the solid content of 58 % at the level of 25 % based on the weight of particles (6.3 % moisture content). As a hardener, 0.4 % of ammonium sulphate and 1ml of cashew nut shell liquid, based on the weight of particles (6.3 % moisture content), was used. Urea-formaldehyde resin was purchased from Watayar Glue Factory in Yangon, Myanmar. Cashew nut shell liquid was collected from Myeik, Tanintharyi Region, Myanmar. The ammonium sulphate was produced from Chengdu Kelong Chemical Reagent Factory, China. Urea-formaldehyde, cashew nut shell liquid and ammonium sulphate are shown in Figure 2.

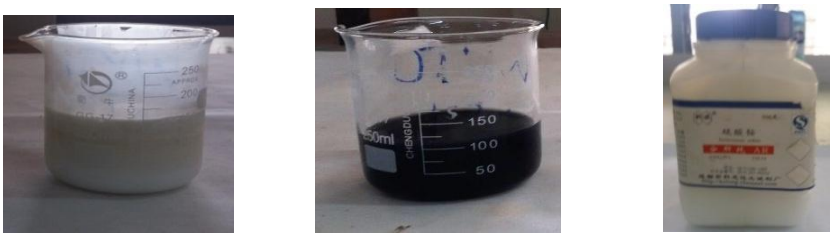

(a) (b) (c)

Figure 2 (a) Urea-formaldehyde, (b) cashew nut shell liquid and (c) ammonium sulphate

Procedure for Preparation of Particleboards

The five types of particleboard panels were made. Pre-weighed 120 g classified size (4 mm, 2 mm, 1 mm, 500 μm and 250 μm) raw material giant reed particles was placed into a Hensel Mixer. Before spraying the UF adhesive, the hardener ammonium sulphate was dissolved at 0.4 % concentration in water and fungicide cashew nut shell liquid 1 mL was blended and

immediately mixed with the adhesive, the glue mixture was then sprayed onto the particles and blended for 5 min at ambient temperature in the Hensel mixer to obtain a homogenized mixture. The mat configuration was one layer. Boards measuring (6" x 6" or 15 cm x 15 cm) were manually formed and pressed in a hydraulic hot press at 2200 psi at 120 °C for 15 min.

The experimental design for preparation of one-layer particleboards is shown in Table 2.

Table 2 Production Parameters of One-layer Particleboards

Parameter	Value
Press temperature (℃)	120
Pressing time (min)	15
Press pressure (psi)	2200
Dimensions (cm)	15x15
Thickness (cm)	0.46 - 0.56
Number of boards of each type	2

Two replicate panels were made for each board type. After pressing, the particleboards were conditioned at ambient temperature about one week in vertical position (Figure 3). The finished particleboards were trimmed to avoid edge effects to a final size of 14.8 cm x 14.8 cm, and then cut into various sizes for properly evaluation according to BS 1811 (1961) and IS 3087 (1965) methods as shown in Figure 4.

Figure 3 Finished particleboards during conditioning at ambient temperature

Figure 4 Particleboards samples stored after the assessment

Some mechanical and physical properties of panels were determined in accordance with their respective methods as shown in Table 3.

Table 3 Tests and Test Specimen Sizes and Number

Test	Specimen size (cm × cm)	Specimen per panel	Method and Equipment
Modulus of rupture	14.8 × 2.5	3	BS:1811-1961
Impact strength	7.5 × 2.5	3	ASTM D – 256 Qualitest Impact 50
Hardness	1.7 ×1.7	3	Wallace Hardness Micro Tester
Tensile strength	14.8 × 2.5	3	Electrohydraulic Tensile Tester
Thickness	14.8 × 2.5	3	Veneer clipper
Density	14.8 × 2.5	3	BS:1811-1961
Moisture content	1.7 × 1.7	3	MOC. 63 U Moisture Analyzer
Water absorption*	2.5 × 2.5	3	IS:3087-1965
Swelling thickness*	2.5 × 2.5	3	IS:3087-1965

*After soaking period 24 h

Results and Discussion

The five types of particleboard (PBS1-PBS5) were prepared by using 25 % urea-formaldehyde, 2 mL (0.4 %) ammonium sulphate, 1 mL cashew nut shell liquid and various particle sizes of giant reed fiber (4 mm, 2 mm, 1 mm, 500 μm and 250 μm).

The mechanical and physical properties of prepared particleboards are shown in Table 4.

Table 4 Mechanical and Physical Properties of Prepared Particleboards

Properties	**PBS1**	**PBS2**	**PBS3**	**PBS4**	**PBS5**	**Reference **Reported**
Modulus of rupture (psi)	8468.8	7013.5	9817.8	10603.9	8611.9	-
Modulus of rupture (kg $cm^{-2)}$	234.9	194.5	272.3	294.1	238.9	100-500
Impact strength (kj m^{-2})	107.7	78.2	68.4	52.3	28.6	-
Hardness (Shore D)	95	95.75	96.5	97.0	98.0	-
Tensile strength (lb)	7	7	7	7	6.5	-
Thickness (cm)	0.56	0.52	0.48	0.46	0.50	-
Density (g cm^{-3})	0.95	0.96	0.98	1.01	1.0	0.40 - 0.80
Moisture content (%)	4.63	5.12	5.16	5.24	5.50	-
Water absorption*(%)	36.74	31.70	31.04	30.01	22.84	20-75
Swelling thickness*(%)	23.21	22.80	20.84	20.23	4.00	5-15

Pressing temperature = 120°C pressing time = 15 min
Pressing pressure = 2200 psi Fiber type = giant reed (internode)
Adhesive type = UF Hardener = ammonium sulphate
Fungicide = CNSL
* = after soaking period 24h
** = FAO (2013)
FAO = Food and Agriculture Organization
PBS1 = particleboard with 4 mm particle size
PBS2 = particleboard with 2 mm particle size
PBS3 = particleboard with 1 mm particle size
PBS4 = particleboard with 500 μm particle size
PBS5 = particleboard with 250 μm particle size

The values of MOR ranged from (194.5 – 294.1) kg cm^{-2}. The particleboards made from five types of particle sizes had MOR values that are sufficiently high to meet the requirements for FAO (2013) standard. Panel (PBS4) having the greatest density gave the greatest values of MOR, suggesting, that the particleboard density plays a very important role on the bending strength, as expected (Figure 5).

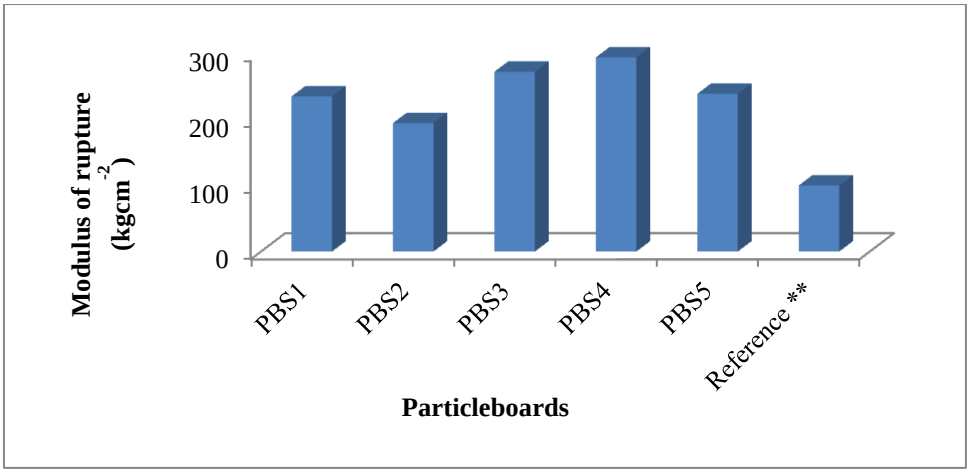

Figure 5 Modulus of rupture of particleboards

From the observation of impact strength of prepared particleboards, it is envisaged that as the size of particles becomes bigger, greater original interaction between the fibers in the particle. Impact strength of particleboard decreases as the particle size of fiber used for particleboard decreases as expected. PBS4 (4 mm) with biggest particle size had the greatest impact strength (Figure 6).

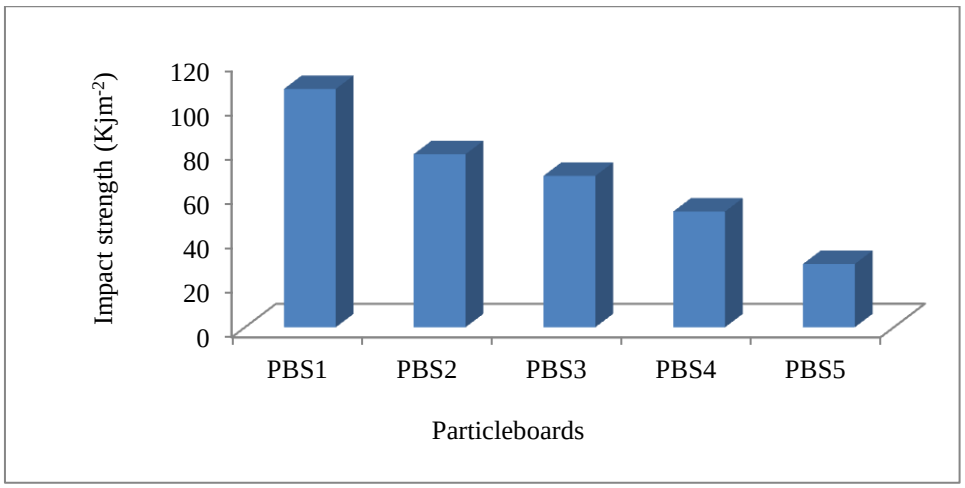

Figure 6 Impact strength of particleboards

It is observed that particleboards with particle sizes (4 mm, 2 mm, 1 mm, 500 μm) have constant tensile strength (7 lb) and decreasing bending period but particleboard with particle size 250 μm has the lower tensile strength (6.5 lb) than that of other four boards.

Hardness of prepared particleboards is gradually increasing from 95 to 98 Shore D. It suggested that particle size of fibers is inversely proportional to the hardness of board formed.

The thickness of the produced particleboards ranges from 0.46 to 0.56 cm. The density ranged from 0.95 to 1.01 gcm^{-3}. Panel PBS4 had the lowest thickness and the highest density, was prepared with the particle size (500μm). It was suggested that these properties may be attributable to an insufficient application of pressure during the compressing. Increasing particle size may be increased thickness and decreased density of board. Kelly (1977) reported that a

higher pressure was required to reach a desired specific gravity for narrow and thicker flakes as opposed to wider and thinner flakes

The water absorption values of particleboards after 24 h soaked in water were 22.84 to 36.74 %. The results fulfilled to FAO (2013) standard. The water absorption values decreased with increasing the board density and decreasing particle size. It was suggested that increasing (WA) of larger particle size panel due to the voids and moistures among the particles.

Particleboards should have a maximum swelling thickness (ST) value of 15 % for 24 h immersion in water (FAO, 2013). Average (ST) of panels following a 24 h immersion ranged from 4.00 to 23.21 %. Panels PBS5 were found to 4 % with swelling thickness value and had the smallest particle size. The ST values decreased with decreasing particle size, because of lesser voids between the particle (Figure 7).

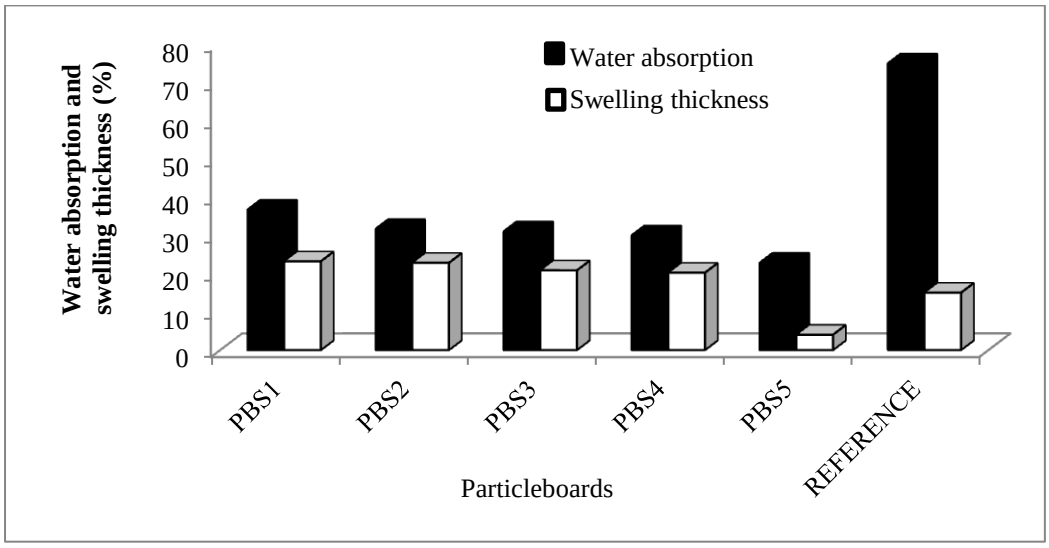

Figure 7 Water absorption and swelling thickness of particleboards

Moisture content of panels ranged from 4.63 % to 5.50 %. The moisture content of particleboard increased as the particle size decreased of fiber due to the greater surface area of particle contact with moisture. The moisture content necessary for fungi growth on the surface of board is 16 % (Burmester, 1974). So, moisture content of board should be reduced to the least as possible.

Surface Morphology of Selected Prepared Particleboards

Surface morphology of particleboards was analyzed by Digital Microscope (50x-500x), China. The micrographs from side view and over view of PBS3 (1 mm) and PBS4 (500 μm) are shown in (Figure 8). It was found that the surface fracture of PBS4 (500 μm) is more uniform, compatible and fibers are not pull out from the surface that is PBS4 has less micropores and microcracks on the surface. This is tend to be more enhanced the MOR, less WA and ST values of particleboard.

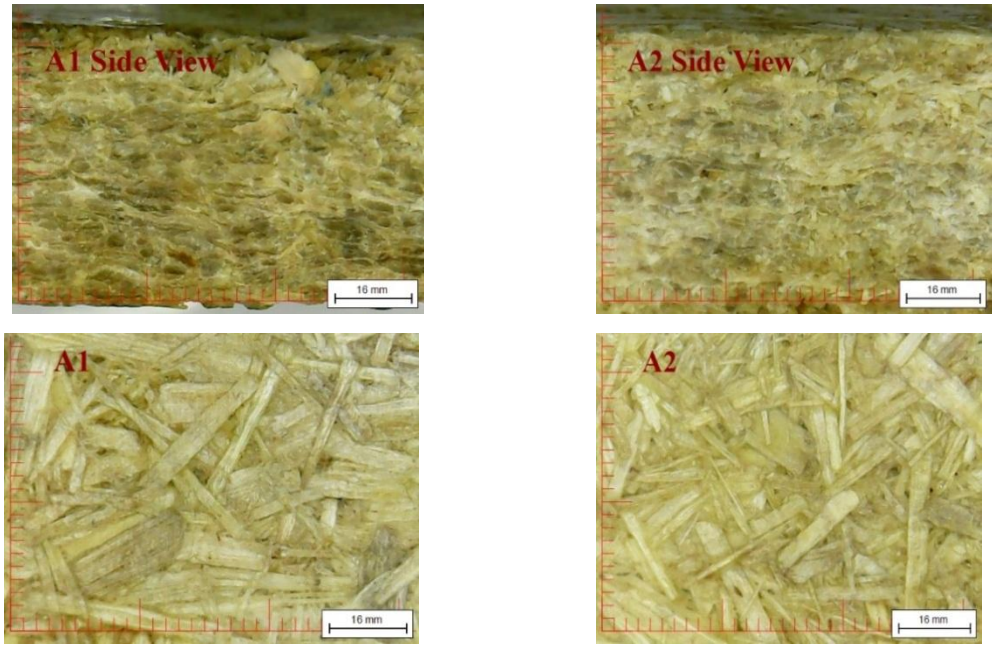

PBS3 (1 mm) PBS4 (500 μm)

Figure 8 Surface micrographs of PBS3 and PBS4 (300x Mag)

Application of the Prepared Particleboards

The finished particleboards were prepared by using giant reed fiber, UF, ammonium sulphate and cashew nut shell liquid to protect the fungi growing on the surfaces. The surface of finished particleboards could also be made attractive by using sun mica laminates. The surface finished particleboards were found to be successful in making of household articles such as ceiling boards, wall partitions and floor underlayment. (Figure 9) shows the photographs of various household articles.

Figure 9 Photographs of household articles

Conclusion

The results presented suggest that it is completely feasibility to manufacture acceptable or high-quality particleboard using giant reed as an alternative lignocellulosic raw material. Since particleboards produced with particle sizes from 4 mm to 250 μm had the most desirable quality and so the production of 500 μm and 250 μm particle sizes are recommended for milling of the culms due to their highest MOR, hardness, density and lowest, thickness, water absorption and

swelling thickness which are fulfilled to FAO (2013), standard. Particle size was found to have a great effect on the properties of UF-bonded giant reed particleboards manufactured from giant reed particles of five different sizes.

Since particleboards are considered quality grade, cost effective and long-life products, could be manufactured for household articles. The use of renewable giant reed fiber for manufacturing particleboards could help to alleviate the scarcity of raw material for the particleboard industry. The present work will contribute to the technological needs for our country: reducing the non-biodegradable pollutants, giving added value of the giant reed culms, preserving potentially the forest depletion and reducing the greenhouse gases emission and creating green world.

Acknowledgement

The authors would like to express their profound gratitude to the Department of Higher Education (Lower Myanmar) Ministry of Education, Yangon, Myanmar for provision of opportunity to do this research.

References

Bell, G.P.(1997). "Ecology and Management of *Arundo donax*, and Approaches to Riparian Habitat Restoration in Southern California", In: Brock, J. H., Wade, M., Pysek, P. and Green, D. (eds.), *Plant Invasions: Studies from North America and Europe,* Blackhuys Publishers Ledien, The Netherlands, pp.103-113

Bisanda, E.T.N., Ogola, W.O. and Tesha, J.V. (2003). "Characerization of Tannin Resin Blends for Particleboard Applications Cement and Concrete Composites". *J. Polym. Mater*., vol. 25, pp. 593-598

Bono, A., Nur. M., Anisuzzaman, S.M., Sualah, S. and Chiew, H.K. (2011). The Performance of MUF Resin with Palm Kernel as Filler. *Advanced Materials Research*, vol. 3, pp. 233-235

Burmester, A. (1974). Simple Methods of Improving Dimensional Stability. (2) Treatment of Wood-based Materials, Technology, Economics. *Holz und Kunststoffverarbeitung,* vol. 9(9), pp. 610-617 (in German)

FAO. (2013). Characteristic Mechanic of Polyester Composite Particleboard with Filler Particle of Areca Nut Fiber, http://www.fao.org/3/a-i4441 e.pdf (Accessed 8 June2013)

Frandsen, P. and Jackso, N. (1994). "The Impact of *Aurndo donax* on Flood Control and Endangered Species", In Jackson, N. E., Frandsen, P and Duthoit, S. (Compliers), *Arundo donax* Workshop Proceedings, 19 November 1993, Ontario, California, USA. Team Arundo and California Exotic Pest Plant Council, Pismo Beach, CA, pp.13-16

Graziani, A. and Steinmanus, S.J. (2009). "Hydrothermal and Thermal Time Models for the Invasive Grass, *Arundo donax*". *Aquatic Botany,* vol. 90, pp. 78-84

Herrera, A.M. and Dudley, T.L. (2003). "Reduction of Riparian Arthropod Abundance and Diversity as a Consequence of Giant Reed (*Arundo donax*) Invasion". *Biological Invasions,* vol. 5, pp.167-177

Kelly, M.W. (1977). "Critical Literature Review of Relationships Between Processing Parameters and Physical Properties of Particleboard", Gen.Tech. Rept. FPL-10. USDA Forest Serv., Forest Prod.Lab., Madison, Wisconsin, USA

Kim, S. (2009). "Environmental-friendly Adhesive for Surface Bonding of Wood-Based Flooring using Natural Tannin to Reduce Formaldehyde and TVOC Emission". *Journal of Hazardous materials*, vol. 100, pp. 744-748

Lee, J.H., Jeon, J. and Kim, S.(2011). "Green Adhesives using Tannin and Cashew Nut Shell Liquid for Environment- friendly Furniture Materials". *Journal of the Korea furniture Society*, vol. 22(3), pp. 219-229

Lewandowski, I., Scurlock, J.M.O., lindvall, E. and Christou, M. (2003). "The Development and Current Status of Perennial Rhizomatous Grasses as Energy Crops in the US and Europe". *Biomass Bioenergy*, vol. 25, pp. 335-361

Mohsen, S.(2011). "Effect of Hardener Type and Particle Size on Formaldehyde Emission Pollution". *International Conference on Environment Science and Engineering* IPCBEE, vol. 8, pp. 242-244

Moran, P.J. and Goolsby, J.A. (2009). "Biology of the Galling Wasp *Tetramesa romana*, a Biological Control Agent of Giant Reed". *Biological Control,* vol. 49(2), pp. 169-179

Sellers,T. (2000). Growing Markets for Engineered Products Spurs Research. *Wood Technology*, vol. 127(3), pp. 40-43

Shatalov, A. A., Quilho, T and Pereira, H. (2001). " *Arundo donax* L. Reed: New Perspectives for Pulping and Bleaching -1. Raw Material Characterization". *TAPPI J.* vol. 84 (11), pp. 1-12

Shatalov, A.A. and Pereira, H. (2005). "Kinetics of Organosolv Delignification of Fiber Crop *Arundo donax* L*". Ind.Crops Prod,* vol. 21(2), pp. 203-210

Sulaiman.S., Yunus, R., Ibrahim, N.A. and Rezaei, F. (2008). "Effect of Hardener on Mechanical Properties of Carbon Fiber Reinforced Phenolic Resin Composites". *Journal of Engineering Science and Technology*, vol. 3(1), pp. 79-86

Tracy, J.L. and Deloach, C.J. (1999). "Suitability of Classical Biological Control for Giant Reed (*Arundo donax*) in the United States", In Bell C., (ed.), *Arduno* and *Saltcedar* Management Workshop Proceedings, 17 June, 1998, California. University of California Cooperative Extension, Holtville.

Ververis, C., Georghiou, K., Christodoulakis, N., Santas, P. and Santas, R. (2004). "Fiber Dimensions, Lignin and Cellulose Content of Various Plant Materials and Their Suitability for Paper Production". *Ind. Crops Prod*, vol. 19, pp. 245-254

Youngquist, J.A.(1999). Wood-based Composites and Panel Products. In: Wood Hand book: Wood as a Engineering Material. Gen. Tech. Rept. FPL-GRT-113. USDA Forest serv., Forest Prod. Lab., Madison, WI, pp. 1-31

Youngquist, J.A. and Hamilton, T.E. (2000). A look at the World's Timber Resources and Processing Facilities. In: Proceedings of the XXI IUFRO world congress 2000, Sub-plenary sessions, Kualalumpur, Malaysia, vol. 1, pp. 183-190

UTILIZATION OF ACTIVATED DURIAN PEEL AS A SORBENT FOR REMOVAL OF DIRECT BLUE DYE FROM AQUEOUS SOLUTION

Htwe Htwe Mar[1], Khin Than Yee[2], Thinzar Nu[3]

Abstract

In the present study, activated durian (*Durio zibethinus* L.) peel was used as a waste sorbent for the colour removal of direct blue dye (Direct Sky Blue FB 100 %, pH = 8.4) from aqueous solution. This research work concerns with the preparation of acid activated durian peel samples (ADP-1 to ADP-5) by using various amounts (1 to 5 % v/v) of hydrochloric acid. According to the results of some physicochemical properties (bulk density and specific surface area), ADP-4 was chosen for removal of direct blue dye. The sorption capacity of ADP-4 was determined as a function of initial concentration, pH, contact time and dosage of sorbent. The maximum removal percent of direct blue dye was found to be 84.308 % at 150 ppm of initial concentration, pH 8, 90 min of contact time and 0.2 g of dosage. This sample was characterized by using FT IR and SEM analyses before and after sorption. The equilibrium data were applied on isotherm models. According to Langmuir and Freundlich isotherms, the monolayer coverage value (Q_o) was found to be 29.499 mg g^{-1} and the adsorption capacity (K_f) was found to be 4.191 mg g^{-1}. The experimental sorption data were fitted both isotherm models and sorption conditions were favourable. ADP-4 is a good sorbent for direct blue dye (Direct Sky Blue FB 100 %) from aqueous solution.

Keywords: Adsorption, adsorption isotherm, dyes, durian peel

Introduction

Numerous numbers of synthetic dyes are being used in various industries such as textile, leather, paper, printing, food, cosmetics, paint, pigments, petroleum, rubber, plastic, pesticide and pharmaceutical industry for different purpose (Sharmaa and Nandib, 2013). Many dyes are toxic to some organisms causing direct destruction of aquatic communities. Some dyes can cause allergic dermatitis, skin irritation, cancer and mutation in human beings and harmful to aquatic life (Bhanuprakash *et al*., 2015).

Removing color from waste water can be done by using several methods. Among these methods, adsorption method using waste sorbent has been found to be superior due to low cost, simplicity of design, flexibility, ease of operation and insensitivity to toxic pollutants (Baseri *et al.*, 2012).

Previous research has shown that the durian peel consists of holo-cellulose, hemi-cellulose and lignin, indicating the feasibility for removing toxic metal ions, dyes or enriching trace elements from aqueous solutions due to the presence of various interesting functional groups on the cellulose (Saueprasearsit, 2011).

The present study is to explore the sorption capability of acid activated durian peel prepared by treating with 4 % HCl (ADP-4) for removal of direct blue dye (Direct Sky Blue FB 100 %) from aqueous solution.

[1] Lecturer, Department of Chemistry, Sagaing University of Education
[2] Lecturer, Department of Chemistry, Myeik University
[3] Associate Professor, Department of Chemistry, University of Yangon

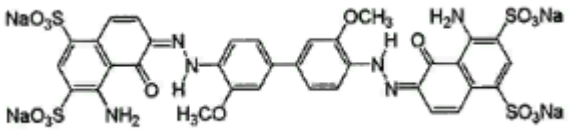

Figure 1 Structure of direct blue dye (Direct Sky Blue FB 100 %)

Materials and Methods

Sample Collection

The durian peels were collected from Tarmwe Market, Tarmwe Township, Yangon Region.

Preparation of Raw Durian Peel Powder

The durian peels were boiled with distilled water. The peels were then dried in oven at 105 ˚C for 12 h. The dried peels were ground to be fine powder by using blender and sieved through 80 mesh sieve. Finally, the raw durian peel powder sample was packed in air-tight container and labeled.

Preparation of Acid Activated Durian Peel Samples (ADP-1 to ADP-5)

10 g of each sample (raw durian peel powder) was soaked with various amounts (1, 2, 3, 4 and 5 % v/v) of hydrochloric acid (100 mL) for 2 h. The samples were washed several times with distilled water until pH 7.0. The obtained five samples were dried in oven at 105 ˚C for 5 h. The samples were then ground to be fine powder by using blender and sieved through 80 mesh sieve. Finally, the acid activated durian peel samples (ADP-1, ADP-2, ADP-3, ADP-4 and ADP-5) were obtained.

Determination of Maximum Wavelengths for Dye Solutions (Methylene Blue and Direct Blue Dye Solutions)

Preparation of stock solutions

Stock dye solutions containing 100 ppm of sorbate were accurately prepared. Methylene blue solutions for determination of specific surface area were prepared by various concentrations ranging from 0.1953 ppm to 6.25 ppm. Direct blue dye solutions for colour removal were prepared by various concentrations ranging from 1.5625 ppm to 50 ppm. In the preparation of dye solutions, distilled water was used as the diluent.

Calibration of dye solutions

To select the maximum adsorption wavelength, for a particular dye, a spectral curve was first plotted by determining the color index (absorbance) of the dye solution as a function of wavelength. In the measurement of the color of the diluted solution, a 1 cm cell was used with distilled water as reference. From the spectral curves, maximum adsorption wavelengths for methylene blue and direct blue dye were observed 605 nm and 550 nm. From the plots of absorbance Vs concentration calibration curve give the slopes of dye solutions (methylene blue and direct blue dye).

Determination of Some Physicochemical Properties of the Five Acid Activated Durian Peel Samples (ADP-1 to ADP-5)

Determination of bulk density

A clean dry 10 mL graduated cylinder was weighed. It was filled with each sample to 10 mL mark and reweighed. The graduated cylinder was placed in a tapping box and the cylinder was tapped gently until there is no more reduction in volume. The minimum volume was recorded and the bulk density was calculated by equation (Bulk density = Weight of sample/ Final volume of sample).

Determination of specific surface area

The specific surface area of the sample was determined by using methylene blue (Langmuir isotherm method)**.** Each sample (0.01 g, 0.02 g, 0.03 g, 0.04 g and 0.05 g) was added to 25 mL of methylene blue solution (40 ppm) individual and was allowed to equilibrate for 60 min in a shaker with 100 rpm. Then, the five sample solutions were kept for 24 h to reach equilibrium. The sample solutions were centrifuged and decanted. The decanted solutions were determined spectrophotometrically at its corresponding λ_{max} (605 nm). The Langmuir plot of C_e / x/m Vs C_e gives a straight line of slope $1/Q_o$. And then the specific surface areas of the samples were calculated by equation $S_{MB} = Q_o \times N_A \times a_{MB} / M_{MB}$ where, x/m is amount of adsorbate adsorbed per unit mass of sorbent (mg g^{-1}), C_e is equilibrium concentration of adsorbate (ppm or mg L^{-1}), Q_o is maximum monolayer coverage capacity (mg g^{-1}), S_{MB} is the specific surface area (m^2 g^{-1}), N_A is Avogadro's number (6.022×10^{23} molecule mol^{-1}), a_{MB} is the occupied surface area of one molecule of methylene blue (120×10^{-20} m^2) and M_{MB} is the molecular weight of methylene blue (373.9 g mol^{-1}).

Sample Selection from the Five Acid Activated Durian Peel Samples

According to the results of some physicochemical properties (bulk density and specific surface area), acid activated durian peel with 4 % HCl (ADP-4) was selected as an sorbent sample for the removal of direct blue dye.

Sorption Studies for the Colour Removal of the Selected Acid Activated Durian Peel (ADP-4)

Effect of initial concentration

Removal of direct blue dye solution by using ADP-4 sample was determined by various initial concentrations from 50 ppm to 300 ppm. Each sample (0.10 g) was added to dye solutions (25 mL) individual and was allowed to equilibrate for 60 min in a shaker with 100 rpm. The sample solutions were centrifuged and decanted. The decanted solutions were determined spectrophotometrically at its corresponding λ_{max} (550 nm). Removal percent of dye was calculated by equation $C_o - C_e / C_o \times 100$ where, C_o = initial concentration (ppm or mg L^{-1}) and C_e = Absorbance / slope = equilibrium concentration (or) final concentration (ppm or mg L^{-1}).

Effect of pH

The effect of pH on the sorption of direct blue dye (150 ppm of initial concentration) was carried out over the pH range from 2 to 10. Dye solutions were adjusted with HCl and NaOH to desire pH. Each sample (0.10 g) was added to dye solutions (25 mL) individual and was allowed

to equilibrate for 60 min in a shaker with 100 rpm. The sample solutions were centrifuged and decanted. The decanted solutions were determined spectrophotometrically at its corresponding λ_{max} (550 nm).

Effect of contact time

The effect of contact time for sorption of dye solutions were determined by keeping other conditions (150 ppm of initial concentration and pH 8). Each sample (0.10 g) was added to dye solutions (25 mL) individual and was allowed to equilibrate for various contact time (30 min to 180 min) in a shaker with 100 rpm. The sample solutions were centrifuged and decanted. The decanted solutions were determined spectrophotometrically at its corresponding λ_{max} (550 nm).

Effect of dosage

The colour removal of dye solutions was determined by various dosages of sample under the optimum conditions (150 ppm of initial concentration, pH 8 and 90 min of contact time). Each sample (0.05 g to 0.35 g) was added to dye solutions (25 mL) individual and was allowed to equilibrate for 90 min of contact time in a shaker with 100 rpm. The sample solutions were centrifuged and decanted. The decanted solutions were determined spectrophotometrically at its corresponding λ_{max} (550 nm).

Characterization of the Selected Acid Activated Durian Peel (ADP-4)

ADP-4 was characterized by modern techniques such as FT IR and SEM analyses before and after sorption.

Results and Discussion

Five Acid Activated Durian Peel Samples (ADP-1 to ADP-5)

The durian peels were collected from Tarmwe Market, Tarmwe Township, Yangon Region. The raw durian peel powder was prepared as described in previous section. Using the raw durian peel powder, the acid activated durian peel samples were then prepared. In the preparation of the acid activated durian peel samples, various amounts (1, 2, 3, 4 and 5 % v/v) of hydrochloric acid were used. Finally, the five acid activated durian peel samples (ADP-1, ADP-2, ADP-3, ADP-4 and ADP-5) were obtained.

Some Physicochemical Properties of the Five Acid Activated Durian Peel Samples (ADP-1 to ADP-5)

Some physicochemical properties (bulk density and specific surface area) of the five acid activated durian peel samples (ADP-1 to ADP-5) were determined by recommended methods. The results are shown in Table 1. From the experimental results, the acid activated durian peel prepared by treating with 4 % HCl (ADP-4) was observed the highest bulk density and specific surface area. The highest bulk density and specific surface area, the more effective sorbent property can exist. Thus, ADP-4 was the more effective than the other four sorbents.

Table 1 Some Physicochemical Properties of the Five Acid Activated Durian Peel Samples (ADP-1 to ADP-5)

Sorbent samples	Bulk density ($g\ cm^{-3}$)	Specific surface area ($m^2\ g^{-1}$)
Acid activated durian peel with 1 % (v/v) HCl (ADP-1)	0.387	244.647
Acid activated durian peel with 2 % (v/v) HCl (ADP-2)	0.396	247.783
Acid activated durian peel with 3 % (v/v) HCl (ADP-3)	0.421	264.755
Acid activated durian peel with 4 % (v/v) HCl (ADP-4)	0.432	268.432
Acid activated durian peel with 5 % (v/v) HCl (ADP-5)	0.406	257.695

Sample Selection from the Five Acid Activated Durian Peel Samples

According to the Table 1 results, the acid activated durian peel prepared by treating with 4 % HCl (ADP-4) was the highest bulk density and surface area. The higher the bulk density of the sorbents, the more porosity on the surface of sorbents can exist. In addition, the higher the surface area, the more effective sorbent property can exist. ADP-4 was selected as the best sorbent sample for removal of direct blue dye.

Colour Removal of Direct Blue Dye by the Selected Acid Activated Durian Peel (ADP-4)

Effect of initial concentration

For this study, initial concentrations of direct blue dye solution were varied from 50 ppm to 300 ppm. The results are shown in Table 2 and Figure 2. It was found that as the removal percent of dye decreases with increasing in initial concentration. This is related to the availability of active sites on the sorbent surface. After 150 ppm of dye solution is reached, the removal percent decreased rapidly. Therefore, 150 ppm of dye solution was chosen as the optimum initial concentration. The removal percent was 46.051 % with respect to 150 ppm of initial concentration.

Table 2 Effect of Initial Concentration on the Removal of Direct Blue Dye by the Selected Acid Activated Durian Peel (ADP-4)

Initial concentration (ppm)	Final concentration (ppm)	Removal percent (%)
50	22.769	54.462
100	48.769	51.231
150	80.923	46.051
200	130.000	35.000
250	175.077	29.969
300	219.692	26.769

pH = 8.4
Dosage = 0.10 g/ 25 mL
Contact time = 60 min
Stirring rate = 100 rpm

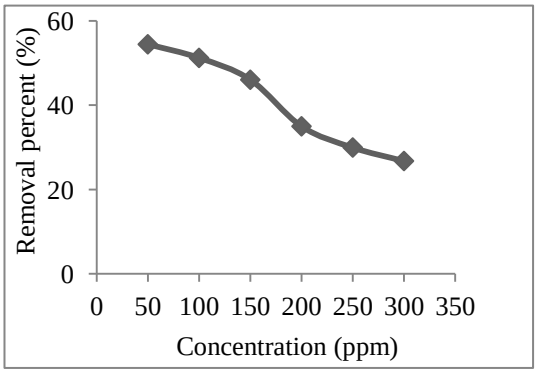

Figure 2 Removal percent of direct blue dye by the selected acid activated durian peel (ADP-4) as a function of initial concentration at pH 8.4, 0.10 g/ 25 mL of dosage and 60 min of contact time

Effect of pH

The effect of pH on the sorption of direct blue dye was carried out over the pH range from 2 to 10. The results are shown in Table 3 and Figure 3. In this experiment, fixed amount of the sample (0.10 g/ 25 mL) and optimum concentration (150 ppm) were used. It can be seen that increase in pH, the removal percent also increases up to pH 8. Beyond pH 8, the removal percent decreases with increasing pH. Almost all the active sites of the sorbent might have been saturated at pH 8. Thus, pH 8 was chosen as optimum pH.

Table 3 Effect of pH on the Removal of Direct Blue Dye by the Selected Acid Activated Durian Peel (ADP-4)

pH	Final concentration (ppm)	Removal percent (%)
2	110.000	26.667
3	102.615	31.590
4	99.692	33.538
5	94.769	36.821
6	88.923	40.718
7	83.231	44.513
8	80.308	46.462
9	81.538	45.641
10	82.769	44.821

Initial concentration = 150 ppm
Dosage = 0.10 g/ 25 mL
Contact time = 60 min
Stirring rate = 100 rpm

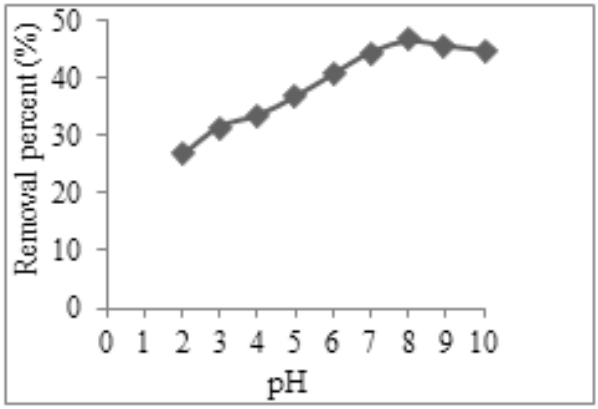

Figure 3 Removal percent of direct blue dye by the selected acid activated durian peel (ADP-4) as a function of pH at 150 ppm of initial concentration, 0.10 g/ 25 mL of dosage and 60 min of contact time

Effect of contact time

At optimum conditions (150 ppm of initial concentration and pH 8), different periods of time (30 min to 180 min) were used for the sorption of direct blue dye by ADP-4. The results are shown in Table 4 and Figure 4. It was found that the removal percent of direct blue dye increases with increasing in contact time. After 90 min contact time had been reached, the removal percent increased slowly. Thus, 90 min was chosen as optimum contact time. The removal percent of dye being adsorbed was 55.692 % at optimum contact time.

Table 4 Effect of Contact Time on the Removal of Direct Blue Dye by the Selected Acid Activated Durian Peel (ADP-4)

Time (min)	Final concentration (ppm)	Removal percent (%)
30	110.923	26.051
60	80.615	46.256
90	66.462	55.692
120	63.077	57.949
150	62.154	58.564
180	59.538	60.308

Initial concentration = 150 ppm
pH = 8
Dosage = 0.10 g/ 25 mL
Stirring rate = 100 rpm

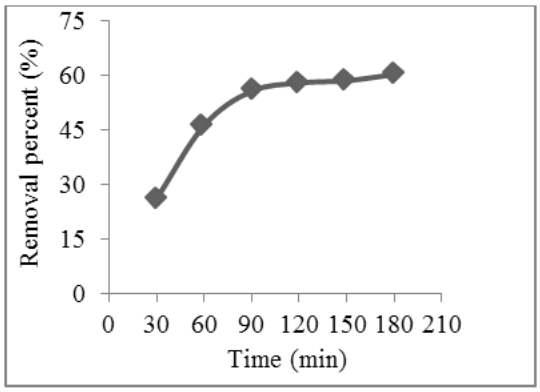

Figure 4 Removal percent of direct blue dye by the selected acid activated durian peel (ADP-4) as a function of contact time at 150 ppm of initial concentration, pH 8 and 0.10 g/ 25 mL of dosage

Effect of dosage

The colour removal of direct blue dye was also determined by various dosages from 0.05 g to 0.35 g under the optimum conditions (150 ppm of initial concentration, pH 8 and 90. min contact time). The results are shown in Table 5 and Figure 5. It was found that the removal percent increases with increasing in sorbent dosage. This is due to the presence of numerous active sites in sorbent. After 0.2 g of sorbent dosage has been reached, the removal percent became steadily increased. Based on the results, 0.2 g was taken as the suitable sorbent dosage for the removal of direct blue dye. The removal percent of dye being adsorbed for 0.2 g of dosage was 84.308 %.

Table 5 Effect of Dosage on the Removal of Direct Blue Dye by the Selected Acid Activated Durian Peel (ADP-4)

Dosage (g)	Final concentration (ppm)	Removal percent (%)
0.05	100.154	33.231
0.10	66.615	55.590
0.15	42.769	71.487
0.20	23.538	84.308
0.25	18.000	88.000
0.30	14.000	90.667
0.35	10.461	93.026

Initial concentration = 150 ppm
pH = 8
Contact time = 90 min
Stirring rate = 100 rpm

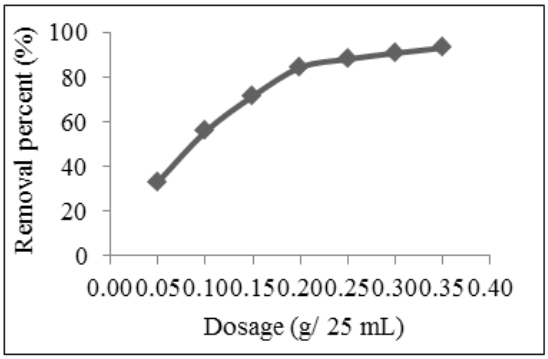

Figure 5 Removal percent of direct blue dye by the selected acid activated durian peel (ADP-4) as a function of dosage at 150 ppm of initial concentration, pH 8 and 90 min of contact time

Characterization of the Selected Acid Activated Durian Peel (ADP-4)

The SEM analysis was performed to observe the surface morphology of the sorbents before and after sorption. Figure 6 (a) shows the surface morphology of ADP-4 before sorption. It was full of cavities due to the modification using activating agent. After sorption, its surface became much smoother and lack of cavities as shown in Figure 6 (b). This is demonstrated that the cavities in the sorbent's surface was almost well occupied with direct blue dye.

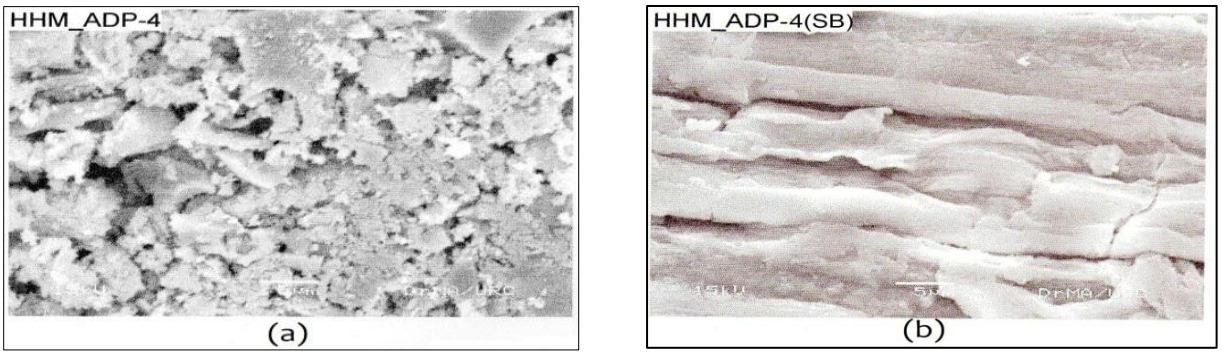

Figure 6 Scanning electron micrographs of the selected acid activated durian peel (ADP-4) (a) before sorption (b) after sorption of direct blue dye

Figures 7 (a) and (b) show the FT IR spectra of ADP-4 before and after sorption of direct blue dye. The peaks at 3337 cm^{-1}, 2921 cm^{-1}, 1631 cm^{-1}, 1429 cm^{-1}, 1369 cm^{-1}, 1315 cm^{-1}, 1240 cm^{-1} and 1156 cm^{-1} were shifted after sorption. It can also be seen that change in intensities of peaks. The facts that generally indicate a process of dye interacts with the sorbent surface. Besides, O-H, C-H and C-O functional groups are involved in sorption process.

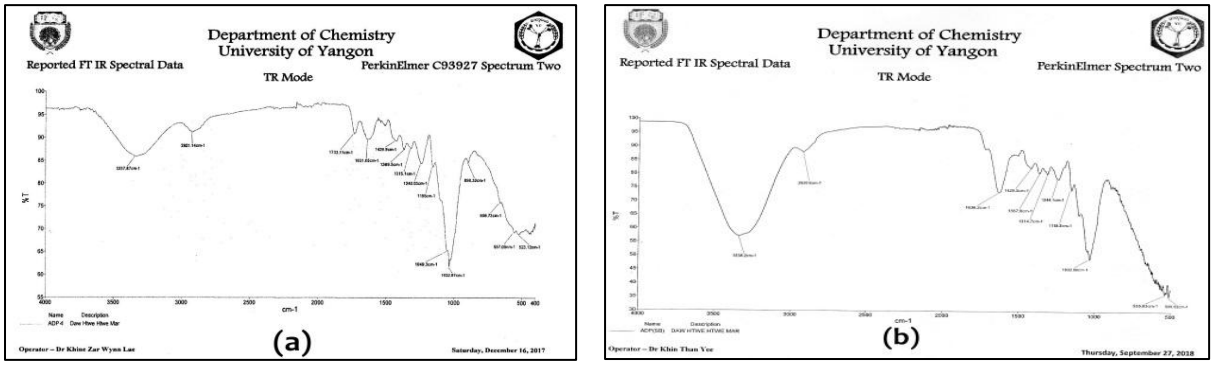

Figure 7 FT IR spectra of the selected acid activated durian peel (ADP-4) (a) before sorption (b) after sorption of direct blue dye

Table 6 FT IR Band Assign of the Selected Acid Activated Durian Peel (ADP-4) before and after Sorption of Direct Blue Dye

Observed wave number (cm^{-1})		*Literature wave number range (cm^{-1})	Band assign
Before sorption	After sorption		
3337	3338	3600-3200	υ_{O-H}
2921	2920	3000-2800	υ_{C-H} (aliphatic)
1733	-	1770-1710	$\upsilon_{C=O}$
1631	1638	1650-1600	$\upsilon_{C=C}$
1429	1426	1470-1350	δ_{C-H} (CH_2 & CH_3 deformation)
1369	1367	1400-1300	δ_{C-H}
1315	1314	1320-1200	υ_{C-O-C} (acid)
1240	1244	1280-1240	υ_{C-O}
1155	1158	1240-1070	υ_{C-O-C}
1049	-	1065-1015	υ_{C-O} in cyclic alcohols
1032	1032	1045-1015	δ_{C-H}
898	-	900-690	δ_{C-H}
659	-	680-620	δ_{C-O-H}
523	535	565-520	$\delta_{C-C=O}$

* Silverstein *et al.*, 1998

Adorption Isotherms

Langmuir isotherm

The Langmuir isotherm assumes that sorption occurs at specific homogeneous sites in the adsorbent and the adsorption capacity of the adsorbent is finite.

Langmuir sorption equation is $x/m = Q_o\, b\, C_e / (1 + b\, C_e)$. The linearized Langmuir equation is given as: $C_e / x/m = (1 / Q_o\, b) + (C_e / Q_o)$ where, x/m is the amount of sorbate adsorbed per unit mass of sorbent (mg g^{-1}), C_e is the equilibrium concentration of adsorbate (mg L^{-1}), Q_o is the maximum monolayer coverage capacity (mg g^{-1}) and b is Langmuir constant (L mg^{-1}) (Nethaji *et al.*, 2013).

Table 7 represents Langmuir data for sorption of direct blue dye by ADP-4 and Langmuir isotherm is shown in Figure 8. From the slope and intercept of the linear plot of the Langmuir isotherm Langmuir constants and separation factor were obtained. The values of the Langmuir constants Q_o and b with the correlation coefficient (R^2) are listed in Table 8. Based on the effect of separation factor on isotherm shape (Figure 8), the R_L value is in the range of $0 < R_L < 1$, which indicates that the sorption of dye solution on ADP-4 was favourable.

Table 7 Langmuir Data for the Sorption of Direct Blue Dye by the Selected Acid Activated Durian Peel (ADP-4)

Weight of sample, m(g)	Final concentration, C_e (mg L^{-1})	Amount of adsorbed, x (mg)	x/m (mg g^{-1})	C_e / x/m (g L^{-1})
0.05	100.154	1.246	24.920	4.019
0.10	66.615	2.085	20.850	3.195
0.15	42.769	2.681	17.873	2.393
0.20	23.538	3.162	15.810	1.489
0.25	18.000	3.300	13.200	1.364
0.30	14.000	3.400	11.333	1.235
0.35	10.461	3.488	9.966	1.050

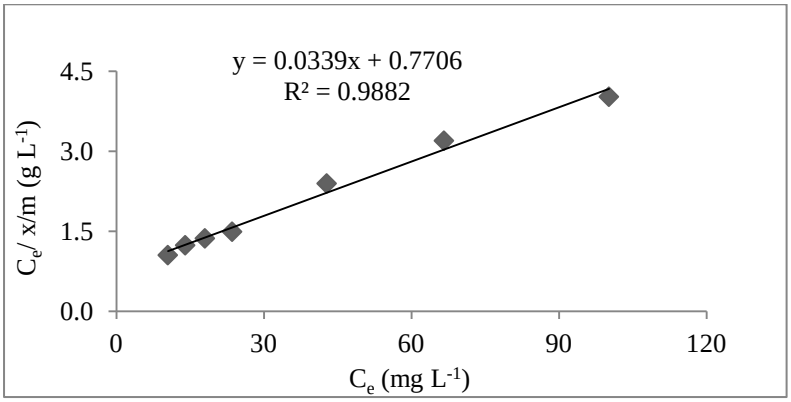

Figure 8 Langmuir isotherm: Sorption of direct blue dye by the selected acid activated durian peel (ADP-4)

Table 8 Langmuir Parameters for the Sorption of Direct Blue Dye by the Selected Acid Activated Durian Peel (ADP-4)

Langmuir parameters			R^2
Q_0 (mg g^{-1})	b (L mg^{-1})	R_L	
29.499	0.044	0.132	0.9882

Freundlich isotherm

The Freundlich isotherm model assumes that the uptake of dyes occurs on a heterogeneous surface by multilayer adsorption and that the amount of adsorbate adsorbed increases infinitely with an increase in concentration.

Freundlich sorption equation is $x/m = K_f C_e^{1/n}$. The linearized Freundlich equation is given as: $\log x/m = \log K_f + 1/n \log C_e$ where, x/m is the amount of sorbate adsorbed per unit mass of sorbent (mg g^{-1}), C_e is the equilibrium concentration of adsorbate (mg L^{-1}), K_f is Freundlich constant (mg g^{-1}) and n is adsorption intensity (L mg^{-1}) (Nethaji *et al.,* 2013).

Table 9 represents Freundlich data for sorption of direct blue dye by ADP-4 and Freundlich isotherm is shown in Figure 9. This figure showed the straight line. The values of the Freundlich constants K_f and 1/n with the correlation coefficient (R^2) are listed in Table 10.

The adsorption intensity (n) value of dye sorption for ADP-4 lies between 1 and 10, thus indicating a favourable.

Table 9 Freundlich Data for the Sorption of Direct Blue Dye by the Selected Acid Activated Durian Peel (ADP-4)

Weight of sample, m (g)	Final concentration, C_e (mg L^{-1})	Amount of adsorbed, x (mg)	x/m (mg g^{-1})	Log C_e	Log x/m
0.05	100.154	1.246	24.920	2.001	1.397
0.10	66.615	2.085	20.850	1.824	1.319
0.15	42.769	2.681	17.873	1.631	1.252
0.20	23.538	3.162	15.810	1.372	1.199
0.25	18.000	3.300	13.200	1.255	1.121
0.30	14.000	3.400	11.333	1.146	1.054
0.35	10.461	3.488	9.966	1.020	0.999

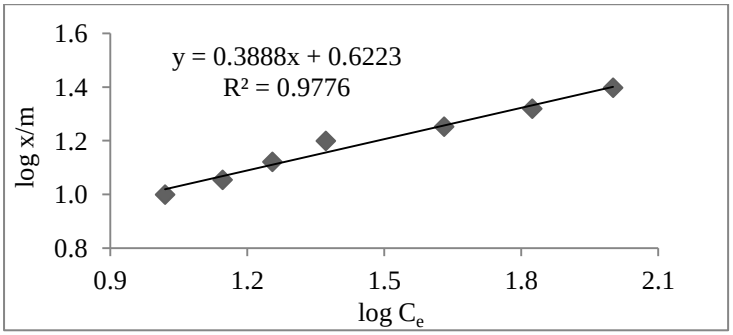

Figure 9 Freundlich isotherm: Sorption of direct blue dye by the selected acid activated durian peel (ADP-4)

Table 10 Freundlich Parameters for the Sorption of Direct Blue Dye by the Selected Acid Activated Durian Peel (ADP-4)

Freundlich parameters		R^2
K_f (mg g^{-1})	n	
4.191	2.572	0.9776

Conclusion

In this study, durian peel as a waste sorbent was used for the removal of direct blue dye (Direct Sky Blue FB 100 %) from aqueous solution. The five Acid activated durian peel samples (ADP-1 to ADP-5) were prepared by treating with various amounts (1 to 5 % v/v) of hydrochloric acid. According to the some physicochemical properties, the acid activated durian peel prepared by treating with 4 % HCl (ADP-4) has the higher bulk density and specific surface area than the other four samples. Thus, ADP-4 was selected as the best sorbent sample for removal of direct blue dye. The effects of various parameters on ADP-4 were investigated in the sorption process. From the results, it was found that 150 ppm of initial concentration, pH 8, 90 min of contact time and 0.2 g in 25 mL of dosage as the optimum conditions. The maximum removal percent of direct blue dye by ADP-4 was observed 84.308 %. In SEM analysis, cavities

from sorbent's surface became much smoother and lack of cavities after sorption of direct blue dye. In FT IR analysis, interaction between dye and sorbent was investigated by the change in intensities and shift of peaks after sorption. O-H, C-H and C-O functional groups participated in sorption process. The adsorption isotherm equations were also applied to check the feasibility of sorption process. From Langmuir isotherm studies, monolayer coverage value (Q_o) was found to be 29.499 mg g^{-1}. From Freundlich isotherm studies, adsorption capacity (K_f) was found to be 4.191 mg g^{-1}. According to these equilibrium data, dye sorbent system fitted both isotherm models and indicated that the sorption conditions were favourable. The results showed that the selected acid activated durian peel (ADP-4) could be used as an effective sorbent for the colour removal of direct blue dye (Direct Sky Blue FB 100 %) from aqueous solution.

Acknowledgements

The authors would like to express their profound gratitude to the Myanmar Academy of Arts and Science for giving permission to submit this paper. We are grateful to Rector Dr Saw Pyone Naing and Pro Rector Dr Myat Myat Thaw from Sagaing University of Education, for their kind encouragement. We also thank to Professor Dr Kathy Myint Thu, Head of Department of Chemistry, Sagaing University of Education, for her help and valuable advice.

References

Baseri, J. R., Palanisamy, P. N. and Sivakumar, P. (2012). "Adsorption of Reactive Dye by a Novel Activated Carbon Prepared from *Thevetia peruviana*". *Int. J. of Chem. Res*. vol. 3 (2), pp. 36-41

Bhanuprakash, M., Belagali, S. L. and Geetha, K. S. (2015). "Removal of Dyes from Aqueous Solution Using Coral Wood Tree Legume as Natural Adsorbent". *An Int. Quarierly J. of Environ. Sci.* vol. 9 (1&2), pp. 123-126

Nethaji, S., Sivasamy, A. and Mandal, A. B. (2013). "Adsorption Isotherms, Kinetics and Mechanism for the Adsorption of Cationic and Anionic Dyes onto Carbonaceous Particles Prepared from *Juglans regia* Shell Biomass". *Int. J. Environ. Sci. Technol*. vol.10, pp. 231-242

Saueprasearsit, P. (2011). "Adsorption of Chromium (Cr^{6+}) Using Durian Peel". *Int. Conference on Biotechnol. & Environ. Management*. vol. 18, pp. 33-38

Sharmaa, N. and Nandib, B. K. (2013). "Utilization of Sugarcane Baggase, an Agricultural Waste to Remove Malachite Green Dye from Aqueous Solutions". *J. Mater. Environ. Sci.* vol. 4 (6), pp. 1052-1065

Silverstein, R. M., Webster, F. X. and Kiemle, D. J. (2005). *Spectrometric Identification of Organic Compounds.* New York: 7^{th} Ed^{n}., John Willey & Sons, Inc. pp. 1-550

INVESTIGATION OF ANTIDIABETIC ACTIVITY AND STRUCTURAL ELUCIDATION OF DIHYDROCHALCONE COMPOUND ISOLATED FROM MYANMAR TRADITIONAL MEDICINAL PLANT, *Grewia nervosa* (Lour.) Panigrahi

Swe Swe Mon[1], Arnt Win[2], Aye Mon Thida Nyo[3]

Abstract

Grewia nervosa (Lour.) Panigrahi was distributed in Bangladesh, India, Sri Lanka, Cambodia, Laos, Thiland, Vietnam, Indonesia, Malaysia and Myanmar and it is locally called in Myanmar as Mya-yar. The roots of Mya-yar were collected from Pyin Oo Lwin Township, Mandalay Region, Myanmar. Antidiabetic effect of methanol extract of root of *G. nervosa* was done at Department of Biotechnology, Mandalay Technological University, Pathein Gyi Township, Mandalay Region, Myanmar. In addition, dihydrochalcone compound was isolated from ethyl acetate extract of the selected sample by thin layer and column chromatography methods. The structure of this compound was elucidated by analysis of NMR spectroscopic and mass spectrometric data.

Keywords: thin layer and column chromatography, dihydrochalcone, Antidiabetic effect, *Grewia nervosa* (Lour.) Panigrahi, NMR

Introduction

Medicinal plants have played an essential role in the development of human culture. Plants are resources of traditional medicines and many of the modern medicines are produced in directly from plants. It has been confirmed by WHO that herbal medicines serve the health needs of about 80 percent of the world's population; especially for millions of people in the vast rural areas of developing countries (Ahmadreza *et al*, 2015).

According to traditional beliefs in Myanmar, there are 96 diseases which afflict humans (Fame Pharmaceuticals, 2012). The belief in turning to nature to heal and cure is strong in nearly all Asian nations and in Myanmar. Traditional medicine treatments have been followed in Myanmar for generations and continue to be popular even today, though more in remote rural areas, not least due to non availability of western medicines. Traditional medicine uses plants and herbs to make powders, gels and tablets for treating disease and body disorders (Goldstein, 2000).

Diabetes mellitus refers to a group of diseases that affect how human body uses blood sugar (glucose). Glucose is vital to human's health because it is an important source of energy for the cells that make up muscles and tissues. It's also brain's main source of fuel. Chronic diabetes conditions include type 1 diabetes and type 2 diabetes. Diabetes symptoms vary depending on how much blood sugar is elevated (Dreschfeld, 1886).

Diabetes is a group of metabolic diseases characterized by hyperglycemia resulting from defects in insulin secretion, insulin action or both. The chronic hyperglycemia of diabetes is associated with long- term damage, dysfunction, and failure of different organs, especially the eyes, kidneys, nerves, heart, and blood vessels (Knowler *et* al, 2002).

Type 1diabetes (insulin-dependent diabetes mellitus) is an autoimmune disease in which the pancreas is unable to produce enough of a hormone called insulin. This reduced insulin production results in a higher than normal level of glucose in the blood – a condition called hyperglycemia (Dillon *et al*, 1936).

[1] Dr, Assistant Lecturer , Department of Chemistry, Sagaing University of Education
[2] Associate Professor, Department of Chemistry, Kyaukse University
[3] Associate Professor, Department of Chemistry, University of Mandalay

This form of diabetes, which accounts for nearly 90- 95 % of those with diabetes, previously referred to as non- insulin- dependent diabetes, type 2 diabetes, or adult-onset diabetes, encompasses individuals who have insulin resistance and usually have relative insulin deficiency (Meena *et al*, 2014).

G. nervosa, belonging to the family Malvaceae, is widely distributed along the Western Ghats of India. Although it has been commonly used in traditional medicine, the medicinal properties have not been scientifically evaluated. This plant contains phytochemical compounds and antioxidant activity. These results suggest that *G. nervosa* would be a potential source for treatment of diabetes and its associated complication such as oxidative stress and inflammation (Meena *et al*, 2014).

The aims of present research work are to evaluate antidiabetic activity and to elucidate the structure of isolated dihydrochalcone compound from root of Myanmar indigenous medicinal plant, *G. nervosa* (Figure 1).

Botanical Description

Figure 1 Leaves and roots of *Grewia nervosa* (Lour.) Panigrahi

Botanical name	: *Grewia nervosa* (Lour.) Panigrahi
Family	: Malvaceae
Myanmar name	: Mya- yar
Part used	: Roots
Distribution	: Bangladesh, India, Sri Lanka, Cambodia, Laos, Thiland, Vietnam, Indonesia, Malaysia and Myanmar (Ayeyarwady, Bago, Mangalay, Taninthayi, Yangon Regions and Mon State) (Panigrahi, 1985)
Medicinal uses	: Diabete mellitus, coughs, indigestion, eczema, itchy, small-pox, typhoid fever, dysentery and syphilitic ulceration of the mouth (Deepa *et al*, 2016)

Materials and Methods

Plant Material

The roots of *Grewia nervosa* (Lour.) Panigrahi, Myanmar named Mya-yar were collected from Pyin Oo Lwin Township, Mandalay Region, Myanmar, in June 2015.

Evaluation of Antidiabetic Activity

The selected *Mus musculus* mice were randomly divided into three groups such as positive control group, tested plant extract group and negative control group. Each group contains three animals. These mice were prepared to cause hyperglycemia by using adrenaline injection (Figure 2). For giving adrenaline injection, the selected mice were fasted overnight. The

animals were given intraperitoneally with adrenaline 0.2 mL/kg body weight in distilled water. They were starved for 4 hr after injection and then they were given 0.5 mL of glucose solution orally at hourly interval to prevent hypoglycemic shock. They were offered unlimited amounts of standard laboratory diet food and water. Mice were fasted for 18 hours prior to drug administration allowing access only to water (Figure 3). Before the drugs and vehicle administration, base line fasting blood sugar levels were measured Ominitest Glucometer in all groups.

In this experiment, the dosage of methanol extract of root of *G. nervosa* was calculated on the body weight basic for each animal. Before giving the extract to the animals, the methanol extract was dissolved in distilled water. After that, the following procedures were done.

1. Blood glucose levels of all mice were measured by Glucometer and test strips.
2. Positive control group was treated with standard drug Glibenclamide 0.5 mg/kg.
3. Sample control group was treated with 0.5 mg/kg of methanol extract sample solution.
4. Negative control group was treated with 0.5 mg/kg of distilled water.

During the experimental procedure, three observations were performed at five times (225 min) of 45 min interval after orally administration of the plant extract, Glibenclamide and distilled water by using Glucometer and test strips. The results were collected from each group for the data analysis.

(a) (b)

Figure 2 (a) Both sexes of 30 g *Mus musculus* mouse
(b) Injected adrenaline subcutaneously

(a) (b)

Figure 3 (a) Oral administration of plant extract
(b) Measured blood glucose level with Omniltest plus glucometer

Extraction and Isolation

The air-dried roots of Mya-yar were percolated with ethanol at room temperature for one month. The ethanol extract was concentrated and the residue (28.1 g) was extracted with ethyl acetate. The ethyl acetate extract was concentrated to produce a residue (2.88 g). The extract was fractionated on a silica gel column using *n*- hexane and ethyl acetate gradient to afford fifteen fractions (frs 1- 12). Fraction 9 was recrystallized by 25 % ethyl acetate in *n*- hexane to yield dihydrochalcone compound (21.5 mg).

Structural Elucidation of Dihydrochalcone Compound

The spectra of isolated pure compound were measured by ^{1}H NMR (500 MHz), ^{13}C NMR (125 MHz), DEPT, HMQC, DQF-COSY, HMBC and EI-MS at Meijo University, Nagoya, Japan.

Results and Discussion

Antidiabetic Activity of Methanol Plant Extract

The mean blood glucose levels of adrenaline induced hyperglycemic mice in methanol plant extract treated group, positive control group and negative control group were shown in Table 1.

Table 1 Antidiabetic Effect of Methanol Extract of Root of Mya-yar on Hyperglycemic Mouse Models

Group	Blood Glucose Level Mean ± SD (mg/dL)					
	0 min	**45 min**	**90 min**	**135 min**	**180 min**	**225 min**
Tested plant extract	119±2.12	252±2.00	162±2.00	126±2.00	134±3.08	123±6.92
Positive control	123±9.33	265±3.24	185±2.35	127±1.58	128±5.79	104±2.35
Negative control	118±2.65	272±2.55	239±2.00	244±1.58	228±1.58	174±2.55

SD = Standard Deviation, Tested plant extract = MeOH extract,
Positive control = Glibenclamide drug, Negative control = Distilled water

The mean blood glucose levels of tested plant extract group, positive control group and negative control group were calculated and the changes in blood glucose levels of all groups are illustrated in Figure 4.

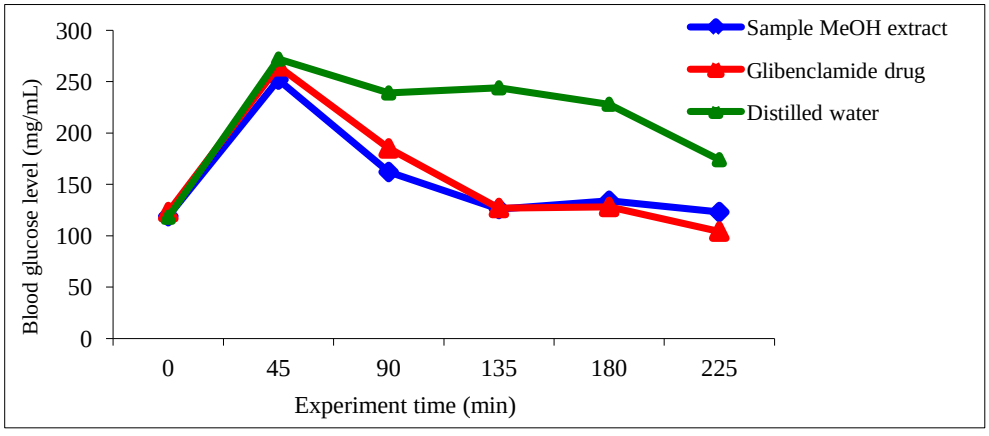

Figure 4 Changes of mean blood glucose levels of test group and control groups

The mean blood sugar levels of tested plant extract group showed hypoglycemic activity against the hyperglycemia response to adrenaline. There was significant reduction of fasting blood sugar level of test group compared with positive control group in this current study at 45, 90, 135, 180 and 225 min.

Determination of Structure of Dihydrochalcone Compound

The structure of isolated pure compound was elucidated by ^{1}H NMR (500 MHz), ^{13}C NMR(125 MHz), DEPT, HMQC, DQF-COSY, HMBC and EI-MS spectra (Figure 5, 6, 7 and 8).

Dihydrochalcone Compound: FT IR (KBr) : (cm^{-1}) 3341.1 (-OH), 3072.6, 3000.6 (=CH), 2931.4, 2834.5 (Sat-H/C), 1657.9 (C=O), 1649.6, 1605.3, 1575.81, 1504.72 (ArH), 1364.4, 1336.7 (C-OH), 1206.73 (C-C-O), 1167.9, 1154.02, 1122.23 (C-O-C): ^{1}H NMR (500 MHz, CD_3OD) δ: 2.86 (2H, t, J= 7.23, H-2), 3.10 (2H, t, J= 7.23, H-3), 6.46 (1H, d, J= 2.42, H-2′), 7.00 (1H, d, J= 8.22, H-5′), 6.39 (1H, dd, J= 2.42, 8.22, H-6′), 6.82 (1H, d, J= 6.80, H-5″), 7.88 (1H, d, J= 6.80, H-6″), ^{13}C NMR (125 MHz, CD_3OD) δ: 201.46 (C-1), 26.75 (C-2), 39.75 (C-3), 122.71 (C-1′), 99.28 (C-2′), 161.05 (C-3′), 159.65 (C-4′), 131.19 (C-5′), 105.26 (C-6′), 129.97 (C-1″), 131.86 (C-2″, 6″), 116.18(C-3″, 5″), 163.68 (C-4″), EI-MS *m/z* (rel.int.): 286 [M^{+}] ($C_{17}H_{18}O_4$).

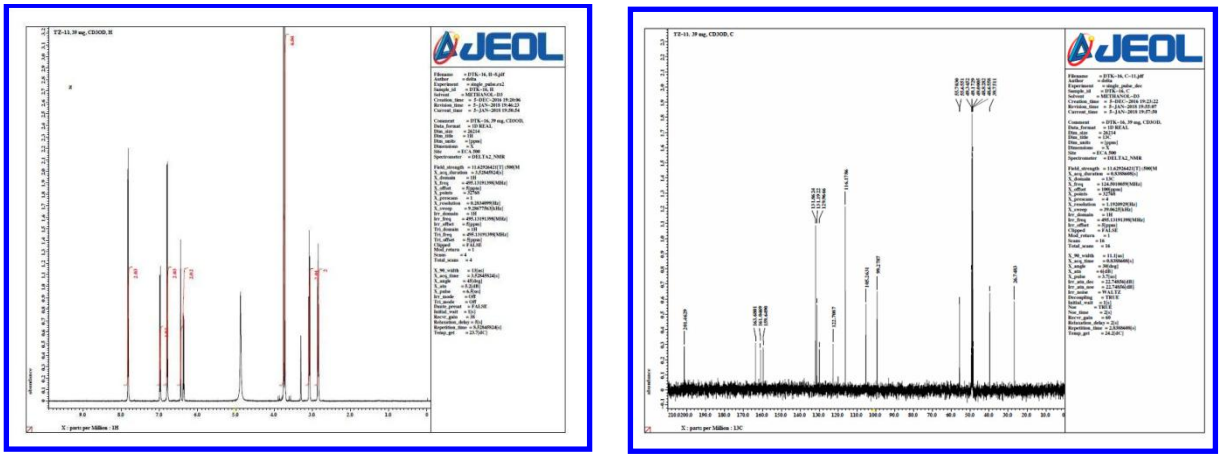

(a) (b)

Figure 5 (a) ^{1}H NMR and (b) ^{13}C NMR spectra of dihydrochalcone compound

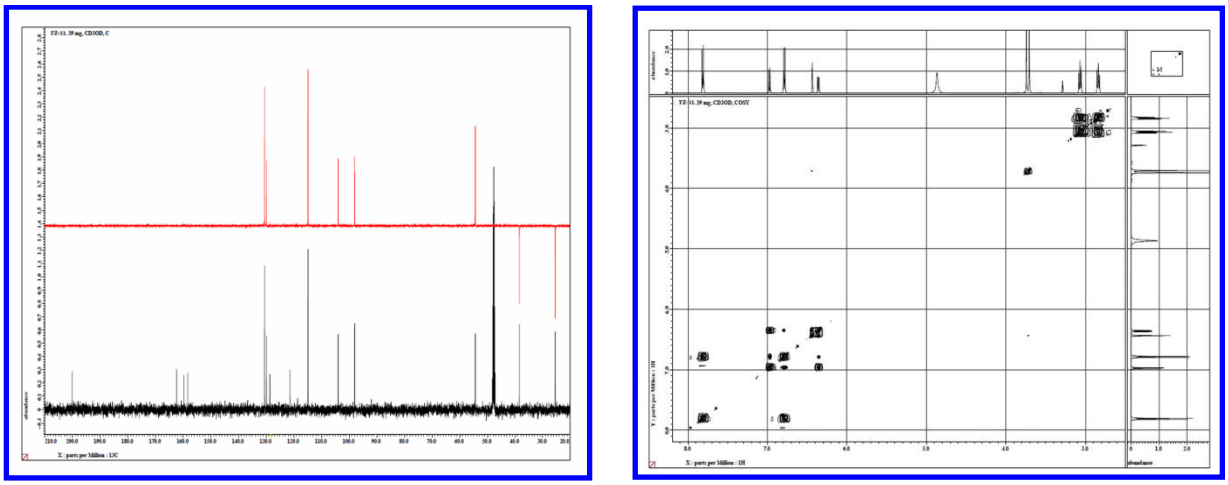

(a) (b)

Figure 6 (a) DEPT and (b) DQF-COSY spectra of dihydrochalcone compound

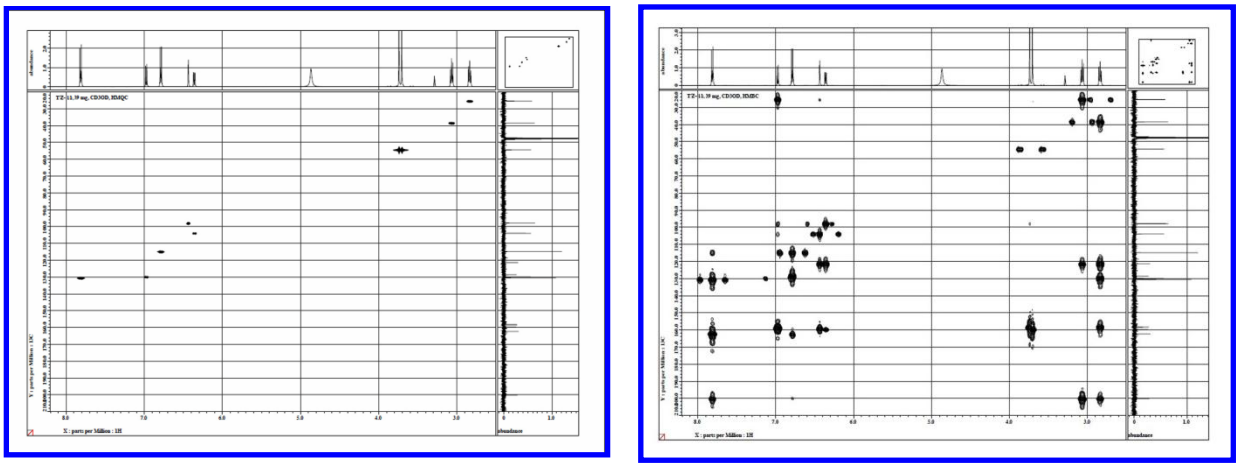

(a) (b)

Figure 7 (a) HMQC and (b) HMBC spectra of dihydrochalcone compound

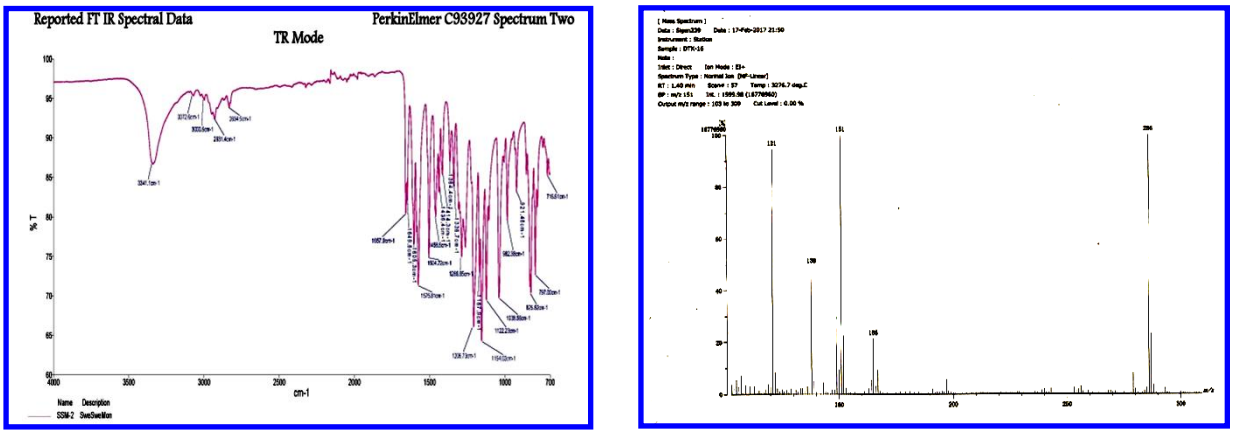

(a) (b)

Figure 8 (a) FT IR and (b) EI-MS spectra of dihydrochalcone compound

According to these spectral data, the molecular formula of this dihydrochalcone compound, yellow needle shape crystal was found to be ($C_{17}H_{18}O_4$) from the observation of a molecular ion peak at *m/z* 286 [M^+] on EI- mass spectrometry. Elucidated structure of isolated compound could be identified with the previous reported data of dihydrochalcone compound.

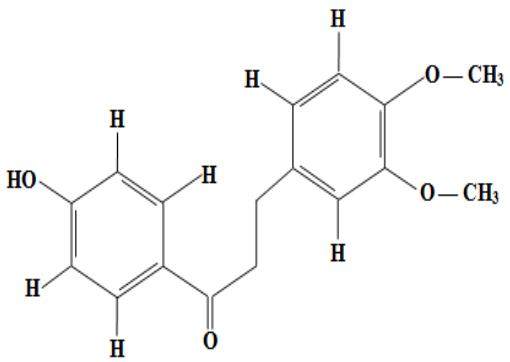

Figure 9 Structure of dihydrochalcone compound

Table 2 ^{13}C, ^{1}H NMR Spectral Data of Dihydrochalcone Compound and ^{1}H -^{13}C, ^{1}H-^{1}H Correlation Exhibited in NMR Spectra in CD_3OD

Carbon.	^{13}C(DEPT)	1H(J,Hz)	HMBC correlation	COSY correlation
1	26.75	2.86	C-1, C-1′	H-3
2	39.75	3.10	C-1, C-1′	H-2
3	55.65	3.73	CH_3, C-3′	-
4	55.70	3.76	CH_3, C-4′	-
5	99.28	6.46	-	H-6′
6	105.26	6.39	C-1′	H-5′, H-2′
7	116.18	6.82	C-1″	H-6″
8	122.71	-	-	-
9	129.97	-	-	-
10	131.19	7.00	C-4′, C-3′	H-6′
11	131.86	7.88	C-4″, C-1	H-5″
12	159.65	-	-	-
13	161.05	-	-	-
14	163.68	-	-	-
15	201.46	-	-	-

Conclusion

In the present investigation, antidiabetic activity of methanol extract of root of Mya-yar was tested by comparing control groups. At the end of the experiment, methanol extract of plant sample was significantly observed to possess the anti-diabetic effect as the standard drug. These results suggest that *Grewia nervosa* (Lour.) Panigrahi would be a potential source for the treatment of diabetes. Moreover, the isolation of dihydrochalcone compound was described. Further studies are required and are in progress here.

Acknowledgements

We wish to express my special thanks to Dr Saw Pyone Naing, Rector and Dr Kay Thi Myint Thu, Professor and Head, Department of Chemistry, Sagaing University of Education for their permission, valuable guidance and encouragement throughout the study. We are very much thankful to Dr Soe Myint Aye, Pro-rector, Myitkyina University and Dr Nwe Nwe Yi, Professor and Head, Department of Biology, Sagaing University of Education, for their helpful and confirmations on scientific name of Mya-yar used in this research. I wish to express our special thanks to our Professors, Dr Yi Yi Myint, Professor and Head and Dr Myint Myint Sein, Professor and Head (Retd:), Department of Chemistry, University of Mandalay for their invaluable help, close supervision, guidance and advice throughout the research work.

References

Ahmadreza, H., Azizollah ,J., Raham, A., and Saleh, H.(2015). "The Application of Medicinal Plants in Traditional and Modern Medicine: The Review of *Thymus vulgaris*", *Internal Journal of Clinical Medicine*, vol. 6, pp. 635-642.

Deepa, M.R., Sheema, D.P., and Udayan, P.S.(2016). "Floristic Diversities and Medicinal Importance of Selected Sacred Groves in Thrissur District, Kerala", *Tropical Plant Research*, vol.3,No.1:pp. 230-242.

Dreschfeld, J., (1886), "The Bradshawe Lecture on Diabetic Coma," *British Medical Journal*, vol. 2, pp. 358-363.

Dillon, E.S., Riggs, H.E., Dyer, W.W.,(1936), "Cerebral lesions in uncomplicated fatal diabetetic acidosis," *American Journal of the Medical Sciences*, vol. 192, No. 3, pp. 360-365.

Fame Pharmaceutical, (2012), "Providing Affordab;e Traditional Medicine". Myanmar.

Goldstein, M.S., (2000), "The Growing Acceptance of Complementary and Alternative Medicine," *Handbook of Medical Sociology*, pp. 284-295.

Knowler, W.C., Barrett, C.E., Gregg, E.W., Fowler, S.E., Hamman, R.F., Lachin, J.M., (2002), "Reduction in the incidence of type 2 diabetes with lifestyle intervention," vol.346, pp. 393-403.

Meena, S.N., Ghadi, S.C., and Janarthanam, M.K.,(2014), "Evaluation of Medicinal Properties of *Grewia nervosa* (Lour.) Panigrahi", *2nd International Conference and Exbition on Pharmacognosy, Phytochemistry & Natural Products*, Goa Universtiy, India.

Panigrahi, G., (1985), "Nomenclatural notes on *Grewia microcos* L. nom. Illeg. (Tillaceae)," vol. 34, pp. 702-703.

A STUDY ON EFFECTS OF GAMMA IRRADIATION ON FRESH CUCUMBER FRUIT (*Cucumis sativus* L.)

Toe Toe Lwin*

Abstract

Cucumber is a versatile food and features in a number of beauty products. This research deals with the study on the effects of gamma irradiation on some physicochemical properties (shelf life, weight loss, pH, moisture, vitamin C) of fresh cucumber fruit due to the highest content of water and light sensitive of vitamin C in it. The sample was collected from Mhawbi market, Yangon Region. This sample was gamma irradiated with 0.5 kGy and 0.7 kGy doses from Co-60 source. The non-irradiated sample was used as comparative study. The shelf life of non-irradiated and two doses of gamma irradiated samples were assessed by changing cucumber skin colour and weight loss at room temperature (29 °C and humidity 74 %). The experimental results revealed that, the shelf life of 0.5 kGy and 0.7 kGy doses of γ irradiated cucumber sample (7 days) was prolonged two times than that of non-irradiated sample (3 days) at room temperature under same condition. At day-2, there were no weight loss of all γ-irradiated samples whereas non-irradiated sample lose 4.5 % of original weight. The moisture contents and pH values of non-irradiated and γ irradiated samples of 0.5 kGy , and 0.7 kGy doses were found to be (97.90 % , 88.89 % , 82.56 %) and (5.67, 5.93, 5.51) by using moisture balance and pH meter. Vitamin C contents of all these samples were found to be 6.34 mg/100g on a fresh weight basis by using iodmetoric titration at day-2. During the storage time, Vitamin C contents of γ irradiated samples of 0.5 kGy, and 0.7 kGy doses were found to be slightly reduced from 6.34 mg/ 100g to 5.37 mg/100g from day-2 to day-5 and from 5.37 mg/100g to 4.29 mg/100g from day-5 to day-7. The pH values of γ irradiated samples of 0.5 kGy , and 0.7 kGy doses were found to be slightly reduced from 5.93 to 4.62 and 5.51 to 4.91 from day-2 to day-7, receptively. From these results, the shelf life of γ irradiated cucumber fruit extended two times than that of control to distribute as fresh product. The vitamin C contents and pH values of irradiated samples are slightly reduced during the storage time.

Keywords: cucumber, Co-60, shelf-life, vitamin C

Introduction

The cucumber (*Cucumis sativus* L.) is a member of the Cucurbitaceae family, along with squash and different kinds of melon (Tatioglu, 1993). Cucumbers are a refreshing, nutritious and incredibly versatile addition to any diet. They are low in calories, fat, cholesterol and sodium but high in water and several important vitamins and minerals (Naganatha and Hartline, 2015). Eating cucumbers may lead to many potential health benefits, including weight loss, balanced hydration, digestive regularity and lower blood sugar levels. They can help prevent dehydration due to consist mostly of water. Dehydration is important for many things including maintaining a healthy intestine, preventing constipation, and avoiding kidney stones. They aid in weight loss due to low in calories, high in water. They help reduce dry skin and blackheads. Therefore, cucumber also features in a number of beauty products (Raaz Maheshwari *et al*., 2014). The food is exposed to doses of ionizing energy, or radiation. At low doses, irradiation is one of the most popular preservation technique used world-wide. On the other hand called "cold pasteurization" because irradiation relies on the energy of ionizing radiation extends a product's shelf life. At higher doses, this process kills insects, moulds, bacteria and other potentially harmful micro-

* Dr, Associate Professor, Department of Chemistry, West Yangon University

organisms. Irradiated food has been exposed to radiation but does not become radioactive itself. The gamma radiation used by Co-60 source is not strong enough to decay the nucleus of even one atom of a food molecule (IAEA, 2003). Finding ways to prevent the deterioration of food and control infection by microorganisms has been a major preoccupation of man over the centuries. Controls such as refrigeration or pasteurization are now common place, and it is expected that one day the technique of food irradiation will also be widely used. Food irradiation can offer a wide range of benefits to food industry and the consumer (ICGFI, 1999).

Materials and Methods

Firstly, the fresh cucumber fruits were collected from Mhawbi Market, Yangon Region. And then, this sample was immediately transported to the Department of Atomic Energy, Ministry of Education, for irradiation. The sample was divided into three groups. Each group contains twenty fresh cucumber fruits. First and second groups were placed in polyethylene bag and treated with two different doses of gamma radiation (0.5 and 0.7 kGy) from Co-60 source which has dose rate of 0.965 kGy/h. Third group involved non-irradiated cucumber (0 kGy) was used as comparative study.

For study on postharvest storage time, the shelf life of two types of γ-irradiated (FCG 0.5, FCG 0.7) and non-irradiated (FCG 0)samples was studied by assessing postharvest changes (colour and weight loss) at room temperature(29 °C and humidity 74 %).

For study on weight loss of each sample during postharvest storage period, periodical weighing was made by using Spring Dial Scale, TL-103.The percentage of weight loss of each sample was calculated by dividing the weight change during storage by the original weight as shown in following.

$$\text{Weight loss (\%)} = [(Wi - Ws)/ Wi] \times 100$$

Where, Wi = initial weight , Ws =weight at sampling period

For study on moisture content of the each sample due to the highest content of water in it, at day-2, about (1) g of each sample was put into a SHIMADZU moisture balance (MOC 63u) and moisture content was obtained automatically.

For study on vary in Vitamin C content in each sample during storage time, a redox titration using iodine solution (or) iodometric titration method (AOAC, 2000) was used. Each fresh juice sample (10 mL) was placed in a conical flask. The solution was titrated with 0.001 M iodine solution. The first appearance of a permanent blue-black coloured due to the starch-iodine complex was taken as the end point. The titration was triplicates and from these results, the ascorbic acid (vitamin C) in the samples was calculated at day-2, day-5 and day-7.

For study on vary in pH values in each sample during storage time, pH value of the each sample was determined by using pH meter at day-2, day-5 and day-7. The electrode was placed in the beaker containing the sample juice of (10 mL) and checked for the reading in the pH meter and waited until to get a stable reading and recorded the pH value.

Results and Discussion

Study on the Effect of γ-Irradiation on Weight Loss of Fresh Cucumber Fruit

Weight loss is one of the physiological parameters used as quality indicator in fruits. The weight loss is because of evaporation of water from the fruit surface as a result of respiration and transpiration. It affects the mainly quality characteristics of fresh, appearance and texture, and these processes are dependent on surrounding temperature and relative humidity (Khattak *et al.*, 2005). Weight losses of non-irradiated and γ-irradiated samples were studied by weighing until deteriorated. According to the results in Table 1, it was found that there were no weight loss of all γ-irradiated samples (FCG 0.5, FCG 0.7) at day-2. They retain their original weight, whereas non-irradiated sample (FCG 0) did not retain its original weight. The percentage of weight loss of all γ-irradiated samples slightly increased in parallel during storage period (7 days). Thus, 0.5 and 0.7 kGy doses of γ-irradiation affect on weight loss of fresh cucumber fruit. It can extend the shelf life of cucumber fruit.

Table 1 Weight Loss of Non-Irradiated and γ-Irradiated Fresh Cucumber Fruit Samples during Different Storage Periods

Storage period (day)	Weight loss (%)		
	FCG 0	FCG 0.5	FCG 0.7
1	0	0	0
2	4.5	0	0
3	4.5	4.5	4.5
4	ND	4.5	4.5
5	ND	4.5	4.5
6	ND	4.5	4.5
7	ND	9.1	9.1

ND = not detected due to deterioration
FCG 0 = Gamma dose of 0 kGy of fresh cucumber fruit (control)
FCG 0.5 = Gamma dose of 0.5 kGy of fresh cucumber fruit
FCG 0.7 = Gamma dose of 0.7 kGy of fresh cucumber fruit

Study on the Effect of γ-Irradiation on Shelf Life of Fresh Cucumber Fruit at Room Temperature

The shelf lives of non-irradiated and γ-irradiated samples were assessed by seeking postharvest deterioration such as (change in colour and weight loss) at room temperature (29 °C and humidity 74 %). The experimental results revealed that the colour of γ-irradiated samples did not significantly change to yellow and retains the freshness during storage period (Table 2, Figure 1). There were no weight loss of all γ-irradiated samples (FCG 0.5, FCG 0.7) at day- 2. Therefore, the shelf life of γ-irradiated (FCG 0.5, FCG 0.7) and non- irradiated (FCG 0) samples were prolonged 7 days and 3 days at room temperature. Hence, the shelf life of γ-irradiated samples were extended two times than that of non-irradiated sample as fresh product.

Table 2 Shelf Life of the Non-Irradiated and γ-Irradiated Fresh Cucumber Fruit Samples at Room Temperature (29 °C and humidity 74%)

No.	Sample	Shelf life at RT (day)
1	FCG 0	3
2	FCG 0.5	7
3	FCG 0.7	7

FCG 0 = Gamma dose of 0 kGy of fresh cucumber fruit (control)
FCG 0.5 = Gamma dose of 0.5 kGy of fresh cucumber fruit
FCG 0.7 = Gamma dose of 0.7 kGy of fresh cucumber fruit

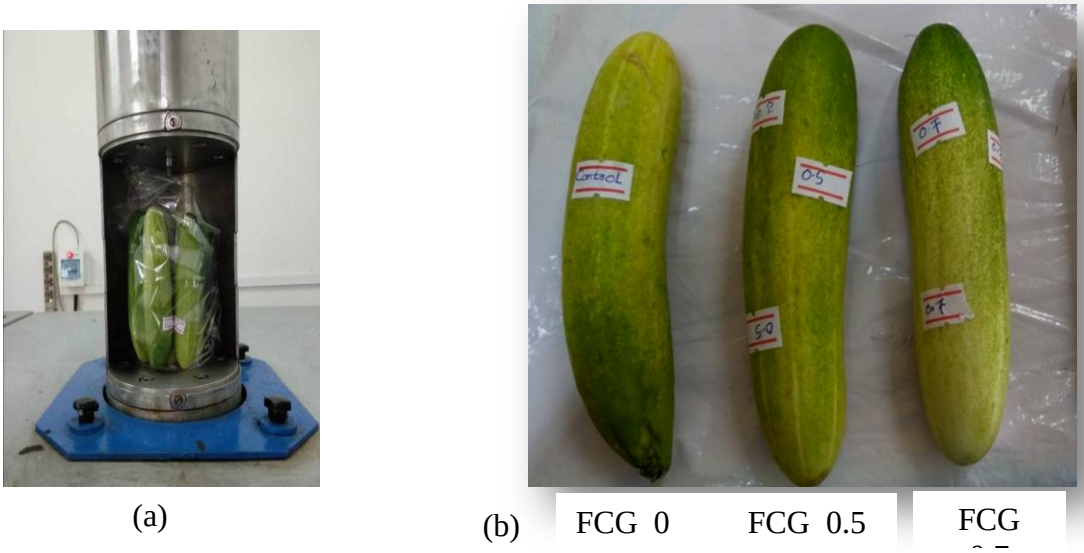

(a) (b)

Figure 1 (a) Gamma irradiation on fresh cucumber fruits at day-1
(b) Observation of the change of the non-irradiated and γ-irradiated fresh cucumber fruits samples during storage at day- 5

Study on the Effect of γ-Irradiation on Moisture Content of Fresh Cucumber Fruit

Water content is a quality factor of food products and is inversely related to its dry matter (total solids). Because food is composed dry matter and moisture. Moisture determination is important in food preservation from microbial growth, sprouting and browning**.** Moisture content recorded depends greatly on the freshness of fruit. Because moisture content is related to the alterations taking place during storage and processing and affects the final quality, it is of direct economic importance to food manufactures and consumers (Pomeranz and Meloan,1978). Therefore, the effect of gamma irradiation on moisture contents of cucumber samples were studied at day- 2. According to the experimental results reported in Table 3, it was found that γ-irradiated samples (FCG 0.5, FCG 0.7) were slightly affected on moisture content of fresh cucumber fruit and the increasing the dose of gamma irradiation, the reducing the moisture content occur. Nevertheless, moisture content of cucumber fruit does not significantly reduce due to the gamma irradiation.

Table 3 Moisture Content of the Non-Irradiated and γ-Irradiated Fresh Cucumber Fruit Samples at Day-2

No.	Samples	Moisture Content (%)
1	FCG 0	97.90
2	FCG 0.5	88.89
3	FCG 0.7	82.56

FCG 0 = Gamma dose of 0 kGy of fresh cucumber fruit (control)
FCG 0.5 = Gamma dose of 0.5 kGy of fresh cucumber fruit
FCG 0.7 = Gamma dose of 0.7 kGy of fresh cucumber fruit

Study on the Effect of γ-Irradiation on pH value of Fresh Cucumber Fruit

Acidity is a major determinant of the taste and quality of most fruits, in combination with sugars and flavor volatiles (Sweeney *et al*., 1970). The pH value of the each sample was determined by using pH meter during storage. From this study (Table 4), it was found that pH values of γ-irradiated samples of different doses did not significantly differ from their control at day-2 and pH values of these samples decreased in parallel during storage period (7 days). This happens whenever food are preserved or stored long-term. Thus, there is no effect of 0.5 and 0.7 kGy doses of γ-irradiation on pH value of fresh cucumber fruit.

Table 4 pH values of the Non-Irradiated and γ-Irradiated Fresh Cucumber Fruit Samples during Different Storage Periods

No.	Samples	pH value		
		Day-2	Day-5	Day-7
1	FCG 0	5.67	ND	ND
2	FCG 0.5	5.93	5.15	4.62
3	FCG 0.7	5.51	4.72	4.91

ND = not detected due to deterioration
FCG 0 = Gamma dose of 0 kGy of fresh cucumber fruit (control)
FCG 0.5 = Gamma dose of 0.5 kGy of fresh cucumber fruit
FCG 0.7 = Gamma dose of 0.7 kGy of fresh cucumber fruit

Study on the Effect of γ-Irradiation on Vitamin C Content of Fresh Cucumber Fruit

Vitamin C (or) ascorbic acid ($C_6H_8O_6$) is a six carbon compound related to glucose. It is a natural water- soluble vitamin. It is found naturally in citrus fruits and many vegetables, cannot be produced or stored by humans and must be obtained in the diet. Ascorbic acid is an essential nutrient in human diets, and necessary to maintain connective tissue and bone. Its biologically active form, vitamin C, functions as a reducing agent and coenzyme in several metabolic pathways. Vitamin C is considered an antioxidant (Mayne, 1994). It is sensitive and can be destroy by heat, light, alkaline pH, cooking, refrigeration and frozen and food preparation (Pauling, 1973). Therefore, vitamin C contents of non-irradiated and γ-irradiated samples of different doses were studied during storage period. From the Table 5, it was found that irradiation with 0.5 and 0.7 kGy doses had no significant effect on vitamin C levels in cucumber fruits at day-2. From the literature survey, this result agree with the irradiation on Melon with 0.5 and 1.0 kGy had no significant effect in vitamin C levels in fruits studied from four harvests

over two consecutive years (Lalaguna, 1998). During the storage time, the vitamin C contents of irradiated samples are slightly reduced. This also happens whenever foods are preserved or stored long-term. Therefore, there is no cause a risk to the health of consumers by using food irradiation.

Table 5 Vitamin C Contents in the Non-Irradiated and γ-Irradiated Fresh Cucumber Fruit Samples during Different Storage Periods

No.	Samples	Vitamin C content (mg/100g)		
		Day-2	Day-5	Day-7
1	FCG 0	6.34	ND	ND
2	FCG 0.5	6.34	5.37	4.29
3	FCG 0.7	6.34	5.37	4.29

ND = not detected due to deterioration
FCG 0 = Gamma dose of 0 kGy of fresh cucumber fruit (control)
FCG 0.5 = Gamma dose of 0.5 kGy of fresh cucumber fruit
FCG 0.7 = Gamma dose of 0.7 kGy of fresh cucumber fruit

Conclusion

In this work, effects of gamma irradiation on the fresh cucumber fruit samples were studied by treatment with 0.5 and 0.7 kGy doses of Co-60 gamma source. From overall results, weight loss, freshness and shelf life of the γ-irradiated fresh cucumber samples are found to be more retained than that of control except slightly reduce moisture contents in them. Moreover, vitamin C content and pH value of gamma irradiated cucumber fruits do not change than that of control at day 2. During the storage time, vitamin C contents and pH value are reduced in these samples as usual. This benefit can be achieved to distribute as fresh product without harmful effect on consumption.

Acknowledgements

The author would like to thank the Department of Higher Education (Lower Myanmar), Ministry of Education, Yangon, Myanmar, for the permission of doing this research. Special thanks are extended to Professor and Head, Dr Hlaing Hlaing Oo and Professor Dr Sanda Khar, Department of Chemistry, West Yangon University for their valuable advice and kind encouragement and for providing research facilities. Thanks are also Daw Thin Thin Soe, Assistant Director, Department of Atomic Energy, Ministry of Education for kindly help to use Co-60 gamma source.

References

AOAC. (2000). "Official Methods of Analysis". Association of Official Analytical Chemists, Manual of Food Quality Control, Washington:17th Ed., pp.714.

IAEA. (2003). "Radiation Processing for Safe, Shelf Stable and Ready to Eat Food". *Processing of a Final Research Coordination Meeting Held in Montreal,* Canada: pp.238-325

ICGFI. (1999). "Consumer Attitudes and Market Response to Irradiated Food". *International Consultative Group on Food Irradiation Policy Document*, Vienna: pp. 1-11

Khattak, A. B., Bibi, N., Chaudry, M. A., Khan, M,. Khan, M. and Qureshi, M. J. (2005). "Shelf Life Extension of Minimally Pocessed Cabbage and Cucumber through Gamma Irradiation". *J.Food Protec*. vol. 68, pp. 105-110

Lalaguna, F. (1998). "Response of Galia Muskmelons to Irradiation as a Quarantine Treatment". .*J .Hort Science*. vol. 33, pp. 118-120

Mayne, P.D. (1994). "Clinical Chemistry in Diagnosis and Treatment". Landon: 6th Ed., Butter and Tanner Ltd., pp. 146-200

Naganatha, S. and Hartline, R. (2015). "Cucumber Nutritional Fact". *J. Veg. Nut* . vol. 15, pp. 1419- 1440

Pauling, L. (1973). " Vitamin C and Common Cold " . London: The Chaucer Press, pp. 29-42

Pomeranz, Y. and Meloan, C. (1978) . "Determination of moisture. In: Food Analysis. Theory and Practice". AVI Publishing Co., Inc., Westport: CT., Rev. Edition, pp. 521-550

Raaz Maheshwari, Laalit Mohan, K.., Malhotra, J., Updhuay, B and Rani, B. (2014). "Invigorating Efficacy of *Cucumis Sativas* for Healthcare & Radiance" *IJCPS*, vol**.** 2 (3), pp. 737

Sweeney, J.P., Chapman,V.J. and Hepner,P.A. (1970). "Sugar, Acid and Flavor in Fresh Fruit". .*J. Am. Dietetic Assoc*. vol.57, pp. 432-435

Tatioglu, T. (1993). "Cucumber Cucumis sativus L. Genetic Improvement of Vegetable Crops". Tarrytown: Pergamon Press Ltd., pp. 197-234

STUDY ON THE PREPARATION OF RUBBER COMPOSITE FROM WASTE TYRE, RUBBER AND NEUTRALIZED WASTE LEATHER PARTICLES

Ko Ko Aung[1], Khin Aye May[2], Kyaw Myo Naing[3]

Abstract

Scrap tyre and waste leather products are major environmental problem for disposal. To overcome this problem, it is needed to reuse into another purpose. Therefore in this research, waste tyre and waste leather were used as filler in rubber compounding which also reduced the cost of production. Waste tyre and waste chrome tanning leather sample (neutralized with ammonia) were collected from tyre shop and leather mill. In this research 6 types of rubber composites RLC I – VI were made by using different amounts of waste tyre and fixed amount of waste leather. All these composites were investigated their physicochemical and physicomechanical properties. In the series of RLC I – VI, RLC VI (100 phr of NR, 100 phr of waste chrome leather neutralized with NH_3 and 600 phr of waste tyre) had the highest tensile strength 6.63MPa, elongation at break 232 %, tear strength 62.0 N/mm and 100 % modulus 6.63 %. RLC VI was more resist to strain and stress. Among the prepared flooring RLC VI was selected due to its highest 100% modulus which resists the pressure and the neutralizing agent (NH_3) used in leather waste did not cause adverse effect on environment. The comparison of surface morphology and thermal resistance of RLC VI and commercial flooring was performed. The surface of RLC VI was smoother than that of commercial flooring. Thermal resistances of both were nearly the same. Weight loss of RLC VI was 65.86 % and commercial was 71.896 %. The cost of prepared flooring was 2710 kyats per 4′×7′ sheet while the commercial was 7500 kyats per sheet. Therefore this prepared rubber composite flooring can be substituted in commercial flooring.

Keywords: waste tyre, waste leather, composites, TG-DTA, SEM, Flooring

Introduction

Mankind has been aware composite materials since several hundred years before Christ and applied innovation to improve the quality of life. Although it is not clear has to how man understood the fact that mud bricks made sturdier houses if lined with straw, used them to make buildings that lasted (Wang, 2011).

Composites that forms heterogeneous structures which meet the requirements of specific design and function, imbued with desired properties which limit the scope for classification. However, this lapse is made up for, by the fact new types of composites are being innovated all the time, each with their own specific purpose like the filled, flake, particulate and laminar composites (Anderson, 2012). Another reason for used as composites materials were high resistance to fatigue and have been high corrosion degradation, high strength or utility ratio (Miracle and Donaldson, 2000).

Materials and Methods

All chemicals used in this research were procured from British Drug House (BDH), England. The chemicals were used as received unless state otherwise. All specific chemicals used were cited detail in each experimental section. The apparatus consist of conventional lab wares, glass wares and modern equipment.

[1] Dr, Lecturer, Department of Chemistry, West Yangon University
[2] Associate Professor, Department of Chemistry, Dagon University
[3] Professor (Retired), Department of Chemistry, Kyaing Tong University

Sampling

Representative rubber smoked sheets were purchased from local markets. Scrap tyre and waste chrome tanning leather were collected from Hlaing Tha Yar Industrial zone, Yangon Region.

Preparation of Scrap Rubber

Vehicle tyre (no more used) was cut with different types of cutting machines to obtain rubber belts. Then, belts were chipped with chipping machine. The rubber chips were ground in the grinding mill to obtain scrap rubber powder.

Preparation of Neutralized Leather Particles

Waste chrome leather shavings, obtained from a local industry, contain chromium (2.5 %) and nitrogen (11.21 %). The untreated leather fibers were dried at 100 °C for 15 min in an air oven and after cooling to ambient temperature, they were shredded into fine particles. The untreated leather particles were acidic in nature which would interfere with the vulcanization of rubber compound (Langmaier *et al.,* 2005). To overcome the acidic nature ammonia was used for neutralizing agent because it was available in local markets and do not affect for environment. After neutralization, the leather particles were separated by filtration and the excess water was removed. The resultant cake was dried in sunlight for 2 days followed by drying in an oven at 100 °C for 15 min (Buljan and Karal, 2011).

Preparation of Rubber Leather Composite

Compounding was done on a 100 phr of natural rubber, 100 phr of neutralized leather particles and 100 to 600 phr of 40 mesh size scrap rubbers. Composite series I to VI are rubber leather composite (RLC) using waste leather neutralized with NH_3. Natural rubber was masticated and after a smooth band was formed on the mill, it was mixed with premix waste leather tyre composites. Softening agent such as aromatic process oil was added to the mixture followed by the addition of antioxidant santoflex 13 (2 phr), zinc oxide and steric acid as activator. It was rolled with roller mill at 60°C to complete mixing. After complete mixing and band formation were ensure, accelerator dibenzothiazldisulpide (MBTS), tetra methyl thiuramdisulphite (TMTD), N- (1,3 dimethyl) –N- phenyl –p-phenylenediamane (6 PPD) and sulphur were added. Appropriate nip gaps were maintained and $3/4^{th}$ cuts were made during the mixing process in order to get uniform compound quality. The schematic diagram for preparation of rubber leather composite is shown in Figure 1 (Ravichandran and Natchimuthu, 2010).

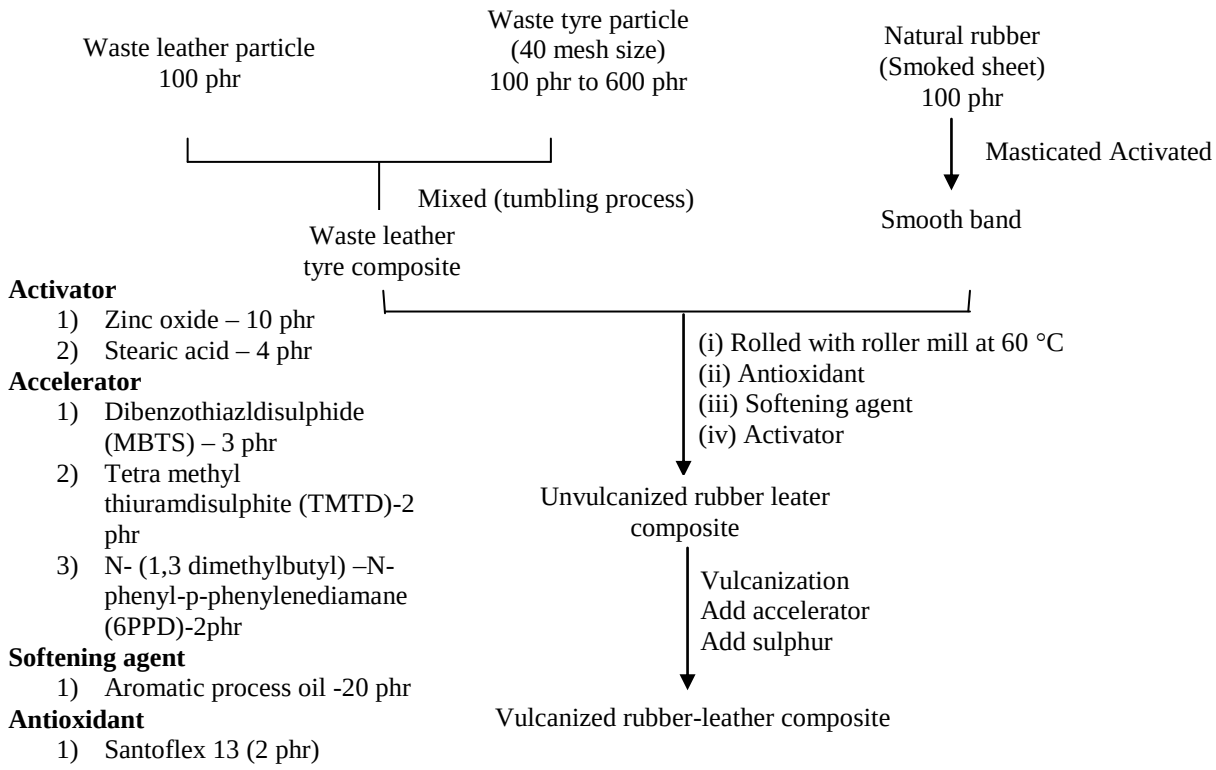

Figure 1 Schematic diagram for preparation of rubber leather composite

Determination of Physicomechanical Properties

Determination of tensile strength and elongation at break

The prepared composite sheets were cut off according to JISK 7127 and the shape and the dimension of the test pieces were prepared. Both ends of the test pieces were firmly clamped in the jaw of tensile strength testing machine. One jaw was fixed and other was movable. The movable jaw moved at the rate of 10 mm/min. the resultant data was recorded on the recorder. This procedure was repeated three times for each composite. The calculation of tensile strength and elongation at break are described in Table 1.

Determination of 100 % modulus

The procedure was the same as procedure for tensile strength and the results are shown in Tables and Figures.

Determination of tear strength

Specimen was cut with single nick (0.05 mm) at the entire of the inner concave edge by a special cutting device using a razor blade. The clamping of the specimen in the jaw of test machine is aligned with travel direction of the grip at the rate of 100 mm/min. The recorder of the machine showed the highest force to tear from a specimen nicked. Tear strength was calculated and described in Table 1. The procedure was repeated three times for each result.

Determination of hardness

The test pieces were placed on the table of instrument. The operating wheel was turned by hand to lower a flat ended circular foot onto the surface of the test piece. After 5 s, the weight of the instrument was pre-set to apply the correct force to foot.

The operating wheel was turned further to apply a known contact force onto foot, followed by a known test force. Hardness is based upon the indentation caused by the test forced. After 30 s, the hardness was directly measured in IRHD on the micrometer gauge. This experiment was repeatedly three times for each composite. The hardness was calculated and described in Table 1(ASTM, 2000).

Physicochemical Characterization of the Prepared Composites
Determination of swelling percent of the prepared composites

The test piece with uniform thickness and volume were used. For the determination of swelling, the test pieces were cut as possible as the same size and weighed. Each piece was placed in each of screw-tight metal capped test bottles (100 mL) containing 50 mL of the selected solvents such as ethanol, gasoline, diesel, engine oil and used engine oil at room temperature. The test piece was taken off from the bottle and blotted with filter paper to remove any adhering oil on sample surface and weighed the sample. The weight gains were measured at 3^{rd}, 6^{th} and 9^{th} days. The swelling percent was calculated and described in Table 2.

Furthermore the prepared composite RLC V and commercial floor were investigated by SEM for surface morphology and TG DTA. All of these techniques were performed at Universities' Research Center, Yangon.

Results and Discussion

The focus of this research was to investigate the effect of filler percent on rubber compounding. The investigation was found on different amounts of filler percent change the physicomechanical and physicochemical properties of composites. To compare the mechanical properties, rubber leather composites were also prepared by using different amount of scrap tyre as filler. The comparisons of physicomechanical properties of 6 types of rubber-leather composites (RLC) were also performed. From the experimental data, composites obtained from scrap tyre as filler showed good oil resistance and heat resistance. Moreover, based on these comparisons, the effective usages of these composites in flooring were also investigated.

Physicomechanical Properties of RLC I to VI

RLC I to RLC VI were prepared by using 100 phr of natural rubber, different amounts (100 – 600 phr) of scrap tyre particle and fixed amount (100 phr) of waste leather (neutralized with NH_3). According to physicomechanical properties RLC VI has the highest tensile strength (6.63 MPa) and elongation at break percent was 232. Thus, it is more resist to strain and stress. Furthermore RLC VI was good 100 % modulus (6.43 %) and the most favorable condition tear strength (62.0 N/mm) (Figure 2).

Table 1 Physicomechanical Properties of Prepared RLC I - VI Samples

Sample	Composition (phr)			Tensile strength (MPa)	Elongation at break (%)	100 % Modulus	Tear strength (N/mm)	Hardness (IRHD)
	*Leather	NR	Waste tyre					
RLC-I	100	100	100	5.30	135	4.89	26.9	76
RLC-II	100	100	200	5.68	156	5.19	34.8	72
RLC-III	100	100	300	5.94	179	5.51	43.9	67
RLC-IV	100	100	400	6.21	200	6.01	52.7	61
RLC-V	100	100	500	6.57	225	6.35	61.5	57
RLC-VI	100	100	600	6.63	232	6.43	62.0	56

* Leather neutralized with NH_3

NR = Natural Rubber

RLC = Rubber leather composite

Natural rubber, NH_3 neutralized leather and100 phr waste tyre composites for RLC I and II, III, IV, V and VI for 200,…., 600 respectively

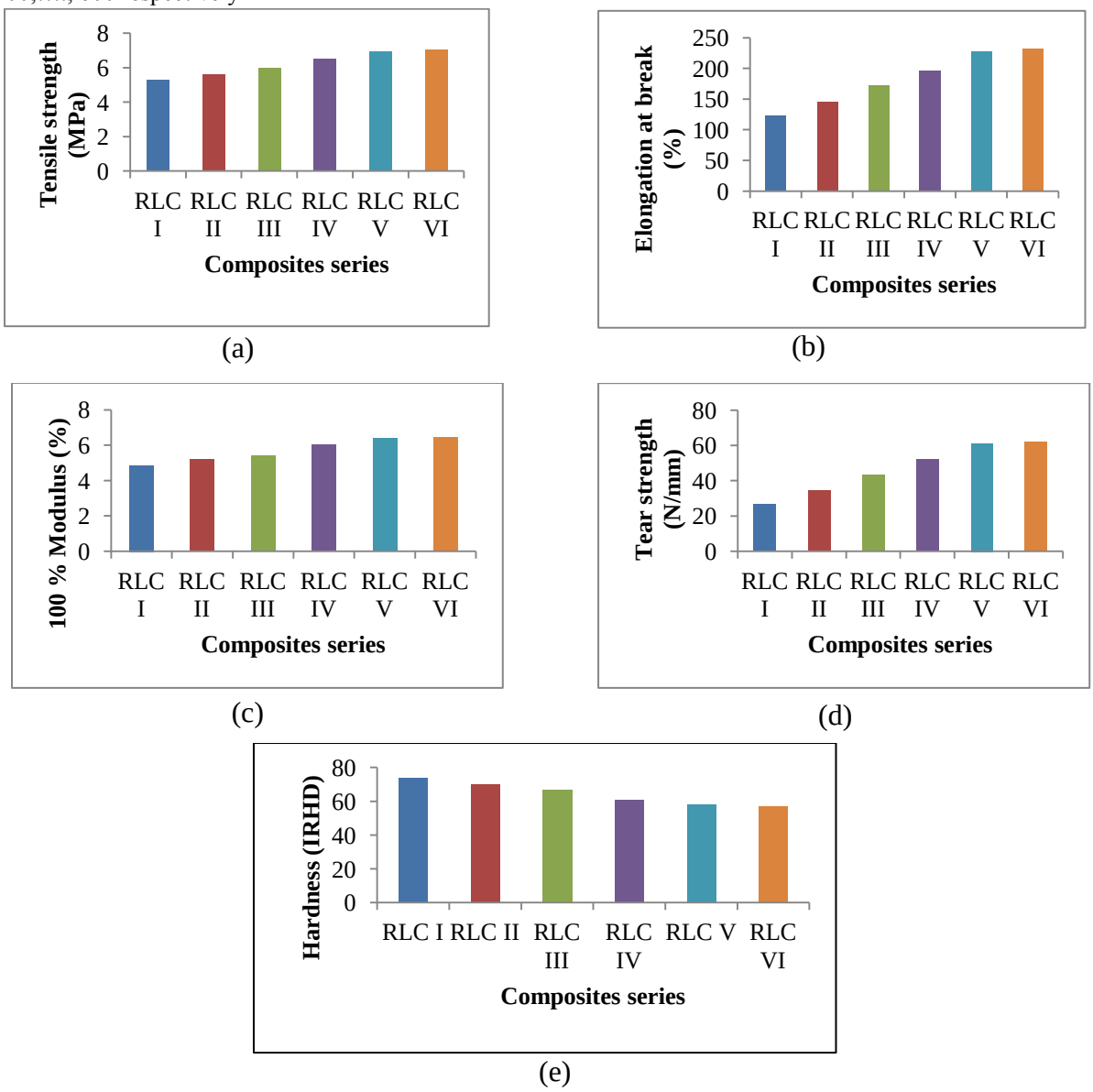

Figure 2 (a) Tensile strength (b) Elongation at break (c) 100 % modulus (d) Tear strength (e) Hardness of prepared composites RlC I to VI versus amount of waste tyre particle

Physicochmical Properties of RLC I to VI

Swelling percentage

For determining the swelling properties, the ethanol, gasoline, diesel, engine oil and used engine oil. Previously weighed sample RLC-VI was soaked in above solvents separately. After soaking for 3 days it was weighed and continued soaking for 6 days and 9 days. Then it was weighed again and again. Finally swelling percents were calculated.

Table 2 shows the results for swelling of prepared rubber composite in selected solvents. This can be attributed to the highly rigid cross-linked polymer nature of composites and non-polar nature of ethanol.

During 9 days of swelling duration, all the composites can absorb the ethanol and the test pieces were swelled. The test pieces become saturated with selected oil that were no increasing in weight after 6 days.

The swelling percent shows, that it can resist spoiling the given solvent on the floor. The swelling percents of these composites after 9 days of duration are also presented in Table 2.

Table 2 Swelling Percent of RLC VI in Different Solvents

Solvents used	Weight (before swelling) (g)	Weight (after swelling) (g)			Swelling percent (%)		
		3 day	6 day	9 day	3 day	6 day	9 day
Ethanol	2.01	2.03	2.04	2.06	1.00	1.49	2.49
Gasoline	2.02	2.21	2.37	2.44	9.41	17.33	20.79
Diesel	2.01	2.25	2.44	2.54	11.94	21.39	26.37
Engine Oil	2.03	2.15	2.25	2.31	5.91	10.84	13.79
Used Engine Oil	2.01	2.10	2.12	2.23	4.48	5.47	10.95

Comparison between TG-DTA thermogram of prepared and commercial floor

The weight lost percent of commercial floor (71.896 %) was greater than prepared floor (65.954 %). Moreover the degradation temperature of commercial floor was 550 °C and the prepared composite was 580 °C. It was shown that the commercial floor is less heat resistance than the prepared floor (Figure 3). Therefore the prepared composite resisted to cigarette and mosquito coil burn.

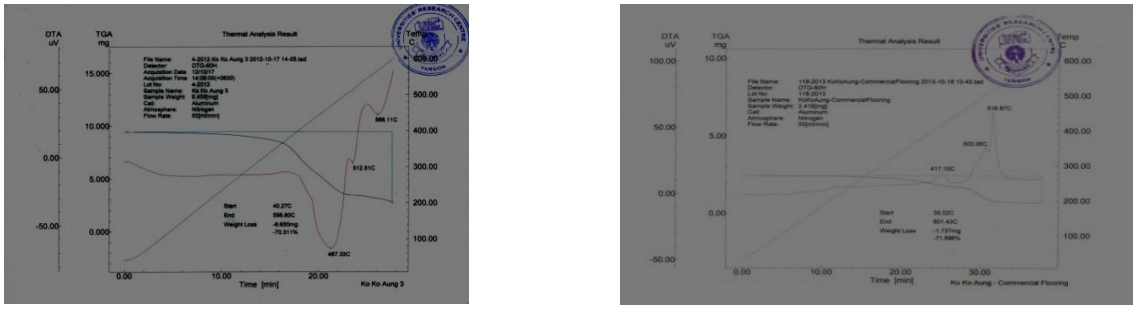

(a) (b)

Figure 3 TG-DTA thermogram of (a) prepared floor and (b) commercial floor

Comparison of SEM image between prepared floor and commercial floor

Figure 4 show the surface image of prepared floor and commercial floor composite. The particle size of prepared floor is smaller than commercial floor. 90 % of particle size was less than 10 μm in prepared floor and in the commercial floor it was has 10μm. The surface of commercial floor composite was found to have has smooth texture particles and ingredients used in the compound were dispersed homogeneously.

(a) (b)

Figure 4 SEM images for (a) prepared floor and (b) commercial floor

Table 3 Estimate Cost for Rubber Floor (for 100 sheets of 4′× 7′ size)

For 2800 sqft	Kyats
Raw materials	
(i) Natural rubber (200 lb x 1200)	240000
(ii) waste leather (200 lb x 15)	3000
(iii) waste tyre (1000 lb x 3)	3000
Chemicals	9000
Electrical cost	1000
Labor cost (3000 x 5)	15000
Total	**271000**

Table 3 shows the estimated cost for 1 rubber sheet is 2710 Kyats. In market the cost of commercial floor (4′× 7′) sheet is 7500 Kyats. Therefore prepared floor composite is 4790 Kyats saved than commercial floor.

Conclusion

From the overall research, the following conclusion could be drawn.

The physicomechanical properties, such as tensile strength, elongation at break, 100 % modulus, tear strength and hardness of 6 composites and physicochemical method (swelling) were examined. Mechanical properties are those physical properties that related to strength, toughness and durability. This RLC-VI has moderately hardness 56 IRHD. Hardness of flooring is the resistance of that flooring to deform under an applied load. RLC-VI has good tensile strength 6.63 MPa. The 100 % modulus of RLC-VI has 6.43 %. If the low modulus (soft) the floor may be good strain, stress or elongation and if the high modulus (hard) the floor may be good stress, load or tensile force. In elongation at break for RLC-VI has 232 %. RLC-VI has high tear strength 62.0 N/mm. So all composite can be used for flooring. For floor decoration, the swelling property of RLC-VI was determined with different solvents such as ethanol, gasoline, diesel, engine oil and used engine oil for rigid cross link polymer nature. Modern techniques were comparatively studied with prepared flooring and commercial flooring. The prepared flooring cost 2710 kyats per (4′× 7′) sheet which is found to be more cost effective than the price of commercial flooring 7500 kyats.

Acknowledgement

The authors wish to thank the Department of Higher Education (Lower Myanmar), Ministry of Education, Yangon, Myanmar, for the financial support of this research programme; and to Dr Daw Hlaing Hlaing Oo, Professor and Head, Department of Chemistry, West Yangon University for her kind provision of the research facilities.

References

American Standard Testing Methods, (1973). *"A Selection Guide and Standard Test Methods for Natural Rubber and its Synthetic Products",* vol. 3(4), pp. 15-25.

Anderson, K.(2012), " *Making Composites from Recycled Tyre Rubber*".

(http://composite.about.com/library/PR/1999/blcsiro1.htm) (Accessed 12 January 2012)

ASTM (2000), *Standard Classification System for Rubber Products in Automotive Application.* vol. 2(3), pp. 25-34

Buljan, J. and Karal, I. (2011). *Introduction to Treatment of Tannery Effluents*. Vienna: United Nations Industrial Development Organization, Austria, pp.1-60

Langmaier, J., Mokere, J.S. and Karnas, R. (2005). "Modification of Chrome-Tanned Leather Waste Hydrolyste with Epichlorhydrin".*Journal of Society of Leather Technologists and Chemists*, vol. 90(5), pp. 29-37

Miracle, D.B. and Donaldson, S.L. (2000). *Introduction to Composites*. New York: Air Force Research Laboratory, USA, pp. 3-14

Ravichandran, K. and Natchimuthu, N. (2010). *Natural Rubber – Leather Composite*. India: Polimeros - natural rubber leather composite, Anna University, vol. 15(2), pp. 1 – 15.

Wang, L. (2011). *Making Complex Composite Materials.*

(http://www.sciencedaily.com/release/2011/05/110526103004)

(Accessed 5 October 2012)

ULTRATHIN IrCo NANODENDRITIC ELECTROCATALYSTS FOR THE OXYGEN EVOLUTION REACTION

Aye Aye Mon[1], GeMeng[2], Junfeng Liu[3]

Abstract

Among the shape-controlled nanostructures of nanocatalysts, nanodendrites (ND) have attracted great interest, because the rich edges and corners atoms resulting from dendrites structure which are conductive for high catalytic activity. In this study, Ir electrocatalysts doped with different amounts of Co were synthesized by an ethylene glycol (EG) reduction method. Ir and IrCo nanocrystals with Ir/Co ratio of 3:1 (IrCo-3:1) showed nanodendrites structure. Among the samples, IrCo-3:1 sample has excellent electrocatalytic activity toward oxygen evolution reaction (OER) in both acid and alkaline conditions with a minimal onset potential (Vs RHE) and a very low Tafelslope than that of IrCo-1:1 and Ir samples. IrCo-3:1 nanodendrites sample also exhibit good stability under both acid and alkaline solution with negligible degradation after 12 h of chronoamperometry test, revealing their excellent stability under OER conditions.

Keywords: IrCo nanodendrites, oxygen evolution reaction, electrocatalysis

Introduction

Renewable sporadic sources, such as solar and winds have a great potential to decrease our dependence on fossil fuel. However, solar and wind energies are alternating and require efficient storage methods for their wide application. A promising large-scale storage way is the conversion of solar and wind into the chemical energy stored in H_2 via the electrochemical water splitting reaction. The water splitting reaction consists of two half reactions, namely, the hydrogen evolution reaction (HER) and the oxygen evolution reaction (OER) (Stern and Hu, 2014). Oxygen evolution reaction (OER) is the process of generating molecular oxygen through electrochemical oxidation of water, and it holds the key to a number of important energy conversion and storage processes, such as water-splitting and rechargeable metal–air batteries (Xu *et al*., 2015; Gong *et al*., 2013; Walter *et al*., 2010). Earth-abundant materials, such as nickel-based and cobalt-based compounds, are widely discovered as boosted catalysts for oxygen evolution reaction (OER) (Chen *et al*., 2016; Lu and Zhao, 2015). Despite significant progress having been achieved, the major challenge problem of non-noble metal-based nanostructured materials established so far is that they still underachieve the Ir and Ru benchmarks for OER (Katsounaros *et al*., 2014; McCrory *et al*., 2013). Another issue related to non-noble metal catalysts for OER that should be specifically mentioned is that they are generally not stable in strongly acidic condition, which largely obstructs their application in proton exchange membrane water electrolyzer (PEMWEs) in which the corrosive acidic environment has to be used (Park *et al*., 2012). Only a few noble metals with good OER activity, such as Ir and Ru, can withstand such a harsh condition (Katsounaros *et al*., 2014; McCrory *et al*., 2013). Compared to Ru, Ir is supposed to be a more ideal catalyst candidate for OER due to its higher stability (Reier *et al.*, 2015). However, the high cost and limited catalytic performance hamper its practical application. Nanocatalysts have obvious advantage in boosting electrochemical catalysis, because of the reduced usage of noble metals but increased catalytically active sites achieved by their high

[1] Dr, Professor, Department of Chemistry, Mohnyin Degree College
[2] Dr, Chemical Resource Engineering, Beijing University of Chemical Technology, Beijing, China
[3] Dr, Professor, Chemical Resource Engineering, Beijing University of Chemical Technology, Beijing, China

surface area to volume ratio (Nesselberger *et al.*, 2011). Doping non-noble metals can reduce the Ir content of electrocatalysts and meanwhile increase their intrinsic activity owing to the synergistic effects between different metals (Chen *etal*., 2014). Kim and co-workers described the synthesis of Ir-ND by the direct surfactant-mediated method, which showed an extremely high OER activity that was about 5.5 times more active than commercial Ir black. These results suggest that engineering noble metals into dendritic structure is an attractive approach for achieving high catalytic performance. However, there has been a little study reported on Ir-ND structure for oxygen evolution reaction (OER) (Lee and Kim, 2011). For example, uniform Ir–Cu nanoframes with highly open structures possessed robust electrocatalytic properties toward OER (Pei *et al*., 2016).

Herein, we report an efficient wet chemical route to prepare ultrathin IrCo nanodendrites. Such interesting structure with accessible sites, maximized surface area and active sites is highly beneficial for enhancing the electrochemical energy conversion. The IrCo nanodendrites also exhibit outstanding stability with limited overpotential change, as revealed by long term chronopotentiometry measurement. To the best of our knowledge, our IrCo nanodendrite is one of the best OER electrocatalysts in both alkaline and acidic conditions reported to date.

Materials and Methods

Preparation and Characterization of 3D IrCo Nanodendrites

All the reagents were of analytical grade, purchased from Beijing Chemical Reagent Factory, and used as received without further purification. In a typical preparation of different ratios of 3D IrCo nanodendrites, 0.2mmol of iridium(III) chloride ($IrCl_3$) and 0.2 mmol of cobalt nitrate ($Co(NO_3)_2{\cdot}6H_2O$) (prepared by adding different amounts of $IrCl_3$ and cobalt nitrate ($Co(NO_3)_2{\cdot}6H_2O$) were dissolved in 6mL of surfactant oleylamine and 2 mL of reducing agent ethanediol under magnetic stirring for 4 h. The resulting homogeneous mixture was transferred to a Teflon-lined stainless-steel autoclave and then heated at 180° C for 12 h before it was cooled to room temperature. The resulting colloidal nanocrystals were collected by centrifugation with 12000 rpm for 20 min and washed by ethanol and cyclohexane for three times before dispersed in cyclohexane. The 3D Ir-Ni and Ir-Cu nanodendrites were also synthesized with the same procedure using $Ni(NO_3)_2.6H_2O$ and $Cu(NO_3)_2.6H_2O$.

The morphology of the as-prepared electrocatalysts was observed on an FEI TecnaiG220 transmission electron microscope (TEM).

Preparation of Catalysts for Electrochemical Characterizations

The prepared 3D IrCo nanodentrite (1 mg) and 5 mg of carbon black were dispersed in 1.5 mL of ethanol, magnetically stirred for 1 h and heated at 200 ℃ for 5 h. Then it was suspended in 40 µL of 5 wt% Nafion by sonication for 30 min to form a homogeneous ink. 5 µL of the catalyst ink (loading amount of ~13.5 µg Ir cm^{-2}) was then loaded onto a glassy-carbon electrode (GCE) (diameter: 5.61 mm, area: 0.247 cm^2) from Pine Instruments.

Electrochemical characterization

Electrochemical characterization of IrCo nanodentrite was performed using a rotating disk electrode (RDE, Pine Research instrument). A three-electrode system controlled by a CHI 660E electrochemistry workstation was employed to carry out the electrochemical measurements

of as prepared samples with different electrolytes such as 0.5M H_2SO_4, 0.05M H_2SO_4, 1M KOH, 0.1M KOH. A glassy carbon electrode (0.196 cm^2) with a thin film of the prepared sample was used as the working electrode. A platinum wire and the saturated calomel electrode (SCE) were used as the counter electrode and reference electrode, respectively. The reference was calibrated against and converted to reversible hydrogen electrode (RHE). The cell was purged with O_2 for 30 min prior to each set of experiments, and then blanketed with O_2 during the experiment. Linear sweep voltammetry was carried out at 5 mV s^{-1}. iR drop was compensated at 95% through the positive feedback using the CHI 660E electrochemistry workstation. The impedance (R) was consistent at multiple potential points (covering both non-OER condition and OER-condition). The Tafel slopes were derived from OER polarization curves obtained at 5mVs^{-1} and 95% iR compensation in all the solutions. Chronopotentiometry was carried out under the same experimental setup without compensating iR drop. All potentials measured were calibrated to RHE using the following equation:

$$E\ (RHE) = E\ (SCE) + 0.241V + 0.0591pH$$

Results and Discussion

Detailed characterization of the prepared IrCo nanodentrites samples with different adding ratios are shown in Figure 1. Typical transmission electron microscopic (TEM) images (Figures 1(a) and 1(b)) show that only Ir and IrCo-3:1samplespossess nanodendrites structure with branch morphology. When the ratio of Ir is decreased to 1:1, the morphology of nanodendrites converted to be nanoparticles (Figure 1(c)). This indicated that Ir plays an important role in the formation of nanodendrites structure. These nanodendrites are monodispersed with an ultrathin average diameter of 2 nm.

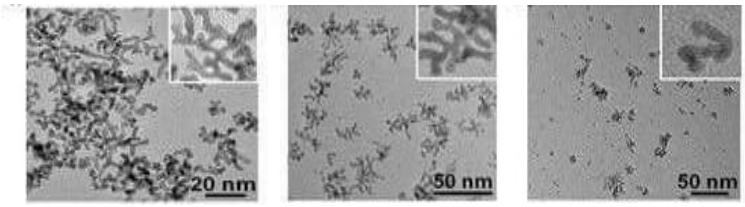

(a) **(b)** **(c)**

Figure 1 TEM images of (a) Ir; (b)IrCo-3:1; (c) IrCo-1:1

Dendritic structure will possess many open sites which allow high catalytic activities. To understand the control mechanism behind the successful synthesis, IrCo-3:1 sample was synthesized by varying the ratio of surfactant oleylamine and reductant ethylene glycol (Figure 2). The results revealed that the combined use of oleylamine and glycol was essential for the successful creation of IrCo nanodendrites. Detailed control experiments show that high-quality nanodendrites could only be obtained in the presence of the specific amount of oleylamine and ethylene glycol (Figure 2(b)). It can be also noted that, nanoparticles were obtained when the ratio of oleylamine to glycol was 1 (Figure 2(a)), and the nanodendrites with poor dispersion and homogeneity were obtained when the ratio increased to 4.3 and 7 (Figures 2(c) and 2(d)).

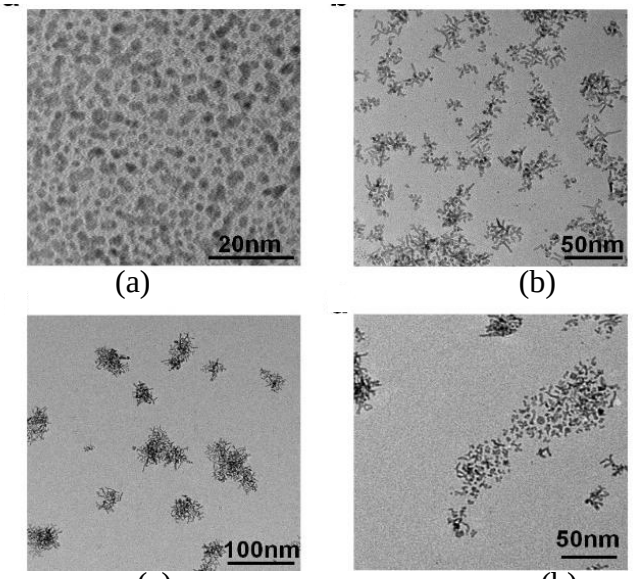

Figure 2 TEM images of IrCo-3:1 prepared with different ratios of oleylamine to glycol (a) 1:1 (b)3:1 (c) 4.3:1 (d) 7:1

To gain in-depth understanding of the formation mechanism, the growth process of Ir superstructure was carefully investigated at different reaction times. Figures 3(a) - 3(c) show the TEM images of the growth intermediates collected at different reaction durations. As shown in Figure 3(a), untidy nanoparticles were formed by the end of the 4h reaction time. As the reaction proceeded for 8h, many branched structures were formed (Figure 3(b)) by combining nanoparticle seeds. Together with the assembling and growth of the branched nanocrystals, nanodendrites were observed after 12 h (Figure 3(c)). Therefore, the growth of the IrCo nanodendrites includes two steps: (i) the initial formation of primary seed crystal at the early stage and (ii) the subsequent self-assembling and growth into nanodendrites to minimize their surface energy at high temperature.

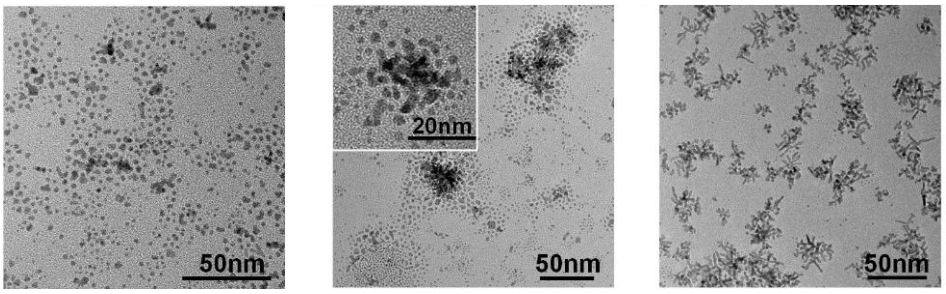

Figure 3 TEM images of IrCo-3:1 prepared at different reaction times: (a) 4h (b) 8h (c) 12h

In order to study the performance of 3D IrCo nanodendrite catalysts, the OER activity in acidic solutions were investigated (Figure 4). Before the electrochemical activity test, the catalysts were scanned at a sweep rate of 50 mV s^{-1} for 20 cycles in the electrolyte until a stable cyclic voltammogram was obtained. The polarization curves were recorded at a slow scan rate of 5 mV s^{-1} and iR compensation. It was found that all the catalysts have higher OER activities in 0.5 M H_2SO_4 than those tested in 0.05 M H_2SO_4. The 3D IrCo-3:1 nanodendrites show the minimal onset potential of ~1.45 V versus RHE in 0.05 M H_2SO_4 and ~1.41 V versus RHE in

0.5 M H_2SO_4 for OER (Figures 4(a) and 4(c)). In 0.5 M H_2SO_4, 3D IrCo-3:1 nanodendrites only need 0.21 V overpotential to achieve 10 mA cm^{-2}, which is better than those of Ir only and IrCo-1:1 sample. Moreover, IrCo-3:1 nanodendrites also exhibit a very low Tafel slope of53 mV dec^{-1} and 57 mV dec^{-1} in 0.05 M H_2SO_4 and 0.5 M H_2SO_4 solution (Figure 4(b) and 4(d)), which is better than the commercial Ir/C (20%). As a comparison, the Ir only samples show lower activity compared with 3D IrCo-3:1 sample, indicating the enhanced catalytic performance of Ir modifying with Co.

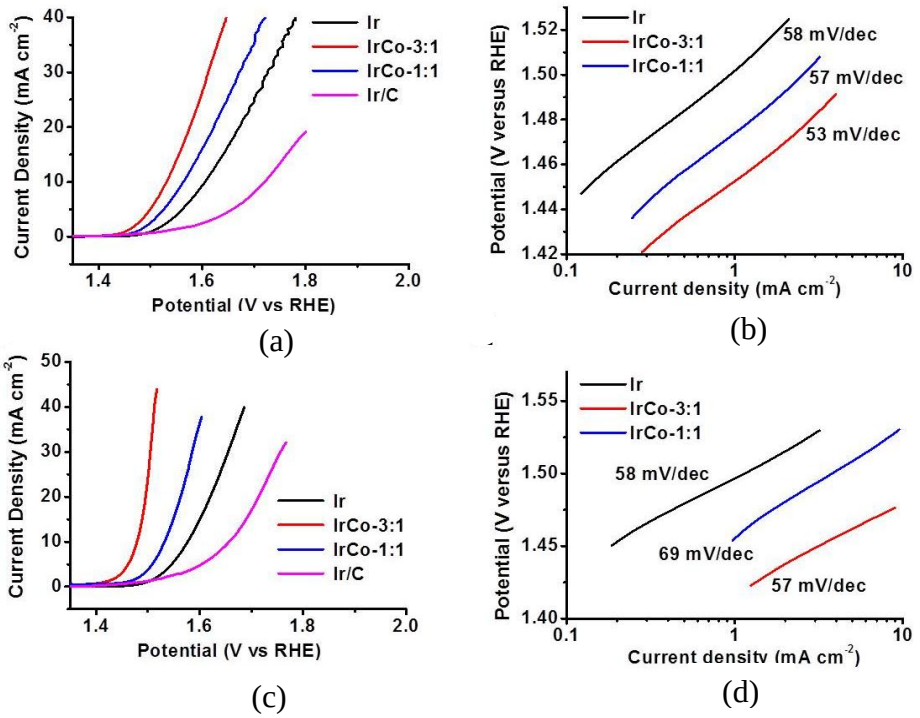

Figure 4 Electrochemical performance of Ir, IrCo-3:1 and IrCo-1:1nanodendrites catalysts in acidic condition. (a) The polarization curves of different catalysts in 0.05 M H_2SO_4 solution at the scan rate of 5 mV s^{-1} with iR-compensation and (b) their Tafel plots at the scan rate of 5 mV s^{-1}. (c) The polarization curves of different catalysts in 0.5 M H_2SO_4 solution at the scan rate of 5 mV s^{-1} with iR-compensation and (d) their Tafel plots at the scan rate of 5 mV s^{-1}.

In 0.1 M KOH and 1 M KOH, IrCo-3:1 nanodendrites also show the lowest onset potential of ~1.49 V and ~1.48 V versus RHE and only requires an overpotential of ~0.31V and ~0.28V to achieve the current density of 10 mA cm^{-2} (Figures 5(a) and (c)). Moreover, IrCo-3:1 nanodendrites also exhibit a very low Tafel slope of 66 mV dec^{-1} and 52 mV dec^{-1} in 0.1 M KOH and 1 M KOH solution (Figures 5(b) and 5(d)). The best activity of IrCo-3:1 sample is mainly because of the combining ultrathin 3D nanodendrite design and Co modified. Both of the OER performances in acidic and alkaline conditions are more preferable than those of most recently reported catalysts, making 3D IrCo nanodendrites among the most active electrocatalyst for OER reported to date.

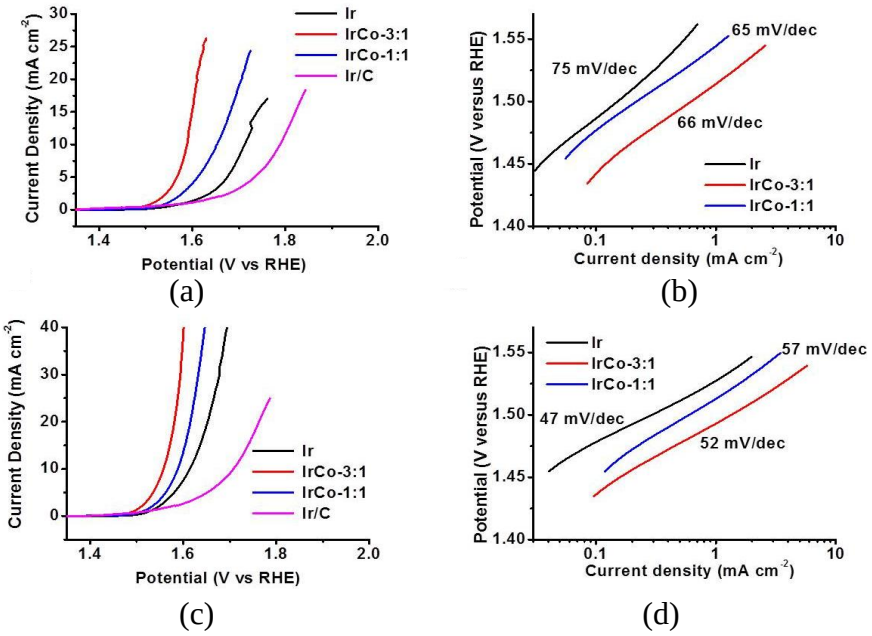

Figure 5 Electrochemical performance of Ir, IrCo-3:1 and IrCo-1:1nanodendrites catalysts in alkaline condition. (a) The polarization curves of different catalysts in 0.1 M KOH solution at the scan rate of 5 mV s^{-1} with iR-compensation and (b)theirTafel plots at the scan rate of 5 mV s^{-1}. (c) The polarization curves of different catalysts in 1 M KOH solution at the scan rate of 5 mV s^{-1} with iR-compensation and (d) their Tafel plots at the scan rate of 5 mV s^{-1}.

The long-term durability of a catalytic electrode is another crucial issue to consider for practical applications. When operating the OER at constant overpotentials, stable corresponding current densities were observed in both 0.05M H_2SO_4 and 0.1 M KOH solution (~2.5 mA cm^{-2}) with negligible degradation (14% and 9%, respectively) after 12 h of testing (Figure 6(a)), revealing their excellent stability under OER conditions. Notably, as shown in (Figure 6(b)), Ir nanodendrites are more stable than IrCo-3:1 sample, which may due to the dissolution of Co in Ir-Co alloy under acidic condition.

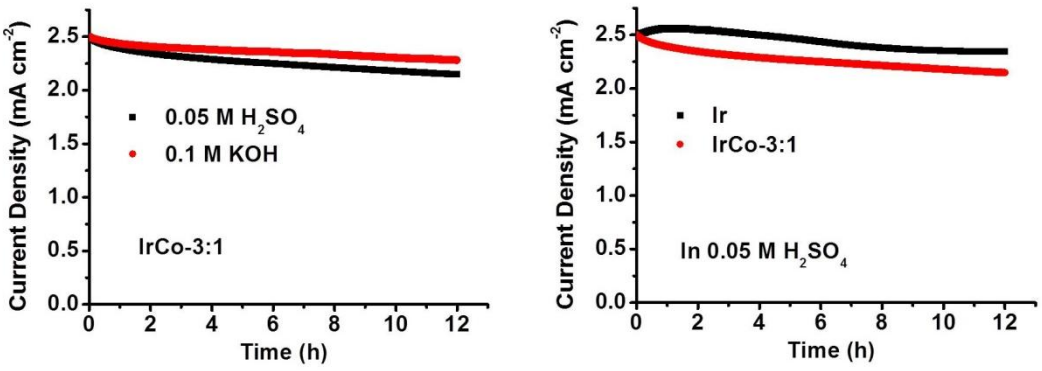

Figure 6 Stability testing of (a) IrCo-3:1nanodendrites sample in 0.05 M H_2SO_4 and 0.1 M KOH solution (b) Ir only and IrCo-3:1 nanodentrites samples in 0.05 M H_2SO_4solutionat constant potentials

Conclusion

In conclusion, Co doped Ir nanodentrites samples of different molar ratios were synthesized by hydrothermal reduction method at different reaction times and were characterized by TEM. Among these samples, only IrCo-3:1 sample at 12 h reaction time possesses nanodentrites structure with branch morphology like Ir only sample. Catalytic activity towards oxygen evolution reaction (OER) of as synthesized catalysts at various electrolytes at broad pH ranges was also investigated. IrCo-3:1 catalyst exhibits an enhanced OER activity compared to IrCo-1:1 and Ir only catalysts due to nanodentrites structure with many active sites on the surface of each branch and modifying of ultrathin nanodentrite Ir with transition metal Co. Given its excellent performance in both alkaline and acidic media, the 3D Ir nanodentrites structure may find broad applications in various water splitting, chemical conversions, and beyond. It is worthy noted that, although the IrCo catalysts contain negligible Co, the modifying effect can change the morphology as well as enhance the electrocatalytic activity.

Acknowledgements

The authors would like to express sincere thanks to Myanmar Academy of Arts and Science for allowing to submit this article. We also indebted to Dr Nyunt Soe, Principalof Mohnyin Degree College.

References

Chen, C., Kang, Y. J., Huo, Z. Y., Zhu, Z. W., Huang, W. Y., Yang, P. D. and Stamenkovic, V. R. (2014). “Highly Crystalline Multimetallic Nanoframes with Three-Dimensional Electrocatalytic Surfaces”. *Science*, vol. 343, pp.1339-1343

Chen, P., Xu, K., Zhou, T., Tong, Y., Wu, J., Cheng, H., Lu, X., Ding, H., Wu, C. and Xie, Y. (2016). "Strong-Coupled Cobalt Borate Nanosheets/Graphene Hybrid as Electrocatalyst for Water Oxidation Under Both Alkaline and Neutral Conditions". *Angew. Chem. Int. Engl.*, vol. 55, pp. 2488-2492

Gong, M., Li, Y. G., Wang, H. L., Liang, Y. Y., Zhou, J. G., Wang, J., Regier, T., Wei, F. and Dai, H. J. (2013). “An Advanced Ni–Fe Layered Double Hydroxide Electrocatalyst for Water Oxidation”. *Am.Chem. Soc*., vol. 135, pp. 8452-8455

Katsounaros, I., Cherevko, S., Zeradjanin, A. R. and Mayrhofer, K. J. (2014). "Oxygen Electrochemistry as Cornerstone for Sustainable Energy Conversion". *Angew. Chem. Int. Ed. Engl.*, vol. 53, pp. 102-121

Lee, W. H. and Kim, H. (2011). “Oxidized Iridium Nanodendrites as Catalysts for Oxygen Evolution Reactions”. *Catal. Commun.*, vol. 12, pp. 408–411

Lu, X. and Zhao, C. (2015). "Electrodeposition of Hierarchically Structured Three-dimensional Nickel-Iron Electrodes for Efficient Oxygen Evolution at High Current Densities". *Nature communications*, vol. 6, pp. 6616

McCrory, C. C., Jung, S., Peters, J. C. and Jaramillo, T. F. (2013). "Benchmarking Heterogeneous Electrocatalysts for the Oxygen Evolution Reaction". *Journal of the American Chemical Society*, vol. 135, pp.16977-16987

Nesselberger, M., Ashton, S., Meier, J.C., Katsounaros, I., Mayrhofer, K.J.J. and Arenz, M. (2011). "The Particle Size Effect on the Oxygen reduction Reaction Activity of Pt Catalysts: Influence of Electrolyte and Relation to Single Crystal Models". *Journal of the American Chemical Society”,* vol.133, pp. 17428-17433

Park, S., Shao, Y., Liu, J. and Wang, Y. (2012). "Oxygen Electrocatalysts for Water Electrolyzers and Reversible Fuel Cells: Status and Perspective". *Energy and Environmental Science*, vol. 5, pp. 9331

Pei, J., Mao, J., Liang, X., Chen, C., Peng, Q., Wang, D. and Li, Y. (2016). "Ir–Cu Nanoframes: One-Pot synthesis and Efficient Electrocatalysts for Oxygen Evolution Reaction". *Chem. Commun*., vol. 52, pp. 3793

Reier, T., Pawolek, Z., Cherevko, S., Bruns, M., Jones, T., Teschner, D., Selve, S., Bergmann, A., Nhan Nong, H., Schlögl, R., Mayrhofer,K J.J. and Strasser, P. (2015). "Molecular Insight in Structure and Activity of Highly Efficient, Low-Ir Ir-Ni Oxide Catalysts for Electrochemical Water Splitting (OER)". *Journal of the American Chemica lSociety* vol. 137, pp. 13031-13040

Stern, L. A., and Hu, X. (2014). "Enhanced Oxygen Evolution Activity by NiO_x and $Ni(OH)_2$ Nanoparticles". *Faraday Discuss*, vol. 176, pp. 363-379

Walter, M. G., Warren, E. L., McKone, J. R., Boettcher, S. W., Mi, Q., Santori, E. A. and Lewis, N. S. (2010)."Solar Water Splitting Cells". *Chem. Rev*., vol. 110, pp. 6446−6473

Xu, K., Chen, P.Z., Li, X.L., Tong, Y., Ding, H., Wu, X.J., Chu, W.S., Peng, Z.M., Wu, C.Z. and Xie, Y. (2015). "Metallic Nickel Nitride Nanosheets Realizing Enhanced Electrochemical Water Oxidation". *J. Am. Chem. Soc.*, vol. 137, pp. 4119–4125

CHARACTERIZATION OF SOIL USED IN POTTERY MAKING OF NWE-NYEIN QUARTER, KYAUK-MYAUNG, SHWEBO DISTRICT, SAGAING REGION

Moe Tin Khaing[1], Nyo Nyo Win[2], Pa Pa San[3]

Abstract

This research is aimed to investigate the physicochemical constituents of soil samples from the well-known glazed pot industry of Nwe-nyein and to characterize these soil samples by advanced spectroscopic techniques. Potters make earthen and glazed pot by mixing too types of soil: yellow soil (sample 1) and red soil (sample 2). They prepare the combined soil (sample 3) by mixing these two types of soil with two: one ratio by weight of yellow and red soil. pH, moisture, colour, electrical conductivity and cations exchange capacity of yellow soil, red soil and combined soil samples were measured by their respective methods to explore their physicochemical properties. Then exchangeable cations analysis informed the cations exchange capacity (CEC), Sodium Adsorption Ratio (SAR), Exchangeable Sodium Percentage (ESP %) and Exchangeable Magnesium Percentage (EMgP %) of tested soil samples and the values of SAR pointed out that all soils were dispersive due to the sodium contents. Textural analysis was done on all soil samples and they were classified as clay. Soluable salt extraction tests were carried out by titration methods to detect the amount of soluble chloride, sulphate, carbonate and bicarbonate but the bicarbonate was not found in all samples. To characterize soil constituents, Energy Dispersive X-ray (EDX) and Scanning Electron Microscopic techniques(SEM) were also applied. According to the EDX results, the highest relative abundance of Si were 42.06 %, 42.55 % and 44.50 % in sample 1, sample 2 and sample 3 respectively and it was followed by the percentages of Fe with 25.92 %, 30.36 % and 28.53 %. Heavy toxic mineral constituents were not found in these soils. SEM examination showed that the crystal like structure of sample 1 and flaky similar soil structures with many porous could be observed in the soil sample 2 and 3. It was concluded that the soil samples used in Nwe-nyein pottery industry were suitable for pottery making and the products of this area were popular in the whole Myanmar.

Keywords: Soil, Cations exchange capacity (CEC), Sodium Adsorption Ratio (SAR), Exchangeable Sodium Percentage (ESP %), Exchangeable Magnesium Percentage (EMgP %)

Introduction

The characteristics common to all clay minerals are derived from their chemical composition, layered structure, and size. There are three definitions of clay: (I) based simply on size, including anything finer than 4 microns be it true clay minerals, quartz, calcite, pyrite or any other substance; this is the "clay" of the grain-size analysis workers, of the sedimentologists and oceanographers; (2) based on composition, defined as one of the hydrous aluminum silicates belonging to the kaolin, montmorillonite or illite groups and also including fine-grained chlorite and vermiculite; (3) the petrographic definition, which includes under the general term "clay", the true clay minerals listed in (21, plus sericite and fine- grained muscovite, biotite and chlorite if finer than about 20 microns, and even the hydrous aluminum oxides "bauxite" and gibbsite (Folk,1974). Grain size distribution of soil classify gravel and sand as coarse grained soil and, silt and clay are categorized as fine grained soil. Soil, particle size < 2 μm is the most determining factor which gives plasticity to

[1] Dr, Associate Professor, Department of Chemistry, Myitkyina University
[2] Dr, Professor, Department of Chemistry, Sagaing University
[3] Dr, Lecturer, Department of Chemistry, Yadanabon University

soil and are called clay particles(Shrestha, 2018). Clay minerals all have a great affinity for water. Some swell easily and may double in thickness when wet. A mixture of a lot of clay and a little water results in a type of mud that can be shaped and dried to form a relatively rigid solid. This property is exploited by potters and the ceramics industry to produce plates, cups, bowls, pipes, and so on. Clay minerals resemble the micas in chemical composition, except the fact that they are fine grained and usually microscopic. Like the micas, clay minerals are shaped like flakes with irregular edges and one smooth side. Glazes are made up of materials that fuse during the firing process making the pot vitreous or impervious to liquids. (Ceramics engineers define vitreous as a pot that has a water absorption rate of less than 0.5%.) Glazes must have three elements: silica, the vitrifying element (converts the raw pottery into a glasslike form)—is found in ground and calcined flint and quartz; flux, which fuses the glaze to the clay; and refractory material, which hardens and stabilizes the glaze. Colour is derived by adding a metallic oxide, including antimony (yellows), copper (green, turquoise, or red), cobalt (black), chrome (greens), iron, nickel, vanadium, and so on. Glazes are generally purchased in dry form by production potters.

Pottery, one of the oldest and most widespread of the decorative arts, consisting of objects made of clay and hardened with heat. The objects made are useful and the importance of pottery production to the local culture and economy facilitates and reinforces common property institutions associated with these goods. The evidence indicates that when rare or scarce "private goods" are integral to a people's livelihoods and culture, common property arrangements can be an effective approach to management (Tucker,201). Nwe-nyein pottery is well known in Myanmar and there is no chemical analysis on the soils from this area. The aim of this research work is to characterize the constituents of soil samples from Nwe-nyein Glazed pottery Industry from Kyauk-Myaung, Shwebo District, Sagaing Region, Myanmar and the location map of the study site is shown in Figure 1.

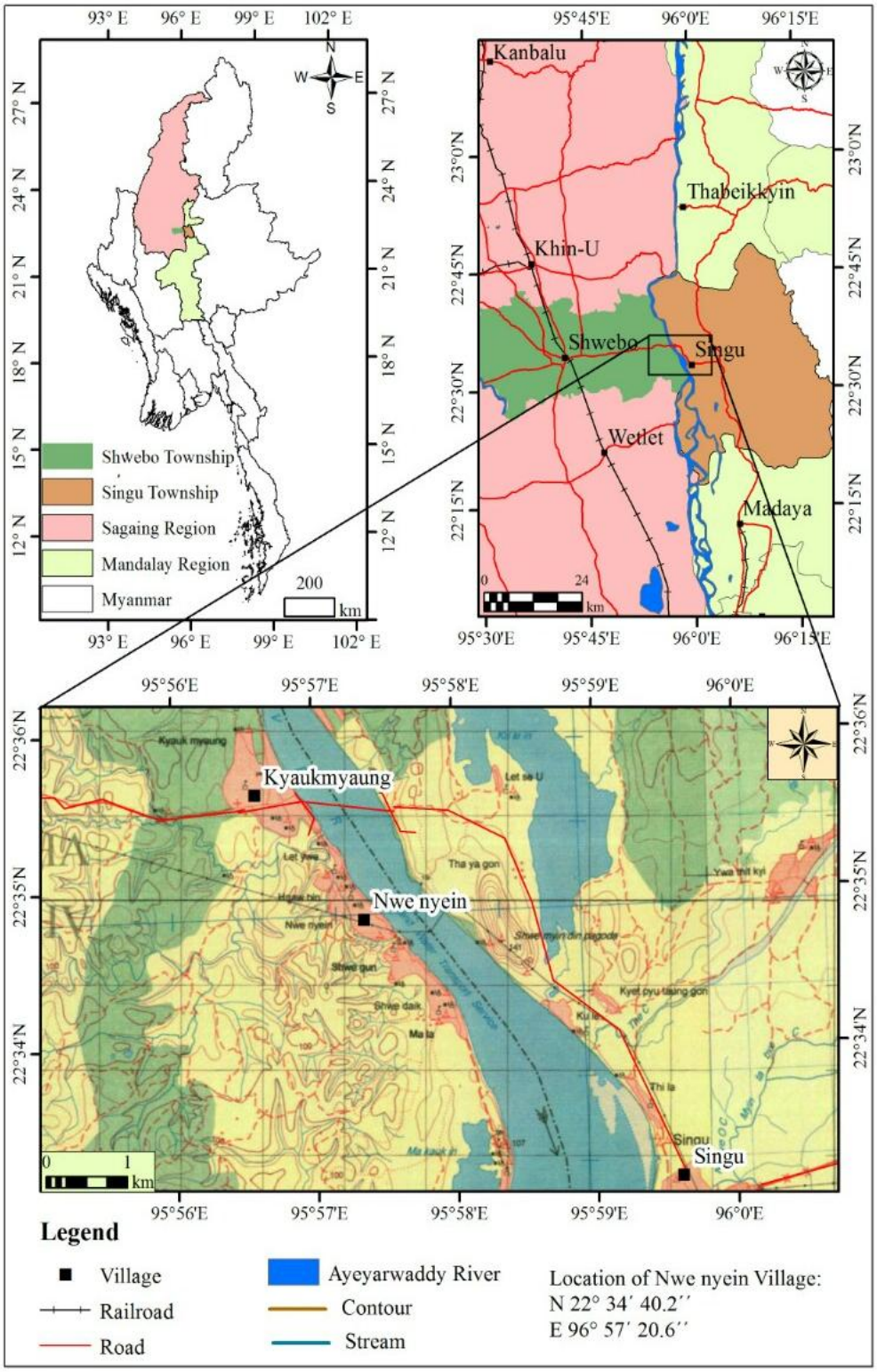

Figure 1 Location map of the study site

Nwe-nyein Pottery

Kyauk-myaung is situated 46 miles north of Mandalay on the west bank of the Ayeyawady River, and 17 miles to the east of Shwebo. It has four large-scale pottery "villages" or complexes and they are Nwe-nyein, Shwe-gon, Shwe-daik, and Malar. Nwe-nyein is the

largest pottery village and it is famous for the production of large glazed pots which can be used to store about 200 litres of water. Potters use two kinds of soils for pottery making and they are red soil and yellow soil. Villagers dig red soil from the floor of the Ayeyawady river and bring yellow soil from the soil deposit which is not far from the villages. Potters needed raw soil material to make pots by mixing yellow and red soils according to weight ratio (2 : 1). In this research, determination of physicochemical properties and characterization of yellow soil, red soil and (2 :1) combined soil were investigated to characterize the constituents of soil samples from the glazed pot industry of Nwe-nyein.

Figure 2 Traditional pottery making procedure of Nwe-nyein industry

(a) Pasting and preparing the soil
(b) Bottom part of a big pot on the potter's wheel
(c) After preparing a big pot
(d) Printing on the pot with chalk glaze
(e) Traditional earthen ash tray
(f) After decorating the tray with chalk
(g) Ready to fire the pots in the kilns
(h) The arrangement of pots in the kilns
(i) Before closing the kilns to fire
(j) Glazed pots products to send into the market
(k) Chemicals used for the preparation
(l) A building decorated with glaze of colour of the glaze

Materials And Methods

Sample Collection

Three soil samples were collected from one of the pottery industries from Nwe-nyein quarter, Kyauk-myaung, Shwebo District, Sagaing Region which is well- known for glazed-pot making in Myanmar. As it can be seen in Figure 3, soil sample-1 is yellow soil, sample-2 is red soil and sample-3 is made by mixing yellow soil and red soil with 2 : 1 ratio by weight of soil sample-1 and sample -2.

Sample-1 yellow soil | Sample -2 red soil | Sample-3 combined soil y : r = 2:1)

Figure 3 Collected samples

Collected soil samples were allowed to dry in air at room temperature. Then these air-dried soil samples were broken up by hand and then they were ground by milling with a wooden roller. After grinding, the soil was screened through a 2mm (10 meshes) sieve. For textural analysis, air-dried soil samples were utilised naturally. The sample was allowed to dry in an electric oven at 105-110°C for about 8 hrs. After cooling it in a desiccator, the loss in weight was determined. From the loss in weight, the percentage of moisture of the sample was calculated. The pH of soil solution was measured by pH meter. The pH meter was calibrated with pH 4.0 and pH 10.0 buffer solution before measurement. The electrical conductivity of the soil samples was determined electrometrically with a calibrated, HACH model electrical conductivity meter. Soil texture was determined by pipette method. The amount of exchangeable calcium and magnesium were determined by titration method at Soil Survey Section, Irrigation Department Yangon. The concentration of exchangeable sodium was detected by using the atomic absorption flame emission spectrophotometer at Soil Survey Section, Irrigation Department Yangon. Characterization of soil samples were done by Energy Dispersive X-Ray Analysis (EDX) and Scanning Electron Microscopic method (SEM). The energy dispersive X-ray spectra (EDX) of the three soil samples were recorded on a Perkin Elmer 700, EDX spectrometer. Morphological structures of sample 1, sample 2 and sample 3 was taken at Chemistry Department, West Yangon University by using Scanning Electron Microscope (JOEL-JSM-5610 Japan), Ion Sputter (JFC-1600).

Results and Discussion

Determination of Physicochemical Properties

Some physicochemical properties of three soil samples were examined and the data obtained were shown in Table 1.

Table 1 Physicochemical Properties of Soil Samples

Sample	pH	Moisture Content (%)	EC (μ mhos/cm)	Colour
1	7.80	1.32	743	pale yellow
2	8.70	1.47	222	red
3	8.60	1.94	779	reddish yellow

Soil sample 1 showed slightly alkaline pH 7.80 and the other two sample 2 and 3 had strongly alkaline pH, 8.70 and 8.60 respectively. Low moisture contents 1.32 and 1.47 were belonged soil sample 1 and sample 2 while soil sample 3 had the higher moisture content (1.94 %). Sample 1 and the combined sample 3 had medium electrical conductivity (EC) (743 and 779 μmhos/cm) but the soil sample 2 had low electrical conductivity (EC) (222 μmhos/cm).

Table 2 Textural Properties

Sample	Composition			
	Sand (%)	Silt (%)	Clay (%)	Texture
1	24	27.5	48.5	Clay
2	15	31.5	53.5	Clay
3	25	33	42	Clay

Soil sample 2 showed the highest clay content, 53.5% and sample 3 had the highest amount of sand and silt percentages, 25% and 33% respectively but all soil samples were informed as clay texture in Table 2.

Table 3 Exchangeable Cation Contents

Sample	meq/100 g of soil							SAR	ESP %	EMgP %	Remark
	Na^+	Ca^{2+}	Mg^{2+}	K^+	Al^{3+}	H^+	CEC				
1	7.30	3.28	1.52	1.23	0.25	0.00	13.58	14.90	53.76	11.19	Dispersive
2	4.43	3.29	1.70	1.61	0.30	0.00	11.33	8.88	39.10	15.00	Dispersive
3	7.30	3.36	1.84	1.28	0.21	0.00	13.78	14.31	52.98	13.35	Dispersive

Low cation exchange capacity was found in all soil samples because they were fallen in the low CEC range 5-15 meq/100 g of soil in Table 3. Relatively unsuitable sodium adsorption ratio between 10-18 were found in the yellow clay sample 1 and the combined sample 3 whereas red clay sample 2 was found as suitable classification of SAR between 1-10 meq/100 g. Increased exchangeable sodium percentage is related to decreased exchangeable magnesium percentage and it can be seen in the results of all soil samples. According to the exchangeable cations analysis, all soil samples were regarded as dispersive soil. But this property is no longer significance during pottery making.

Table 4 Extracted Soluble Salts

No	Parameter (meq/L)	Sample 1	Sample 2	Sample 3
1	CL^-	0.67	0.35	0.46
2	SO_4^{2-}	5.53	0.05	6.40
3	CO_3^{2-}	0.00	0.00	0.00
4	HCO_3^-	0.80	1.60	0.80

Water soluble salts were determined and the results were observed as shown in Table 4. Sample 1 contained the highest CL^- salt (0.67). Medium content of sulphate salts was observed in sample 1 (5.53). Sample 2 showed the lowest SO_4^{2-} contents (0.05 meq/L) while sample 3 gave the highest SO_4^{2-} value (6.40 meq/L) of soil solution. Sample 2 possesses the double HCO_3^- content (1.6 meq/L) of the other two samples (0.80 meq/L). Water soluble CO_3^{2-} was not found in all tested soil samples.

Scanning Electron Microscopic Examination

SEM images of soil samples were measured by scanning electron microscopic analysis and the result obtained were informed in Figures 4, 5 and 6.

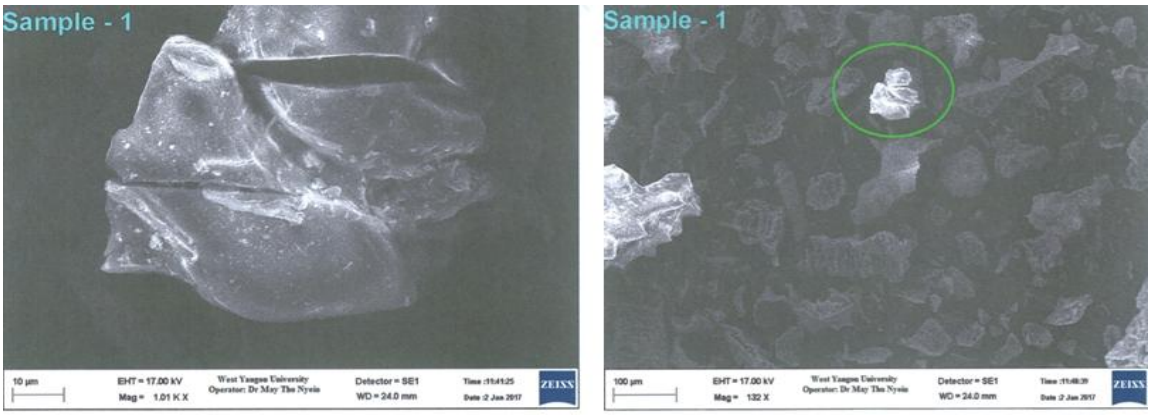

Figure 4 Morphological structure of soil sample 1

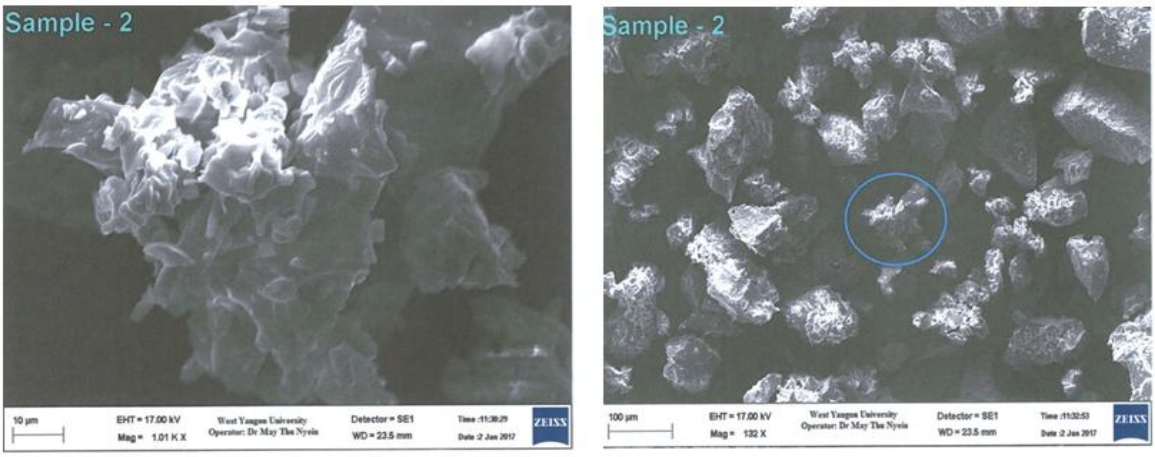

Figure 5 Morphological structure of soil sample 2

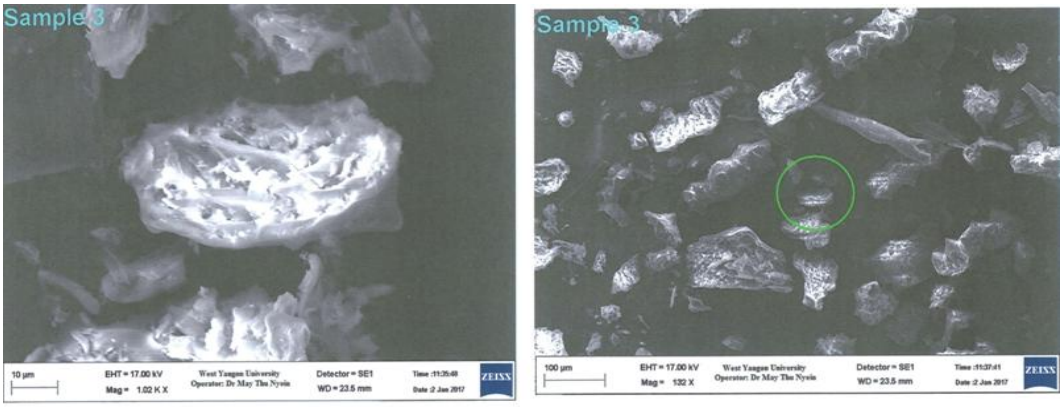

Figure 6 Morphological structure of soil sample 3

In these SEM photograms, soil sample 2 and 3 gave flaky structures with many micropores but sample 1 was found as crystal like structure.

Elemental Composition of Soil Samples

Determination of elemental composition of soil samples was carried out by Energy Dispersive X-ray analysis. The resulting relative abundant compositions in percentage of tested soil samples were displayed in Table 5. The highest Ca contents (9.342 %) was observed among these three soil samples and also the highest Al amount (14.83 %) was determined in soil sample 2. The composition of major elements such as Si, Fe and K of all soil samples do not differ significantly.

Table 5 Elemental Composition of Soil Samples

No	Element	%Composition		
		Sample 1	Sample 2	Sample 3
1	Si	42.064	42.554	44.500
2	Fe	25.922	30.355	28.526
3	Ca	9.342	1.546	2.831
4	Al	7.997	14.826	13.824
5	K	6.794	6.958	6.695
6	S	4.397	0.490	0.431
7	Ti	2.297	2.359	2.240
8	Zr	0.259	-	-
9	Mn	0.232	0.272	0.381
10	Sr	0.201	0.216	0.178
11	Cr	0.107	0.066	0.071
12	Zn	0.086	0.127	0.098
13	V	0.083	0.119	0.121
14	Ni	0.073	-	-
15	Cu	0.055	0.065	0.060
16	Rb	0.050	-	-
17	Y	0.042	0.048	0.045

Conclusion

Ceramics and earthenware created by Nwe-nyein pottery industry are still in common use in many parts of everyday life of Myanmar people. Most are in the form of cooking pots, flower pots, drinking water pots and food and water storage pots. Drinking water pots are earthenwares and it is convenient to use these pots to filter heavy toxic minerals of ground water and other unneeded impurities. Glazed pot or in Myanmar we called San-Oh is being made by applying specific elevated temperature (>1000 °C). Analyzed soil samples from Nwe-nyein complex have not been investigated scientifically before. This study revealed that the determination of pH, moisture, color, electrical conductivity, cations exchange capacity, texture, soil mineralogical constituents and characterization of soil morphology. Particle size distribution was also measured to classify the texture. According to physiochemical properties of pottery soils, they do not contain hazardous toxic metals and all results data support that these soils are suitable to use in pottery making. Another detail research should be carried out on pottery soil by using other additional advanced spectroscopic techniques to do a complete survey and long term assessment. Finally, traditional pottery making of Nwe-nyein area was still needed to maintain this art and encourage with advanced technology and all kinds of supplements for local people as soon as possible.

Acknowledgements

The authors would like to thank to Department of English for the correction of grammar and usage error and also Higher Education (Naypyidaw), Ministry of Education for supporting fund. The authors would like to express gratitude to Rector Dr Aye Kyaw and Pro-rectors Dr Khin Ma Ma Tin and Dr Myinzu Min, Yadanabon University for providing necessary resources. The authors would like to express our gratitude to Daw Myint Myint, Professor and Head, Department of English for hercorrection and edition of written English errors. We owe a great deal of gratitude to Dr Hlaing Haling Myat, Professor and Head, Department of Chemistry, Yadanabon University for her invaluable suggestions, kind guidance and encouragement for carrying out this research project.

References

Folk, R.L. (1974*). Petrology of Sedimentary Rocks*, Austin, Texas, Hemphill Publishing Company, p.89.

Lajunen, L.H. (1997). *Spectrochemical Analysis by Atomic Absorption and Emission*, Cambridge, the Royal Society of Chemistry, British Library.

Lieutenant Kyaw Thu Hein, (2011). *Elemental Analysis of Dolomitic Limestone Samples by Various Methods*, MSc Thesis, Chemistry Department, University of Mandalay (Unpublished)

Zunbul, B. (2005). *AAS, XRD, SEM, EDS and FTIR Studies of the Effect of Calcite and Magnesite on the Uptake of* Pb^{2+} *Ions by Natural Kaolinite and Clinoptilolite*, MSc Thesis, Graduate School of Engineering and Sciences of İzmir Institute of Technology

Shrestha R., Prajapati R. S. and Maskey P. N. (2018). Basic Properties of Soil of Bhaktapur Pottery, *International Journal of Science and Engineering Investigations*, vol 7, (78), pp.75-78, ISSN:2251-8843

Tucker, C. M. (2010). "Private Goods and Common Property: Pottery Production in a Honduran Lenca Community", *Human Organization*, Vol.69 (1), pp 43-53

STUDY ON TRADITIONAL MEDICINE (SETKUPALA No.2) FOR EYE DISEASES

Shwe Sin[1], Khin Myint[2]

Abstract

This research was studied on determination of antioxidant activity, toxicity of some elemental content, and antimicrobial activity of Traditional Eye Medicine, Setkupala (No.2) manufactured by Ministry of Health. In this work, the sample was collected from Myanmar Traditional Medicine shop, Yangon. Percent inhibition of the watery extract was tested by DPPH assay method. IC_{50} value of the sample was calculated by linear regression excel program. From the results, it is noted that IC_{50} values of Setkupala (No.2) had slight antioxidant activity. The elemental content of the sample was investigated by EDXRF and AAS methods. Iron content was higher than Selenium, Zinc, and Manganese in the sample whereas the content of Arsenic and Lead were present in the highest toxic elements. The contents of Iron, Arsenic, and Lead in the samples based on one oral dose (five tablets) per day were over the maximum permissible level of WHO standard. In the determination of antimicrobial activity, *Bacillus subtilis* (N.C.T.C- 8236), *Bacillus pumilus (*N.C.I.B-8982), *Staphylococcus aureus* (N.C.P.C- 6371), *Pseudomonas aeruginosa* (6749), *Candida albicans*, and *E.*coli (N.C.I.B- 8134) strains were used Antimicrobial activity test was done by using agar well diffusion method. According to the study of antimicrobial activity, it was clearly noticed that the different extracts of Setkupala (No.2) were effective against the different strains.T herefore, Setkupala (No.2)had antimicrobial activity. From the phytochemical investigation, it is found that the carbohydrates, glycosides, phenolic compounds, reducing sugars, saponins and tannins were present in the sample. Moreover, the sample was examined by FT IR and HPLC method.

Keywords: Setkupala (No.2), antioxidant activity, elements, antimicrobial activity, FT-IR, HPLC

Introduction

Most of the traditional medicines have provided for public health sector. Among the traditional medicines for the treatment of eye disorder, Setkupala (No.2) is a well-known oral medicine. It is composed of *Cinnamomum tamala* sp. (Karaway), *Elettaria cardamomum* Maton. (Pharlarnge),, *Semecarpus anacardium* L. F. (Chee thee), *Saussurea affinis*, *Sperng* sp. (Pannoot), *Myristica fragrans* Houtt. (Zardeikpho), *Syzygium aromaticum* L. Merr. & Perry (Layhyin), *Hydnocarpus kurzii* (King.) Warburg (Kalaw thee), *Rauwolfia serpentina* Benth. (Bonmayazar), *Plumbago rosea* L. (Kantgyokni), *Piper longum* L. (Peikchin), *Gentiana kurroo*,Royle. (Hsapale), *Nigella sativa* L. (Samonnet), *Carallia brachiate* (lour.) Merr. (Maniawga), *Foeniculum vulgare* Gaertn. (Samonsabah), *Trachyspermum ammi* L. (Samonphyu), *Anethum sowa* Roxb. (Samonnyo), *Foeniculum vulgare* Mill. (Samonphwe), *Lepidium sativum* L. (Samonni), *Cassia acutifolia* Delile. (Pwaygaing), *Capparis sepiaria* L. (Hsoogauknet), *Ferula foetida sp.* (Sheingo, Latex), *Aloe sp.* (Moke Khar), Borax, (Letchah meebauk). This medicine can reinforced not only eye diseases but also hypertension, paralysis, and arthritis. Therefore, it was need to study the effectiveness of Setkupala No.2 because traditional practitioners rely upon the Setkupala No.2 medicine to cure ailments.

[1] Dr, Associate Professor, Department of Chemistry, University of Mandalay
[2] Lecturer, Department of Chemistry, Sittwe University

Materials and Methods

Determination of Antioxidant Activity

In this experiment, the sample was collected from the traditional herbal shop from Ministry of Health, Yangon. The antioxidant activity was studied on watery extract of selected sample Setkupala (No.2) by DPPH free radical scavenging assay. 0.002 % DPPH solution was prepared in the brown coloured bottle by dissolving 2 mg of DPPH powder in the EtOH 100 mL. It was stored in the refrigerator for no longer than 24 h. About 4 mg of watery extract and 10 mL of EtOH were thoroughly mixed by shaker. Then, stock solution was obtained. Desired concentrations 400 μg mL^{-1}, 200 μg mL^{-1}, 100 μg mL^{-1}, 50 μg mL^{-1}, 25 μg mL^{-1} and 12.5 μg mL^{-1} of watery extract were prepared from this stock solution by dilution with appropriate amount of EtOH. The stock solution (100 μg mL^{-1}) of the sample was prepared by dissolving 1 mL of sample solution in 9 mL of EtOH. This stock solution was twofold serially diluted with EtOH to get the sample solutions with the concentration of 50, 25, 12.5, 6.25, 3.125, 1.56, and 0.78 μg mL^{-1}. The blank solution was prepared by mixing the sample solution 1.5 mL with 1.5 mL of EtOH. The control solution was prepared by mixing 1.5 mL of 0.002 % DPPH solution and 1.5 mL of EtOH using shaker. DPPH radical scavenging activity was determined by UV spectrophotometric method. The control solution was prepared in the brown bottle by mixing 1.5 mL of 0.002 % DPPH solution and 1.5 mL of ethanol using shaker. The sample solution was also prepared by mixing thoroughly 1.5 mL of 0.002 % DPPH solution and 1.5 mL of each of the test sample solution. The bottles were allowed to stand at room temperature for 30 min. After 30 min, the absorbance of these solutions was measured at 517 nm and the percentage of radical scavenging activity (% RSA) was calculated by the following equation.

$$\% RSA = \frac{A_{control} - (A_{sample} - A_{blank})}{A_{control}} \times 100$$

where, % RSA = % radical scavenging activity of test sample,
$A_{control}$ = absorbance of DPPH in EtOH solution,
A_{sample} = absorbance of sample solution with DPPH solution, and
A_{blank} = absorbance of sample solution with EtOH solution.

The antioxidant power (IC_{50}) is expressed as the test substance concentration (μg/mL) that result in a 50 % reduction of initial absorbance of DPPH solution and that allows to determine the concentration. IC_{50} (50% inhibitory concentration) values were calculated by linear regressive excel program. Similarly, the standard, ocuvite (western medicine), was determined above procedure. The standard deviation was also calculated by the following equation:

$$\text{Standard Deviation (SD)} = \sqrt{\frac{(\bar{x} - x_1)^2 + (\bar{x} - x_2)^2 + \ldots (\bar{x} - x_n)^2}{(n-1)}}$$

Determination of Elements by Energy Dispersive X- ray Fluorescence Spectrometry

The powdered sample was fabricated into pellet. The pellet sample was placed in the sample chamber of EDX- 700 spectrometer that can be measured the sixteen samples at a time and analyzed in PC based multi - channel analyzer using EDX- 700 software.

Determination of Elements by Atomic Absorption Spectrophotometry

Atomic absorption spectrophotometer (Perken Elma Analyst 800) was used for determination of elements. About 1 g of ash sample was accurately weighed and dissolved in 5 mL of 20 % of concentrated hydrochloric acid. The resulting solution of ash sample was evaporated to dryness and dissolved in 6 mL of 20 % HCl solution (volume by volume) followed by centrifugation. The centrifugate was decanted and the clear solution was made up to 100 mL with deionized water. The resultant solution 10 mL was pipette accurately and made up to 100 mL again with deionized water. The sample solution prepared was now ready for analysis of mineral elements by AAS (Lajunen, 1991).

Determination of Antimicrobial Activity

The strains used in this study were *Bacillus subtilis* (N.C.T.C-8236), *Bacillus pumilus* (N.C.I.B-8982), *Staphylococcus aureus* (N.C.P.C-6371), *Pseudomonas aeruginosa* (6749), *Candida albicans*, and *E.*coli (N.C.I.B-8134). Antimicrobial activity test was done by using agar disc diffusion method. The ethyl alcohol, petroleum ether, ethyl acetate, n-butanol and aqueous extracts were impregnated in agar disc for about five minutes. Then the incorporated discs with extracts were placed on the nutrient agar medium seeded with 0.25 mL of each microorganism suspension by sterile forceps. Inoculated plates with different indicator cultures were incubated at 37 °C in an incubator for 24 h. After overnight incubation, the developing zone of inhibition on agar medium were measured by a plastic ruler and recorded.

Phytochemical Investigation

In the phytochemical test, the sample was examined by using Mayer's reagent, Dragendorff's reagents and Wagner's reagents for alkaloids, by using concentrated hydrochloric acid and magnesium ribbon for flavonoids, by bromothymol blue indicator for organic acids, by Benedict's reagent for reducing sugars, by acetic anhydride and concentrated sulphuric acid for steroids (Robison, 1983), by spraying with ninhydrin reagent for α– amino acids, by using 2 % chloride solution and 1 % gelatin solution for tannin (Marini-Bettolo *et al*, 1981), by using sodium picrate solution for cyanogenic glycosides, by using 10 % lead acetate solution for glycosides (Trease, 1980), by using vigorously shaking with distilled water for saponins, by using iodine solution for starch (M-Tin Wa, 1970), by using 10 % α- naphthol for carbohydrates, by using acetic anhydride and concentrated sulphuric acid for steroids, by using 5 % ferric chloride solution for phenolic compounds, (Vogel, 1966).

FT IR Spectroscopic Analysis

The Fourier transform infrared spectrum of ethyl acetate extract of the sample was measured as KBr pellet and recorded on Perkin Elmer GX FT IR Spectrophotometer at the Universities' Research Centre (URC).

HPLC Analysis

Chemicals

All the chemicals used were of Analytical Reagent grade. Solvents used were HPLC grade from Hua Co., Najing, China. The water used was distilled and deionized by using Millipore system.

Sampling

The solutions extracted were filtered by 0.45 μm filter. 1 mL each ethyl acetate solutions extracted then were dried by eppendorf vacufuge plus vacuum concentrator and mixed with 1 mL of concerned mobile solution. After that, 20 μL each solution was added in the vial.

Chromatographic conditions

C 18 column (4.5 × 250 & 5 μm particles) (Phecda) was used as stationary phase. The mobile phase consisted of 0.1 % formic acid buffer (A) and acetonitrile (B) was carried out gradient elution as follows; 5 min, 80%(A); 25 min, 30%(A); 35 min, 30% (A) The flow rate was 1.0 mL/min and the injection volume was kept 20 μL. The chromatograms were recorded at 265 nm and column temperature was maintained at 25° C throughout the study period. Different samples prepared as well as mobile phase were filtered using 0.45 μm filter and degassed by ultrasonication (Metrex) prior to use.

Results and Discussion

Antioxidant Activity of Sample Extract

In this work, DPPH (2, 2- diphenyl-1- picryl- hydrazyl) radical scavenging assay was used to assess the antioxidant activity for watery extract of Setkupala (No.2). The absorbance of different concentrations was measured at 517 nm by using UV spectrophotometer. Absorbent measurement was carried out in three times for each solution and mean values obtained were to calculate percent inhibition of oxidation by the equation. In the average values of percent inhibition, IC_{50} (50 % inhibitory concentration) values in μg mL^{-1} were calculated by linear regressive excel program. The results of sample are shown in Table 1.

According to literature, the lower the IC_{50} value is the higher the antioxidant activity. 50 % inhibitory concentration of Setkupala (No.2) was 27.37 μg mL^{-1} and standard (ocuvite, western medicine) was 172.61 μg mL^{-1}. Therefore, the antioxidant activity of Setkupala (No.2) was six times higher than that of ocuvite medicine.

Table 1 Antioxidant Activity of Setkupala (No.2)

Sample	Inhibition of Various Concentration of Watery Extract						IC_{50} µg/mL
	12.5 µg/mL	25 µg/mL	50 µg/mL	100 µg/mL	200 µg/mL	400 µg/mL	
Watery Extract	26.43 ±1.18	49.07 ±1.29	82.40 ±1.51	84.39 ±0.43	78.42 ±0.54	77.43 ±0.32	27.37
Standard (Ocuvite)	10.05 ±3.47	17.98 ±3.82	17.81 ±5.08	21.16 ±0.92	60.84 ±8.21	67.40 ±6.28	172.61

Elemental Analysis

Setkupala (No.2) was studied by Energy Dispersive X-Ray Fluorescence technique and Atomic Absorption Spectrophotometry for the determination of elements. The X-ray fluorescent analysis is widely accepted as a standard method for elemental analysis. It is observed that calcium, potassium, silicon, sulphur, iron, strontium, thallium, manganese, zirconium, rubidium, zinc, copper, and nickel were present in Setkupala (No.2) by EDXRF. The relative abundance of elements is shown in Table 2. The spectrum from EDXRF determination is shown in Figure 1. From the data, it can be seen that percentage of calcium is the highest amount in Setkupala (No.2) and the second highest amount is potassium. silicon, sulphur and iron are the third highest amount. The trace amount of strontium, thallium, manganese, zirconium, rubidium, zinc, copper, and nickel are present in the medicine. In this work, a total of 7 elements were determined. Iron, selenium, zinc, and manganese are some of antioxidant nutrient elements whereas some toxic elements are arsenic, lead, and cadmium. Atomic absorption spectrophotometric analysis showed that Setkupala (No.2) contained 0.0363 % of iron, 0.0005 % of selenium, 0.0005 % of zinc, 0.0001 % of manganese, 0.0084 % of arsenic, 0.0028 % of lead, and 0.0001 % of cadmium. The calculation results of percentage and compositions of elements per different tablets per day are also shown in Table 3. From the literature, it was known that the permissible level of elements were 150 µg/day of iron, 200 µg/day of selenium, 2800 µg/day of zinc, 2300 µg/day of manganese, 50 µg/day of arsenic, 21 µg/day of lead, and 6 µg/day of cadmium (WHO, 1996). According to daily medical dosage for Setkupala (No.2), a dose for a day is 4/5 tablets for adult. Therefore, it is suitable for two tablets a dose instead of five tablets a dose because the contents of iron, arsenic and lead in five tablets are over the permissible levels and the two tablets a dose are under the maximum permissible level according to WHO standard.

Table 2 Relative Abundance of Elemental Contents in Setkupala (No.2)

No	Element	Relative Abundance (%)
1	Ca	39.265
2	K	28.911
3	Si	11.730
4	S	11.419
5	Fe	7.136
6	Sr	0.485
7	Ti	0.478
8	Mn	0.228
9	Zr	0.115
10	Rb	0.082
11	Zn	0.067
12	Cu	0.050
13	Ni	0.034

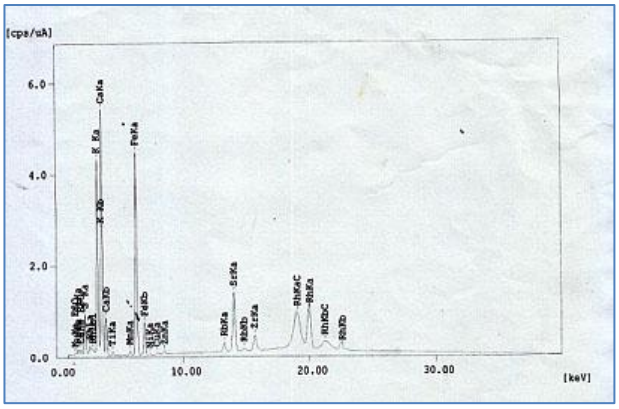

Figure 1 EDXRF spectrum of Setkupala (No.2)

Table 3 Elemental Contents in Setkupala (No.2) Determined by AAS (based on dried sample)

No.	Elements	Content (%)	Content (x 10^{-6}) mg per day					
			One tablet	Two tablets	Three tablets	Four tablets	Five tablets	WHO (1996)
1.	Fe	0.0363	108	218	326	435	544	150
2.	Se	0.0005	0.14	0.28	0.42	0.55	0.69	200
3.	Zn	0.0005	1.6	3.22	4.83	6.44	8.05	2800
4.	Mn	0.0001	0.28	0.56	0.86	1.16	1.46	2300
5.	As	0.0084	25.1	50.1	76.4	100	126	50
6.	Pb	0.0028	8.36	16.7	25.1	33.7	41.8	21
7.	Cd	0.0001	0.31	0.63	0.94	1.26	1.57	6

Antimicarobial Activity

The organism strains such as *Bacillus subtilis*, *Bacillus pumilis*, *Staphylococcus aureus*, *Pseudomones aeruginosa*, *Candida albicans* and *E.coli* species were used for testing the antimicrobial activity of fractions separated from Setkupala (No.2). The antimicrobial activity was tested by agar disc method. The inhibition zones of various extracts are shown in Table 5. It is clearly noted that EtOAc and n-BuOH extract of Setkupala (No.2) possessed antimicrobial activity against all strains tested. In addition, all the fractions were found to be active against *B.subtilis and Staphylococcus aureus* species. However, all fractions were more active against *Staphylococcus aureus* than *B.subtilis.* Especially, n-BuOH extract possessed significantly high antimicrobial activity.

Pseudomonas aeruginosa can cause devastating infections in the human eye. It is one of the most common causes of bacterial keratitis. EtOAc extract showed total activity against *P. aeruginosa. Candida albican* can cause conjunctivitis. Visual disturbance may include blurring, sensitivity to light and eye pain. *S.aureus* always has the potential to cause diseases, including

boils and pimples, wound infections, pneumonia, septicemia, food intoxication and toxic shock syndrome. Symptoms of *E.coli* infection are nausea or vomiting, severe abdominal cramps, watery or very bloody diarrhea, fatigue, fever (Jacobson and Silverma, 2009).

Therefore, Setkupala (No.2) can prevent the above diseases because it possessed antibacterial activity.

Table 4 Results of Antimicrobial Activity of Crude Extracts of Setkupala (No.2)

No.	Fraction	*B. subtilis*	*S. aureus*	*P.aeruginosa*	*B. pumilus*	*C.albicans*	*E.coli*
1.	P_1	++ (16 mm)	+++ (23 mm)	-	-	-	-
2.	P_2	++ (17 mm)	+++ (22 mm)	-	-	-	-
3.	P_3	++ (18 mm)	+++ (24 mm)	+++ (25 mm)	++ (17 mm)	++ (17 mm)	+++ (24 mm)
4.	P_4	++ (17 mm)	+++ (23 mm)	++ (17 mm)	+++ (24 mm)	+++ (26 mm)	+++ (25 mm)
5.	P_5	++ (16 mm)	+++ (23 mm)	-	-	-	-

P_1 = EtOH extract
P_2 = Petether extract
P_3 = EtOAC extract
P_4 = n-BuOH extract
P_5 = Aqueous

Agar well - 10 mm
(+) = 10 mm ~ 14 mm (mild activity)
(++) = 15 mm ~ 19 mm (medium activity)
(+++) = 20 mm above (high activity)
(–) = negative

Phytochemical Study

Phytochemical study revealed the presence of carbohydrates, glycosides, phenolic compounds, reducing sugars, saponins, and tannins in Setkupala (No.2).

Study on FT IR spectrum.

The band assignments of FT IR spectrum of ethyl acetate extract are presented in Table 5. The broad band at 3359 cm^{-1} is attributed to O-H stretching vibration. Asymmetric and symmetric C-H stretching vibrations of methyl group absorb at 2923 cm^{-1}, 2854 cm^{-1}. A strong band occurred at 1708 cm^{-1} is assigned as a stretching vibration of C=O which is conjugated to aromatic ring. A peak at 1603 cm^{-1} indicates the C=C stretching vibration of alkenic group. Strong bands at 1456 cm^{-1} and 1377 $cm^{-1}$are attributed to the O-H bending vibration.

Table 5 Assignment for FT IR Spectrum of Ethyl Acetate Extract of Setkupala (No.2)

Wavelength (cm^{-1})	**Assignment**	**Possible Compounds**
3359	-OH stretching	Phenolic compounds, glycosides, or alkaloids
2923, 2854	-CH stretching	Aliphatic chains
1708	C=O stretching	Aromatic ring
1603	C=C stretching	Unsaturated carbonyl compounds
1456, 1377	C-H bending	Aliphatic chains

Analysis of Setkupala (No.2)

The sample was determined by HPLC-MS (TOF) Agilent Mass Hunter, Workstation Software B.04.00). According to the result, it could be known that the peaks showed at the retention time 3.317 min, 6.317 min, and 6.57 min respectively. Then the Agilent Mass Hunter software interpreted at 144.0908 m/z, 218.1219 m/z, and 287.1758 m/z for these peaks. As they were studied by library, that might be possible compounds indicated that N-Acetyl-dl-alanine methyl amide, Ethanol, 2,2'-oxybis-, dipropanoate and 1-Serine, N, O-bis (pivaloyl)-, methyl ester compounds might be present in the Setkupala (No.2).

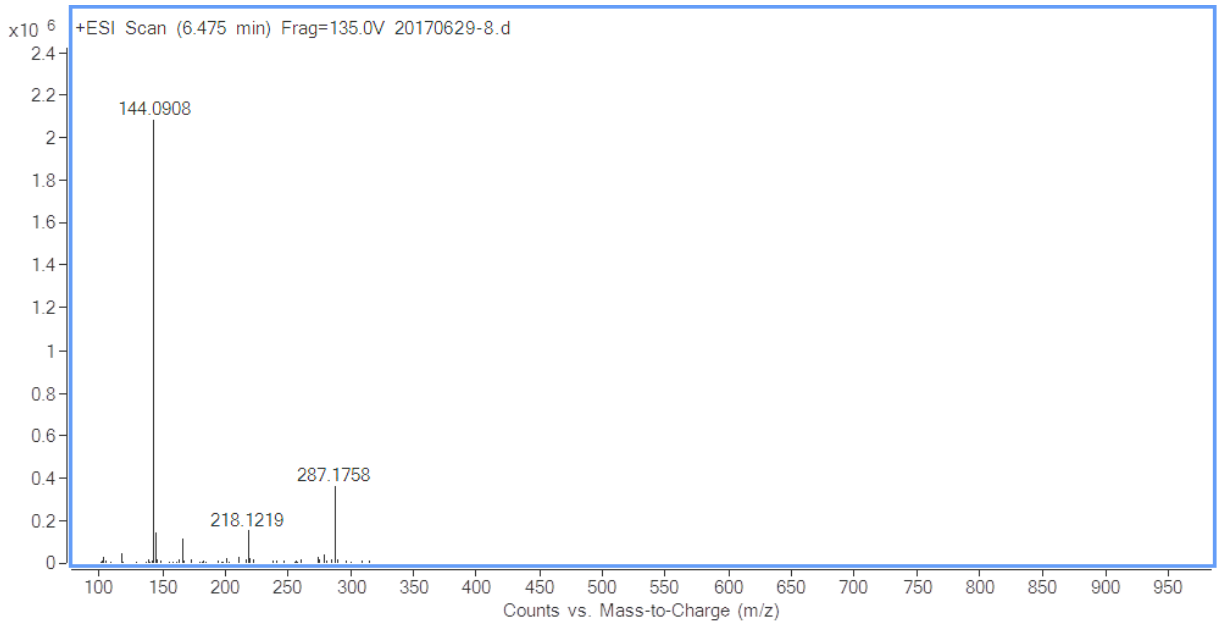

Figure 2 Spectrum review of chromatogram result of Setkupala (No.2)

Conclusion

According to phytochemical study, Setkupala (No.2) reveals that it contains carbohydrates, glycosides, phenolic compound, reducing sugars, saponins, and tannins.

From the study of elemental analysis, it is found out that Setkupala (No.2) contains chlorine, potassium, silicon, sulphur, iron, strontium, titanium, manganese, zirconium, rubidium, zinc, copper, and nickel by EDXRF. Moreover, iron, selenium, zinc, manganese, arsenic, lead, and cadmium were studied by AAS method. Composition of the some elements for a dose was under the maximum permissible level of WHO standard. However, the amount of iron, arsenic, and lead in a dose or five tablets was over the maximum permissible level. According to the data, it is suggest that the two tablets were a suitable dose per day. On the other hand, it should be continued that the elemental content of ingredients of Setkupala (No.2) should be determined and the amount of ingredients which have high toxic level will be reduced in the formulation.

By the study of antimicrobial activity, it was clearly noted that the different extracts of Setkupala (No.2) were effective against some pathogenic microorganisms such as *Bacillus subtilis, Staphylococcus aureus, Pseudomonas aeruginosa, Bacillus pumilus, Candida*

albicans and *E.coli sp.* Therefore, Setkupala (No.2) has antimicrobial activity. Furthermore, it possess higher antioxidant activity than that of western medicine, ocuvite. And it was seen that N-Acetyl-dl-alanine methylamide, Ethanol, 2,2'-oxybis-, dipropanoate and 1-Serine, N, O-bis (pivaloyl)-, methyl ester compounds might be present in the Setkupala (No.2) by HPLC-MS (TOF).

Acknowledgements

The authors would like to acknowledge to Professor Dr Yi Yi Myint (Professor and Head), Chemistry Department, University of Mandalay, for her kind encouragement and invaluable suggestions. We also would like to express our profound gratitude to the Department of Higher Education, Ministry of Education, Myanmar, for provision of opportunity to do this research and Myanmar Academy of Arts and Science for allowing to present this paper.

References

Jacobson, J. and Silverma, S. (2009). *Pathogenesis of Bacterial Infections*. New York: pp. 55 - 289

Lajumen, L. H. J. (1991). Spectrochemical Analysis by Atomic Absorption and Emission. London: The Royal Society of Chemistry, British Library, pp. 57

Marini - Bettolo, G. B., Nicole, H. M. and Palamia, M.(1981). "Plant Screening by Chemical and Chromatographic Procedure Under Field Conditions". *J. Chromato.,* vol. 45, pp. 121- 123

Robison, T. (1983). *The Organic Constituents of Plants*. USA: 5th Ed., Cordus Press, pp. 63 - 64

M-Tin-Wa. (1972). "Phytochemical Screening, Methods and Procedures". *Phytochemical Bulletin of Botanical Society of America* **5**(3): pp. 4 - 10

Trease, G. E.(1980). *Pharmacology*. London. 1st Ed., Spottiswoods Ballantyne Ltd., pp. 108

Vogel, A.I. (1966). *A Text Book of Practical Organic Chemistry*. London: 3th Ed., Language Book and Longman Group Co., Ltd., pp. 453 - 454

WHO. (1996). "Trace Elements in Human Nutrition and Health", Geneva: pp.37 - 287

STUDY ON COMPARATIVE ADSORPTION EFFICIENCIES OF RICE STRAW AND COCONUT HUSK (FIBRE) BY USING CONGO RED DYE

Hta Hta Win*

Abstract

Adsorption of congo red from aqueous solution onto rice straw (RS) and coconut husk fibre (CCH) under batch conditions was investigated. Before sorption process, the physicochemical properties of RS and CCH fibre such as moisture content, ash content, bulk density and pH were determined by standard methods. The samples was characterized by SEM. Adsorption was studied as a function of amount of adsorbent, contact time, pH and various concentrations with time. It was carried out at pH 6. A synthetic solution of 25 mg/L of the dye was used. The optimum contact time was 120 min and 0.2g was a suitable dose of sorbent.The sorption properties of congo red were spectrophotometrically determined.The highest removal percent of congo red by rice straw powder (80.31%) and coconut husk fibre powder (74.96%) were observed.

Keywords: Rice straw, Coconut husk, Sorption, Congo red

Introduction

Pollution; environmental pollution, the addition of any substance (solid, liquid, or gas) or any form of energy (such as heat, sound, or radioactivity) to the environment at a rate faster than it can be dispersed, diluted, decomposed recycled or stored in some harmless form. The major kinds of pollution are air pollution, water pollution, and land pollution. Water pollution is the presence of harmful materials in water, such as sewage, dissolved materials, waste from farms, factories and crude oil spilled from oil tankers (Adamson, 1967). The three main substances that pollute water are nitrates from fertilizers, sewage and detergents. Most dye materials are irritants to the skin, eyes, and respiratory system and may be toxic by inhalation and ingestion (Bharathi and Remesh, 2013). Synthetic dyes are extensively used in textile dyeing, paper printing, color photography, pharmaceutical, food, cosmetic and other industries (Sharma*et al*., 2010). Rice is the world's second largest cereal crop and produces the largest amount of crop residues (Soest, 2006). Rice, rice husk and rice straw are the main products of rice cultivation and processing. Rice straw and coconut husk (fibre) are considered extremely effective for the removal of impurities (Binod, *et al.,* 2010). The initial dye concentration, pH, contact time and dosage effects were studied aiming to obtain the best adsorption capacity by rice straw powder and coconut husk powder. Dried rice straw and dried coconut husk biomass were prepared using low cost carbon source rice straw powder and coconut husk powder biomass were used as adsorbents for the removal of acidic dye (Congo red) from aqueous solution.The aim of the research work is to study the adsorptions efficiencies of rice straw powder and coconut husk fibre powder to be used as effective sorbents for the colour removal of acidic dye (Congo red).

Materials and Methods

Sampling and Preparation

The rice straw and the coconut husk were collected from Kanpya Village, Magway Township, Magway Region. Firstly the samples were cut into small pieces. Then they were washed with tap water to remove the attached dusts and other impurities. The washed rice straw

* Dr, Associate Professor, Department of Chemistry, University of Magway

and coconut husk were dried and ground in the mechanical grinder to form the fine powder. The powder was sieved and a size fraction in the range of less than 100 μm was used in all the experiments. This powder was soaked (0.01 g/mL) in 5% w/v bleaching powder for 24 hours. The mixture was filtered and the powder residue was continuously washed with distilled water until the pH of the solution is nearly neutral. This filtered biomass was first dried at room temperature and then in oven at 60 ºC for 6 hours. Figure 1 (a) and (b) shows the photographs of rice straw powder and coconut husk fibre powder. The dried biomass rice straw powder and coconut husk powder were stored in air-tight glass bottles to protect them from moisture.

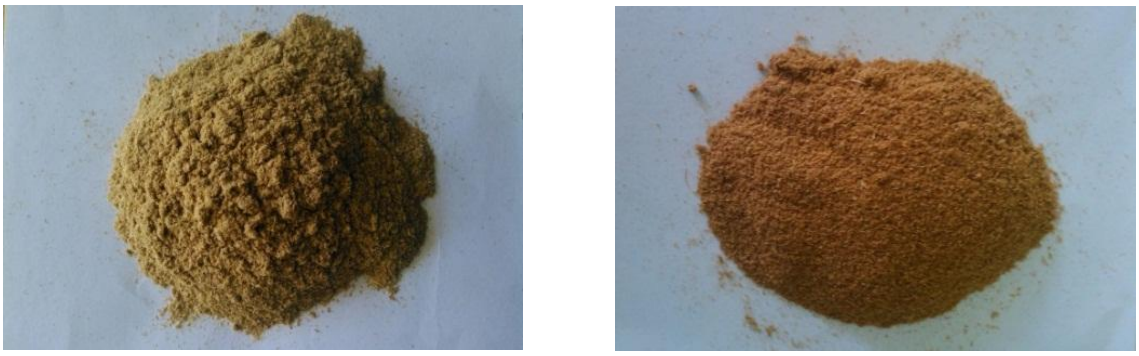

(a) (b)

Figure 1 Photographs of (a) rice straw powder (b) coconut husk fibre powder

Determination of Physicochemical Properties of Rice Straw and Coconut Husk

The physicochemical properties of RS and CCH fibre such as moisture content, ash content, bulk density and pH were determined by standard methods.

Characterization of Rice Straw and Coconut Husk by SEM

The surface morphologies of RS and CCH fiber were studied by SEM. The SEM micrographs were taken with (JEOL-JSM-5610, Japan).

Sorption Studies of Congo Red by Rice Straw and Coconut Husk

A stock solution of 100 mg/L (congo red solution) was prepared by dissolving 100 mg in 1 L distilled water. By serial dilution, the dye solutions congo red within the concentration range of 0.80 mg/L to 50 mg/L were prepared.

Determination of Maximum Absorption Wavelength of Congo Red Solution

The spectrophotometer was first calibrated with blank solution of distilled water. Maximum wavelength of congo red solution (25 mg/L) was determined by spectrophotometer at various wavelengths.

Construction of a Standard Calibration Curve

Series of standard (congo red) solution were prepared by serial dilution. The absorbance of standard solutions was measured at the wavelength of 500 nm by means of spectrophotometer. The standard calibration curve was constructed by plotting the absorbance versus concentration of the congo red solution.

Effect of pH on Adsorption of Congo Red by Two Types of Sorbents

The solution of congo red (25 mg/L) was prepared and the range of pH (3-8) was adjusted by the adding of 0.1 M sodium hydroxide and (0.1 M) hydrochloric acid. Each 50 mL of congo red solution was mixed with 0.2 g of adsorbent (rice straw powder or coconut husk fibre powder) in the flasks. The flasks were shaken with electronic shaker at room temperature for 2 h and the sample solution was prepared by filtration. The residual content of congo red in the filtrate was determined by spectrophotometrically.

Effect of Initial Concentration on Adsorption of Congo Red by Rice Straw and Coconut Husk

Accurately weighed sample (0.2 g) was placed in separate conical flasks. Then 50 mL of congo red solution initial concentration (5 mg/L- 40 mg/L) was added into each conical flask and was shaken with electric shaker. The residual content of congo red in the solution was determined by spectrophotometrically.

Effect of Contact Time on Adsorption of Congo Red byRice Straw and Coconut Husk

Accurately weighed sample (0.2 g) was placed in separate conical flasks. Then 50 mL of congo red solution (25 mg/L) was added into each conical flask and was shaken with electric shaker. The contact time was varied at interval of 20 min, 40 min, 60 min, 80 min, 100 min, 120 min, 140 min and 160min. The sample solution was separated by filtration. The residual content was determined by spectrophotometrically.

Effect of Dosage on Adsorption of Congo Red byRice Straw and Coconut Husk

The samples of various masses ranging from 0.01 g - 0.30 g were separately placed in the conical flask and 50 mL of standard congo red solution (25 mg/L) was added into each conical flask. In order to attain complete equilibrium, the solutions were shaken with electric shaker for one hour at room temperature. The sample solutions were removed from the sorbent by filtration. The residual content of congo red in the solution was determined by spectrophotometrically.

Results and Discussion

Physicochemical Properties of Rice Husks and Coconut Husks

The resulting data of rice straw powder and coconut husk fibre Powdersuch as moisture content, ash content, bulk density and pH value are presented inTable1. According to the results, it was observed that moisture content (%) of rice straw powder is lower than coconut husk fibre powder and ash content (%), bulk density (gcm^{-3}) and pH of rice straw powder are greater than coconut husk fibre powder.

Table 1 Physicochemical Properties of Rice Straw Powder and Coconut Husk Fibre Powder

No.	Sample	Moisture content (%)	Ash Content (%)	Bulk Density (gcm^{-3})	pH
1.	Rice straw powder	7	18	0.21	7.69
2.	Coconut husk fibre powder	10	3	0.08	7.35

Characterization of Rice Straw Powder and Coconut Husk Fibre Powder by SEM

SEM measurement for surface analysis was carried on rice straw powder and coconut husk fibre powder samples. The SEM micrographs displaying the surface morphology of rice straw powder and coconut husk fibre powder are shown in Figures 2 (a) and (b). In this micrograph, sponges like shaped particle and their sizes (10 μm) were observed.

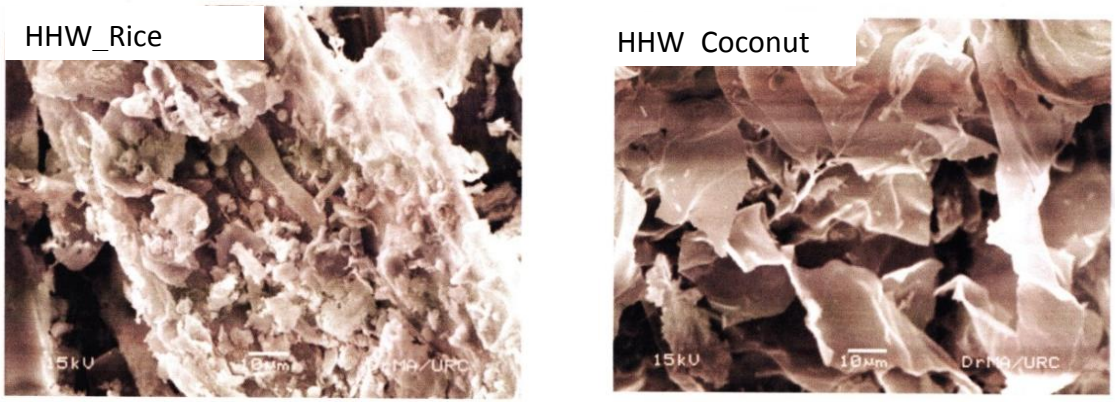

(a) (b)

Figure 2 SEM images of (a) rice straw and (b) coconut husk

Determination of Wavelength of Maximum Absorption of Congo Red Solution

Wavelength of maximum absorption of congo red solution (25 mg/L) was determined by spectrometer at various wavelengths. From the curve of absorbance versus wavelength (Figure 3), it was found that the maximum wavelength (λ_{max}) of congo red is 500 nm.

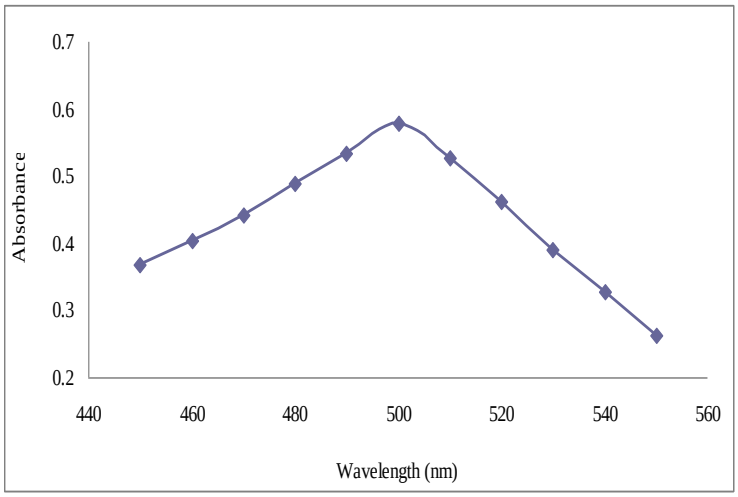

Figure 3 Maximum absorbance wavelength for congo red

Construction of Standard Calibration Curve of Congo Red

Series of standard solution were prepared by serial dilution. The absorbance of standard solutions was measured at the wavelength of 500 nm by means of spectrophotometer, spectrum curve for congo red is presented inFigure4. The data from 0.80 mg/L to 25 mg/L follows the Lambert Beer's Law, but beyond 25 mg/L it deviates from Lambert Beer's Law.

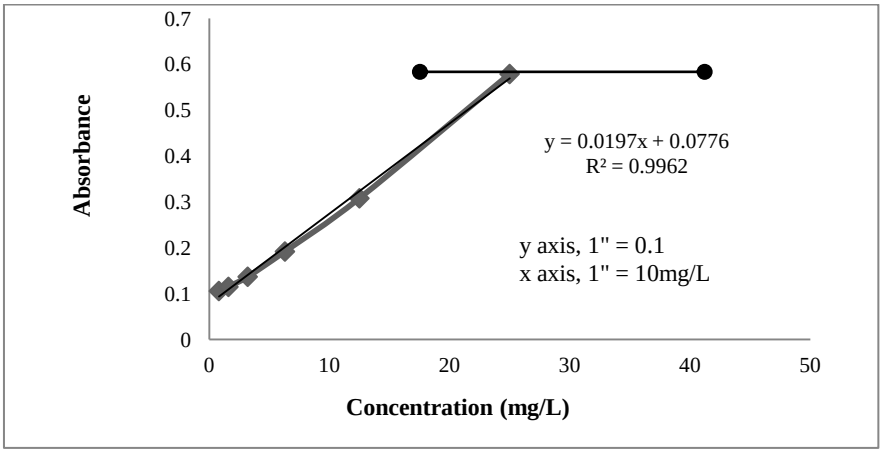

Figure 4 Calibration curve for congo red at λ_{max} = 500 nm

Sorption Properties of Congo Red by Rice Straw Powder and Coconut Husk Fibre Powder

During the sorption process, solute is transferred from solution of the solid phase where its concentration increase until a dynamic equilibrium is reached. The concentration of solute (dye) in the sorbent depends not only on the concentration in solution, but also on some parameters that may influence potentially the sorption equilibria. Dye molecules contain after strongly acidic or basic groups (e.g., sulphonic); which degree of dissociation remains virtually unchanged over a wide pH range.

Effect of pH

The pH of aqueous solution is an important parameter in the adsorption process and thus the effect of pH has been studied by varying it in the range of 3.0 – 8.0. Effect of pH on sorption of congo red by using rice straw powder and coconut husk fibre powder is presented in Figure 5. The maximum percent removals of congo red by rice straw powder and coconut husk fibre powder were observed at pH 6 and decreased substantially with increasing of pH. According to the results, it was found that rice straw powder gave the higher removal percent than that of coconut husk fibre powder at pH 6.

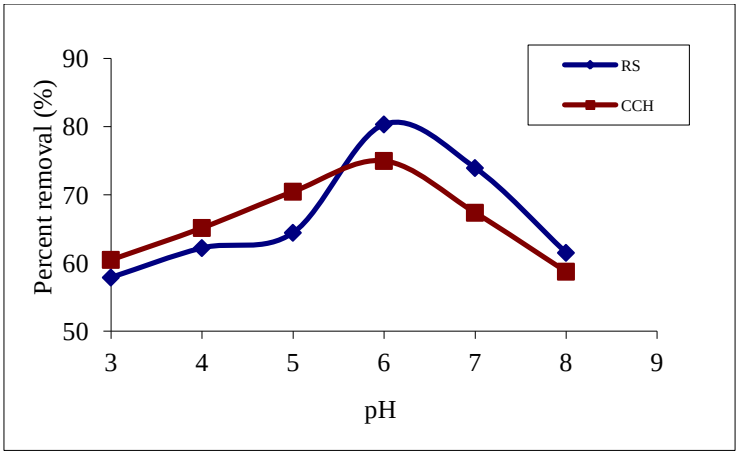

Figure 5 Effect of pH on sorption of congo red by using rice straw powder and coconut husk fibre powder

Effect of Initial Concentration

The effect of initial concentration on percent removal of congo red by rice straw powder and coconut husk fibre powder was studied when other parameters (dosage of sorbent and contact time) were kept constant and varied the initial concentrations ranging from 5 to 40 mg/L. The effect of initial concentration on adsorption of congo red by rice straw powder and coconut husk fibre powder is shown in Figure 6.It can be seen that the lower the initial concentration of congo red solution, the sorption is higher and the higher concentration of adsorbate the sorption capacity is lower.

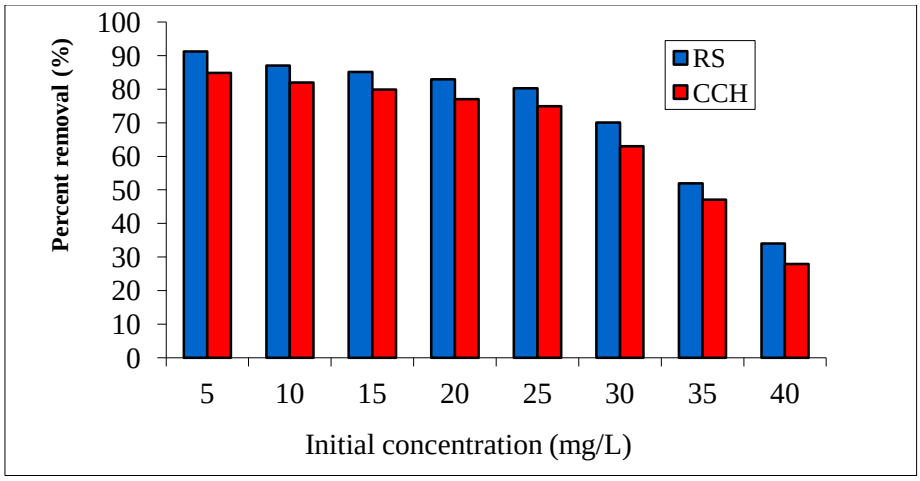

Figure 6 Effect of initial concentration on adsorption of congo red by rice straw powder and coconut husk fibre powder

Effect of Contact Time

The effect of contact time on the extent of adsorption of congo red by rice straw powder and coconut husk fibre powder is shown in Figure 7. The extent of adsorption increase with time of 20 min and attained equilibrium at 120 min when using initial concentration of 25 mg/L at pH 6.

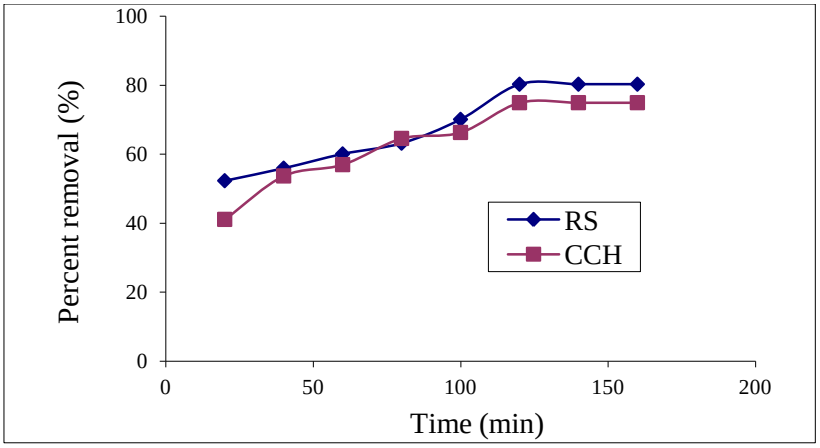

Figure 7 Effect of contact time on the removal of congo red by using rice straw powder and coconut husk fibre powder

Effect of Dosage

In the investigation of effect on dosage on the removal of congo red, the dose sorbent (rice straw powder and coconut husk fibre powder) were varied from 0.01 g to 0.30 g in 50 mL of congo red solution. The effect of dosage of sorbent on the removal of congo red by using rice straw powder and coconut husk fire powder is shown in Figure 8. According to the resulting data, the highest removal percent of congo red were observed when 0.2 g of rice straw powder and coconut husk fibre powder were used. This increase of percentage of adsorption can be explained by the presence of high number of adsorption sites on the area of adsorbent.

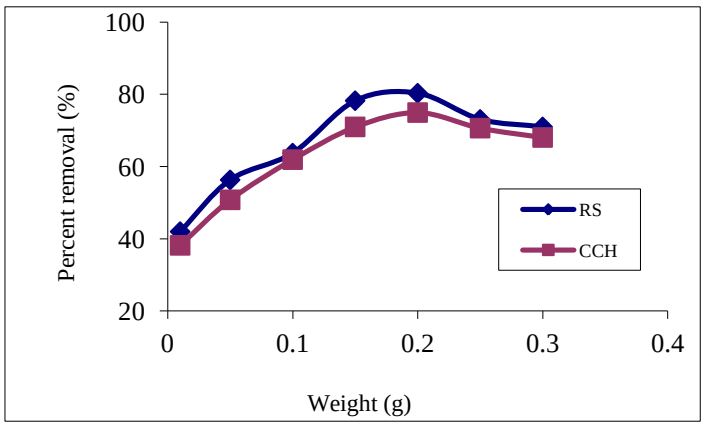

Figure 8 Effect of dosage of sorbent on the removal of congo red byusing rice straw powder and coconut husk fibre powder

Conclusion

In this study, congo red was removed from aqueous solution by rice straw powder and coconut husk fibre powder. Rice straw and coconut husk fibre were collected from Kanpya Village, Magway Township, Magway Region.

The physicochemical properties of rice straw powder and coconut husk fibre powder such as moisture content 7% and 10%, ash content 18% and 3%, bulk density 0.21 g cm^{-3} and 0.08 g cm^{-3} and pH 7.69 and 7.35 were determined respectively.

From SEM micrographs, it was observed that porosity of rice straw powder was higher than that of coconut husk fibre powder. Sorption study was carried out spectrophotometrically. The effects of sorption parameters in the process of sorption were studied with respect to pH, initial concentration, contact time and dosage method.

According to the experimental results, it was found that the highest removal percents of congo red by rice straw powder were (80.31%) and coconut husk fibre powder were (74.96%) when using (0.2g) of sorbents in 50 mL of 25 mg/Linitial congo red solution of pH 6 for 120 min. Thus, rice straw powder and coconut husk fibrepowder can be used as effective sorbents for the removal of acidic dye from aqueous solution.

It was found that rice straw powder (80.31%) had greater sorption efficiency than coconut husk fibre powder (74.96%).

Acknowledgements

The author wish to thank the Myanmar Academy of Arts and Science for allowing to present this paper and Professor and Head, Dr Thidar Aung and Professor Dr Htay Htay Win, Department of Chemistry, Magway University for their provision and suggestions of the research facilities.

References

Adamson, A. W. (1967). *Physical Chemistry of Surface*. New York: 2nd Ed., Interscience Publishers. pp. 301-303

Bharathi, K. S. and Remesh, S. T. (2013). "Removal of Dyes using Agricultural Waste Water as Low-cost Adsorbents: Review".*Appl Water Sci.,* vol. 31, pp. 773-790

Binod, P., Sindhu, R., Singhania, R. R., and Devi, L. (2010)."Bioethanol Production from Rice Straw.An Overview".*BioresourceTechnol.*, vol. 101, pp.4767-4774

Sharama, P., Kaur, R., Baskar, C. and Chung, W. J. (2010)."Removal of Methylene Blue from Aqueous Waste using Rice Husk and Rice Husk Ash".*Desalinatia*, vol. 259, pp.249-257

Soest, P. J. V. (2006). "Rice Straw, the Role of Silica and Treatments to Improve Quality".*Aim, Feed Sci. Technol*., vol. 103, pp.137-171

STRUCTURE ELUCIDATION OF A PURE ORGANICCOMPOUND ISOLATED FROM THE BARK OF *ADINA CORDIFOLIA* HOOK.F (HNAW)

Kyu Kyu Maw,[1] Hla Myo Min,[2] Myint Myint Sein[3]

Abstract

One of Myanmar indigenous medicinal plant, *Adina cordiforlia* Hook.f (Hnaw) was selected for chemical analysis. A pure organic compound was isolated from the bark of Hnaw by using advanced separation methods such as Thin Layer and Column Chromatography. The yield percent of this pure green crystal compound was found to be 2.35 % based upon the ethyl acetate crude extract. The pure isolated organic compound responds medium activity on *Bacillus pumilus* and *E. coli* and low activities against *Staphylococcus aureus*, *Pseudomonas aeruginosa* and *Candida albicans*. The molecular formula of the pure compound was determined as $C_{22}H_{22}O_8$ by using some spectroscopic techniques such as FT IR, ^{1}H NMR (500 MHz), ^{13}C NMR (125 MHz), DQF-COSY, HMQC, HMBC and EI-Mass spectral data. Hydrogen deficiency index of this compound is 12. Finally, the complete structure of this pure compound as dimer of 2-hydroxy-4-ethoxy cis-coumaric acid was elucidated by employing DQF-COSY, ^{1}H NMR splitting patterns, coupling constant (J- value) and HMBC spectroscopic studies.

Keywords: *Adina cordiforlia* Hook.f, Thin Layer and Column Chromatography, Spectroscopic techniques

Introduction

In ancient times, medicinal plants have been used all over the world as unique sources of medicines. Many medicinal plants represent a rich source of drugs individually or in combination have been recommended in various medical treaties for the cure of different diseases (Kirtikar and Basu, 1933).

Thousands of indigenous plants have been used by man from prehistoric times on all continents for relieving and curing ailments. In spite of tremendous development in the field of allopathy medicinal plants and their derivatives still remain one of the major sources of drugs in modern and traditional systems throughout the world playing a major role in medicinal therapy. In India about 7300 plant species are used in traditional health care systems. 90% of the medicinal plants which find place in day to day uses, many of these, are used as herbal remedies. The expanding domestic and global demand of herbal remedies. The expanding domestic and global demand of herbal products has put the native medicinal plant resources under significant stress (Kumari, 2013).

In this study, a pure bioactive organic compound was isolated from the bark of *Adina cordifolia* Hook.f belonging to the family, Rubiaceae, locally known as Hnaw by applying modern separation methods such as Thin Layer and Column Chromatography. Furthermore, the structure of this bioactive compound was elucidated by using some modern spectroscopic methods such as FT IR, ^{1}H NMR (500 MHz), ^{13}C NMR (125 MHz), DQF-COSY, HMQC, HMBC and EI-Mass spectrometry.

[1] Dr, Lecturer, Department of Chemistry, University of Magway
[2] Dr, Professor, Department of Chemistry, University of Mandalay
[3] Dr, Professor (Retd.), Department of Chemistry, University of Mandalay

Botanical description of *A. cordifolia* (Figure 1) was shown as follows:


Figure 1 Plant and bark of *Adina cordifolia* Hook.f (Hnaw)

Family	-	Rubiaceae
Botanical name	-	*Adina cordifolia* Hook.f.
Myanmar name	-	Hnaw
English name	-	Yellow Teak
Medicinal uses	-	inflammation, urinary retention, wounds and ulcers, skin diseases, infection, dysentery, fever and burning sensation

Materials and Methods

The following advanced instruments were used in the characterization of the sample as well as in the structure elucidation of the pure compound.

1. UV lamp (Lambda 40, Perkin Elmer Co, England)
2. FT IR spectrometer (Shimadzu, Japan)
3. NMR spectrometer (500 MHz) (JEOL, Japan)
4. EI-Mass spectrometer

The chemicals used were analytical grade reagents. They were produced from British Drugs House (BDH) London and Merck, Germany. Analytical preparative thin layer chromatography was performed by using precoated silica gel (Merck, Co. Inc. Kieselgel 60 F_{254}). Silica gel (70 to 230 mesh ASTM) was used for column chromatography.

Sample Collection

The bark of Hnaw for experiment was collected from Bu-ta-lin Township, Sagaing Region, Myanmar. The samples were cut into small pieces and allowed to air dry. Then the dried pieces were stored in a well-stoppered bottle and used throughout the experiment.

Extraction and Isolation of Pure Organic Compound

Air dried sample (800 g) was percolated with 95 % ethanol (2.7 L) for two months. The extracted solution was filtered and evaporated in air. Then, it was re-extracted with ethylacetate (200 mL) and resulting solution was evaporated. The ethylacetate crude extract (6.5 g) was obtained.

The ethylacetate crude extract (6.5 g) was fractionated by column chromatography over silica gel with various ratios of n-hexane and ethylacetate from non-polar to polar. Totally (283) fractions were obtained. Each fraction was checked by TLC. The same R_f value fractions were combined. Three combined fractions were collected. Major combined fraction (II) gave only one spot on TLC and UV active. Pure green crystal (0.1526 g) was obtained. The yield percent of this pure compound (KKM-1) was found to be 2.35 % based upon the ethylacetate crude extract.

Screening of Antimicrobial Activities of the Pure Isolated Compound

Antimicrobial activities of the pure isolated compound were determined by agar-well diffusion method on six tested organisms such as *Bacillus subtilis, Staphylococcus aureus, Pseudomonas aeruginosa, Bacillus pumilus, Candida albicans* and *E. coli* respectively.

Identification of the Pure Isolated Compound

The pure isolated compound was identified by modern spectroscopic techniques such as FT IR, ^{1}H NMR (500 MHz), ^{13}C NMR (125 MHz), DQF-COSY, HMQC, HMBC and EI-Mass spectrometry.

Results and Discussion

Screening of Antimicrobial Activities of the Pure Isolated Compound

Antimicrobial activities of the pure isolated compound were determined by agar-well diffusion method on six tested organisms. The pure isolated organic compound responds medium activity on *Bacillus pumilus* (16 mm) and *E.coli* (18 mm) and low activities against *Staphylococcus aureus* (13 mm), *Pseudomonas aeruginosa* (12 mm) and *Candida albicans* (12 mm). The results are shown in Table 1 and Figure 2.

Table 1 Antimicrobial Activities of the Pure Isolated Compound

Sample	Solvent	Inhibition zone diameters (mm) against different microorganisms					
		I	**II**	**III**	**IV**	**V**	**VI**
Pure Compound	EtOH	-	13 (+)	12 (+)	16 (++)	12 (++)	18 (++)

Agar well~10 mm
10 mm~14 mm(+)
15 mm~19 mm(++)
20 mm above (+++)

Organisms
I. *Bacillus subtilis*
II. *Staphylococcus aureus*
III. *Pseudomonas aeruginosa*
IV. *Bacillus pumilus*
V. *Candida albicans*
VI. *E. coli*

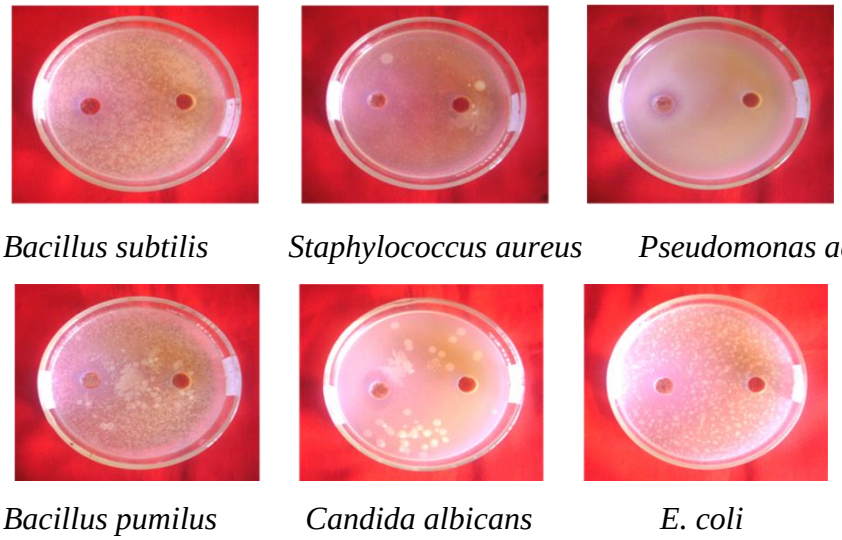

Figure 2 Screening of antimicrobial activities of the pure isolated compound

Identification of the Pure Isolated Compound

The ethyl acetate crude extract was separated by chromatography on a silica gel column using n-hexane and ethyl acetate with various ratios from non-polar to polar to obtain pure organic compound, dimer of 2-hydroxy-4-ethoxy cis-coumaric acid.

Molecular Formula of the Pure Isolated Compound

The molecular formula of the pure isolated organic compound could be determined by some spectroscopic methods such as FT IR, ^{1}H NMR (500 MHz), ^{13}C NMR (125 MHz), DQF-COSY, HMQC, HMBC and EI-Mass spectrometry (Figure 3 to Figure 8).

According to FT IR spectrum (Figure 3) the characteristic bands at 3170 cm^{-1}, 2962 cm^{-1}, 2913 cm^{-1}, 1681 cm^{-1}, 1604 cm^{-1}, 1566 cm^{-1}, 1404 cm^{-1}, 1234 cm^{-1}, 1130 cm^{-1}, 1033 cm^{-1}, 829 cm^{-1} and 756 cm^{-1} showed that the pure isolated compound contains –OH group, sp^3 hydrocarbon, carbonyl group, aromatic benzenering, allylic hydrocarbon, gemdimethyl group, C–CO – O stretching vibration, C–C–O stretching vibration of alcohol group, C–O–C stretching vibration of ether group, trans or E and cis or Z alkenic groups, respectively (Silverstein *et al*., 2005).

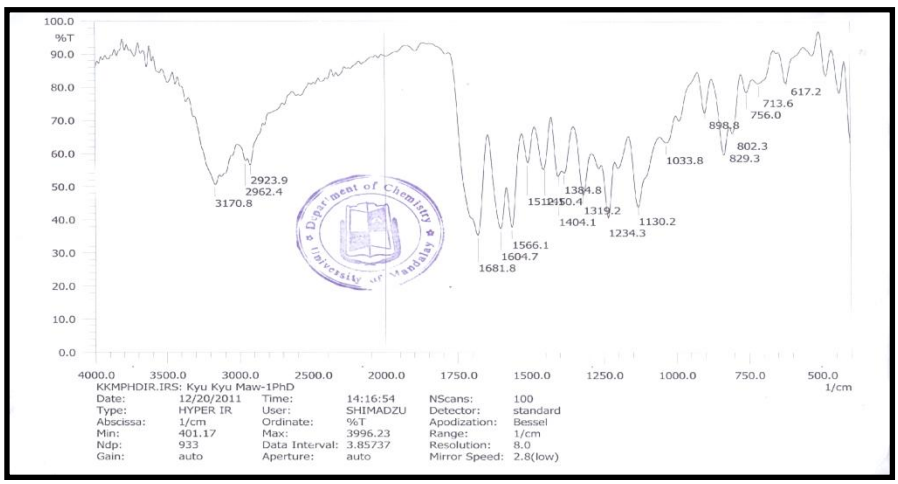

Figure 3 FT IR spectrum (KBr) of the pure isolated compound

^{1}H NMR (500 MHz) spectrum (Figure 4) represents the chemical shift values, splitting pattern and coupling constant (J-values) of protons. According to this spectrum, the pure isolated compound contains 9 protons (Timothy, 1999).

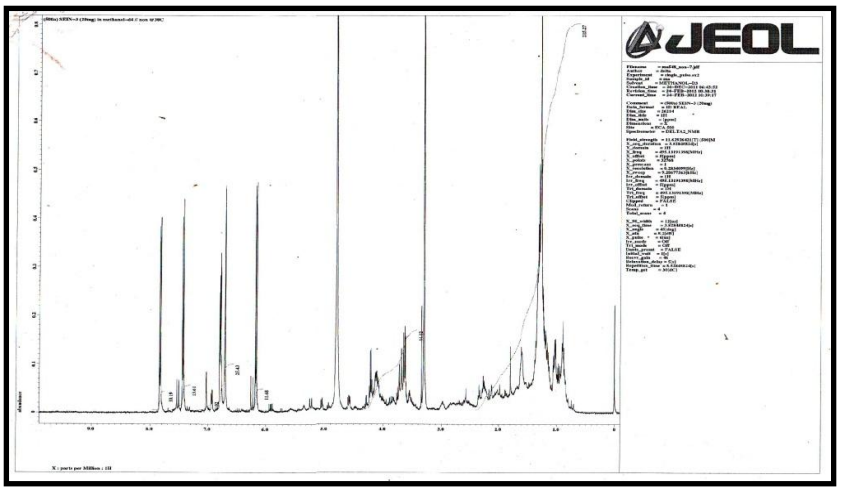

Figure 4 ^{1}H NMR spectrum (500 MHz, MeOH) of the pure isolated compound

^{13}C NMR spectrum (Figure 5) represents the total number of carbons. According to this spectrum, the pure isolated compound contains 11 carbons.

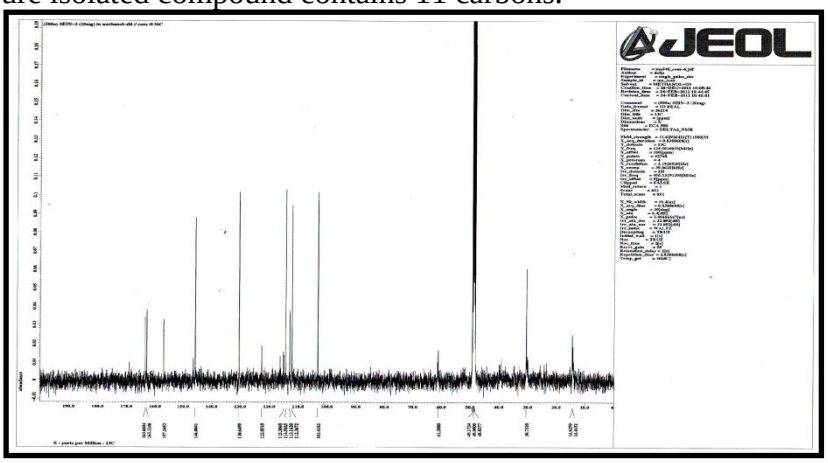

Figure 5 ^{13}C NMR spectrum(125 MHz, MeOH) of the pure isolated compound

The DEPT spectrum (Figure 6) confirms the number of carbons, protons and kinds of carbons containing in this compound (Silverstein *et al*., 2005).

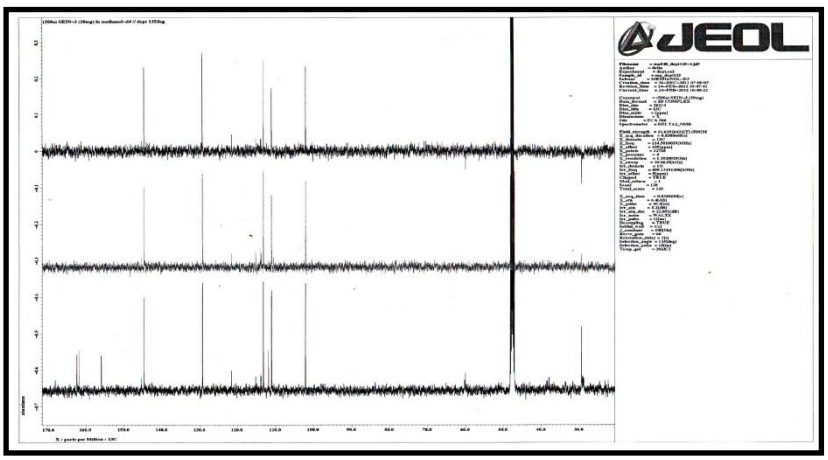

Figure 6 DEPT spectrum of the pure isolated organic compound

The HMQC spectrum (Figure 7) gives rise to the proton- carbon direct correlation (Timothy, 1999).

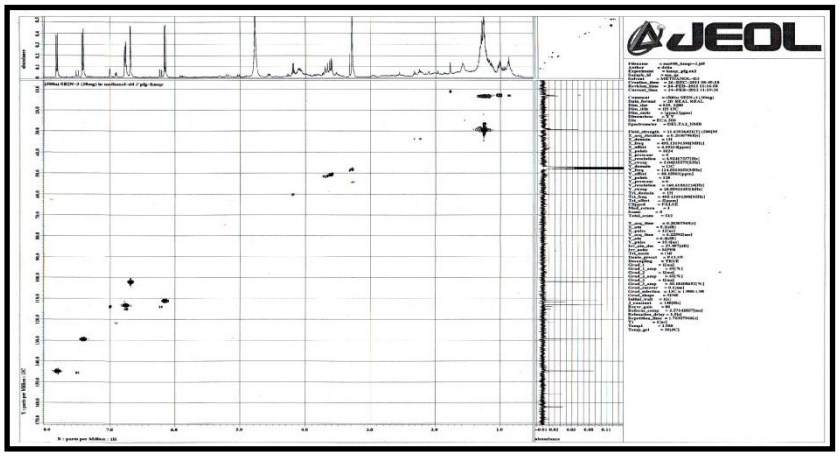

Figure 7 HMQC spectrum of the pure isolated organic compound

In addition EI-MS spectrum (Figure 8) of this compound shows the molecular ion peak at m/z 414 which implies the molecular mass of compound (Porter and Baldas, 1971).

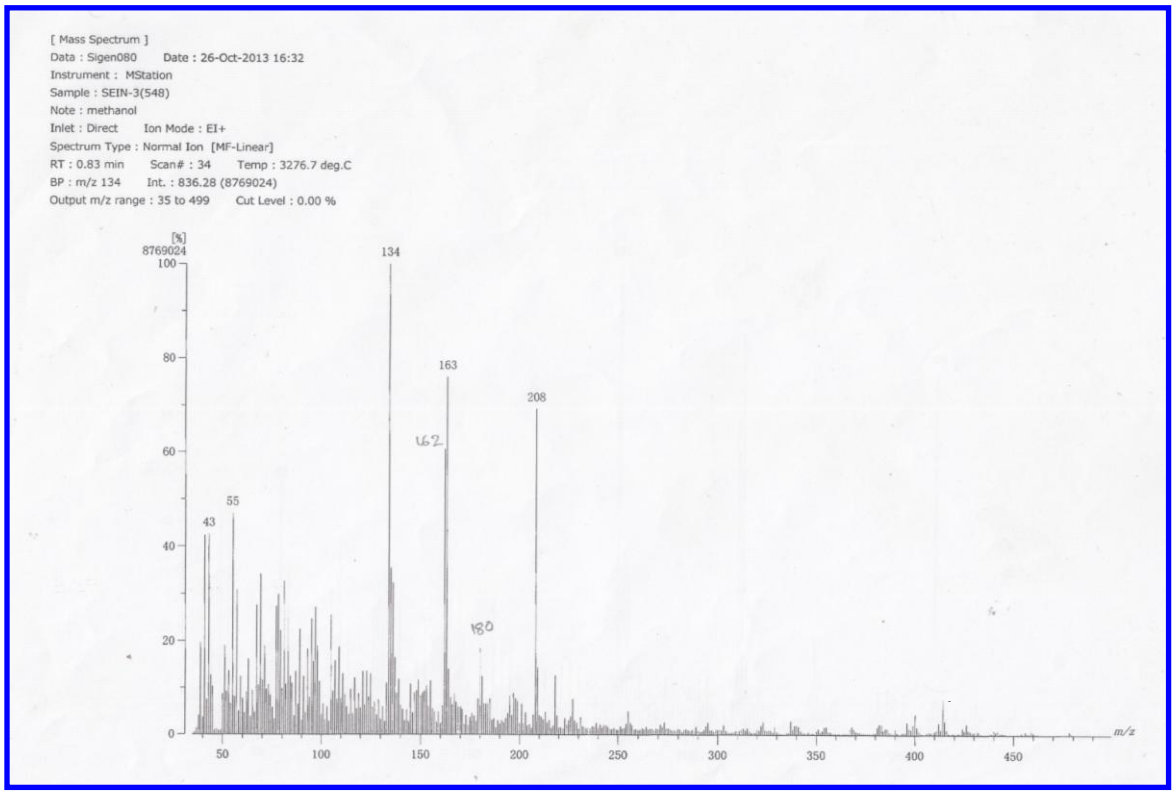

Figure 8 EI-MS spectrum of the pure isolated organic compound

According to ^{1}H NMR and ^{13}C NMR spectral data, the partial molecular formula is $C_{11}H_9$ and the partial molecular mass is 141.

In accordance with FT IR assignment, the pure compound should consist of at least one carbonyl group, one -OH group and one ether functional group.

Hence, the extended molecular formula is $C_{11}H_{10}O_3$ and extended partial molecular mass is 190.

However, in EI-Mass spectrum, the molecular ion peak m/z at 414 which represents the molecular mass of this pure compound. According to EI-Mass spectrum and the previous spectrums (^{1}H NMR , ^{13}C NMR, DEPT and HMQC), the compound is suggested to exist as a dimer.

Therefore, the extended molecular formula become to be $C_{22}H_{20}O_6$ and its molecular mass is 380.

Hence, the remaining partial molecular mass = 414 – 380 = 34. It should be two –OH groups.

Thus, the real molecular formula of this pure compound (KKM- 1) is $C_{22}H_{22}O_8$ which agrees with the nitrogen rule.

$$\text{Hydrogen Deficiency Index (HDI)} = 22 - \frac{22}{2} + 1$$

$$= 12$$

Structure Elucidation of the Pure Isolated Compound

The structure elucidation of the pure isolated compound could be determined by ^{1}HNMR, DQF-COSY, HMQC and HMBC spectral data (Figure 9 and Figure 10).

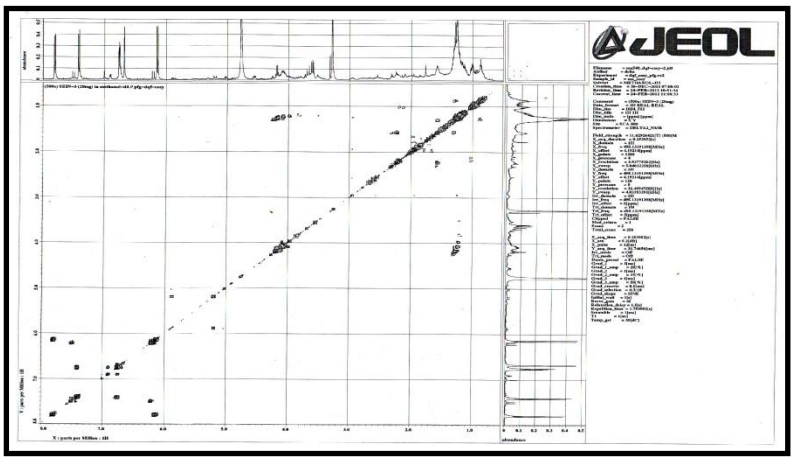

Figure 9 DQF-COSY spectrum of the pure isolated organic compound

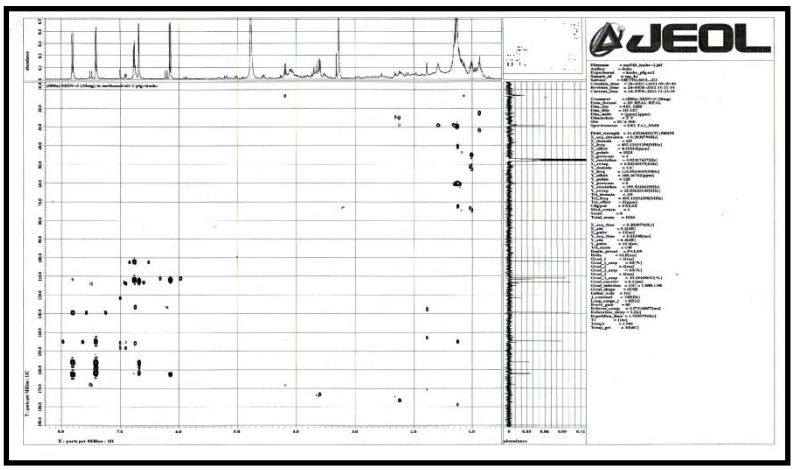

Figure 10 HMBC spectrum of the pure isolated organic compound

The substituted benzene fragment could be assigned by DQF-COSY (Figure 9), HMQC (Figure 7) and HMBC (Figure 10) spectra respectively. In the fragment a , the ortho orientation of two aromatic protons (δ 6.78 ppm and δ 7.44 ppm) and the meta orientation of two aromatic protons (δ 6.78 ppm and δ 6.69 ppm) could be confirmed by ^{1}H NMR splitting patterns and coupling constants J values.

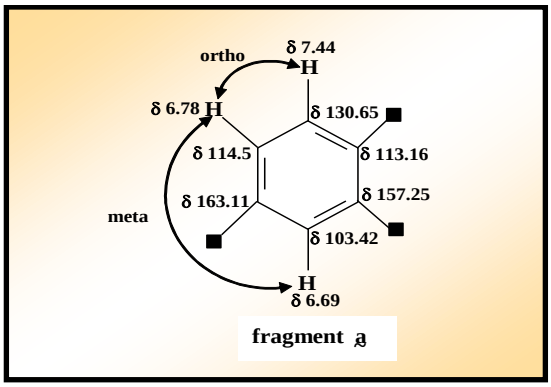

On the other hand, the alkenic fragment could be assigned by DQF-COSY, HMQC, HMBC spectra. It can be confirmed by ^{1}H NMR splitting pattern and coupling constant (J values) which indicates that the two alkenic protons (δ 7.83 ppm and δ 6.17 ppm) exist as cis position to each other (Fragment b).

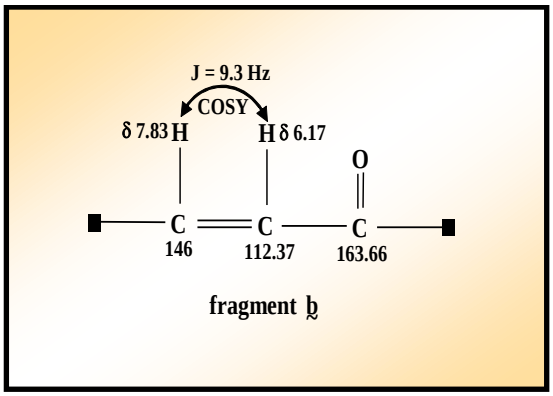

The observation of downfield chemical shift of one of alkenic protons (δ 7.83 ppm) is consistant with the theoretical resonance contribution structures caused by carbonyl group next to them, as shown below.

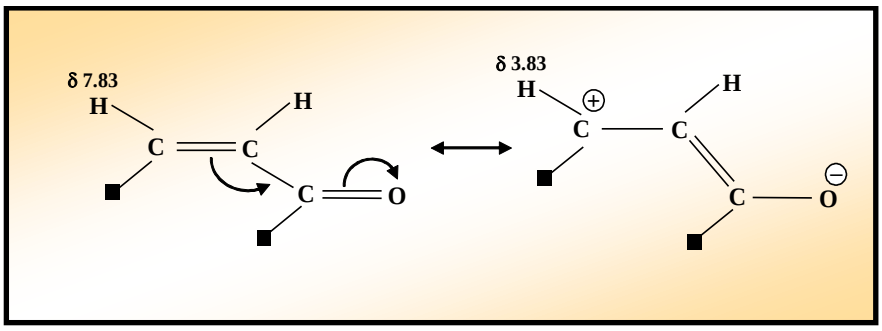

Moreover, the ethylenylhydroxy (–O–CH_2–CH_2–) fragment could be elucidated by DQF-COSY and HMQC spectra (Fragment c).

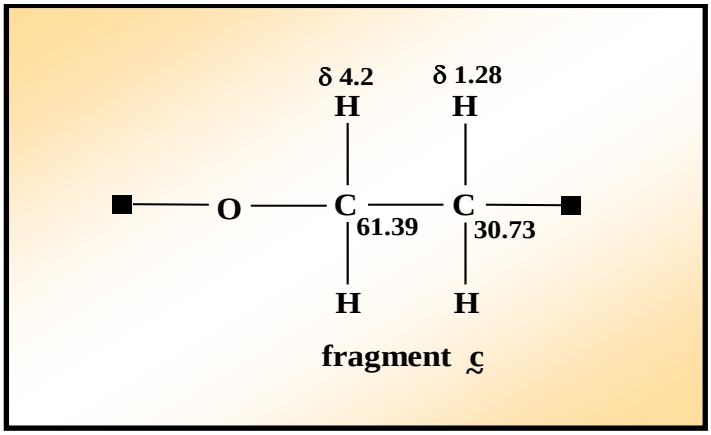

The combination of fragments a, b and c gives the gross molecular structure (fragment d̲) shown below.

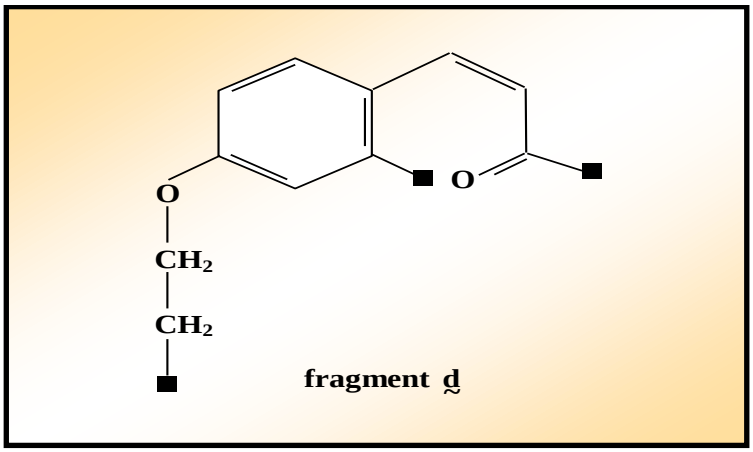

According to the FT IR spectrum, the reasonable attachment of two hydroxy groups to the downfield chemical shift aromatic quaternary carbon (δ 157.25 ppm) and the carbonyl carbon (δ 163.66 ppm) produces the following fragment e.

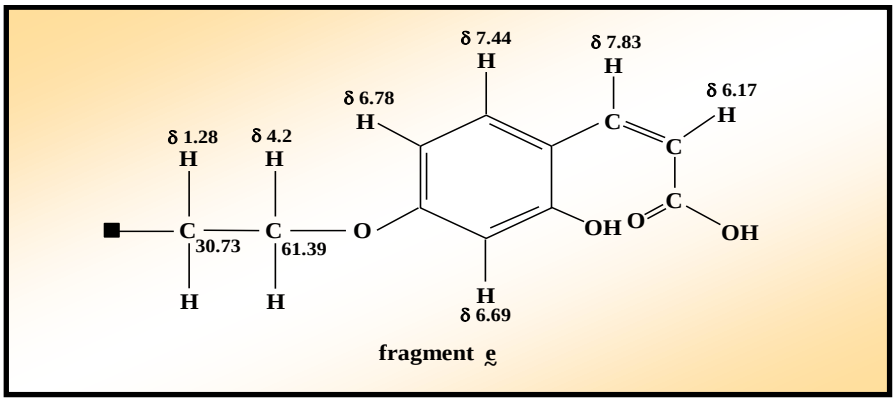

In the FT IR spectrum, the unusual lower frequency of –OH functional group at 3170.8 cm^{-1} and the carboxylic carbonyl group at 1681.8 cm^{-1} is assigned to be formation of intramolecular hydrogen bonding in this fragment, as described below.

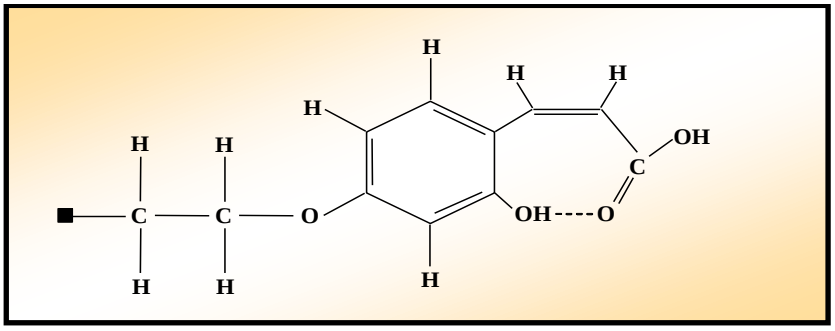

There are anomalous stretching frequencies of –OH and – CO – groups observed in FT IR spectrum. Carboxylic group – OH shows normal pattern (broad) and position (between 3200 – 2500 cm^{-1}). But phenolic – OH shows very much lower frequency 3170.8 cm^{-1}. At the same time, carboxylic carbonyl also shows very lower frequency value 1681.8 cm^{-1} if it is compared with its normal value 1740 cm^{-1}.

One factor which tend to lower the stretching frequency of carbonyl is due to the presence of conjugated system. However this effect will not decrease the frequency down to 1681.8 cm^{-1}. So there must be other factor that causes carboxylic acid carbonyl frequency. These unusual lower frequencies of phenolic – OH and carboxylic carbonyl group are assigned to be presence of intramolecular hydrogen bonding within the compound, as shown below.

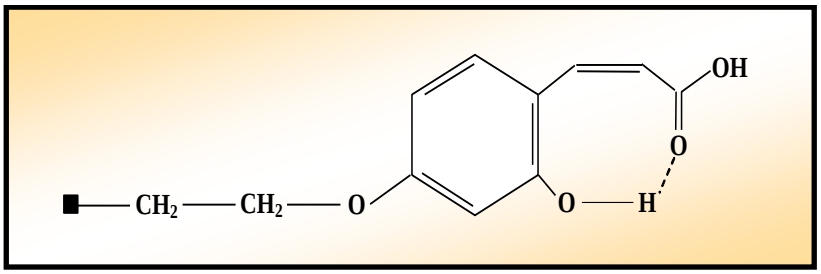

Formation of intramolecular hydrogen bonding well accounts for observed lower frequencies of both –OH and C = O stretching vibration.In EI-Mass spectrum, the observation of the apparent peak at m/z 208 implies the following molecular structure.

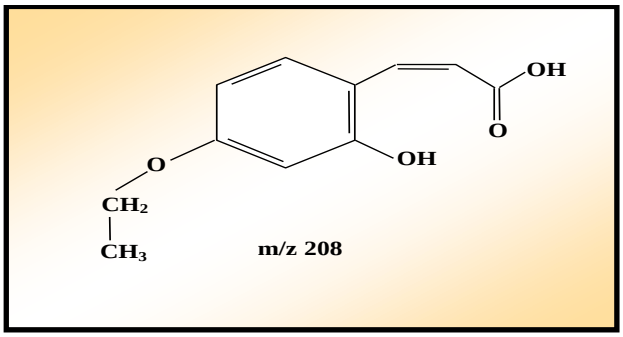

However, the absence of methyl carbon in the DEPT spectrum and the occurrence of the molecular ion peak at m/z 414 indicates that the compound is suggested to exist as a dimer as described below.

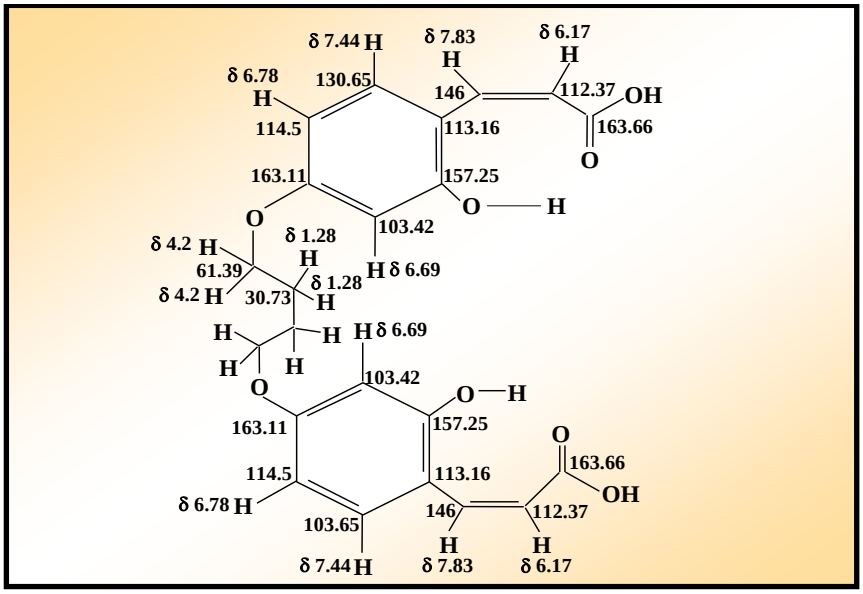

Complete structure of the pure isolated compound

The IUPAC name of the pure compound isolated from the bark of *A. cordifolia* (Hnaw) is dimer of 2-hydroxy-4-ethoxy cis-coumaric acid.

Conclusion

In this research, the bark of *A. cordifolia* (Hnaw) was selected for chemical analysis. Green crystals (2.35 %) could be isolated from ethyl acetate crude extract in pure state. The molecular formula and the complete structure of the isolated compound were determined by some spectroscopic methods. This elucidated structure as dimer of 2-hydroxy-4-ethoxy cis-coumaric acid was then confirmed by mass fragmentation behaviours in EI-Mass spectral data. When antimcrobial activities of pure compound was determined, it exhibited medium activities against on *Bacillus pumilus* and *E.coli* and low activities against *Staphylococcus aureus, Pseudomonas aeruginosa* and *Candida albicans*.

Acknowledgements

The authors wish to thank the Myanmar Academy of Arts and Science for allowing to present this paper and Professor and Head, Dr Thidar Aung and Professor Dr Htay Htay Win, Department of Chemistry, Magway University for their provision and suggestions of the research facilities.

References

Kirtikar, K. R. and Basu, B. D. (1993). *Indian Medicinal Plants*. India: L.M. Basu, Allahadbad, pp. 1347-1348

Kumari, A. and Sharma, R. A. (2013). "A Review on *Millingtonia Hortensis* Linn.", *International Journal of Phamaceutical Sciences Review and Research,* vol. 9 (2), pp. 85-92

Porter, Q.N. and Baldas, J. (1971). *Mass Spectrometry of Heterocyclic Compounds.* New York: Wiley-Inter Science, a Division of John Wiley and Sons. Inc

Silverstein, R.M., Webster, F.X. and Kiemle, D.J. (2005). *Spectrometric Identification of Organic Compound.* New York: 7th Edition, John Wiley and Sons Inc, pp. 127-244

Timothy, D.W. (1999). *High Resolution NMR Techniques in Organic Chemistry*. New York: Pergamon, An Imprint of Elsevier Science

FATTY ACIDS IN AVOCADO OIL AND NUTRITIONAL, ANTIOXIDANT AND ANTIMICROBIAL ASSESSMENT OF THE PULP

Sandar Moe[1], Ei Thandar Ngon[2]

Abstract

Avocado (*Persea americana* Mill.) fruits contain many nutritional components which have medicinal importance as well. The oil (81%) from the fruit pulp was extracted by Soxhlet extraction with petroleum ether. The fatty acids in the oil were identified by GC-MS analysis by NIST spectral library. Eleven fatty acids were identified in the ester fraction: two unidentified acids; myristic acid; palmitoleic acid; palmitic acid; linoleic acid; petroselinic acid; oleic acid, as well as (11Z)-11-octadecenoic acid, stearic acid andisostearic acid, in the increasing order of retention time up to 23 min. One long chain alcohol and one free fatty acid were also suggested to be present in the pulp oil by FT IR. Avocado pulps were then analyzed for nutritional values present by using AOAC methods. The observed data revealed that avocado pulp had high energy value (344 kcal/100g). Moisture content (5.56 %) and ash content (5.23 %) were calculated in dried sample of avocado pulp. Protein, fat, fiber and carbohydrate contents were 6.55 %, 4.18 %, 8.14 % and 70.34 %, respectively. Agar well diffusion method was adapted to determine the antimicrobial activity of the avocado pulp extracts (PE, MeOH, EtOAc, EtOH and H_2O). The MeOH, EtOAc and EtOH extracts of avocado pulp were active against *Bacillus subtilis, Staphylococcus aureus, Bacillus pumilus, Candida albicans*and *Escherichia coli* while PE and H_2O extracts were inactive on all the tested microorganisms. All the extracts were inactive on *Pseudomonas aeruginosa.* In addition, the antioxidant activity of avocado pulp was slightly higher in the watery extract (IC_{50} = 19.32 µg/mL) than the ethanol extract (IC_{50} = 21.84 µg/mL) by DPPH assay method. The present study therefore confirms the nutritional and medicinal values of the avocado produced in Taunggyi.

Keywords: Avocado, fatty acids, nutritional values, antimicrobial activity, antioxidant activity

Introduction

There is currently great popular interest in natural products, which has motivated the search for a new sauce of bioactive compounds that can be beneficial for human consumption that can be beneficial for human consumption in place of synthetic compounds used in food industry as additives, and can contribute to the reduction of generated waste giving them a much more beneficial destination (Rodriguez-Carpena *et al.,* 2011). The avocado (*Persea americana* Mill.) is a fruit with antioxidant and antibacterial properties, produced in almost all tropical and subtropical regions of the world (Kate and Lucky, 2009). The avocado has an olive-green peel and thick pale yellow pulp that is rich in fatty acids such as linoleic, oleic, palmitic, stearic, linolenic, capric and myristic acids. This fruit is normally used for human consumption, but it also has been used as medicinal plant in Mexico and elsewhere in the world (Dreher and Davenport, 2013). The aim of this research was to study the fatty acid composition and nutritional values of avocado pulp oil and to evaluate the antioxidant and antimicrobial activity of avocado pulp.

[1] Dr, Associate Professor, Department of Chemistry, Taunggyi University
[2] Demonstrator, MRes, Department of Chemistry, University of Medicine (Taunggyi)

Materials and Methods

Plant Material

Fresh avocadopulps were collected from vegetable and fruit Myoma Market Taunggyi Township. The plant material was identified and authenticated at Department of Botany, Taunggyi University. The pulps were cut into small pieces and dried at room temperature. This sample was ground into powder in an electric blender and stored in airtight container.

Extraction of Avocado Pulp Oil

The powdered sample of pulp fruit (Avocado) (60 g) was weighed placed in a thimble made from Whatman paper No. 1 and then placed in a Soxhlet extractor. Petroleum ether was poured into the extractor until some of it overflowed into the flask. Petroleum ether was heated by means of a water bath. The extraction was assumed to be complete when a small amount of extract placed on a watch glass did not leave any residue on evaporation of solvent. Duration of about 5 h was required for the complete extraction during which time the petroleum ether was recycled about 30 times. The petroleum ether was removed by simple distillation until the stickey mass obtained. The above procedure was repeated with another two portions of the pulp fruit sample (180 g). The extracts were combined and then concentrated by distilled yielding brownish yellow colour crude extract (80.43 g).

Transesterification of Avocado Pulp Oil to Methyl Ester

The molecular weight of avocado pulp oil was taken as 880 g/mol, which was supposed to be a reasonable estimate (Watson, 2014). Avocado oil (11.2 g, or 25 mL) was placed in a 250 mL round-bottom flask, mixed with KOH (6 pellets, *i.e.*, *ca* 600 mg),about 5.4% of the mass of oil, and then with methanol (2.5 g, calculated mass corresponding to 6:1 molar ratio of methanol to oil, *i.e.*., twice the stoichiometric amount). The flask was then fitted with a reflux condenser and the mixture was stirred-heated in a water bath (bath temperature 65 - 70 °C) placed on a magnetic stirrer heater for 45 min with rapid stirring to ensure good mixing between the methanol and the avocado oil. At the end of the reaction, a clearer and less viscous mixture was obtained, indicating formation methyl esters from the original oil. This was also shown by the TLC (silica gel; hexane-diethyl ether-acetic acid, 85:15:1) using anisaldehyde-sulphuric acid spraying reagent. Methyl esters migrated a little higher (R_f 0.72) than the original oil (R_f 0.64) (Figure 1).

To the reaction product mixture the calculated volume (8 mL) of 1.25 M acetic acid was added slowly to neutralize the KOH. Then the mixture was stirred vigorously for a few minutes and then transferred to a 250 mL separatory funnel. Upon standing, separation of two distinct layers was observed. The lower layer of glycerol was drained out and the top layer was poured into an Erlenmeyer flask, dried over anhydrous sodium sulphate and filtered into a tared round-bottom flask. From the mass of the dried transesterified oil (8.0 g), the yield was calculated (yield 76.2 %). The crude reaction mixture (0.6 g) was fractionated on a silica gel column (40 g, diameter 1.7 cm) by eluting with hexane-diethyl ether-acetic acid (85 : 15 : 1). Three fractions A, B and C were obtained. The purified methyl ester mixture A was submitted for GC-MS analysis, as well as for recording the FT IR spectra. The fractions B and C were also submitted for recording FT IR spectra.

Figure 1 Co- TLC chromatogram of transesterified and original avocado pulp oils

Determination of Nutrient Values of Avocado Pulp

The nutrient values (moisture, ash, fiber, fat, protein, carbohydrate and energy value) of avocado pulp were determined by AOAC methods at Union of Myanmar Federation of Chambers of Commerce and Industry (UMFCCI).

Preparation of Extracts

Sample of avocado pulp (20 g) was made into small pieces and subjected for homogenization for MeOH, EtOH, PE, and water. The obtained extracts were filtered with filter paper. The filtrates obtained were evaporated at rotary evaporator at 50 ˚C. The extracts were used to determine antioxidant and *in vitro* antimicrobial activities.

Preparation of Sample Solution

Sample (4 mg) and 10 mL of EtOH were thoroughly mixed by shaker. The mixture solution was filtered and the stock solution was obtained. The sample solutions (40, 20, 10, 5, 2.5, 1.25, 0.625 μg mL^{-1} concentration) were prepared from this stock solution by dilution with appropriate amount of EtOH.

Free Radical Scavenging Activity by DPPH Method

The effect on DPPH radical was determined using the method by Marinova and Batchvarov (2011). The control solution was prepared by mixing 1.5 mL of 60 M DPPH solution and 1.5 mL of EtOH using shaker. The test sample solution was also prepared by mixing thoroughly 1.5 mL of 60 M DPPH solution and 1.5 mL of sample solution. The mixture solutions were allowed to stand at room temperature for 30 min. Then, the absorbance of these solutions was measured at 517 nm by using UV-7504 spectrophotometer. Absorbance measurements were done in triplicate for each concentration and then mean values so obtained were used to calculate percent inhibition of oxidation by the following equation. The capability to scavenge the DPPH radical was calculate using the following equation:

$$\% \text{ Inhibition} = \frac{A_{control} - A_{sample}}{A_{control}} \times 100$$

Where, $A_{control}$ = absorbance of control solution

A_{sample} = absorbance of tested sample solution.

IC_{50} value was calculated by linear regressive excel program. The results are described in Table 3 and Figures 9 and 10.

Screening of Antimicrobial Activity

Nutrient agar was prepared according to the method described by Cruickshank (1975). Nutrient agar was boiled and 20–25 mL of the medium was poured into the test tube and plugged with cotton wool and sterilized at 121°C for 15 min in an autoclave. After this, the tubes were cooled down to 30–35 °C and poured into sterilized petridishes and 0.1–0.2 mL of the test organisms were added into the dishes. The agar was allowed to set for 2–3 h; then 10 mm agar well was made by the help of sterilized agar well and cutter. After that, about 0.2 mL of the sample was introduced into the agar well and incubated at 37°C for 24 h. The inhibition zone which appeared around the agar well indicated the presence of antimicrobial activity.

Results and Discussion

Extraction of Avocado Oil

Extraction of avocado pulp oil was carried out by transesterification method and yield percentage was determined to be 81 %.

Analysis of Fatty Acids in the Avocado Pulp Oil

To investigate the fatty acids making up the glyceride of avocado pulp oil by GC-MS, they need to be converted to a more volatile compound. Thus in the present work methyl esters of the fatty acids were prepared by transesterification reaction.

In a transesterification reaction, alcoholysis is done using a small amount of base such as KOH or K_2CO_3 as a catalyst. The reaction is reversible and excess amount of alcohol (methanol in the present work) is used to drive the reaction to completion to give another ester (fatty acid methyl esters or FAMEs in the present work). This is unlike hydrolysis of ester under basic condition, where the carboxylic formed is irreversibly deprotonated to a salt, namely a soap; the base is consumed as part of the reaction product. It may be noticed that transesterification requires a catalytic amount of base, whereas a stoichiometric amount of base is needed for saponification. Transesterification and saponification are illustrated below for trimyristin, which is a major constituent of nutmegs.

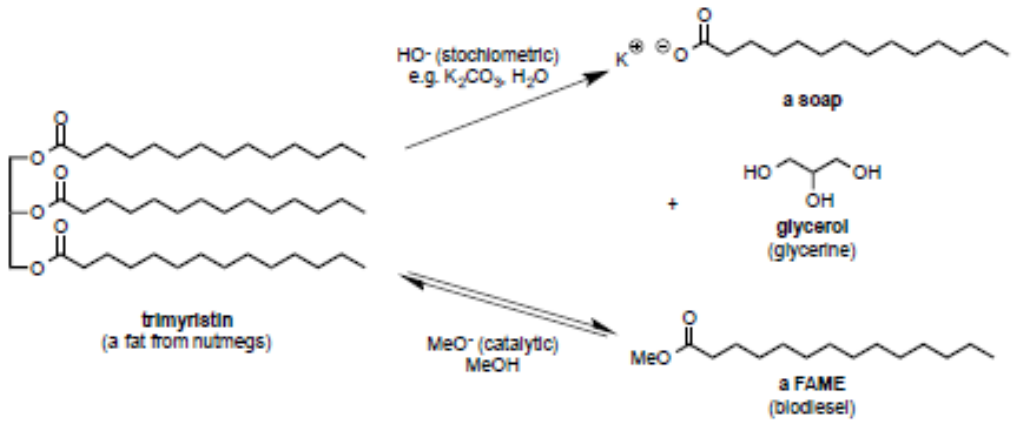

The crude transesterified oil (0.6 g) was fractionated on a silica gel (40 g) in a glass (diameter 1.7 cm) column by eluting with the solvent system,n-hexane-diethyl ether-acetic acid, (85:15:1), yielding a major fraction of a colourless clear oil **A** (R_f 0.72, purple on heating with anisaldehyde-sulphuric acid reagent) (0.2 g, yield 33 %, based on crude transesterified oil) supposed to be the pure mixture containing only methyl esters of fatty acids making up the glycerides of the avocado oil investigated.

This fraction was obtained by combining individually collected fractions to yield fraction B (yellow crystals, R_f 0.28 purple spot with anisaldehydesulphuric acid) (4 mg, yield 0.66 %, based on crude transesterified oil) and fraction C (oily, R_f 0.91, purple spot with anisaldehyde-sulphuric acid) (0.9 mg, yield 0.15 % based on crude transesterified oil (Figures 2 and 3).

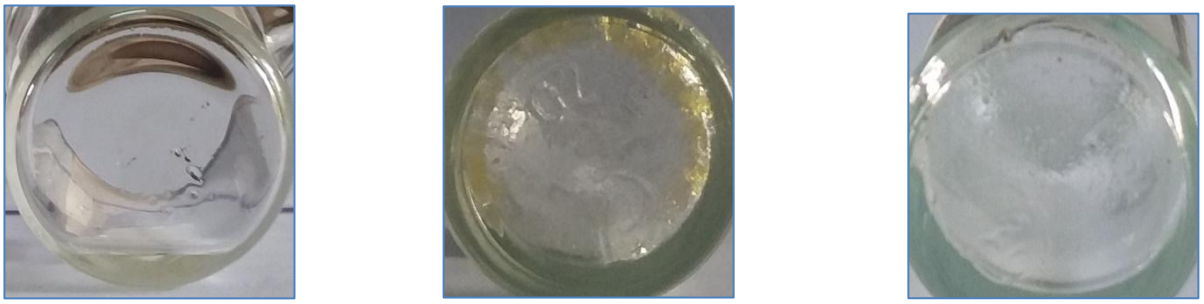

Fraction A
Methylated ester

Fraction B
Free acid

Fraction C
Long chain alcohol

Figure 2 Photographs of fractions A, B, C from avocado pulp oil

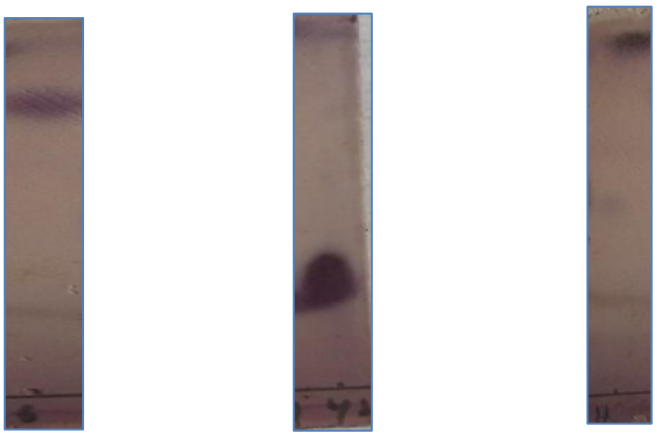

A B C

Solvent reagent - Anisaldehyde - conc: sulphuric acid
Solvent system - n-hexane : EtOAc : CH_3COOH
85 : 15 : 1
R_f value of A, B, C - 0.7201, 0.2972, 0.9189

Figure 3 Thin layer chromatograms of the fractions A, B, C

Analysis of Ester Fraction A

Fraction A is the methyl esters of the fatty acids making up the glycerides in the avocado pulp oil and GC-MS analysis showed the variety of these fatty acids.

First fraction A was first confirmed by its IR spectrum as esters (Figure 6 and Table 1). Next, the variety of methyl esters was indicated by GC-MS analysis of A. Thus, methyl ester of palmitic, palmitoleic and myristic acid are shown to be present in A (Figures 4 and 5a). Furthermore, two more fatty acids were also shown to be present by GC-MS (Figure 5b). Unfortunately, presence of the reported (Kadam and Salunkhe, 1995) major ester, methyl oleate could not be shown. This is supposedly caused by stopping too early the elution time, before methyl oleate could be eluted.

Analysis of fractions B and C

From their FT IR spectra, fraction B was shown to be fatty acid (Figure 7 and Table 1). As shown by TLC (Figure 3) they are present as free acids in the original avocado pulp oil. Similarly, fraction C was deduced as long chain alcohol (s) (Figure 8 and Table 1).

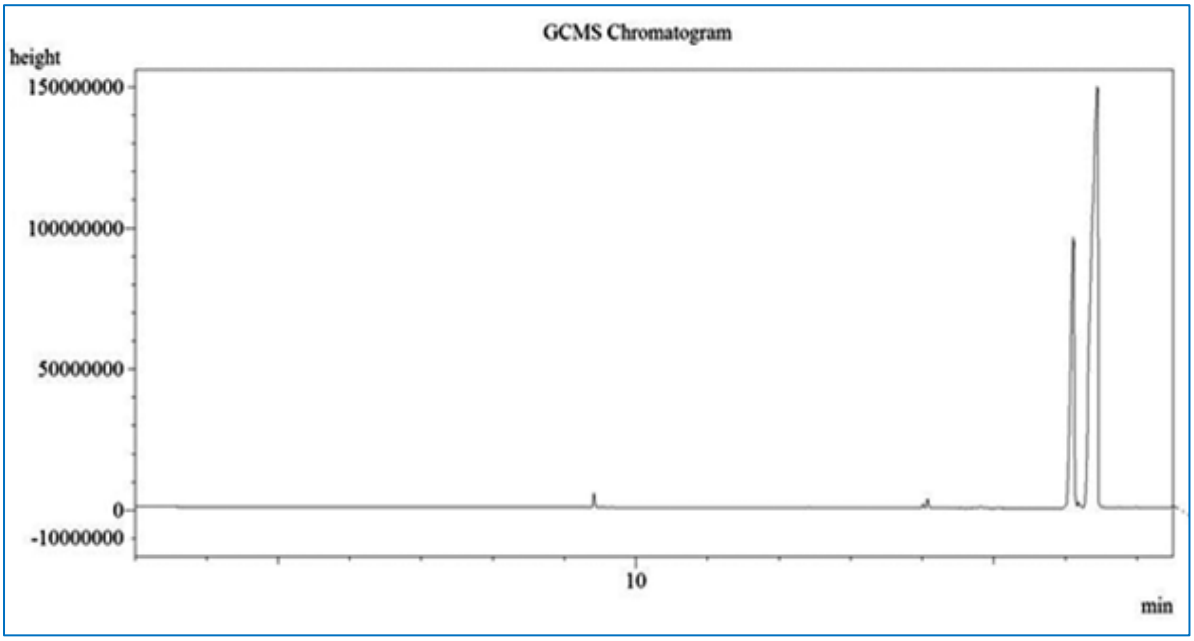

Figure 4 Gas chromatogram of separated methyl esters fraction A

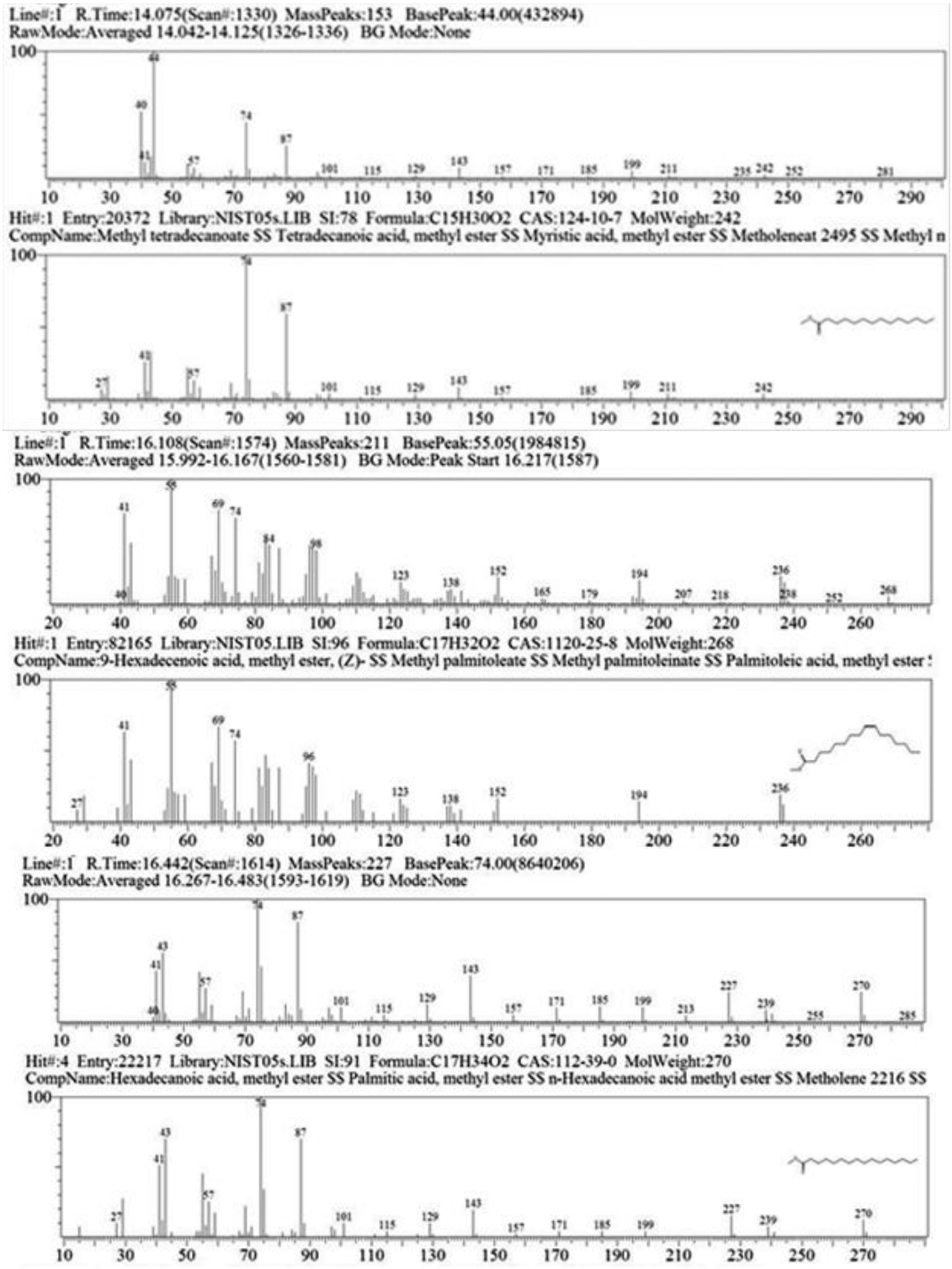

Figure 5a Identification of methyl esters of myristic (RT 14.075 min), palmitoleic (RT 16.108 min), and palmitic (RT 16.442 min) acids by comparison of the EI mass spectra of GC eluted compounds with respective library standard compounds

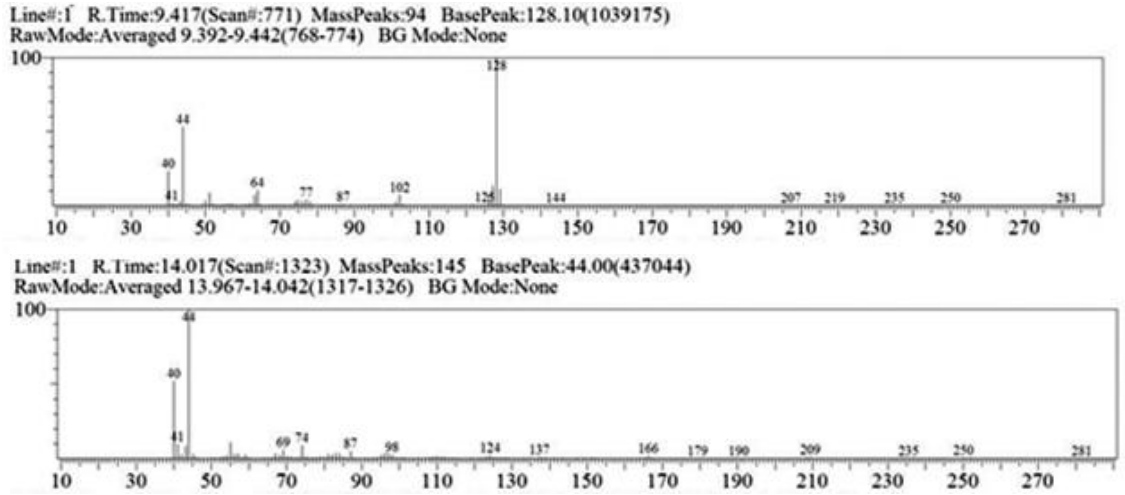

Figure 5b EI mass spectra of methyl esters of two unidentified fatty acids eluted with retention times 9.417 and 14.017 min from GC

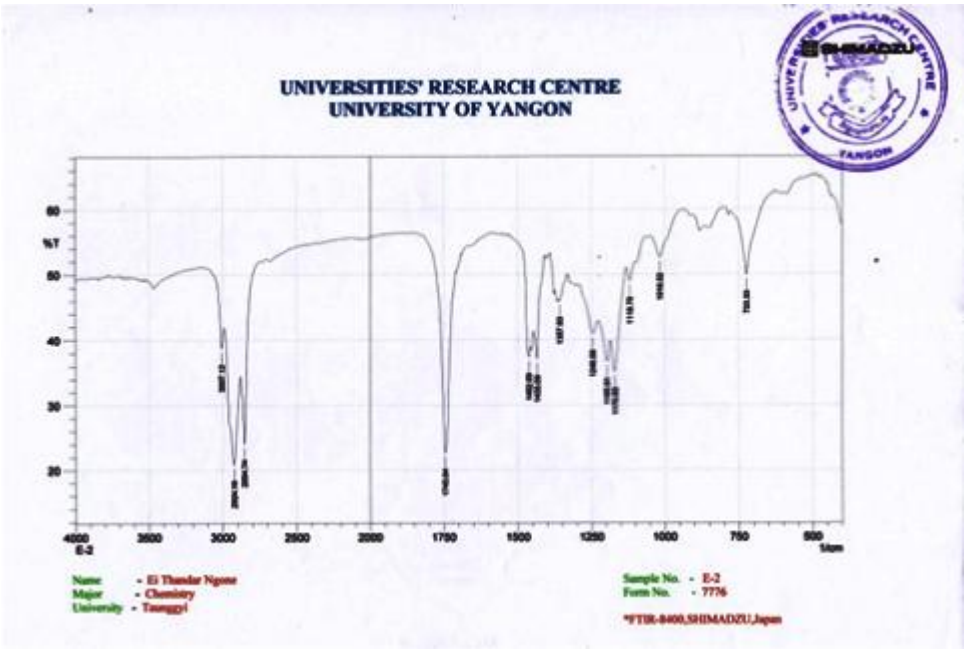

Figure 6 FT IR spectrum of isolated compound A from avocado pulp oil

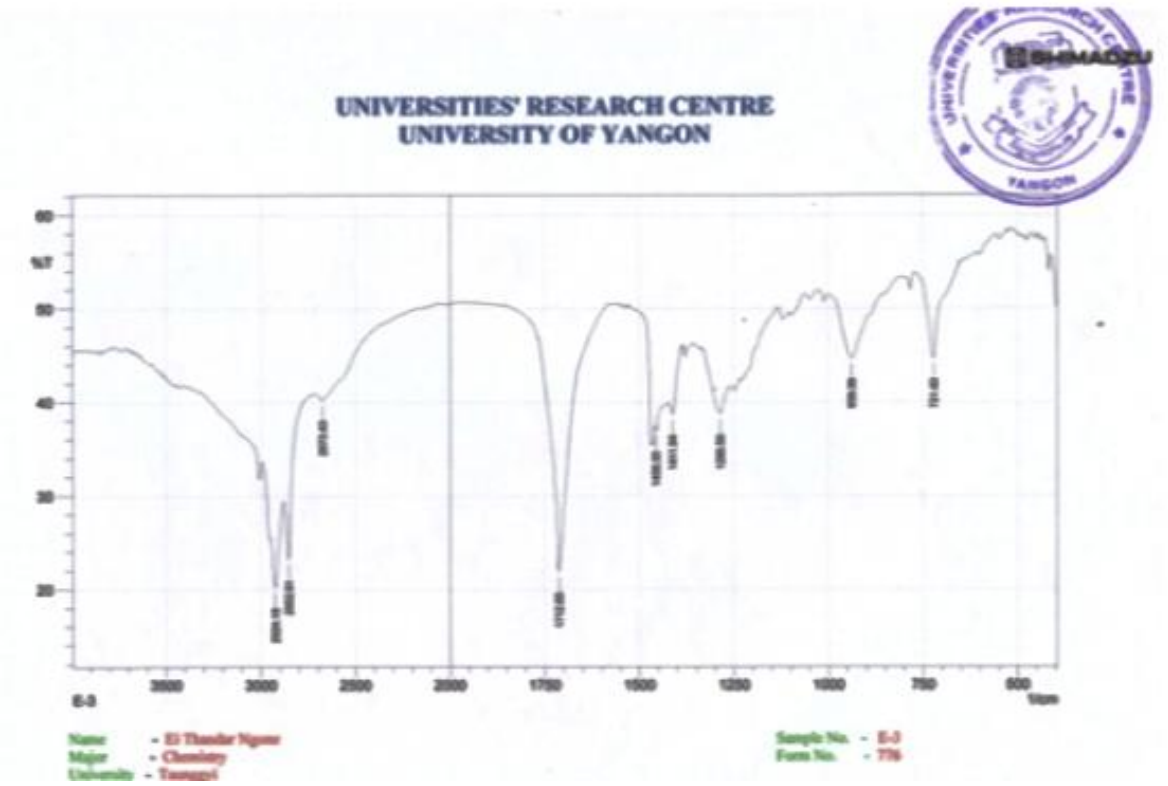

Figure 7 FT IR spectrum of isolated compound B from avocado pulp oil

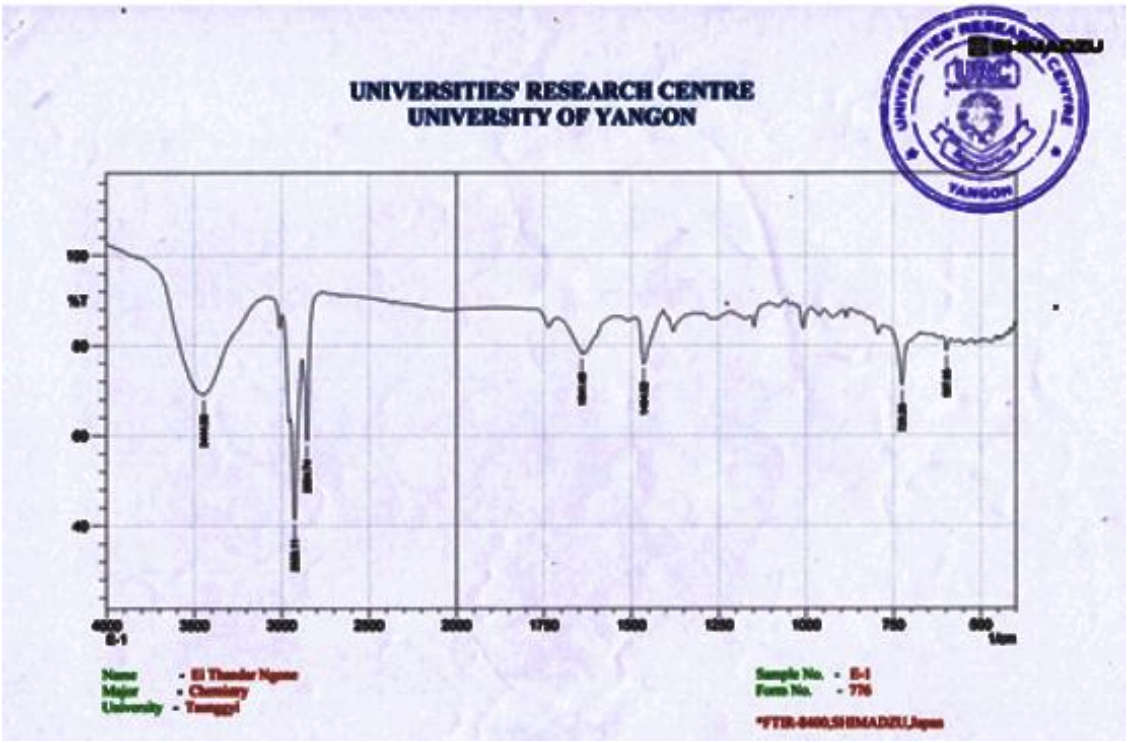

Figure 8 FT IR spectrum of isolated compound C from avocado pulp oil

Table 1 FT IR Spectral Data of the Fractions A, B and C from Avocado Pulp Oil

Sample code	Wavenumber (cm^{-1})								
	ν_{O-H}	$\nu_{=C-H}$	ν_{C-H}	$\nu_{C=O}$	$\nu_{C=C}$	$\delta_{as\ C-H}$	$\delta_{s\ C-H}$	ν_{C-O}	$\delta_{oop\ =C-H}$
A	-	3007	2924, 2854	1745	-	1462	1357	1195, 1170, 1016	723
B	3500-2500	3007	2924, 2852	1712	-	1456	1375	1286	939,721
C	3444	3007	2926, 2854	-	1641	1464	1375	1010	725

Nutrient Values of the Avocado Pulp

The nutritional values such as moisture, ash, crude fibre, fat, protein and carbohydrate in the avocado pulp fruit were estimated according to the AOAC methods conducted at UMFCCI. The results are shown in Table 2.

Table 2 Nutrient Values of Pulp of *Persea americana* Mill.

No.	Test Parameter	Test Method	Proximate Composition (%)
1	Moisture	AOAC	5.56
2	Ash	AOAC	5.23
3	Protein	AOAC (Kjeldahl Method)	6.55
4	Crude Fibre	AOAC (Fibre Cap Method)	8.14
5	Fat	AOAC(Buchi Soxhlet Method)	4.18
6	Total Carbohydrate	By difference	70.34
7	Energy value (kcal/100 g)		344

Antioxidant Activity of Crude Extracts of Avocado Pulp

Antioxidant benefits our health by cleaning free radicals out of our bloodstream. Different antioxidants benefit different parts of the body. Antioxidant activity of 95% ethanol, water extracts and standard ascorbic acid were estimated by measuring the DPPH radical scavenging activity of different concentrations of extracts. It is based on the reduction of colour of free radical DPPH in ethanolic solution by different concentration of samples. In this experiment, seven different concentrations 0.625, 1.25, 2.5, 5, 10, 20 and 40 μg/mL of each crude extract in ethanol and standard ascorbic acid in water were used. Determination the absorbance of each solution was measured at 517 nm using UV-visible spectrophotometer. The DPPH is a stable free radical to decolourize in the presence of antioxidants. The DPPH free radical contains an odd electron, which is responsible for the absorbance at 517 nm and also for a visible deep purple colour. When DPPH accepts an electron donated by an antioxidant compound, the DPPH is decolorized which can be quantitatively measured from the charges in absorbance. It was found that as the concentrations were increased, the absorbance values were decreased. The radical scavenging activity of crude extracts was expressed in term of percent inhibition and IC_{50} (50% inhibition concentration) values. The IC_{50} values were calculated after linear regression analysis

of the observed inhibition percentage Vs concentration of sample, where lower IC_{50} values indicated antioxidant activity.

The IC_{50} values for crude extracts and standard ascorbic acid are shown in Table 3, Figures 9 and 10. The IC_{50} values of water, ethanol and standard ascorbic acid were observed to be 19.32, 21.84 and 1.22 µg/mL, respectively. The IC_{50} value of water extract is lower than that of ethanol extract. All extracts showed very mild antioxidant activity when compared to standard ascorbic acid (1.22 µg/mL).

Table 3 % RSA (Radical Scavenging Activity) and IC_{50} Values of Crude Extracts of Avocado Pulp

No.	Extract	% RSA (mean ± SD) in different concentrations (µg/mL)							IC_{50} (µg/mL)
		0.625	1.25	2.5	5	10	20	40	
1	Ethanol	26.61 ±0.75	29.94 ±0.21	31.67 ±0.52	35.97 ±0.21	43.10 ±0.98	49.41 ±0.84	56.06 ±0.32	21.84
2	Watery	25.99 ±0.55	28.55 ±0.48	32.85 ±0.21	35.00 ±2.12	41.03 ±0.43	50.66 ±0.24	63.13 ±0.79	19.32
3	Ascorbic acid	25.92 ±0.79	51.14 ±0.75	60.43 ±0.32	72.07 ±0.60	77.20 ±1.15	83.09 ±0.12	90.23 ±0.72	1.22

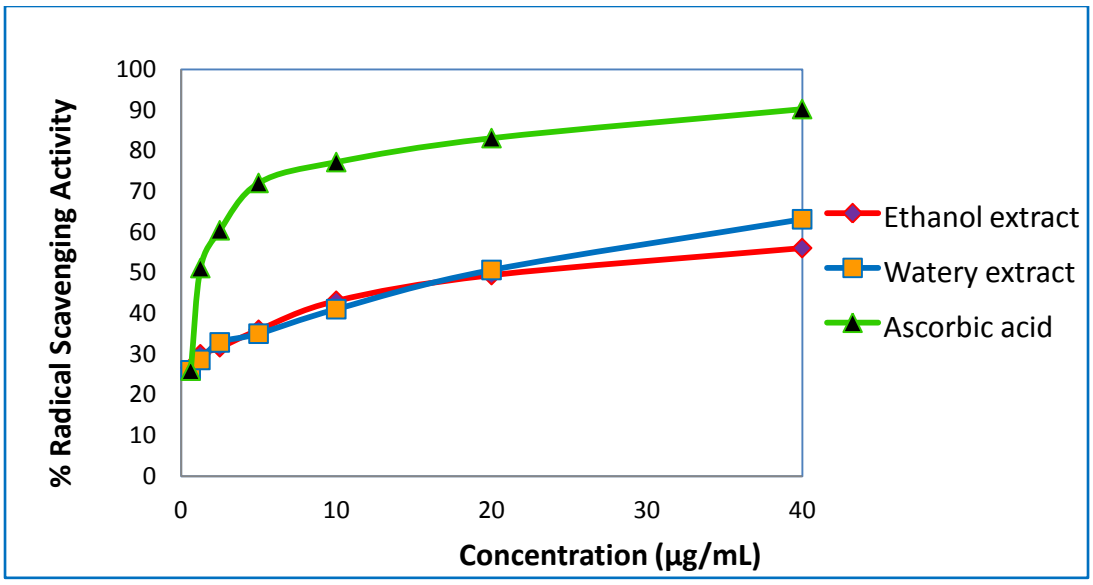

Figure 9 Radical scavenging activity of different concentrations of crude extracts of avocado pulp

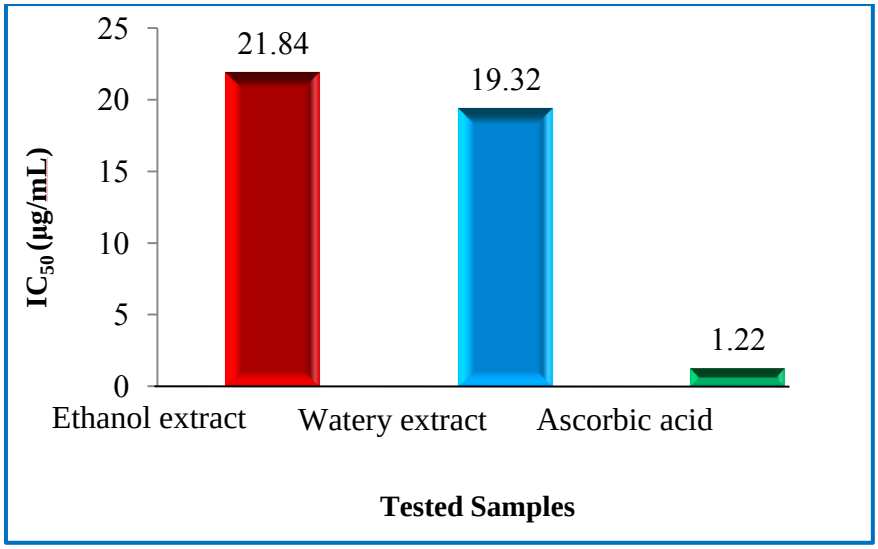

Figure 10 A bar graph of IC_{50} values of crude extracts of avocado pulp

Antimicrobial Activity of Crude Extracts by Agar Well Diffusion Method

The crude extracts were tested against six pathogenic microorganisms by using agar well diffusion method. MeOH, EtOAc and EtOH extracts of the pulp were active by agar well diffusion method on the five microbial species tested namely *Bacillus subtilis*, *Staphylococcus aureus, Bacillus pumilus, Candida albicans* and *Escherichia coli* but inactive on *Pseudomonas aeruginosa*. Non-polar extract PE and H_2O extracts were inactive by agar well diffusion method on the six microbial species. The photograph of inhibition zone diameters of different crude extracts against the six species of organisms tested are shown in Figure 11, and the results are summarized in Table 4.

Table 4 Antimicrobial Activity of PE, EtOAc and H_2O Extracts from Pulp of Avocado Pulp by Agar Well Diffusion Method

No.	Extracts	Diameter of Zone of Inhibition against different microorganisms (mm)					
		I	II	III	IV	V	VI
1	Pet-Ether	–	–	–	–	–	–
2	MeOH	13 (+)	13 (+)	–	12 (+)	13 (+)	13 (+)
3	EtOAc	11 (+)	12 (+)	–	13 (+)	11 (+)	12 (+)
4	EtOH	12 (+)	13 (+)	–	12 (+)	12 (+)	12 (+)
5	H_2O	–	–	–	–	–	–

Agar well – 10 mm
10 mm ~ 14 mm (+)
15 mm ~ 19 mm (++)
20 mm above (+++)

Organisms
I – *Bacillus subtilis*(N.C.T.C-8236)
II – *Staphylococcus aureus*(N.C.P.C-6371
III – *Pseudomonas aeruginosa*(6749)
IV – *Bacillus pumilus*(N.C.I.B-8982)
V – *Candida albicans*
VI – *Escherichia coli* (N.C.I.B-8134)

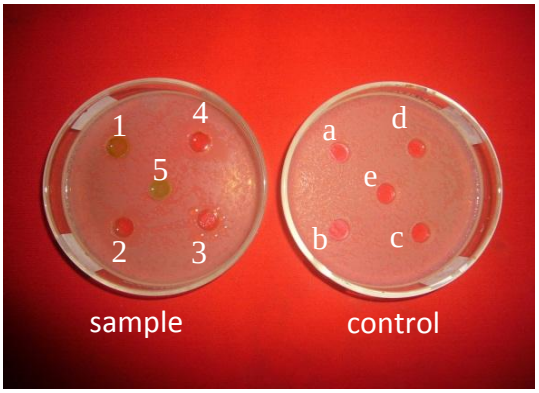

Bacillus subtilis

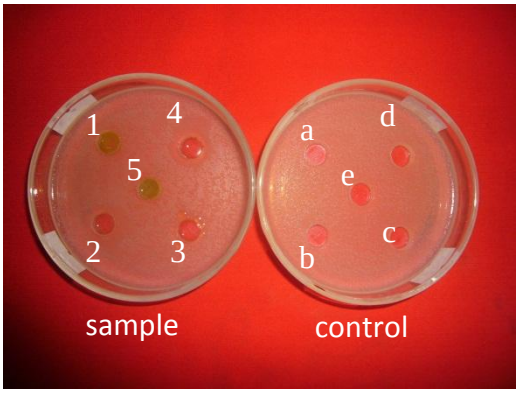

Staphylococcus aureus

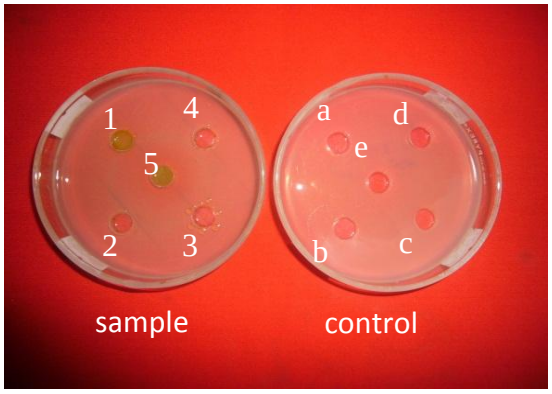

Pseudomonas aeruginosa

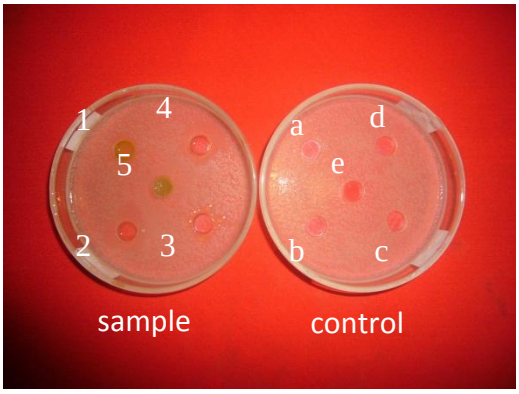

Bacillus pumilus

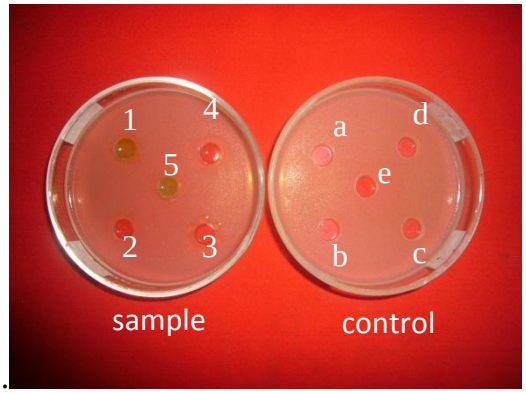

Candida albicans

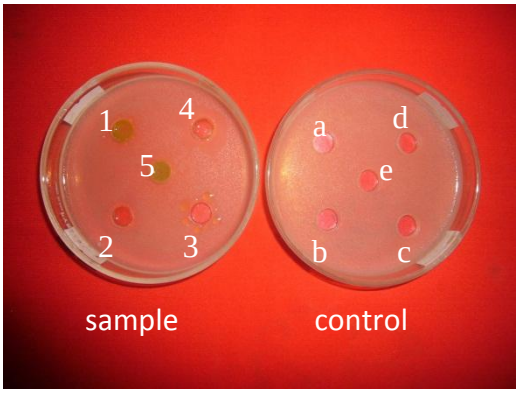

Escherichia coli

1 – PE extract

2 – MeOHextract

3– EtOAcextract

4 – EtOHextract

5 – H_2O extract

a – PE control

b – MeOH control

c – EtOAc control

d – EtOH control

e – H_2O control

Figure 11 Antimicrobial screening of PE, MeOH, EtOAc, EtOH and H_2O extracts from the avocado pulp by agar well diffusion method

Conclusion

Avocado pulp oil (81 %) was extracted by Soxhlet extraction with petroleum ether. GC-MS analysis of avocado oil after transesterification to fatty acid methyl esters, showed the presence of eleven fatty acids namely, myristic, palmitoleic, palmitic, linoleic, petroselinic, oleic, [11z]-11-octadecenoic, stearic, isostearic acids and two unidentified acids. Moreover, a long chain alcohol and a free fatty acid were also identified by FT IR in the avocado pulp oil. The nutritional values of avocado pulp were moisture (5.56%), ash (5.23 %), protein (6.55 %), fiber (8.14 %), fat (4.18%), carbohydrate (70.34 %) and energy value (344 kcal/100g). The antioxidant activity activity of the avocado pulp by DPPH assay was slightly higher in the water extract (IC_{50} = 19.32 µg/mL) than the ethanol extract (IC_{50} = 21.84 µg/mL). In the screening of antimicrobial activity, against *B. subtilis,S. aureus, B. pumilus, C. albicans* and *E. coli*, the ethanol, methanol and ethyl acetate extracts of Avocado pulp were active, whereas petroleum ether and water extracts were inactive on all the tested microorganisms. Therefore, avocado species can be taken as a good source of nutritious food.

Acknowledgements

The authors would like to thank the Myanmar Academy of Arts and Science for allowing to present this paper and Professor and Head Dr Ah Mar Yi and Professor U Myint Ngwe, Department of Chemistry, Taunggyi University for their kind encouragement.

References

Cruickshank, R., Duguid, J.P., Marimion, B.P. and Swain, R.H. (1975). "*Medical Microbiology, the Practice of Medical Microbiology*". Edinburgh: 12th Ed., Churchill Livingstone, p.11.

Dreher, M.L. and Davenport, A.J. (2013). "Hass Avocado Composition and Potential Health Effects". *Crit. Rev. Food Sci. Nutr.*, vol. 57(7), p.738-750.doi: 10.1080/ 10408398.2011.556759

Kate, I.E. and Lucky, O.O. (2009). "Biochemical Evaluation of the Tradomedicinal Uses of the Seeds of *Persea americana* Mill. (Family :Lauraceae)". *World Journal Medical Sciences*, vol. 4(2), p. 143-146.

Kadam, S.S. and Salunkhe, D.K. (1995). "Avocado in Handbook of Fruit Science and Technology: Production, Composition, Storage and Processing". New York Marcel Dekker Inc., p. 363-375

Marinova, G. and Batchvarov, V. (2011). "Evaluation of the Methods for Determination of the Free Radical Scavenging Activity by DPPH". *Bulgarian Journal of Agricultural Science*, vol. 17, p. 11-24.

Rodriguez-Carpena, J., Morcuende, D., Andrade, M.J., Kylli, P. and Estevez, M. (2011). "Avocado *(Persea americana* Mill.) Penolics, *in Vitro* Antioxidant and Antimicrobial Activities and Inhibition of Lipid and Protein Oxidation in Porcine Patties".*Journal of Agricultural and Food Chemistry*, vol. 59(10), p. 5625-5635.

Watson, D.A. (2014). "Biodesel". http://www.udel.edu/chem/dawatson/classes/chem (Accessed 12 August 2015).

REFINING OF WASTE FRIED PALM OIL BY MODIFIED BENTONITE CLAYS

Tha Zin Win[1], Kyi San Aye[2], Hlaing Hlaing Oo[3]

Abstract

Frying of foods is the most commonly used in the food preparation. Without any treatment, the fried oil can be used for a few days and must be discarded after such time. The useful life of fried palm oil can be increased by the refining with various adsorbents, natural adsorbents and modified adsorbents. In this paper, the natural bentonite clay and modified acid activated bentonite clay were used for refining of waste fried palm oils. The natural bentonite clay was collected from Kyaukpadaung Township. The essential parameters such as acid value, peroxide value, iodine value and saponification value of before and after refined fried oils were investigated. The completely refined fried oil showed the properties of the acid value, peroxide value, iodine value and saponification values were evenly spread between 1.39 to 1.54 mg g^{-1}, 2.28 to 2.62 meq kg^{-1}, 100.33 to 109.75 mg g^{-1} and 142.72 to 152.73 mg KOH g^{-1} respectively. These results were under permitted level for edible palm oil. Moreover, the determination of incremental adsorption capacity of acid activated bentonite clay sample using 3 % H_2SO_4, it can be resilient in refining process within 18h long frying time of waste fried palm oil. This experimental work found that locally available natural bentonite clay can be modified for the use of efficient and effective refining material to the waste fried palm oil.

Keywords: Fried palm oil, bentonite, activated bentonite, refining, adsorbent

Introduction

Bentonite clay is an aluminiumphyllosilicate, which consists mostly of the mineral montomorillonite. Bentonite clay enormously abundant in nature has been considered as a potential source of adsorbent for removing, colour pigments from edible oils. Surface modified the clay samples have high potential to provide an alternative to most widely used activated carbon (Chaisena and Rangsriwatananon, 2004). The surface modification of bentonite can be carried out by thermal activation and acid activation processes. Thermal processing change the structure and composition upon heating and largely depends on the particle size and the heating regime (Sennour *et al*., 2009).The another method by treating bentonite clay with inorganic acids at high temperature is termed acid activated clays. The cost of production of acid activated clays is low. The acid activation of the clays alters the physical properties, such as, enhancing the surface area and average pore volume (Lian *et al*., 2009).Palm oil is commonly used for cooking due to its high saturation (oxidative stability) of the refined product when it was frying. Palm oil is one of the few highly saturated vegetable fats and does not contain cholesterol, although saturated fat intake does increase a person's LDL (Low-density lipoprotein) and HDL (High-density lipoprotein) cholesterol. Refining of fried palm oil is done to remove unwanted minor components that make oils unappealing to consumers, while trying to cause the least possible damage to the neutral oil as well as minimum refining loss. The components to be removed are all those glyceridic and non-glyceridic compounds that are detrimental to the flavour, colour, stability or safety of the refined oils (Ruiz-Mendez and Dobarganes, 1999).

[1] Dr, Assistant Lecturer, Department of Chemistry, Yangon University of Distance Education
[2] Dr, Associate Professor, Department of Chemistry, Bago University
[3] Dr, Professor and Head, Department of Chemistry, West Yangon University

The aim of this research was to increase the usefulness of waste fried palm oil by refining process using natural and modified bentonite clay.

Materials and Methods

This experimental work concerned with the refining of waste fried palm oil by modified bentonite clays. In this work, the raw natural bentonite (NBN) clay was collected from the Kyaukpadaung Township, Mandalay Region and it was modified by acid modification and heat activation process. Waste fried palm oil used in this study was bought from local market. All chemicals used in this experiment were procured from British Drug House (BDH) Chemicals Ltd., Poole, England.

Preparation of Adsorbent Materials

(a) Natural bentonite clay sample preparation

Firstly, foreign matters were removed from raw natural bentonite clay sample and then soaked in distilled water and dried at 105 ºC for 4 h. The samples were ground and sieved with 125 μm mesh. The natural bentonite clay powders were stored in desiccators for further study of characterization and modification.

(b) Modification of Natural Bentonite Clay Sample

(i) Acid modification

The prepared natural bentonite clay sample (50 g) was treated with 500 mL of 1 to 5 % sulphuric acid (analytical grade) at 90 °C for 4 h in a stirred glass. After the acid treatment, the samples were filtered and washed with distilled water until neutral. The samples were dried at 105 °C for 5 h and ground to pass through a 75 μm sieve. The dried acid activated bentonite was kept in a desiccator containing silica gel for further study of characterization and modification oil bleaching.

(ii) Heat activation

The natural bentonite clay sample (50 g) was calcined in the range of temperature 100, 200, 300, 400 and 500 °C for 1 h. The heat activated bentonite clays sample was stored in desiccators for further study of characterization and modification.

Refining of Waste Fried Palm Oil

The refining process contains four steps. There are degumming process, neutralization process, bleaching process and deodorization process. For the degumming of waste fried palm oil, oil sample (300 mL) was placed in a conical flask and the flask was heated to 60-70 °C, and then 50 mL of water was added and mixed about for 30 min. The solution was taken out and removed the hydrated gums by centrifugal separation method. The sample was filtered off. Then, the resulted water degumming oil was continued for neutralization process. 1 M NaOH 20 mL was added in 300 mL degummed oil with a reaction time of around 30 min at slow stirring and temperature around 80 °C, the water phase is eliminated by centrifugation and the oil was with water to remove the remaining soap. Then, the resulted neutralized oil was carried on the

bleaching process. In this process, 5 g each of natural and two modified bentonite clays were separately put in each conical flask and 50 mL of waste fried palm oil was added to each flask. The flasks were heated at 80, 100, 120, 140 ºC temperatures and 30, 45, 60, 75, 90 min bleaching time. The samples were filtered by vacuum flask using vacuum pump. Then, the quality of bleaching fried oil samples was analyzed. For deodorization process, the bleached oil 50 mL was added with 5 g of bamboo powder and stirred and filtered. Then finally, deodorized oil was obtained.

Determination of Incremental Adsorption Capacity of Acid Activated Bentonite Clay Sample

The experimental procedure of frying and refining were carried out repeatedly for 5 batches without changing acid activated bentonite clay. During the first refining process, (fried oil of first time refining process) designated as RFO 1. And then, this first refined oil (RFO 1) was fried again to obtain the colour like as first collected fried oil sample. The frying duration was as long as 5 h (FO 2). The obtained fried oil was refined again the same as above procedure and the resulted fried oil was designated as RFO 2 (fried oil of second time refining process). Similar procedure was made 5 h frying duration for RFO 2 designated as FO 3. Similarly, another 5 h frying duration for RFO 3 designated as FO 4 and the last frying duration 3 h for (RFO 4) and designated as FO 5 which was again refined (RFO 5). Finally, total 18 h frying durations were studied without changing acid activated bentonite clay adsorbent. The acid value, peroxide value, iodine value and saponification values of the oil samples were determined.

Characterization of Bentonite Clay Samples and Waste Fried Palm Oil

The characterization of natural bentonite (NBN) and modified bentonite clay samples were performed by XRD (Rigaku-D-Max-2200, Japan, URC, UY, Myanmar) and SEM (JOEL-JSM-5610 series, Japan, URC, UY, and Myanmar). In addition, XRD analysis of commercial bentonite clay and standard bentonite clay were carried out to compare with modified bentonite clay sample. Waste fried palm oil samples before and after refining process were analyzed conventional methods to determine the acid value, peroxide value, saponification value and iodine value.

Results and Discussion

In this research, natural bentonite clay sample, Kyaukpadaung Township, Mandalay Region, was used for the experimental work. From the XRD results, the particle size of natural bentonite clay sample compared with those of the commercial bentonite and standard bentonite are presented in Table 1. Because of the smallest particle size among these three, the natural bentonite clay sample was chosen to modify for the refining process.

Table 1 The Particle Size of Three Different Types of Bentonite Clay Samples

No.	Sample	Particle size (nm)	Source
1.	Natural bentonite clay	69.0063	Kyaukpadaung Township
2	Commercial bentonite clay	99.8983	Pyoneiyar Star Co. Ltd.
3	Standard bentonite clay	78.7160	Chemistry Department, UY

The natural bentonite clay sample was modified by acid activation method and heat activation method. The natural bentonite clays and acid activated bentonite clays at different sulphuric acid concentrations are presented in Table 2.

Table 2 Original Bentonite Clays and Acid Activated Bentonite Clays with Different Sulphuric Acid Concentrations

Sample	Concentration of H_2SO_4 % W/V	Code No.
Natural or untreated bentonite clay	-	NBN
Acid Activatied bentonite Clays	1	AABN 1
Acid Activatied bentonite Clays	2	AABN 2
Acid Activatied bentonite Clays	3	AABN 3
Acid Activatied bentonite Clays	4	AABN 4
Acid Activatied bentonite Clays	5	AABN 5

The natural bentonite clay sample is brown colour in nature. After acid treatment, the colour observations of acid activated bentonite clays were changed from brown, grey till the AABN 3 has whitish colour. The grey colour of bentonite could be due to the relatively some amount of cations such as Al^{3+} and Fe^{3+} which still remained after the activation The Whitish colour could be due to the replacement of metal ions such as Al^{3+}, Fe^{3+} and Ca^{2+} in the clay with H^{+} (Lian *et al*., 2009).

Table 3 Heat Activated Bentonite Clays at Different Temperatures

Sample	Activated Temp °C	NBN
Natural or untreated bentonite clay	-	NBN
Heat activated bentonite clay	100	HABN 1
Heat activated bentonite clay	200	HABN 2
Heat activated bentonite clay	300	HABN 3
Heat activated bentonite clay	400	HABN 4
Heat activated bentonite clay	500	HABN 5

The heat activated bentonite clays at different temperatures are presented in Table 3. After thermal activation of natural bentonite clay, the colour changed from brown to dark colour. The heat activated bentonite clay is darker than acid activated bentonite clay. This is because of the clay minerals generally calcined prior to their use in order to remove any impurities or

moisture attached to the clay particles. Consequently, the adsorbed and hydrated water, and impurities attached to bentonite clay were removed in the dehydration stage (Sennour *et al*., 2009).

From XRD pattern, the particle size of natural bentonite clay (NBN), acid modified and heat activated bentonite clay samples were determined by using Debye Scherrer equation (Yildiz *et al*., 2004). The resulted data are presented in Table 4. The particle size of natural bentonite clay is 69.0063 nm. After acid activation of natural bentonite clays, the particle sizes of AABN 1 to AABN 5 were in the range of 40.2970 to 46.5531 nm while HABN 1 to HABN 5 have in the particle size distribution range of 50.3280 to 60.2873 nm. The acid activated bentonite clay samples are more preferable to the refining process for the waste fried palm oil because of their smaller particle sizes than those of heat activated clay samples.

Table 4 Average Crystallite Grain Size of Bentonite Clay Samples by XRD

Sr. No.	Type of Bentonite	Average Crystallite Grain Size D (nm)
1.	NBN	69.0063
2.	AABN 1	46.5531
3.	AABN 2	44.0213
4.	AABN 3	40.2970
5.	AABN 4	41.8983
6.	AABN 5	42.1289
7.	HABN 1	60.2873
8.	HABN 2	50.3280
9.	HABN 3	57.4430
11	HABN 4	53.6349
11	HABN 5	52.1015

NBN = Natural Bentonite
AABN = Acid-Activated Bentonite
HABN = Heat-Activated Bentonite

Among acid activated samples, activated with 3 % H_2SO_4, AABN 3 gave the smallest average crystallite grain size (40.2970 nm). It can be explained that consolidation or agglomeration of smaller particles occurs by modification of bentonite with sulphuric acid. According to this trend, particles lose their clay mineral property due to both activation processes. The acid activation caused the creation of new pores having lower diameters than those of the original and heat activated bentonite clays (Yildiz *et al*., 2004). The particle size distributions of the original and activated bentonite clays showed that the acid activation strongly affected the particle size of the clays.

The surface morphologies of natural bentonite clay, acid activated bentonite clays and heat activated bentonite clays magnification using SEM are presented in Figures 1 and 2.

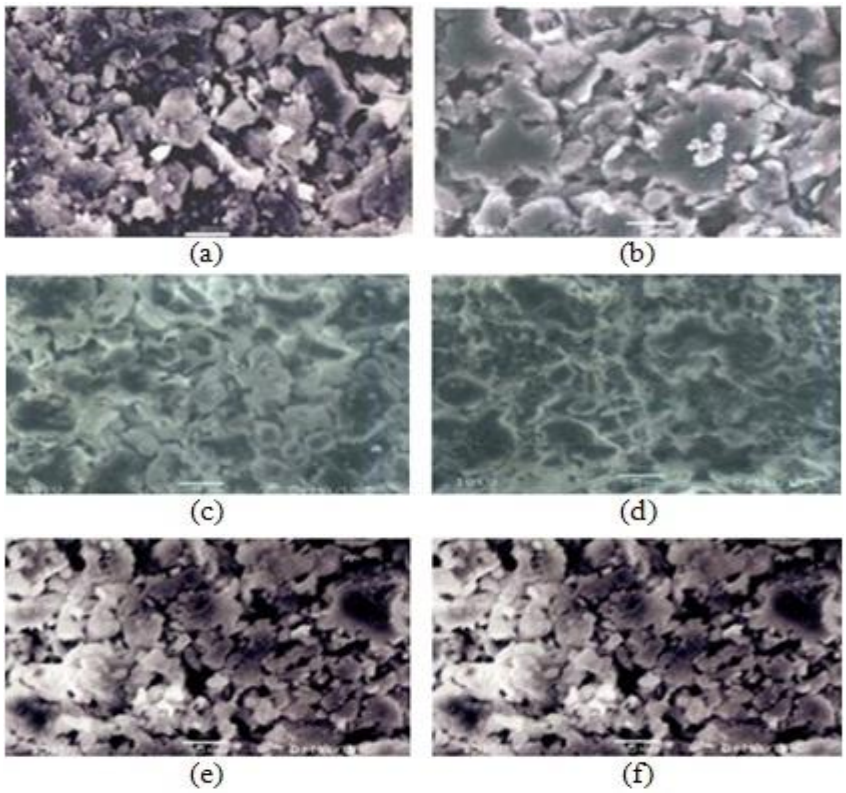

Figure 1 SEM Micrographs of (a) NBN (b) AABN 1 (c) AABN 2 (d) AABN 3 (e) AABN 4 (f) AABN 5

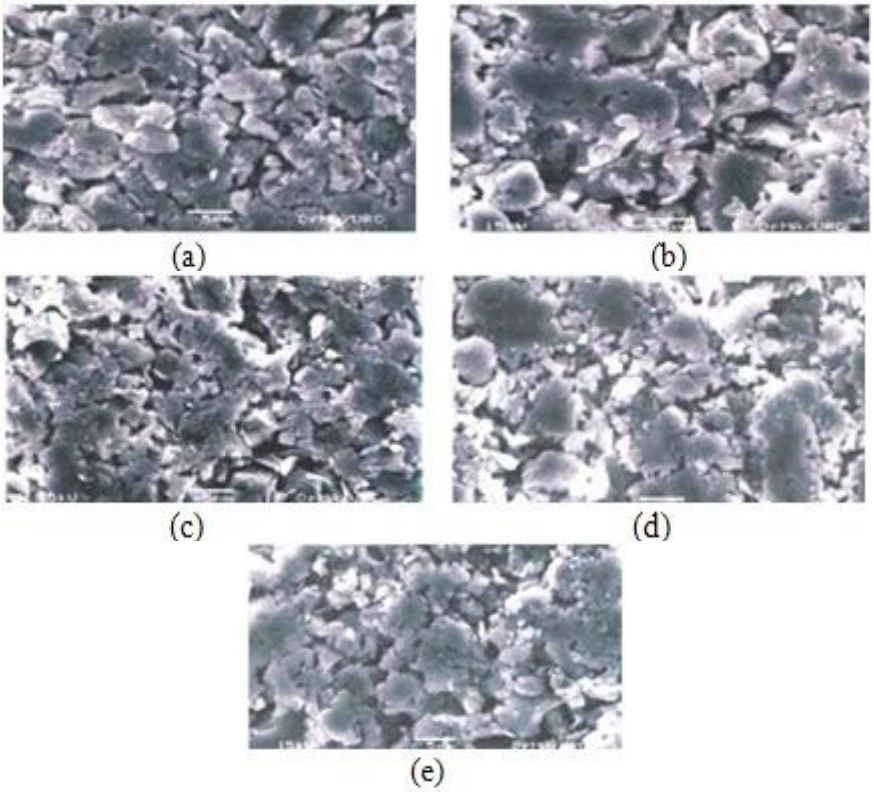

Figure 2 SEM Micrographs of (a) 100 °C (HABN 1) (b) 200 °C (HABN 2) (c) 300 °C (HABN 3) (d) 400 °C (HABN 4) (e) 500 °C (HABN 5)

According to these figures, an acid activation creates voids in the bentonite making the clay surface more porous as increase in acid concentration till the acid activation at 3 % H_2SO_4 and becomes highly porous. The formation of smaller pores takes place as the impurities are removed and the exchangeable cations are replaced by H^+ ions. Further increase in acid concentration (4 % H_2SO_4 and 5 % H_2SO_4) reduced the porosity rendering clay surface rather flat and clumps of uneven surface can be seen along with some that flakes of low porosity. Heating beyond 200 °C resulted in the gradual decrease in porous nature in heat activated bentonite and the interlayer spaces may have collapsed resulting in more tightly bound structure with reduction in porous structure at 500 °C. From XRD and SEM results, using acid activation 3 % H_2SO_4 for refining of waste fried palm oil gave the best results for this experiment.

In the refining procedure, the optimum temperature and duration time were studied for AABN 3 bentonite clay modified with 3 % H_2SO_4. The results are presented in Table 5 and Table 6. According to the literature, the higher the acid value found, the higher the level of free fatty acid which translates into decreased oil quality (Yang *et al*., 2006). The peroxide value is a measure of oxidation during storage. The peroxide value determines the extent to which the oil has undergone rancidity, thus it could be used as an indication of the quality and stability of fats and oils.

From these observations, the optimum results for the refining process are 100 ºC temperature and 45 min time duration.

Table 5 Acid Values and Peroxide Values of the Fried Oil (F.O) Treated with AABN 3 at Different Treated Temperatures

Sr. No.	Treated Temperature (°C)	Acid Value (mg g^{-1})	Peroxide Value (meq kg^{-1})
1	80	2.26	10.80
2	100	1.80	3.60
3	120	2.36	18.00
4	140	2.14	21.60
5	F.O	16.83	39.60

(dosage 5 g, time 1h)

Table 6 Acid Values and Peroxide Values of the Fried Oil (F.O) Treated with AABN 3 at Different Treated Times

Sr. No.	Treated Time(min)	Acid Value (mg g^{-1})	Peroxide Value (meq kg^{-1})
1	30	1.80	3.90
2	45	1.52	3.60
3	60	1.73	7.20
4	75	1.94	10.80
5	90	2.68	18.00
6	F.O	16.83	39.60

(temperature 100 °C, dosage 5 g)

The step by step colour change of waste fried palm oil during refining process using 3 % H_2SO_4 (AABN 3) are presented in Table 7. Initial colour was dark brown and finally the decolourization of waste fried palm oil was observed. The overall refining process (4 steps) took 3.5 h for this experiment.

Table 7 The Colour Observation of Waste Fried Palm Oil in Refining Process

Steps No.	Refining Process	Colour	Time/ h
1	waste fried palm oil	dark brown	-
2	after degumming process	brown	½
3	after degumming and neutralizing process	yellow	1
4	after degumming, neutralizing and bleaching process	colourless	2

In the determination of incremental capacity of acid activated bentonite clay sample, the experimental procedure of repeatedly frying and refining without changing bentonite were carried out. The resiliency of AABN 3 with fried time is presented in Table 8.

Table 8 The Resiliency of Acid Activated Bentonite Clay Sample with Repeated Fried Time of Waste Palm Oil

Code No.	Fried time/h	Resiliency of acid activated bentonite clay/h
RFO1	-	-
RFO 2	5	5
RFO 3	5	10
RFO 4	5	15
RFO 5	3	18

Some essential parameters of oil samples after the repeated frying and refining with AABN 3. The result data are presented in Table 9.

According to Table 9, the acid value, peroxide value, iodine value and saponification value of waste fried palm oil (FO) sample were 16.38 mg g^{-1}, 39.6 meq kg^{-1}, 12.34 mg g^{-1} and 209.81 mg KOH g^{-1} respectively. Alternatively, the acid value, obtained for refined oil sample (RFO 1 to RFO 5) ranged from 1.39 to 1.54 mg g^{-1}, respectively.

Table 9 Some Essential Parameters of Oil Samples after the Repeated Frying and Refining with AABN 3

Properties	Sample							
	FO	**RFO 1**	**RFO 2**	**RFO 3**	**RFO 4**	**RFO 5**	**PO**	**Standard Range (Yang *et al*., 2006)**
Acid Value (mg g^{-1})	16.38	1.54	1.49	1.43	1.42	1.39	1.47	< 4
Peroxide Value (meq kg^{-1})	39.6	2.28	2.31	2.49	2.62	2.52	2.25	< 10
Iodine Value (mg g^{-1})	12.34	106.13	108.44	109.75	105.83	100.33	80.75	101-150
Saponification Value (mg $KOHg^{-1}$)	209.81	144.11	142.72	142.78	151.62	152.73	151.47	151-165

FO = Fried Oil PO = Palm Oil

The acid value of edible oil is lower than 4 mg g^{-1} (Yang *et al*., 2006). Therefore, the observed acid values were under allowable limit for edible oil after refining process.

The peroxide value of obtained refined oil sample ranged from (RFO 1 to RFO 5) 2.28 to 2.62 meq kg^{-1}. The lower peroxide value in the bleached fried oil suggests that the oil can be stored for a long time without deterioration. Oil with high peroxide value are unstable and become easily rancid oil having higher peroxide value (within 20-40 meq kg^{-1}).The iodine value obtained for RFO 1 to RFO 5 were between 100.33 and 109.75 mg g^{-1}. High iodine value in oil shows that the oil has good qualities of edible oils. The saponification values obtained for RFO 1 to RFO 5 were between 142.72 to 152.77 mg KOH g^{-1} respectively. The high saponi-fication value 209.81 for waste fried oil was significantly decreased to 142.72 mg KOH g^{-1} after refining process and it was under permitted level for edible palm oil. Therefore, it was found that refining of fried oil samples investigated were not contaminated until 18 h long frying time and were distributed under allowable limit for edible oil. Thus, the fried oil was extensively frying duration 18 h due to refining process including AABN 3 was used as adsorbent.

Conclusion

In the present research, modified bentonite material from Kyaukpadaung Township, Mandalay Region was evaluated in refining process to incremental frying time. In this study, two types of modification of natural bentonite clay, acid activation and heat activation were carried out. Acid modification of natural bentonite is preferred to the refining process for the waste fried palm oil. From XRD and SEM results, acid activated bentonite clay (AABN3) due to the smallest particle size and highly porous surface. The changes of surface properties of local bentonite clays after acid activation was observed that 3 % H_2SO_4 (AABN 3) gave the best results for the refining process. Moreover, the determination of incremental adsorption capacity of acid activated bentonite clay sample using 3 % H_2SO_4 can be resilient in refining process within 18 h long frying time. The degree of enhancement of frying time for fried palm oil greatly influenced by the use of acid activated bentonite clays. Thus, the acid modified bentonite from Kyaukpadaung, Mandalay Region can be a low cost adsorbent for refining of waste fried palm oil.

Acknowledgments

The authors would like to express their profound gratitude to the Department of Higher Education (Yangon Office), Ministry of Education, Myanmar, for provision of opportunity to do this research and Myanmar Academy of Arts and Science for allowing to present this paper.

References

Chaisena, A. and Rangsriwatananon, K. (2004). "Effects of Thermal and Acid Treatments on Some Physico-chemical Properties of Lampang Diatomite". *Suranaree Journal of Science and Technology*, vol.1(4), pp.289-299

Lian, L., Guo,L. and Guo, C.(2009). "Adsorption of Congo Red from Aqueous Solution on Ca-bentonite". *J. Hazardous Materials*, vol.161, pp.126-131

Ruiz-Mendez, M.V. and Dobarganes, M.C.(1999)."Olive Oil and Olive Pomace Oil Refining".*Oleagineux, Corps gras, Lipids*,vol.6, pp.56-60

Sennour, R., Mimane, G., Benghalem, A. and Taleb,S. (2009). "Removal of Persistent Pollutant Chlorobenzene by Adsorption onto Activated Montmorillonite". *Appl. Clay Sci.*, vol.43, pp.503-506

Yang, T., Wen, X.D., Li, J. and Yang, L. (2006). "Theoretical and Experimental Investigations on the Structures of Purified Clay and Acid-Activated Clay". *Appl. Surface Sci.*, vol.252, pp.6154-6161

Yildiz, N., Aktas, Z. and Calimli, A. (2004). "Sulphuric Acid Activation of Calcium Bentonite". *Particulate Sci. and Tech*., vol.22, pp.21-33.

STUDY ON NUTRITIONAL VALUE AND ANTIDIABETIC ACTIVITY OF *SWIETENIA MACROPHYLLA* KING SEED (MAHOGANY)

Khine Khine Lin[1] , Myat Hsu Mon[2]

Abstract

This research deals with the study on nutritional value and antidiabetic activity of seed of *Swietenia macrophylla* King (Mahogany). Mahogany fruits were collected from Hinthada University campus. In the preliminary phytochemical investigation, it was found that alkaloids, phenolic compounds, flavonoids, steroids, terpenoids, tannins, saponins, carbohydrates, reducing sugars, glycosides and trace amount of cyanogenic glycosides were present in the seed whereas α- amino acid was not detected. Determination of the nutritional values of the seed provided 24.03 % of crude fat, 14.70 % of protein, 13.03 % of dietary fiber, 8.45 % of moisture, 3.15 % of ash and 36.64 % of carbohydrate. According to ED-XRF analysis, the elemental composition of the seed was found to be potassium (1.145 %), phosphorus (0.526 %), sulphur (0.227 %), calcium (0.190 %), iron (0.004 %) and minor components (0.002 %) of Mn, Zn and Cu. After that, the antidiabetic activity of the seed was evaluated by alpha amylase inhibition assay method. IC_{50} values of the extracts were found to be 0.069 mg/mL of ethanol, 0.096 mg/mL of ethyl acetate and 0.168 mg/mL of water extracts.

Keywords: *Swietenia macrophylla* King Seed, phytoconstituents, nutritional values, antidiabetic activity, IC_{50}

Introduction

In the plant kingdom, there are thousands of plants known and unknown, that yield medicine or drugs of great use to man. According to the World Health Organization (WHO), more than 80 % of the world's population in developing countries relies on traditional medicine for their primary health care needs. Natural products from medicinal plants, either as pure compounds or as standardized extracts from medicinal plants provide unlimited opportunities for new drug leads because of the unmatched availability and chemical diversity of bioactive principles from the plant Kingdom(Sasidharan *et al*., 2011). Myanmar is a country considered to be rich in medicinal plants genetic resources. *Swietenia macrophylla* King is one of the valuable medicinal plant in Myanmar.

It is beautiful, lofty, evergreen hardwood timber species of the family Meliaceae. The plant is native to America, Mexico, South America and India. It is extended in most tropical countries especially in Brazil, Philippines, Peru, Malaysia, Singapore and Myanmar.

Medicinal Uses of *Swietenia macrophylla* King

Abundance health benefit that the seeds have is mainly because the seeds contain huge amount of flavonoids and saponins. Especially, the seed extracts have medical efficacy. The seeds have many uses such as in the treatment of hypertension, against chest pain, insect repellent, relieve constipation and menstrual pain, lessen the cholesterol level, increase appetite, fight free radical, prevent colon cancer, boost the immune system and against leishmaniasis. The seeds are very bitter in taste and it has effective in lowering blood sugar level especially if suffer from diabetes. A decoction of the crushed seeds of *S.macrophylla* is also used to treat skin

[1] Dr, Lecturer, Department of Chemistry, West Yangon University

[2] MSc Student, Department of Chemistry, Hinthada University

aliments and wounds. The seed extracts are used to cure malaria, anemia, diarrhoea, dysentery, eczema, rheumatism, cancer, cough, cold and fever (Goh *et al*., 2011).

Nowadays, they are more widely available often in capsule form, as a dietary supplement. People grind the seeds into powder and drink them with water. For diabetics, taking half of tea spoon powdered *S.macrophylla* seed with warm water before a meal may help keep their blood sugar steady. These make them become nutritionally rich, as rich as ginseng. Furthermore, it has possessed a wide array of biological properties such as antidiabetic, anti-microbial, anti-inflammatory, anti-mutagenic, antioxidant, antifungal, antibacterial and anti-obesity activities. In addition, it also contains many natural nutrients that can sustain a healthy body and increase the overall energy of the human body such as protein, minerals, vitamins, fiber, carbohydrates, folic acid, essential fatty acid and so on. Seed kernels yield oil which is very bitter and purgative. The essential oils which are extracted from Mahogany seeds are also used to re-vitalize skin (Amitava *et al*., 2006).

The leaf decoction is used against nerve disorders and bleeding. It contains a sizeable amount of total phenolic, tannins and flavonoid contents. Leaves of *S.macrophylla* have been reported significantly for the prescription of febrifuge, colds, cataract and diarrhoea. The leaves have also been found anti-diabetic, anti-bacterial, anti-oxidant, anti-microbial, anti-fungal, anti-diarrhoeal, anti-malarial and anti-inflammatory (Hasnash *et al*., 2009).

Traditionally, the bark decoction of *S. macrophylla* is used to treat anemia, diarrhoea, dysentery, fever, tuberculosis, loss of appetite and toothache. The bark contains tannin and may serve as an anti-pyretic, tonic and astringent for wounds. In addition, its bark is used for curing psoriasis, hypertension, diabetes, malaria and epilepsy as a folk medicine. It can be inhibited growth of cancer tumors (Panda *et al*., 2010).

The photograph of *S. macrophylla* is shown in Figure 1.

Botanical Characteristics of *Swietenia macrophylla* King

Family	: Meliaceae
Genus	: *Swietenia*
Species	: *macrophylla*
Scientific name	: *Swietenia macrophylla*
English name	: Big leaf mahogany
Myanmar name	: Mahogany
Part used	: Seed

Figure 1 Photographs of *S. macrophylla*

Materials and Methods

Sample Preparation

The fruits of the *S. macrophylla* (Mahogany) were collected from Hinthada University Campus, Ayeyawady Region. The plant was identified by Department of Botany, Hinthada University. The seeds were obtained after removing the hard shell of the fruits. The collected *S. macrophylla* seeds were dried under shadow for four weeks. The dried seeds were ground into powdered form with electric grinder and stored in air tight container to prevent moisture and other contamination.

Determination of Nutritional Value

The nutritional values such as protein, fiber, fat and carbohydrates were also determined. The fat content was determined by the soxhlet extraction method. The protein and fiber content were also studied by acid alkali treatment. The quantitative analyses for the determination of total ash and moisture contents have been done according to AOAC methods (AOAC 1990). The relative abundance of the elements present in seed of the *S. macrophylla* was also determined by Energy dispersive X-ray fluorescence spectrometer (Shimadzu EDX-900).

Investigation of Antidiabetic Activity on the Seed of *S. macrophylla* by α Amylase Assay

Preparation of crude extract by successive solvent extraction method

100 g of the dried seed sample was extracted with petroleum ether (350 mL) by Soxhlet extractor for about 3 h. Then the defatted residue was refluxed with 350 mL of respective solvents (ethanol , ethyl acetate).The soluble portion of the each solvent was obtained by filtration the mixture of the sample. This procedure was repeated for three times. The combined extracts were evaporated under reduced pressure by means of a rotatory evaporator until one third of original volume was remained. Then the mixture was transferred into the porcelain basin and evaporated until the crude extract was obtained. Different crude extracts of ethanol and ethyl acetate were obtained.

The preparation of watery crude extract of the seed sample was carried out according to above procedure.

Screening of antidiabetic activity on the seed of *S.macrophylla*

Accurately weighed, 80 mg of each crude extract was dissolved in 10 mL of buffer solution and thoroughly mixed by shaker. Then it was diluted to 100 mL to obtain the stock solution. Desired concentrations of 0.8 mg/mL, 0.4 mg/mL, 0.2 mg/mL, 0.1 mg/mL, 0.05 mg/mL and 0.025 mg/mL of each solution were prepared from this stock solution by serial dilution with appropriate amount of buffer solution.

Alpha-amylase inhibition activity was determined by UV spectrophotometric method. 1.0 mL of test sample in different concentrations (0.8 mg/mL, 0.4mg/mL, 0.2mg/mL, 0.1 mg/mL, 0.05 mg/mL and 0.025 mg/mL) and 1.0 mL of α-amylase solution were added into each test tube. Then all the test tubes were incubated for 10 min at 25 ℃. After incubation, 1.0 mL of 1 % starch solution was also added and incubated again for 5 min at 25 ^{o}C. After that, 2 mL of

dinitrosalicylic acid was added into these test tubes. The test tubes were again incubated in boiling water for 5 min and cooled at room temperature. The sample solutions were obtained.

Control solution was prepared by using the same procedure replacing the test sample with distilled water.

Blank solution was also prepared without addition of α-amylase replaced by equal amount of buffer solution.

The sample solution, control solution and blank solution were allowed to stand at room temperature for 30 min. After 30 min the absorbance of these solutions were measured by UV spectrophotometer at 540 nm. Absorbance measurement were done in triplicate for each solution and then mean values so obtained were used to calculate percent inhibition of α-amylase by the equation. The IC_{50} value (50 % inhibition concentration) were also calculated by linear regressive excel program.

$$\%\text{Inhibition} = \frac{A_{\text{control}} - (A_{\text{test sample}} - A_{\text{Blank}})}{A_{\text{control}}} \times 100$$

% Inhibition = percent inhibition of sample

$A_{control}$ = absorbance of control solution

A_{sample} = absorbance of sample solution

A_{blank} = absorbance of blank solution

Results and Discussion

Nutritional Values of *S.macrophylla* Seed

The fat content of the sample was determined by the Soxhlet extraction method and was found to be 24.03 %. In addition, the sample was also studied for fiber content by acid alkali treatment and protein content by AOAC method. The carbohydrate, fat, protein and fiber contents for *S.macrophylla* seed were found to be 36.64 %, 24.03 %, 14.70 % and 13.03 %, respectively. All the results are shown in Table 1. The greater amount of fat (24.03 %) and protein (14.70 %) in the seed can helps to maintain body temperature, absorb the nutrients and provide energy. Moreover, fiber content (13.03 %) in the seed lowers cholesterol level, maintain body weight and relieve constipation in the body.

The total ash in the sample is the inorganic residue remaining after the organic matter has been burnt away. The moisture content of sample determined by oven dried method was found to be 8.45 % and ash content by using muffle furnace was 3.15 %.

Elemental Compositions of *S.macrophylla* Seed by EDXRF Spectrometry

The relative abundance of elements present in *S.macrophylla* seed determined by EDXRF spectrometer showed 1.145 % for K, 0.526 % for P, 0.227 % for S, 0.190% for Ca, 0.004 % for Fe, 0.002 % for Mn, Zn, and Cu. All the results are represented in Table 2. The EDXRF spectrum obtained is shown in Figure 2. It can be seen that potassium is the major elements in Mahogany seed. Potassium plays many important roles within the body. Potassium is crucial to cardiovascular and nerve functions in our body. It is particularly important for the ability of our skeletal and smooth muscles to contract. But it can be lost in diuretic therapy for edema or hypertension.

Table 1 Some Nutritional Values of *S.macrophylla* Seed

No.	Components	Content (%)
1.	Fat	24.03
2.	Protein	14.70
3.	Fiber	13.03
4.	Moisture	8.45
5.	Ash	3.15
6.	Carbohydrate	36.64

Table 2 Relative Abundance of some Elements in *S. macrophylla* Seed by EDXRF Method

No	Elements	Relative Abundance (%)
1.	Potassium(K)	1.145
2.	Phosphrous (P)	0.526
3.	Sulphur (S)	0.227
4.	Calcium (Ca)	0.190
5.	Iron (Fe)	0.004
6.	Manganese (Mn)	0.002
7.	Zinc (Zn)	0.002
8.	Copper (Cu)	0.002
9.	Hydrocarbon (CH)	97.902

West Yangon University
Chemistry Department

EDX Report

Report No.

Sample Information

Sample Name	mahogony
Meas. Date	2018/03/05 13:19:59
Comment	with mylar film
Group	powder CH balance
Operator	Dr Cherry Ohn

Measurement Condition

Channel	kV	uA	Filter	Acq.	Collimator	10mm	Atmos.	Air
Na-U	50	79-Auto	----	0 - 40	Analysis	0.00-40.00	Time	Live- 60 DT% 30

Quantitative Result

Analyte	Result		Std.Dev.	Calc.Proc	Line	Intensity
K	1.145	%	[0.009]	Quan-FP	K Ka	34.0869
P	0.526	%	[0.030]	Quan-FP	P Ka	1.0411
S	0.227	%	[0.006]	Quan-FP	S Ka	1.4917
Ca	0.190	%	[0.002]	Quan-FP	CaKa	10.0850
Fe	0.004	%	[0.000]	Quan-FP	FeKa	2.8701
Mn	0.002	%	[0.000]	Quan-FP	MnKa	0.9128
Zn	0.002	%	[0.000]	Quan-FP	ZnKa	3.1246
Cu	0.002	%	[0.000]	Quan-FP	CuKa	2.2877
Rb	0.000	%	[0.000]	Quan-FP	RbKa	1.5553
COH	97.902	%	[------]	Balance	--------	--------

Profile

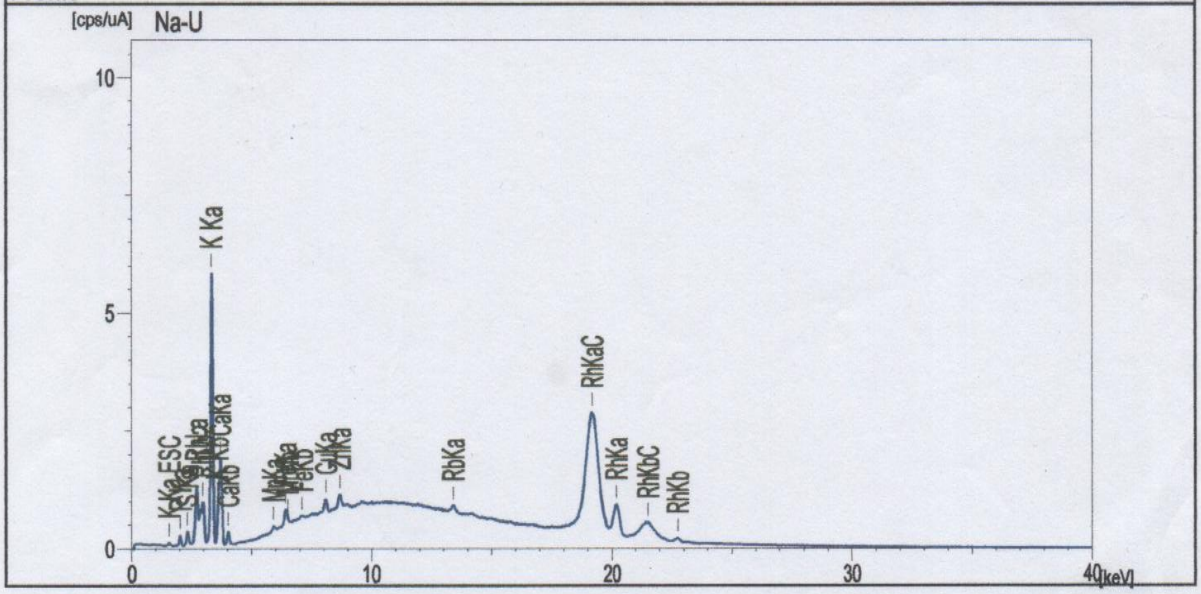

Figure 2 EDXRF spectrum of *S. macrophylla* Seed

Antidiabetic Activity of *S. macrophylla* Seed

The antidiabetic activity of the seed sample was studied by α - amylase inhibition assay. Alpha-amylase is an enzyme that cleaves an internal glycosidic bond within a poly or oligosaccharide. It catalyzes the hydrolytic cleavage of polysaccharides into absorbable monosaccharides. The inhibition of α-amylase decreases rate of hydrolytic cleavage of carbohydrate and slows the elevation of blood sugar in the body. Therefore, the percentage of α-amylase inhibition represents for antidiabetic activity of the sample and expressed in terms of IC_{50} value (50 % inhibition concentration). The lower IC_{50} value showed the higher α-amylase inhibition (greater antidiabetic activity). All the extracts of the seed possesses inhibition property. The inhibition percentage and IC_{50} value of the different extracts of the seed were represented in Table 3. Among the extracts, ethanol extract possesses higher inhibition percent due to lower IC_{50} value of 0.069 mg/mL. The graphical representation of IC_{50} values of the extracts is shown in Figure 3.It was found that IC_{50} value of ethanol extract (0.069 mg/mL) is not much differ from the IC_{50} value of standard Acarbose (Antidiabetic drug).

Therefore, the seed of *S.macrophylla* can be used as an antidiabetic agent in the treatment of diabetes mellitus.

Table 3 α –Amylase Inhibition Percentage and IC_{50} Values of Different Extracts of Seed of *S. macrophylla*

Extracts	Inhibition (%) (Mean ± SD) in different concentrations (mg/mL)						IC_{50} (mg/mL)
	0.025	0.05	0.1	0.2	0.4	0.8	
Ethyl acetate	33.00±1.7	42.85± 1.5	50.61±1.9	63.63±1.6	67.47±1.7	77.52±1.2	0.096
Ethanol	37.50±1.9	45.20±0.44	57.89±1.5	66.67±1.1	77.77±1.7	80.09±1.3	0.069
Watery	29.82±1.7	44.44±1.5	48.71±0.3	50.61±0.7	57.44±0.2	61.54±0.4	0.168
Acarbose	40.86±1.5	52.37±1.7	59.62±1.6	68.48±0.9	79.65±0.8	82.77±1.3	0.047

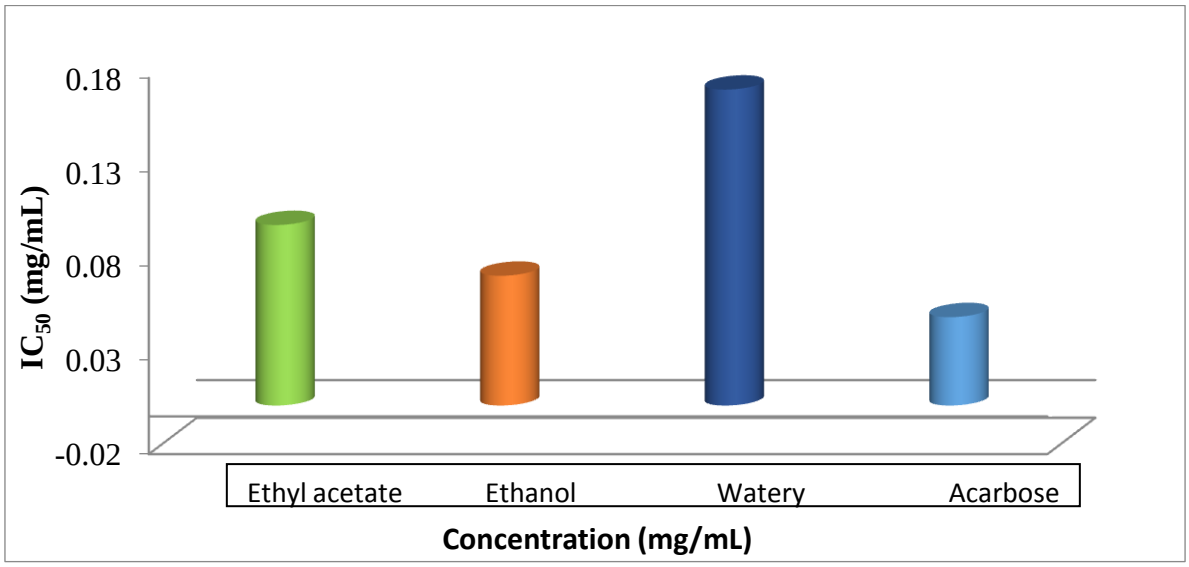

Figure 3 A bar graph of IC_{50} values of crude extracts of *S. macrophylla* seed compared with standard acarbose

Conclusion

The nutritional values and elemental composition of seed of *S. macrophylla* (Mahogany) from Myanmar were studied by AOAC method and ED-XRF Spectrometry. It was observed that 24.03 % of crude fat, 14.70 % of protein, 13.03 % of dietary fiber, 8.45 % of moisture, 3.15 % of ash and 36.64 % of carbohydrate were present in dried seed sample. The greater amount of fats , protein and fiber in *S.macrophylla* seed are essential nutrients for the body processes, brain development and nerve function. The elemental composition of the Mahogany seed by EDXRF showed potassium (1.145 %), phosphorous (0.526 %), sulphur (0.227 %), calcium (0.190 %), iron (0.004 %) and of Mn, Zn, and Cu (0.002 % each). The seed of Mahogany also possesses potassium (1.145 %) than the other elements. Potassium is one of the most common mineral and plays a vital role in heart function. In medicine, the natural sources rich in potassium are low in sodium, helping to maintain normal blood pressure. It is crucial to cardiovascular and nerve functions. Antidiabetic activity (α-amylase inhibition) was exhibited in terms of IC_{50} value. Ethanol extract showed the lowest IC_{50} value (0.069 mg/mL) followed by ethyl acetate (0.096 mg/mL), and watery (0.168 mg/mL). The lower the IC_{50} value, the greater the antidiabetic activity. The present study scientifically proved that the seed of Mahogany possesses antidiabetic property. This finding provides the Mahogany seed contains valuable natural nutrients for healing and improve the blood circulation system in the body. Therefore, *S. macrophylla* seed is considered rare privilege of any herbaceous plant in the world.

Acknowledgements

The authors would like to express their profound gratitude to Myanmar Academy of Arts and Science for allowing to present this paper. We also express ours appreciation to Professor and Head, Dr Hlaing Hlaing Oo, Professor Dr Sanda Khar, Department of Chemistry West Yangon University for their kind supervision and encouragement to present this research work.

References

Amitava, D., Sunilson, J. A. J., Kiran, N. and Rejitha, G (2009). "Antinociceptive Activity of the fruit of *Swietenia macrophylla* King". *journal of Pharmacy Research*, vol. 2(9), pp.1367-1369

AOAC, (1990). *Official and Tentative Methods of Analysis the Association of Official Agriculture Chemists.* Washington D C : 11th Ed., pp. 526

Goh, H.B. and Abdul, A. H. (2011). "In Vitro Cytotoxic Potential of *Swietenia macrophylla* King Seeds against Human Carcinoma Cell lines". *J of Medicinal Plants Res*., vol. 5(8), pp.1395-1404

Hanash, O., Tan, S. K., Wong, K. C., Boey, P. L. and Ibrahlm, P. (2009). "Antimicrobial and Antioxidant Activities of *Swietenia macrophylla* leaf extracts". *As.J.Food Ag-Idn*, vol. 2(02), pp.181-188

Panda S.P., Bera, S., Haldar P. K., Adhikary, S., Kandar C C (2010). "Antidiabetic and Antioxidant Activity of *Swietenia macrophylla* King in Streptozotocin-induced Diabetic Rats". *Pharmaceutical Biology*, vol. 48(9),pp. 974-979

Sasidharan, S., Chen,Y., Saravaran, D., Sundram, K. M. and Latha, L. Y (2011). "Extraction, Isolation and Characterization of Bioactive Compounds from Plant's Extracts". *Afr J Tradit Complement Altern Med*., vol. 8(1), pp.1-10

PREPARATION OF ORGANIC FERTILIZERS FROM KITCHEN WASTES AND MEAL CAKES

Toe Toe Khaing[1], Myat Lay Nwe[2], Khin Myo Myint[3], Thida Tin[1],
Win Win Khaing[4], Moe Myat Myat[5]

Abstract

Organic fertilizers are easily biodegradable and do not affect environmental pollution. They are carbon-based compounds that can increase the productivity and growth quality of plants. They have various benefits over chemical fertilizers. In this research, four organic fertilizers were prepared using kitchen vegetable wastes with peanut meal cake (OF-1, OF-2) and kitchen vegetable wastes with sesame meal cake (OF-3, OF-4) under aerobic and anaerobic conditions. The physicochemical properties of prepared organic fertilizers such as pH value, moisture content, available phosphorus content, available potassium content and organic carbon content were determined. The available nitrogen content in prepared organic fertilizers was measured by alkaline permanganate method. The results from determination were compared with two commercial organic fertilizers. The amount of available nitrogen in OF-1, OF-2, OF-3 and OF-4 were 1.67 %, 1.57 %, 1.45 % and 0.88 % respectively. The available nitrogen content of all prepared organic fertilizers was found to be higher than those of two commercial organic fertilizers. The carbon- nitrogen ratios of the prepared organic fertilizers were calculated. The results from prepared organic fertilizers showed that aerobic condition gave high efficiency. Furthermore, the elemental analysis of four prepared organic fertilizers was examined by EDXRF (Energy Dispersive X-ray Fluorescence) spectroscopy. Silicon was found to be the highest value in all prepared organic fertilizers.

Keywords: Organic fertilizers, chemical fertilizers, kitchen vegetable wastes, meal cake, aerobic condition,

Introduction

Fertilizers are sources of plant nutrients that can be added soil as supplement for its natural fertility. There is usually a very dramatic improvement in both quantity and quality of plant growth when appropriate fertilizers are added. Proper use of fertilizer leads to the production of more nutritious food. Overuse of chemical fertilizer changes the acidity of soil (Secth and Arama, 1986).

Kitchen waste is defined as left-over organic matter from restaurants, hotels and household (Li *et al*., 2009). Tons of kitchen wastes are produced daily in highly populated areas. Kitchen wastes entering the mixed-municipal waste system are difficult to process by standard means, such as incineration, due to the high moisture content (Kuo and Cheng, 2007). Organic matter from kitchen waste can be transformed into useful fertilizer and biofuel (Ma *et al*., 2009).

Meal cakes resulted after extraction of oil from oil seeds were used in food processing, animal food and fertilizer. Meal cakes contain about 50 percent of protein and other functional components.

[1] Dr, Associate Professor, Department of Engineering Chemistry, Mandalay Technological University
[2] Dr, Associate Professor, Department of Engineering Chemistry, Technological University , Kyaing Tong
[3] Dr, Associate Professor, Department of Chemistry, Shwe Bo University
[4] Dr, Associate Professor, Department of Chemistry, Bamaw University
[5] Dr, Associate Professor, Department of Engineering Chemistry, Myanmar Aerospace Engineering University

Organic fertilizers may contribute substantially to improving yield, soil quality and reducing the environmental impacts of conventional farming. These components have been used in sustainable agriculture and to provide nutrients for plant growth and development.

In this research, organic fertilizers were prepared using some kitchen wastes, meal cakes, chicken dung, soil and straw. Then, some physicochemical properties of prepared organic fertilizers were determined by standard methods.

Materials and Methods

Samples Collection

Vegetable wastes were collected from local market, Maha Aungmyae Township, Mandalay Region. The peanut and sesame mealcakes, chicken dung and rice straw were collected from Taung Pyone Gyi Village, Patheingyi Township, Mandalay Region. Soil was also collected from Shangalay Kyune Village, Mandalay Region.

Vegetable wastes were cut into small pieces and rotten in the plastic bag for about one day and then used throughout experiment. The chicken dung was dried under the sunlight. Dried chicken dung were pounded and sieved with 60 mesh sieve to become chicken dung powder. This condition was ready to use. Soil was ground and sieved with 60 mesh sieve to get soil powder. Straws were cut into small pieces. Two different kinds of commercial organic fertilizers, Shwe Zeewa and Naychi (denoted as commercial 1 and commercial 2 respectively) were purchased from agricultural shop. Figure 1 shows the materials for preparing organic fertilizers.

Preparing the Barrel for Aerobic Condition

The plastic containers with lids were taken. Three holes (1 cm in diameter) were made around the top third and the bottom third of the barrel, at a distance of 6 cm from each other. Another hole (1 cm in diameter) was made in the base of the barrel to seep the liquid from the decomposing organic matter from the barrel.

Preparing the Barrel for Anaerobic Condition

Plastic container with lid having same capacity as used in barrel for aerobic condition was taken. There was no hole in the container.

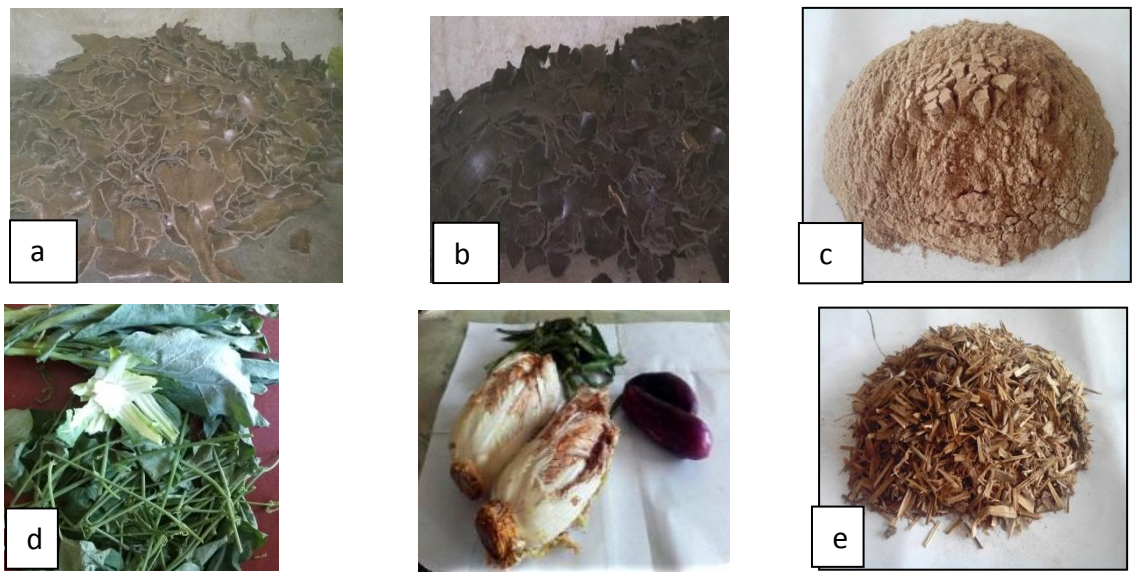

Figure 1 (a) Peanut meal cake (b) sesame meal cake (c) soil (d) kitchen waste and (e) rice straw

Preparation of Effective Microorganism Solution

Effective microorganism (EM) solution was prepared from vegetable waste with chicken dung at room temperature. The fermentation time took about one month to obtain effective microorganism (EM) solution. This EM solution was prepared before doing the organic fertilizers.

Preparation of Organic Fertilizer

Four different kinds of organic fertilizers were prepared, such as

(i) aerobic and anaerobic conditions by using selected kitchen wastes and peanut meal cake (Prepared Organic Fertilizers, OF-1 and OF-2).

(ii) aerobic and anaerobic conditions by using selected kitchen wastes and sesame meal cake (Prepared Organic Fertilizers, OF-3 and OF-4).

The layer for compost

For composing in layers, the following successive layers were piled on top to this.

1. A layer of 1 kg of straw
2. A layer of 1 kg of kitchen wastes
3. A layer of 1 kg of meal cake
4. A layer of 1 kg of soil
5. A layer of 1 kg of EM solution

These types of layers were repeated three times. Finally 1 kg of the straw was put on these layers. The water was sprinkled over the layers for anaerobic condition, and plastic container was enclosed. They were allowed to decompose for two months.

Turning over for the sample under aerobic conditions

During decomposition the layers were turned over regularly, in order that it remained well aerated and all the materials were converted into compost. The first turning over was done after two weeks. The second turning over took place after two weeks. Then each turning over was done after one week. If necessary, water was sprinkled over the container during the process. After two months, decomposition was complete because the plant materials were changed into an unrecognizable crumbly dark mass. However, some straws do not decompose completely.

Determination of Yield Percent of the Prepared Organic Fertilizers

The prepared organic fertilizers were dried and the yield percent of these were determined based upon the total weight of selected materials used.

Determination of Some Physicochemical Properties of the Prepared Organic Fertilizers

Some physicochemical properties of prepared organic fertilizers and another two commercial organic fertilizers were determined by standard methods as shown in Table 1 (AOAC, 1990; AOAC, 2000; Emerson, 1997; Vogel, 1961).

Table 1 Methods for Determination of Some Physicochemical Properties of the Prepared Organic Fertilizers

No.	Parameter	Method
1	pH	Using pH meter
2	Moisture content	Oven drying method
3	Available nitrogen	Alkaline permanganate method
4	Available phosphorus	Olsen's method
5	Available potassium	Atomic absorption spectroscopic method
6	Organic carbon	Walky and Black's method
7	Elemental contents	EDXRF method

Results and Discussion

The Yield Percent of Prepared Organic Fertilizers

The yield percent of the prepared organic fertilizers were calculated based upon the total weight of used materials and shown in Table 2. The yield percent were found to be in the range of 35.54-64.52 %. The yield percent is good for preparation of organic fertilizer.

Table 2 Yield Percent of the Prepared Organic Fertilizers

No.	Prepared Organic Fertilizers	Yield percent (%)
1	OF-1(prepared organic fertilizer with peanut meal cake under aerobic condition)	35.54
2	OF-2 (prepared organic fertilizer with peanut meal cake under anaerobic condition)	64.52
3	OF-3 (prepared organic fertilizer with sesame meal cake under aerobic condition)	39.08
4	OF-4 (prepared organic fertilizer with sesame meal cake under anaerobic condition)	59.30

The pH and Moisture Values of the Prepared Organic Fertilizers

Table 3 shows pH and moisture values of the prepared organic fertilizers. According to the values of pH, prepared organic fertilizers under aerobic condition using both meal cakes were slightly alkaline, but under anaerobic condition were nearly neutral. The results of moisture in all prepared organic fertilizers were significantly lesser than two commercial organic fertilizers.

Table 3 The pH and Moisture Values of Prepared Organic Fertilizers and Commercial Organic Fertilizers

No.	Organic Fertilizer	pH	Moisture (%)
1	OF-1	7.85	3.53
2	OF-2	7.17	6.20
4	OF-3	7.79	3.67
5	OF-4	7.18	4.86
6	Commercial-1	7.67	35.23
7	Commercial-2	7.46	42.76

Elemental Composition of the Prepared Organic Fertilizers

The elemental composition of prepared organic fertilizers was determined by EDXRF spectroscopy and the results are shown in Table 4. The elemental analysis indicates that prepared organic fertilizers contain a number of minerals. The amount of silicon was the highest in all prepared organic fertilizers. EDXRF results give only the relative abundance of elements present in prepared fertilizers.

Table 4 Relative Abundance (%) of Elemental Composition of Prepared Organic Fertilizers (EDXRF method)

No	Elements	Relative Abundance (%)			
		OF-1	OF-2	OF-3	OF-4
1	Al	2.223	2.970	3.080	4.376
2	Si	11.02	12.05	11.970	12.230
3	P	0.556	0.566	0.458	0.286
4	S	0.137	0.127	0.095	0.046
5	Cl	1.536	1.520	1.636	1.429
6	K	2.603	2.001	2.891	2.098
7	Ca	2.011	2.084	1.174	1.176
8	Ti	0.244	0.246	0.259	0.359
9	V	0.006	0.006	0.006	0.007
10	Cr	0.005	0.005	0.005	0.007
11	Mn	0.063	0.066	0.068	0.057
12	Fe	2.547	2.567	2.665	3.254

Available N, P, K of Prepared Organic Fertilizers

The determination of available nitrogen, phosphorus and potassium values of prepared organic fertilizers was performed using standard methods and results are shown in Table 5.

Table 5 Available N, P, K Values of Prepared Organic Fertilizers and Commercial Organic Fertilizers

No.	Organic Fertilizer	Available N (%)	Available P (%)	Available K (%)
1	OF-1	1.67	1.06	2.27
2	OF-2	1.57	1.04	1.18
3	OF-3	1.45	2.03	1.93
4	OF-4	0.88	1.14	1.14
5	Commercial-1	0.86	0.55	0.46
6	Commercial-2	1.43	0.41	0.68

According to the results from the determination of N, P and K values, it can be observed that available N, P and K contents of all prepared organic fertilizers were higher than those of both commercial organic fertilizers. Therefore, all prepared organic fertilizers can supply more amount of N, P and K. These could be used for leaf crops like cabbage which required abundant nitrogen. Moreover, the prepared organic fertilizers using peanut and sesame meal cakes under aerobic condition contained higher amount of potassium and phosphorus. These are good for seed bearing plants and root crops which required a good amount of potassium and phosphorus.

Organic Carbon Value and Carbon-nitrogen Ratio of the Prepared Organic Fertilizers

The examination of amount of organic carbon and carbon-nitrogen ratio of prepared organic fertilizers were carried out. The results are shown in Table 6. The carbon-nitrogen ratios of prepared organic fertilizers under aerobic condition were higher than those of anaerobic condition.

For preparing organic fertilizer under aerobic condition is good to yield more amount of organic carbon.

Table 6 Organic Carbon Value and Carbon-nitrogen Ratio of Prepared Organic Fertilizers and Commercial Organic Fertilizers

No.	Organic Fertilizer	Organic Carbon (%)	Carbon-nitrogen ratio
1	OF-1	13.45	8.05
2	OF-2	8.33	5.31
3	OF-3	14.27	9.84
4	OF-4	5.38	6.11
5	Commercial-1	4.88	5.67
6	Commercial-2	11.89	8.31

Conclusion

In this research work, organic fertilizers were prepared under two conditions (aerobic and anaerobic) using vegetable wastes, peanut and sesame meal cakes, soil and rice straw. EM (effective microorganism) solution was also supplied.

The yield percent of prepared organic fertilizers were found to be 35.54-64.52 %. From the determination of pH value, it can be seen that prepared organic fertilizers under anaerobic condition were nearly neutral but under aerobic condition were slightly alkaline. All prepared organic fertilizers were found to be less moisture content.

The elemental analysis indicates that prepared organic fertilizers contain a number of minerals. The amount of silicon was the highest value in all prepared organic fertilizers.

According to the results from the determination of N, P and K values, it can be observed that available N, P and K contents of all prepared organic fertilizers were higher than those of both commercial organic fertilizers. Moreover, the amount of potassium in OF-1(2.27 %) and phosphorus in OF-3(2.03 %) show that aerobic condition is good efficiency for preparation of organic fertilizer. Carbon-nitrogen ratios of prepared organic fertilizers were found to be in the range of 5.31-9.84.

The organic fertilizer should be used widely in agriculture instead of chemical fertilizer or mixing with chemical fertilizer because of their low cost, good fertility of the soil and supplying more trace elements. The obvious advantages of prepared organic fertilizers over other organic fertilizers are economically viable, convenient and effective. Therefore, prepared organic fertilizers have great potential for applications and can also help in waste management and keeping environment clean.

Acknowledgements

We would like to thank the Myanmar Academy of Arts & Science for allowing to present this research paper. We would like to express the gratitude to Dr Sint Soe, Rector, Mandalay Technological University for his interest and encouragement on our research work. We also thank to Dr Yi Yi Myint, Professor and Head, Department of Chemistry, University of Mandalay and Dr Myat Myat Mon, Professor and Head, Department of Engineering Chemistry, Mandalay Technological University, for their kind help and invaluable advice for this research work.

References

AOAC. (1990). *Official Methods of Analysis*. Virginia: Association of Official Analytical Chemists, Arlington

AOAC. (2000). *Official Methods of Analysis.* Virginia: Association of Official Analytical Chemists, Arlington

Emerson, P. (1997). *Soil Characteristics*. London: Mc Graw-Hill Book Co, Inc.

Kuo, W. and Cheng, K.(2007). "Use of Respirometer in Evaluation of Process and Toxicity of Thermophillic Anaerobic Digestion for Treating Kitchen Waste". *Bioresource Technology*,vol. 98, pp.1805-1811

Li, R., Chen, S., Li,X., Lar J., He, Y. and Zhu, B. (2009). "Anaerobic Codigestion of Kitchen Waste with Cattle Manure for Biogas Production". *Energy and Fuels*, vol. 23, pp. 2225-2228

Ma, H., Wang, Q., Qian D., Gong, L. and Zhang, W. (2009). "The Utlization of Acid-tolerant Bacteria on Ethanal Production from Kitchen Garbage". *Renewable Energy*, vol. 34, pp. 1466-1470

Secth, S. and Arama, B.C. (1986). *Hand Book on Fertilizer Usage*. New Delhi: 6th Edition. The Fertilizer Association of India

Vogel, A. I. (1961). *Quantitative Inorganic Analysis*. London: 3rd Ed. Longman and Green Co. pp.236

ASSESSMENT OF TUBE-WELL WATER QUALITY FROM KYAUKTAN VILLAGE, MINBU TOWNSHIP, MAGWAY REGION

Thwe War Aung*

Abstract

This study deals with the determination of physicochemical properties, trace elements and bacteriological analysis of tube-well water. The tube-well water samples were collected from two sites of Kyauktan Village, Minbu Township. Water samples were analysed from the study area, seasonally in 2018. The physicochemical properties such as the temperature, pH, the electrical conductivity (EC), the turbidity, total dissolved solids, total alkalinity, chloride concentration and salinity of all water samples were measured. The pH values of the collected samples were higher in summer than the other two seasons. The total dissolved solids values were high in rainy season. The total hardness values, dissolved oxygen (DO), biochemical oxygen demand (BOD) and chemical oxygen demand (COD), of water samples were also determined. Some trace elements such as, lead and cadmium were analyzed by Atomic Absorption Spectrophotometer (AAS). Arsenic was detected by Arsenator. The bacteriological analysis of total coliform and *Escherichia coli* was done in the collected water samples. The total coliform and *Escherichia coli* counts were higher in rainy season than other seasons. The experimental results obtained were compared with the WHO standards for human health. The aim of this research is to study water quality for human consumptions and to prevent environmental pollution in this study area.

Keywords: drinking water quality, physicochemical properties, trace elements, bacteriological analysis

Introduction

Water is a transparent and nearly colourless chemical substance that is the main constituent of Earth's streams, lakes, and oceans, and the fluids of most living organisms. Analysis of quality of water is one of many important aspects in the environmental control. As well as the human population of water increases, the human consumption of water also increases. And then pollution of water also increases. There are many parameters that define quality of water. The most some importance of these are the temperature, pH, the electrical conductivity (EC), the turbidity, total dissolved solids, total alkalinity, chloride concentration, salinity, sulphate and nitrate. The natural water analysis for physical, chemical properties including trace element contents are very important for public health studies especially for children (Aminur, 2015).

Tube-Well is a type of ground water. Water well along 100-200 mm (3.9-7.9) inches wide stainless steel tube or pipe bored in underground aquifer (Gupta *et al.*, 2010). In this research, the physicochemical properties, the trace elements and the bacteria examination of tube-well water from Kyauktan Village were carried out.

Kyauktan Village is a village in Minbu Township, Magway Region. People who lives in this village always use these tube-well water for drinking, washing, domestic uses and agricultural purposes. Therefore, the present work is aimed to study water quality of tube-well water from Kyauktan Village, Minbu Township, Magway Region.

* Dr, Lecturer, Department of Chemistry, Magway University

Materials and Methods

Collection of Samples

Tube-well water samples were collected from two sites of Kyauktan Village, Minbu Township, Magway Region. Water samples were collected from the tube-wells at the depth of 7620 mm and 9100 mm, respectively. Three liters of each water sample was taken by means of polyethylene bottles for physicochemical determination. The samples were stored in laboratory and temperature was maintained at 25 ^{o}C (Sulieman, 2010).

Physicochemical Examination of Water Samples

The physicochemical properties of water samples were determined by the following procedures (APHA, 2012).

Determination of temperature

The temperature of water samples was measured by using a thermometer.

Determination of electrical conductivity

The conductivity of water samples was measured by using a conductivity meter within two hours after sampling.

Determination of total dissolved solids

50 mL of water sample was transferred to porcelain crucible and weighed and then evaporated to dryness in an oven to obtain constant weight.

Determination of turbidity

10 mL of distilled water was filled to the colorimeter tube. A filter (415 nm) was placed into slot of colorimeter. This tube was inserted into the chamber and covered. Then, 0 % T and 100 % T were adjusted with controls. This tube was used as the 100 % T blank. 10 mL of water sample was filled to another colorimeter tube and then capped. The test sample was inserted into chamber, covered and measured percent T as soon as reading stabilized.

Determination of pH

The pH of water samples was measured by using a pH meter within two hours after sampling.

Determination of hardness by EDTA titrimetry

10 mL of water sample was added to 100 mL conical flask. 1 to 2 mL of buffer solution at a pH of 10.0 was added to the sample. And then 1 to 2 drops of Erichrome Black T (EBT) indicator solution was added and titrated with ethylene diamine tetra acetic acid (EDTA) titrant to change in colour from wine red to blue.

Determination of total alkalinity (TA) of drinking water samples by titrimetry

Ten mL of water sample was pipetted into a 100 mL conical flask. Two drops of phenolphthalein indicator were added and titrated against 0.1 M HCl. When the solution became colourless and phenolphthalein alkalinity (PA) was calculated as $CaCO_3$ (mg/L) using the equation. A is the volume of titrant (mL) used in the titration. Methyl orange was added to the same flask and continued titration till the colour changed from yellow to orange. The total volume of titrant corresponds to total alkalinity (TA) as $CaCO_3$ (mg/ L). B is the total volume of titrant (mL) consumed with both the indicators.

$$\text{Phenolphthalein Alkalinity (PA)} = \frac{\text{A} \times \text{Molarity of acid} \times 50000}{\text{Volume of sample (mL)}}$$

$$\text{Total Alkalinity (TA)} = \frac{\text{B} \times \text{Molarity of acid} \times 50000}{\text{Volume of sample (mL)}}$$

Determination of biochemical oxygen demand (BOD)

Two bottles 100 mL with lid were taken and cleaned well. 25 mL sample was put into each bottle and 75 mL of distilled water was added to each of the bottles. Then the bottles were closed well. One bottle was kept in the incubator at (20-22) ^{o}C for 5 days. Then 10 mL of manganese sulphate solution and 2 mL of alkali-iodide solution were added to the other bottle well below the surface of the liquid by using a syringe. Then the bottle was closed and mixed by inverting the bottle several times. When the precipitate settled leaving a clear supernatant above the precipitate it was shaken again slowly by inverting the bottle, and when setting had produced at least 50 mL supernatant, 8 mL of concentrated H_2SO_4 were added. Then the bottle was closed and mixed by gentle inversion until dissolution was completed. Then 100 mL of the sample was titrated with 0.05 M $Na_2S_2O_3$ solution until a pale-yellow solution was obtained. Then 2 mL of freshly prepared starch solution was added and titration was continued until a blue colour appeared. The procedure was then repeated using 100 mL distilled water (blank). Then the procedure was repeated for incubated sample.

Determination of chemical oxygen demand by permanganate method

Water sample (10 mL) was taken in a 100 mL conical flask. Then 5 mL of concentrated H_2SO_4 was added and 1 g of copper sulphate was also added. Then 3 mL of prepared 1 M $KMnO_4$ solution was added to the mixture and the bottle was immersed in boiling water for 30 min while keeping the surface of the boiling water at the higher level than the surface of the sample. Then, 3 mL of prepared 1 M sodium oxalate solution was added and immediately titrated with 1 M potassium permanganate until violet colour appeared. Then the procedure was repeated for the blank separately under same condition using 10 mL of distilled water instead of 10 mL of sample.

Determination of some trace elements by AAS

Some elements such as lead and cadmium content of water sample were analyzed by AAS (Atomic Absorption Spectroscopy). Arsenic content was detected by using Arsenator.

Bacteriological examination of tube-well water sample

Bacteriological examination of tube-well water sample was done at the Public Health Laboratory, Ministry of Health and Sports, Mandalay.

Results and Discussion

Nature of the Sampling Sites

Tube-Well drinking water samples were collected from two sampling sites of Kyauktan Village, Minbu Township, Magway Region. Their locations and depth of tube-wells are shown in Table 1 and Figure 1.

Table 1 Location of the Sampling Sites

Sampling Site	Location	Latitude and Longitude	Depth of Tube-Well (mm)
I	Magyitan	North latitude 20˚10' and East longitude 94˚ 50'	7620
II	Yaymyetsu	North latitude 20˚45' and East longitude 95˚12˚	9100

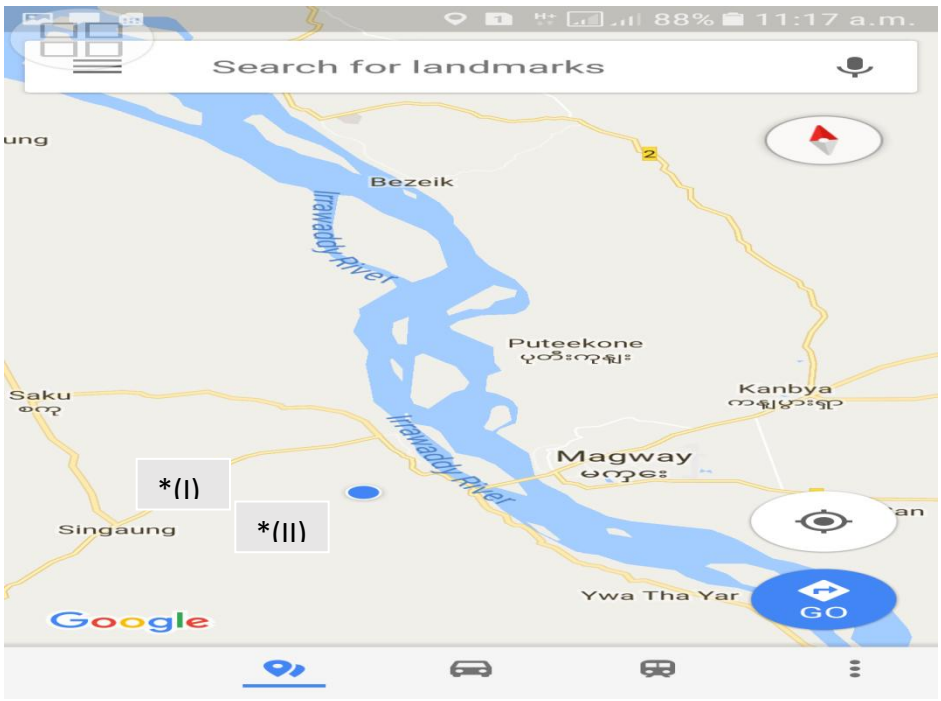

Figure 1 Map of sample collecting sites ***(I)** Magyitan, ***(II)** Yaymyetsu

Physical Parameters of Drinking Tube-Well Water from Two Sites of Kyauktan Village, Minbu Township

The physical parameters such as temperature, pH, electrical conductivity, total dissolved solids, and turbidity were determined at March**,** 2018 in summer, July, 2018 in rainy season and at December, 2018 in winter. The results were described in (Table 2 and Figure 2).

In Table 2, the physical properties of tube-well water samples were found to be changed in three seasons. But, the temperatures of drinking tube-well water samples were found to be same and the pH value of sample (II) was higher than that of sample (I) in all seasons. The electrical conductivity of sample (II) in rainy season was found to be the highest and the total dissolved solids of sample (II) in rainy season was also found to be the highest. The turbidity values of samples (I) and (II) were found to be < 5 FTU in all seasons.

Table 2 Some Physical Parameters of Tube-Well Water Samples in Three Seasons, 2018, Compared with WHO Standards (2008)

Parameters	Sample I			Sample II			WHO Standard (2008)
	Winter	Summer	Rainy Season	Winter	Summer	Rainy Season	
Temperature (ºC)	30	29	28	30	29	28	20-30
pH	7.3	7.1	7.3	7.8	7.5	7.6	6.5-8.5
Electrical Conductivity ($\mu S\ cm^{-1}$)	615	670	1200	650	780	1500	<1500
Total Dissolved Solid (ppm)	212	340	870	200	400	990	1000
Turbidity (FTU)	< 5	< 5	< 5	< 5	< 5	< 5	5

The relationship between electrical conductivity and total dissolved solids is shown in Figure 2. The electrical conductivity values of sample (I) are lower than that of sample (II) in all three seasons. The total dissolved solids of sample (I) are also lower than that of sample (II). It was observed that the electrical conductivity of tube-well water sample increases, the total dissolved solids also increases in three seasons. The electrical conductivity values are directly proportional to total dissolved solids (Gorde and Jadhav, 2013).

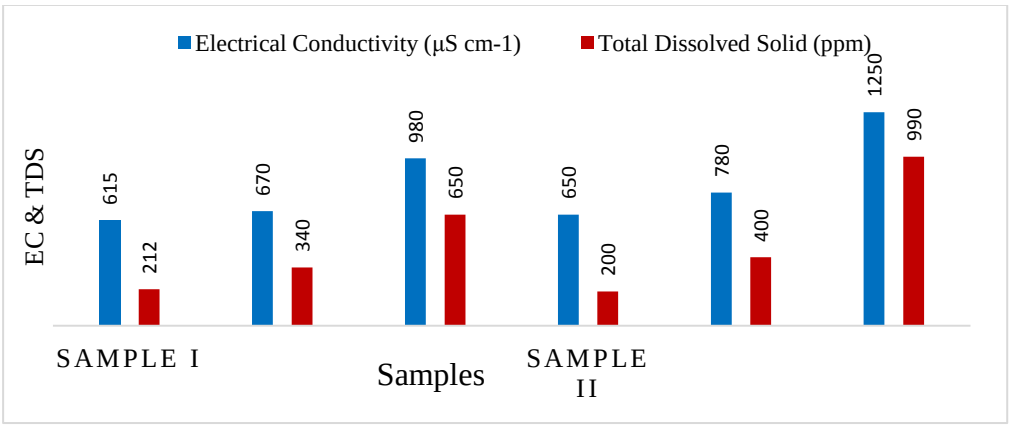

I Magyitan II Yaymyetsu

Figure 2 The relationship between electrical conductivity and total dissolved solids of drinking tube-well water samples

Some Chemical Parameters of Drinking Tube-Well Water

The chemical parameters such as total hardness, total alkalinity, dissolved oxygen, biochemical oxygen demand, chemical oxygen demand, chloride ion concentration and salinity

were determined in three seasons of 2018. The results are described in Table 3 and Figures 3, 4, 5, 6, 7 and 8. The total hardness and total alkalinity values of sample (II) were found to be higher than that of sample (I). The dissolved oxygen values of sample (I) was found to be higher than that of sample (II) at this study time. From BOD and COD determination, sample (I) has lower values than sample (II). The chloride and salinity values of sample (II) were found to be higher than that of sample (I).

Table 3 Some Chemical Parameters of Tube-Well Water Samples in Three Seasons, 2018

Parameters	Sample I			Sample II			WHO Standard (2008)
	Winter	Summer	Rainy	Winter	Summer	Rainy	
Total Hardness (mg L^{-1})	36	32	36	105	110	125	300
Total Alkalinity (ppm)	150	120	155	165	170	182	600
DO (ppm)	4.2	4.0	4.5	3.8	2.7	1.5	4-6
BOD (ppm)	1.6	0.5	1.8	1.9	2.2	4.8	2-4
COD (ppm)	2	2	3	3	2	7	15
Chloride (ppm)	33	35	106	53	40	116	250
Salinity (ppm)	0.15	0.25	0.69	0.22	0.35	0.78	0.4

The total hardness, total alkalinity and chloride values of water samples in winter are shown in Figure 3. From this Figure 3, total hardness, total alkalinity and chloride values of sample (I) are lower than that of sample (II).

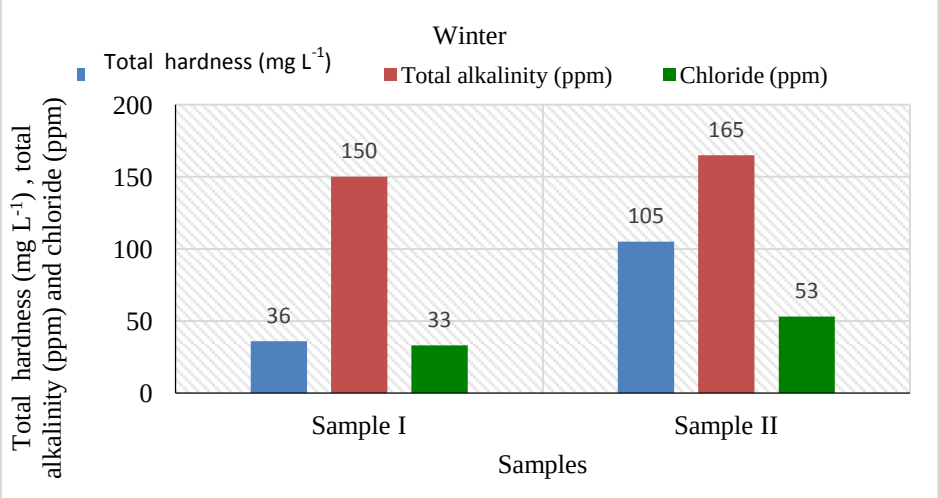

Figure 3 The total hardness, total alkalinity and chloride values of drinking tube-well water samples in winter

Figure 4 shows total hardness, total alkalinity and chloride values of water samples in summer. The total hardness and total alkalinity of sample (I) are lower than that of sample (II). But chloride value of sample (II) is slightly higher than that of sample (I).

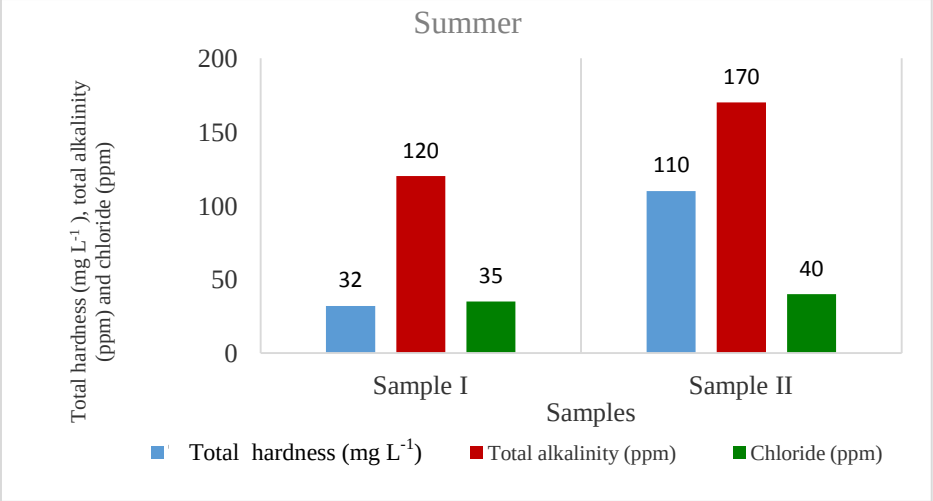

Figure 4 The total hardness, total alkalinity and chloride values of drinking tube-well water samples in summer

The total hardness, total alkalinity and chloride values of water samples in rainy season are shown in Figure 5. The total hardness and total alkalinity of sample (II) are obviously higher than that of sample (I) in rainy season. This may be due to the flooding of water near these tube-wells in rainy season.

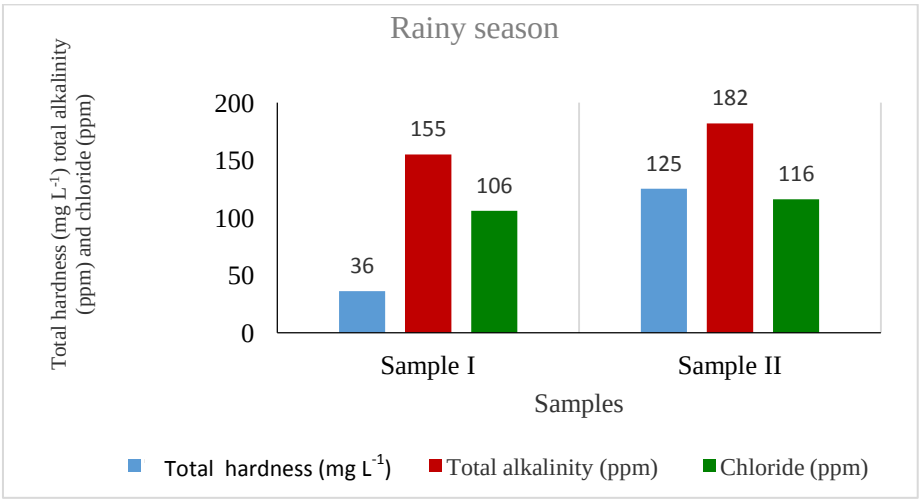

Figure 5 The total hardness, total alkalinity, chloride and salinity values of drinking tube-well water samples in rainy season

DO, BOD and COD values of water samples in winter, summer and rainy season are shown in Figure 6, 7 and 8. DO values of sample (I) are higher than that of (sample II) in all three seasons. BOD values of sample (I) are lower than that of sample (II) in all three seasons. COD values of sample (I) are lower than that of sample (II) in winter and rainy season. But COD of sample (I) and (II) are the same value of 2 ppm in summer.

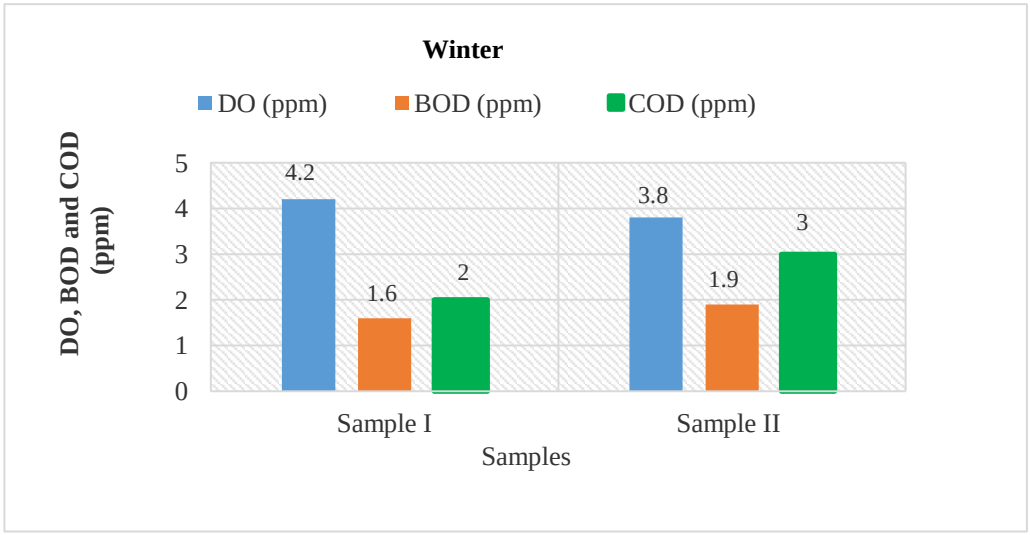

Figure 6 The DO, BOD and COD values of drinking tube-well water samples in winter

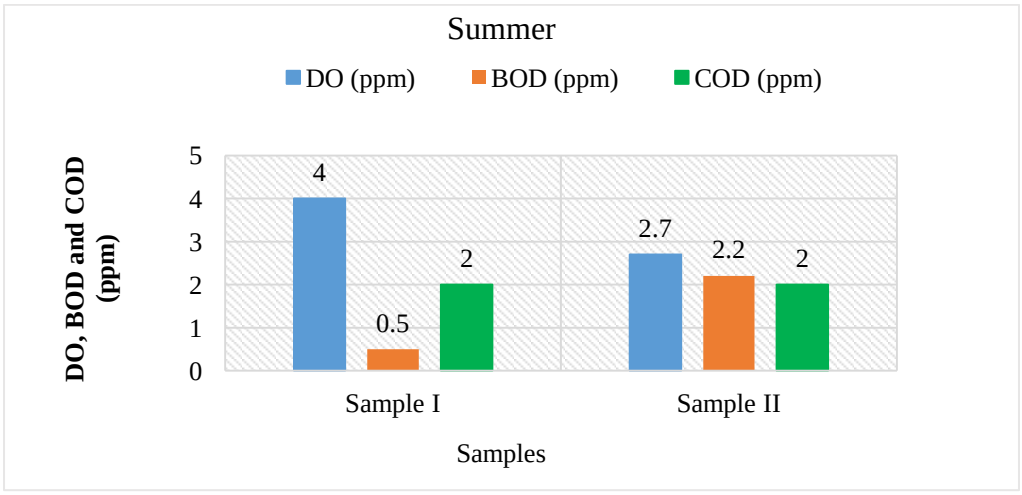

Figure 7 The DO, BOD and COD values of drinking tube-well water samples in summer

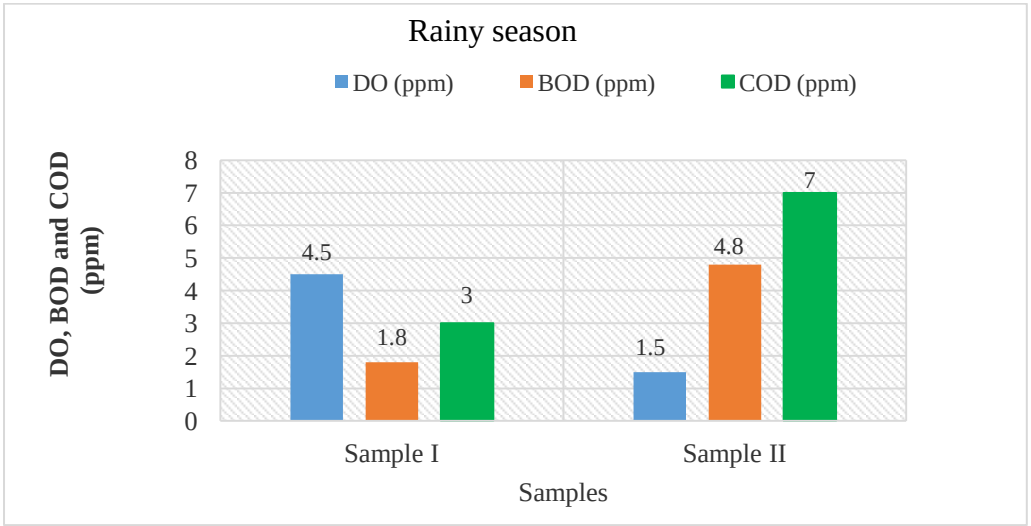

Figure 8 The DO, BOD and COD values of drinking tube-well water samples in rainy season

Trace Elements of Tube-Well Water Samples

Some elements such as lead and cadmium were analyzed by Atomic Absorption Spectrophotometer (AAS). Arsenic was detected by Arsenator. It was found that the amount of trace elements were not changed during the experimental period (2018).

Bacteriological Examination of Tube-Well Water Samples

Some bacteriological analyses such as coliform and *Escherichia coli* were done at the Ministry of Health and Sports, Public Health Laboratory. The results are described in Table 4.

Table 4 Bacteriological Examination of Water Samples in Three Seasons, 2018

Parameters	Sample I			Sample II		
	Winter	Summer	Rainy	Winter	Summer	Rainy
Probable Coliform Count (cfu/mL)	0/5	0/5	2/5	2/5	1/5	5/5
Escherichia coli Count	Non-Isolated	Non-Isolated	Isolated	Isolated	Isolated	Isolated
Remark	Satisfactory	Satisfactory	Un-Satisfactory	Un-Satisfactory	Un-Satisfactory	Un-Satisfactory

Coliform and *Escherichia coli* were not detected in Sample (I) in winter and summer. In rainy season, sample (I) was found to have 2/5 coliform count and *Escherichia coli* was also isolated. But sample (II) was found to have coliform count and *Escherichia coli* was detected in all three seasons.

Conclusion

In this research, the study of physicochemical properties of dinking tube-well water from two sites of Kyauktan Village, Minbu Township, Magway Region was done. The physicochemical parameters such as temperature, electrical conductivity, total dissolved solids, turbidity, pH, hardness, alkalinity, biological oxygen demand, chemical oxygen demand, chloride ion and salinity content were determined. In addition, some trace elements such as arsenic, lead and cadmium were analyzed. The electrical conductivity values of tube-well water samples show that this water has been good for drinking. The pH values of sample (II) were found to be slightly alkaline at three seasons. From the hardness values of water samples, sample (I) may be soft water (< 50 mg L^{-1}) and sample (II) may be slightly hard (100-150 mg L^{-1}). The total alkalinity of sample (II) was found to be higher than that of sample (I) in all seasons. The BOD value of sample (II) was found to be highest at rainy seasons. This may be due to the flooding in rainy seasons. The COD for water samples are lower than the standard values. The trace elements determination, arsenic was found to be 0 ppb. Lead and cadmium were not detected. From the examination of bacteria, sample (I) shows the presence of *Escherichia coli* (2/5) at rainy season and thus it was un-satisfactory in rainy season. In summer and winter, *Escherichia coli* was not isolated and sample (I) was used for satisfactory. *Escherichia coli* in sample (II) was found in all three seasons. Thus sample (II) may be used un-satisfactory for all seasons. In summary, sample (I) may be used for drinking and domestic uses at summer and winter. But it must be used after boiling in rainy seasons. For sample (II), it may be used for agricultural uses. It may be used for drinking after the water had been boiled and any appropriate treatment.

Acknowledgements

The authors wish to thank the Myanmar Academy of Arts and Science for allowing to present this paper and Professor and Head, Dr Thidar Aung and Professor Dr Htay Htay Win, Department of Chemistry, Magway University for their provision and suggestions of the research facilities.

References

Aminur, R. (2015). "Physicochemical and Bacteriological Analysis of Drinking Tube-Well Water from Some Primary School, Magura, Bangladesh to Evaluate Suitability for Students''. *Int. Journal of Applied Science and Engineering Research*, vol.4 (5), pp. 735-748

APHA. (2012). "*Standard Methods for the Examination of Water*''. Washington DC: 22nd Edition, American Public Health Association, pp. 38-50

Gorde, S.P. and Jadhav, M.V. (2013). "Assessment of Water Quality Parameters: A Review''. *Journal of Engineering Research and Applications*, vol.3 (6), pp. 2029-2035

Gupta, N., Shikha, B. and Patra, B. A. (2010). "Physicochemical Analysis of Drinking Water Quality from 32 Locations in Delhi''. *Journal of Indian Water Works Association,* vol.3 (6), pp.124-235

Sulieman, E.I. (2010). "Chemical, Physicochemical and Physical Properties of Wastewater from the Sudanese Fermentation Industry''. *Int. Journal of Applied Science and Engineering Research*, vol.4 (5), pp. 735-748

WHO. (2008). ''Guidelines for Drinking-Water Quality, Volume **1**, Recommendations''. Geneva: 3rd Edition, World Health Organization, pp. 53

[1]STUDY ON PRELIMINARY PHYTOCHEMICAL SCREENING, ANTIBACTERIAL AND ANTIOXIDANT ACTIVITIES OF *PIPER BETLE* L. (BETEL VINE)

Su Lay Yee[1], Tin Tin Myo[2]

Abstract

The present study was carried out to investigation of preliminary phytochemical constituents, antibacterial activity and antioxidant activity of *Piper betel* L. leaf (*Piperaceae*) commonly known as betel vine. The plant is locally known as Kun in Myanmar. Phytochemical investigation of *P. betle* leaf revealed the presence of alkaloids, glycoside, carbohydrate, amino acid, phenolic compound, flavonoid, steroid, terpenoid, saponin, tannin, starch, reducing sugar and organic acid. From the results of antibacterial activity assay, it was observed that ethyl acetate and ethanol extracts of *P. betle leaf* have high antibacterial activity against *Bacillus subtilis*, *Staphylococcus aureus*, *Pseudomonas aeruginosa*, *Bacillius pumilus* and *E. coli*. Screening of antioxidant activity was done by DPPH free radical scavenging assay by using UV spectroscopic method. The IC_{50} values for the ethanol and ethyl acetate extracts were 54.61 µg/mL and 70.53 µg/mL, for watery extract was 105.80 µg/mL. The smaller the IC_{50} value the greater the antioxidant activity. Ethanol extract of *P. betle* showed the more effective results.

Keywords: *Piper betle* L., phytochemical, antibacterial activity, antioxidant activity

Introduction

Betel (*Piper betle* L.) is locally known as Kun and Betel vine in English. It belongs to the genus *Piper* of the *Piperaceae* family. Its heart-shaped leaves can grow up to the size of 18 cm in length and 12 cm in width. This plant is cultivated most parts of South India, Bengal, Sri Lanka, Myanmar and Thailand for its leaves. The *P. betle* leaves are the most important plant part and it possesses medicinal, religious and ceremonial value in Southeast Asia. In India, it is customary to serve *P. betle* leaves on various social, cultural and religious occasions and is also offered to guests as a mark of respect (Warrier *et al.,* 1995). Fresh *P. betle* leaves are chewed together with areca nut and slaked lime as natural tonic and breath refresher. Aqueous extracts of *P. betle* leaves have also been shown to reduce the adherence of early dental plaque bacteria (Razak *et al*., 2006). As well as use as a mouth freshener, the leaves are used for wound healing and digestive and pancreatic lipase stimulant activities in traditional medicine (Periyanayagam *et al*., 2012). A preliminary study has reported *P. betle* leaves extracts contain large numbers of bioactive molecule like polyphenols, alkaloids, steroids, saponins and tannins. Antioxidant, anti-bacterial and anti-fungal, antiinflammatory, anti-diabetic and radioprotective activities of *P. betle* leaves have also been reported (Chakraborty and Shah, 2011).

Scientific Classification

Family	:	Piperaceae
Genus	:	*Piper*
Species	:	*P.betle*
Botanical name	:	*Piper betle* L.
Common name	:	Betel vine
Myanmar name	:	Kun

[1] Dr, Associate Professor, Department of Chemistry, Shwebo University
[2] Dr, Lecturer, Department of Chemistry, Kyaing Tone University

The photographs of *P. betle*. (Kun) plant and leaves are shown in Figure 1.

Figure 1 *P. betle* (Kun) plant and leaves

Phyto-constituents of *P. betle*

P. betle are one of the highly investigated plants and phytochemical studies show that *P. betle contains* a wide variety of biologically active compounds whose concentration depends on the variety of the plant, season and climate (Kumar, 1999). The specific strong pungent aromatic flavour in leaves is due to phenol and terpene like bodies. The quality of the leaf depends upon the phenolic content, i.e., more the phenolic content betters the leaf quality. Recently many researches work shows the *P. betle* leaves contains starch, diastases, sugars and an essential oil composing of safrole, allyl pyrocatechol monoacetate, eugenol, terpinen-4-ol, eugenyl acetate, etc. as the major components (Razak *et al.*, 2006). Phytochemical investigation on leaves revealed the presence of alkaloids, carbohydrate, amino acids, tannins and steroidal components. The middle part of the leaf contains largest quantity of Tannin. The terpenoids include 1, 8-cineole, cadinene, camphene, caryophyllene, limonene, pinene, Chavicol, ally pyrocatechol, carvacrol, safrole, eugenol and chavibetol are the major phenols found in betel leaf. Eugenol was identified as the antifungal principle in the oil. The fresh new leaves contain much more amount of essential oil diastase enzyme and sugar as compare to old leaves (Harborne, 1984).

Materials and Methods

Collection of Sample

In the present research, the *P. betle* leaves were collected from Kun Gyan Kone Township, Yangon Region. The leaves were washed and air dried for two weeks. Then, the dried leaves were powdered in a grinding machine. The powdered sample was stored in air-tight bottle, so as to prevent moisture changes and contamination.

Preliminary Phytochemical Investigation

The *P. betle* leaves were screened for the presence of various bioactive principles. Phytochemical investigations were performed to know the different types of chemical constituents such as alkaloids, glycosides, carbohydrates, α-amino acids, phenolic compounds, flavonoids, steroids, terpenoids, saponins, tannins, cyanogenic glycosides, starch, reducing sugars, organic acids and quinones according to the appropriate reported procedure ((Harborne, 1984). After treating the test solution with specific reagents, the tests were detected by virtual observation of colour change or precipitate formation.

Screening of Antibacterial Activity of Various Extracts from *P. Betle* L.

The antibacterial activities of different crude extracts such as petroleum ether, ethyl acetate, ethanol and water extracts were determined against five bacteria such as *Bacillus subtilis, Bacillus pumilus, Staphylococcus aureus, Pseudomonas aeruginosa,* and *Escherichia coli* species by employing agar well diffusion method at Pharmaceutical Research Department, Ministry of Industry, Yangon, Myanmar (Mar Mar Nyein *et al.*, 1991).

Antioxidant Activity Assay

Screening of antioxidant activity of the crude extracts (aqueous and ethanol) of *P. betle* leaves were carried out by DPPH free radical scavenging assay using UV spectroscopic method (Brand-Williams *et al*., 1995). Ascorbic acid was used as a standard. Absorbance measurements were done in triplicate for each sample solution. Absorbance values obtained were used to calculate % inhibition, 50 % inhibitory concentration (IC_{50}) and standard deviation. Lower absorbance of the reaction mixture indicates higher free radical scavenging activity.

Results and Discussion

Preliminary Phytochemical Investigation

Phytochemical investigations were carried out on the petroleum ether, ethyl acetate, ethanol and water extracts of *P. betle* leaves sample using standard procedures to identify the constituents. The preliminary phytochemical investigation of *P. betle* leaves was carried out to view the different types of chemical constituents present in the leaf according to the procedures. From results, it was observed that alkaloids, glycosides, carbohydrates, α-amino acids, phenolic compounds, flavonoids, steroids, terpenoids, saponins, tannins, starch, reducing sugars and organic acids were present in the leaves of *P. betle* (Table 1). The phytochemical compounds such as flavonoids, tannin, phenolic compounds and saponins have potentially significant application against bacteria. Many phytochemicals are antioxidants such as flavonoids, polyphenols and have been found to possess different pharmacological properties. The *P. betle* leaf has biologically active principles.

Screening of Antibacterial Activity of Crude Extracts from *Piper betle L.*

In vitro screening of antibacterial activity of various extracts such as petroleum ether, ethyl acetate, ethanol and watery extracts from *P. betle* leaves were done by agar well diffusion method (Figure 2). In this investigation, the extracts were tested against five bacteria such as *B. subtilis, B. pumilus, S. aureus, P. aeruginosa* and *E. coli.* All extracts of *P. betle* were active on tested bacteria. The petroleum ether extract was found low activity on the all organisms and watery extract was found to be low activity aganist *B. subtilis, B. pumilus, S. aureus* and *E. coli* species. Ethyl acetate extract show the highest activities on *P. aeruginosa* and *E. coli*. But ethyl acetate extract showed the medium activities on others microorganisms. In ethanol extract, exception of *P. aeruginosa* showed the highest activities on tested bacteria (Table 2).

Table 1 Results of Phytochemical Investigation on *P. betle* Leaf

Sr No.	Chemical Constituents	Test Reagent	Observation	Inference
1	Alkaloids	(i) Dragendorff's	Orange ppt.	+
		(ii) Mayer's	White ppt.	+
2	α-Amino acids	Ninhydrin	Purple colour solution	+
3	Carbohydrates	Molisch's	Violet ring	+
4	Cyonogenic Glycoside	Sodium picrate	No change	-
5	Flavonoids	Shinoda's	Pink solution	+
6	Glycosides	10 % lead acetate	Brown ppt.	+
7	Organic acids	Bromocresol green	Yellow solution	+
8	Phenolic compound	5 % ferric chloride	Brown ppt.	+
9	Quinones	Hydrochloric acid	Yellow colour solution	+
10	Reducing sugars	Benedict's	Light green ppt.	-
11	Saponins	Foam test	Marked frothing	+
12	Starch	Iodine	Blue colour solution	+
13	Steriods	Liberman Burchard	Greenish yellow solution	+
14	Tannins	Ferrous sulphate	Green ppt	+
15	Terpenoids	Liberman Burchard	Pink ppt.	+

(+) = presence (-) = not detected

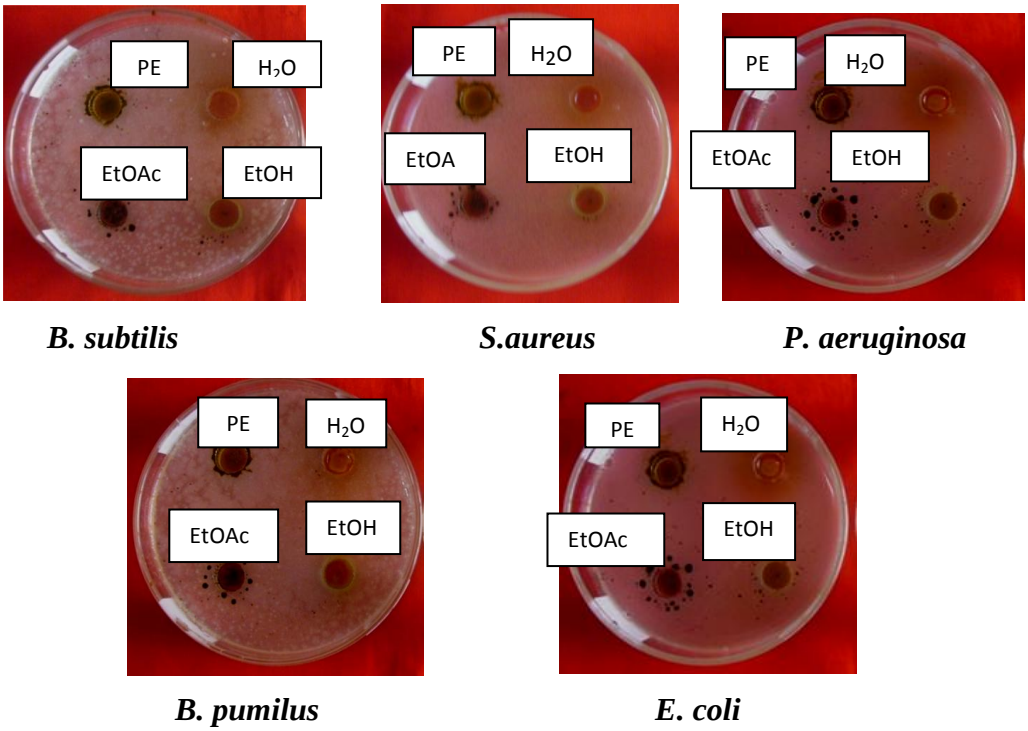

B. subtilis ***S.aureus*** ***P. aeruginosa***

B. pumilus ***E. coli***

Figure 2 Inhibition zones indicating the antibacterial activities of various crude extracts of *P. betle* against tested bacteria

Table 2 Inhibition Zone Diameters of *P. betle* Leaf Extracts

Microbial Strains	Inhibition zone diameters of different extracts (mm)			
	PE	EtOAc	EtOH	H_2O
B. subtilis	14(+)	19 (++)	22 (+++)	13 (+)
S. aureus	13 (+)	19 (++)	20 (+++)	14 (+)
P. aeruginosa	13 (+)	20 (+++)	17 (++)	16 (++)
B. pumilus	12 (+)	19 (++)	20 (+++)	14 (+)
E. coli	13 (+)	20 (+++)	24 (+++)	14 (+)

(+) = 10-14 mm (low activity), (++) =15-19 mm (moderate activity)
(+++) = 20 mm and above (high activity), (−) = no zone of inhibition
Agar well diameter = 8 mm

Antioxidant Activity of Extracts of *P. betle*

The crude extract of watery, ethanol and ethyl acetate extracts were taken for screening of antioxidant activity by determination of DPPH free radical scavenging property by using UV spectroscopic method. The percent oxidative inhibition values of crude extracts were measured at different concentrations. From these experimental results, it was found that as the concentrations were increased, the absorbance values were decreased, i.e., increase in concentration and increase in radical scavenging activity of crude extracts expressed in term of % inhibition (Table 3). IC_{50} values in µg/mL were calculated by linear regression equation. DPPH free radical scavenging activity of extracts of *P. betle* was clearly indicated that ethanol extract of the leaves of *P. betle* had the higher activity than that of watery and ethyl acetate extracts. The IC_{50} value for the ethanol extract was 54.61 µg/mL, those for watery and ethyl acetate extracts were respectively 105.8 µg/mL and 70.53 µg/mL, and that of standard ascorbic acid was 35.81 µg/mL (Table 4). The smaller the IC_{50} value the greater the antioxidant activity. Ethanol extract of *P. betle has* higher activity because the IC_{50} value of ethanol extract was much lesser than that of watery and ethyl acetate extracts.

Table 3 Percent Radical Scavenging Activity (% RSA) of Extracts of *P. betle* Leaf and Standard Ascorbic Acid

Concentration (µg/mL)	% RSA			
	H_2O extract	EtOH extract	EtOAc extract	Ascorbic acid
12.5	17.20	28.46	28.89	37.85
25	29.22	39.82	40.58	43.57
50	41.88	48.93	45.05	57.85
100	48.70	59.64	56.51	62.85
200	71.10	74.06	71.49	76.42

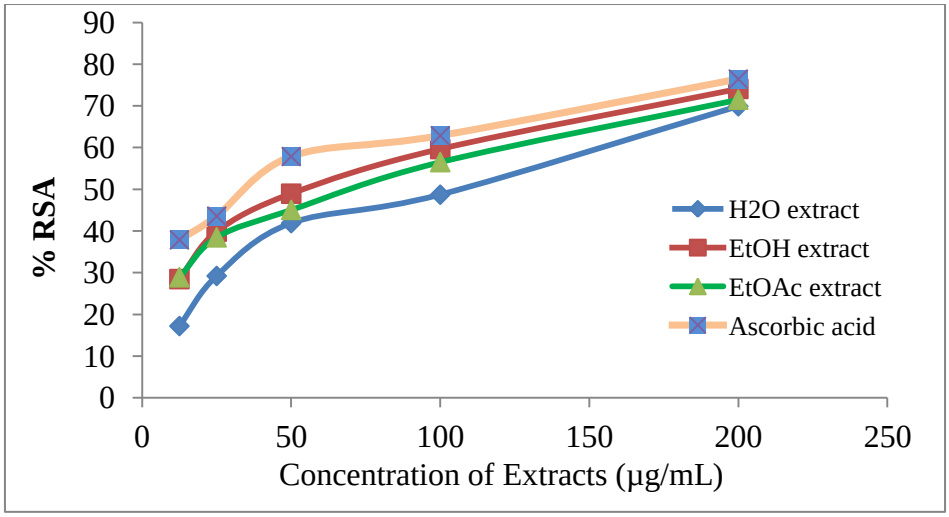

Table 4 IC_{50} Values of Extracts of *P. betle* Leaf and Standard Ascorbic Acid

Sample	IC_{50} (µg mL^{-1})
EtOH extract	54.61
EtOAc extract	70.53
H_2O extract	105.80
Ascorbic Acid	35.81

Conclusion

Herbal medicines are valuable and readily available resources for primary health care. *P. betle* leaves are also used as traditional medicine around the world. According to this research, *P. betle* leaves contain various bioactive compound. Based on this study, various extracts of leaves exhibited antibacterial activity against various gram positive and gram-negative pathogens. In this study, antibacterial activity and antioxidant activity of ethanol extracts are likely to show good relationship. Ethanol extract showed the highest activities on tested microorganisms and DPPH radical scavenging activity with the IC_{50} value of 54.61 µg/mL compared to other extracts of P. *betle* leaf in this study.

Acknowledgements

The authors would like to thank the Department of Higher Education, Ministry of Education, Myanmar, for the permission of doing this research. We would like to express deep sense of gratitude to Dr Hlaing Hlaing Oo, Professor and Head (Reteired), Department of Chemistry, West Yangon University for their kind provision of the research facilities. Special thanks are extended to Professor and Head, Dr Kyu Kyu Swe, Department of Chemistry, Shwebo University for her kind encouragement.

References

Brand-Williams, W., Cuvelier, M.E. and Berset, C. (1995). "Use of a Free Radical Method to Evaluate Antioxidant Activity". *LWT-Food Sci. Technol.*, vol. 28, pp.25-30

Chakraborty, D. and Shah, B. (2011). "Antimicrobial, Antioxidative and Anti-Hemolytic Activity of *Piper Betel* Leaf Extracts". *International Journal of Pharmarcy and Pharmaceutical Sciences*, vol. 3, pp.192-198

Harborne, J. B. (1984*). Phytochemical Methods, A Guide to Modern Techniques of Plant Analysis*. New York, 2nd Edition, Chapman and Hall, pp.120-160

Kumar, N. (1999). "Betelvine (*Piper betle* L.) Cultivation". *Indian Journal of History of Science*. vol. 34, pp. 19-32

Mar Mar Nyein, Chit Maung, Mya Bwin and Tha, S.J. (1991). "*In Vitro* Testing of Various Indigenous Plant Extracts on Human Pathogenic Bacteria". *Myanmar Health Science Research Journal*, vol. 3, pp. 89-99

Periyanayagam, K., Adeesan, M., Kavimani, S. and Vertiselval, T. (2012). "Pharmacognostic and Phytochemical Profile of Leaves of *Piper betle.* L.". *Asian Pacific J. Topical Biomed*. vol. 6 pp. 506-510

Razak, F.A, Othman R.Y and Haji, Z.H.A. (2006). "The Effect of *Piper betle* and *Psidium Guajava* Extracts on The Cell-Surface Hydrophobicity of Selected Early Settlers of Dental Plaque". *J. Oral Sci*., vol. 48, pp. 71–75

Warrier P.K., Nambair, V.P.K. and Ramankutty, C. (1995). *Indian Medicinal Plants: A Compendium of 500 Species*, India: Arya Vaidya Sala, Kottakal, Kerala; Orient Longman, pp-485-500

FOCUSING ON THE ELEMENTAL CONTENTS, ANTIOXIDANT ACTIVITY AND CYTOTOXICITY OF *RHODODENDRON ARBORETUM* W.W.SM (TAWNG ZA LAT NI) FLOWER

Myint Myint Khaing[1], Win Min Than[2], Wah Wah Khaing[2], Moh Moh Naing[3], Cherry Aung[3], Yee Wai Phyo[4]

Abstract

Rhododendron arboreum W.W.Sm (Tawng Za Lat Ni) is one of the landmarks of Chin State. Local people use it as a salad, wine and other kinds of native foods. This research focused on phytoconstituents, elemental contents, antioxidant activity and cytotoxicity of flowers of *R. arboreum* (Tawng Za Lat Ni) that were investigated by UV -Visible spectrophotometer, animal test model (*Artemia salina*) and some modern techniques. Moreover, the elemental contents of these flowers were analyzed by Energy Dispersive X ray Fluorescence (EDXRF) Method that showed the presence of K, Si, Ca, Fe, Mn, Cu and Zn. According to antioxidant activity test, IC_{50} of Tawng Za Lat Ni flower was 4.57μg/mL indicating the presence of antioxidant substances that can bond with and stabilize free radicals helping to prevent the damage they cause to the body, thereby reducing the risk of cancer. The cytotoxic effect of ethanol extract of flowers was examined by brine shrimp assay (*Artemia salina*) and Tawng Za Lat flowers were not found to have cytotoxic effect (and considered to be safe for consumption.

Keywords: *R. arboreum,* antioxidant activity, cytotoxic effect, brine shrimp assay, *Artemia salina*

Introduction

Traditional medicines are made from plants, animal products and minerals (Still, 2003; Healing Base, 2011). However, medicinal plants and plant derived medicines are widely used in traditional cultures all over the world and they are becoming increasingly popular in modern society. Plants have been particularly used as medicine for health and survival of man (Petrovska, 2012). The knowledge of the development of ideas related to the usage of medicinal plants as well as the evolution of awareness has increased the ability of pharmacists and physicians to respond to the challenges that have emerged with the spreading of professional services in facilitation of man's life. Myanmar traditional knowledge and medicine is believed to be able to cure all of these diseases by using ingredients such as fresh or dried roots, stems, leaves, buds and flowers. Traditional medicine continues to be widely practiced by the majority of the population, partly as a supplement and partly as an alternative to modern medicine.

Scientists all over the country had to test various herbs on modern scientific lines with a view to proving claims of proper selection of medicinal plant. The general research methods includes proper selection of medicinal plants, preparation of crude extracts, biological screening, detailed chemopharmacological investigations, toxicological and clinical studies, standardization and use of active moiety as the lead molecule for drug design. *Rhododendron* species have long been used in traditional medicine. Animal studies and in vitro research has identified possible

[1] Dr, Associate Professor, Department of Engineering Chemistry, Technological University, Kalay
[2] Lecturer, Department of Engineering Chemistry, Technological University, Kalay
[3] Assistant Lecturer, Department of Engineering Chemistry, Technological University, Kalay
[4] Demonstrator, Department of Engineering Chemistry, Technological University, Kalay

anti-inflammatory and hepatoprotective activities which may be due to the antioxidant effects of flavonoids or other phenolic compounds and saponins.

Rhododendron species are found in Sino Himalayas, southern and northeastern China, Japan, Myanmar, Thailand, Indonesia, Malaysia, Phillipines and New Guinea (Bhattacharyya, 2011) . In Myanmar, *Rhododendron arboreum* flower (white and red) is the famous landmark of Mt. Victoria as well as Chin State (Ong *et al*., 2018). Most species have brightly coloured flowers which bloom from late winter through to early summer (Turner and Wasson, 1997). Rhododendron species have long been used in traditional medicine (Popescu and Kopp, 2013). Scientific classification of *R. arboreum* (Tawng Za Lat Ni) (Figure 1) is as follows (Madhvi *et al*., 2019).

Family name	-	Ericaceae
Scientific name	-	*Rhododendron arboreum* W.W.Sm
Myanmar name	-	Tawng Za Lat Ni
English name	-	Rose Apple
Medicinal uses	-	Anti-inflammatory, hepatoprotective activities
Distribution	-	Hilly region (Chin State) in Myanmar
Part used	-	Flowers

(a) (b)

Figure 1 (a) Tawng Za Lat tree and (b) Flowers of Tawng Za Lat Ni

This research focused on the phytochemicals, elemental contents, antioxidant activity and cytotoxicity of the flowers of *Rhododendron arboreum* W.W.Sm (Tawng Za Lat Ni) that is suitable for local traditional food of Chin ethnic group.

Materials and Methods

Sample Collection

Flowers of Tawng Za Lat Ni were collected from Chin State, Myanmar. The flowers were identified at Department of Botany, University of Mandalay. The collected flowers were dried in the shade for two weeks and then, 300 g of the flower samples were dissolved in 2.5 L of ethanol.

Phytochemical Tests of *R. arboreum* (Tawng Za Lat Ni)

In order to know the type of chemical constituents consisting in the Tawng Za Lat Ni flower, phytochemical tests were carried out according to the reported methods (Evans,1996).

Elemental Analysis of *R. arboreum* (Tawng Za Lat Ni)

The elements present in Tawng Za Lat Ni flowers were examined by Energy Dispersive X-ray Fluorescence Spectroscopy (EDXRF) (SPECTRO XEPOS EDXRF Spectrometer, Germany) at the Department of Chemistry, Monywa University.

Determination of Antioxidant Activity of *R. arboreum* (Tawng Za Lat Ni)

In this study, DPPH (2,2-diphenyl-1-1-picryl hydrazyl) free radical scavenging assay has been chosen to evaluate the free radical scavenging effectiveness of crude extract of Tawng Za Lat Ni flower (Marinova and Batchvarov, 2011) at Department of Biotechnology, Mandalay Technological University.

Sample solutions of Tawng Za Lat Ni flowers extract were prepared by dissolving 3.125 mg of flower extract in 100 mL of ethanol to obtain 31.25 μg/mL and then it was serially diluted to obtain 15.625, 7.812, 3.906, 1.953 μg/mL solutions.

The control solution prepared by mixing 1.5 mL of 0.002 % DPPH solution and 1.5 mL of ethanol, and the sample solution prepared by mixing 1.5 mL of 0.002 % DPPH solution and 1.5 mL of test sample solution were incubated at room temperature and shaken on a shaker for 30 min. After incubation, the absorbance values of different concentrations of tested samples were measured at 517 nm. Absorbance measurements were used to calculate the percentage of radical scavenging activity (% RSA) by the following equation:

$$\% \text{ RSA} = [A_{DPPH} - (A_{sample} - A_{blank})/ A_{DPPH}] \times 100$$

where,

$\%$ RSA = % radical scavenging activity of test sample
A_{DPPH} = absorbance of DPPH in EtOH solution
A_{sample} = absorbance of sample + DPPH solution
A_{blank} = absorbance of sample + EtOH solution.

Ascorbic acid was taken as a standard for preparation of standard curve with different concentrations (2.000,1.000, 0.500,0.250 and 0.125 μg/ mL).

Determination of Cytotoxicity by Hatching of Brine Shrimp Larvae

Dried cysts of *Artemia salina* (brine shrimp) were hydrated for 30 min in sterile distilled water and then cysts were suspended in 400 mL of sterile artificial sea water with salinity 0.33 ppt. A 60 watt lamp was positioned upon it to provide a direct light and warmth throughout the embryogenesis. Filtered air was passed through the cooled solution to reoxygenate the medium.

Free swimming nauplii started to appear after 12 h and most of the eggs became hatched into free swimming forms by 24 h. The nauplii were collected using a Pasteur pipette with a nozzle of at least 1 mm in diameter.

Sample solutions of Tawng Za Lat Ni flowers extract were prepared by dissolving 100 mg of flower extract in 100 mL of ethanol to obtain 1000 μg/mL and then it was serially diluted to obtain 500, 250, 125 and 62.5 μg/mL solutions.

Brine shrimp toxicity test was determined by the methods of Mayer *et al* (1982). Firstly, 1 mL each of the diluted extract solutions (test solution) was added to vials and thirty nauplii were collected with Pasteur pipette from the hatching container and were transferred to each vial carrying over the minimum amount of sea water. The vials with solvent and potassium dichromate solutions were also filled with thirty nauplii as controls.

The vials were restored in the dark room while the temperature was controlled at25 ± 1^{o}C. After 24 h incubation in the dark room, the vials were taken out for counting of nauplii. Nauplii were considered dead if they immobilized at the bottom of the vials. Counting of dead and alive nauplii in each vial was made to get LD_{50} for each flower ethanol extract (Sahgal *et al*., 2010). Based on the percentage of the mortality, the 50% lethality dose (LD_{50}) to the nauplii was determined by using the graph of mean percentage mortality versus the log of concentration.

Results and Discussion

Phytochemicals Present in *R. arboreum* (Tawng Za Lat Ni) Flower

The results of the phytochemical screening of *Rhododendro**n** arboreum* (Tawng Za Lat Ni) flowers are shown in Table 1. According to above table, flowers of Tawng Za Lat Ni contains alkaloids, tannins, flavonoids, terpenes, glycosides, phenolic compounds, polyphenols and reducing sugars

Table 1 Phytochemicals present in *R. arboreum* (Tawng Za Lat Ni) Flowers

No	Test	Reagent	Observation	Result
1	Alkaloids	(1) Wagner's reagent	Brown ppt	+
		(2) Dragendorff's reagent	Orange ppt	+
2	Tannins	10% $FeCl_3$,dil H_2SO_4	Yellow brown colour solution	+
3	Saponins	Distilled water	No froth like comb	-
4	Flavonoids	Conc: HCl, Mg turning,heat	Pink colour solution	+
5	Terpenes	$CHCl_3$, Acetic anhydride, conc: H_2SO_4	Deep pink colour solution	+
6	Glycosides	10% Lead acetate	White ppt	+
7	Steroids	Acetic anhydride, conc: H_2SO_4	No green colour solution	_
8	Phenolic compounds	10% $FeCl_3$	Greenish blue colour	+
9	Polyphenols	1% $FeCl_3$, 1% $K_3Fe(CN)_6$	Greenish blue colour	+
10	Reducing sugars	Benedict solution	Orange	+

(+) = present of constituent, (-) = absence of constituent

Elemental Analysis of *R. arboreum* (Tawng Za Lat Ni) Flowers by EDXRF Method

The relative abundance of some elements present in flowers of Tawng Za Lat Ni was analyzed by EDXRF method. The results obtained are listed in Table 2. According to the EDXRF report, there are eleven elements found in the flowers of Tawng Za Lat Ni. Among them, potassium is the most abundant element that is very suitable for human body that decreases the risk of stroke, lowers blood pressure, protects against loss of muscle mass, preserves bone mineral density and reduces the formation of kidney stones.

Antioxidant Activity of *R. arboreum* (Tawng Za Lat Ni) Flowers

The antioxidant activity of ethanolic extract of sample was determined by DPPH free radical scavenging assay. Ascorbic acid was used as standard and the result of IC_{50} value of the standard ascorbic acid (0.39 μg/mL) is shown in Table 3. According to Table 4 and Figure 2 it was found that the ethanolic extract scavenged DPPH radical . In DPPH screening assay that IC_{50} value of sample was found to be 4.57 μg/mL which was a little higher than that of standard ascorbic acid (IC_{50} 0.39 μg/mL). So, the sample extract has less antioxidant activity than the standard ascorbic acid. Tawng Za Lat Ni flowers contained phenolic compounds providing them the potential of scavenging free radicals. The sample has a suitable antioxidant activity for the treatment of cancer and hepatic diseases.

Table 2 Relative Abundance of Some Elements Present in Tawng Za Lat Ni Flowers

No	Elements	Symbols	Relative abundance (%)
1	Potassium	K	0.678
2	Silicon	Si	0.158
3	Phosphorus	P	0.109
4	Sulphur	S	0.105
5	Calcium	Ca	0.084
6	Iron	Fe	0.006
7	Manganese	Mn	0.004
8	Copper	Cu	0.002
9	Titanium	Ti	0.001
10	Zinc	Zn	0.001
11	Gold	Au	0.001

Table 3 Results of IC_{50} value of the standard Ascorbic Acid

Concentration (μg/mL)	Mean Absorbance	Mean % Inhibition	IC_{50} (μg/mL)
0.125	0.3593	41.21401	
0.250	0.3204	47.57853	
0.500	0.2871	53.02683	0.39
1.000	0.2541	58.42605	
2.000	0.2189	64.18521	

Table 4 Results of IC_{50} Value of the Tawng Za Lat Ni Flowers

Concentration (μg/mL)	Mean Absorbance	Mean % Inhibition	IC_{50} (μg/mL)
1.950	0.2250	45.21549	
3.900	0.2184	46.82250	
7.800	0.1908	53.54273	4.57
15.625	0.0951	76.84441	
31.250	0.0194	95.27636	

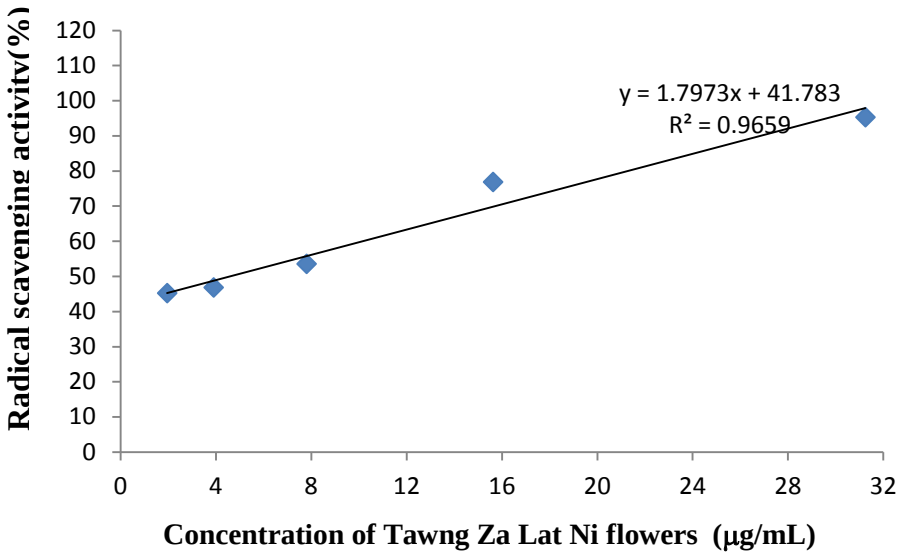

Figure 2 Plot of radical scavenging activity as a function of concentration of Tawng Za Lat Ni flowers

Toxicity Testing of the Tawng Za Lat Ni Flowers Using Brine Shrimp

Toxicity of the test samples was tested by using brine shrimp (*Artemia salina*) . Brine shrimp toxicity test results are shown in Table 5. Plotting of mortality percentage versus log of concentration of Taung Za Lat Ni flower extract demonstrates a linear correlation (Figure 3). Furthermore, there is a direct proportional relation between the concentration of the Taung Za Lat Ni flower extract and the degree of lethality (R^2 = 0.9917). LD_{50} value of Taung Za Lat Ni flower extract was calculated as > 1000 µg/mL. LD_{50} is the amount of a material, given all at once, which causes the death of 50% (one half) of a group of test animals (brine shrimp). The LD_{50} is one way to measure the short-term poisoning potential (acute toxicity) of a material. According to Meyer's toxicity index, the sample with LD_{50} < 1000 µg/mL are considered as toxic, while the sample with LD_{50} > 1000 µg/mL are considered as non-toxic (Meyer *et al*., 1982). Thus, Taung Za Lat Ni flower were found to be noncytotoxic in the brine shrimp bioassay so that they can be used for human consumption.

Table 5 Mortality Percentage of *R. arboreum* (Tawng Za Lat Ni) Flowers by Brine Shrimp Test

Concentration C (µg/mL)	Log C	Alive	Dead	Accumulated Alive	Accumulated Dead	Ratio/ Death: Total	Mortality (%)
1000	3	1	29	1	75	75 : 76	0.987
500	2.69897	13	17	14	46	46 : 60	0.767
250	2.39794	18	12	32	29	29 : 61	0.475
125	2.09691	20	10	52	17	17 : 69	0.246
62.5	1.79588	23	7	75	7	7 : 82	0.085

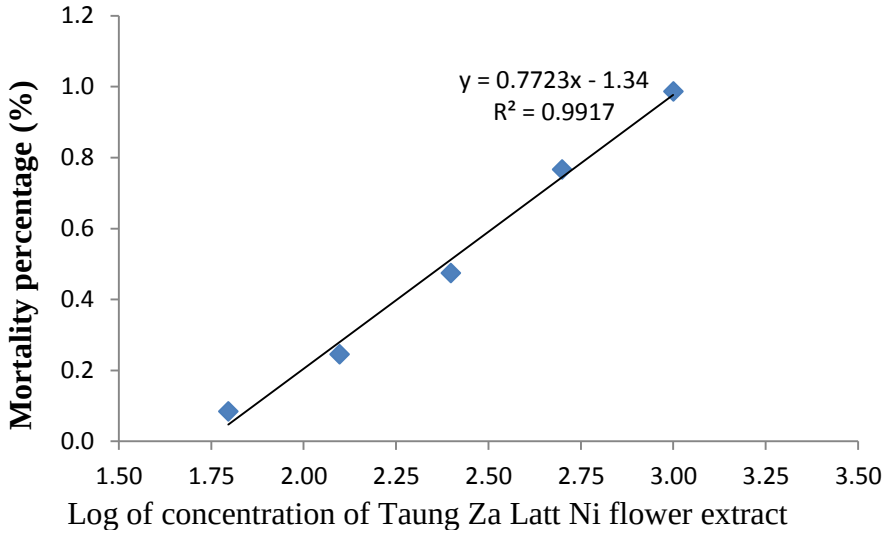

Figure 3 Plot of mortality percentage as a function of log concentration of Tawng Za Lat Ni flowers extract

Conclusion

In this research work, the phytochemical constituents of *R. arboreum* (Tawng Za Lat Ni) flower consists of secondary plant products such as alkaloids, tannins, flavonoids, terpenes, glycosides, phenolic compounds, polyphenols and reducing sugars by phytochemical assays. According to EDXRF report, there are eleven elements that are found in these sample flowers in which potassium constituent is the highest percentage among elements. IC_{50} value of Tawng Za Lat Ni flower is 4.57 μg/mL and thus, it has less antioxidant activity than the standard ascorbic acid (IC_{50} =μg/mL). However, it has a moderate amount of antioxidant activity. Brine shrimp assay showed that *R. arboretum* (Tawng Za Lat Ni) flower was noncytotoxic. *Rhododendron* flowers have a number of health benefits and have full potency to be utilized in the food and beverage industry.

Acknowledgements

We would like to acknowledge to the Ministry of Education for the research funding of our group as well as we also send great thanks to our principal, Dr Thant Zaw Oo who provide research needs and encourage our group to carry out this research. We also send a gratitude to Dr Nanda Kyaw Thu, lecturer at the Department of Botany, Mandalay University for his kind help for the classification of Tawng Za Lat flower.

References

Bhattacharyya, D. (2011**).** "Rhododendron Species and Their Uses with Special Reference to Himalayas- A Review". *Assam University Journal of Science & Technology: Biological and Environmental Sciences*. vol. 7 (1), pp. 161–167

Evans, W.C.(1966) . *Trease Evans Pharmacognosy*. London: 14th Ed, WB Saunders Ltd, pp.119- 159

Healing Base. (2011). *The Use of Metals and Minerals in Ayurvedic and Siddha Medicine.* www.healingbase.com/the-use-of-metals-minerals-in. (Accessed 28 July 2019)

Marinova, G. and Batchvarov, V. (2011). "Evaluation of the Methods for Determination of the Free Radical Scavenging Activity by DPPH". *Bulgarian Journal of Agricultural Science*, 17 (1) , pp.11-24

Meyer, B. N., Ferrigni, N. R., Putman, J. E., Jacbsen, L. B., Nicols, D. E. and McLaughlin, J. L. (1982) . "Brine Shrimp : A Convenient General Bioassay For Active Plant Constituents**".** *Plant Medica*., vol. 45, pp. 31- 34

Ong, H.G., Ling, S.M., Win, T.T.M., Kang, D.H., Lee, J.H. and Kim,Y.D.(2018). "Ethnobotany of Wild

Medicinal Plants Used by the Müün Ethnic People: A Quantitative Survey in Southern Chin State, Myanmar". *Journal of herbal medicine*, vol. 13, pp. 91-96

Petrovska, B.B.(2012). "Historical Review of Medicinal Plants' Usage". *Pharmacogn Rev.* , vol.,6(11), pp. 1–5

Popescu, R. and Kopp, B. (May 2013). "The Genus Rhododendron: An Ethnopharmacological and Toxicological Review". *J Ethnopharmacol.*, vol.147 (1), pp. 42–62

Sahgal, G., Ramanathan, S. , Sasidlharan, S. M., Mordi, S., Ismail, S. and Mansor, S. M. (2010). "Brine Shrimp Lethality and Acute Oral Toxicity Studies on *Swietenia mahagoni* (Linn.) Jacq. Seed Methanolic Extract". *Pharmacognosy Research*, vol. 2, pp. 215-220

Still, J.(2003). "Use of Animal Products in Traditional Chinese Medicine: Environmental Impact and Health Hazards". *Complement Ther Med*., vol.11(2), pp.118-122

Turner Jr., R.J. and Wasson, E. (1997). *Botanica: The Illustrated A-Z of Over 10,000 Garden Plants and How to Cultivate Them.* USA: 1st ed., Better World Books, p. 742

STUDY ON NUTRITIONAL VALUES, TOTAL PHENOLIC AND FLAVONOID CONTENTS AND EVALUATION OF ANTIMICROBIAL AND ANTIOXIDANT ACTIVITIES OF ETHANOLIC EXTRACT OF FRUITS OF *Trapa natans* L. (Kywe-gaung-thee)

Aye Mon Thida Nyo[1], Arnt Win[2], Mar Pi Myint[3] and Khon Nam[4]

Abstract

In this research work, the fruits of *Trapa natans* L., Myanmar name Kywe-gaung-thee were selected for determination of some nutritional values, minerals contents, total phenolic content, total flavonoid content, antimicrobial activity and antioxidant activity. The fruits of *T. natans* (Kywe-gaung-thee) were collected from Pathein-gyi Township, Mandalay Region, Myanmar. Firstly, some nutritional values of fruits of *T. natans* such as moisture, ash, pH, protein, fiber and fat were determined by AOAC method. The mineral contents were also determined by EDXRF technique. Moreover, the total phenolic content of fresh fruit of *T. natans* was measured by Folin – Ciocalteau reagent and total flavonoid content was measured by $AlCl_3$ method with UV visible spectrophotometer. Furthermore, the antimicrobial activities of three solvent extracts of selected sample were tested by agar well diffusion method on six microorganisms such as *Bacillus subtilis, Staphylococcus aureus, Pseudomonas aeruginosa, Bacillus pumilus, Candida albicans* and *E.coli*. In addition, the antioxidant activity of the ethanolic extract of selected sample was evaluated by DPPH (1,1- diphenyl-2- picryl hydrazyl) assay method.

Keywords - *Trapa natans* L., nutritional values, total phenolic content, total flavonoid content, antimicrobial activity, antioxidant activity

Introduction

Trapa natans L. is commonly known as "Water Chestnut". Water chestnut is one of the most popular vegetables used in Asia, due to its special feature and medicinal values which, it is found in Taiwan, China and parts of South East Asia (Chandana *et al.*, 2013). *T. natans* is an aquatic floating herb which belongs to the family Lythraceae. It has flaxuose stem, ascending in the water; the submerged parts are furnished with numerous opposite pairs of green root-like spreading pectin ate organs. Leaves are alternate, crowed on the upper part of the stem, 3.8-5 cm long. Flowers are few, auxiliary, solitary, pure white (Adkar *et al.*, 2014).

The fruit is covered with a thick jet black outer cover shaped like a horn protruding from the head of the buffalo. The outer cover is hard, making it quite difficult to peel off to obtain the white meat (edible portion) inside (Gani *et al*., 2015). It contains some vitamins like thiamine, riboflavin, nicotinic acid, vitamin C, vitamin A, D-amylase and considerable amount of phosphorylases. The water chestnut is used in many Ayurvedic preparations as nutrient, appetizer, astringent, diuretic, aphrodisiac, tonic, cooling and anti-diarrheal agent. It is also useful in lumbago sore throat, bilious affections, bronchitis, fatigue and inflammation. The whole herb has been reported for hepatoprotective activity, antimicrobial activity, antibacterial activity, antitumor activity, antioxidant activity and free radical scavenging activity (Chandana *et al*., 2013).

1. Dr, Associate Professor, Department of Chemistry, University of Mandalay
2. Associate Professor, Department of Chemistry, Kyaukse University
3. Assistant Lecturer, Department of Chemistry, University of Mandalay
4. M Sc Candidate, Department of Chemistry, University of Mandalay

In addition to this, the juice of the fruit has been used for diarrhea and dysentery. It is also said to have cancer-preventing properties. The antibiotic and antioxidant properties are important attributed to *T. natans* as a medicinal plant (Aidew, L. and Buragohain, A. K., 2014).

Fruits of *T. natans* are important sources of polyphenolic antioxidants that have high free radical scavenging properties being associated with protective effects against coronary heart disease, cancer diseases, neurodegenerative diseases and osteoporosis (Roni *et al*., 2016).

In this research work, the fruits of *T. natans* (Kywe-gaung-thee) were selected for determination of nutritional values, mineral contents, total phenolic content, total flavonoid content, antimicrobial activity and antioxidant activity.

Botanical Description of *Trapa natans* L.

(a) (b) (c)

Figure 1 (a) Plant, (b) flower and (c) fruits of *Trapa natans* L.

Family name	:	Lythraceae (Loosetrife family)
Genus	:	*Trapa*
Species	:	*natans*
Scientific name	:	*Trapa natans* L.
Myanmar name	:	Kywe-gaung-thee
English name	:	Water Chestnut, Water Caltrop (Takano, A. and Kadono, Y., 2005)
Part used	:	Fruit
Medicinal uses	:	Tonic, debility, emaciation, asthma, cracked heels, diarrhea, dysentery, bilious affections, piles, leucorrhoea and menorrhagia. (Sofowora, A., 1993)

Material and Methods

Sample Collection

Trapa natans L. fruits were collected from Pathein-gyi Township, Mandalay Region, Myanmar. Fresh fruits were washed thoroughly under running tap water, and fruit coat was removed. The fleshy, white edible part was gently rinsed with distilled water. After then, the sample was crushed with mortar and pestle into pieces.

Determination of Nutritional Values of Fruits of *T. natans*

Nutritional values of *T. natans* were measured by AOAC (Association of Official Analytical Chemists) method.

Determination of Mineral Contents from Fruits of *T. natans*

Mineral contents in fruits of *T. natans* were determined by EDXRF method, at the Department of Chemistry, Monywa University.

Quantitative Determination of Total Phenolic and Flavonoid Content of *T. natans*
Preparation of fresh fruit juice solution of *T. natans*

The fresh fruit sample (100 g) was blended. The blended sample was homogenized with about 350 mL of distilled water. 393 mL of sample solution were obtained. Then the solution was filtered and the filtrate was centrifuged two times and the clear solution was used for the measurement of total phenolic and flavonoid content.

Preparation of standard gallic acid stock solution

10 mg of the standard gallic acid was taken in a test tube. 10 mL of distilled water was added to the standard compound. 1 mL of this standard solution was taken in another test tube. The volume of this solution was made up to 10 mL with distilled water (Slinkard and Singleton, 1977).

Construction of calibration curve of standard gallic acid

The prepared gallic acid solution was taken by micro pipette into a series of test tubes 20 μL, 40 μL, 60 μL, 80 μL and 100 μL, respectively. The volume was made up to 1.6 mL with distilled water in each tube. And then 100 μL of Folin - Ciocalteau reagent and 300 μL of saturated Na_2CO_3 (20 %) solution were added. After each standard solution was heated in the water bath at 40 ºC for 30 min and then cooled at room temperature. The absorbance values of prepared standard gallic acid solutions were measured by UV visible spectrophotometer at 765 nm with respect to the blank solution. The calibration curve for standard gallic acid is shown in Figure 4.

Determination of total phenolic content of *T. natans*

The total phenolic content of fresh fruit juice was measured by using the Folin-Ciocalteau method. Firstly, 40 μL of expressed juice was taken in a test tube. It was made up to 1.6 mL with distilled water. 100 μL of Folin-Ciocalteau reagent was mixed and then 300 μL of saturated Na_2CO_3 (20 %) solution was added.

The mixture was heated in a water bath at 40 °C for 30 min and then cooled at room temperature. The absorbance of this prepared sample solution was measured at 765 nm using a UV spectrophotometer. The assay was carried out in triplicate. The results are shown in Table 4. The total phenolic content of *T. natans* juice was expressed as mg gallic acid equivalent per 100 g fresh weight (Slinkard and Singleton, 1977).

Construction of calibration curve of standard quercetin

10 mg of the standard quercetin was taken in a test tube. 100 mL of MeOH was added to the standard compound. The stock solution was obtained. It was diluted with MeOH in various ratios to obtain four different of concentrations, such as 25 μg/mL, 50 μg/mL, 75 μg/mL, and 100 μg/mL respectively. Then, 4.0 mL of solution was prepared for each concentration. 0.5 mL of each standard quercetin solution was taken in 5 mL test tube and 1.5 mL methanol, 0.1 mL of

10 % aluminium chloride, 0.1 mL of 1 M potassium acetate and 2.8 mL distilled water were added separately to each tube.

These tubes were left at room temperature for 30 min after which the absorbance of the reaction mixture was measured at 415 nm with UV/ Visible spectrophotometer. The calibration curve was plotted by using the resulted absorbance data of standard quercetin solutions at concentrations 25 μg/ mL to 100 μg/ mL in methanol.

Determination of total flavonoid content of *T. natans*

The total flavonoid content of fresh fruit juice was measured by aluminium chloride ($AlCl_3$) method using quercetin as a standard. Firstly, 0.5 mL of fresh fruits juice was taken in test tube and 0.1 mL of 10 % aluminium chloride, 0.1 mL of 1M potassium acetate and 4.3 mL distilled water were added into it. This tube was left at room temperature for 30 min after which the absorbance of the reaction mixture was measured at 415 nm with UV/Visible spectrophotometer. The assay was performed in triplicate. The results are shown in Table 4. The total flavonoid content of fresh fruit juice was expressed as mg quercetin equivalent (QE)/100g fresh weight (Bag *et al*., 2015).

Determination of Antimicrobial Activities of Fruits of *T. natans*

Antimicrobial activities of various solvent extracts of *T. natans* were investigated by employing agar well diffusion method at Pharmaceutical Research Department (PRD) in Yangon. The solvents used were n-hexane, ethyl acetate and ethanol. Tested organisms are *Bacillus subtilis, Staphylococcus aureus, Pseudomonas aeruginosa, Bacillus pumilus, Candida albicans* and *E. coli.*

Determination of Antioxidant Activity of Ethanol Extract of Fruits of *T. natans*

The antioxidant activity of ethanol extract of fruits of *T. natans* (Kywe-Gaung-Thee) was determined by DPPH (1, 1- Diphenyl - 2 -picryl - hydrazyl) Radical Scavenging Assay method.

Sample solution was prepared by thoroughly mixing 2 mL of 60 μM DPPH solution and 2 mL of test sample solution. The solution was then allowed to stand at room temperature for 15 min. Control solution was prepared by mixing 1.5 mL of 60 μM DPPH solution and 1.5 mL of 95 % ethanol. The solution was then allowed to stand at room temperature for 15 minutes. Blank solution was prepared by mixing 1.5 mL of test sample solution and 1.5 mL of 95 % ethanol. The solution was then allowed to stand at room temperature for 15 min. Absorbance values of these solutions were measured at 517 nm by using UV-visible spectrophotometer. Experiment was done in triplicate for the ethanol extract of fruits of *T. natans.* Percent inhibition was calculated by using the following equation.

$$\% \text{ inhibition} = \frac{\text{DPPH}_{\text{alone}} - (\text{Sample} - \text{Blank})}{\text{DPPH}_{\text{alone}}} \times 100$$

Where, % inhibition = percent inhibition of test sample
DPPH alone = absorbance of DPPH solution
Sample = absorbance of sample solution
Blank = absorbance of blank solution

Finally, IC_{50} (50 % inhibition concentration) was determined by using liner regressive excel program. Ascorbic acid was used a standard for comparison purpose.

Results and Discussion

In this section, the results obtained from the experimental works such as nutritional values, mineral contents, total phenolic content, total flavonoid content, antimicrobial activity and antioxidant activity of the fruits of *T. natans* are discussed.

Nutritional Values of Fruits of *T. natans*

Some nutritional compositions of *T. natans* such as moisture, ash, pH, fat, fiber and protein content were determined by AOAC method and observed data are listed in Table 1.

Table 1 Results of Nutritional Values of Fruits of *T. natans*

No.	Parameter	Observed data	Analytical method	Apparatus used
1	Moisture (%)	5.3	Gravimetric method	Temperature controlled oven
2	Ash (%)	1.7	Loss of weight in ignition	Temperature controlled oven, Muffle furnace
3	pH	6.8	-	pH meter
4	Fat (%)	2.1	Petroleum ether extraction	Soxhlet extractor (SOX-412)
5	Fiber (%)	2.3	Enzymatic gravimetric method	Autocleaved and microwave heated
6	Protein (%)	1.24	Macro kjeldahl method	Protein analyzer

According to this table, the results obtained in nutritional values are moisture 5.3 %, ash 1.7 %, pH - 6.8, fat 2.1 %, fiber 2.3 % and protein 1.24 %. All of the resulting data were obtained by triplicate measurements. Mean value was described for each.

Mineral Contents in Fruits of *T. natans*

Figure 2 and Table 2 shows that potassium was the highest amount in the sample. Decreasing order of mineral content is K > P > S > Si > Ca > Fe > Cu > Mn > Zn. Therefore fruits of *T. natans* contain the essential minerals for human health. There is no toxic material contained in the selected sample.

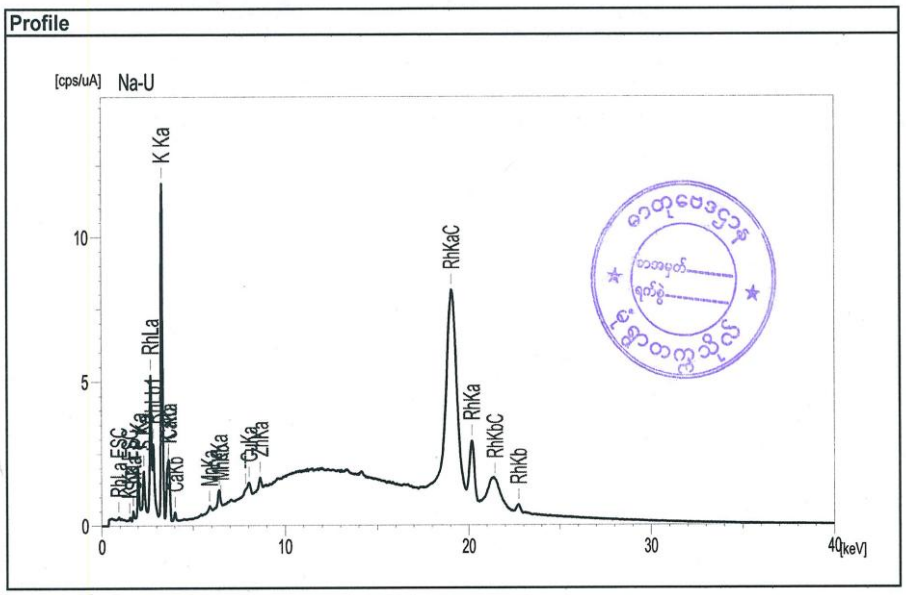

Figure 2 EDXRF spectrum of dried fruits of *T. natans*

Table 2 The Results of Mineral Contents in Fruits of *T. natans*

No.	Elements	Symbols	Relative Abundances (%)
1.	Potassium	K	0.672
2.	Phosphorus	P	0.308
3.	Sulphur	S	0.143
4.	Silicon	Si	0.114
5.	Calcium	Ca	0.068
6.	Iron	Fe	0.003
7.	Copper	Cu	0.002
8.	Manganese	Mn	0.002
9.	Zinc	Zn	0.001

Total Phenolic Content of Fruits of *T. natans*

Determination of total phenolic content was carried out by Folin-Ciocalteau reagent by using UV spectrophotometer at 765 nm.

The standard gallic acid solutions at concentration 2 to 10 μg/mL in distilled water were measured to know their absorbance by PD-303 UV visible spectrophotometer. The calibration curve was plotted against by using the resulting data of standard gallic acid solution as shown in Figure 4.

The total phenolic content was determined by Folin-Ciocalteau reagent using spectrophotometer. The total phenolic content of fruits of *T. natans* was calculated from the standard curve prepared from different concentrations of gallic acid in which the simple spectrophotometric procedure was followed for the working standard. The total phenolic content of fruits of *T. natans* was found to be 70.24 ± 1.68 mg/100 g fresh weight.

Total Flavonoid Content in *T. natans*

The calibration curve was plotted against by using the resulting data of standard quercetin solution as shown in Figure 5. The results of total flavonoid content are described in Table 4.

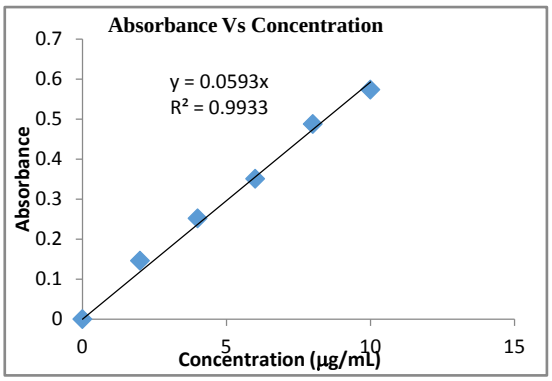

Figure 4 Absorbance Vs concentration curve for standard gallic acid solution

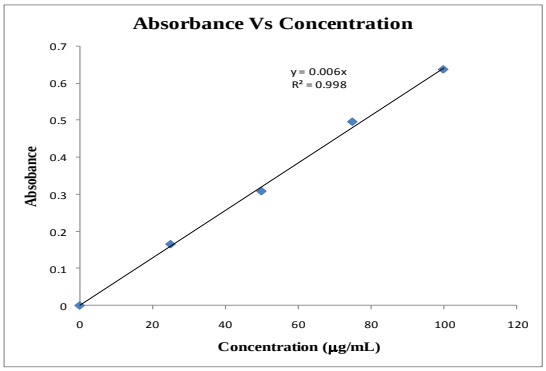

Figure 5 Absorbance Vs concentration curve for standard quercetin solution

Table 3 The Total Phenolic and Flavonoid Contents of Fruits of *T. natans*

Name of Sample	Phenolic Content (mg/100g) Mean ± Standard Deviation	Flavonoid Content (mg/100g) Mean ± Standard Deviation
Fresh Fruits of *Trapa natans* L.	70.24 ± 1.68	13.04 ± 0.19

In accordance with these results, the total phenolic and flavonoid content of these fresh fruit solutions were found to be 70.24 ± 1.68 mg/100 g and 13.04 ± 0.19 mg/100 g fresh weight respectively.

Antimicrobial Activities of Fruit of *T. natans*

Antimicrobial activities of the fruit of *T. natans* (Kywe-gaung-thee) were tested by agar well diffusion methods on six selected organisms (Figure 4). The results are shown in Table 4.

Table 4 Results of Antimicrobial Activities of Fruit of *T. natans*

Extracts	Diameter of Inhibition Zone (mm)					
	I	II	III	IV	V	VI
n-hexane	13 (+)	13 (+)	12 (+)	14 (+)	13 (+)	14 (+)
EtOAc	15 (++)	25 (+++)	28 (+++)	25 (+++)	22 (+++)	26 (+++)
EtOH	20 (+++)	17 (++)	16 (++)	17 (++)	17 (++)	15 (++)

Agar well – 10 mm
10 mm ~ 14 mm (+)
15 mm ~ 19 mm (++)
20 mm above (+++)

Micro-organisms
I = *Bacillus subtilis*
II = *Staphylococcus aureus*
III = *Pseudomonas aeruginosa*
IV = *Bacillus pumilus*
V = *Candida albicans*
VI = *E. coli*

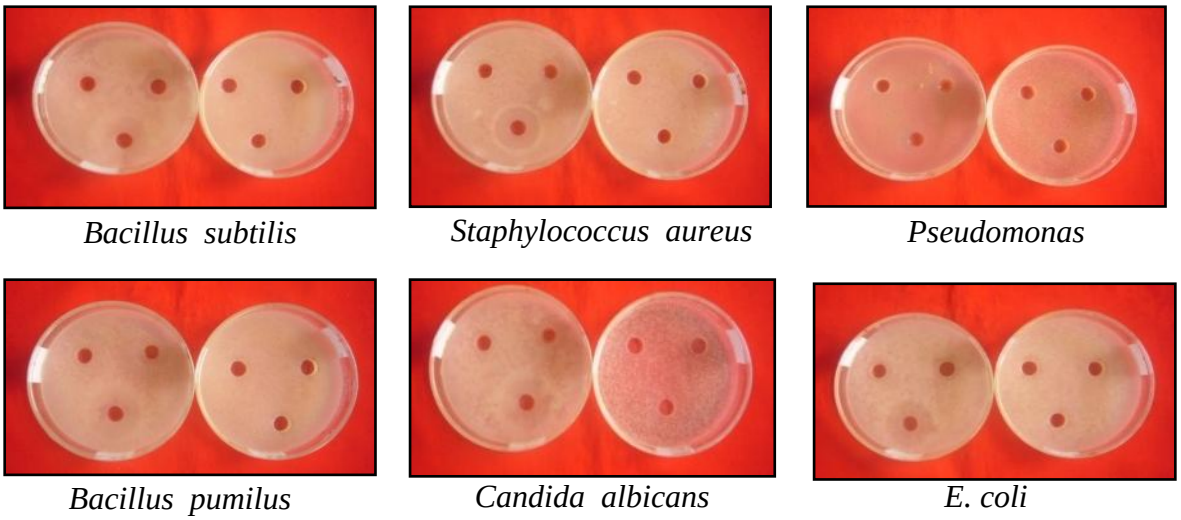

Figure 3 Antimicrobial activities of various solvents (n-hexane, ethanol, ethylacetate) extracts of *T. natans* and control solutions

According to these results, ethanol extract of fruit of *T. naptans* responds high activity on *Bacillus subtilis* and medium activities on remaining five organisms and ethylacetate extract gives high activities on all tested organisms except *Bacillus subtilis*. n-Hexane extract of selected sample has low activities on all tested organisms. Therefore, polar solvent extracts of *T. naptans* responds more antimicrobial activities than non-polar solvent extract.

Antioxidant Activity of Fruits of *T. natans*

The result of antioxidant activity using DPPH assay in standard ascorbic acid is shown in Table 5 and Figure 6. IC_{50} value was calculated by using linear regressive equation.

Table 5 Percent Oxidative Inhibition of Various Concentration of Standard Ascorbic Acid

Ascorbic acid concentration (µg/mL)	% inhibition	IC_{50} (µg/mL)
50	89.936	
25	64.103	
12.5	53.840	11.98
6.25	45.350	
3.125	36.378	

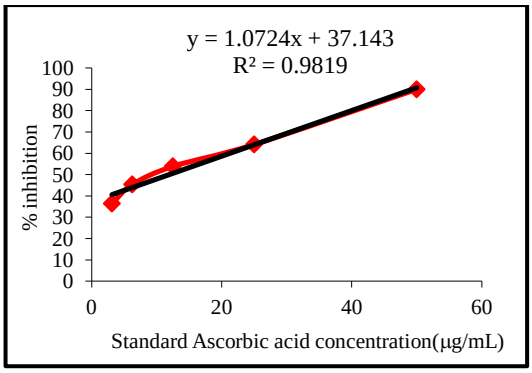

Figure 6 % Inhibition Vs different concentration of standard ascorbic acid

The antioxidant activity of ethanolic extract of the fruit of *T. natans* is shown in Table 6 and Figure 7. IC_{50} value of selected sample was also calculated by using linear regressive equation.

Table 6 Percent Oxidative Inhibition and IC_{50} Value of *T. natans*

Sample concentration (μg/mL)	% inhibition	IC_{50} (μg/mL)
100	58.228	62.80
50	48.101	
25	42.025	
12.5	38.734	
6.25	33.418	

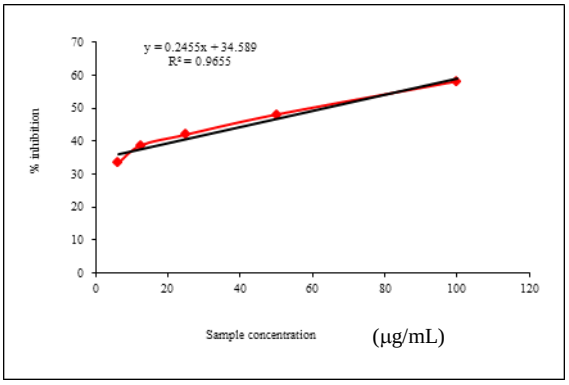

Figure 7 % Inhibition Vs different concentration of sample solution

The IC_{50} values of ethanolic extract of fruit of *T. natans* is 62.80 μg/mL which gives significant activity compared to standard ascorbic acid, IC_{50} 11.98 μg/mL.

Conclusion

In this research work, the edible parts of the fruits of *T. natans* (Water chestnut), Myanmar named Kywe-gaung-thee were selected for chemical investigations. According to the results of present studies, the fruits of *T. natans* were found to contain good nutritional values, nontoxic mineral contents and high antimicrobial activities. Especially, the fruit of *T. natans* was found to be the rich source of phenolic compounds which support the preventing cancer and other serious diseases. The relative property of phenolic compounds is antioxidant activity. Hence, the ethanolic extract of *T. natans* gave significant antioxidant activity compared to the standard ascorbic acid. The fruit of *T. natans* is not popular fruit in Myanmar. But it has very good potency for human health. Moreover, it is cheaper than other popular fruits. Therefore, the fruit of *T. natans* should be edible for health.

Acknowledgements

We are extremely grateful to Dr Thida Win, Rector, University of Mandalay and Professor Dr Yee Yee Myint, Head of Department of Chemistry, University of Mandalay, Myanmar for their permitting, understanding, kind helps and good guidance on our research studies. We also thank to Dr Than Than Aye, Professor and Head (Rtd.) and Dr Kyae Mon Lwin, Professor, Head of Department of Chemistry, Kyaukse University for their permitting and supporting the some research facilities throughout our research works.

References

Adkar, P., Dongare, A., Ambavade, S., and Bhaskar, V. H. (2014). "*Trapa bispinosa Roxb*: A Review on Nutritional and Pharmacogical Aspects", pp. 1-13.

Aidew, L. and Buragohain, A. K. (2014). "Antimycobacterial and Antioxidant Activities of the Fruits of *Trapa natans* L. var. *Bispinosa* Reveal its Therapeutic Potential". *AJPCT*, vol.2 (10), pp. 1234-1245

AOAC (2000). "Official Methods of Analysis".17th Edition, The Association of Official Analytical Chemists, USA. Methods 925.10, 65.17, 974.24, 992.16.

Bag, G. C., Grihanjali, D. P. and Bhaigyabati, T. (2015). "Assessment of Total Flavonoid Content and Antioxidant Activity of Methanolic Rhizome Extract of Three Hedychium Species of Manipur Valley*". Int. J. Pharm. Sci. Rev. Res*., vol. 30 (1), pp. 154-159

Chandana, M., Rupa, M. and Chakraborthy, G. S. (2013). "A Review on Potential of Plants Under Trapa species" *IJRPC*, vol. 3, (2), pp. 502-508

Gani, A., Rasool N., Shah, A., Ahmad, M., Gani, A., Wani, T. A., Wani, I. A. , Wani, S. M. and Masoodi, F. A. (2015). "DNA Scission Inhibition, Antioxidant, and Antiproliferative activities of Water Chestnut (*Trapa natans*) Extracted in Different Solvents". *CyTA-Journal of Food*, vol. 13, (3), pp. 415-417

Roni, B., Verma, D., Bhati, I., Chharang, H. and Mahoshwari, R. K. (2016). "Health Benefits of Scrumptious Water Chestnuts / Water Caltrop (*Trapa natans* L.)". *Int. Arch. App. Sci. Technol (IAASCA*); vol. 7 (3), pp. 32 - 35.

Slinkard, K. and Singleton, V. L. (1977). "Total Phenol Analysis: Automation and Comparison with Manual Methods". *American Journal of Enology and Viticulture*, vol.28, pp. 49-55.

Sofowora, A. (1993). " Medicinal Plants and Traditional Medicine in Africa", New York, John Wiley and Sons Limited, vol. 2, pp. 96-106.

Takano, A. and Kadono, Y. (2005). "Allozyme Variations and Classification of *Trapa* (Trapaceae) in Japan". *Aquat Bot*, vol.33, pp. 108-118.

PHENOLIC CONTENT, ANTIOXIDANT AND ANTITUMOUR ACTIVITIES AND ISOLATION OF A PHENOLIC COMPOUND FROM THE BARK OF *ALSTONIA SCHOLARIS* L. (TAUNG-MA-YO)

Khin Maw Maw[1], Swe Zin Myint[2], Saw Hla Myint[3]

Abstract

The present work focused on the determination of total phenol content, antioxidant activity and screening of anti-tumour activity of some crude extracts of the bark of *Alstonia scholaris* L. (Taung-ma-yo). Moreover, the research deals with the isolation of a phenolic compound by column chromatography and identification of the isolated compound by UV and FT IR. The total phenol contents of crude extracts of 70 % ethanol (99.33 μg GAE/mg) and water (61.5 μg GAE/mg) were determined by spectrometric Folin-Ciocalteu reagent (FCR) method .The antioxidant activity of 70 % ethanol extract (IC_{50} value of 27.75 μg/mL) and water extract (IC_{50} value of 90.56 μg/mL) of the bark sample was determined by DPPH assay method. Preliminary screening of anti-tumour activity of crude extracts of ethyl acetate, 70 % ethanol and water was carried out by Potato Crown Gall test. It was observed that, of the three doses, i.e., 0.05, 0.1 and 0.15 g/disc each extract tested, the minimum dose showing activity was 0.15 g for ethyl acetate extract and 0.05 g for 70 % ethanol extract on day 5. On day 7, tumours appeared for the ethyl acetate extract but not for the 70 % ethanol extract as observed under microscope and by staining with iodine solution. Column chromatographic separation of ethyl acetate extract by gradient elution with pet ether, ethyl acetate and methanol yielded a compound (A_1) having R_f value of 0.45 on silica gel layer with pet ether : ethyl acetate (2.5 : 7.5, v/v). UV spectra of isolated compound (A_1) showed that it was to be a phenolic compound by alkaline red shift and also supported by FT IR spectrum.

Keywords *: Alstonia scholaris* L., phenol content, anti-oxidant activity, anti-tumour activity

Introduction

Herbal medicine contains natural substances that can promote health and reduce illness. There are many herbs, which are used to treat cardiovascular problems, liver disorders, central nervous system, digestive and metabolic disorder. The plant, *Alstonia scholaris* L., invites attention of the researcher worldwide for its pharmacological activities ranging from antimalarial to anticancer activities (Bhanu *et al*., 2013).

A.scholaris (Taung-ma-yo) belonging to family Apocynaceae, is a medium to large tree. It has wide occurrence in the Asia Pacific region from India, Srililanka, through mainland South East Asia and Southern China, throughout Malaysia to Northern Austria and Salomon island (Anubha and Yashwant, 2015). *A. scholaris* contains some of the important alkaloids such as echitamine, tubotaiwine, akuammicine, echitamidine, picrinine (Kalaria *et al*., 2012). The bark of the *A. scholaris* is used in Ayurvedic medicine to treat fever, malaria, troubles in digestion, tumors, ulcers, asthma and so forth.

Some biological properties of *A.scholaris* such as antimicrobial, antidiarrheal, antimalarial, anticancer, and antioxidant activities have been studied (Baliga, 2010). The present study was performed to investigate phenolic content, antioxidant and antitumour activities from bark of *A. scholaris*. The presence of alkaloids, phenolic compounds and flavonoids have also

[1] Lecturer, 1 PhD, Department of Chemistry, Dagon University
[2] Dr, Lecturer, Department of Chemistry, Dagon University
[3] Dr, Part time Professor, University of Yangon

been reported by many workers. A phenolic compound was also isolated and characterized especially in this study.

The report may be divided into five portions, (i) preparation of different crude extracts (ii) determination of phenolic content (iii) investigation of antioxidant activity and antitumour activity (iv) isolation of compounds (v) identification of an isolated compound.

Materials and Methods

Collection and Preparation of Plant material

The bark of *Alstonia scholaris* L. was collected from Kamayut Township, Yangon Region. The bark samples were transformed into powder and stored in air-tight container.

Preparation of Crude Extracts

The dried powdered sample (50 g) was percolated in 70 % ethanol about 3 days. After 70 % ethanol extract was filtered, again percolated and filtered in this solvent, until the extracted sample become faint.

The collected filtrates (70 % ethanol extract) obtained were concentrated by rotatory evaporator to get concentrated 70 % ethanol residue. Some ethanol extract was used to determine the activities. The other ethanol extract was then partitioned with ethyl acetate about five times. Resultant ethyl acetate extracts were concentrated and used to isolate some compounds.

Some dried powdered sample was also extracted in warm water and boiled in water bath for one hour. After boiling, water extract was filtered and dried. Watery extract were used to detect some activities.

Preliminary Phytochemical Test

A few grams of dried bark powder of *A. scholaris* was subject to the tests of alkaloids, α-amino acids, carbohydrates, flavonoids, glycosides, phenolic compounds, reducing sugars, saponins, starch, steroid, tennis and terpenoids according to the standard procedures (Marini-Bettolo *et al*.,1981).

Preparation of Solution and Determination of Total Phenol Content

The amount of total phenolics in ethanol and water extracts was determined by the spectrometric Folin-Ciocalteu reagent method. Gallic acid was used as a standard and the total phenolics were expressed as μg/mL gallic acid equivalents. For this purpose, the calibration curve of gallic acid was drawn (Figure 1).Standard solution having concentrations (3.125, 6.25, 12.5, 25, 50, 100 μg/mL) of gallic acid were prepared. The sample solutions (70 % EtOH and water extract) were also prepared by dissolving 10 mg of crude extracts in 10 mL of ethanol. Each sample (1 mL) was introduced into test tube and mixed with 5 mL of a 10 fold dilute Folin-Ciocalteu reagent and incubated for about 5 min. To each test tube, 4 mL of 1 M sodium carbonate was added and the test tubes were kept at room temperature for 2 h. Absorbance of standard solution and sample solutions was measured at λ_{max} 765nm (Vance *et al*., 2003).

Screening of Antioxidant activity

DPPH (1,1-diphenyl-2-picryl-hydrazyl) radical scavenging assay was chosen to assess the antioxidant activity of plant materials. This assay has been widely used to evaluate the free radical scavenging effectiveness of various flavonoids and polyphenol in food systems (Lee and Shinbamoto, 2001 ; Thaw Thaw Zin, 2016).

Different concentrations (3.125, 6.25, 12.5, 25, 50, 100 and 200 μg/mL) of Standard Ascorbic Acid solution and sample (crude extracts of 70% ethanol and water) solutions were prepared. The concentrations of the solutions were serially diluted with appropriate amount of ethanol. DPPH (0.002 %) solution was also prepared by dissolving DPPH (0.002 g) in 100 mL ethanol.

The control solution was prepared by mixing 1.5 mL of 0.002 % DPPH solution and 1.5 mL of 95 % ethanol using vortex mixer. The sample solutions and standard solution were also prepared by mixing thoroughly 1.5 mL of 0.002 % DPPH solution and 1.5 mL for each concentration of test sample solutions and standard solution respectively. The solutions were allowed to stand at room temperature for 30 min. After 30 min, the absorbance of these solutions was measured at 517 nm by using UV spectrophotometer. Absorbance measurements were done in triplicate for each solution and then mean values so obtained were used to calculate percent inhibition of oxidation by the following equation (Tomoko, 1998).

$$\text{Percent Inhibition} = \frac{A_{control}(A_{sample} - A_{blank})}{A_{control}} \text{ x } 100\,\%$$

Preliminary Screening of Anti-tumour Activity

The antitumour activity screening of different crudes such as ethyl acetate, 70 % ethanol, and watery extracts of bark of *A. scholaris* was carried out against *Agrobacterium tumefacien* by Potato Crown Gall test of Potato Disc Assay method at the Pharmaceutical Research Department Ministry of Industry, Yangon, Myanmar. Fresh, disease free potato tubers were obtained from local market and transferred within 48 h to the laboratory. Tubers of moderate sizes were surface-sterilized by immersion in 50 % sodium hydrochlorite (Clorox) for 20 min. The ends were removed and soaked for 10 min in Clorox. A core of the tissue was extracted from each tuber by using surface-sterilized (ethanol and flame) 1.5 cm wide cork borer. And, 2 cm pieces were removed from each end and discarded and the remainder of the cylinder is cut into 0.5 cm thick discs with a surface-sterilized cutter. The discs were then transferred to 1.5 % agar plates (1.5 g of petri dish). Each plate contained three discs. The procedure was done in the clean bench in the sterile room, 50 mL, 100 mL and 150 mL of this solution of each extract was separately dissolved in 2 mL of dimethyl sulphoxide (DMSO); the solution was filtered through Millipore filters into a sterile tube 0.5 mL of this solution was added to 1.5 mL of sterile distilled water and 2 mL of broth culture of *A. tumefaciens* strain (48 h culture containin 3.5×10^9 cells/mL) were added aseptically. Controls were made as mentioned above procedure.

Using a sterile disposable pipette, 1 drop (0.05 mL) from these tubes was used to inoculate each potato disc, spreading it over the disc surface. The process of cutting the potatoes and incubation must be conducted within 30 min. the plates were sealed with tape to minimize moisture loss and incubated at room temperature for 12 days. After incubation, Lugol's solution (I_2-KI) was added and the tumors were counted with a microscope and compared with control.

The antitumor activity was examined by observation of tumor produced or not within 5 days and 7 days (Priestman and Edwards, 1953).

Extraction and Isolation of Bioactive Compound

The crude extracts from the bark of *A. scholaris* were obtained by percolating with 70 % ethanol and then further partitioning with ethyl acetate.

For the clear separation of bioactive compounds from the ethyl acetate extract was done by thin layer chromatography, different ratios of pet ether and ethyl acetate solvent systems were used. The visualization of separated constituents was examined under UV_{254} and UV_{365} nm, and by spraying with 5 % $FeCl_3$ solution.

Individual constituents from ethyl acetate extract were isolated by column chromatography. A column (diameter 1.84 cm and height 28 cm) was packed using 0.7 g of ethyl acetate extract and 25 g of silica gel. The gradient elution solvents were pet ether and ethyl acetate from the ratio (2.5 : 7.5) to ethyl acetate and methanol (9:1).

Results and Discussions

Pytochemicals constitute one of the most numerous and widely distributed groups of substances in the plant kingdom. Plants produce chemicals known as secondary metabolites that are not directly involved in the process of growth but acts as deterrents to insects and microbial attack. In the present work, phytochemical tests were carried out by test tube methods. It was observed that alkaloids, ∝-amino acids, carbohydrates, flavonoids, glycosides, phenolic compounds, reducing sugars, saponins, steroids, tennins and terpenoids were present and starch was absent in the bark sample. Therefore, the bark of *A.scholaris* is rich in phytochemicals.

Phenolic compounds are a class of antioxidant agents which act as free radical terminators and their bioactivities may be related to their abilities to chelate metals, inhibit lipoxygenase and scavenge free radicals (Karamian and Ghasemlou, 2013). The amount by total phenol was determined with the Folin-Ciocalteu reagent. Gallic acid was used as a standard compound and the total phenols were expressed as μg GAE/mg using the standard curve equation : $y=0.0068x + 0.168$, $R^2 = 0.9993$, where y is absorbance at 760 nm and x is total phenolic content in the extracts of *A.scholaris* expressed in mg/mL. Table 1 and Figure 1 show the variation of mean absorbance with concentration of Gallic acid. Table 2 shows the contents of total phenols that were measured by Folin Ciocalteu reagent in terms of gallic acid equivalent. The total phenol contents were found in 70 % ethanol extract (99.33 μg GAE/mg) and watery extract (61.5 μg GAE/mg).

The efficiency of antioxidant potential of different extracts depends on its ability to scavenge free radicals either by donating hydrogen atom to the oxidizing free radical or decrease the energy of the antioxidant radical that prevents the autooxidation of the antioxidant radical into additional free radicals. Therefore in order to assess the antioxidant potential of extracts of *A. scholaris*, total antioxidant capacity was determined. In the present study, 70 % ethanol extract was observed to have significant (IC_{50}- 27.75 μg/mL) higher antioxidant activity value as compared to watery extract (IC_{50}- 90.56 μg/mL) of *A. scholaris*. The results of radical scavenging activity and IC_{50} values of standard Ascorbic Acid, 70 % ethanol and watery extracts of bark of *A. scholaris* are shown in Table 3 and Figure 2.

The antitumour activity screening of different crude extracts (ethyl acetate, 70 % ethanol, water)of the bark of *A. scholaris* was carried out against *Agrobacterium tumefaciens* by Potato Crown Gall test or Potato Disc Assay method. The results are given in Table 4. Among the results, 70 % ethanol extract inhibited (0.05 g to 0.15 g during 5 days and 7 days) against the formation of tumour cell.

The ethyl acetate crude extract was fractionated by column chromatography. Gradient elution by increasing polarity using pet ether, ethyl acetate and methanol mixture was performed. One of the combined fractions (14-70) having R_f = 0.45 was eluted by the solvent system pet ether:ethyl acetate (2.5:7.5). This combined fraction was found to be one of the phenolic compounds by spraying with 5 % $FeCl_3$. The TLC profiles are shown in Figure 3. This was confirmed by UV and FT IR (Figures 4 and 5, Tables 5 and 6). According to the results, the isolated fraction (compound A_1) is a phenolic compound by alkaline red shift in UV and also supported by FT IR spectrum.

Table 1 Absorbance of Gallic Acid Standard Solution at λ_{max} 765 nm

Concentration (μg/mL)	3.125	6.25	12.5	25	50	100
Absorbance	0.188	0.205	0.252	0.352	0.506	0.851

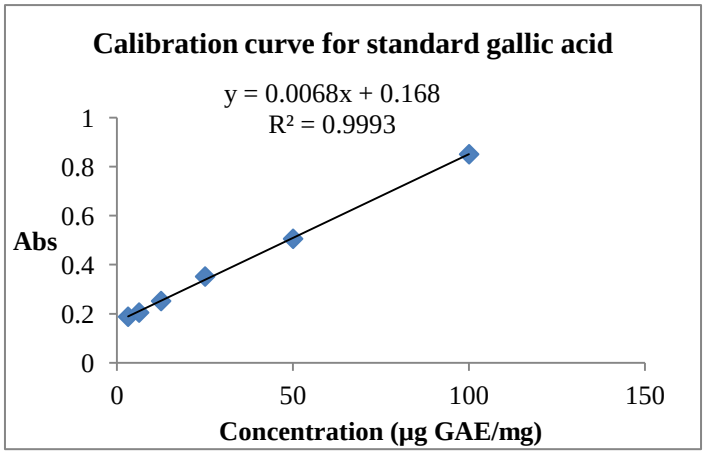

Figure 1 Standard gallic acid calibration curve at λ_{max} 765 nm

Table 2 Total Phenol Contents of 70 % Ethanol and Watery Extracts of the Bark of *Alstonia scholaris* L. (Taung-ma-yo)

No.	Extracts	TPC (μg GAE/mg)
1	Water	61.5
2	70 % Ethanol	99.33

Table 3 % RSA (Radical Scavenging Activity) and IC_{50} Values of Crude Extracts of Bark of *A.scholaris* and Standard Ascorbic Acid

Tested sample	% RSA (mean ±SD) in different concentrations (μg/mL)							IC_{50} (μg/mL)
	3.125	6.25	12.5	25	50	100	200	
70 % Ethanol extract	41.45 ± 6.88	47.50 ± 2.50	47.35 ± 1.04	49.71 ± 1.88	52.36 ± 1.46	70.36 ± 0.21	81.12 ± 3.34	27.75
Watery extract	20.5 ± 2.71	31.42 ± 4.38	30.68 ± 1.25	33.92 ± 0.42	37.32 ± 0.63	52.95 ± 1.46	71.1 ± 0.42	90.56
Standard Ascorbic acid	33.2 ± 0.92	57.66 ± 1.99	88.34 ± 0.88	94.22 ± 1.33	95.87 ± 1.55	96.17 ± 0.22	96.31 ± 0.44	5.27

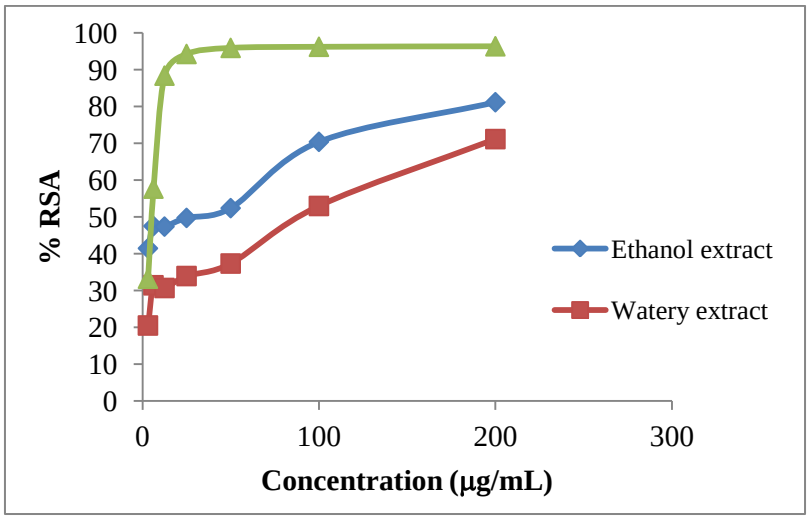

Figure 2 % RSA Vs concentration of crude extracts of bark of *A.scholaris* and standard ascorbic acid and

Table 4 Anti-tumour Activity of Crude Extracts from Bark of *Alstonia scholaris* L.

Sample	Tumour formation (5 days)			Tumour formation (7 days)		
	0.05 g	0.1 g	0.15 g	0.05 g	0.1 g	0.15 g
Ethyl acetate extract	+	+	-	+	+	+
70 % Ethanol extract	-	-	-	-	-	-
Watery extract	+	+	+	+	+	+
Control	++			++		

(++) Formation of tumour

(+) Some formation of tumour

(-) No formation of tumour

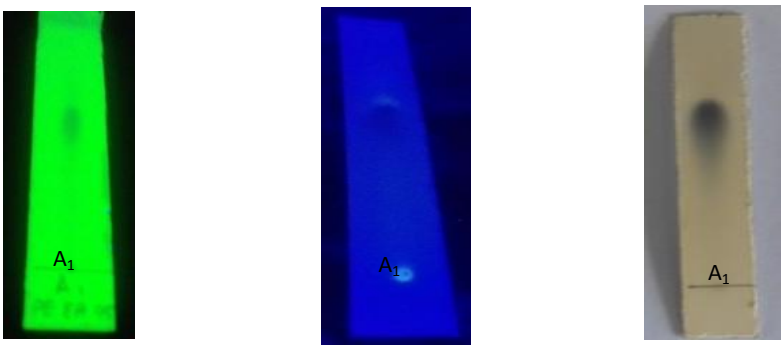

under UV_{254} nm under UV_{365} nm spraying with 5 % $FeCl_3$

Solvent system – Pet ether : Ethyl acetate (2.5:7.5)

Figure 3 TLC profiles of isolated compound (A_1) from ethyl acetate extract under UV_{254} nm, UV_{365} nm and 5 % $FeCl_3$

Table 5 Assignment of the UV Spectra of the Isolated Compound (A_1)

Medium	λ_{max} (nm)	Electronic Transition	Remark
MeOH	218, 253, 290	$\pi \rightarrow \pi^*$	Alkaline red shift Thus a phenolic compound
MeOH + NaOH	213, 273, 297	$\pi \rightarrow \pi^*$	

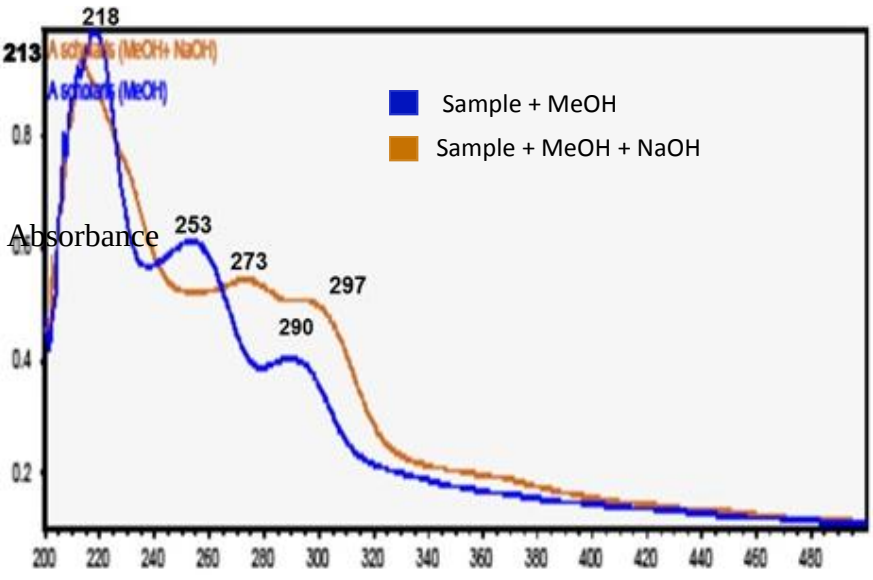

Figure 4 UV spectra for isolated compound from Bark of *Alstonia scholaris* L.

Table 6 FT IR Spectral Data of Isolated Compound (A_1) from Bark of *Alstonia scholaris* L.

No	Wavenumber (cm^{-1})	Vibrational mode	Remark
1	3327	O-H stretching	OH group attached on aromatic ring
2	3079	C-H stretching	Aromatic CH stretching
3	2922, 2852	C-H stretching	CH group in CH_3, CH_2, CH
4	1712	C=O stretching	Conjugated Carbonyl
5	1604, 1494, 1461	C=C stretching	C=C on aromatic ring
6	1186	C-O stretching	C-O group directly attached to aromatic ring

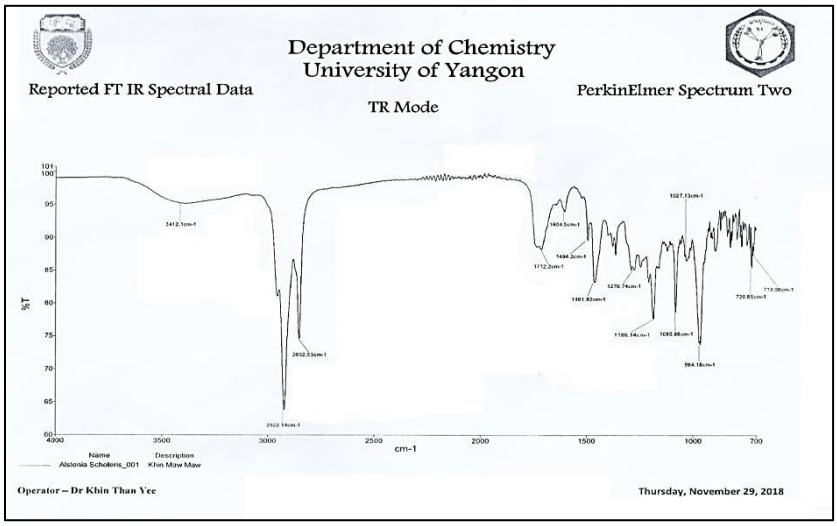

Figure 5 FT IR spectrum of isolated compound obtained from bark of *Alstonia scholaris* L. (Neat)

Conclusion

From the overall assessment for the present work concerning with the chemical and bioactivity investigation on the *Alstonia scholaris* L. (Taung-ma-yo) bark, the following inferences could be deduced. In the present work on the bark sample, preliminary phytochemical tests revealed the presence of alkaloids, α-amino acids, carbohydrates, flavonoids, glycosides, phenolic compounds, reducing sugars, saponins, steroids, tannins and terpenoids in it. Total phenol content (TPC) of 70 % ethanol crude extract was 99.33 μg GAE/mg and that of water extract was 61.6 μg GAE/mg. Thus, 70 % ethanol extract showed higher phenol contents than watery extract. The antioxidant activity of crude extract in bark sample was screened by DPPH assay method. IC_{50} value of 70 % ethanol extract was 27.75 μg/mL and that of watery extract was 90.56 μg/mL. So, ethanol extract showed more potent antioxidant activity than watery extract. Antitumour activity of crude extracts was investigated by Potato Crown Gall test. Ethyl acetate, 70 % ethanol and watery extracts were used to investigate against tumour cells within 5 days and 7 days. Among three extracts, ethanol extract showed the highest anti-tumour activity. Moreover, isolation of bioactive constituent fractions in bark sample was examined by thin layer chromatographic method. Isolated compound was eluted in the solvent system pet ether : ethyl acetate (2.5:7.5) by column chromatography. This compound was a phenolic which was confirmed by spraying reagent, UV and FT IR.

Acknowledgement

The authors would like to thank the Department of Higher Education (Yangon office), Ministry of Education, Yangon, Myanmar, for the permission of doing this research and for allowing to write this paper. Our deepest gratitude is expressed to Dr Win Naing, Rector, Dagon University, for his encouragement, Dr Nu Nu Yi and Dr Nay Thwe Kyi, Prorectors, Dagon University, for their invaluable advices and Dr Cho Cho Win, Professor and Head, Dr Hnin Hnin Than, Professor, Department of Chemistry, Dagon University for their helpful advice, valuable suggestions and provision of research facilities at the Department of Chemistry, Dagon University.

References

Anubha, A. and Yashwant, R. (2015). "Review: Phytochemistry, Ethanobotanical and Pharmacological activities of *Alstonia scholaris* R.Br (Apocynaceae)". *International Journal of Advanced Research*, vol. 3 (8), pp. 584 – 590

Baliga, M.S. (2010). "*Alstonia scholaris* Linn R .Br in the Treatment and Prevention of Cancer: Past, Present, and Future". *Integr. Cancer Ther*., vol. 9(3), pp. 261-269

Bhanu, P., Chakraborthy, G.S. and Nandini, M. (2013). "Complete Aspects of *Alstonia schotaris*". *IJPRIF*., vol . 5 (1), pp. 17-26

Kalaria, P., Payal, G., Manodeep,C. and Jagadish, K. (2012). "A Phytopharmacological Review of *Alstonia scholaris* : A Panoramic Herbal Medicine". *IJRAP*., vol. 3 (3), pp. 367-370

Karamian, R. and Ghasemlou, F. (2013). "Screening of Total Phenol and Flavonoid Content,Antioxidant and Antimicrobial Activities of the Methanolic Extracts of Three Silence Species from Iron". *Intl J Agri Crop Sci.*, vol. 5 (3), pp. 305 – 312

Lee, K. G. and Shibamoto. T. (2001). "Antioxidant Property of Aroma Extract Isolated from Clove Buds". *Food Chem*., vol. 74, pp. 443–448

Marini-Bettolo, G.B., Nicoletti, M. and Patamia, M. (1981). "Plant Screening by Chemical and Chromatographic Procedure under Field Conditions". *J. Chromatography*, vol. 213, pp. 113-127

Priestman, J. and Edwards, F.C.G. (1953). *Aids to Qualitative Pharmaceutical Analysis*. London : 1st Edition, Wilkins Co. Baltimore, pp. 98

Thaw Thaw Zin. (2016). *A Phytochemical and Medico–Chemical Investigation of Ginkgo billoba L. (Kabar-Oo) Leaves and Coptis teeta Wall. (Khan. Tauk) Rhizomes.* Ph.D. Dissertation, Department of Chemistry, University of Yangon

Tomoko, Y. (1998). "HPLC Method for Evaluation of the Free Radical Scavenging Activity of Foods by using 1, 1-Diphenyl 2-Picryl Hydrazyl". *Biochem*., vol. 62(6), pp. 1201 – 1204

Vance, C.P., Javanraedi, J., Stushnoff, C., Locke, E. and Vivanco, J. M. (2003). "Antioxidant Activity and Total Phenolic Contents of Iranian Ocimum accessions". *Food Chemistry*. vol. 83, pp. 547-550

ANTIMICROBIAL ACTIVITY AND PHYTOCHEMICAL CONSTITUENTS OF *EMBLICA OFFICINALIS* GAERTN. (ZI-BYU) AND *TERMINALIA CHEBULA* RETZ. (PHAN-KHA)

San San Aye[1], Ei Ei San[2], Ni Ni Than[3]

Abstract

Developing countries, where dysentery and diarrhea are endemic, depend strongly on traditional medicine as a source for inexpensive treatments because it is based on plants which are abundantly available in these countries. Consequently, Myanmar medicinal plants (Zi-Byu and Phan-Kha) which are used for the treatment of dysentery and diarrhea in Myanmar were selected to study in order to find the scientific basis for such use. Polar and non-polar extracts of the selected fruits were tested on six microorganisms by agar well diffusion technique. Phytochemical examination for types of organic constituents present in Zi-Byu and Phan-Kha fruits were carried out. The polar extracts of Zi-Byu and Phan-Kha showed antimicrobial activities (17 mm - 40 mm) against all the six microorganisms tested. Gallic acid (0.9 %) and β-sitosterol (0.36 %) were isolated from Zi-Byu and Phan-Kha, respectively. The isolated gallic acid was identified by UV, FT IR, ^{1}H NMR, ^{13}C NMR and mass spectrometry. β-sitosterol isolated from Phan-Kha was confirmed by authentic β-sitosterol and also compared with melting point determination. Moreover, isolated gallic acid showed antimicrobial activity (12 mm - 15 mm) against *Staphylococcus aureus*, *Candida albicans* and *Mycobacterium* species.

Keywords*:* antimicrobial activities, gallic acid, β-sitosterol, phytochemical

Introduction

Emblica officinalis Gaertn. (Zi-Byu)

The medicinal plant, *Emblica officinalis* Gaertn. (Zi-Byu), belonging to the family, Euphorbiaceae, is commonly known as 'Amla' or 'amlaki' in Bengali and 'Indian gooseberry' in English. This species is medium sized deciduous tree with 8-18 meters height (Rai **et al**., 2012). Amla is rich in fiber, carbohydrate, iron and is reported as the richest source of vitamin C (Singh **et al**., 2011). Supplements of fresh amla fruit is very favorable to individuals suffering from anemia. The juice of fresh amla fruit is given as diuretic, anti-bilious remedy and as a tonic. It is also helpful in over thirst, dyspepsia, burning sensation and other complaints of digestive system (Kumar *et al.,* 2012).

Terminalia chebula Retz. (Phan-Kha)

Terminalia chebula Retz. of the family Combretceae is an important tree of pharmaceutical and trade value. It is distributed in the forests of Northern India, Eastern India and the Southern Peninsula. The fruit of the plant is rich in tannin and commonly known as myrobalan or chebulic myrobalan. In Indian pharmacopoeia, fruit of *T. chebula* is extensively used as adjuvants to other medicines in almost all diseases e.g jaundice, splenopathy, hiccough, cephalagia, epilepsy, leprosy and as astringent, anti-inflammatory, digestive, cardiotonic (Phetkate *et al.,* 2012). Effect of tannin from *T. chebula* on the infectivity of potato virus X was also reported.

[1] Dr, Associate Professor, Department of Chemistry, University of Yangon
[2] Dr, Assistant Lecturer, Department of Chemistry, University of Yangon
[3] Dr, Professor and Head, Department of Chemistry, University of Yangon

The present research work deals with antimicrobial screening of polar and non-polar extracts and the column chromatographic isolation of some organic constituents of *E. officinalis* and *T. chebula* fruits.

Materials and Methods

Plant materials

The fruits of Zi-Byu and Phan-Kha were collected from local market in Yangon Region. These samples were ground to get a fine powder by grinding machine. The drug powders were then stored in an air-tight container.

Preparation of crude extracts

100 g of each dried powdered sample were percolated in 500 mL of petroleum ether (PE, 60-80 °C) for one week and filtered. This procedure was repeated for three times. Then the filtrate was concentrated by a vacuum rotatory evaporator to get respective PE extract. Similarly, ethyl acetate, acetone and 80 % EtOH extracts of each dried powdered sample were prepared according to the above procedure. In the preparation of watery extract; 100 g of each dried powdered sample were soaked in 500 mL of distilled water into the conical flask. These flasks were boiled on water bath for 6 h and filtered. This process was carried out for three times. The combined filtrates were to dryness over a water bath at 100 °C to get the corresponding watery extract.

Antimicrobial screening

Antimicrobial activity of the prepared crude extracts was determined by agar well diffusion method. Four small holes of 10 mm diameter each were cut out in the inoculated agar to place samples to be tested. The volume of each sample placed in each well was 0.1 mL. The petridish was then incubated at 37 ºC for 48 h, and the diameters of clear inhibition zones around the wells, if appeared, were measured (Finegold and Martin, 1982).

Isolation of compound from *E. officinalis* (Zi-Byu)

The dried fruit powder (50 g) was soaked overnight in 200 mL of PE at room temperature (Harborne, 1984). The mixture was filtered and the filtrate (PE extract) kept for later use; the residue was extracted with 500 mL of 70 % EtOH by maceration for one week and the EtOH extract was evaporated to dryness in rotary evaporator. The residue was dissolved in 2 M hydrochloric acid solution and hydrolyzed for 45 min on a boiling water bath. The mixture was cooled and filtered. The filtrate was extracted with ethyl acetate. The ethyl acetate layer was concentrated to dryness in rotary evaporator and the residue ("flavonoid" extract) was used for column separation. Thus, ethyl acetate extract (0.6 g) was chromatographed on a silica gel column using toluene: ethyl acetate (7:3) solvent mixture as eluent. Finally, three main fractions were obtained. Fraction No.3 yielded compound 1 as pure crystals (0.9 % gallic acid) upon evaporation at room temperature. The isolated compound 1 was identified by spectroscopic method (^{1}H, ^{13}C and MS). The NMR spectra (^{1}H, ^{13}C) of isolated compound was recorded in Pyridine with TMS as internal standard at 400 MHz for ^{1}H, and at 100 MHz for ^{13}C NMR. Moreover, mass spectrum (ESI-FT-ICR) of isolated compound was recorded by a Bruker Apex III Fourier transform ion cyclotron resonance (FT-ICR) mass spectrometer.

Isolation of compound from *T. chebula* (Phan-Kha)

The dried fruit powder (50 g) was extracted with petroleum ether (60-80 ºC) for about one week by percolation method followed by filtration. PE extract of Phan-Kha was fractionated by column chromatography using PE: ethyl acetate (9:1, 5:1) as eluent. Finally, colorless crystals of β-sitosterol (0.36 %) were isolated. β-sitosterol is one of several phytosterols with chemical structure similar to that of cholesterol. It is a white, waxy with a characteristic odour. The isolated compound was subjected to Co-TLC analysis with a standard β-sitosterol sample. The chromatogram was developed in the chosen solvent system for the compound isolated. After the plate has dried, the R_f value of isolated sample was measured. Localization of spot was made by viewing directly under UV 254 nm and 365 nm light. And then, it was treated with 5 % H_2SO_4, anisaldehyde-H_2SO_4 and ceric sulphate followed by heating, respectively.

Results and Discussion

Antimicrobial activity

In the present work, the samples were tested on six strains of microorganisms which include *Bacillus subtilis, Staphylococcus aureus, Pseudomonas aeruginosa, Bacillus pumilus, Candida albicans* and *Mycobacterium* species. The measurable zone diameter, including the agar well diameter, shows the degree of antimicrobial activity. It was found that the polar extracts of *E. officinalis* and *T. chebula* showed antimicrobial activities against all the six microorganisms tested (Figure 1 and Table 1 and Figure 2 and Table 2). It was also observed that, the PE extracts of *E. officinalis* and *T. chebula* did not show any antimicrobial activity. The gallic acid isolated from Zi-Byu indicated the antimicrobial activity against *Staphylococcus aureus, Candida albicans* and *Mycobacterium* species (12 mm-15 mm). According to the experimental results, antimicrobial activity of ethyl acetate crude extracts (40 mm) of Zi-Byu fruit was found to be more potent against *Bacillus subtilis* than 80 % EtOH crude extracts (26 mm) of Phan-Kha fruits. The larger the inhibition zone diameter, the greater is the antimicrobial activity.

Identification of isolated compounds

The two compounds namely gallic acid and β-sitosterol were isolated from Zi-Byu fruits and Phan-Kha fruits, respectively.

1 (Gallic acid): White crystalline compound (0.9 %), mp. 230 ºC (225-230 ºC) (Merck Index, 2001); UV(nm): 228, 262, 284; FT IR ν_{max}^{kBr} cm^{-1}: 3418 ($^{\upsilon}$O-H), 1701 ($^{\upsilon}$C=O), 1618, 1451, 1246, 1027; ^{1}H NMR (400 MHz, Pyridine-d5) δ (ppm): 8.11(s) (Figure 3); ^{I3}C NMR (100 MHz, pyridide-d5) δ (ppm): 169.50, 147.48, 110.45 (Figure 4); ESI - FT-ICR mass spectrum m/z (%): M-H, 169 (Figure 5).

2 (β-sitosterol): The isolated compound was UV inactive. It was identified by some colour tests on TLC, 5 % H_2SO_4, ceric sulphate solutions and anisaldehyde H_2SO_4 were employed as spraying agents followed by heating. It was also identified by comparison study (Co-TLC) with standard β-sitosterol (Figure 6). The same R_f values (0.27) were observed for the isolated compound and standard β-sitosterol with PE: EtOAc (5:1). The coloration of isolated compound was found to be identical with that of standard β-sitosterol with each spraying reagent. It gave violet, brown and bluish-purple colors when it was treated with 5 % H_2SO_4, anisaldehyde-H_2SO_4 and ceric sulphate followed by heating, respectively.

β-sitosterol: Colorless needle (0.36 % yield, mp. 138-140 ºC), FT IR ν_{max}^{kBr} cm^{-1}: 3400 ($^{\upsilon}$O-H), 2939-2877 ($^{\upsilon}$C-H), 1643 ($^{\upsilon}$C=C), 1049 ($^{\upsilon}$C-O).

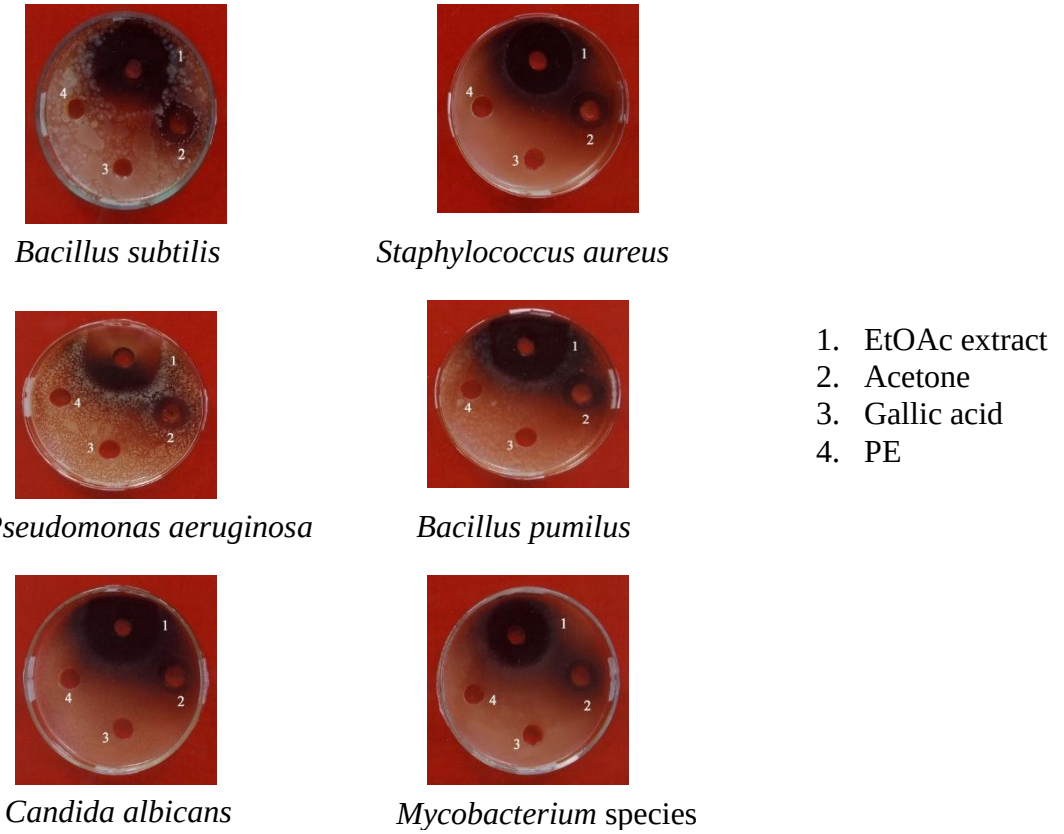

Bacillus subtilis *Staphylococcus aureus*

Pseudomonas aeruginosa *Bacillus pumilus*

Candida albicans *Mycobacterium* species

Figure 1 Agar well diffusion tests of *E.officinalis* (Zi-Byu) fruit extract on six microorganisms

Table 1 Results of Antimicrobial Activity of Zi-Byu Fruit

No	Organisms	Inhibition zone diameter (mm)			
		PE	**Gallic acid**	**Acetone**	**EtOAc**
1.	*Bacillus subtilis*	–	–	20	40
2.	*Staphylococcus aureus*	–	15	20	35
3.	*Pseudomonas aeruginosa*	–	–	17	40
4.	*Bacillus pumilus*	–	–	20	38
5.	*Candida albicans*	–	12	19	38
6.	*Mycobacterium species*	–	12	18	33

* Agar well -10 mm, No activity (–)

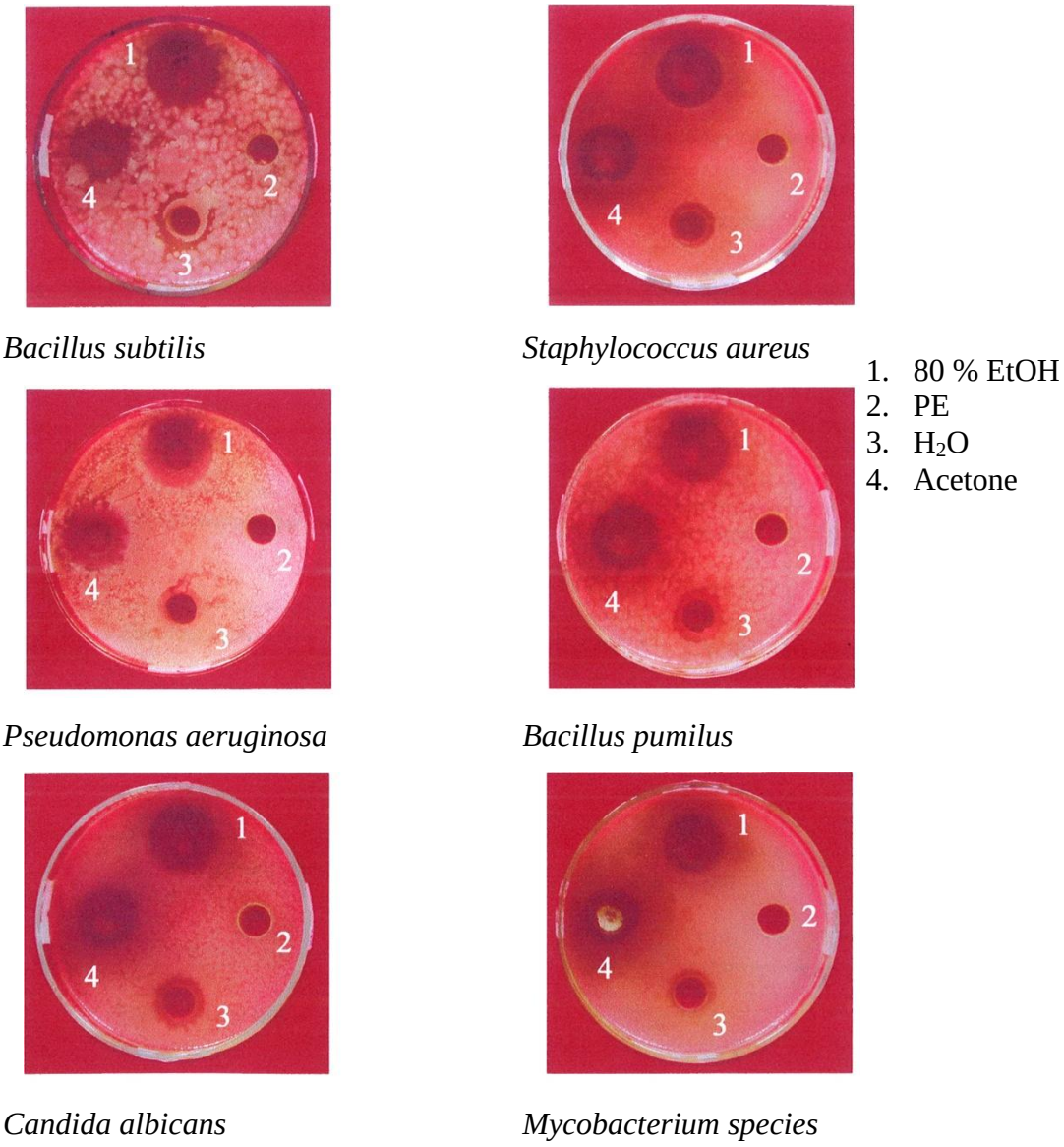

Figure 2 Agar well diffusion tests of *T. chebula* (Phan-Kha) fruit extracts on six microorganisms

Table 2 Results of Antimicrobial Activity of Phan-Kha Fruit

No	Organisms	Inhibition zone diameter (mm)			
		PE	**80 % EtOH**	**Acetone**	**H_2O**
1	*Bacillus subtilis*	–	26	22	20
2	*Staphylococcus aureus*	–	23	20	15
3	*Pseudomonas aeruginosa*	–	22	19	15
4	*Bacillus pumilus*	–	24	25	18
5	*Candida albicans*	–	24	21	17
6	*Mycobacterium species*	–	20	19	17

* Agar well-10 mm, (–) No activity

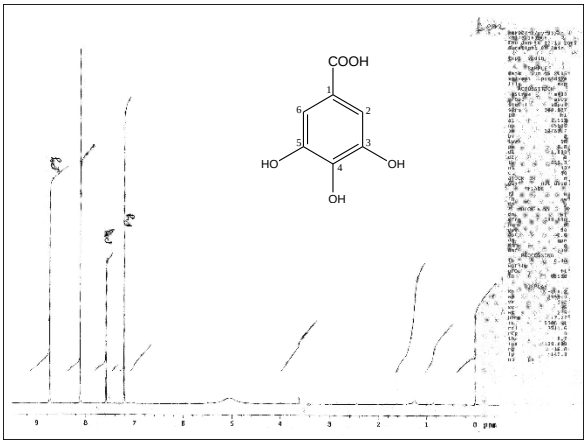

Figure 3 ^{1}H NMR spectrum of isolated gallic acid from *E. officinalis* (Zi-Byu)

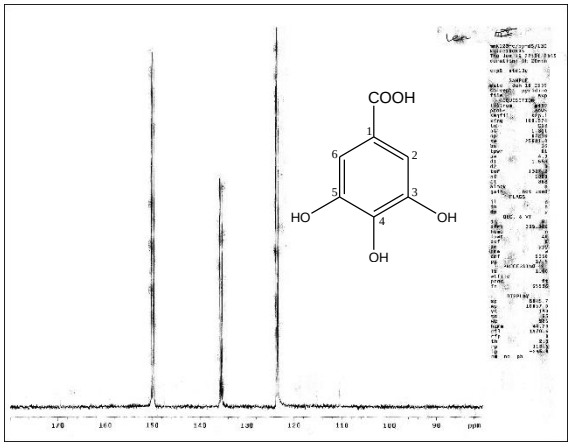

Figure 4 ^{13}C NMR spectrum of isolated gallic acid from *E. officinalis* (Zi-Byu)

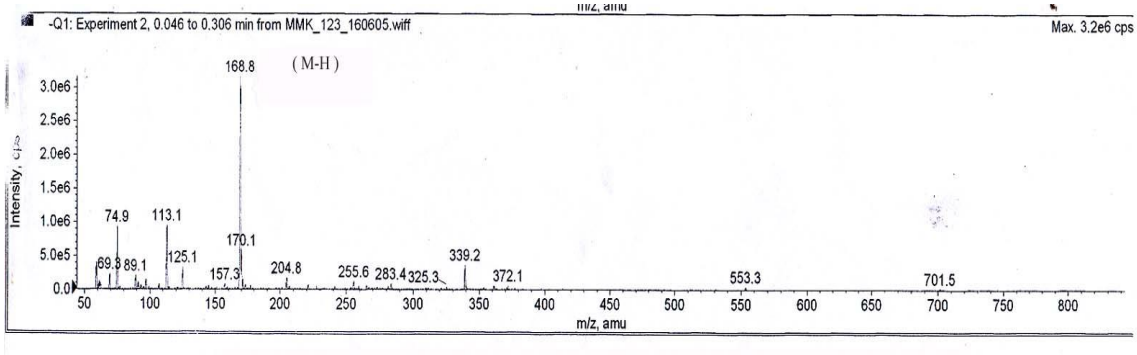

Figure 5 ESI-FT-ICR mass spectrum of isolated gallic acid from *E. officinalis* (Zi-Byu)

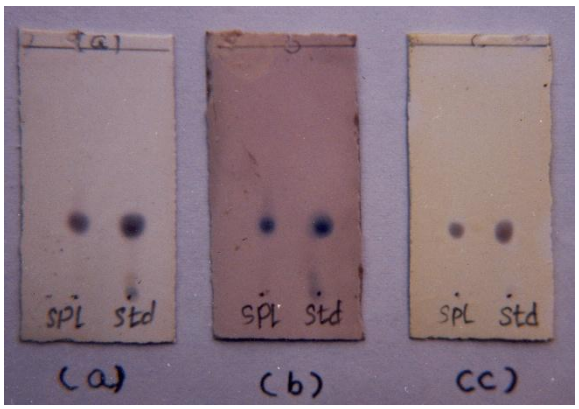

SPL = Sample
Std = standard β-sitosterol
Spraying agents
(a) = 5 % H_2SO_4
(b) = Anisaldehyde H_2SO_4
(c) = $CeSO_4$
Stationary phase: Silica gel
Mobile phase : PE: EtOAc (5:1)

Figure 6 Thin layer chromatograms of isolated β–sitosterol from *T. chebula* (Phan-kha)

Conclusion

From the present research work on "Comparative studies of antimicrobial activity and phytochemical constituents of *E. officinalis* (Zi-Byu) and *T. chebula* (Phan-Kha)", the following conclusions can be drawn.

Crude extracts have been prepared from Zi-Byu and Phan-kha by using non-polar and polar solvents. The antimicrobial activity of the crude extracts was screened by *in vitro* method

using agar well diffusion techniques on six microorganisms which include *Bacillus subtilis, Staphylococcus aureus, Pseudomonas aeruginosa, Bacillus pumilus, Candida albicans* and *Micobacterium* species. Polar extracts of Zi-Byu and Phan-Kha showed antimicrobial activity against all tested microorganisms (17 mm - 40 mm). However, non-polar extracts of both fruits did not show antimicrobial activity. In the case of *Bacillus subtilis* and *Pseudomonas aeruginosa*, ethyl acetate extract of Zi-Byu fruit has more antimicrobial activity than acetone extract. 80 % ethanol extract of Phan-Kha has higher antimicrobial activity than acetone extract against *Bacillus subtilis, Staphylococcus aureus, Pseudomonas aeruginosa, Candida albicans* and *Mycobacterium species.* From the experimental results, Zi-Byu (40 mm) has more pronounced antimicrobial activity than Phan-Kha fruit (26 mm). Colorless crystal of gallic acid (0.9 %) was obtained from ethyl acetate extract of Zi-Byu by column chromatographic method. It was confirmed by UV, FT IR, ^{1}H NMR, ^{13}C NMR and mass spectrometry. Pet-ether extract of Phan-Kha was separated by column chromatographic method to give β-sitosterol (0.36 %). It was confirmed by standard β-sitosterol and melting point determination. Moreover, isolated gallic acid from Zi-Byu also showed antimicrobial activity (12 mm-15 mm). Gallic acid is a well-known natural antioxidant. Therefore, gallic acid containing Zi-Byu fruit may be used as natural antioxidant and antimicrobial agents.

Acknowledgements

The authors would like to express their profound gratitude to the Department of Higher Education, Ministry of Education, Yangon, Myanmar, for provision of opportunity to do this research and Myanmar Academy of Arts and Science for allowing to present this paper.

References

Finegold, S. M. and Martin, W. J. (1982). *Diagnostic Microbiology*. London: The C.V. Mosby Co.

Harborne, J.B. (1984). *Phytochemical methods*. *A Guide to Modern Techniques of plant Analysis*, London: Chapman and Hall

Kumar, K.P.S., Bhowmik, D., Dutta, A., Yadav, A.P., Paswan, S., and Srivastava, S. (2012). Recent Trends in Potential Traditional Indian Herbs *Emblica officinalis* and Its Medicinal Importance. *J. Pharmacog and Phytochem*. vol.1 (1), pp. 24-32

Merck Index. (2001). *An Encyclopedia of Chemicals and Drugs*, USA: 13th Edition, Merck and Co., Inc., p. 772

Phetkate, P., Kummalue, T. and Kietinun, S. (2012). Significant Increase in Cytotoxic T Lymphocytes and Natural Killer Cells by Triphala: A Clinical Phase I Study. Evidence Based Complementary and Alternative Medicine. vol. 2, pp. 1-6

Rai, N., Tiwari, L., Sharma, R.K. and Verma, A.K. (2012). Pharmaco-botanical Profile on *Emblica officinalis* Gaertn. *A Pharmacopoeial Herbal Drug*. *STM Journals*. vol. 1(1), pp. 29-41

Singh, E., Sharma, S., Pareek, A., Dwivedi, J., Yadav, S. and Sharma, S. (2011). Phytochemistry, Traditional Uses and Cancer Chemo Preventive Activity of Amla (*Phyllanthus emblica*): *The sustainer. J. App. Pharma. Sci*. vol. 2 (1), pp.176-183

PREPARATION AND CHARACTERIZATION OF BISMUTH FERRITE ($BiFeO_3$) NANOPARTICLES BY SOL-GEL METHOD

Thuzar Nyein[1], Zaw Naing[2], Khin Than Yee[3], Cho Cho[4]

Abstract

This research work was concerned with the preparation and characterization of bismuth ferrite ($BiFeO_3$), a trigonal or rhombohedral distorted perovskite structure, by sol-gel method. In this method, $BiFeO_3$ powder was prepared by using bismuth(III) nitrate and iron(III) nitrate as starting materials. The precursor powders were calcined at different temperatures (450, 550, 650 and 750 °C) for 4 h. The prepared samples were characterized by XRD, TG-DTA and FT IR and SEM techniques. The calcined temperature of 550 °C was selected as optimum temperature due to high crystallinity and average nanocrystallite size. Some physicochemical properties (pH, moisture, bulk density, porosity and surface area) of the prepared $BiFeO_3$ powder sample calcined at 550 °C were also determined.

Keywords: $BiFeO_3$ powder, Sol-gel method, XRD, TG-DTA, FT IR, SEM techniques

Introduction

Multiferroic materials are of particular interest due to the co-existence of ferromagnetic and ferroelectric properties (Awan and Bhatti, 2009). Among varies multiferroics, bismuth iron oxide ($BiFeO_3$/BFO) is the only material that shows both ferroelectric and antiferromagnetic properties at room temperature. There is an increasing need for magnetic nanoparticles for different applications that could be solved through high performance technique production large quantities of nanoparticles (Dwita and Wijaya, 2016). In particular, bismuth nanoparticles are expected to play important role in a variety of relevant applications like an enhancing spontaneous magnetization, high super conductivity, high tech magnetic tape, photovoltaics, spintronics and field of magnetism (Selbach *et al*., 2007). This ferroic material can be synthesized by different methods such as co-precipitation method, sol-gel method, microwave assisted method, hydrothermal method, solvothermal method and micro emulsion method (Freitas, 2013).

Among these methods, sol-gel method is one of the methods to synthesize nanoparticles are very simple and relatively clean materials. $BiFeO_3$ nanoparticle was prepared by sol-gel method using bismuth nitrate and ferric nitrate are dissolved with 2-methoxy ethanol, citric acid and acetic acid. The synthesized bismuth ferrite ($BiFeO_3$) nanoparticle was characterized by XRD, TG-DTA, FT IR and SEM techniques (Chunlin *et al.*, 2012). Unit cell of $BiFeO_3$ can be described by hexagonal, trigonal, rhombohedral and cubic structures. From a structural point of view, the room temperature structure of $BiFeO_3$ is a highly rhombohedrally distorted perovskite or trigonal structure with space group R_3c (Johari, 2011). The aim of the present research work is to study the role of the prepared bismuth ferrite ($BiFeO_3$) nanoparticle powder by sol-gel method and its characterization.

[1] Assistant Lecturer, Department of Chemistry, Maubin University
[2] Dr, Associate Professor, Department of Chemistry, Dagon University
[3] Dr, Lecturer, Department of Chemistry, Myeik University
[4] Dr, Professor, Department of Chemistry, University of Yangon

Materials and Methods

Materials and Methods of Analysis

Ferric nitrate nanohydrate ($Fe(NO_3)_3.9H_2O$) with 98 % purity, bismuth nitrate pentahydrate ($Bi(NO_3)_3.5H_2O$) with 98% purity and other reagents were purchased from commercial sources with analytical grade and used as received. Labwares and glasswares facilities were used at Chemistry Laboratory of Yangon University and also at the Maubin University and Universities' Research Center, Lower Myanmar, Yangon Region. Instruments employed were hot plate magnetic stirrer, oven, furnace and spectrophotometer. The methodologies and techniques used were carried out according to the procedures given in the recommended texts and literatures.

Preparation of Bismuth Ferrite ($BiFeO_3$) Powder by Sol-Gel Method

Bismuth nitrate pentahydrate [$Bi(NO_3)_3.5H_2O$] and ferric nitrate nanohydrate [$Fe(NO_3)_3.9H_2O$] were mixed with mole ratio of 1:1 and dissolved in 2-methoxy ethanol. After the solution became transparent it was continued to stir one hour at room temperature. Citric acid ($C_6H_8O_7$) as a chelating agent and acetic acid were added. Then the resulting solution was transparent, blackish red and clear. Furthermore, solution was heated at temperature 80 °C on a hot plate under continuous stirring condition until all the liquid evaporated. There was an immense evolution of brown fumes, towards the end of the reaction a fluffy brown mass (gel) was obtained at the base of the beaker. The obtained gel was calcined at 450, 550, 650 and 750 °C for 4 h.

Characterization of the Prepared Bismuth Ferrite ($BiFeO_3$) Powder

The average crystallite size of prepared bismuth ferrite ($BiFeO_3$) nanoparticles were determined from XRD pattern by using Scherrer equation. XRD model was Rigaku X-ray diffractometer, RINT 2000 P/C software at no. 9240 J 101, Japan. Thermal stability of prepared bismuth ferrite ($BiFeO_3$) nanoparticles was examined by Shimadzu DTG 60 H operated under nitrogen and oxygen atmosphere. The FT IR spectra of prepared bismuth ferrite ($BiFeO_3$) nanoparticles were recorded by using Shimadzu, IR Prestige-21, (Japan) FT IR spectrophotometer at Department of Chemistry, University of Yangon. The surface morphology of the prepared bismuth ferrite ($BiFeO_3$) nanoparticles were observed on a JSM 5610 LV scanning microscope, JEOL Ltd., Japan.

Determination of Some Physicochemical Properties of the Prepared Bismuth Ferrite ($BiFeO_3$) Powder

Determination of pH

The sample (about 1 g) was placed into a Pyrex 200 mL beaker and 100 mL of distilled water was added. The content of the beaker was heated at 80 ˚C for 10 min. The beaker and content were gently shaken and the sample was filtered. The filtrate was cooled at room temperature and pH of the sample was determined by using a pH meter.

Determination of free moisture content

Moisture content (%) was determined by the oven method at 110 ± 5 ˚C. An accurately weighed sample (about 1 g) was added to a pre-dried and cooled dish with a cover. The uncovered dish is placed in an electric oven, and dried at 110 ± 5 ˚C for 2 h. After heating the cover was placed in position and in desiccator for cooling. And weighing which was repeated until a constant weight was obtained. The moisture percent is represented by the loss in weight

Determination of bulk density

A clean dry 10 mL graduated cylinder was weighed. It was then filled with the dry sample to the 10 mL mark and reweighed. The graduated cylinder was placed in a tapping box and the cylinder was tapped gently until there was no more reduction in volume. The minimum volume was recorded and the bulk density was calculated.

Determination of porosity

The porosity of sample was measured by dry-wet method. About 1 g of the dry sample was placed in a beaker and 0.8 mL of distilled water was added. The sample was equilibrated with distilled water for 24 h and then was determined by dividing the amount of water adsorbed with the amount of the dry sample.

Determination of surface area by methylene blue adsorption test

A stock solution of methylene blue was prepared by dissolving 0.1 g of methylene blue in 1 L distilled water. By serial dilution, the methylene blue solutions within the concentration ranged from 10 ppm to 100 ppm were prepared. Analyses were carried out spectrometrically by using Cary 60 UV-visible spectrophotometer. Different concentrations of dye solution were prepared and accurate weight (0.1 g) of sample was equilibrated with an appropriate concentration of the test solution and the surface area was calculated.

Results and Discussion

Preparation of Bismuth Ferrite ($BiFeO_3$) Powder by Sol-Gel Method

Molar ratio (1:1) of bismuth nitrate pentahydrate and ferric nitrate nanohydrate were mixed. The mixture was dissolved in 2-methoxy ethanol and then citric acid (a chelating agent) and acetic acid were added after stirring 1 h at room temperature. After continuous stirring, all the liquid were evaporated. At the end of the reaction a fluffy brown mass (gel) was obtained and calcined at 450, 550, 650 and 750 °C for 4 h.

Characterization of Prepared Bismuth Ferrite ($BiFeO_3$) Powder by Sol-Gel Method

XRD analysis

The XRD diffractograms of prepared bismuth ferrite ($BiFeO_3$) powder by sol-gel method are illustrated in Figure 1. The average crystallite sizes of prepared sample calcined at different temperatures were calculated using XRD spectra and Debye-Scherrer equation. It was observed that the crystallite size increases with increasing temperature which may be due to the growth of particles size but the sample calcined at 550 °C was selected as optimum temperature because the sample $BiFeO_3$ has high crystallinity and average crystallite size 42.21 nm from XRD result and 41.05 nm by using Debye Scherrer equation (Table 1).

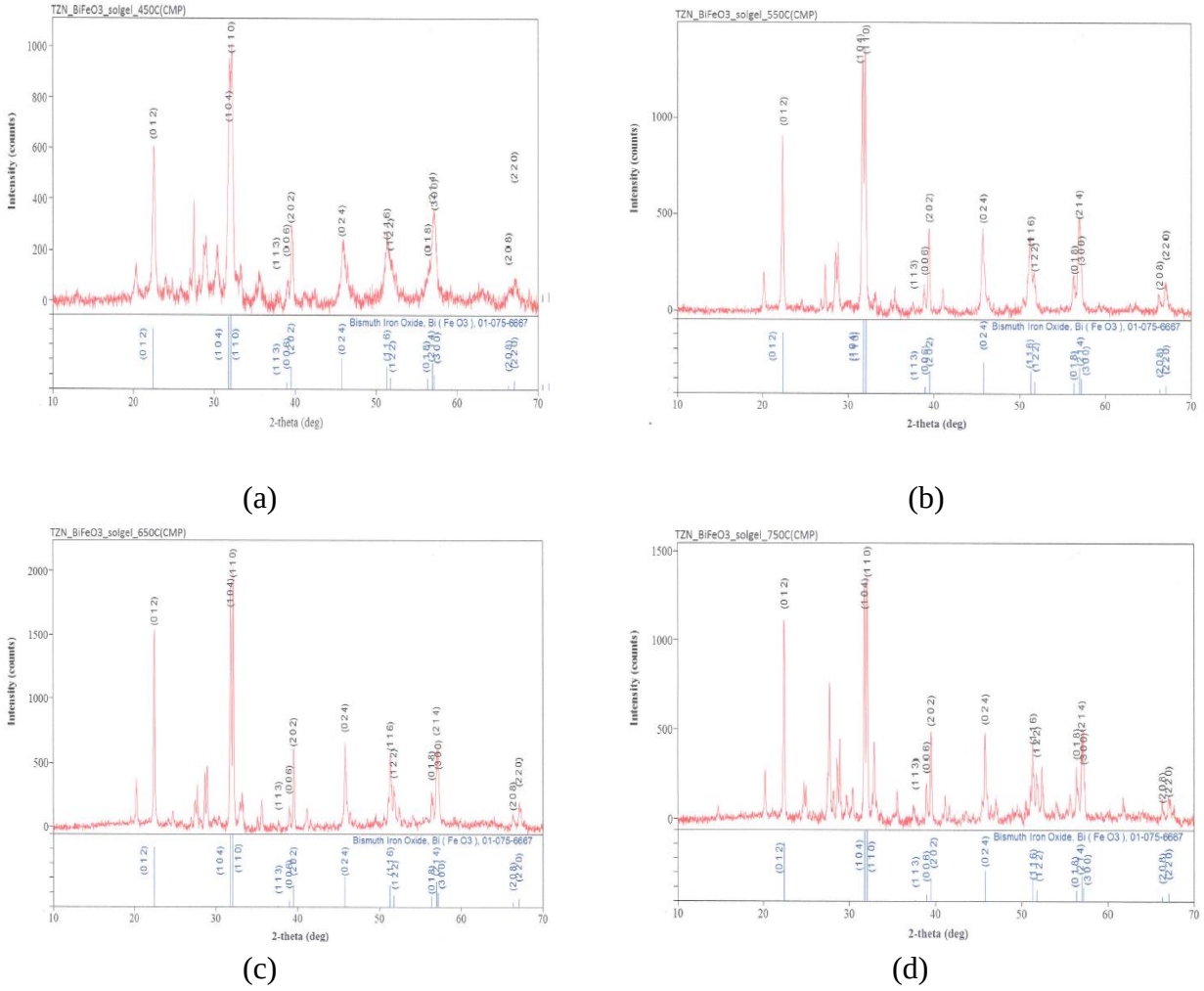

Figure 1 X-ray diffractograms of prepared $BiFeO_3$ powder calcined at (a) 450 °C (b) 550 °C (c) 650 °C (d) 750 °C for 4 h

Table 1 Average Crystallite Sizes of the Prepared $BiFeO_3$ Powder Calcined at Different Temperatures for 4 h

Temperature (°C)	Average crystallite size (nm)		Lattice Parameters (A)			Crystal System
	XRD data	Debye Scherrer Equation	a	b	c	
450	59.31	65.34	5.5474	5.5474	13.7895	Trigonal
550	42.21	41.05	5.5770	5.5770	13.8694	Trigonal
650	61.48	56.79	5.5756	5.5756	13.8621	Trigonal
750	65.34	59.78	5.5729	5.5729	13.8573	Trigonal

Thermal analysis

The TG-DTA thermograms of prepared $BiFeO_3$ powder by sol-gel method are illustrated in Figure 2. The weight loss percent of prepared samples at different temperatures was very low. Thermal stability of all prepared samples was observed above the temperature of 550 °C (Table 2).

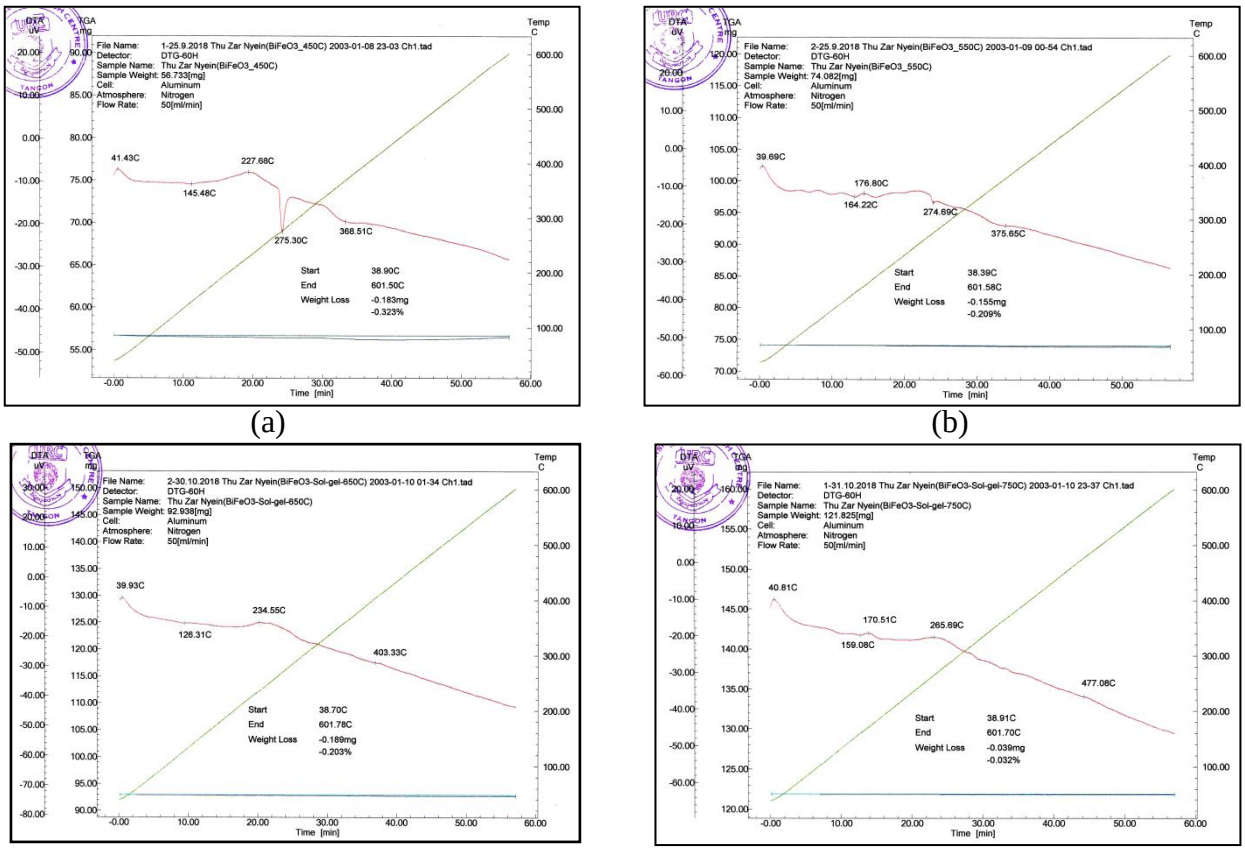

Figure 2 TG-DTA thermograms of prepared $BiFeO_3$ powder calcined at (a) 450 °C (b) 550 °C (c) 650 °C (d) 750 °C for 4 h

Table 2 Thermal Analysis of Prepared $BiFeO_3$ Powder Calcined at Different Temperatures for 4 h

Temperature (°C)	Weight loss (%)
450	0.323
550	0.209
650	0.203
750	0.032

FT IR spectral analysis

The FT IR spectra of prepared bismuth ferrite ($BiFeO_3$) powder by sol-gel method are illustrated in Figure 3. Stretching vibration of Bi-O and Fe-O chemical bonds of prepared sample at 550 °C was observed in wave number 527 and 845 cm^{-1}. There is no O-C-O symmetric stretching in the sample (Table 3).

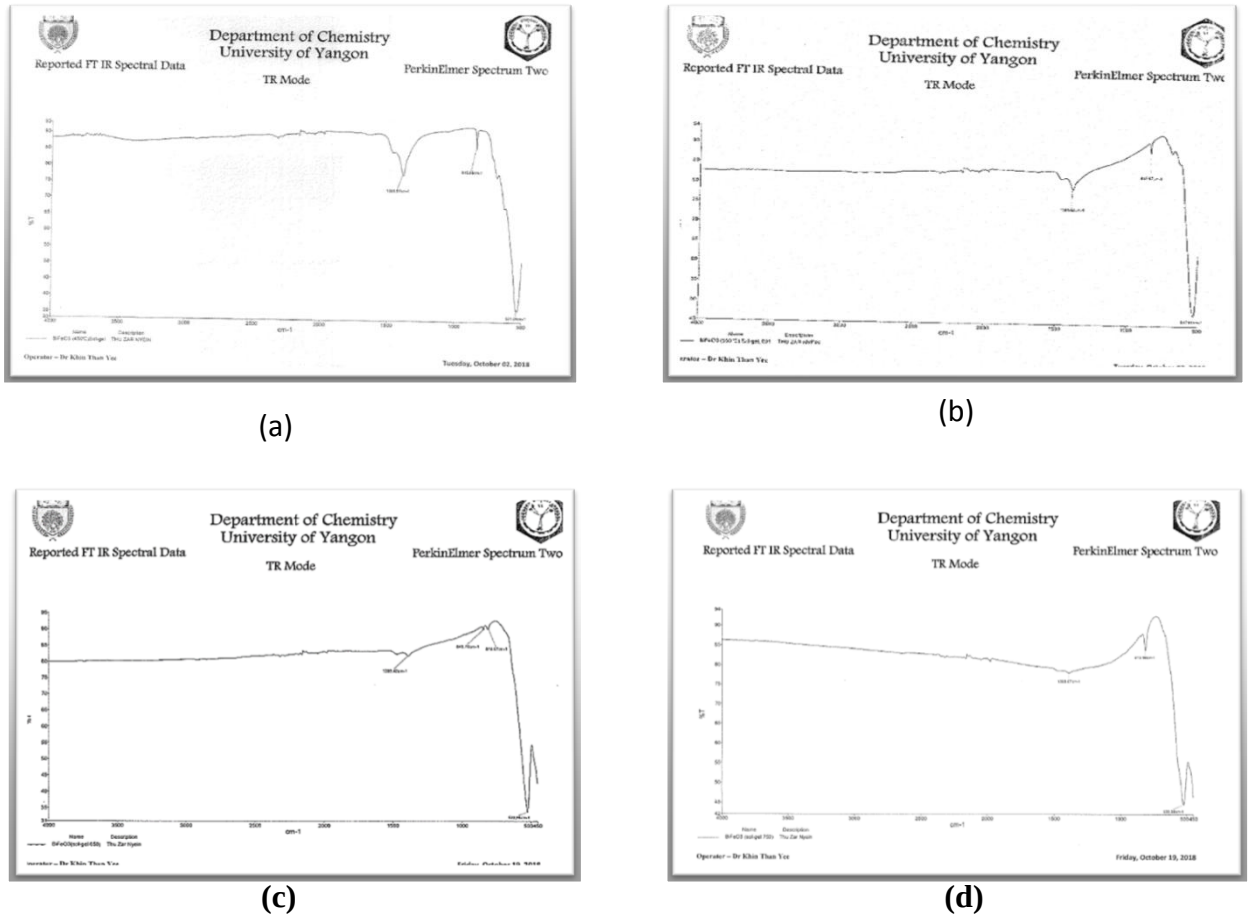

Figure 3 FT IR spectra of the prepared $BiFeO_3$ powder calcined at (a) 450 °C (b) 550 °C (c) 650 °C (d) 750 °C for 4 h

Table 3 FT IR Spectral Data of Prepared $BiFeO_3$ Powder Calcined at Different Temperatures for 4 h

Observed Wavenumber (cm^{-1})					
Temperatures (**°C**)				Literature Wavenumber (cm^{-1})	Band Assignment
450	550	650	750		
531	527	522	522	*970 - 450	Bi–O & Fe–O stretching
845	845	846	813		
1390	-	-	-	**1450 - 1350	O – C – O symmetric stretching

*(Silverstein, 2003 and ** Nakamoto, 1970)

SEM analysis

The SEM micrograph of prepared $BiFeO_3$ powder calcined at 550 °C (optimum temperature) indicated that the continuous distribution of spherical shapes with clear grain boundaries and the formation of well defined pores in the sample.

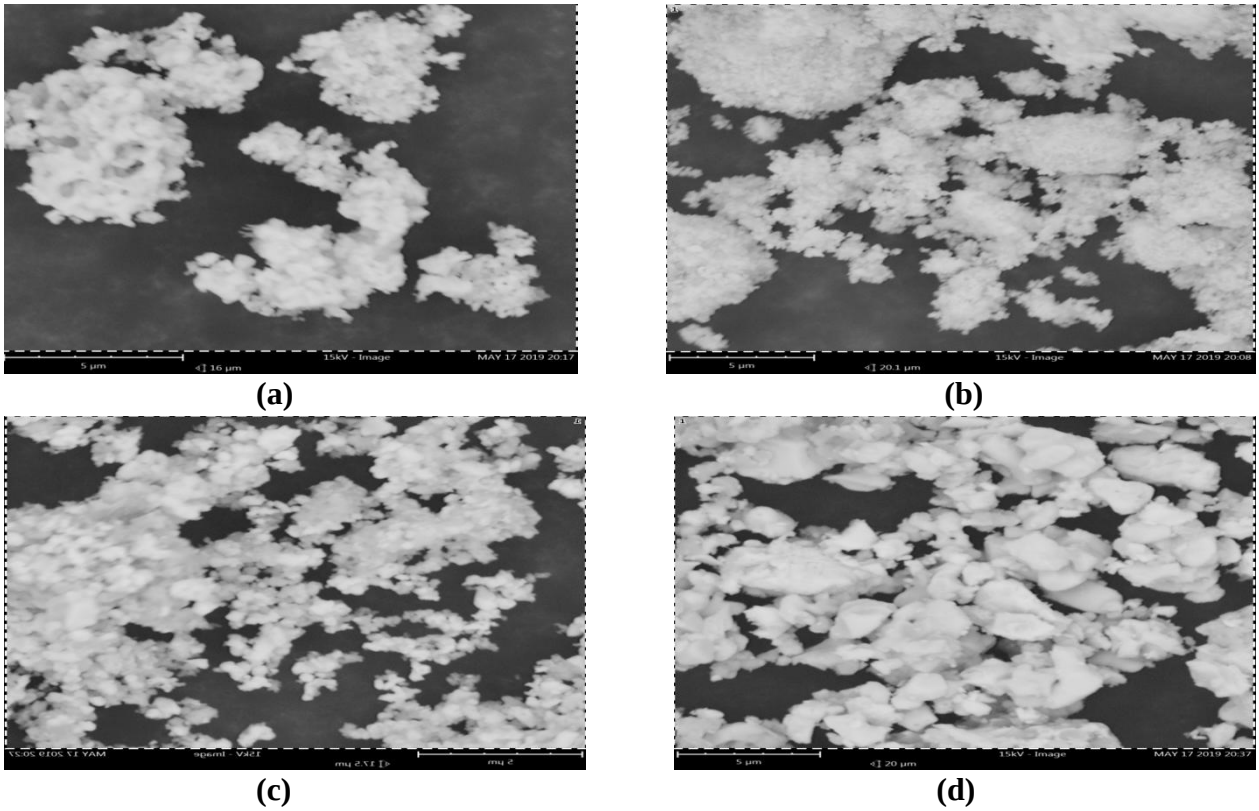

Figure 4 SEM micrographs of prepared $BiFeO_3$ powder calcined at (a) 450 °C (b) 550 °C (c) 650 °C (d) 750 °C for 4 h

Aspect of Physicochemical Measurement of the Prepared $BiFeO_3$ Powder Calcined at 550 °C for 4 h by Sol-gel Method

The physicochemical properties of prepared $BiFeO_3$ powder calcined at 550 °C for 4 h by sol-gel method were pH, moisture, bulk density, porosity and surface area (Table 4). The sample showed nearly neutral (pH~ 6.80) and the moisture percent and bulk density were 0.11 % and 1.25 g cm^{-3}. So, it was found that the lesser the moisture percent the better the crystallinity. The porosity and surface area of the sample indicated 85 % and 342 m^2 g^{-1}. Thus, the large surface area and porosity revealed the good nanoparticles for photodegradation, electrical application (semiconductors), optical devices and electrochemical cells.

Table 4 Physicochemical Properties of Prepared $BiFeO_3$ Powder Calcined at 550 °C for 4 h by Sol-gel Method

Sample	pH	Moisture (%)	Bulk density (g cm^{-3})	Porosity (%)	Surface area (m^2 g^{-1})
$BiFeO_3$	6.80	0.11	1.25	85	342

Conclusion

Bismuth ferrite ($BiFeO_3$) nanoparticles was successfully prepared by sol-gel method at different temperatures. The resulting nanoparticles were characterized by XRD, TG-DTA, FT IR and SEM techniques. From the characterization studies, it can be concluded that the prepared bismuth ferrite ($BiFeO_3$) nanoparticles may be useful as good adsorbent for photodegradation, semiconductor for electrical application and sensor for optical properties.

Acknowledgements

The authors would like to thank the Department of Higher Education, Yangon, Myanmar for allowing to carry out this research work. Profound gratitude is especially thankful to Ministry of Education, Myanmar and Professor Dr Ni Ni Than, Head of Department of Chemistry, University of Yangon for providing all the departmental facilities.

References

Awan, M. and Bhatti, A. (2009). "Room-temperature Multi-ferrociy in Off-Stoichiometric $BiFeO_3$ Ceramics Prepared by Melt-phase Sintering". *Nucleus*, vol. 46(4), pp. 465-471

Chunlin, F., Meng, H., Wei, C. and Xiaoling, D. (2012). "Preparation of Bismuth Ferrite Nanopowders at Different Calcination Temperatures". *J. Ceramic Processing Research*, vol. 13(5), pp. 561-564

Dwita, S. and Wijaya, M. (2016). " Synthesis of Bismuth Ferrite Nanoparticle and Single Phase by Sol-gel Process for Multiferroic Material". *ARPN. J. Engineering and Applied Sciences*, vol. 11(2), pp. 901-905

Freitas, V. F. (2013). "Structural Phase Relations in Perovskite-structured $BiFeO_3$ Based Multiferroic Compounds". *J. Adv. Ceram*., vol. 2(2), pp. 103–111

Johari, A. (2011). "Synthesis and Characterization of Bismuth Ferrite Nanoparticles". *AKGEC. J. Technol*., vol. 2(2), pp. 17-20

Nakamoto, K. (1970). *Infrared Spectra of Inorganic and Coordination Compounds.* New York: 2nd Edition, Wiley Interscience Publication

Selbach, S.M., Tybell, T., Einarsud, M.A. and Grande, T. (2007). "Size Dependent Properties of Multiferroic Bismuth Ferrite Nanoparticles". *Chem. Mater*., vol. 19(26), pp. 6478-6484

Silverstein, R.M., Webster, F.Z. and Kiemle, D.J. (2003). *Spectrometric Identification of Organic Compounds.* New York: 7th Edition, JohnWiley and Sons Inc.

INVESTIGATION ON SOME BIOACTIVITIES AND THE NUTRIENTS OF *NEPHELIUM LAPPACEUM* L. (KYET-MAUK) SEEDS

Zin Thu Khaing[1], Ye Myint Aung[2], Ei Ei Moe[3]

Abstract

Nephelium lappaceum L. (*Sapindaceae*) popularly known as Kyet-mauk in Myanmar which is one of the traditional medicinal plant. So, *N. lappaceum* (Kyet-mauk) seeds were chosen for this research work. The present research work was designated to evaluate the antioxidant, antidiabetic, antimicrobial and cytotoxic activities of *N. lappaceum* seed. The preliminary phytochemical investigation by test tube method revealed the presence of alkaloids, α–amino acids, carbohydrates, flavonoids, glycosides, organic acids, phenolic compounds, reducing sugars, saponins, starch, tannins and terpenoids. Cyanogenic glycosides and steroids were not found in *N. lappaceum* seed. Investigation on nutrients (moisture, ash, fat, protein, fiber and carbohydrate) of *N. lappaceum* seed has been carried out by AOAC method. An energy value (Kyet-mauk) seed was found to be 430.07 kcal/100 g on the basis of dried sample. The mineral contents: K, Ca, Fe, Zn, Mn, Cu, and Rb were relatively observed by EDXRF spectroscopy. Among them, potassium content of the sample was the highest (49.528 %). In the screening of the antioxidant activity by DPPH method, IC_{50} values of ethanol and watery extracts were found to be 16.34 μg/mL and 17.31 μg/mL, respectively. *In vitro* α-amylase inhibitory activity of ethanol and watery extracts was investigated by using the starch-iodine method. The percent inhibition of α-amylase activity of ethanol extract (IC_{50} = 80.58 μg/mL) and watery extract (IC_{50} = 178.86 μg/mL) indicated the superiority of ethanol extract over watery extract. The total phenol contents (TPC) of ethanol and watery extracts of *N. lappaceum* seed were determined by FCR method. The TPC contents of ethanol and watery extracts were respectively observed to be (79.88 ± 2.86 μg GAE/mg) and (30.73 ± 7.65 μg GAE/mg). The antimicrobial activities of the various crude extracts (petether, acetyl acetate, ethanol and watery extracts) of *N. lappaceum* seed sample were determined against six strains of microorganisms by agar well diffusion method. The ethanol extract showed the antimicrobial activity with the inhibition zone diameters range 10 ~ 14 mm against six microorganisms such as *B. subtilis, S. aureus, P. aeruginosa, B. pumilus, C. albicans and E. coli*. The cytotoxicity of ethanol and watery extracts of *N. lappaceum* seed were evaluated by brine shrimp cytotoxicity bioassay. The LD_{50} values of ethanol and watery extracts were $LD_{50} >\geq 1000$ μg /mL.

Keywords: *Nephelium lappaceum* L., nutritional values, antioxidant activity, α-amylase inhibition activity, antimicrobial activity, cytotoxicity

Introduction

The term “medicinal plant” includes various types of plants used in herbalism ("herbology" or" herbal medicine"). It is the use of plants for medicinal purposes, and the study of such uses. Nowadays, herb refers to any part of the plantlike fruit, seed, stem, bark, flower, leaf, stigma or a root, as well as a non-woody plant. Earlier, the term “herb” was only applied to non-woody plants, including those that come from trees and shrubs. These medicinal plants are also used as food, flavonoid, medicine or perfume and also in certain spiritual activities. Plants have been used for medicinal purposes. Traditional systems of medicine continue to be widely practiced on many accounts. Population rise inadequate supply of drugs, prohibitive cost of treatments, side effects of several synthetic drugs and development of resistance to currently used

[1] Dr, Lecturer, Department of Chemistry, University of Yangon
[2] Dr, Professor & Head, Department of Chemistry, Pathein University
[3] MSc Candidate, Department of Chemistry, University of Yangon

drugs for infectious diseases have led to increase emphasis on the use of plant materials as a source of medicines for a wide variety of human ailments. Treatment with medicinal plants is considered very safe as there is no or minimal side effects. The use of herbal is independent of any age groups and the sexes. This is the reason why herbal treatment is growing in popularity across globe. These herbs that have medicinal quality provide rational means for the treatment of many internal diseases, which are otherwise considered difficult to cure. Moreover, some plants are considered as important source of nutrition and as a result of that they are recommended for their therapeutic values (Zahid , 2016 and Thomas *et al.*,1998). The use of herbal remedies is more prevalent in patients with chronic diseases such as cancer, diabetes, asthma and end-stage renal disease (WHO, 1991).

Description and Distribution of *Nephelium lappaceum* L.

N. lappaceum known as rambutan is one of variety tropical fruit which commonly consumed in south-east Asia (Figure 1). The rambutan is a medium-sized tropical tree in the family *Sapindaceae*. It is an evergreen tree growing to a height of 12–20 m. Rambutan tree loves the tropical climates, around 22-30 ºC and is sensitive to temperatures below 10 ºC. The rambutan is native to the Malay-Indonesian region and other tropical regions of Southeast Asia. Fruit is around to oval single seeded berry (3-6 cm long and 3-4 cm broad). The leathery skin is from green to red (rarely orange or yellow). The single seed is glossy brown 1–1.3 cm, with a white basal scar. Flowers are greenish white, fragrant, very small, without petals and borne on axillary panicles. Leaves are pinnate and elliptic (Suganthi and Josephine, 2016). Trees begin flowering from March to May and August to October. Fruits mature from 15 to 18 weeks after flowering. The rambutan fruit can be used in a wide range of products including beverages, dairy products, desserts, jams and gum. It is an important commercial crop in Asia, where the fruits are consumed fresh, canned in syrup, or processed, and appreciated for its refreshing flavor and exotic appearance. There is now been a steady increase in the production of rambutan canned in syrup with an increase in the commercial production of rambutan for canning purposes (Manaf *et al*., 2013).

Botanical Aspect of *Nephelium lappaceum* L. (Kyet-mauk)

Family	-	*Sapindaceae*
Genus	-	*Nephelium* L.
Species	-	*N.lappaceum*
Botanical name	-	*Nephelium lappaceum* L.
Myanmar name	-	Kyet-mauk
English name	-	Rambutan
Part used	-	Seeds

(a)

(b)

(c)

Figure 1 Photographs of (a) Plant (b) Fruit(c) Seeds of *Nephelium lappaceum* L. (Kyet-mauk)

Medicinal Uses and Chemical Constituents of *N. lappaceum* (Kyet mauk)

The rambutan is a rich source of vitamins and minerals that aids in losing weight, strengthening bones, and also offers anti-parasitic properties. The leaves can be juiced and used for a healthy scalp. The bark is known to cure sores. In addition, it also possesses biological activities such as antioxidant and antimicrobial. The rambutan seeds are useful to enhance skin texture and to against diabetes (Sukmandari *et al*., 2017).

A single light brown rambutan seed contains the saturated and unsaturated fatty acids. The arachidic acid is saturated fatty acid. The oleic acid, monounsaturated omega-9 fatty acid reduces blood pressure, increases good cholesterol and cuts the risk of developing ulcerative colitis. The arachidonic acid, polyunsaturated omega-6 fatty acid increases protein synthesis resulting in increased aerobic capacity and muscle hypertrophy (De *et al*., 2014 and Rajasekaram *et al*., 2013).

Rambutan seeds are not poisonous and contain carbohydrate, fats, proteins, which can meet the needs of the body of nutrients. There is now a convenient source of rambutan seeds for fat extraction. The fat has been used in cooking and the manufacture of soap. The fat contains oleic and arachidic acids as the dominant fatty acids. Rambutan seed fat also has the potential for conversion into a biodiesel or fuel extender because of its high cetane index (67.1). Rambutan roots, bark and leaves have various uses in medicine and in production of dye (Manaf *et al*., 2013). Rambutan has antioxidant activity and high phenolic content. Therefore, we conducted our research to evaluate antioxidant and hypoglycemic activity of rambutan's seed extract. The aim of the research here is to study on the Myanmar traditional herbs that play a very important role in the development of new drugs. The objective of this research is to find out the potential antioxidant, anti-diabetes and antimicrobial of herbal drugs.

Material and Methods

Sample Collection and Preparation of *N. lappaceum* (Kyet-mauk)

The *N. lappaceum* (Kyet-mauk) seeds were collected from Belin Township, Mon State. The sample was identified at Department of Botany, University of Yangon. The collected samples were washed, peeled leathery skin and edible skin then the seeds were cut into small pieces, dried at room temperature and ground into powder by motor. The sample was stored in air-tight container to prevent moisture changes and other contamination.

Preliminary Phytochemical Investigation of *N.lappaceum* (Kyet-mauk) Seeds

In order to find out the types of phyto-organic constituents such as alkaloids, α-amino acids, carbohydrates, cyanogenic glycosides, flavonoids, glycosides, organic acids, phenolic compounds, reducing sugars, saponins, starch, steroids, tannins, and terpenoids in the sample, preliminary phytochemical tests were carried out according to the appropriate methods. Various crude extracts (pet-ether, ethyl acetate and ethanol)of *N. lappaceum* were prepared for TLC screening, which were loaded on the precoated TLC silica gel plate and the chromatography was carried out by using an appropriate standard solvent system for *N. lappaceum* . The developed chromatograms were first inspected under UV-254 nm and 365 nm light and then sprayed with detecting reagents to classify the compounds present and their functional groups.

Qualitative Elemental Analysis by Energy Dispersive X-ray Fluorescence (EDXRF) Spectrometry

About 1 g of dried sample was fabricated into the pellet. The sample was placed in the sample chamber of EDX-720 spectrometer that can measure the sixteen samples at the same time. The chamber was pumped up to vacuum. The pressure was about 88 pa and the detector temperature is about 170 °C. Therefore, liquid nitrogen needs to be added at the time of analysis. Rhodium target was used in (Shimadzu EDX-720) spectrometer Universities' Research Center, University of Yangon. Each sample was run for a counting time of about 100 seconds and the spectrum obtained was stored using EDX-720 software (Griken, 1993).

Determination of Nutrients of *N. lappaceum* (Kyet-mauk) Seeds

Nutritional values such as moisture content, ash content, fat content, fiber content, protein content, carbohydrate content and energy value of the selected sample were determined by AOAC method (AOAC, 2002).

Preparation of Ethanol and Watery Extracts from *N. lappaceum* (Kyet-mauk) Seeds

The dried powder sample (100 g) was percolated with 95% ethanol (500 mL) for one week and filtered. This procedure was repeated for three times. The combined filtrate containing plant constituents were evaporated under reduced pressure by means of a rotary evaporator. Consequently, 95% ethanol soluble extract was obtained. The 95 % ethanol extract was then partitioned with pet-ether (60-80 °C) (500 mL) by using separatory funnel. The pet-ether fraction was removed under reduced pressure in a rotary evaporator. The pet-ether extract was obtained. The defatted residue was then extracted 3 times with 95 % ethanol (500 mL) for one week by percolation. Removal of the solvent from combined ethanol fractions provided ethanol crude extract. Watery extract of three samples was prepared by boiling 100 g of sample with 500 mL of distilled water for 6 h and filtered. It was repeated three times and the filtrates were combined followed by heating on water bath and sand bath to give watery extract. Each extract was stored in refrigerator for screening of biological activities.

Determination of Antioxidant Activity of Ethanol and Watery Extracts of *N. lappaceum* (Kyet-mauk) Seeds by DPPH Free Radical Scavenging Assay

The free radical scavenging activity of crude extracts of *N. lappaceum* (Kyet-mauk) seeds was measured by using DPPH free radicals scavenging assay (Marinova and Batchvarov, 2011). DPPH radical scavenging activity of ethanol and watery extracts of Kyet-mauk seeds was determined by UV-visible spectrophotometer. The control solution was prepared by mixing 1.5 mL of 0.002 % DPPH solution and 1.5 mL of ethanol in the brown bottle. The blank solution was prepared by mixing the sample solution 1.5 mL with ethanol 1.5 mL.The sample solution was also prepared by mixing 1.5 mL of 0.002 % DPPH solution and 1.5 mL of test sample solution with the concentrations of 40, 20, 10, 5, 25, 1.25 μg/mL. These bottles were incubated at room temperature and were shaken on shaker for 30 min. After 30 min, these solutions were measured at 517 nm and the percentage of radical scavenging activity (% RSA) was calculated by the following equation.

$$\% \text{ RSA} = [\{(A_{DPPH} - A_{sample}) - A_{blank}\} / A_{DPPH}] \times 100$$

Where, % RSA = % radical scavenging activity of test sample

A_{DPPH} = absorbance of DPPH in EtOH solution

A_{sample} = absorbance of sample+ DPPH solution

A_{blank} = absorbance of sample + EtOH solution

The antioxidant power (IC_{50}) is expressed as the test substances concentration (μg/mL) that result in a 50 % reaction of initial absorbance of DPPH solution and that allows to determine the concentration. IC_{50} (50 % inhibition concentration) values were calculated by linear regressive excel program.

Determination of α-Amylase Enzyme Inhibition Activity of Ethanol and Watery Extracts of *N. lappaceum* (Kyet-mauk) Seeds and Standard Acarbose

Alpha-amylase activity can be measured for *in-vitro* by hydrolysis of starch in the presence of α-amylase enzyme. This process was quantified by using iodine, which gives blue colour with starch. The reduced intensity of blue colour indicates the enzyme-induced hydrolysis of starch into monosaccharide. If the substance/extract possesses α-amylase inhibitory activity, the intensity of blue color will be more. In other words, the intensity of blue colour in test sample is directly proportional to α-amylase inhibitor activity (Mandal and Reddy, 2016). Alpha-amylase activity was carried out by starch-iodine method. 10 μL of α-amylase solution (0.025 mg/mL) was mixed with 390 μL of phosphate buffer (0.02 M containing 0.006 M NaCl, pH 7.0) with different concentrations of extracts (400, 200, 100, 50, 25 and 12.5 μg/mL). After incubation at 37 °C for 10 min, 100 μL of starch solution (1 %) was added, and the mixture was re-incubated for 1 h. Next, 0.1 mL of 1 % iodine solution was added, and after adding 5 mL distilled water, the absorbance was taken at 565 nm. Sample, substrate and α-amylase blank determinations were carried out under the same reaction conditions. Inhibition of enzyme activity was calculated as (%) = (A-C) ×100/ (B-C), where, A = absorbance of the sample, B = absorbance of blank (without α-amylase), and C = absorbance of control (without starch).

$$\% \text{ Inhibition} = \frac{A_{Sample} - A_{Control}}{A_{Blank} - A_{Control}} \times 100$$

Where, A_{Sample} = absorbance of test sample solution

$A_{Control}$ = absorbance of control solution

A_{Blank} = absorbance of blank solution

Determination of Total Phenolic Content of *N. lappaceum* (Kyet-mauk) Seeds by FCR Method

One of the antioxidative factors, total phenolic content (TPC) was measured by spectrophotometrically according to the Folin-Ciocalteu method (Reynertson, 2007). Frist, 1 mL of different concentration of Gallic acid solution (20, 10, 5, 2.5, 1.25 and 0.625 μg/mL) was mixed with 5 mL of diluted F-C reagent (FCR: H_2O, 1:10) and incubated for 5 min. To each tube, 4 mL of 1M sodium carbonate was added and the tubes were kept in room temperature for 15 min and the UV absorbance of reaction mixture was read at λ_{max} 765 nm. A standard curve

was prepared by plotting the absorbance against concentration of Gallic acid. The phenolic content in each sample was estimated by Folin–Ciocalteu method. Each extract (1 mg) was mixed with 1 mL of distilled water. To this, 5 mL of F-C reagent (1:10) was added and incubated for 5 min. To each tube, 4 mL of 1M sodium carbonate was added and the tubes were kept in room temperature for 15 min and the UV absorbance of reaction mixture was read at λ_{max}765 nm. The blank solution was prepared as the above procedure by using distilled water instead of sample solution. Total phenolic content was estimated as µg Gallic acid equivalents (GAE)/mL of different extracts.

Determination of Antimicrobial Activity of Various Crude Extracts of *N.lappaceum* (Kyet-mauk) Seeds

Antimicrobial activities of various crude extracts such as PE, EtOAc, EtOH, and H_2O were investigated by agar well diffusion method at the Pharmaceutical Research Department (PRD), Ministry of Industry, Yangon.

The agar well diffusion method was used to test the antimicrobial action of the extracts on 24 h broth culture of the organisms used. Nutrient agar (4.6 g) and agar (1 g) were dissolved in 20 mL distilled water. The resulting nutrient agar medium was autoclaved at 121°C for 15 min and cooled in water bath (40 °C). After cooling, bacteria suspension of each bacteria strain (0.02 mL) was added and poured into Petri dishes. The seeded plates were allowed to dry in room temperature for 10 min. A standard cork borer of 10 mm diameter was used to cut uniform wells on the surface of the solid medium. The extracts of PE, EtOAc, EtOH, and H_2O (1 g) of each were dissolved in 1 mL of their respective solvent. Each of the different crude extracts (0.15 mL) were filled into the wells and incubated at 37 °C for 18-24 h. Antimicrobial activity in terms of zones of inhibition (mm) was recorded after 24 h of incubation (Lawrence *et al.*, 2009).

Determination of Cytotoxicity by Brine Shrimp Lethality Bioassay of *N.lappaceum* (Kyet-mauk) Seeds

Artificial sea water (9 mL) and (1 mL) of different concentrations of samples and standard solutions were added to each chamber of ice tray. Alive brine shrimp(10 nauplii) were taken with pasteur pipette and placed into each chamber. They were incubated at room temperature about 24 h. After 24 h, the number of dead or survive brine shrimp was counted and 50 % of lethality dose (LD_{50}) was calculated (Sahagal *et al*., 2010).

Results and Discussion

Phytochemical Constituents of *N. lappaceum* (Kyet-mauk) Seeds

According to the phytochemical tests in order to know their types present in the selected sample, alkaloids, α-amino acids, carbohydrates, flavonoids, glycosides, phenolic compounds, reducing sugars, saponins, starch, tannins, terpenoids and organic acids were found to be present. Cyanogenic glycosides and steroids were absent. Cyanogenic glycosides act as selective cytotoxic agents. Longer period of intake of the small number of cyanogenic glycosides in daily food have led to chronic toxicity.

Nutrients in *Nephelium lappaceum* L. (Kyet-mauk) Seeds

Nutrients in (Kyet-mauk) seeds sample were investigated by standard AOAC methods. The nutrients 7.30 % of moisture, 1.82 % of ash, 30.53 % of fat, 11.71 % of protein, 21.53 % of fiber, 27.11 % of carbohydrate and energy value 430.07 cal /100 g

were detected. So, rambutan seeds are not poisonous and contain carbohydrate, fats, proteins, which can meet the needs of the body of nutrients.

Elements Present in *N. lappaceum* (Kyet-mauk) Seeds by Energy Dispersive X ray Fluorescence (ED-XRF) Spectrometry

X-ray spectroscopy permits simultaneous analysis of light elements to heavy elements. Simadzu EDX-720 spectrometer can analyze the elements from Na to U under vacuum condition. In this work, relative abundance of elements present in seeds of *N.lappaceum* was determined by EDXRF spectrometer. K (49.528 %), Ca (38.818 %), Fe (4.651 %), Zn (2.264 %), Mn (1.892 %), Cu (1.752 %), and Rb (1.095 %) were observed. Among them, potassium content of the sample was the highest (49.528 %). High potassium decreases the risk of stroke, lower blood pressure, protects against loss of muscle mass, preserves bone mineral density and reduces the formation of kidney stones.

Antioxidant Activity of Ethanol and Watery Extracts of *N.lappaceum* (Kyet-mauk) Seeds by DPPH Radical Scavenging Assay

The antioxidant activity of ethanol and watery extracts of *N.lappaceum* seeds was evaluated by DPPH (1, 1-diphenyl-2-picryl-1-hydrazyl) radical scavenging assay. According to the procedure as described by (Marinova and Batchvarou, 2011), ascorbic acid was used as standard. Colorimetry with DPPH, a stable free radical, has been reported as a simple method for evaluation of the free radical scavenging activity. It tends to capture hydrogen from the antioxidant. Due to its free radical, the ethanolic DPPH solution is violet and absorbs at 517 nm. The colour changes upon neutralization of this free radical from violet to pale yellow by daylight. The decolouration of the initial colour is proportional to the test substances having anti-radicalizing power. Preliminary test for radical scavenging activity by DPPH method based on the change in colour of crude extracts. The absorbance of different concentrations (40, 20, 10, 5, 2.5, 1.25 μg/mL) of tested samples were measured at maximum absorption of wavelength 517 nm by using UV-7504 spectrometer. Absorbance was measured in triplicates for each solution. Ethanol extract (IC_{50} = 16.34 μg/mL) was found to be more potent than watery extract (IC_{50} = 17.31 μg/mL) comparing to standard ascorbic acid (IC_{50} = 2.25 μg/mL). The higher the antioxidant activity of ethanol extract of Kyet-mauk seeds possessed due to the lower IC_{50} value. Ethanol extract of Kyet-mauk seeds was found to be lower effective than standard ascorbic acid (IC_{50} = 2.25 μg/mL) (Table 1 and Figures 2 and 3).

Table 1 Percent Radical Scavenging Activity and IC_{50} Values of Ethanol and Watery Extracts of *N.lappaceum* (Kyet-mauk) Seeds and Standard Ascorbic Acid

Samples	% Inhibition (Mean ± SD) In Different Concentration (µg/mL)						IC_{50} (µg/mL)
	1.25	2.5	5	10	20	40	
Ethanol extract	7.550 ± 1.410	10.540 ± 0.403	26.070 ± 1.410	40.880 ± 1.007	55.270 ± 5.641	61.540 ± 0.403	16.34
Water extract	7.410 ± 0.403	9.690 ± 0.806	21.510 ± 0.202	39.740 ± 0.604	52.710 ± 0.806	59.120 ± 0.604	17.91
Ascorbic acid	34.360 ± 0.000	53.860 ± 0.000	62.380 ± 0.000	66.870 ± 0.000	72.750 ± 0.010	82.500 ± 0.000	2.25

IC_{50} = 50 % Inhibition Concentration

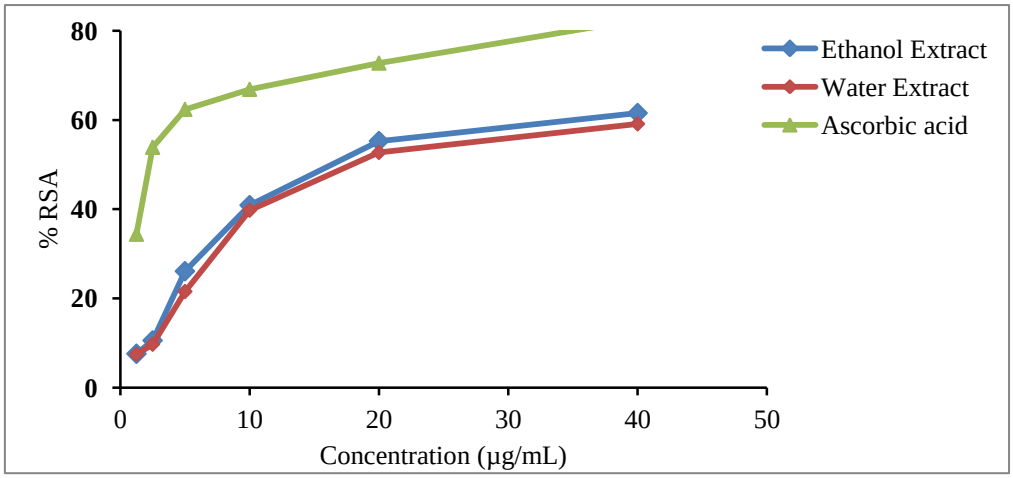

Figure 2 %RSA of ethanol and watery extracts of *N.lappaceum* (Kyet-mauk) seeds and standard ascorbic acid

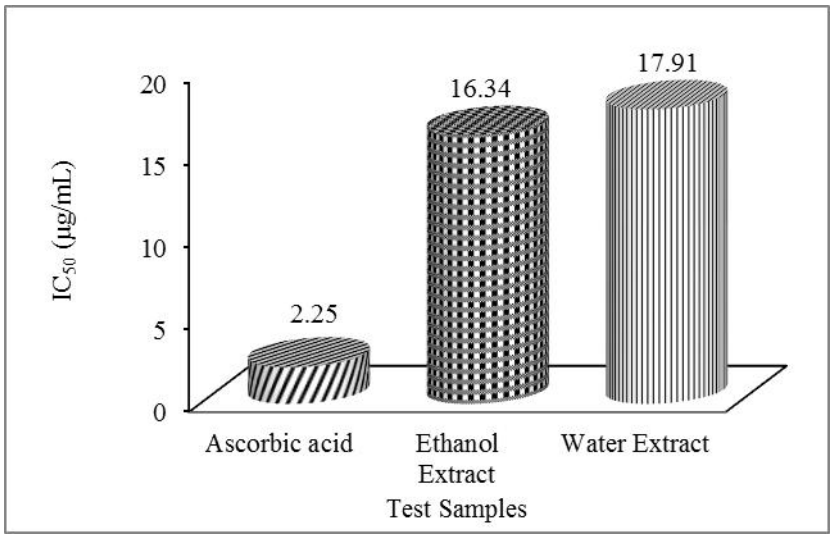

Figure 3 A bar graph of IC_{50} values of ethanol and watery extracts of *N.lappaceum* (Kyetmauk) seeds

α-Amylase Enzyme Inhibition Activity of Ethanol and Watery Extracts of *N. lappaaceum* (Kyet-mauk) Seeds

In the present study, α-amylase inhibitory activities of ethanol and watery extracts of *N.lappaaceum* (Kyet-mauk) seeds were investigated. The percentage inhibition of the α-amylase by ethanol and watery extracts were studied in a concentrations of 400, 200, 100, 50, 25, 12.25 µg/mL respectively. α-Amylase activity was measured *in vitro* by hydrolysis of starch in presence of α-amylase enzyme. This process was quantified by using iodine, which gives blue colour with starch. The reduced intensity of blue colour indicates the enzyme-induced hydrolysis of starch into monosaccharides. If the substance/extract possess α-amylase inhibitory activity, the intensity of blue colour will be more. In other words, the intensity of blue colour in test sample is directly proportional to α-amylase inhibitory activity. The treatment goal of diabetic patients is to maintain near normal levels of glycemic control, in both fasting and post-prandial conditions (Matsui *et al*., 2001). α-Amylase catalyzed the hydrolysis of α-1, 4-glycosidic linkage of starch, glycogen and various oligosaccharides. Alpha-glycosidase further breaks down the disaccharides to simple sugars, readily available for intestinal absorption. The inhibition of their activity in the digestive tract of humans is considered to be effective tool to control diabetes. In addition, these effects may lead to diminish absorption of monosaccharides (Hara and Honda *et al.*, 1990). Therefore, effective and nontoxic inhibitors of alpha-amylase and alpha-glucosidase have long been sought.

The percent inhibitions of α-amylase activity of ethanol and watery extracts were 80.58 µg/mL and 178.86 µg/mL that indicated the superiority of ethanol extract over watery extract (Table 2 and Figures 4 and 5). These extracts exhibited lower activity than standard acarbose (IC_{50} = 13.59 µg/mL). Inhibition of α-amylase could lead to reduction in postprandial hyperglycemia in diabetic condition (Mandal *et al*., 2016).

Table 2 α-Amylase Enzyme Inhibitions and IC_{50} Values of Ethanol and Watery Extracts of *N.lappaaceum* (Kyet-mauk) Seeds and Standard Acarbose

Sample	% Inhibition (mean ± SD) in different concentration (µg/mL)						IC_{50} (µg/mL)
	12.5	25	50	100	200	400	
Water extract	17.647 ± 0.003	21.307 ± 0.008	34.756 ± 0.006	39.809 ± 0.006	52.727 ± 0.026	56.604 ± 0.025	178.86
Ethanol extract	21.929 ± 0.004	35.315 ± 0.008	41.667 ± 0.009	55.285 ± 0.008	65.000 ± 0.012	71.569 ± 0.001	80.58
Std-Acarbose	48.110 ± 2.270	69.800 ± 1.900	73.150 ± 0.630	83.000 ± 4.110	90.160 ± 4.430	93.060 ± 2.210	13.59

IC_{50} = 50 % Inhibition Concentration

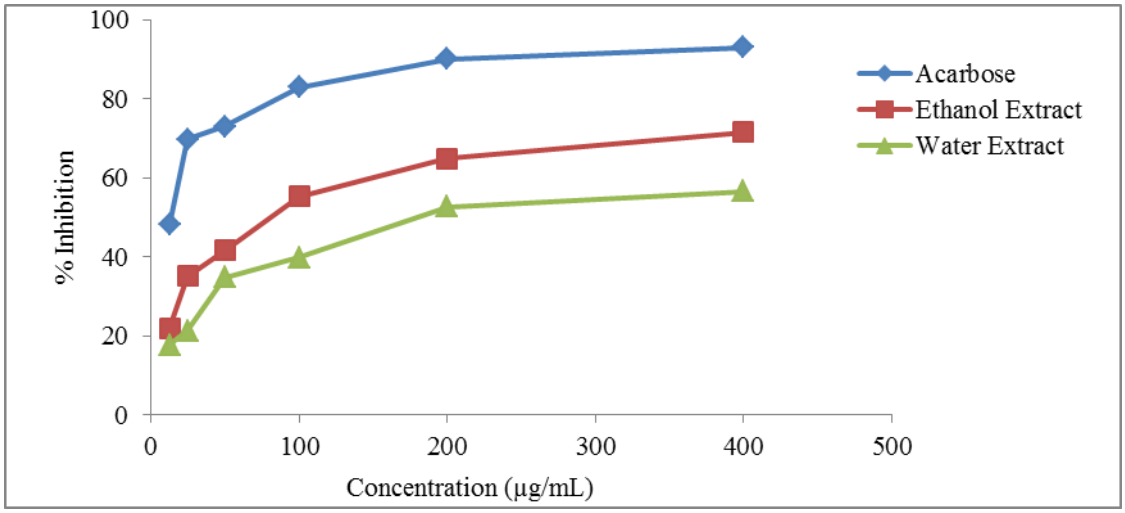

Figure 4 α-Amylase enzyme inhibition activities of watery and ethanol extracts of *N.lappaaceum* (Kyet-mauk) seeds and standard acarbose

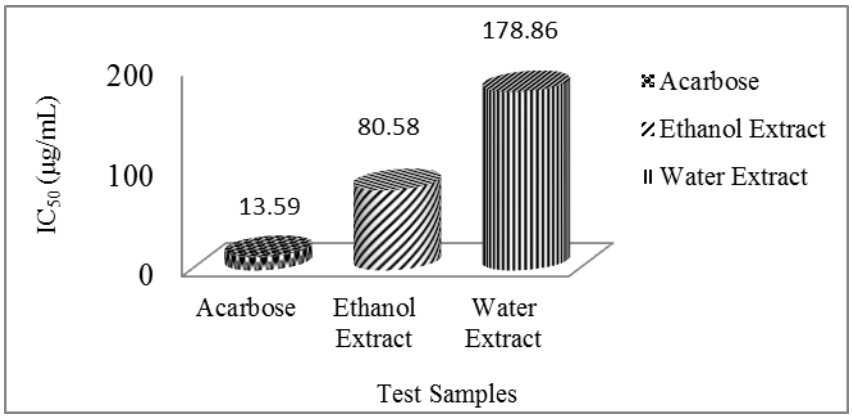

Figure 5 A bar graph of IC_{50} (µg/mL) of watery and ethanol extracts of *N.lappaaceum* (Kyet-mauk) seeds and standard acarbose

Total Phenol Contents of Ethanol and Watery Extracts of *N. lappaceum* (Kyet-mauk) Seeds by Folin-Ciocalteu Reagent (FCR)

In this study, the total phenolic contents of (Kyet-mauk) seeds were measured at 765 nm colorimetrically by Folin-Ciocalteu method. The TPC content of ethanol extract (79.88 ± 2.86 µg GAE/mg) was found to be higher than watery extract (30.73 ± 7.65 µg GAE/mg). Several studies have described the antioxidant properties of medicinal plants which are rich in phenolic compounds. They possessed biological properties such as antigaging, anticarcinogen and antiflammation (Zainol *et al*., 2003). These correlations indicated that high total phenol contents in ethanol extract contributed to high in antiradical scavenging activity and α-amylase inhibition activity of ethanol extract (Table 3 and Figure 6).

Table 3 Total Phenol Content (TPC) of Ethanol and Water Extracts of *N. lappaaceum* (Kyet-mauk) Seeds

No.	Extracts	TPC (µg GAE/mg ± SD)
1	Ethanol extract	79.880 ± 2.860
2	Water extract	30.730 ± 7.650

GAE = Gallic acid equivalent

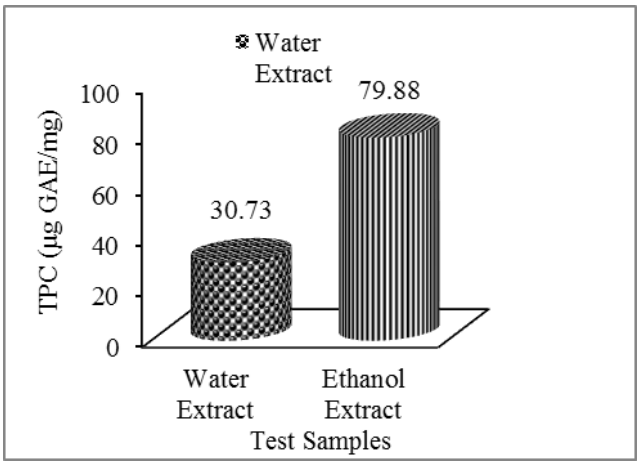

Figure 6 A bar graph of total phenolic contents of ethanol and watery extracts of *N. lappaaceum* (Kyet-mauk) seeds

Antimicrobial Activity of Various Crude Extracts of *N. lappaceum* (Kyet-mauk) Seeds by Agar Well Diffusion Method

Antimicrobial activities of *N. lappaceum* (Kyet-mauk) seeds crude extracts such as PE, EtOAc, EtOH and H_2O were investigated by agar well diffusion method. The microorganisms tested were *B. subtilis, S. aureus, P. aeruginosa, B. pumilus, C. albicans and E. coli.* The diameter of agar well was 10 mm. When comparing different antimicrobial agents to known concentration, the inhibitory zone diameter is taken as a measure of antimicrobial activity. The larger the diameter, the higher the antimicrobial activity of the test agents. EtOH extract showed the antimicrobial activity with the inhibition zone diameter range between 10~14 mm against six microorganisms such as *B. subtilis, S. aureus, P. aeruginosa, B. pumilus, C. albicans and E. coli*. EtOAc extract inhibited all microorganisms. Water extract inhibited five microorganisms except *E. coli*. PE extract showed the activity on *B. subtilis*, *S. aureus*, *P. aeruginosa, C. albicans* and non-activity on other microorganisms. Ethanol extract had more antimicrobial activity than EtOAc, watery and PE extracts (Table 4).

Table 4 Inhibition Zone Diameter of Various Crude Extracts of *N. lappaceum* (Kyet-mauk) Seeds

No.	Microorganisms	Diameter of inhibition zone (mm)			
		PE extract	EtOAc extract	EtOH extract	H_2O extract
1.	*Bacillus subtilis*	11 (+)	11 (+)	11 (+)	11 (+)
2.	*Staphylococcus aureus*	11 (+)	11 (+)	12 (+)	12 (+)
3.	*Pseudomonas aeruginosa*	11 (+)	12 (+)	13 (+)	14 (+)
4.	*Bacillus pumilus*	−	11 (+)	11 (+)	12 (+)
5.	*Candida albicans*	11 (+)	11 (+)	12 (+)	11 (+)
6.	*Escherichia coli*	−	11 (+)	12 (+)	−

Diameter of agar well = 10 mm 10 mm ~ 14 mm (+)

Cytotoxicity of Ethanol and Watery Extracts of *N. lappaceum* (Kyet-mauk) Seeds by Brine Shrimp Lethality Bioassay

The brine shrimp assay is very useful tool for the isolation of bioactive compounds from plant extracts (Ramachandran, 2011). The method is attractive because it is very simple, inexpensive and low toxin amounts are sufficient to perform the test in the micro well scale. It is considered as useful tool for preliminary assessment of toxicity. It has also been suggested for screening pharmacological activities of plant extracts (Prashith, 2012).

The ten nauplii of brine shrimp (*Artemiasalina*) are used for each chamber. The cytotoxicity effect was expressed as LD_{50} values (50% Lethality Doses). The percentage of dead brine shrimp in 1000, 100, 10, 1 µg/mL concentration for watery extract were 36.67 %, 26.67 %, 16.67 %, 6.67 % and ethanol extract were 46.67 %, 30.00 %, 23.33%, 13.33%. LD_{50} values of both watery and ethanol extracts were $LD_{50} > 1000$ µg/mL(Table 5). Standard Caffeine did not show cytotoxicity until 1000 µg/mL concentration whereas cytotoxicity of standard $K_2Cr_2O_7$ was LD_{50} = 55.01 µg/mL. According to results, the rambutan seeds are not poisonous until 1000 µg/mL concentration. The LD_{50} was reported to be greater than 5000 mg kg^{-1} of extract (Rohman, 2017).

Table 5 Cytotoxicity of Different Concentration of Ethanol and Watery Extracts of *N. lappaceum* (Kyet-mauk) Seeds

Test samples	% of Dead brine shrimp in different concentration of sample				LD_{50} (µg/mL)
	1	10	100	1000	
Ethanolextract	13.33	23.33	30.00	46.67	>1000
Wateryextract	6.67	16.67	26.67	36.67	>1000
$K_2Cr_2O_7$	40.33	43.33	56.67	100.00	55.01
Caffeine	0	0	0	0	0

No. of brine shrimp = 10

Conclusion

The research finding revealed the presence of alkaloids, α–amino acids, carbohydrates, flavonoids, glycosides, organic acids, phenolic compounds, reducing sugar, saponin, starch, tannin and terpenoids. Cyanogenic glycosides and steroids were absent in Kyet-mauk seeds. The nutritional values determined by AOAC method indicated that 7.30 % of moisture, 1.82 % of ash, 30.53 % of fat, 11.71 % of protein, 21.53 % of fiber and 27.11 % of carbohydrate based on the dry weight. And also 430.07 kcal/100g of energy value was observed in Kyet-mauk seeds. The mineral contents such as K, Ca, Fe, Zn, Mn, Cu and Rb of Kyet-mauk seeds powder sample were quantitatively determined by EDXRF. Among them, the potassium content of this sample was the highest (49.528 %).

DPPH (1, 1-diphenyl-2-picrylhydrazyl) radical scavenging assay showed that ethanol extract (IC_{50} = 16.34 µg/mL) of Kyet-mauk seeds was more effective than watery extract (IC_{50} = 17.91 µg/mL) in antioxidant activity and it was also observed to be comparable with the standard ascorbic acid (IC_{50} = 2.25 µg/mL). The percent inhibition of *in vitro* α-amylase inhibition activity of ethanol and watery extracts of (Kyet-mauk) seeds was investigated by starch-iodine method. The IC_{50} values of ethanol and watery extracts were found to be 80.58 µg/mL and 178.86 µg/mL respectively. These activities of extracts were found to be lower than that of standard acarbose (IC_{50} = 13.59 µg/mL). The total phenol content (TPC) of ethanol and watery extracts of Kyet-mauk seeds were determined by FCR method. According to the results, the superiority of antioxidant and α-amylase inhibition activities of ethanol extracts over watery extracts of Kyet-mauk seeds was correlated with the total phenol content of ethanol extract.

EtOH and EtOAc extracts showed the antimicrobial activity with the inhibition zone diameter range between 10 ~ 14 mm against all six microorganisms - *Bacillus subtilis, Staphylococcus aureus, Pseudomonas aeruginosa, B. pumilus, C. albicans and E. coli*. Water extract inhibited five microorganisms except *E. coli.* PE extract showed the activity on *B. subtilis, S. aureus, P. aeruginosa, C. albicans* and non-activity on other microorganisms.

According to cytotoxicity test it was observed that the LD_{50} values of both ethanol and watery extracts were LD_{50}>1000 µg/mL. Therefore, the Kyet-mauk seeds fat and oil extracts are practically non-toxic.

Since previous and present studies suggest that *N. lappaceum* L. (Kyetmauk) seeds have shown potential as sources of natural antioxidants, further studies need to be directed to isolate and characterize antioxidant active compounds from the extracts which could be responsible for antioxidant and antidiabetic activities. Finally, the present study provided to justify the traditional claim of herbs for antioxidant, antimicrobial and antidiabetic activities. This plant may essentially contain herbal bioactive compounds, inhibitory enzyme activities and some bioactivities.

Acknowledgements

The authors would like to thank the Department of Higher Education, Ministry of Education, Yangon, Myanmar, for the permission of doing this research and also to the Myanmar Academy of Arts and Science for allowing the present of this paper.

References

AOAC. (2002). "Official Method of Analysis". *International Food Research Journa*l, vol.17, pp. 423-432

De, S. P. S., Luben, R., Shrestha, S. S., Khaw, K. T. and Hart, A. R (2014). "Dietary Arachidonic and Oleic Acid Intake in Ulcerative Colitis Etiology: A Prospective Cohort Study Using 7 – day Food Diaries". *International Food Research Journal, vol.* 26 (1), pp. 11-8

Griken, R. and Markowictz, E. (1993). *Quatification in XRD Analysis of Internal Thickness Samples.* New York: 1st Ed., Marcel Dekken Inc., pp. 339-358

Hara, Y., and Honda, M. (1990). "The Inhibition of α-Amylase by Tea Polyphenols". *Agric. Biol. Chem.*, vol. 54, pp. 1939-1945

Lawrence, R., Priyanka, T. and Ebenezer, J. (2009). "Isolation, Purification and Evaluation of Antibacterical Agents from *Tamarindus indica* L. (Magyi) Pulp". *J. Microbial*, vol. 40, pp. 906-915

Manaf, Y. N. A., Marikkar, J. M. N., Long, K. and Ghazali, H. M. (2013). "Physico-Chemical Characterization of the Fat from Red-Skin Rambutan (*Nephelium lappaceum* L.) Seed*", Journal of Oleo Science*, vol. 62 (6), pp. 335-343

Mandal, A. and Reddy, P. J. M. (2016). "*In vitro* Alpha Amylase Inhibitory Activity of Ethanol and Hot Water Extracts of Polyherbal Formulation". *World Journal Pharmaceutical Research*, vol. 5 (1), pp. 968-971

Matsui, T., Ueda, T. Oki, Terahara, K., and Matsumoto, N. (2001). "Glycosidase Inhibitory Action of Natural Acylated Anthocyanins". *J. Agri. Food Chem*., vol. 49, pp. 1948-1951

Marivona, G. and Batchvarov, V. (2011). "Evaluation of the Methods for Determination of the Free Radical Scavenging Activity by DPPH". *Bulg. J. Agric. Sci.*, vol. 17 (1), pp. 11-24

Prashith, K. T. R., Raghavendra, L. and Vinayaka, K. S. (2012). "Cytotoxic Activity of Croton gibsonianus Nimm. Grah". *Scienc, Technology and Arts Research Journal*, vol.1 (1), pp. 57-59

Rajasekaram, A., Ganesam, S., Kamini, N. C., Lavanya, C., Yoon, L. and Oh, H. S. (2013). "Anti-nocieptive, CNS, Antibacterial and Antifungal Activities of Methanol Seed Extracts of *Nephelium laplpaceum* L.". *Journal of Oriental Pharmacy and Experiment Medicine*, vol.13 (2), pp. 149-157

Ramachandran, S., Vamsikrishma, M., K. V. Gowthami, K. V., Heera, B. and Dhanaraju, M. D. (2011). "Assessment of Cytotoxicity Activity of Agave cantula Using Brine Shrimp (*Artemia salina*) Lethality Bioassay". *Asian Journal of Scientific Research*, vol. 4 (1), pp. 90-94

Reynertson, K. A. (2007). "*Phytochemical Analysis of Bioactive Constiuents from Edible Myrtaceal Fruits*", PhD (Dissertation), New York, The City University, vol. 98

Rohman, A. (2017). "Physico-chemical Properties and Biological Activities of Rambutan (*Nephelium lappaceum* L.) Fruit". *Research Journal of Phytochemistry*, vol. 11, pp. 66-73

Sahagal, G., Ramanathan, S., Sasidharan, S., Mordic, S. M. S., Ismailu, S. (2010). "A Cute Oral Toxicity Studies on *Swieteniamahagoni* (Linn). Jacq. Seed Methanolic Extract", *Pharmacognosy Res*., vol. 2, pp. 215-220

Suganthi, A. and Dr. Josephine, M. R. (2016). "*Nephelium lappaceum* L.: An Overview". *International Journal of Phamaceutical Science and Research*, vol. 1 (5), pp. 36-39

Sukmandari, N. S., Dash, G. K., Jusof, W. H. W. and Hanafi, M. (2017). "A Review on *Nephelium lappaceum* L.". *Research Journal of Pharmacy and Technology*, vol.10 (8), pp. 2819-2827

Thomas, J., Joy, P., and Skaria, P. (1998). *Medical Plants*. India: 1st Ed., Kerala, pp. 3-4

WHO. (1991). *Guidelines for the Assessment of Herbal Medicines, Programme on Traditional Medicine*. Geneva: 1st Ed., World Health Organization, pp. 91-94

Zahid., H. (2016). "Introduction and Importance of Medicinal Plants and Herbs", *World Journal of Pharmaceutical Research*, vol. 5 (9), pp. 317-326

Zainol, M. K., Hamid, A. A., Yusef, S. and R. Muse, R. (2003). "Antioxidant Activity and Total Phenolic Compounds of Leaf, Root and Petiole of Four Accessions of *Centellaasiatica* (L.) Urban". *Food Chemistry*, vol. 81, pp. 575-58

CHARACTERIZATION OF MODIFIED CHITOSAN-ALGINATE-STARCH-GLYCEROL/ SORBITOL COMPOSITE MEMBRANES AND THEIR ANTIMICROBIAL ACTIVITIESZ

Nan Yu Nwe[1], Zaw Naing[2], Khin Than Yee [3], Cho Cho[4]

Abstract

The chitosan-alginate-starch composite membranes (CAS 1- 4), modified chitosan-alginate-starch-glycerol composite membranes (CASG 1- 4) and modified chitosan-alginate-starch-sorbitol composite membranes (CASS 1- 4) were prepared by using casting and autoclaving methods. These membranes have smooth surfaces, highly transparent and pale yellow colour. The mechanical properties such as tensile strength, elongation at break and tear strength of these prepared membranes were determined. Based on the mechanical properties of the prepared composite membranes: CAS-3, CASG-2 and CASS-2 composite membranes were chosen for further studies. The selected composite membranes were characterized by FT IR and SEM analyses. SEM micrographs of composite membranes showed their significant nature of surface morphologies. The antimicrobial activities of these membranes were tested by agar well diffusion method as to apply these membranes for biomedical applications.

Keywords: composite membranes, mechanical properties, antimicrobial activities

Introduction

Chitin is the most abundant nitrogen containing biopolymers in nature and it is found widely in the shells of crabs, lobsters, krill and shrimp (Wibowo *et al.*, 2004). It is a linear polysaccharide consisting of ideally (1→4) linked 1-2-acetamido-2-deoxy- β-D- glucopyranose. Chitosan is a linear polysaccharide consisting of (1→4) linked 2-amino- 2-deoxy-β-D-glucopyranose. Chitosan is produced by alkaline N- deacetylation of chitin (Mohanty *et al.*, 2002). Chitosan is very similar to chitin. Chitosan is a white to light yellow colour, insoluble in water but it is readily soluble in dilute aqueous organic acid such as acetic acid, propionic acid, formic acid and lactic acid. The term biopolymers refer to naturally occurring large polymeric molecules, such as proteins, nucleic acids and polysaccharides, which are essential components of all living systems. The same term is also used to describe synthetic polymer prepared from identical on similar monomers or subunits to those which make up the natural polymers. Natural biopolymers are receiving much attention due to their biocompatibility and biodegradability (Peter, 1995). Biodegradation is the degradation and assimilation of organic polymers and other compounds by the action of living organisms. Sodium alginate is the common commercial algin which is the alkali metal salt of alginic acid. Alkali metal salts of alginic acid as well as the ammonium, magnesium and lower amine salts are water soluble. The soluble alginates are strongly hydrophilic colloids, yielding highly viscous solution at low concentration (Whistler *et al*., 1997). Sodium alginate fits in a divalent cation such as calcium leading to the formation of calcium alginate beads (Draget, 2000). The resultant structure of linked chains is called an egg-box model. Calcium alginate beads were synthesized through a cross-linking reaction between sodium alginate and calcium chloride solutions. The effect of calcium concentration on the bead

[1] 3- PhD, Lecturer, Department of Chemistry, Maubin University
[2] Dr, Associate Professor, Department of Chemistry, Dagon University
[3] Dr, Lecturer, Department of Chemistry, Myeik University
[4] Dr, Professor, Department of Chemistry, University of Yangon

strength and chemical stability were investigated (Gotoh *et al.,* 2004). Composites consist of two (or more) distinct constituents or phases, which when mixed together result in a material with entirely different properties from those of the individual components. Typically, a manmade composite would consist of a reinforcement phase of stiff, strong material, frequently fibrous in nature, embedded in a continuous matrix phase. As a biopolymer, it is readily procession into membranes, hollow fibers and beads as well as sponges from its aqueous acid solution. Chitosan's unique properties make it useful for a broad variety of industrial and biomedical applications. In the present study, modified chitosan-alginate-starch cross-linked composite membranes were prepared to be used for medical purposes.

Materials and Methods

Sample Collection

Chitosan sample was purchased from Shwe Poe Co. Ltd., Hlaing Tharyar Township, Yangon Region.

Starch was prepared from maize grain, *Zea mays* L. and this sample was procured from Insein Market, Yangon Region.

Preparation of Chitosan-Alginate-Starch (CAS) Composite Membranes

Chitosan-alginate-starch (CAS) composite membrane was prepared by following procedure. Firstly, chitosan 1.5 % (w/v) was dissolved in 1 % (v/v) acetic acid solution and stirred for 1 h to obtain the clear homogeneous chitosan solution. Secondly, sodium alginate 3 % (w/v) and starch solution 0.3 % (w/v) were prepared individually and then they were mixed and stirred for 30 min. Finally, chitosan solution was added to these mixture solution and stirred for 1 h. The resulting prepared solutions were poured onto melamine plates and membranes were allowed to dry at room temperature for one week to obtain the respective composite membranes. By using various concentrations of starch [0.1 %, 0.2 %, 0.3 % and 0.4 % (w/v)], chitosan-alginate-starch (CAS) composite membranes were prepared and denoted as CAS-1, CAS-2, CAS-3 and CAS-4, respectively.

Preparation of Chitosan-Alginate-Starch-Glycerol (CASG) Composite Membranes

Modified chitosan-alginate-starch-glycerol (CASG) composite membranes were prepared by using optimum amounts of 1.5 % (w/v) chitosan, 3 % (w/v) sodium alginate, 0.3 % (w/v) starch solution and 0.10 % (w/v) glycerol. The glycerol was also used as plasticizer for flexibility of membranes. The resulting modified composite solutions were autoclaved at a pressure of 0.1 MPa and 121 ± 1 ˚C for 1 h. The CASG composite membranes were prepared by using various percentages of glycerol 0.05 %, 0.10 %, 0.15 % and 0.20 % and the prepared membranes were denoted as CASG-1, CASG-2, CASG- 3 and CASG-4, respectively.

Preparation of Chitosan-Alginate-Starch-Sorbitol (CASS) Composite Membranes

Modified chitosan-alginate-starch-sorbitol (CASS) composite membranes were prepared by using optimum amounts of 1.5 % (w/v) chitosan, 3 % (w/v) sodium alginate, 0.3 % (w/v) starch solution and 0.10 % (w/v) sorbitol. The sorbitol was also used as plasticizer for flexibility of membranes. The resulting modified composite solutions were autoclaved at a pressure of

0.1 MPa and 121 ± 1 ˚C for 1 h. The CASS composite membranes were prepared by using various percentages of sorbitol 0.05 %, 0.10 %, 0.15 % and 0.20 % and the prepared membranes were denoted as CASS-1, CASS-2, CASS-3 and CASS-4, respectively.

Mechanical Properties

Determination of thickness

Thickness of the prepared CAS, CASG and CASS composite membranes was measured by using NSK Micrometer. The thickness of the membranes was measured at 5 points (center and 4 corners) using digital micrometer.

Determination of tensile strength and elongation at break

The prepared CAS, CASG and CASS composite membranes were cut off according to JIS K 7127 (1987) and the shape and dimension of test pieces were obtained. The both ends of test pieces were firmly clamped in the jaw of testing machine. One jaw was fixed and the other was moveable. The rate of moveable jaw was hold 100 mm/min. The resulting data was shown at the recorder. This procedure for tensile strength was repeated for three times. The resulting data are presented in Tables 1, 2, 3 and Figures 1, 2, 3.

Determination of tear strength

The specimen was cut off by using die-cutting. Specimen was cut with a single nick (0.05 mm) at the entire of the inner concave edge by a special cutting device using a razor blade. The clamping of the specimen in the jaw of test machine was aligned with travel direction of the grip in 100 mm/min. The order of the machine showed the highest force to tear from a specimen nicked. The procedure was repeated three times for each result. The resulting data are described in Tables 1, 2, 3 and Figures 1, 2, 3.

FT IR analysis

The selected composite membranes: CAS-3, CASG-2 and CASS-2 were analyzed by using Shimadzu, IR Prestige-21, (Japan) FT IR spectrophotometer at the Department of Chemistry, University of Yangon. The FT IR spectrometer was calibrated by blank scanning between 1000 and 4000 cm^{-1} with resolution of 1 cm^{-1} and 3 scans/ sample. The membranes were directly mounted in the light path of the spectrometer for scanning. The FT IR spectral assignment data of prepared membranes are given in Table 4 and Figure 4.

SEM analysis

The selected composite membranes CAS-3, CASG-2 and CASS-2 were characterized by scanning electron microscope, (JEOL Ltd., Japan). The sample was attached to double-sided carbon tap on the same holder and coated with 200 nm platinum with a sputter coater JFC- 1600 auto fine coater. An accelerated voltage of 20 kV and secondary electron was used, then the micrograph was taken with a JEOL Super Mini Cup Ex-54143 MSK. SEM micrographs are shown in Figures 5.

Screening of Antimicrobial Activities of the Selected Composite Membranes by Agar Well Diffusion Method

The selected composite membranes : CAS-3, CASG-2 and CASS-2 were tested with *Bacillus subtilis, Staphylococcus aureus, Pseudomonas aeruginosa, Bacillus pumilus, Candida albicans and E. coli* species to investigate the nature of antimicrobial activity. After preparing the bacteriological media, the dried membranes were placed on the agar with flamed forceps and gently pressed down to ensure proper contact. The plates were incubated immediately or within 30 min after incubation. After overnight incubation at 37 ˚C, the results observed are shown in Table 5 and Figure 6.

Results and Discussion

Aspect of Film Preparation

In the present work, the modified chitosan membranes were prepared by solution-casting from solution of chitosan in dilute acetic acid, sodium alginate solution and starch solution in various concentrations. In this process, chitosan was used as the base polymer. Chitosan as such do not have enough mechanical strength required for a wound dressing material, however, it has antimicrobial property as well as wound healing capacity. To give better tensile strength to the end product, sodium alginate and starch were added and to give flexibility to the composite glycerol and sorbitol were added. Both chitosan and sodium alginate have wound healing ability but their abilities were decreased when these two were mixed. So, starch solution was used to upgrade the healing ability. The gel forms by chemical reaction when the sodium alginate was dissolving in water. The special property of alginates is the ability to form films of sodium alginate. The colour of the chitosan-sodium alginate-starch film varied slightly to yellow with increasing chitosan content.

Mechanical Properties

The mechanical properties such as tensile strength, tear strength and elongation at break are important parameters for showing the nature of membranes. The mechanical properties of CAS 1-4, CASG 1-4 and CASS 1-4 composite membranes are shown in Tables 1, 2, 3 and Figures 1, 2, 3. The more the tensile strength of membrane, the higher is the elasticity of the membrane. This means to point out that CAS-3, CASG-2 and CASS-2 composite membranes are more flexible and more elastic than the others.

Table 1 Mechanical Properties of the Chitosan-Alginate-Starch (CAS) Composite Membranes Containing Various Concentrations of Starch

Membrane	Tensile strength (MPa)	Elongation at break (%)	Tear strength (kNm^{-1})
CAS- 1	12.50	19.00	68.00
CAS- 2	18.30	10.00	21.00
CAS- 3	19.50	38.00	32.90
CAS- 4	9.80	25.00	44.30

CAS- 1= Chitosan (1.5 %) +Alginate (3.0 %) +Starch (0.1 %) w/v
CAS- 2= Chitosan (1.5 %) +Alginate (3.0 %) +Starch (0.2 %) w/v
CAS- 3= Chitosan (1.5 %) +Alginate (3.0 %) +Starch (0.3 %) w/v
CAS- 4= Chitosan (1.5 %) +Alginate (3.0 %) +Starch (0.4 %) w/v
Thickness = ~ 0.10 mm

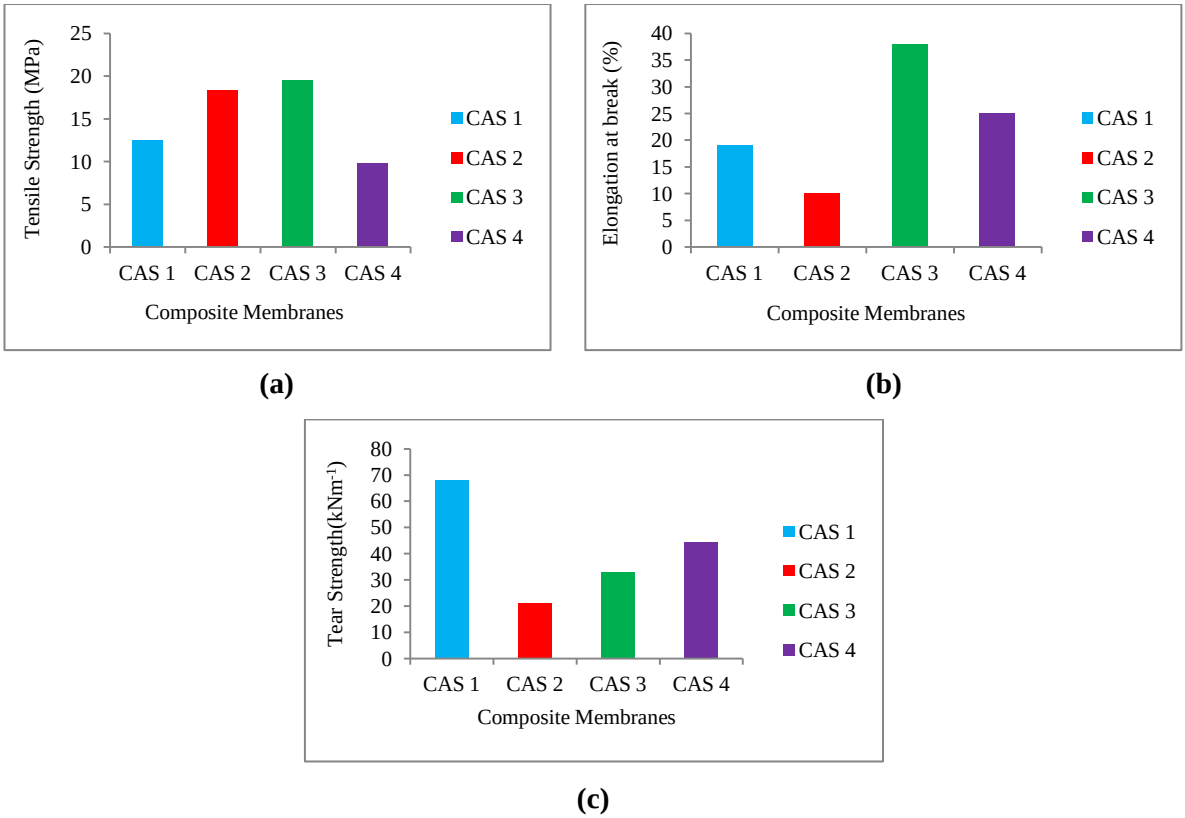

(a) **(b)**

(c)

Figure 1 Mechanical properties of the chitosan-alginate-starch (CAS) composite membranes (a) tensile strength (b) elongation at break and (c) tear strength

Table 2 Mechanical Properties of the Chitosan-Alginate-Starch-Glycerol (CASG) Composite Membranes Containing Various Concentrations of Glycerol

Membrane	Tensile strength (MPa)	Elongation at break (%)	Tear strength (kNm^{-1})
CASG- 1	16.00	13.00	15.70
CASG- 2	20.50	18.00	42.50
CASG- 3	13.20	15.00	20.00
CASG- 4	9.20	32.00	14.40

CASG- 1 = Chitosan (1.5 %) +Alginate (3.0 %) +Starch (0.3 %) +Glycerol (0.05 %) w/v
CASG- 2 = Chitosan (1.5 %) +Alginate (3.0 %) +Starch (0.3 %) +Glycerol (0.10 %) w/v
CASG- 3 = Chitosan (1.5 %) +Alginate (3.0 %) +Starch (0.3 %) +Glycerol (0.15 %) w/v
CASG- 4 = Chitosan (1.5 %) +Alginate (3.0 %) +Starch (0.3 %) +Glycerol (0.20 %) w/v
Thickness = ~ 0.10 mm

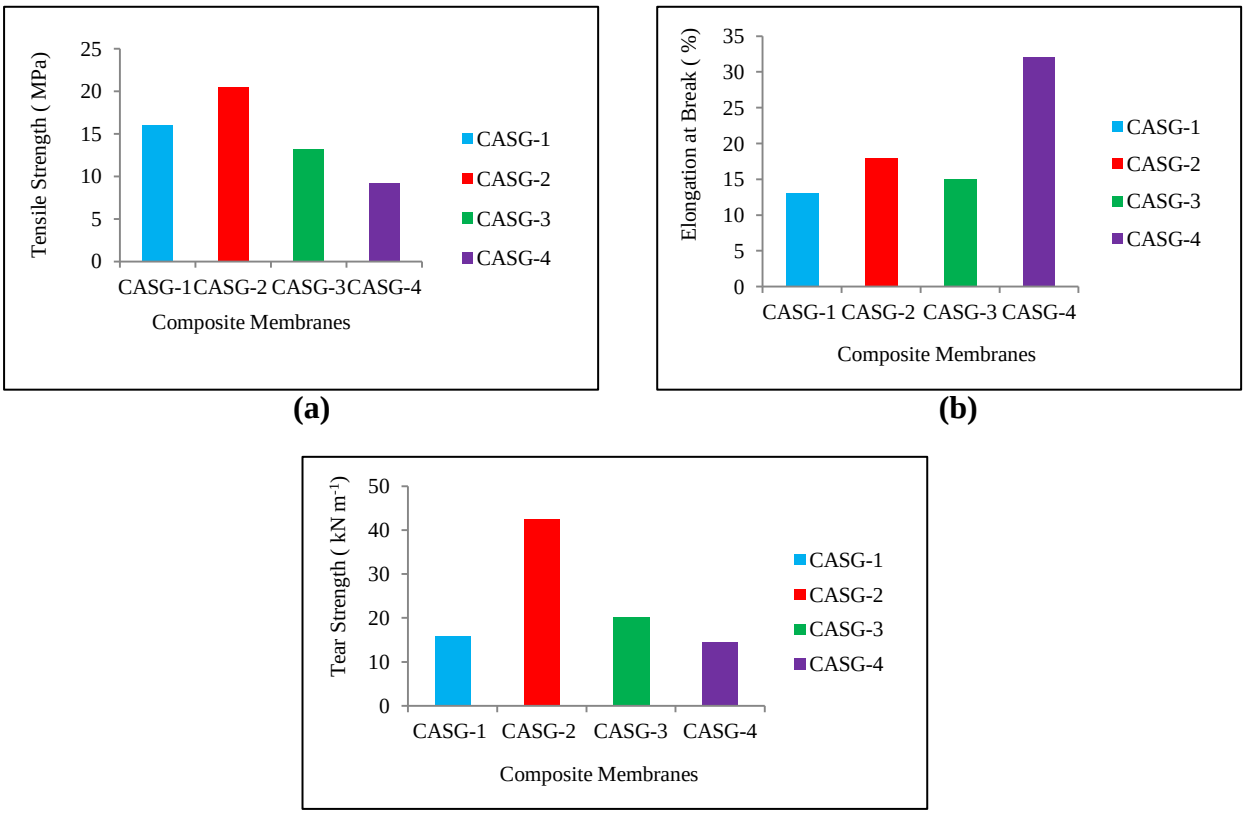

Figure 2 Mechanical properties of the chitosan-alginate-starch-glycerol (CASG) composite membranes (a) tensile strength (b) elongation at break and (c) tear strength

Table 3 Mechanical Properties of the Chitosan-Alginate-Starch-Sorbitol (CASS) Composite Membranes Containing Various Concentrations of Sorbitol

Membrane	Tensile strength (MPa)	Elongation at break (%)	Tear strength (kNm^{-1})
CASS- 1	18.80	18.00	9.00
CASS- 2	30.00	17.00	16.00
CASS- 3	10.80	16.00	17.00
CASS- 4	26.30	25.00	7.00

CASS- 1 = Chitosan (1.5 %) +Alginate (3.0 %) +Starch (0.3 %) + Sorbitol (0.05 %) w/v
CASS- 2 = Chitosan (1.5 %) +Alginate (3.0 %) +Starch (0.3 %) + Sorbitol (0.10 %) w/v
CASS- 3 = Chitosan (1.5 %) +Alginate (3.0 %) +Starch (0.3 %) + Sorbitol (0.15 %) w/v
CASS- 4 = Chitosan (1.5 %) +Alginate (3.0 %) +Starch (0.3 %) + Sorbitol (0.20 %) w/v
Thickness = ~ 0.10 mm

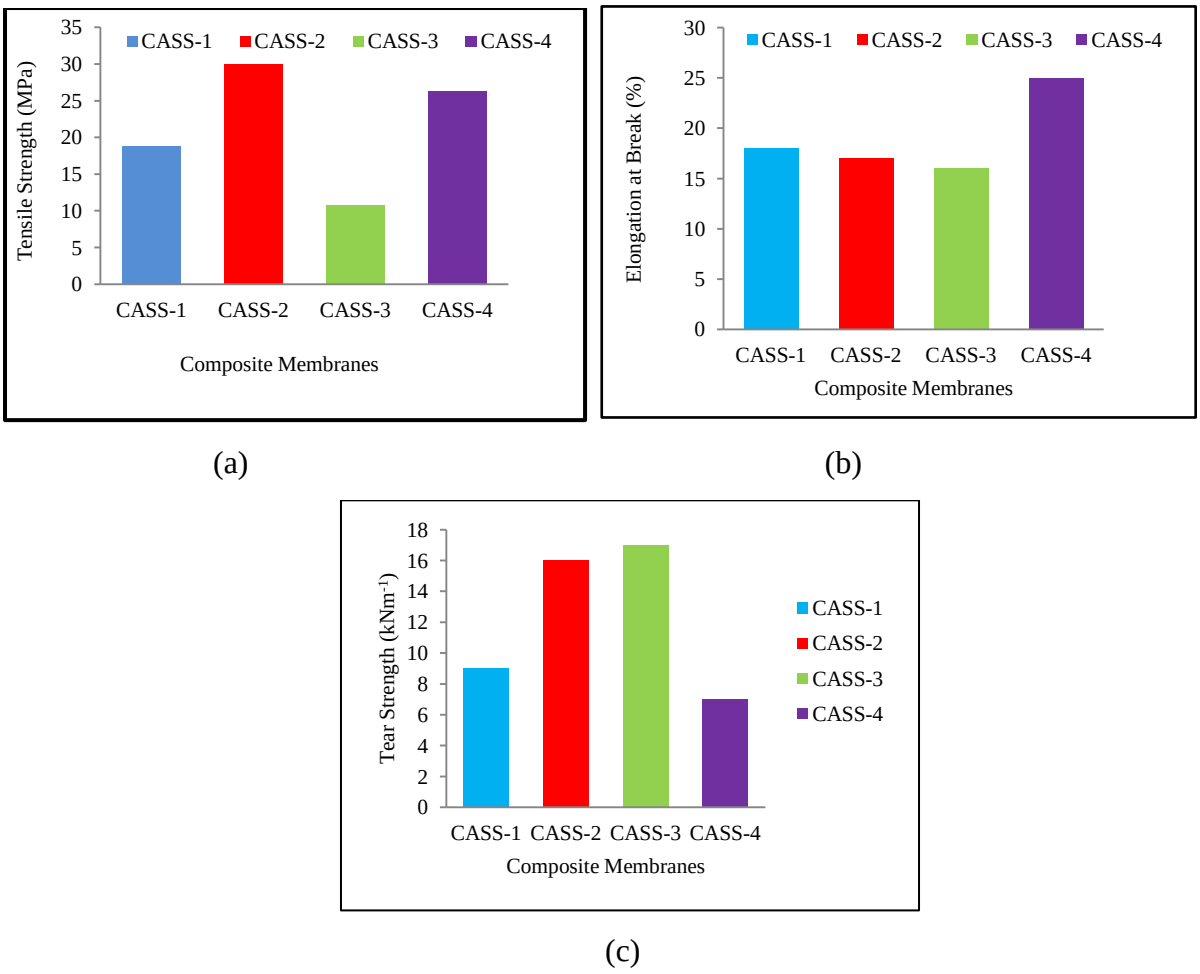

Figure 3 Mechanical properties of the chitosan-alginate-starch-sorbitol (CASS) composite membranes (a) tensile strength (b) elongation at break and (c) tear strength

Characterization of the Selected Composite Membranes

FT IR analysis

FT IR spectroscopic studies allowed to analyze the characteristic bands corresponding to the vibrations of the hydroxyl, carbonyl, amide, amine and ester groups. The FT IR spectra of selected composite membranes: CAS-3, CASG-2 and CASS-2 are shown in Figure 4 and Table 4. The broad bands at 3264, 3291, 3307 cm^{-1} in spectra of all samples are attributed to the OH stretching, which overlap with N-H stretching in the same region. The peaks at 2921, 2923 cm^{-1} are due to the C-H stretching vibration. The strong peaks at 1641, 1632, 1640 cm^{-1} are due to the O-H bending vibration. The sharp peaks at 1544, 1555, 1553 cm^{-1} range in spectra represent N-H bending in secondary amide. The sharp peaks at near 1408, 1322, 1413 cm^{-1} correspond to vibrations of COO- stretching groups. The sharp peaks at 1019, 1028, 1087 cm^{-1} range in spectra represent the C-O-C stretching vibration of primary alcohol and cyclic ether (Muzzarelli and Peter, 1973; Silverstein and Webster, 1998).

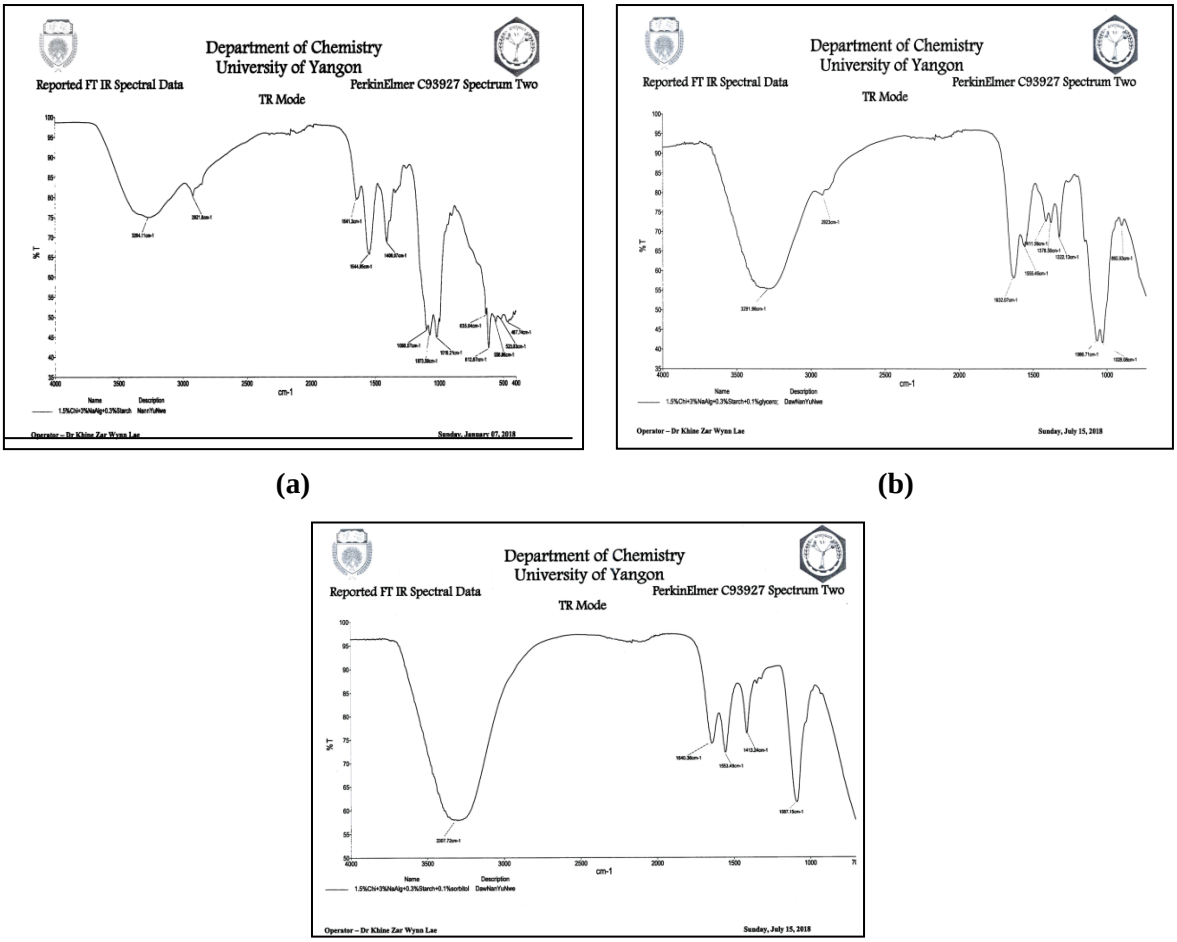

(a) **(b)**

(c)

Figure 4 FT IR spectra of the selected composite membranes (a) CAS-3 (b) CASG-2 and (c) CASS-2

Table 4 FT IR Band Assignments of the Selected Composite Membranes: (CAS-3, CASG-2 and CASS-2)

Observed wave number (cm^{-1})			* Literature wave number (cm^{-1})	Remark
CAS-3	**CASG-2**	**CASS-2**		
3264	3291	3307	3450-3225	O-H stretching and N-H stretching vibration
2921	2923	-	2940-2820	C-H stretching vibration
1641	1632	1640	1870-1650	O-H bending vibration
1544	1555	1553	1625-1430	N-H bending in secondary amide
1408	1322	1413	1425-1390	COO- stretching vibration
1019	1028	1087	1045-1015	C-O-C stretching vibration of CH_2OH, cyclic ether

*Muzzarelli and Peter, 1973; Silverstein and Webster, 1998

(b) SEM analysis

The SEM images revealed that the surface morphologies of membranes vary with the ratios of constituents in the selected composite membranes. SEM micrographs of CAS-3, CASG-2 and CASS-2 composite membranes are shown in Figure 5. The SEM micrographs indicated that CAS-3 composite membranes showed more sponge like nature and cluster form which enhances sorption property of membrane and CASG-2 composite membrane showed surface nature uniformly pores or voids and homogeneous nature and CASS-2 composite membrane showed scabrous and patchy surface morphologies.

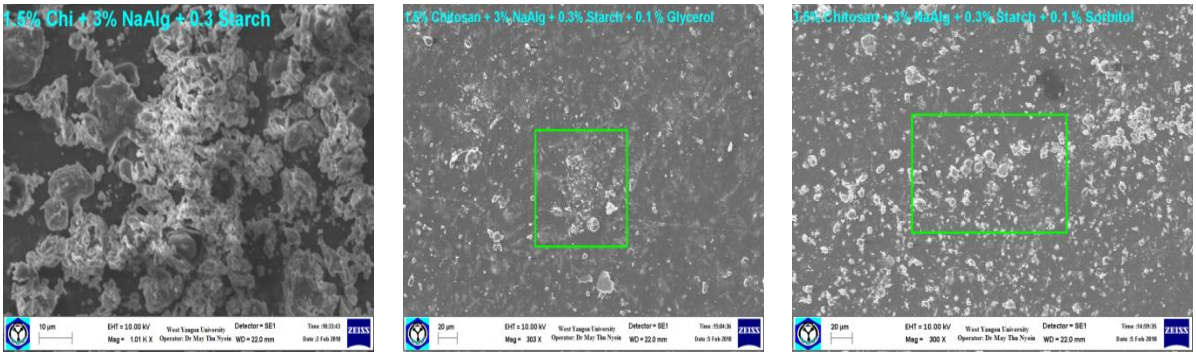

(a) (b) (c)

Figure 5 SEM micrographs of the selected composite membranes: (a) CAS-3 (b) CASG-2 and (c) CASS-2

Antimicrobial Activity of the Selected Composite Membranes by Agar Well Diffusion Method

Antimicrobial activities of the selected composite membranes: CAS-3, CASG-2 and CASS-2 were studied. These selected membranes were tested on six different strains of human pathogenic bacteria, *Bacillus subtilis*, *Staphylococcus aureus*, *Pseudomonas aeruginosa*, *Bacillus pumilus*, *Candida albicans*, and *E. coli*. To strengthen the finding, the antimicrobial activity of the all selected membranes was determined by agar well diffusion method. Antimicrobial activities of the all selected membranes were evaluated based on the diameters of clear inhibition zone surrounding the agar well. The selected CAS-3, CASG-2 and CASS-2 composite membranes showed medium antimicrobial activities in the range of inhibition zone diameters (13~19 mm). Among them, the modified CASG-2 composite membrane showed that highest activity against six microorganisms (14~19 mm). The resulting data are shown in Table 5 and Figure 6.

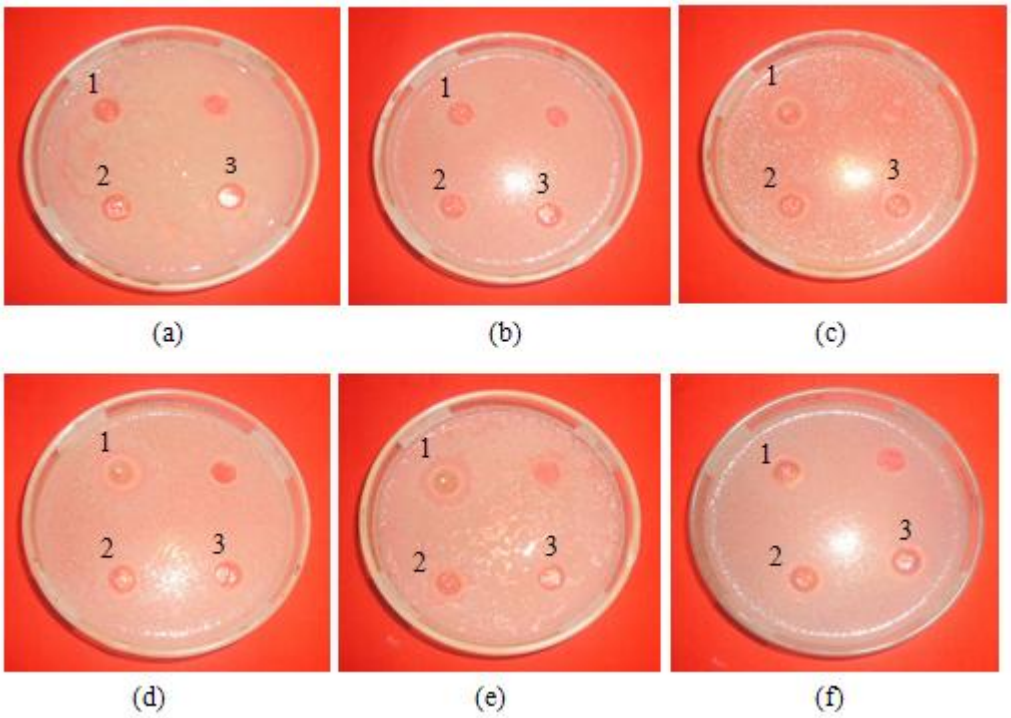

Figure 6 Antimicrobial activities of the selected (1) CASG-2 (2) CAS-3 and (3) CASS-2 composite membranes

(a) *Bacillus subtilis* (d) *Bacillus pumilus*
(b) *Staphylococcus aureus* (e) *Candida albicans*
(c) *Pseudomonas aeruginosa* (f) *E. coli*

Table 5 Antimicrobial Activities of the Selected Composite Membranes: CASG-2, CAS-3 and CASS-2

Membranes	**Inhibition zone diameters (mm) of the samples against different organisms**					
	(a)	**(b)**	**(c)**	**(d)**	**(e)**	**(f)**
CASG-2	14(+)	15(++)	17(++)	18(++)	19(++)	16(++)
CAS-3	13(+)	14(+)	17(++)	16(++)	18(++)	16(++)
CASS-2	13(+)	14(+)	16(++)	14(+)	14(+)	15(++)

Ager well – 10 mm
10 mm ~ 14 mm (+)
15 mm ~ 19 mm (++)
20 mm above (+++)

Organisms
(a) *Bacillus subtilis* (N.C.T.C-8236)
(b) *Staphylococcus aureus* (N.C.P.C-6371)
(c) *Pseudomonas aeruginosa* (6749)
(d) *Bacillus pumilus* (N.C.I.B-8982)
(e) *Candida albicans*
(f) *E. coli* (N.C.I.B-8134)

Conclusion

In this study, polymer blended membranes consisting of chitosan, sodium alginate, starch and glycerol/ sorbitol solution were prepared. The various types of chitosan-alginate-starch composite membranes and modified chitosan-alginate-starch-glycerol/ sorbitol composite membranes were prepared by blending, casting and solvent evaporating technique under

autoclaving conditions of 121 ˚C and 0.1 MPa in a time frame of 1 h. These membranes showed clear, smooth surface, flexible, highly transparent and light yellow colour.

Based on the mechanical properties such as tensile strength, elongation at break (%) and tear strength, the optimum condition was achieved by using 1.5 % (w/v) chitosan, 3.0 % (w/v) sodium alginate, 0.3 % (w/v) starch solution, 0.1 % (w/v) glycerol/ sorbitol. According to mechanical properties, CAS-3, CASG-2, CASS-2 composite membranes were selected to be used for biomedical applications.

FT IR analysis, indicated that the functional groups were present of selected CAS-3, CASG-2, CASS-2 composite membranes. SEM micrographs revealed the similar pattern of pores distribution on the surface of these membranes. CAS-3 composite membranes showed more sponge like nature and cluster form which enhances sorption property of membrane and CASG-2 composite membrane showed surface nature uniformly pores and homogeneous nature and CASS-2 composite membrane showed scabrous and patchy surface.

The antimicrobial activities of selected CAS-3, CASG-2, and CASS-2 composite membranes were tested by agar well diffusion method. The selected CAS-3, CASG-2 and CASS-2 composite membranes showed antimicrobial activities. Especially, CASG-2 composite membrane showed the highest activity on six microorganisms.

According to these results, the modified CASG-2 composite membrane is more suitable to be used as burn wound healing due to its mechanical properties and antimicrobial activity.

Acknowledgements

The authors would like to express their profound gratitude to the Department of Higher Education, Ministry of Education, Yangon, Myanmar, for provision of opportunity to do this research and Myanmar Academy of Arts and Science for allowing to present this paper.

References

Draget, K. I. (2000). *Alginates, In. Handbook of Hydrocolloid*. Cambridge: Philips G.O., Williams P.A (Eds.), Woodhead Publishing

Gotoh, T., Matsushima, K. and KiKuchi, K. I. (2004). "Chemospheres". *International Journal of Science*, vol. 55, pp. 57-64

Mohanty, A. K., Misr, M. and Drzal, L. T. (2002). "Sustainable Biocomposite from Renewable Resources: Opportunities and Challenges in the Green Materials World". *J. Polym. Environ.,* vol. 10, pp. 19 -26

Muzzarelli, R. A. A. and Peter, M. G. (1973). *Chitin Handbook*. Germany: 8th Ed., Bremen, European Chitin Society

Peter, M. G. (1995). "Applications and Environmental Aspects of Chitin and Chitosan". *J. Macromol. Sci.,* vol. 32, pp. 629 – 641

Silverstein, R. M. and Webster, F. X. (1998). *Spectrometric Identification of Organic Compound*. New York: 6th Ed., John Wiley and Sons

Whistler, R. L. and BeMiller, J. N. (1997). *Carbohydrate Chemistry for Food Scientists.* St. Paul, Minn: Eagan Press

Wibowo, S., Velzquez, G. Savant, V. and Torres, J. (2004). "Surimi Wash Waste Water Treatment for Protein Recovery: Effect of Chitosan Alginate Complex Concentration and Treatment Time on Protein Adsorption". *Food Science and Technology,* vol. 66, pp. 319-322

PREPARATION, CHARACTERIZATION AND APPLICATION OF NANOSILICA AND NANOSILICA XEROGEL FROM BAMBOO LEAVES

Phyu Phyu Lwin[1], Thinzar Nu[2], Khin Aye May[3]

Abstract

Giant bamboo (Wa-bo-gyi) is the largest member of the grass family in Myanmar. In this research, the preparation and characterization of the nanosilica extracted from bamboo leaves (*Dendrocalamas giganteus* Munro, Wa-bo-gyi) were studied. At first, bamboo leaves ash was prepared from bamboo leaves by calcination at various temperatures with different times. Characterization of bamboo leaves ash samples was carried out by using EDXRF, XRD, SEM and FT IR techniques. The XRD data for all of these synthesized samples showed the silica with nanosize. From EDXRF analysis, the presence of SiO_2, K_2O, P_2O_5, CaO of bamboo leaves was found. The maximum relative abundance of SiO_2 was found to be 52.29 % at the calcination temperature of 1000 °C for 2 h. The physicochemical properties of the selected sample (calcined at 1000 °C for 2 h), were 0.37 % of moisture, 3.08 % of ash, 1.44 g/mL of bulk density and 10.03 pH of Silica xerogel powder was prepared from the selected sample by using 1 M NaOH and 6 M H_2SO_4 solution. The prepared silica powder was characterized by EDXRF, XRD, SEM and FT IR analyses. The particle size of xerogel was slightly increased (30.5 nm) and the relative abundance of silica was significantly promoted to 84.15 %. The selected sample was introduced into the formulation of cement. The quality of cement (soundness, normal consistency, setting time, compressive strength and tensile strength) improved when mixing with the selected ash sample.

Keywords: *Dendrocalamas giganteus* Munro, nanosilica, xerogel

Introduction

Bamboo is probably the fastest-growing and highest yielding natural resource and construction material available to mankind. However, the use of bamboo generates other residues not used as fibers, such as the bamboo leaf. In some countries, significant amounts of bamboo are processed, generating high volumes of solid waste. These wastes are often burnt in open landfills, negatively impacting the environment.

The main objective of the present work is to extract nanosilica from natural sources bamboo leaves. In the present research, the bamboo leaves sample was collected from Mayangone Township, Yangon Region. The preparation to get bamboo leaves ash was worked in muffle furnace from 400 and 900 °C for 1 h and 2 h, respectively. In addition, the ash sample was also prepared at 1000 °C for 1 h, 2 h, 3 h and 4 h.

Bamboo leaves ash is black or grey colour. By controlling the burning conditions like temperature and time, amorphous silica of ultrafine size and reactivity will be produced. Bamboo leaves ash is formed by silica with a completely amorphous nature (Aye Aye Aung, 2014). Silica (SiO_2) is the major component in bamboo ash and other oxides such as CaO, K_2O , Al_2O, SO_3, Fe_2O_3, MgO and MnO are present in it (Cocina, 2010).

[1] Lecturer, Department of Chemistry, Dagon University
[2] Dr, Associate Professor, Department of Chemistry, University of Yangon
[3] Dr, Associate Professor, Department of Chemistry, University of Yangon

Nanosilica has been prepared through dissolution and precipitation process. The dissolution of silica was carried out by using an alkali leaching process (1 M NaOH) to partially dissolved carbonaceous materials. The resulting sodium silicate was filtered and dried in an oven for 24 h at 100 °C. The precipitation of silica from sodium silicate solution was carried out using 6 M H_2SO_4 at the pH of 7 and left for aging 12 h. The obtained silica gel was centrifuged and washed with hot water and dried at 80 °C for 24 h to get silica powder (Vaibhav, 2014).

Nanosilica is used mainly in concrete mixture for construction industry, nanosilica possess more pozzolanic nature (Itler, 1979). It has the capability to react with the free lime during the cement hydration and forms C-S-H get giving strength, impermeability and durability to concrete. In addition, nanosilca can be widely used porcelain, plaster, batteries, paints, adhesives, cosmetics, glass, steel, chemical fiber and environmental protection to upgrade the quality (Wang, 2004).

Materials and Methods

Sample Collection and Preparation

Bamboo leaves were collected from Mayangone Township, Yangon Region. Bamboo leaves were washed with water several times to remove dirt particles. They were dried at room temperature for two weeks.

Preparation of Bamboo Leaves Ash from Bamboo Leaves

Silicon dioxide reduction was conducted by ashing the bamboo leaves in two stages, first by combusting the dried bamboo leaves and then ashing using a muffle furnace. Dried bamboo leaves were weighed and burned in open space for pre-ash sample. Then this pre-ash was calcined in a muffle furnace at a temperature of 400 °C, 500 °C, 600 °C, 700 °C, 800 °C and 900 °C with holding time of 1 h and 2 h, respectively. The obtained ash samples were designated as BLA-1(1) and BLA-1(2) for calcination temperature of 400 °C and calcination time of 1 h and 2 h, respectively. Similarly, BLA-2(1) and BLA-2(2), BLA-3(1) and BLA-3(2), BLA-4(1) and BLA-4(2), BLA-5(1) and BLA-5(2), BLA-6(1) and BLA-6(2) were prepared at the calcination temperature of 500 °C, 600 °C, 700 °C, 800 °C and 900 °C, respectively. In addition, the char was calcined in a furnace at a temperature of 1000 °C with holding time of 1 h, 2 h, 3 h and 4 h until it became a grey ash and which were respectively denoted as BLA-7(1), BLA-7(2), BLA-7(3) and BLA-7(4). Once calcined, the ash was ground and sieved with 60 mm mesh. The sample was put in sealed plastic bag and this bag was stored in the desiccator at room temperature.

Characterization of the Prepared Bamboo Leaves Ash Samples (BLAs)

The prepared ash samples were characterized by EDXRF, XRD, SEM and FT IR analyses. According to the results of analyses, BLA-7(2) was selected for the preparation of nanosilica xerogel.

Analyses of Physicochemical Properties of BLA-7(2)

Some physicochemical properties such as moisture content, ash content, bulk density and pH of the selected sample BLA-7(2) were determined by conventional methods.

Preparation of Nanosilica Xerogel from Bamboo Leaves Ash BLA-7 (2)

A 2 g of bamboo leaves ash (the selected sample) and 20 mL of 1 M NaOH solution were mixed in a beaker (250 mL, pyrex). The mixed solution was set up for 24 h. Then obtained sodium silicate solution was filtered with Whatmann No. 41 filter paper into a beaker and dried in an oven for 24 h at 100 °C. The precipitation of silica from sodium silicate solution was made by adding 6 M H_2SO_4 to pH 7 and 24 h. The precipitated nanosilica was carefully centrifuged and washed with hot water to avoid the loss of residue. The residue on the filter paper was washed with hot water several times. Finally, the residue was dried in an oven at 80 °C for 24 h to give silica xerogel powder.

Characterization of Silica Xerogel

The prepared silica xerogel powder was characterized by EDXRF, XRD, SEM and FT IR analyses**.**

Results and Discussion

Preparation of Bamboo Leaves Ash

Bamboo leaves were collected from Mayangone Township, Yangon Region. The collected sample was washed with water, air dried in an open vessel and pre-ashed on electrical hot plate for 2 h. Then the pre-ashed sample of bamboo leaf was calcined in muffle furnace at the temperatures of 400 - 900 °C for 1 h and 2 h and 1000 °C for 1 - 4 h respectively to obtain bamboo leaves ash. Totally 16 ash samples were prepared. The percent yields of ash from the Wa-bo-gyi samples were obtained in the range of 1.24 – 46.0 %.

Characterization of Bamboo Leaves Ash

EDXRF analysis

The elemental composition of bamboo leaves ashes were determined by EDXRF analysis. These spectra showed that SiO_2, K_2O, CaO and P_2O_5 are the major constituents in BLA samples. Other oxides such as MnO, Fe_2O_3, CuO, TiO_2 and PbO in BLA were also found below 1 %. The silica percent of different bamboo leaves ashes are shown in Table 1.

Table 1 Relative Abundance of Silica in the Different Bamboo Leaves Ash by EDXRF Analysis

Sr. No.	Sample	Calcination time (h)	Calcination temperature (°C)	SiO_2 (%)
1	BLA-1(1)	1	400	31.279
2	BLA-1(2)	2	400	35.073
3	BLA-2(1)	1	500	33.862
4	BLA-2(2)	2	500	34.703
5	BLA-3(1)	1	600	31.809
6	BLA-3(2)	2	600	32.983
7	BLA-4(1)	1	700	30.597
8	BLA-4(2)	2	700	33.862
9	BLA-5(1)	1	800	37.258
10	BLA-5(2)	2	800	35.388
11	BLA-6(1)	1	900	40.374
12	BLA-6(2)	2	900	45.662
13	BLA-7(1)	1	1000	35.264
14	BLA-7(2)	2	1000	52.290
15	BLA-7(3)	3	1000	41.430
16	BLA-7(4)	4	1000	50.972

Among these 16 ash samples, the maximum relative abundance of SiO_2 was achieved to be 52.29 % at the calcination temperature of 1000 °C for 2 h. So BLA-7(2) is silica rich sample. BLA-7(2) was selected for the preparation of nanosilica xerogel powder.

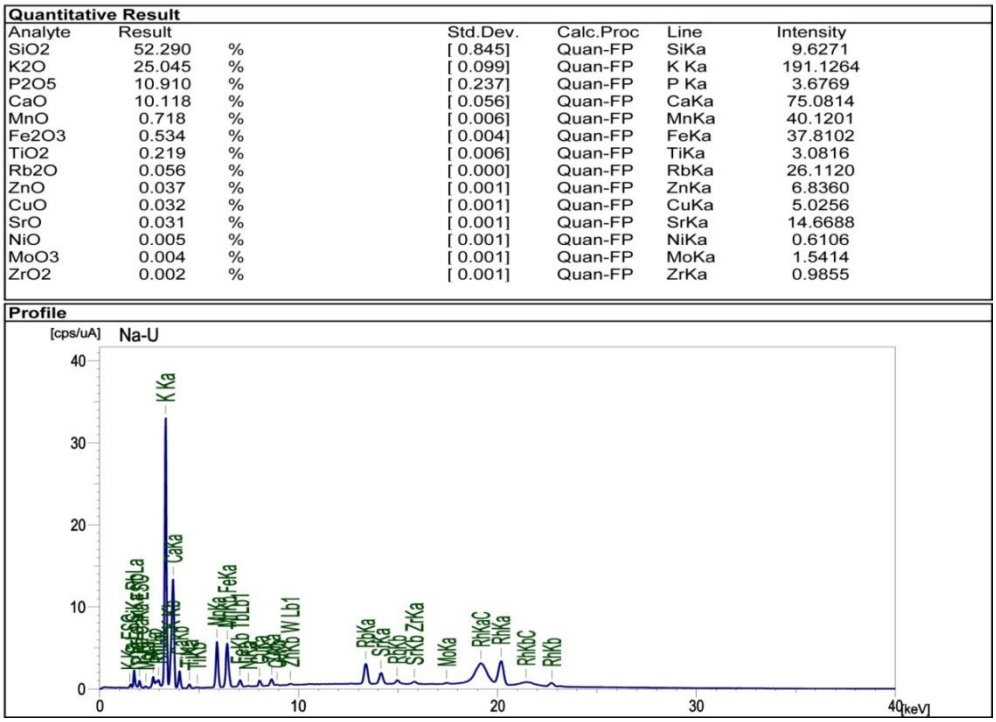

Quantitative Result

Analyte	Result		Std.Dev.	Calc.Proc	Line	Intensity
SiO2	52.290	%	[0.845]	Quan-FP	SiKa	9.6271
K2O	25.045	%	[0.099]	Quan-FP	K Ka	191.1264
P2O5	10.910	%	[0.237]	Quan-FP	P Ka	3.6769
CaO	10.118	%	[0.056]	Quan-FP	CaKa	75.0814
MnO	0.718	%	[0.006]	Quan-FP	MnKa	40.1201
Fe2O3	0.534	%	[0.004]	Quan-FP	FeKa	37.8102
TiO2	0.219	%	[0.006]	Quan-FP	TiKa	3.0816
Rb2O	0.056	%	[0.000]	Quan-FP	RbKa	26.1120
ZnO	0.037	%	[0.001]	Quan-FP	ZnKa	6.8360
CuO	0.032	%	[0.001]	Quan-FP	CuKa	5.0256
SrO	0.031	%	[0.001]	Quan-FP	SrKa	14.6688
NiO	0.005	%	[0.001]	Quan-FP	NiKa	0.6106
MoO3	0.004	%	[0.001]	Quan-FP	MoKa	1.5414
ZrO2	0.002	%	[0.001]	Quan-FP	ZrKa	0.9855

Figure 1 EDXRF spectrum of BLA-7(2)

XRD analysis

X-ray powder diffraction (XRD) is a analytical technique primarily used for phase identification of a crystalline material and can provide information on unit cell dimensions. X-ray diffraction is a common technique for the study of crystal structures, atomic spacing and crystallite size. Almost all of the diffractograms indicated that the prepared ash samples were crystalline nature and mixture of different types of silica. The diffractograms of BLA samples, the diffraction angles (2q) of all the major peaks were observed around 20° and 30° which are the presence of quartz and tridymite phase. The crystallite sizes of these 16 ash samples were calculated by Scherrer equation. The sizes of all samples were observed within the range of nano scale. The crystallite size of BLA-7(2) was found to be 19.6 nm. It was found to be the smallest crystallite size among 16 ash samples. Therefore BLA-7(2) was selected for the preparation of nanosilica xerogel powder. Figure 2 shows the XRD diffractogram of BLA-7(2) sample.

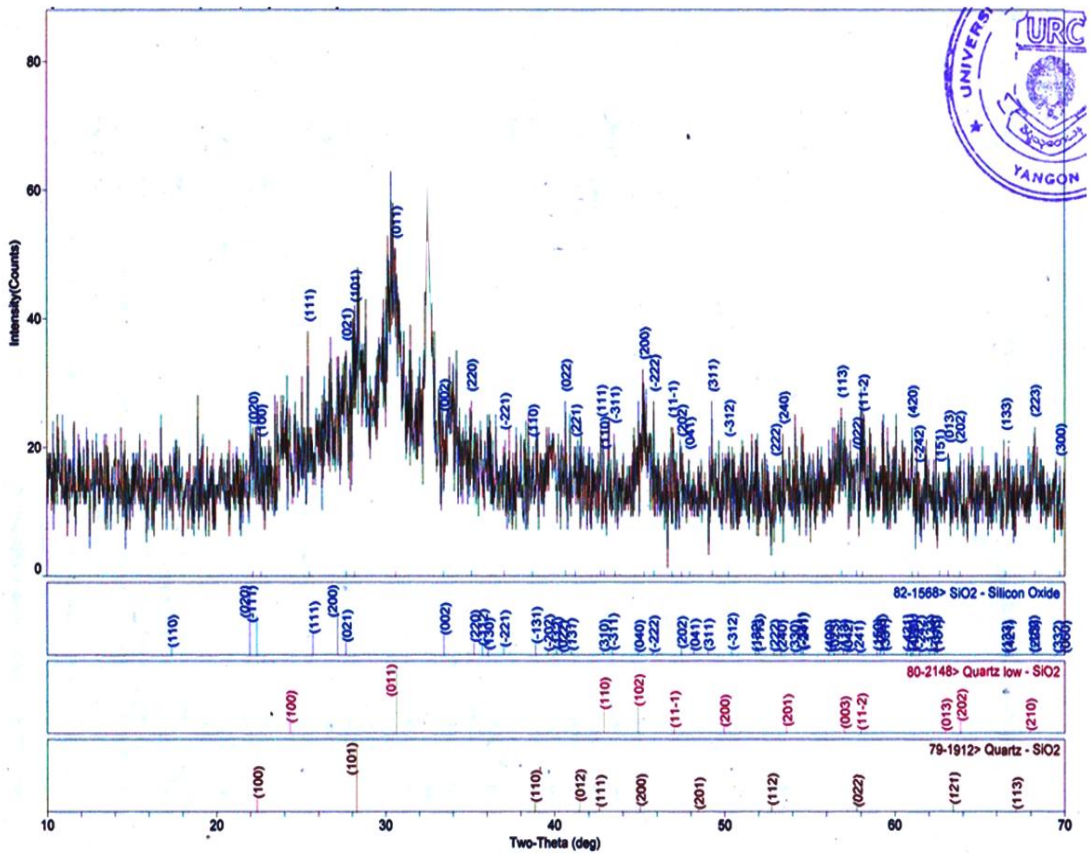

Figure 2 XRD diffractogram of BLA-7(2)

SEM analysis

The SEM micrographs of bamboo leaves ash samples showed porous nature at the calcinations temperature of 400 - 900 °C, however with rising calcinations temperature and calcinations time the ash samples (1000 °C for 1 h, 2 h , 3 h and 4 h) were seen to be more rigid.

At lower temperature of calcinations at 400 °C, 500 °C, the semi-ash or primary char of bamboo leaves did not show well defined pores. At the temperatures of 600 °C, 700 °C, 800 °C and 900 °C the surface morphology of the bamboo leaves ash were observed a distinct appearance of pores. The bamboo leaves ash at these temperatures were used as good sorbent for the removal of heavy metals and degradation of organic dye. At higher calcination temperature (at 1000 °C), the bamboo leaves were found to be completely changed to ash. At the calcination temperature 1000 °C, the samples were more rigid than the previous samples. Figure 3 shows the SEM micrograph of BLA-7(2).

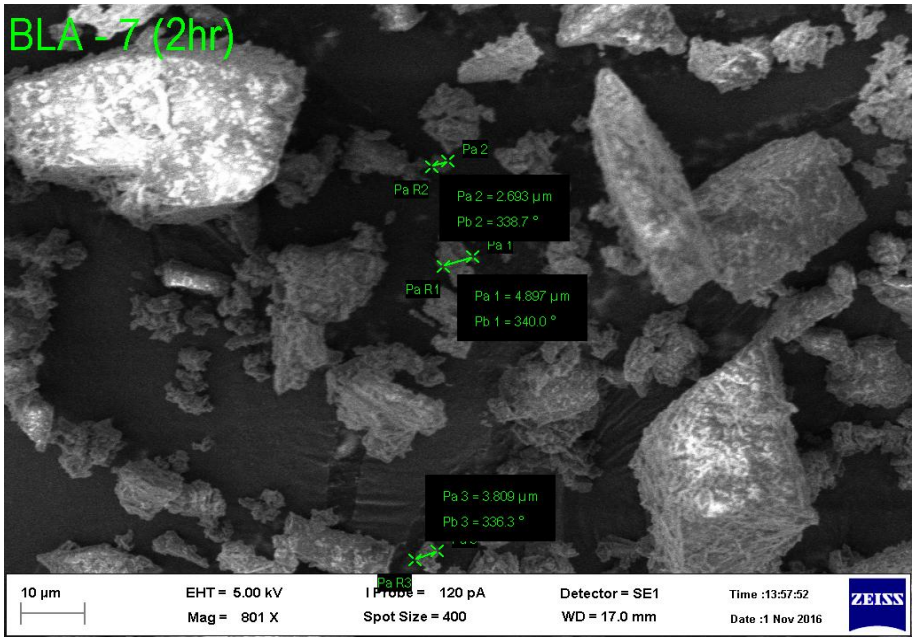

Figure 3 SEM micrograph of BLA-7(2)

FT IR analysis

Figure 4 shows the FT IR spectrum of BLA-7(2). The wave number at 3477 cm^{-1} is related to stretching vibration of Si-OH group. The wave number at 1661 cm^{-1} is related to bending vibration of Si-OH group. The wave number at 1057 cm^{-1} was observed as asymmetric stretching vibration of Si-O-Si group. The wave number at 616 cm^{-1} was observed as bending vibration of Si-O bond. FT IR data assignments are shown in Table 2.

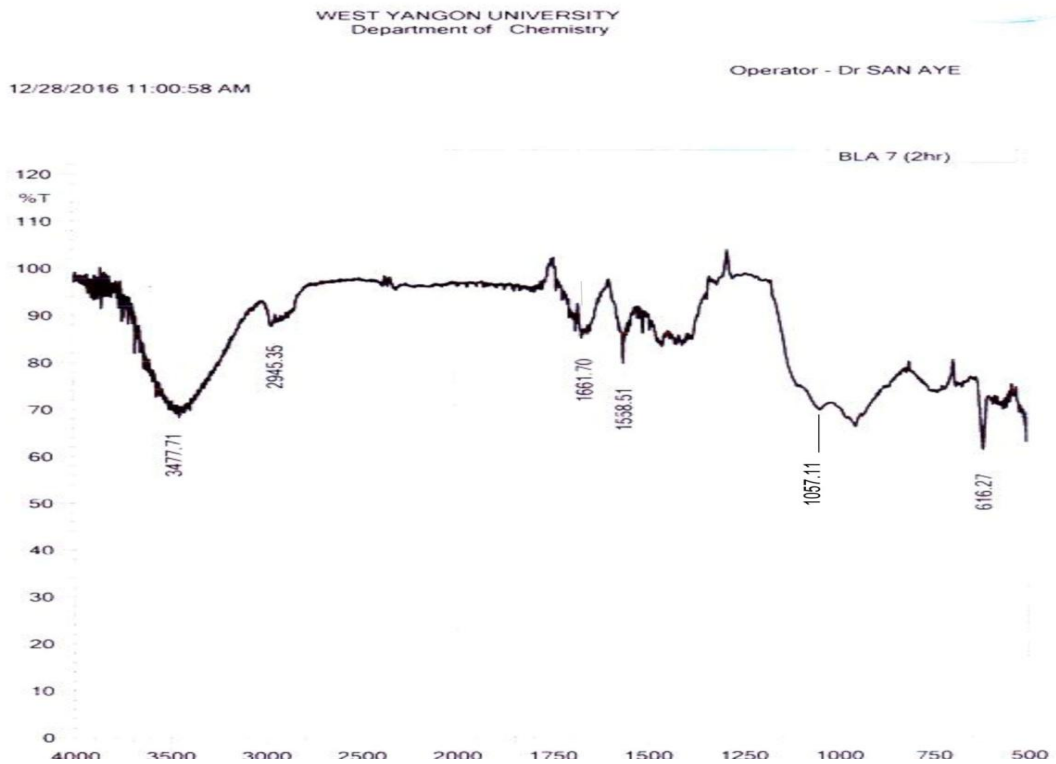

Figure 4 FT IR spectrum of BLA-7(2)

Table 2 Band Assignment for FT IR Spectrum of BLA-7(2)

Band No.	Observed wave no.(cm^{-1})	* Literature wave no.(cm^{-1})	Band Assignment
1.	3477	3700-3200	n_{Si-OH}
2.	1661	1750-1650	d_{Si-OH}
3.	1057	1200-700	$n_{Si-O-Si}$
4.	616	<650	d_{Si-O}

* Nakamoto, 1986; Amutha *et al.*, 2010

Physicochemical Properties of BLA-7(2)

Some physicochemical properties of BLA-7(2) are relevant to moisture content, ash content, bulk density and pH. The moisture content 0.37 %, bulk density 1.44 g mL^{-1} and pH value (10.03) of BLA-7(2) sample (3.08% yield) were obtained. So this sample was found to be in base nature.

Characterization of Nanosilica Xerogel Powder

Nanosilica xerogel powder was prepared from BLA-7(2) by dissolution and precipitation method. The prepared xerogel powder was characterized by EDXRF, XRD, SEM and FT IR techniques.

EDXRF analysis of nanosilica xerogel powder

The EDXRF spectrum of xerogel powder is described in Figure 5. The comparison of the relative abundance of some oxides in BLA-7(2) and nanosilica xerogel powder are shown in Table 3. In the preparation of nanosilica by calcination of bamboo leaves, the maximum silica percent was observed as 52 % in BLA-7(2) but it was promoted to 84 % in nanosilica xerogel powder. Therefore this process (xerogel formation process) gave the silica rich substance.

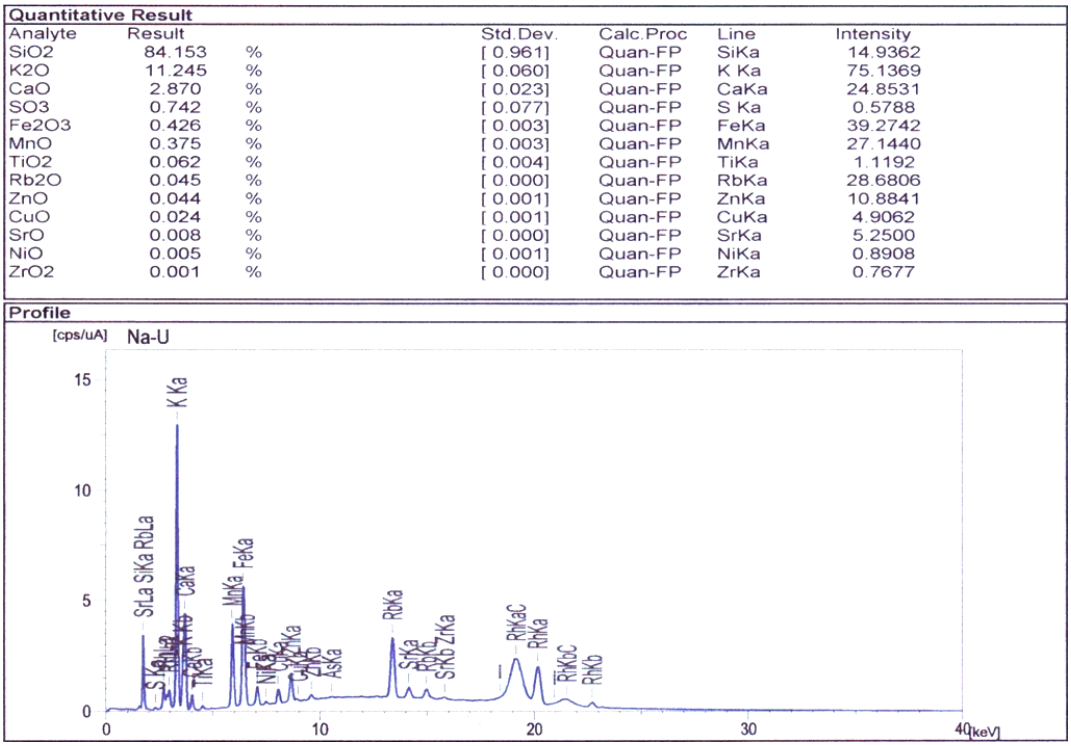

Quantitative Result

Analyte	Result		Std.Dev.	Calc.Proc	Line	Intensity
SiO2	84.153	%	[0.961]	Quan-FP	SiKa	14.9362
K2O	11.245	%	[0.060]	Quan-FP	K Ka	75.1369
CaO	2.870	%	[0.023]	Quan-FP	CaKa	24.8531
SO3	0.742	%	[0.077]	Quan-FP	S Ka	0.5788
Fe2O3	0.426	%	[0.003]	Quan-FP	FeKa	39.2742
MnO	0.375	%	[0.003]	Quan-FP	MnKa	27.1440
TiO2	0.062	%	[0.004]	Quan-FP	TiKa	1.1192
Rb2O	0.045	%	[0.000]	Quan-FP	RbKa	28.6806
ZnO	0.044	%	[0.001]	Quan-FP	ZnKa	10.8841
CuO	0.024	%	[0.001]	Quan-FP	CuKa	4.9062
SrO	0.008	%	[0.000]	Quan-FP	SrKa	5.2500
NiO	0.005	%	[0.001]	Quan-FP	NiKa	0.8908
ZrO2	0.001	%	[0.000]	Quan-FP	ZrKa	0.7677

Figure 5 EDXRF spectrum of silica xerogel powder

Table 3 Comparison of the Relative Abundance of some Oxides in BLA-7(2) and Silica Xerogel Powder Prepared from BLA-7(2)

Sample	Relative abundance of some oxides (%)			
	SiO_2	K_2O	P_2O_5	CaO
Nanosilica (BLA-7(2))	52.290	25.045	10.118	10.919
Nanosilica Xerogel	84.153	11.245	-	2.870

XRD analysis of nanosilica xerogel powder

Figure 6 is the XRD diffractogram of nanosilica xerogel powder. According to XRD results, nanosilica xerogel consists essentially of tridymite form of silica, which is the crystalline nature. The crystallite size of these sample was calculated by Scherrer equation and the result was observed within the range of nano scale. The average crystallite size of xerogel was found to be 30.5 nm. When the preparation of nanosilica xerogel powder, the crystallite size was larger than that of BLA-7(2) but the percent composition of nanosilica in xerogel powder was very much higher than that of BLA-7(2).

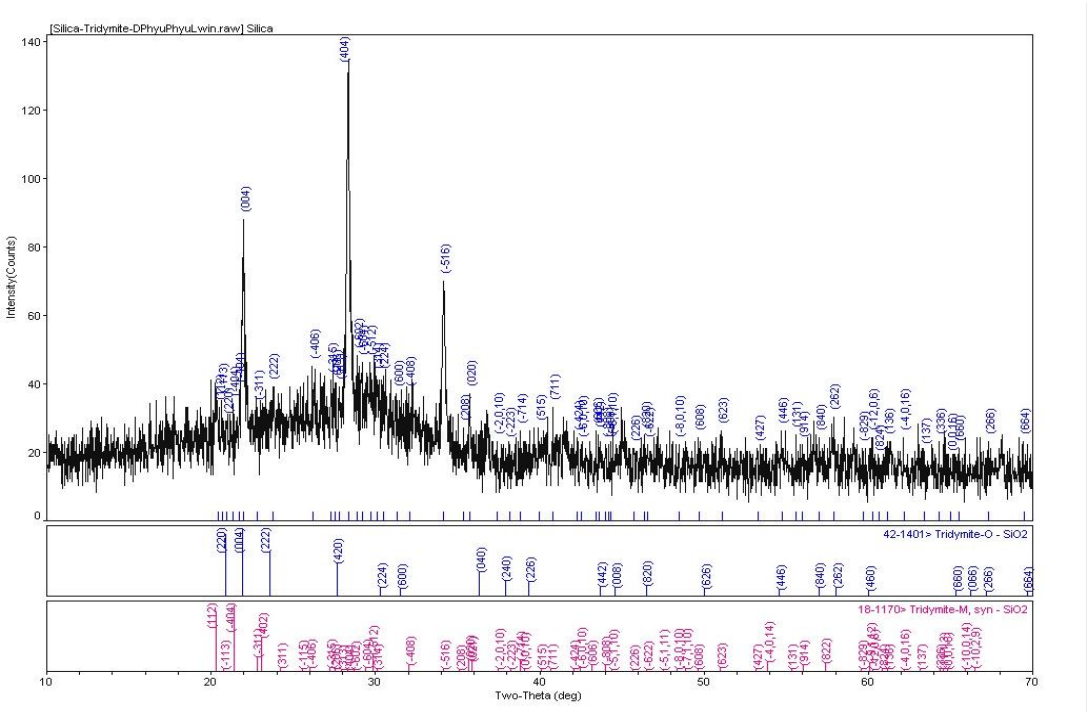

Figure 6 XRD diffractogram of silica xerogel powder

SEM analysis of nanosilica xerogel powder

The SEM micrographs of nanosilica xerogel are presented in Figures 7 (a) and (b). It indicated that xerogel powder has porous nature.

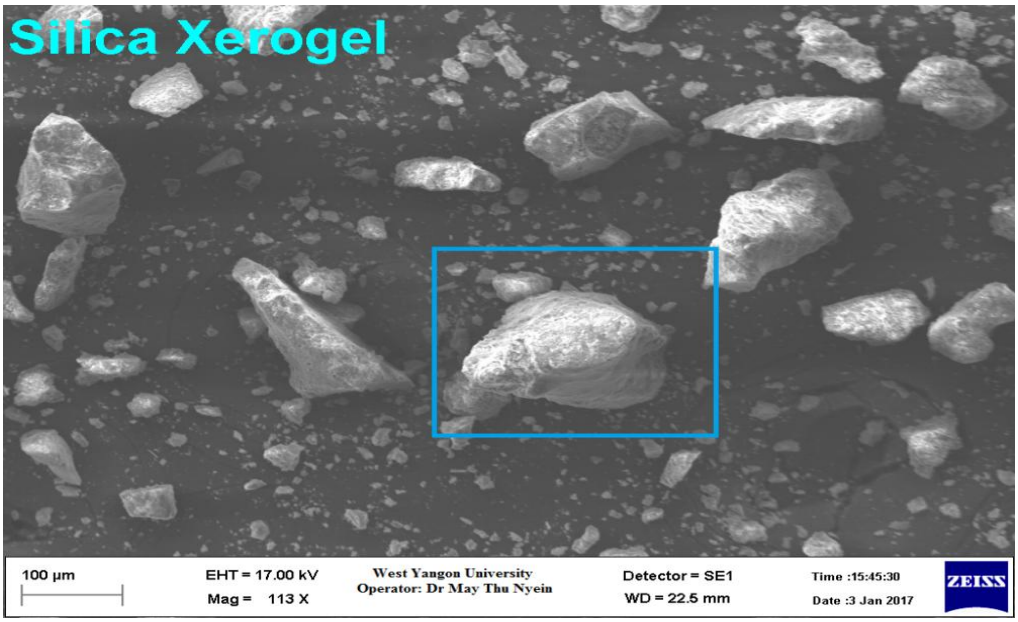

Figure 7(a) SEM micrograph of silica xerogel (Magnification 113 x)

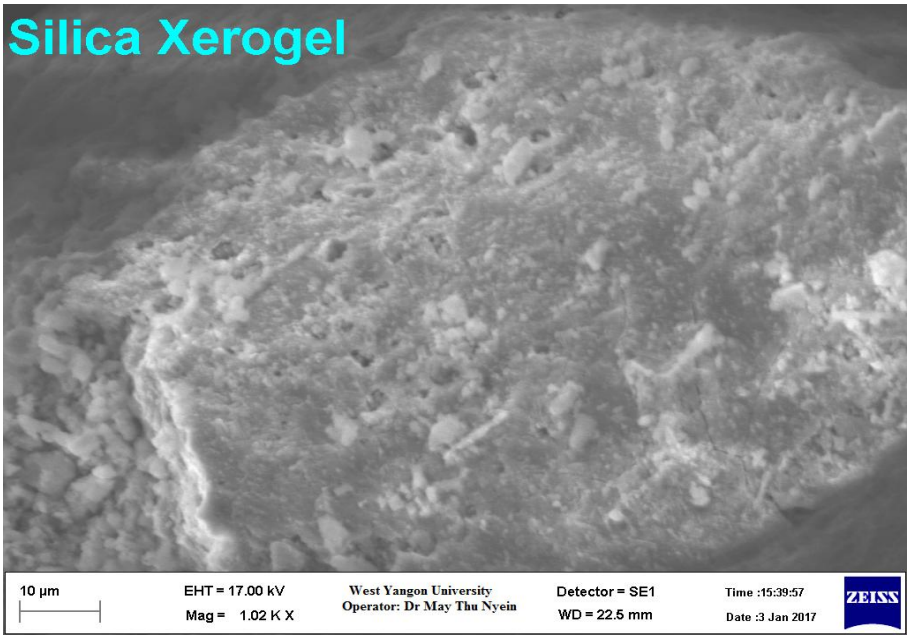

Figure 7(b) SEM micrograph of silica xerogel (Magnification 1020 x)

Table 4 Comparison of the Crystallite Size of BLA-7(2) and Silica Xerogel Powder

No.	Sample	2q (degree)	FWHM (degree)	Calculated (nm)
1	Nanosilica (BLA-7(2))	30.601	0.420	19.6
2	Nanosilica Xerogel	28.353	0.268	30.5

FT IR analysis of nanosilica xerogel powder

The characterization of prepared nanosilica xerogel was studied by FT IR spectrophotometer. Figure 8 and Table 5 show the FT IR spectrum and its band assignment of nanosilica xerogel. The possible assignment for the band at 3357 cm^{-1} is stretching vibration of OH bond in Si-OH group. The band at 1631 cm^{-1} indicates the bending vibration of OH bond in Si-OH group. The band at 1047 cm^{-1} is stretching vibration of Si-O asymmetric bond in Si-O-Si group.

.

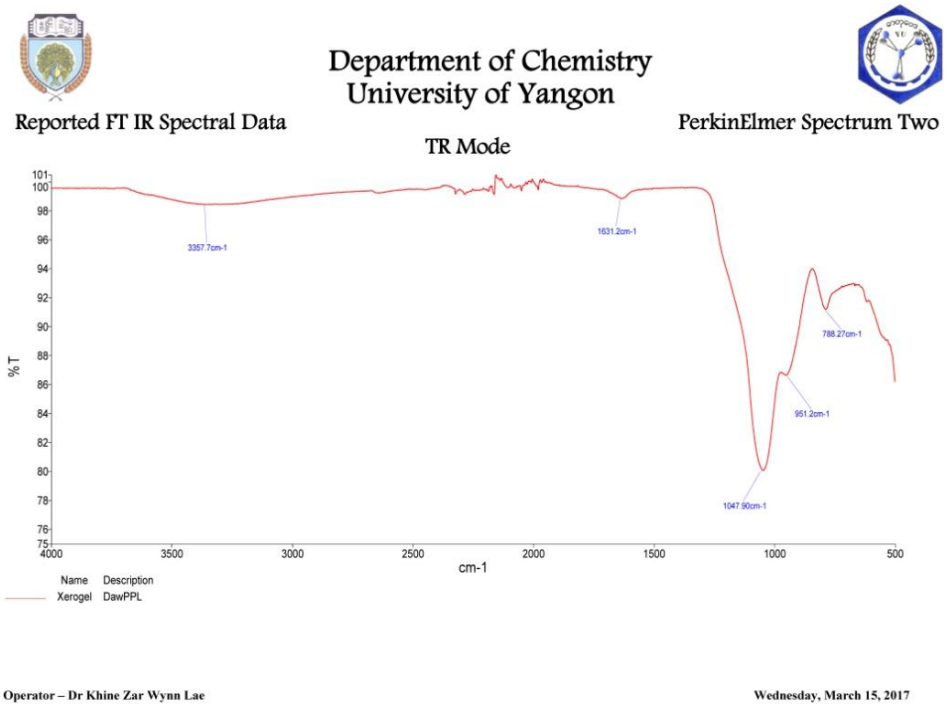

Figure 8 FT IR spectrum of silica xerogel

Table 5 Band Assignment for FTIR Spectrum of Nanosilica Xerogel

Band No.	Observed Wave No. (cm^{-1})	*Literature Wave No. (cm^{-1})	Band Assignment
1.	3357	3700-3200	n_{Si-OH}
2.	1631	1750-1600	d_{Si-OH}
3.	1047	1200-1000	$n_{Si-O-Si}$
4.	951	1200-700	n_{Si-OH}
5.	788		$n_{Si-O-Si}$

*****Nakamoto, 1986; Amutha *et al.*, 2010

Physicomechanical Analysis of Cement Containing 5 % BLA-7 (2) (5 %BLA Cement)

The quality of 5 % BLA cement (soundness, normal consistency, setting time, compressive strength and tensile strength) were improved when mixing with the selected ash sample.

Table 6 Physicomechanical Properties of Cement (Alpha) and BLA Cement

Sample	Normal Consistency (%)	Setting Time (min)		Soundness (mm)	Compressive strength (MPa)		Tensile strength (psi)	
		Initial	Final		7 days	28 days	7 days	28 days
Cement (Alpha)	28.5	150	256	1.6	11.3	15.7	230	243.3
BLA Cement	30.8	171	234	1.0	15.6	16.7	230	270

Conclusion

In this research, an attempt was made to produce nanosilica from *Dendrocalamas giganteus* Munro (wa-bo-gyi) bamboo leaves ash. The formation of nanosilica in bamboo leaves ash depends not only on the calcination temperature but also calcination time. At low calcination temperature, the colour of ashes was observed dark-grey; depending upon the proportion of unburnt carbon present. The ash obtained at 800 °C was almost grey colour. The bamboo leaves was calcined at 1000 °C, the ash was observed white.

This study indicated that the maximum relative abundance of SiO_2 can be produced by maintaining the calcinations temperature at 1000 °C under calcination time for 2 h (BLA-7(2)). The yield percent of this sample was 3.08 %.

BLA-7(2) was characterized by EDXRF, XRD, SEM and FT IR techniques. From EDXRF result, the maximum relative abundance of silica was found to be 52.29 % and small amount of other trace oxides. XRD analysis of this sample was observed crystalline nature and crystallite size was 19.6 nm. From the SEM analysis it was found that this sample has porous nature. FT IR analysis showed the presence of Si-OH, Si-O-Si and Si-O bond.

The production of high purity silica from BLA-7(2) was studied by dissolution and precipitation method. From EDXRF analysis, the relative abundance of silica was distinctly increased from 52.29 to 84.15 % and other constituent oxides were decreased. From the XRD analysis, the silica xerogel powder was found to be crystalline nature and tridymite phase from the ICDD search/match process. Its crystallilte size was 30.5 nm. From the SEM analysis, silica xerogel powder has porous nature. In the FT IR data of silica xerogel sample, the presence of Si-OH and Si-O-Si groups were found in the prepared silica xerogel.

The physical and mechanical properties of 5 % BLA cement and alpha cement such as normal consistency, setting time, compressive strength and tensile strength were also determined. It was found that the normal consistency of 5 % BLA cement was higher than alpha cement. The increase in normal consistency was observed that it needed larger amount of water than the alpha cement. This is because of 5 % BLA mixture with the cement presents more porous nature and hence tends to absorb more water.

The setting time of 5 % BLA cement and alpha cement were compared. It can be observed that the addition of 5 % BLA in the cement speeds up setting time. The soundness test

result of 5 % BLA mixing with cement is 1 mm, which is well within the limiting value of 10 mm specified by BS12 (British Standard).

The compressive strength of 5 % BLA blended cement was increased from 11.3 MPa to 15.6 MPa after 7 days, and from 15.7 MPa to 16.7 MPa after 28 days. The tensile strengths of BLA blended cement and alpha cement were found to be the same value after 7 days. But they were found to be increased from 243.3 psi to 270.0 psi after 28 days.

From the experimental results of compressive strength and tensile strength, it can be inferred that addition of 5 % BLA enhance the quality of cement.

Acknowledgements

The authors would like to express their profound gratitude to the Department of Higher Education, Ministry of Education, Nay Pyi Daw, Myanmar, for provision of opportunity to do this research and Myanmar Academy of Arts and Science for allowing to present this paper.

References

Amutha, K., Ravibasker, R and Sivakumar, G. (2010). "Extraction, Synthesis and Characterization of Nanosilica from Rice Husk Ash". *International Journal of Nanotechnology and Applications,* vol.4, pp. 61-66

Aye Aye Aung. (2014). *A Study on Cross-Linked Iron Doped Silica Composite from Bamboo Leaf Ash for the Removal of Toxic Metal Ions*. Yangon: PhD Dissertation, Chemistry Department, Yangon University

Cocina, E. V. (2010). "Pozzolanic Behaviour of Bamboo Leaves Ash: Characterization and Determination of the Kinetic Parameters". *Cement & Concrete Composites*, vol. 33, pp. 68-73

Itler, R.K. (1979). *The Chemistry of Silica.* New York: John Wiley and Sons, Inc., 230-233

Nakamoto, K. (1986). *Infrared and Raman Spectra of Inorganic and Coordination Compounds*. New York: John Wiley and Sons, Inc., pp. 1087-1088

Vaibhav,V. (2014). "Agricultural Waste as a Source for the Production of Silica Nanoparticles". *Elsevier,* vol. 24, pp. 308-316

Wang, K. (2004). "Bionanotechnology Based on Silica Nanoparticles". *Journal of Medicinal Research Review,* vol. 139(5), pp. 515-520

PREPARATION AND CHARACTERIZATION OF CELLULOSE NANOFIBRES FROM PINEAPPLE LEAF FIBRES AND SUGARCANE BAGASSE

Htet Htet Than Sein[1], Khin Than Yee[2], Myo Maung Maung[3], Mya Theingi[4]

Abstract

The aim of the study was to extract cellulose nanofibres (CNF) from pineapple leaf fibres (PALF) and sugarcane bagasse (SCB). The CNF was isolated from PALF and SCB by mechanical treatments and chemical treatments using alkaline, acids and inorganic salts. The physicochemical properties of prepared samples such as moisture content, ash content, pH and solubility were determined conventionally. Yield percent of pineapple leaf cellulose nanofibres (PALCNF) was higher than that of sugarcane bagasse cellulose nanofibres (SCBCNF). The raw samples and prepared samples were characterized by XRD, FT IR, EDXRF and SEM analysis to confirm as cellulose nanofibres. Crystallinity index percent of the prepared cellulose nanofibres was investigated by using XRD analysis. According to the XRD investigation, PALCNF and SCBCNF have the sharp diffraction peak is 2θ value at 22˚ and the amorphous diffraction peak is 2θ value at 18˚. It could be noticed that cellulose was present in the form of cellulose. Based on the FT IR spectrum, there are several peaks in raw samples which are not found in the spectrum of cellulose nanofibres. The EDXRF table shows the elemental constituents of the untreated raw samples and the CNF after chemical treatment. The SEM analysis showed that the PALCNF has fibrous nature and the SCBCNF has irregular aggregated shape fibrils.

Keywords: Cellulose nanofibres, pineapple leaf cellulose nanofibres, sugarcane bagasse cellulose nanofibres, chemical treatment

Introduction

Cellulose is an organic compound with the formula $(C_6H_{10}O_5)_n$, a polysaccharide consisting of a linear chain of several hundred to many thousands of β(1→ 4) linked D-glucose unit (Lavanya *et al.,* 2011). Cellulose is the most abundant polymer on Earth. It consists of glucose-glucose linkages arranged in linear chains where C-1 of every glucose unit is bonded to C-4 of the next glucose molecule. Cellulose in nanometers or nanocellulose has a size range from 10 nm to 350 nm (Kadla and Gilbert, 2000).

Cellulose, an important structural component of plants, have received much attention because of their low density, nonabrasive, combustible, nontoxic, low cost and biodegradable properties. Cellulose fibres have some disadvantages such as moisture absorption, quality variations, low thermal stability and compatibility with the hydrophobic polymer matrix. However, production of nanoscale cellulose fibers and their application in composite materials have gained increasing attention due to their high strength and stiffness combined with low weight, biodegradability and renewability.

The cellulose fibres can be classified into three groups. They are following.

(i) **Leaf fibre :** abaca, cantala, curaua, date palm, henequen, pineapple, sisal, banana;

(ii) **Seed fibre :** cotton; bast: flax, hemp, jute, ramie; fruit: coir,kapok, oil palm;

(iii) **Grass fibre :** alfa, bagasse, bamboo; stalk: straw (cereal).

[1] PhD Candidate, Department of Chemistry, University of Yangon
[2] Dr, Lecturer, Department of Chemistry, University of Myeik
[3] Dr, Lecturer, Department of Chemistry, Dagon University
[4] Dr, Lecturer, Department of Chemistry, University of Yangon

The bast and leaf (the hard fibers) types are the most commonly used in composite applications. Commonly use plant fibres include cotton, jute, hemp, flax, ramie, sisal, coir, henequen and kapok. Cotton contains much of cellulose in it (around 90%), how in wood, plant leaves and stalks, it is found in combination with other materials, such as lignin and hemicelluloses (Chandrahasa *et al.,* 2008).

Pineapple leaf fibres (PALF) are an important natural fiber that exhibit high specific strength and stiffness. The PALF observed to have the high percentage of α-cellulose content (81.27 %) and low percentage of hemicellulose (12.31 %) and lignin (3.46 %) content. The α-cellulose is purified with steam treatment correlated with acid treatment processes (Cherian *et al.,* 2011).

Sugarcane bagasse (SCB) contains cellulose (40-50 %), much of which is in the crystalline structure. Another component in sugarcane bagasse is hemicellulose as much as (25-35 %) which is amorphous polymer and mainly composed of xylose, arabinose, galactose, and mannose. The rest is mostly lignin with about (18-24 %) (Wulandari *et al.,* 2016).

There are two basic approaches for creating nanostructurs – bottom-up method and top down method. The bottom up method involves construction on a molecular scale from scratch using atoms, molecules and nanoparticles building blocks. The top down method involves the disintegration of macroscopic material to a nanoscale by the following methods: mechanical (e.g., grinding), chemical (e.g., partial hydrolysis with acids or bases), enzymatic (e.g., treatment with enzymes hydrolyzing cellulose, hemicellulose, pectin and lignin) and physical (e.g., techniques using focused ion beams or high–power lasers). In this paper, the top down method was used for production of cellulose nanofibres.

The top down approach deals mainly with the removal of non-cellulosic compounds to obtain pure cellulose and then mechanically treating it to get cellulose nanofibres. The treatment basically involves alkaline hydrolysis to remove pectin and lignin followed by bleaching to get rid of hemicellulose and lastly acid hydrolysis to remove mineral traces and to hydrolyze amorphous cellulose, providing the required nanofibres (Nohwar *et al.,* 2016).

Materials and Methods

Sample Collection

Pineapple leaf was collected from Shaw Pyar Village, Pathein Township and sugarcane bagasse was collected from Hledan Market. Other requiring chemicals were purchased from chemical store. Distilled water was used as the solvent in all analyses.

Extraction of Pineapple Leaf Fibres

Pineapple leaf fibres from the leaves can be done in two ways, namely the manual and mechanical methods. The most common and effective is the manual method. Firstly, pineapple leaves were washed with water. The manual process used a plate or whittle with no sharp knife to remove the skin leaves still attached to the fibres surface. After that, the fibres were washed with water and dried in sunlight or using the oven. Dry fibres were cut into small pieces (Adam *et al.,* 2016).

Preparation of Cellulose Nanofibres from Pineapple Leaf Fibres

PALF were treated with 2 % (w/v) NaOH (fibres to liquor ratio1:10) in an autoclave and kept under 138 kPa pressure for a further period of 1 hour. Pressure was released immediately. The fibres were removed from the autoclave, and the fibres were washed in distilled water until it was rid of alkali. The steam exploded fibers were bleached using a mixture of NaOH and glacial CH_3COOH (27 g/L and 78.8 g/L, respectively) and a mixture of 1:3 NaClO solutions. The bleaching was repeated six times. After the bleaching the fibres were thoroughly washed in distilled water and dried. The steam exploded bleached fibres were treated with $H_2C_2O_4$ of 11 % (w/v) concentration in an autoclave until it attained a pressure of 138 kPa. The pressure was released immediately. The autoclave was again set to reach 138 kPa and the fibres were kept under that pressure for 15 min. The pressure was released and the process repeated eight times. The fibres were taken out washed until the washings no longer decolorized $KMnO_4$ solution to make sure that the washings are free from acid. The proceeded nanofibrils were suspended in distilled water and kept stirring with a mechanical stirrer for about 4 h until the fibres are dispersed uniformly (Cherian *et al.,* 2011).

Preparation of Cellulose Nanofibres from Sugarcane Bagasse

Sugarcane bagasse was dried in sunlight and then cut into small pieces. The cut bagasse was milled to become powder. The powder of bagasse was bleached with sodium hypochlorite for 6 h with constant stirring at 45 °C to remove the lignin. The residue was washed with distilled water until a neutral pH. The neutral residue was refluxed with 17.5 % sodium hydroxide for 3 h with constant stirring at 45 °C to remove hemicellulose. The residue of this process was also washed until reach a neutral pH, and it was dried at room temperature for 2-3 days. Isolated cellulose from sugarcane bagasse was hydrolyzed with sulfuric acid with a ratio of cellulose to sulfuric acid 1:25. The hydrolysis of cellulose with 10 % (v/v) H_2SO_4 at 40 ˚C for 10 min. The hydrolysis process was quenched by adding 10-fold excess distilled water (250 mL) to the reaction mixture. A colloidal suspension which produced was centrifuged at 6500 rpm for 30 minutes. Then, it was dialyzed for 5 days to neutralize and eliminate the sulfate ions. The neutral colloidal suspension was sonicated for 10 minutes to homogenize the generated cellulose nanofibres (Wulandari *et al.,* 2016).

Characterization of the Prepared Samples

The physicochemical properties (moisture, ash, pH and solubility) of cellulose nanofibres prepared from pineapple leaf fibres and sugarcane bagasse were determined. The crystallinity index was calculated by using XRD analysis. The structural characterization of PALCNF and SCBCNF were characterized using FT IR. The elemental constituents in samples were analyzed by EDXRF analysis. The morphological structure of prepared samples were characterized by SEM.

X-ray diffraction (XRD) analysis was carried out using Rigaku X-ray Diffractometer, RINI 2000/PC software, Cat. No 9240 J 101, Japan. Copper tube with nickel filter was used. The diffraction pattern was recorded in terms of 2θ in the range of 10-70 °.

FT IR spectrum was recorded in the range of 4000-400 cm^{-1} by using 8400 SHIMADZU, Japan FT IR spectrophotometer.

Elemental EDXRF analysis on the prepared sample was done by using Shimadzu model EDX-800 EDXRF spectrometer.

The scanning electron microscopy (SEM) images were recorded by using JSM-5610 Model SEM, JEOL-Ltd., Japan.

Results and Discussion

Physicochemical Properties of PALCNF and SCBCNF

Table 1 shows the physicochemical properties (moisture, ash, pH and solubility) of cellulose nanofibres obtained from pineapple leaf fibres and sugarcane bagasse. In this table, PALCNF was a significant higher content of moisture, ash and yield percent than that of SCBCNF. The moisture content of cellulose was within the acceptable range (10 – 13.5 %) for high quality cellulose and standards for food application. The ash content is greater than 0.2 % which is recommended for high quality cellulose. The pH value falls within the acceptable range (6-7) for cellulose used in the pharmaceutical, cosmetics and food industries. Cellulose has strong affinity and hydrogen bonding through the Vander Wal's force itself; hence it is very stable and insoluble in water.

Table 1 Physicochemical Properties of PALCNF and SCBCNF

Physicochemical Properties	PALCNF	SCBCNF
moisture (%)	10.11	9.84
ash (%)	0.53	0.01
pH	6.5	6.8
solubility	Insoluble	Insoluble
yield percent (%)	40.26	9.6

PALCNF = Pineapple leaf cellulose nanofibres
SCBCNF = Sugarcane bagasse cellulose nanofibres

XRD Analysis

XRD analysis was conducted to analyze the crystallinity of raw samples and preparation of samples. The crystallinity index percent (C_I) was calculated using the following equation, by measuring the peak height of the crystalline region (I_{200}) and the amorphous region (I_{am}).

$$C_I\ (\%) = \frac{I_{200} - I_{am}}{I_{200}} \times 100\ \%$$

I_{200} is the maximum intensity of the peak for the crystalline cellulose ($2\theta = 22^{\circ}$-24°). I_{am} represent the intensity of diffraction of the noncrystalline material for the amorphous cellulose ($2\theta = 16^{\circ}$-18°). Figures 1(a) and (b) show XRD diffractograms of the raw PALF and PALCNF. Figures 2 (a) and (b) show XRD diffractograms of the raw SCB and SCBCNF. From the graph it can be seen that the raw samples are amorphous in nature and after the pretreatment crystallinity in the material is achieved, as also with acid hydrolysis. The amorphous nature of raw samples is due to the presence of large amounts of lignin, hemicellulose and other. After acid hydrolysis, the structural changes in crystallinity.

The crystallinity index percent for all samples was calculated by peak height method and represented as shown in Table 2. From the XRD result, the crystallinity index of the PALF was calculated as 75.12 % and increased in case of PALCNF to 89.05 %. Similarly, the increase the crystallinity index percent from 42.5 % for the SCB to 65.28 % for the SCBCNF. In both samples, it was found that the increase the value of C_I from raw sample to prepared CNF was undoubtedly attributed to the removal of hemicellulose and lignin in amorphous region and remaining amorphous parts was removed during acid hydrolysis.

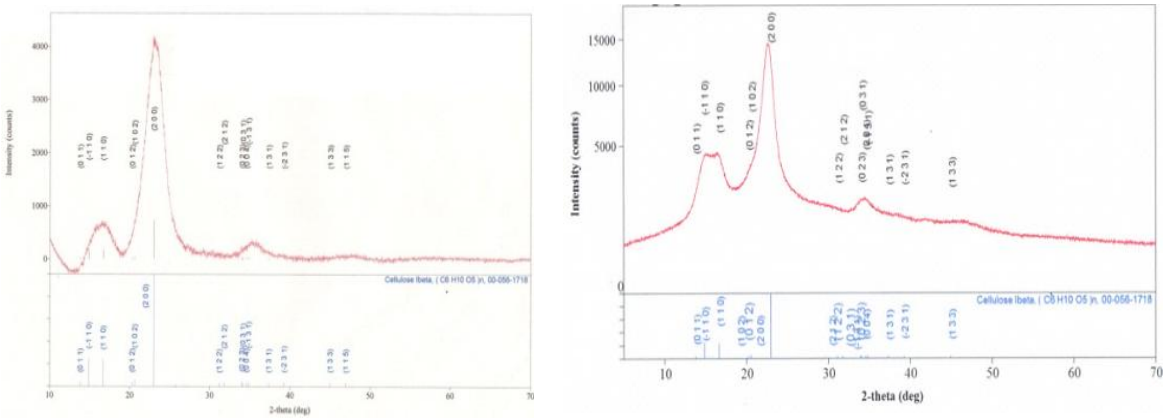

(a) (b)

Figure 1 XRD diffractograms of (a) raw pineapple leaf fibres PALF
(b) pineapple leaf cellulose nanofibres PALCNF

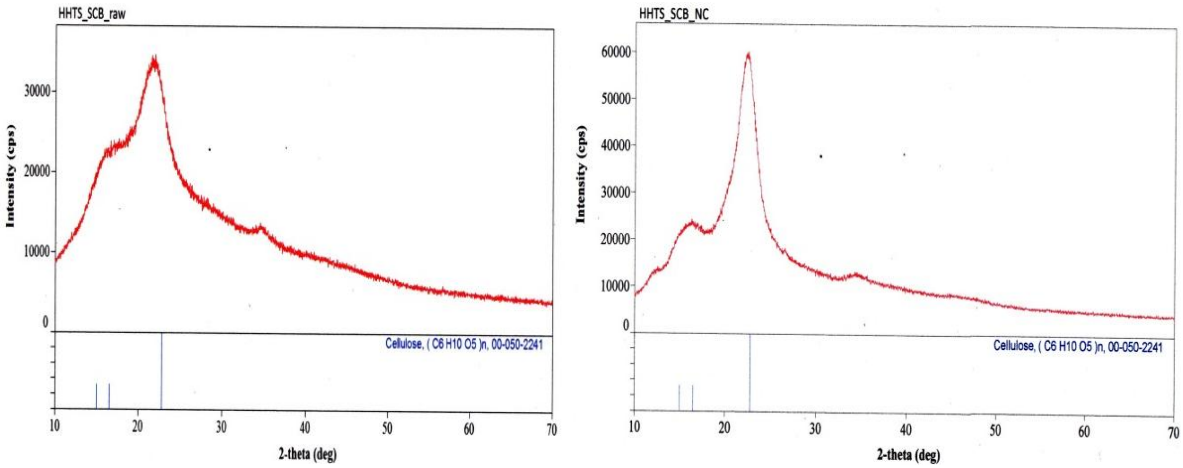

(a) (b)

Figure 2 XRD diffractograms of (a) raw sugarcane bagasse SCB
(b) sugarcane bagasse cellulose nanofibres SCBCNF

Table 2 Crystallinity Index Percent of the Raw Samples and Prepared Cellulose Nanofibres

Samples	Crystallinity Index (%)
PALF (raw)	75.12
PALCNF	89.05
SCB (raw)	42.5
SCBCNF	65.28

FT IR Analysis

FT IR spectroscopy was used to show that the lignin and hemicellulose have been removed during the preparation of cellulose fibres through analysis of its functional group. Figures 3 (a) and (b) present the result of the FT IR analysis of raw PALF and chemical treated PALCNF. Figures 4 (a) and (b) also present the FT IR spectra of raw SCB and SCBCNF. Based on the FT IR spectra, there are several peaks in the raw samples which were not found in the spectra of cellulose nanofibres. The peaks are 1244 cm^{-1}, 1248 cm^{-1}, 1514 cm^{-1}, 1587 cm^{-1}, 1729 cm^{-1} and 1730 cm^{-1}. The absorption peaks of 1244 cm^{-1} and1248 cm^{-1} appeared due to the C-O stretching vibration of aryl group in lignin. The spectrum presented characteristic peaks in the 1514 cm^{-1} and 1587 cm^{-1} corresponding to the aromatic skeletal vibration. The C=O stretching vibration of carboxylic groups of hemicellulose and lignin is around 1729 cm^{-1} and 1730 cm^{-1}. In CNF, the spectral bands of 1428 cm^{-1}, 1426 cm^{-1} and 897 cm^{-1} show significantly the presence of cellulose. PALCNF and SCBCNF have the same functional groups. The band assignments of raw samples and chemical treatment of CNF are described in Table 3.

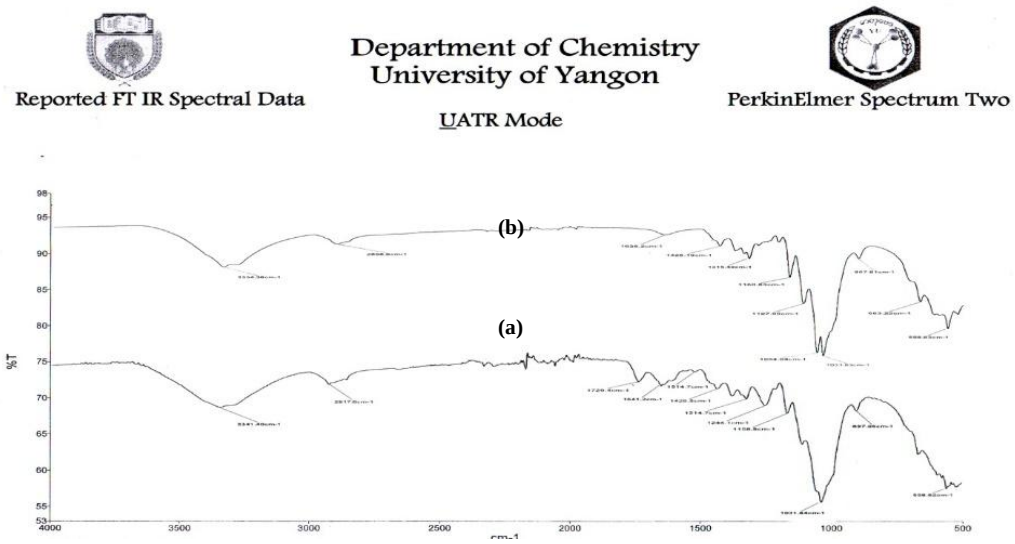

Figure 3 FT IR spectrum of (a) raw pineapple leaf fibres PALF
(b) pineapple leaf cellulose nanofibres PALCNF

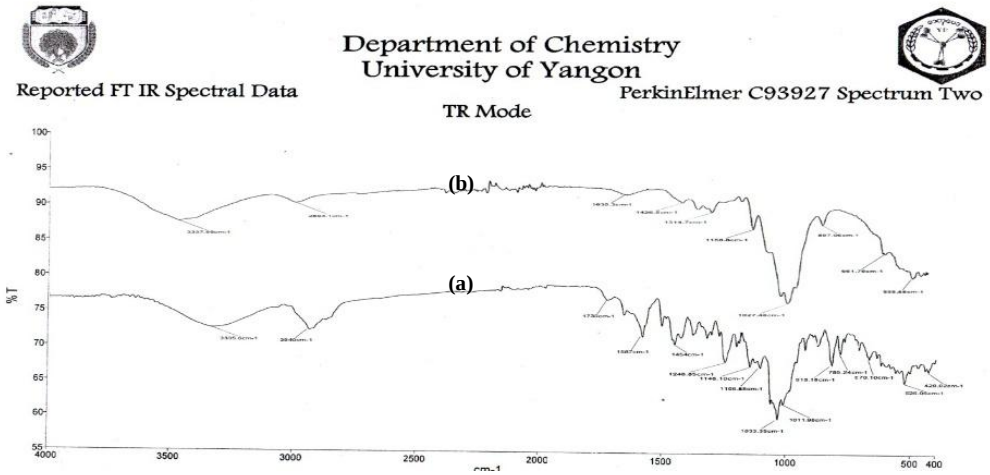

Figure 4 FT IR spectrum of (a) raw sugarcane bagasse SCB
(b) sugarcane bagasse cellulose nanofibres SCBCNF

Table 3 FT IR Band Assignments of the Raw Samples and the Prepared Cellulose Nanofibres

Observed wavenumber (cm^{-1})				*** Literature wavenumber (cm^{-1})**	**Band Assignment**
Raw PALF	**PALCNF**	**Raw SCB**	**SCBCNF**		
3431	3334	3335	3337	3600-3200	O-H stretching
2918	2890	2940	2894	2980-2850	C-H stretching (ketone and carbonyl)
1729	**-**	**1730**	**-**	**1765-1715**	**C=O stretching of ester**
1641	1638	-	1635	1665-1620	O-H bending
1514	**-**	**1587**	**-**	**1600-1500**	**C=C stretching (aromatic ring in lignin)**
1427	**1428**	**1455**	**1426**	**1430-1420**	**CH_2 scissoring motion in cellulose**
1314	1315	-	1314	1310-1250	C-O-C stretching (antisymmetric)
1244	**-**	**1248**	**-**	**1310-1210**	**C-O stretching (aryl group in lignin)**
1158	1160	1148	1158	1160-1000	C-O-C stretching (symmetric)
1031	1054	1033	1027	1050-1000	C-O stretching in cyclic alcohol
897	**897**	**818**	**897**	**937-897**	**β (1-4) glycosidic linkage between the glucose unit in cellulose**

***** Silverstein *et al*., 2003

EDXRF Analysis

Energy dispersive X-ray fluorescence was used for the elemental analysis of raw samples and prepared CNF from PALF and SCB. Figures 5 (a) and (b) show the EDXRF spectra of raw PALF and PALCNF. Figures 6 (a) and (b) also show the raw SCB and SCBCNF. In both raw samples contain many amount of metals. The CNF have the main costituents of (COH) and impurity of sulphur and other the trace metals. Other smaller peaks are Al, Si, K, Ca, Fe, Cu and Zn. They are negligible contents. This elemental impurity is due to the acid (H_2SO_4) hydrolysis of cellulose fibres and remaining after dialysis of CNF having sulphate group to some extent. The elemental constituents in raw samples and prepared CNF are described in Table 4.

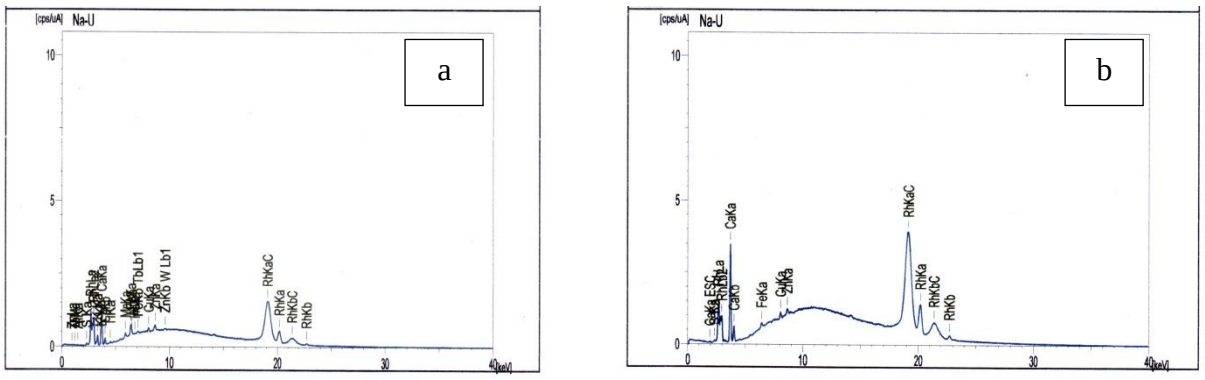

Figure 5 EDXRF spectra of (a) raw pineapple leaf fibres PALF
(b) pineapple leaf cellulose nanofibres PALCNF

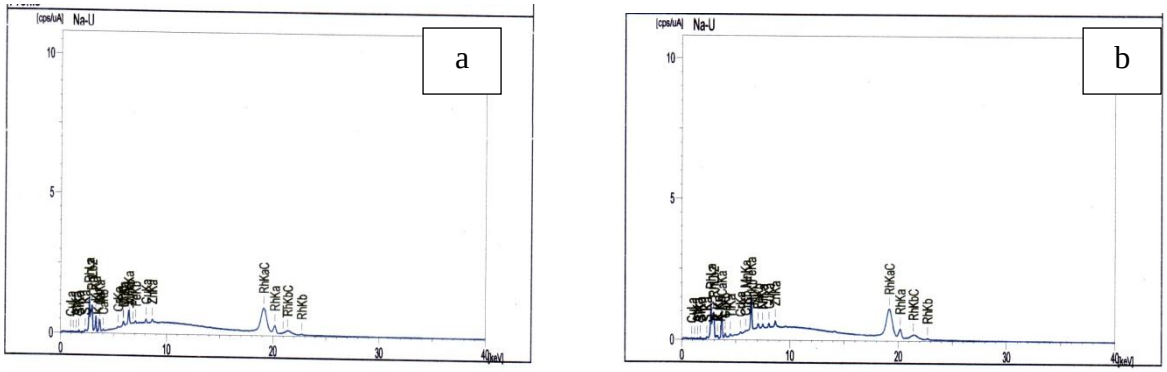

(a) (b)

Figure 6 EDXRF spectra of (a) raw sugarcane bagasse SCB
(b) sugarcane bagasse cellulose nanofibers SCBCNF

Table 4 Relative Abundance of Elements in Raw Samples and Prepared Cellulose Nanofibres from Pineapple Leaf Fibres and Sugarcane Bagasse

Elements	Relative Abundance (%) of Elements in Raw Samples and Cellulose Nanofibres			
	Raw PALF	PALCNF	Raw SCB	SCBCNF
Al	1.190	-	1.239	1.215
Si	-	-	0.528	0.526
K	0.059	-	0.103	0.018
S	0.066	0.68	0.080	0.064
Ca	0.135	0.322	0.044	-
Fe	0.004	0.002	0.005	-
Mn	0.003	-	0.002	-
Cr	-	-	0.001	-
Cu	0.001	0.001	0.001	-
Zn	0.001	0.001	0.001	-
HO	0.002	-	-	-
Ti	0.002	-	-	-
COH	98.537	99.606	97.996	98.057

SEM Analysis

In order to further investigate the structural changes in the fibres, SEM micrographs of the PALF and PALCNF are shown in Figures 7 (a) and (b). According to the SEM image, it is clear that the average diameter of PALCNF is lower than that of PALF. Because PALCNF is the removal of hemicellulose, lignin and pectin after chemical treatment and then to convert nanocellulose after acid hydrolysis. They have fibrous nature.

Figures 8 (a) and (b) also show SEM micrographs of the SCB and SCBCNF. The diameter of the original sugarcane bagasse fibre was much bigger than that of the chemical treatment sample. On treating with the bleaching agent the lignin is removed through complex formation. On subsequent treatment with alkali the hemicellulose is hydrolyzed and becomes water soluble. Finally, the sulphuric acid hydrolysis usually could cleavage the remaining amorphous regions of the cellulose.

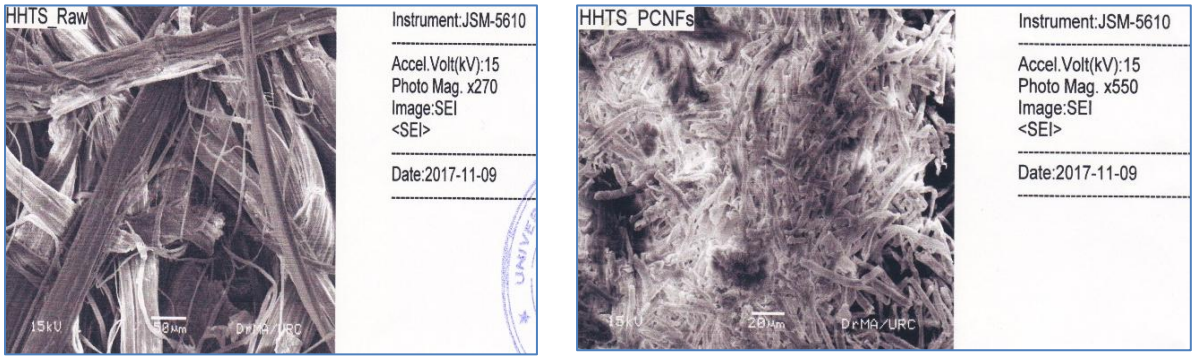

(a) (b)

Figure 7 SEM micrographs of (a) raw pineapple leaf fibres PALF
(b) pineapple leaf cellulose nanofibres PALCNF

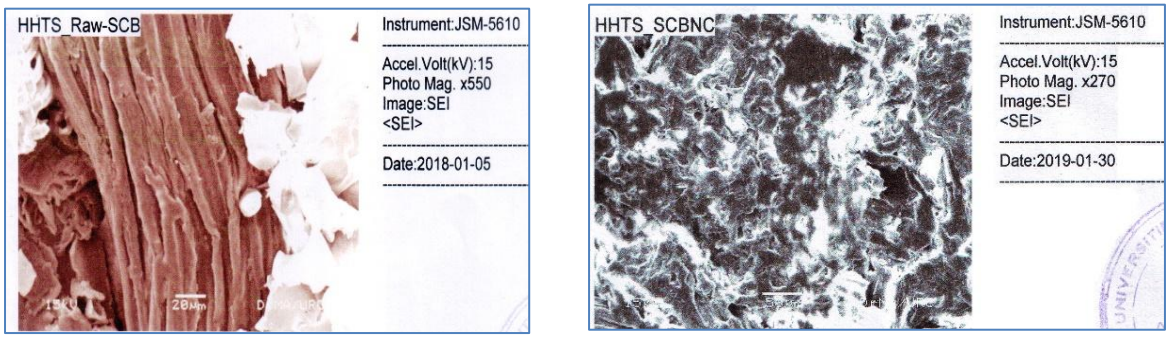

(c) (b)

Figure 8 SEM micrographs of (a) raw sugarcane bagasse SCB
(b) sugarcane bagasse cellulose nanofibres SCBCNF

Conclusion

In this study, cellulose nanofibres can be obtained from prepared cellulose from pineapple leaf fibres and sugarcane bagasse followed by acid hydrolysis. The extracted of CNF and raw samples are investigated to determine the physicochemical properties (moisture, ash, pH and solubility) and the spectrophotometric properties (XRD, FT IR, EDXRF and SEM). The pH values of PALF and SCBCNF to be 6.5 and 6.6 respectively, were found. The pH value falls within the acceptable range (6–7) for cellulose used in the pharmaceutical, cosmetics and food industries. From XRD analysis, the crystallinity index of raw samples and CNFs was calculated. It was found that the increase of crystallinity index of the prepared CNF was due to the partially removal of hemicellulose and lignin. FT IR spectroscopy helps to identify the changes in chemical compound of natural fibres before and after the chemical treatments. Analyzing the

spectra, it is evident that there was no remaining lignin in the obtaining cellulose nanofibers. This arises from the absence of the absorption bands related to the aromatic ring vibrations (1600-1500 cm^{-1}). The spectral bands observed at 1428 cm^{-1}, 1426 cm^{-1}, 897 cm^{-1} represent significant cellulose. Moreover, the bands at 1160 cm^{-1}, 1158 cm^{-1}, 1054 cm^{-1} and 1027 cm^{-1} are observed in pure cellulose. According to the SEM image, the surface morphology of PALF and PALCNF composed of several microfibrils. Elemental analysis (EDXRF) showed 0.068 % and 0.064% sulfur impurity in CNFs along other main components in PALCNF and SCBCNF. PALF has the thread-like structure. PALCNF exhibits rod-like structure. SCB is also exhibits plate like lamella structure but SCBCNF has irregular aggregated shape fibrils. From these observation, the yield percent of cellulose nanofibres obtained from pineapple leaf fibres (40.26 %) is greater than that of sugarcane bagasse (9.6 %). Moreover, the cellulose nanofibres prepared from pineapple leaf fibers has higher crystallinity index percent (89.05 %) than that of sugarcane bagasse (65.28 %). This investigation shows that this chemical process was more efficient and effective process for the preparation of cellulose nanofibres from PALF and SCB.

Acknowledgements

The authors would like to express their profound gratitude to the Department of Higher Education, Ministry of Education, Yangon, Myanmar, for provision of opportunity to do this research and Myanmar Academy of Arts and Science for allowing to present this paper.

References

Adam, A., Yusof, Y. and Yohya, A. (2016). "Extraction of Pineapple Leaf Fibre : Josapine and Moris". *Journal of Enginnering and Applied Science*, vol. 11(1), pp. 161-165

Chandrahasa, R., Rajamane, N. P. and Jeyalakshmi, J. (2008). "Development of Cellulose Nanofibres from Coconut Husk". *International Journal of Emerging Technology and Advanced Engineering*, vol. 4(4), pp. 88-93

Cherian, B. M., Leao, A. L., Souza, S. F. D., Costa, L. M. M., Olyveira, G. M. D., Kottaisamy, M., Nagaragin, E. R. and Thomas, S. (2011). "Cellulose Nanocomposites with Nanofibres Isolated from Pineapple Leaf Fibers for Medical Applications". *Carbohydrate Polymer*, vol. 86, pp. 1790-1798

Kadla, J. F. and Gilbert, R. D. (2000). "Cellulose Structure : A Review". *Cellulose Chemistry Technology*, vol. 34, pp. 197-216

Lavanya, D., Kulkarni, P. K., Dixit, M., Raavi, P. K. and Krishna, L. N. V. (2011). "Sources of Cellulose and Their Application – A Review". *International Journal of Drug Formulation and Research*, vol. 2(6), pp. 19-34

Nohwar, N., Upasham, S., Nair, S. and Vallavhajosyula, S. S. (2016). "Cellulose Nanofibres: From Nature to Biotechnological Solution". *International Journal of Current Biotechnology*, vol. 4(4), pp. 1-6

Silverstein, R. M., Webster, F. X. and Kiemle, D. J. (2003). *Spectrometric Identification of Organic Compounds*. New York: 7th Edition, John Wiley and Sons, Inc.

Wulandari, W. T., Rochliadi, A. and Arcana, I. M. (2016). "Nanocellulose Prepared by Acid Hydrolysis of Isolated Cellulose from Sugarcane Bagasse". *Materials Science and Enginnering*, vol. 107, pp. 1-7

FERMENTATION PROCESS, ANTIMICROBIAL ACTIVITY AND PHYSICOCHEMICAL ANALYSIS OF KEFIR GRAINS FERMENTED MILK, GRAPE (*VITIS VINIFERA* L.) AND APPLE (*MALUS PUMILA*) JUICES

Aye Khaing Soe[1], Phyu Phyu Win[2], Saw Hla Myint[3]

Abstract

The purpose of this study was to prepare low alcoholic fruit beverages through fermentation of grape juice and apple juice with kefir grains and optimum conditions for fermentation has been studied. The present study includes phytochemical investigation of selected fruits (grape and apple), antimicrobial activity and some physicochemical analysis of kefir fermented milk and fruits juice such as pH, titratable acidity, alcohol content, reducing sugar content and total soluble solids were determined. During the12 - 48 h of incubation, pH values of the fermented milk kefir and fruits-based beverages ranged from 5.8 to 3.0. These pH values were similar to those previously reported for kefir beverage. The antimicrobial activity of water kefir, apple juice kefir, grape juice kefir and milk kefir was screened with microorganisms such as three Gram positive bacteria - *Bacillus subtilis*, *Bacillus pumilus*, *Staphylococcus aureus*, two Gram negative bacteria - *Escherichia coli*, *Pseudomonas aeruginosa* and a fungus *Candida albicans* by agar well diffusion method. Milk kefir exhibited higher antimicrobial potency against the test organisms with inhibition zone diameters ranged between 20mm - 25 mm. Apple juice kefir and grape juice kefir also exhibited antimicrobial potency against the test organisms with inhibition zone diameters ranged between 18 mm - 23 mm.

Keywords : Kefir, kefir grains, probiotics, grape, apple, fermentation, antimicrobial activity

Introduction

Fermented foods and beverages play an important role in the human diet as they provide essential as well as contribute towards prevention of diseases. Lactic acid bacteria and yeasts are a major group of microorganism associated with fermented products. Some of the microorganisms, known as probiotics, confer health properties to human health. Thus, many different types of fermented foods and beverages containing probiotics are produced around the world to support wellness and health. (Athanasiadis *et al*., 2004) Probiotics are live microorganisms that have a beneficial effect on the host intestinal microbial balance. Advantages of probiotics are support body's ability to sbsorb nutrients and fight infection, support the immune system and help reduce chronic inflammation in digestive tract, treat high cholesterol and antibiotic associated diarrhoes. Lactic acid bacteria (LAB) and bifidobacteria are the most common types of probiotics.

Kefir is a unique fermented probiotic beverage produced by kefir grains (a mixture of lactic acid bacteria, acetic acid bacteria, and yeast). Kefir is nutrient-dense, with plenty of protein, B vitamins, potassium and calcium. It is incredibly beneficial for digestion and gut health. Kefir grains are multi-species natural starter culture, consisting of lactic acid bacteria (LAB), acetic acid bacteria and yeasts. Both the bacteria and yeast are surrounded by a polysaccharide matrix, called kefiran, which is a water-soluble branched glucogalactan, creating

[1] 2PhD Candidate, Department of Chemistry, University of Yangon
[2] Dr, Associate Professor, Department of Chemistry, Dawei University
[3] Dr, Professor (Retd.), Department of Chemistry, University of Yangon

complex symbiotic community and widely used in fermented dairy products and beverages. It is very complex probiotic.

There are essentially two main types of kefir, and they differ in multiple ways. The two types of kefir are water kefir and milk kefir (Witthuhn *et al*., 2005).

Water kefir is a sour, alcoholic, and carbonated fermented beverage of which the fermentation is started with water kefir grains as inoculum. Water kefir grains consist of polysaccharide and contain microorganisms responsible for the water kefir fermentation. Its light and fizzy and can be flavored with any juice, tea or herbs. Fruit juice kefir is a delicious containing the probiotics benefits of kefir. The selected fruits for fermentation are grapes and apple fruits. Grapes are versatile fruits used in a wide range of popular fruits. It contains high levels of vitamins C, K and copper, good levels of vitamins B6, B2, B1, iron and potassium. The nutrients in grapes may help protect against cancer, eye problems, cardiovascular disease, and other health conditions. Grapes are suitable for people with diabetes, as long as they are accounted for in the diet plan. Apples are one of the most popular fruits in the world. They're also highly nutritious, high in vitamin C, fiber and several antioxidants which helps prevent absorption of dietary-LDL or bad cholesterol in the gut. Apples are low in calories; 100 g of fresh fruit slices provide just 50 calories. This fruit is good for diabetics, blood sugar regulation, protecting bones, boost brain power, aids weight loss (Joshi *et al.*, 2006).

Milk kefir is a fermented milk drink made with a yeast/bacterial fermentation starter of kefir grains. It is prepared by inoculating cow, goat, or sheep milk with kefir grains. Drinking of milk kefir is a healthy, fermented food with a consistency comparable to drinkable yogurt. It is a slightly sour, deliciously creamy and refreshing. Milk grains feed on lactose in milk (Guarner *et al*., 2005).

Various types of kefir beverages have been chosen for this research because fermented foods and beverages play an important role in the human diet as they provide essential nutrients as well as contribute towards prevention of diseases. In this research work, screening of phytochemical constituents, antimicrobial activity and physicochemical analysis of different kefir beverages were carried out.

Materials and Methods

Sample Collection

Water kefir grains (Figure 1) and milk kefir grains (Figure 2) were purchased from the NIHON KEFIA Co., Ltd, Japan. Grape samples were collected from Thirimingalar Market, Yangon Region, originally from Yamethin Township, Mandalay Region and apple samples were also collected from Myitkyina Township, Kachin State.

Botanical Aspect of grape

Botanical name	:	*Vitis vinifera* L.
Family	:	Vitaceae
Genus	:	Vitis
Species	:	Vinifera

Figure 1 Water kefir grains

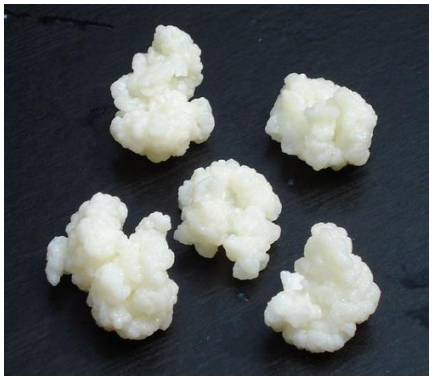

Botanical Aspect of apple

Botanical name	:	*Malus pumila* Mill.
Family	:	Rosaceae
Genus	:	Malus
Species	:	*M.*pumila

Figure 2 Milk kefir grains

Preliminary Phytochemical Investigation of Grape and Apple Juice

In order to find out the types of organic constituents present in the grape and apple fruits samples, preliminary phytochemical investigation was carried out according to the appropriate reported methods.

Investigation of the Development of Fermented Apple and Grape Juice Kefir Beverages Using Kefir Grains as a Starter Culture

Processing of water kefir

Water kefir grains (ca. 4 g) were added in a beaker or glass jar and then water and sugar (sucrose 4 g and distilled water 250 mL) were added. The gas jar was sealed with clean clothes and allowed to culture for 12 to 48 h at room temperature, then the kefir grains were removed to give the water kefir recipes (Figure 3).

Figure 3 Preparation of water kefir recipes

Preparation of fruit juice water kefir

The fermented water kefir (1F) was poured into a large glass jar or beaker and was added to each jar 60 mL of fruit juice or fresh fruit (apple or grape) and then allowed the kefir ferment for another 12 h (2 F). As the fruit was metabolized by kefir grains, the colour change was noticed in 24 h.

Processing of milk kefir

Milk kefir grains (ca. 4 g) were added in a jar and then fresh milk (250 mL) was added. The glass jar was sealed with clean clothes and allowed to culture for 12 to 48 h at room temperature, then the kefir grains were removed, resulting the milk kefir recipes (Figure 4).

Figure 4 Preparation of milk kefir recipes

Physicochemical Analysis of Kefir Beverages

Determination of pH

The pH values of kefir beverages were determined by pH meter.

Determination of total soluble solids content

Total soluble solid (ºBrix) content of kefir beverages was measured in units of degrees Brix by using ABBE refractometer.

Determination of acidity

200 mL of boiled and cooled distilled water was placed into a 50 mL conical flask and added 1mL phenolphthalein and titrated against 0.1 M sodium hydroxide until definite pink end point. Then 5 mL of grape juice sample was added and titrated against 0.1 M sodium hydroxide solution until same distinct end point. (Nummer, 2008). The volume of NaOH was noted and calculated with following equation:

$$\text{Titratable acidity A as tartaric acid } (\text{g}/100\ \text{mL}) = \frac{(\text{V})\ (\text{M})\ (75)\ (100)}{1000\ (\text{v})}$$

V = mL of sodium hydroxide solution used for titration
M = molarity of sodium hydroxide
v = sample volume (mL)

Determination of reducing sugar content

Reducing sugar content of kefir beverages was measured by Lane and Eynon method. (Leung et *al*., 1984).

Determination of alcohol content

Alcohol content of kefir beverages was measured by distillation method.

Screening of Antimicrobial Activities of Different Kefir Beverages by Agar Well Diffusion Method

Screening of antimicrobial activity

Antimicrobial activity of different kefir beverages (water kefir, milk kefir, apple and grape juice kefir) was tested against six pathogenic microorganisms by using agar well diffusion method. The extent of antimicrobial activity was measured from the diameter zone of inhibition. (Cruickshank et *al*., 1975)

Test organisms

Basic test organisms used in the research were kindly supplied by the Fermentation Department, Pharmaceutical Research Department, Ministry of Industry 1, and Yangon Region. These include *Bacillus subtilis, Bacillus pumilus, Staphylococcus aureus, Escherichia coli, Pseudomonas aeruginosa* and *Candida albicans*.

Procedure

Nutrient agar was prepared according to the method described by Cruickshank et al., 1975. Nutrient agar was boiled and 20-25 mL of the medium was poured into the test tube and plugged with cotton wool and sterilized at 121 ºC for 15 min in the autoclave. After this, the tubes were cooled down to 30-35 ºC and poured into the sterilized petri dishes and 0.1-0.2 mL of the test organisms were added into the dishes. The agar was allowed to set for 2-3 h; then 10 mm agar wells were made by the help of sterilized agar well cutter. After that, about 0.2 mL of the sample was introduced into the agar well and incubated at 37 ºC for the 24 h. The inhibition zone which appeared around the agar well, indicated the presence of antimicrobial activity.

Results and Discussion

Preliminary Phytochemical Investigation of Apple and Grape Fruits

Preliminary Phytochemical analysis was performed in order to know different types of chemical constituent present in the fruit samples. The results were summarized in Table 1.

Both of the sample showed the presence of alkaloids, glycosides, flavonoids, carbohydrates, tannins, phenolic compounds, α-amino acids, reducing sugars, organic acid and saponins whereas steroid is absent in both grape and apple fruits. Terpenoids is present in apple fruits but absent in grape fruits.

Table 1 Results of Phytochemical Investigation of Grape and Apple Fruits

No.	Types of compounds	Extract	Test reagents	Observation	Remark	
					Grape	Apple
1	Alkaloids	1 % HCl	Mayer's Wagner's	red ppt yellow ppt	+ +	+ +
2	α-Amino acids	H_2O	Ninhydrin	violet colour spot	+	+
3	Carbohydrates	H_2O	10% α-naphthol and conc: H_2SO_4	red ring violet ring	+	+
4	Flavonoids	H_2O 70 % EtOH	dil:NH_3, conc: H_2SO_4 Mg turning and conc: HCl	yellow colour pink colour	+ +	+ +
5	Glycosides	H_2O	10% lead acetate	white ppt	+	+
6	Terpenoids	$CHCl_3$	Acetic anhydride & conc: H_2SO4	no pink colouration	-	+
7	Phenolic compounds	H_2O	1% $FeCl_3$	green colour deep blue colour	+	+
8	Reducing sugars	dil H_2SO_4	Benedict's solution	brick red ppt	+	+
9	Saponins	H_2O	Distilled water	frothing	+	+
10	Organic acids	H_2O	Bromocresol green	yellow colour	+	+
11	Steroids	PE	Acetic anhydride and conc H_2SO_4	no colouration	-	-
12	Tannins	H_2O	0.1 % $FeCl_3$	greenish yellow	+	+

(-) = absence, (+) = presence

Physicochemical Analysis of Different Kefir Beverages

Physicochemical analyses such as pH, reducing sugar content and acidity content, total soluble solids content and alcohol content of different kefir beverages were determined by reported methods and it was found that longer incubation period, higher acidity content and alcohol content but lower pH value, total soluble solid content and reducing sugar content.

pH

pH values of kefir beverages obtained from different fermentation times were measured by pH meter. The pH value of water kefir was ranged from 5.8 to 3.4.The pH value of milk kefir was ranged from 4.1 to 3.3. The pH value of grape juice kefir was ranged from 3.3 to 3.0. The pH value of apple juice kefir was ranged from 3.4 to 3.0 respectively. This suggests the oxidation of the alcohol to acid upon keeping longer incubation time. These results are reported in Table 2.

Table 2 pH Value of Water Kefir, Milk Kefir, Grape Juice Kefir and Apple Juice Kefir

No.	Samples	pH values			*Literature value
		12 h	24 h	48 h	
1	Water kefir	5.8	3.8	3.4	6.0-3.5
2	Milk kefir	4.1	3.7	3.3	
3	Grape juice kefir	3.3	3.0	3.0	
4	Apple juice kefir	3.4	3.3	3.0	

Acidity

Acidity content of kefir beverages obtained at different fermentation times were measured by titration method. The acid value of water kefir was ranged from 5.8 to 9.71.The acid value of milk kefir was ranged from 3.3 to 4.1. The acid value of grape juice kefir was ranged from 18.3 to 66.27. The acid value of apple juice kefir was ranged from 25.35 to 46.12 respectively. In this research, highest acidity content was observed in grape juice kefir. These results are reported in Table 3.

Table 3 Acidity of Water Kefir, Milk Kefir, Grape Juice Kefir and Apple Juice Kefir

No.	Samples	Acidity content (%)		
		12 h	24 h	48 h
1	Water kefir	5.8	6.8	9.71
2	Milk kefir	3.3	3.7	4.1
3	Grape juice kefir	18.3	39.57	66.27
4	Apple juice kefir	25.35	35.93	46.12

Alcohol content

Alcohol content of kefir beverages obtained from different fermentation times were measured by distillation method. The alcohol content of water kefir was ranged from 0.1 to 0.44.The alcohol content of milk kefir was ranged from 0.05 to 0.4. The alcohol content of grape juice kefir was ranged from 1.0 to 1.81. The alcohol content of apple juice kefir was ranged from 0.4 to 1.20 respectively. During the 12 h, 24 h and 48 h of incubation, alcohol content of fermented water kefir, milk kefir, apple juice kefir and grape juice kefir was increased. Highest alcohol content was observed in grape juice kefir. These results are reported in Table 4.

Table 4 Alcohol Content of Water Kefir, Milk Kefir, Grape Juice Kefir and Apple Juice Kefir

No.	Samples	Alcohol content (%)		
		12 h	24 h	48 h
1	Water kefir	0.1	0.2	0.44
2	Milk kefir	0.05	0.15	0.4
3	Grape juice kefir	1.0	1.48	1.81
4	Apple juice kefir	0.4	0.66	1.20

Total soluble solid content

Total soluble solid (ºBrix) content content of kefir beverages was measured in units of degrees Brix by using ABBE refractometer. The total soluble solid content of water kefir was ranged from 1.3 to 0.3. The total soluble solid content of milk kefir was ranged from 3.0 to 1.9. The total soluble solid content of grape juice kefir was ranged from 7.8 to 5.00. The total soluble solid content of apple juice kefir was ranged from 8.4 to 6.25 respectively. In this research, when longer incubation period were observed lower total soluble solid content. These results are reported in Table 5.

Table 5 Total Soluble Solid (ºBrix) Content of Water Kefir, Milk Kefir, Grape Juice Kefir and Apple Juice Kefir

No.	Samples	Total soluble solid (ºBrix)		
		12 h	24 h	48 h
1	Water kefir	1.3	0.85	0.3
2	Milk kefir	3.0	2.6	1.9
3	Grape juice kefir	7.8	6.25	5.00
4	Apple juice kefir	8.4	7.00	6.25

Reducing sugar content

Reducing sugar content of kefir beverages obtained different fermentation times were measured by Lane and Eynon method. The reducing sugar content of water kefir was ranged from 4.8 to 1.9.The reducing sugar content of milk kefir was ranged from 4.1 to 3.3. The reducing sugar content of grape juice kefir was ranged from 5.1 to 2.76. The reducing sugar content of apple juice kefir was ranged from 3.5 to 3.64 respectively. In this research, when longer incubation period were observed lower reducing sugar content. But highest reducing sugar content was observed in apple juice kefir .These results are reported in Table 6.

Table 6 Reducing Sugar Content of Water Kefir, Milk Kefir, Grape Juice Kefir and Apple Juice Kefir

No.	Samples	Reducing Sugar content (%)		
		12 h	24 h	48 h
1	Water kefir	4.8	3.0	1.9
2	Milk kefir	4.1	3.7	3.3
3	Grape juice kefir	5.1	4.05	2.76
4	Apple juice kefir	3.5	3.84	3.64

Antimicrobial Activity of Water Kefir, Apple Juice Kefir, Grape Juice Kefir and Milk Kefir against on Six Species of Microorganisms

Antimicrobial activity of water kefir , apple juice kefir, grape juice kefir and milk kefir were screened on six different strains of microorganisms such as *Bacillus subtilis*, *Bacillus pumilus*, *Staphylococcus aureus*, *Escherichia coli*, *Pseudomonas aeruginosa* and *Candida albicans* by agar well diffusion method. It was found that milk kefir exhibited higher antimicrobial potency against *Bacillus subtilis*, *Staphylococcus aureus*, *Pseudomonas aerugino* and *Escherichia coli* with inhibition zone diameters ranged between 20 mm - 25 mm. But Milk kefir showed no activity on *Bacillus pumilus* and *Candida albicans.* Apple juice kefir and grape juice kefir also exhibited antimicrobial potency against the test organisms with inhibition zone diameters ranged between 18 mm - 23 mm. Therefore, prepared kefir beverages showed the antimicrobial activity and it may be used for the treatment of diseases infected by the microorganisms such as diarrhea, dysentery and urinary infections.The result of antimicrobial activities of different kefir beverages samples are reported in Table 7 and Figures 5 to 10.

Table 7 Antimicrobial Activity of Water Kefir , Apple Juice Kefir, Grape Juice Kefir and Milk Kefir against on Six Species of Microorganisms

No.	Sample	Inhibition zone diameters (mm) against different microorganisms					
		A	**B**	**C**	**D**	**E**	**F**
1	Water Kefir	12(+)	13(+)	23(+++)	14(+)	15(++)	13(+)
2	Milk Kefir	20(+++)	20(+++)	20(+++)	-	-	25(+++)
3	Apple Juice Kefir	23(+++)	22(+++)	23(+++)	23(+++)	20(+++)	23(+++)
4	Grape Juice Kefir	21(+++)	20(+++)	20(+++)	20(+++)	20(+++)	18(++)
5	(-) Control	-	-	-	-	-	-

Agar well - 10 mm
10mm ~ 14 mm (+)
15 mm ~ 19 mm (++)
> 20 mm above (+++)

A = *Bacillus subtillis*
B = *Staphylococcus aureus*
C = *Pseudomonas aeruginosa*
D = *Bacillus pumilus*
E = *Candida albicans*
F = *E.coli*

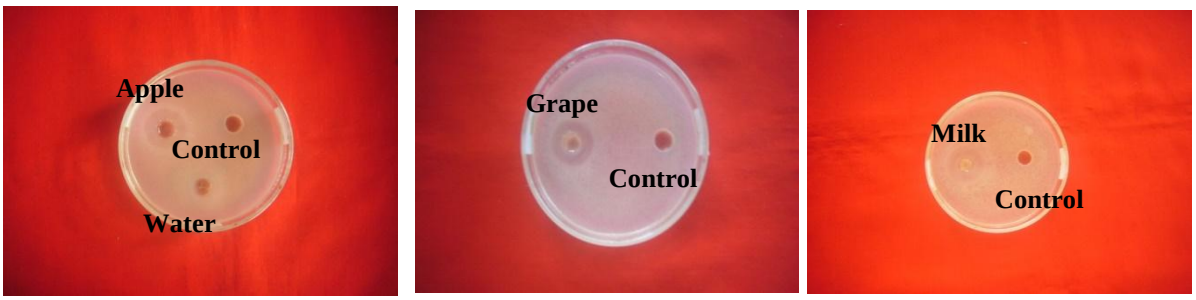

Figure 5 Antimicrobial screening of water kefir, apple juice kefir, grape juice kefir and milk kefir against *Bacillus subtillis* by agar well diffusion method

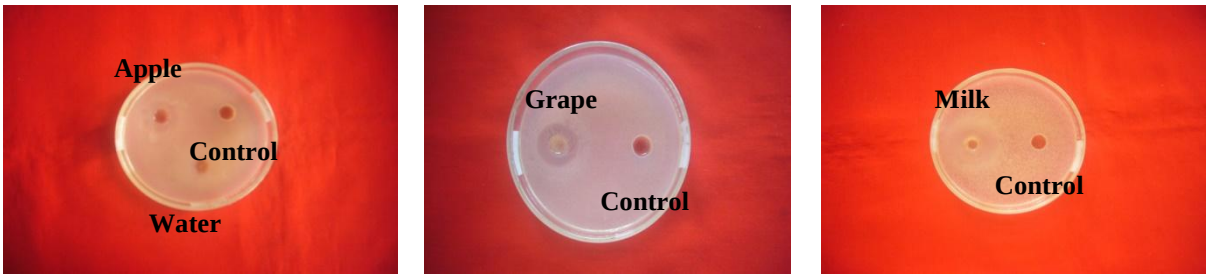

Figure 6 Antimicrobial screening of water kefir, apple juice kefir, grape juice kefir and milk kefir against *Staphylococcus aureus* by agar well diffusion method

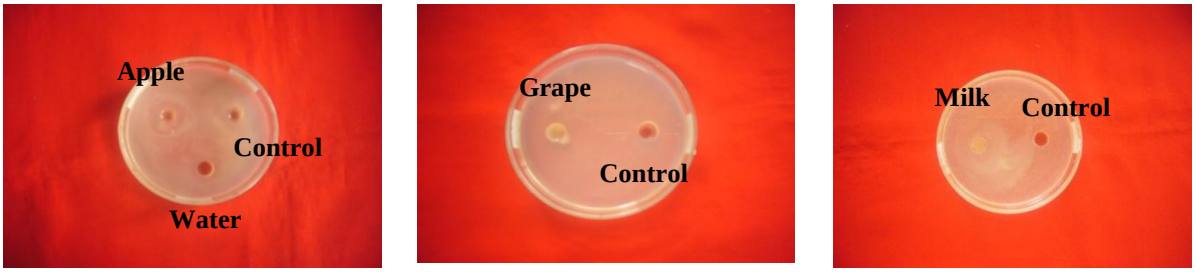

Figure 7 Antimicrobial screening of water kefir, apple juice kefir, grape juice kefir and milk kefir against *Pseudomonas aeruginosa* by agar well diffusion method

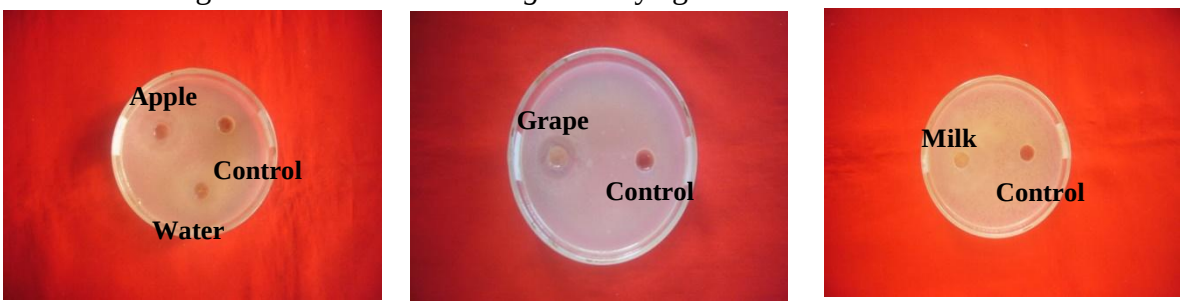

Figure 8 Antimicrobial screening of water kefir, apple juice kefir, grape juice kefir and milk kefi against *Bacillus pumilus* by agar well diffusion method

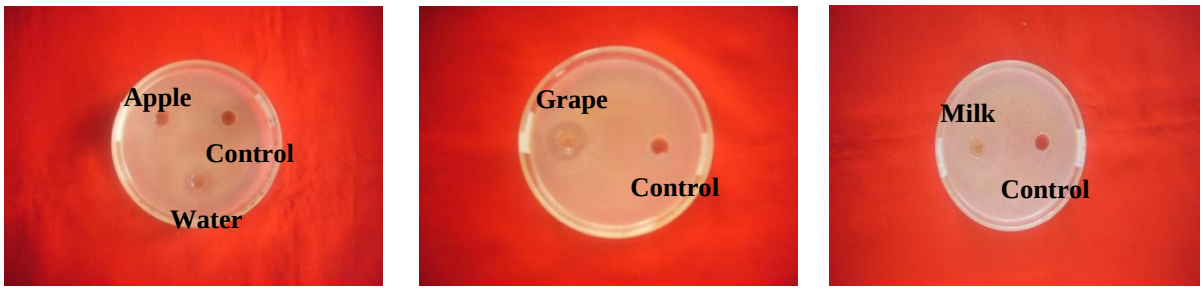

Figure 9 Antimicrobial screening of water kefir, apple juice kefir, grape juice kefir and milk kefir against *Candida albicans* by agar well diffusion method

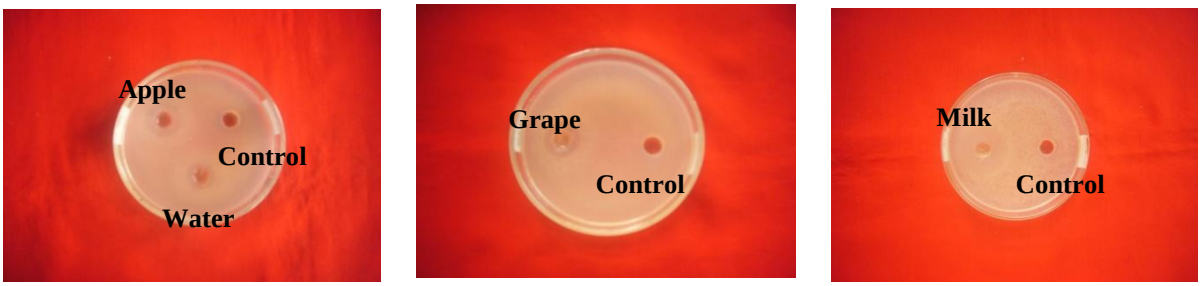

Figure 10 Antimicrobial screening of water kefir, apple juice kefir, grape juice kefir and milk kefir against *E.coli* by agar well diffusion method

Conclusion

The preliminary phytochemical investigation indicated the presence of alkaloids, glycosides, flavonoids, carbohydrates, tannins, phenolic compounds, α-amino acids, reducing sugars, organic acid and saponins in grape and apple fruits. Steroid was found to be absent in both grape and apple fruits. Terpenoids was found to be present in apple fruits but absent in grape fruits.

From the determination of the some physicochemical properties of kefir beverages, pH values of the fermented water kefir, milk kefir and fruits-based beverages ranging from 5.8 to 3.0 during the 12 h, 24 h and 48 h of incubation,. These pH values were similar to those previously reported for kefir beverage. During the 12 h, 24 h and 48 h of incubation, acidity content of different kefir beverages were increased from 3.3 % to 46.12 %, alcohol content was increased from 0.05 % to 1.81%, total soluble solid (TSS) content and reducing sugar content was reduced from 8.4 ºBrix to 0.3 ºBrix and 5.1 % to 1.9 %, respectively.

From antimicrobial screening tests, almost all of the kefir beverages (water kefir, milk kefir, grape Juice kefir and apple Juice kefir) exhibited antibacterial and antifungal activities.

Among them, milk kefir showed higher potency with inhibition zone diameter up to 25 mm on *Bacillus subtilis, Staphylococcus aureus, Pseudomonas aeruginosa* and *Escherichia coli*. Apple juice kefir and grape juice kefir also exhibited antimicrobial potency with inhibition zone diameter up to 23 mm against on all test organisms. Thus kefir beverages may be useful in the treatment of bacterial and fungal infections owing to its effective antibacterial and antifungal actions.

Acknowledgements

The authors would like to thank the Myanmar Academy of Art and Science for allowing to present this research work and Dr Ni Ni Than, Head of Department of Chemistry, University of Yangon, for allowing me to use the research facilities.

References

AOAC. (2000), *Official and Tentative Methods of Analysis, Association of Official Analytical Chemists*, Washington DC : 17th Ed., pp. 150-152

Athanasiadis, I., Paraskevopoulou, A., Blekas G. and Kiosseoglou. V. (2004). "Development of a Novel Whey Beverage by Fermentation with Kefir Granules Effect of Various Treatments". *Biotechnology Progress*., vol. 20, pp. 1091-1095

Beshkova, D., Simova, E. D., Simov, Z. I., Frengova, G. I. and Spasov, Z. N. (2002). "Pure Cultures for Making Kefir". *Food Microbiol*, vol. 19, pp. 537-544

Cruickshank, R., Duguid, J.P., Marmion, B.P. and Swain, R.H.A. (1975) *Medical Microbiology*, The Practice of Medical Microbiology. 12th Ed, vol. II, pp.96-150

Guarner, F., Corthier, G., Salminen, S., Koletzko, B. and Morelli., L. (2005). "Should Yoghurt Cultures be Considered Probiotic?". *Br J Nutr*., Vol. 93(6), pp. 783– 86.

Joshi, V. K., Sharma S. and Rana. N. S. (2006). "Production, Purification, Stability and Efficacy of Bacteriocin from Isolates of Natural Lactic Acid Fermentation of Vegetables". *Food Technol. Biotechnol.*, vol. 44, pp. 435-439

Leung, David, W. M., Thorpe and Trevor, A. (1984). "Interference by edta and calcium ions of the 3,5-dinitrosalicylate reducing sugar assay". Phytochemistry. Pergamon Press., vol 23 (12), pp. 2949–2950

Marini-Bettolo, G. B., Nicole, H. M. and Palamia. M. (1981). "Plant Sc reening by Chemical and Chromatographic Procedure Under Field Condition". *J. Chromatog*., pp. 121-123

M-Tin Wa. (1972). "Phytochemical Screening Methods and Procedure". *Phytochemical Bulletin of Botanical Society of America Inc*., vol. 5(3), pp. 4-10

Nummer, B.A. (2008). "Food Acidity and Safety". *Food Safety*, vol. 1, pp. 1-4

Shi, J., Yu, J., Pohorly J. E. and Kakuda. Y. (2003). "Polyphenolics in Grape Seeds—Biochemistry and Functionality". *Journal of Medicinal Food*, Vol. 6 (4), pp. 291-299.

Witthuhn, R. C., Schoeman, T. and Britz, T. J. (2005). "Characterisation of the Microbial Population at Different Stages of Kefir Production and Kefir Grain Mass Cultivation". *Int. Dairy J*., vol. 15, pp. 383-389

ISOLATION AND CHARACTERIZATION OF α-AMYLASE DURING GERMINATION OF MAIZE GRAINS (*ZEA MAYS* L.)

Khin Sandar Linn[1], Myat Kyaw Thu[2], Thaw Thaw Win[3]

Abstract

α-Amylase (EC 3.2.1.1) break down long-chain carbohydrate, ultimately yielding maltotriose and maltose. In this research, α-amylase from germinating maize grains was extracted by using sodium chloride and acetate buffer pH 5.6 solution. Qualitative examination of α-amylase activity in the solution was carried out by using iodine staining method. Soluble starch was used as a substrate for α-amylase activity determination by measuring the absorbance of maltose using UV-visible spectrophotometer. α-Amylase activities during germinating of maize grains were studied by determining the daily enzyme activity. The maximum α-amylase activity was found on third day of growth. The protein content of enzyme solution was determined by Biuret method. The specific activity of enzyme solution was calculated to be 12.035 μmol min^{-1} mg^{-1}. The enzyme unit (EU) of crude α-amylase was found to be 165.01 EU per gram of maize grains. The optimum pH of α-amylase was found to be 5.6 in acetate buffer and optimum temperature was found to be 60 °C. The values of K_m and V_{max} treated statistically using the linear regression method were compared with various graphically methods (Michaelis-Menten, Lineweaver-Burk, Eadie-Hofstee and Hanes-Wilkinson). The K_m and V_{max} values of α-amylase were found to be 0.192×10^{-2} g mL^{-1} and 1.978×10^{-3} M min^{-1}, respectively, from Lineweaver-Burk plot. The reaction order (n) for α-amylase was calculated to be 1.203 proving that the reaction order is first order. The activation energy (E_a) of α-amylase-catalyzed reaction was calculated to be 4.977 kcal mol^{-1}. In this research, cassava sample was used as a starch source for the preparation of maltose. The maltose content in the prepared sample was determined by using Dinitrosalicylic acid method.

Keywords : Germinating maize grains, α-amylase, soluble starch, maltose

Introduction

Maize (*Zea mays* L.) is a major staple food grain throughout the world, particularly in Africa, Latin America and Asia. Maize is a tropical plant (Fox and Manley, 2009) which requires warm temperatures. The maximum size of kernels is reputedly 2.5 cm. An ear commonly holds 600 kernels. The grains are about the size of peas, and adhere in regular rows around a white, pithy substance, which forms the ear. α-Amylase is a protein enzyme (EC 3.2.1.1) that hydrolyses alpha bonds of large, alpha-linked polysaccharides, such as starch and glycogen, yielding glucose and maltose (Hussain *et al*., 2013).

Cereal α-amylases are known as enzyme originates from cereals grain such as wheat, barley, maize, rye etc. (Muralikrishna and Nirmala, 2005). It plays a dominant role in starch metabolism during grain development as well as germination. α-Amylases (endo-1,4-α-D-glucan glucohydrolase) are extracellular enzymes that randomly cleave the 1,4-α-D-glucosidic linkages between adjacent glucose units in the linear amylose chain (Anto *et al*., 2006).

Amylases are one of the main enzymes used in industry. Such enzymes hydrolyze the starch molecules into polymers composed of glucose units. Amylases have potential application in a wide number of industrial processes such as food, fermentation and pharmaceutical industries (Souza and Magalhaes, 2010). α-Amylases can be obtained from plants, animals and

[1] Dr, Assistant Lecturer, Department of Chemistry, University of Yangon
[2] Dr, Professor, Department of Chemistry, University of Yangon
[3] MSc, Department of Chemistry, University of Yangon

microorganisms. The production of α-amylase is essential for conversion of starches into oligosaccharides. Starch is an important constituent of the human diet and is a major storage product of many economically important crops such as wheat, rice, maize, tapioca, and potato. Starch-converting enzymes are used in the production of maltodextrin, modified starches, glucose, maltose and fructose syrups.

Cassava starch is used as a starch source and enzymic hydrolysis of starch was carried out by using crude α-amylase from maize grain. The maltose content was measured by dinitrosalicylic acid method. The production of sugar syrups by enzymatic method is among the most advanced food technologies, characterized by higher yields, wide range of products, higher product quality and energy economy (Blanchard and Katz, 1995).

The aim of this research was to study the isolation and characterization of α-amylase during germination of maize grains.

Materials and Methods

Materials

Maize Grains samples and cassava starch were purchased from local shop, Yangon Region. Bovine Serum Albumin (BSA) was purchased from Sigma Aldrich, England. All other chemicals used were of analytical reagent grade. In all investigations, the recommended standard methods and techniques involving both conventional and modern methods were provided.

Sample Preparation and Extraction of α-Amylase from Maize Grains

Maize grains (Figure 1) were placed in wet sand and kept at room temperature. After day 1 of germination, maize grains (10 g) were taken and α-amylase was extracted with sodium chloride and acetate buffer pH 5.6 solution. The partially purified α-amylase was qualitatively examined by iodine staining method for its α-amylase activity. Soluble starch was used as a substrate for α-amylase activity determination by measuring the absorbance of maltose using UV-visible spectrophotometer. Similarly, the same procedure was carried out after day 2, 3, 4, 5, 6, 7, 8 and 9 germination. Protein content was determined by Biuret method using Bovine Serum Albumin (BSA) as standard at 550 nm. Specific activity was calculated by using enzyme activity and protein content.

(a) (b)

Figure 1 (a) Maize seeds (b) After third day germination

Characterization of α-Amylase from Maize Grains

α-Amylase properties of optimum pH, optimum temperature and effect of reaction time were determined by dinitrosalicylic acid method. The enzyme kinetic parameters of K_m, V_{max} and reaction order of α-amylase-catalyzed reaction were determined by dinitrosalicylic acid method (Mohamed *et al*., 2009).

Application of α-Amylase from Maize Grains

Cassava sample was used as a starch source for the preparation of maltose. The maltose content in the prepared sample was determined by using dinitrosalicylic acid method (Blanchard and Katz, 1995).

Results and Discussion

Extraction of α-Amylase from Maize Seed

In this work, crude α-amylase was extracted from germinated maize seed (Kigel *et al*., 1995). After day 1, germinated maize was taken and extracted with salt solution. Similarly, the same procedure was carried out after day 2, 3, 4, 5, 6, 7, 8 and 9 germination.

Qualitative Examination of α-Amylase by Using Iodine Staining Method

The iodine staining method is well suited for extensive kinetic analysis of purified enzyme (Normera, 1986). Thus, qualitative examination of α-amylase was done by using iodine staining method (Harper, 1977). In this work, a blank solution containing the mixture of starch and distilled water showed deep blue colour with iodine solution, whereas solution mixture containing the enzyme and starch solutions showed no colour with iodine solution (Figure 2). Therefore, α-amylase enzyme isolated from germinated maize hydrolyzes the starch by breaking down the α-glucosidic bond.

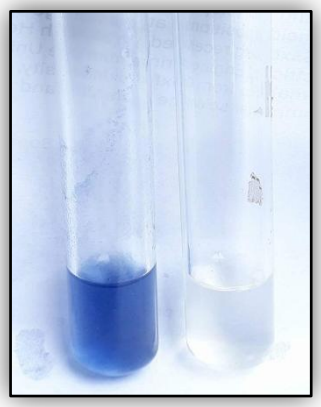

(a) **(b)**

Figure 2 Gelatinized starch solution treated with iodine solution
(a) without enzyme (control)
(b) with enzyme after 10 min at RT

Construction of Calibration Curve for Determination of Maltose Liberated from α-Amylase Action by DNS Method

Maltose can be used as a standard for estimating reducing sugar in unknown samples (Mohamed *et al*., 2009). Maltose reduces the pale yellow coloured alkaline 3,5-dinitrosalicylic acid (DNS) to the orange-red coloured, 3-amino 5-nitro salicylic acid. This intensity change in colour is measured using a UV-visible spectrophotometer as the absorbance at 540 nm wavelength. It was found that the nature of the plot of absorbance *vs.* concentration of maltose (Table 1 and Figure 3) was a straight line passing through the origin showing that Beer's Law was obeyed.

Table 1 Relationship between Absorbance and Concentration of Standard Maltose Solution

No.	Concentration of maltose (mM)	Absorbance at 540 nm
1	2.777	0.169
2	2.222	0.130
3	1.666	0.105
4	1.111	0.063
5	0.555	0.032
6	0.278	0.013

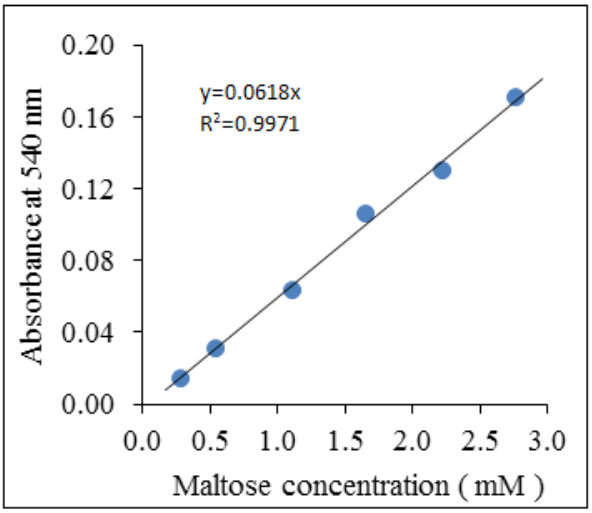

Figure 3 Plot of absorbance as a function of standard maltose concentration

Variation of α-Amylase Activity in Germinated Maize

During germination, a number of enzymes are synthesized and play a role in the complex process of maize production (Thoma, 1971). Especially enzyme degrading carbohydrate, α-amylase and proteins are formed. In this work, the maximum α-amylase activity was determined from the amount of maltose formed during the α-amylase-catalyzed reaction in the time scale of 1 to 9 days. The plot of α-amylase activity *vs.* day of germination (Table 2 and Figure 4) showed that the activity increased with the days and a maximum was reached at 3 days. Finally, the activity decreased with the increased in germination day. The maximum α-amylase activity was found to be 7.675 μmol min^{-1} mL^{-1} at day 3. α-Amylase was isolated from germinated maize by extraction with aqueous solution (acetate buffer).

Table 2 Relationship between Day of Germination and α-Amylase Activity

Germination (Day)	α-Amylase activity (μmol min^{-1} mL^{-1})
1	3.475
2	4.865
3	7.675
4	4.311
5	3.970
6	3.896
7	3.875
8	3.600
9	3.253

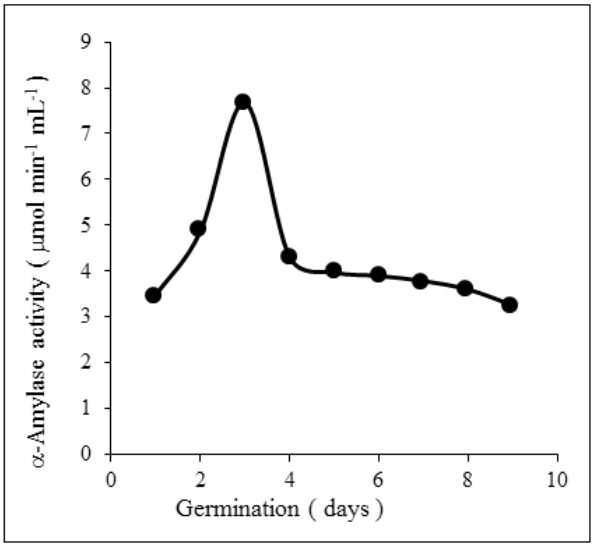

Figure 4 Variation of α-amylase activity with day of germination

Calibration Curve for Protein Determination by Biuret Method

Before determining the proteins content in sample solutions, it is necessary to construct a calibration curve by using standard protein concentration and their absorbance at 550 nm (Savary *et al.*, 1969). In this work, bovine serum albumin (BSA) was used as a standard protein. The different absorbance values were obtained for various standard protein solutions by using a UV-visible spectrometer. It was found that the nature of the plot of absorbance at 550 nm *vs.* concentration of protein (mg $mL^{-1)}$ (Table 3 and Figure 5), was a straight line passing through the origin showing that Beer's Law was obeyed.

Table 3 Relationship Between Absorbance and Concentration of Bovine Serum Albumin (BSA) Solutions

No.	Absorbance at 550 nm	Protein Concentration (mg mL^{-1})
1	0.006	0.024
2	0.014	0.048
3	0.022	0.072
4	0.030	0.098
5	0.035	0.120

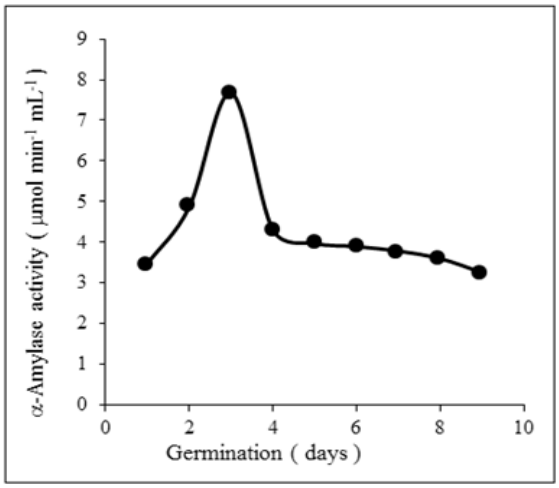

Figure 5 Calibration curve for standard protein solution

α-Amylase Activity, Protein Content and Specific Activity of the Enzyme Solution in α-Amylase by Biuret Method

α-Amylase activity was determined from the amount of maltose formed during the α-amylase-catalyzed reaction using starch as the substrate, according to the DNS method. The enzyme unit (EU) of crude α-amylase was found to be 160.01 EU per gram of maize grain. The protein content was determined by Biuret method. The protein content was observed to be 0.6377 mg mL^{-1}. Specific activity is the total activity divided by total protein. Specific activity was calculated by dividing the number of units/mL by the protein concentration in mg/mL to get μmol/min/mg. The specific activity was calculated to be 12.035 μmol min^{-1} mg^{-1}.

Optimum pH of α-Amylase Activity

At an optimum pH, an enzyme's activity is greatest. At pH above and below optimum pH, the activity of the enzyme is reduced and reaction rates are slower (Charles, 2007). In this work, different buffers of pH value 3.6 to 6.5 were used to determine the activity of the prepared α-amylase sample. The nature of the activity *vs.* pH curve of the enzyme (Table 4 and Figure 6) was obviously found to be unsymmetrical and the optimum pH was obtained at pH 5.6 with starch as substrate.

Table 4 Relationship between α-Amylase Activity and pH of Buffer Solution

Buffer	pH	α-Amylase activity (μmol min^{-1} mL^{-1})
Acetate	3.6	1.952
Acetate	4.0	3.941
Acetate	4.4	5.202
Acetate	4.8	5.796
Acetate	5.2	6.190
Acetate	5.6	7.479
Sodium Phosphate	6.0	3.556
Sodium Phosphate	6.5	4.554

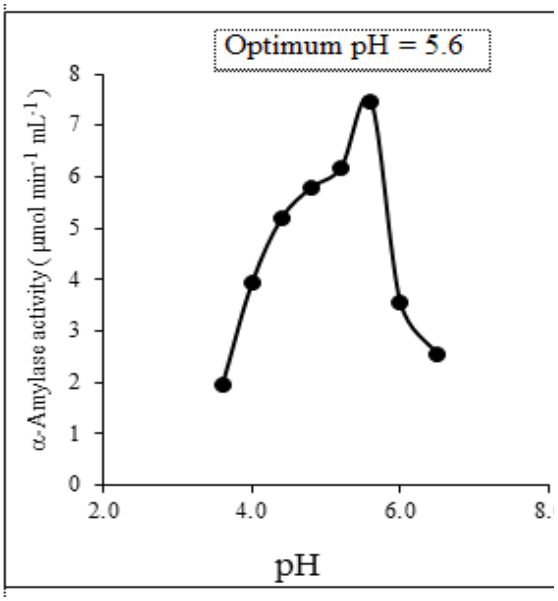

Figure 6 Plot of α-amylase as a function of pH solutions

Optimum Temperature of α-Amylase Activity

In this study, the effect of the temperature on the α-amylase activity was investigated in the temperature range from 40 to 90 ºC. The optimum temperature for α-amylase was found to be 60 ºC in acetate buffer pH 5.6 (Table 5 and Figure 7). The activation energy of α-amylase-catalyzed reaction was calculated by using Arrhenius equation (Atkins, 1994). Table 6 shows the relationship between temperature and velocity of α-amylase-catalyzed reaction. Figure 8 shows the graph for determination of activation energy and Arrhenius constant. By using the constant substrate concentration throughout the experiment, rate constant (K) in Arrhenius equation can

be substituted by velocity of the α-amylase-catalyzed reaction. The activation energy (E_a) was determined to be 4.977 kcal mol^{-1} from linear regression method.

Table 5 Relationship between α-Amylase Activity and Temperature of the Solution at pH 5.6

Temperature (°C)	α-Amylase Activity (μmol min^{-1} mL^{-1})	Velocity x 10^{-3} (M min^{-1})
40	5.434	1.208
45	6.004	1.334
50	6.803	1.512
55	8.452	1.878
60	9.117	2.206
70	6.899	1.533
80	5.619	1.249
90	5.243	1.165

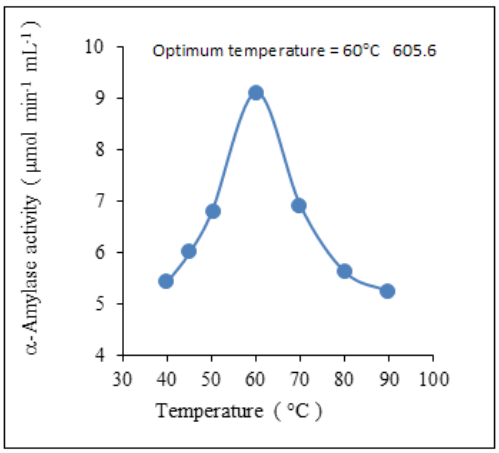

Figure 7 Plot of α-amylase activity as a function of temperature of the solutions at pH 5.6

Table 6 Relationship between Temperature and Velocity of theα-Amylase-catalyzed Reaction

Temperature (°C)	Temperature (K)	1/T (10^{-3} K^{-1})	Velocity × 10^3 (M min^{-1})	Log V
40	313	3.195	1.208	-2.9179
45	318	3.145	1.334	-2.8748
50	323	3.096	1.512	-2.8024
55	328	3.048	1.878	-2.7263
60	333	3.003	2.026	-2.6934

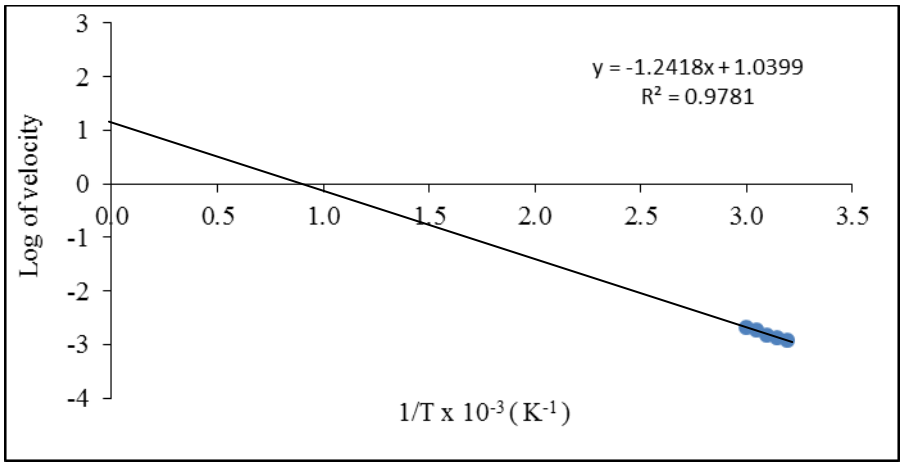

Figure 8 Plot of log of velocity as a function of 1/T for Germinated maize α-amylase

Effect of Reaction Time on α-Amylase-catalyzed Reaction

Among other conditions which control the rate of enzyme reaction, reaction time is an important factor in the determination of enzyme activity (Anderson, 1972).

In this work, the action of the α-amylase on soluble starch was studied in acetate buffer of pH 5.6. The amount of maltose liberated during the various reaction times of 3, 5, 10, 15, 20, 25, 30 and 35 min were determined by dinitrosalicylic acid method (Table 7). Figure 9 shows the plot of velocity of α-amylase reaction as a function of reaction time. At the beginning of the reaction (during 15 min), the reaction is very fast. Then, velocity decreased steadily. Therefore, in sequence studies, reaction time of 10 min was used for initial velocity measured in enzyme kinetic.

Table **7 Relationship between Reaction Time and Velocity of α-Amylase -catalyzed Reaction**

No	Reaction Time (min)	Concentration (mM)	Velocity (mM min^{-1})
1	3	12.012	4.004
2	5	12.159	2.432
3	10	16.711	1.671
4	15	16.793	1.119
5	20	17.484	0.874
6	25	17.763	0.711
7	30	17.993	0.599
8	35	18.272	0.522

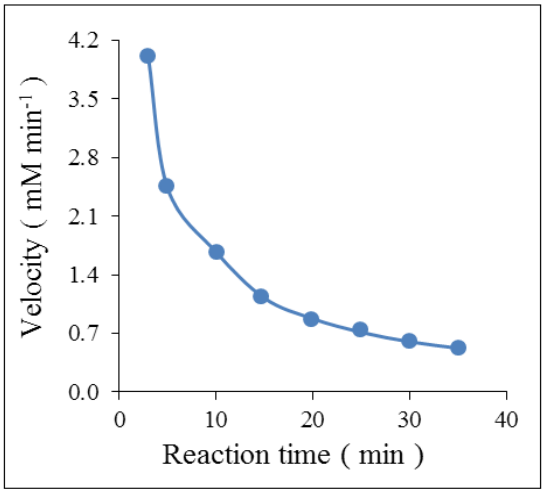

Figure 9 Plot of velocity of α-amylase-catalyzed reaction as a function of reaction time

Effect of Enzyme Concentration on α-Amylase-catalyzed Reaction

The activity of an enzyme is determined by the enzyme concentration (Walsh, 1968). As the enzyme concentration increases the rate of reaction increases linearly, because there are more enzyme molecules available to catalyze reaction. The validity of enzyme assay method was tested using different volume of enzyme. The enzyme activity was found to have a linear relationship with different volumes of enzyme solution ranging between 0.05 to 0.2 mL of enzyme (Table 8 and Figure 10).

Table 8 Relationship between α-Amylase Activity and Enzyme Concentration

No.	Enzyme solution (mL)	α-Amylase activity (μmol min^{-1} mL^{-1})
1	0.05	3.415
2	0.10	6.367
3	0.15	8.945
4	0.20	12.09

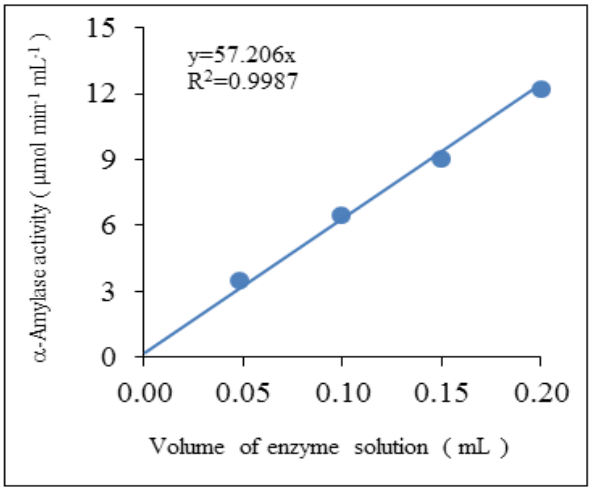

Figure 10 Plot of α-amylase activity as a function of volume of α-amylase solution of enzyme solution

Effect of Substrate Concentration on α-Amylase-catalyzed Reaction

In the present work, the velocities of enzyme reaction measured at different levels of starch concentration and their reciprocal values are shown in Table 9. The Michaelis-Menten plot of V *vs.* [S] is shown in Figure 11. If the concentration of starch was increased, the rate if reaction also increased until a point was reached where the enzyme was working as fast as it could; that was, it was transforming its maximum number of starch molecules each minute. At this point, the enzyme was said to be saturated, and further increases in the concentration of the starch would not increased the rate of reaction. The enzyme could worked no faster.

Most common transform is the Lineweaver-Burk plot which is also called double reciprocal plot (1/V vs 1/[S]) (Figure 12). From this Lineweaver-Burk plot K_m and V_{max} values were found to be 0.192×10^{-2} g mL^{-1} and 1.978×10^{-3} M min^{-1}, respectively. Figure 13 shows the Eadie-Hofstee plot of V vs V/[S]. K_m and V_{max} values obtained by this plot were 0.126×10^{-2} g mL^{-1} and 1.863×10^{-3} M min^{-1}, respectively. Hanes-Wilkinson plot, an alternative plot of [S]/V vs [S] based on Hanes equation gave a straight line as shown in Figure 14. From this plot, K_m and V_{max} values were calculated to be 0.114×10^{-2} g mL^{-1} and 1.843×10^{-3} M min^{-1}, respectively. Comparison of kinetic parameters of the α-amylase enzyme from different methods is shown in Table 10.

Table 9 Relationship between Substrate Concentration and Velocity of α-Amylase-

No.	$[S]\times10^{-2}$ (g mL^{-1})	$-[S]\times10^{-2}$ (g mL^{-1})	$1/[S]\times10^{2}$ (g^{-1} mL)	$V\times10^{-3}$ (M min^{-1})	$1/V\times10^{3}$ (M^{-1}min)	V/[S] (M min^{-1} g^{-1} mL)	$[S]/V\times10$ (gmL^{-1} M^{-1} min)
1	0.50	-0.50	2.000	1.219	0.820	2.438	0.410
2	0.75	-0.75	1.333	1.481	0.676	1.975	0.506
3	1.00	-1.00	1.000	1.676	0.597	1.676	0.597
4	1.25	-1.25	0.800	1.695	0.589	1.356	0.737
5	1.50	-1.50	0.667	1.719	0.582	1.146	0.873
6	1.75	-1.75	0.571	1.739	0.575	0.994	1.006

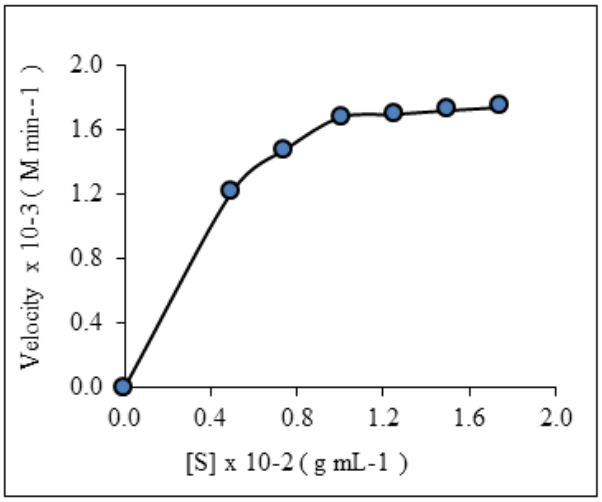

Figure 11 Michaelis-Menten plot used for graphic evaluation of V_{max} and K_m for crude α-amylase

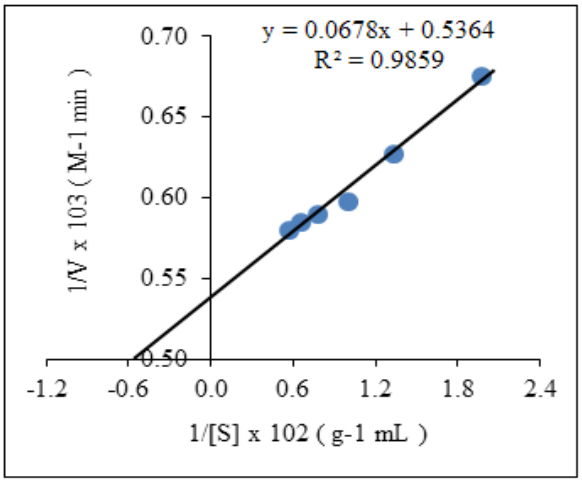

Figure 12 Lineweaver-Burk plot of 1/V *vs.* 1/[S] used for graphic evaluation V_{max} and K_m for crude α-Amylase

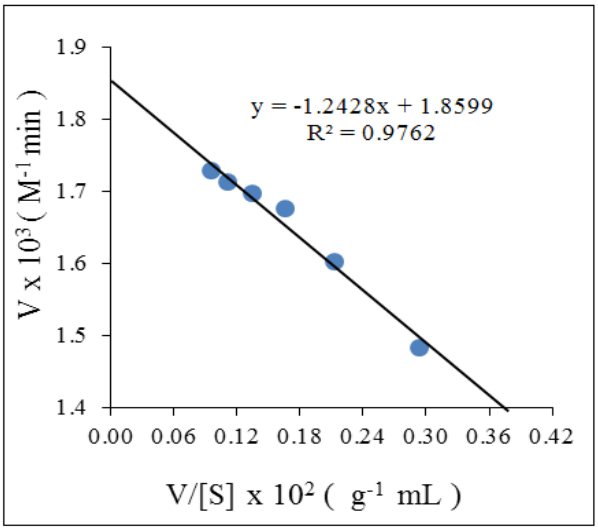

Figure 13 Eadie-Hofestee plot of V *vs.* V/[S] used for graphic evaluation of V_{max} and K_m for crude α-amylase

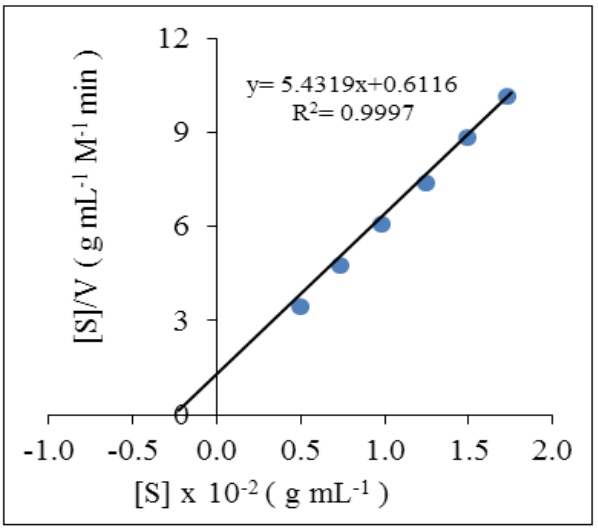

Figure 14 Hanes-Wilkinson plot of [S]/V *vs.* [S] used for graphic evaluation V_{max} and K_m for crude α-amylase

Table 10 Comparison of Kinetic Parameters of the α-Amylase Enzyme from Different Methods

No.	Methods	$V_{max} \times 10^{-3}$ (M min^{-1})	$K_m \times 10^{-2}$ (g mL^{-1})
1	Michaelis-Menten	1.739	0.285
2	Lineweaver-Burk	1.978	0.192
3	Eadie-Hofstee	1.863	0.126
4	Hanes-Wilkinson	1.843	0.114

Effect of

Reaction Order on α-Amylase-catalyzed Reaction

Reaction order refers to the number of molecules involved in forming a reaction complex that is component to proceed to product (s). A reaction characterized by the conversion of one molecules of A to one molecules of B with no influence from any other reactant or solvent is a first-order reaction (Martin, 1993). The plot of Log V/(V_{max}–V) *vs*. Log [S] will give a straight line from which reaction order (n) value can be computed from the slope (Tale 11 and Figure 15). The reaction order (n) for α-amylase was calculated to be 1.2033 proving that the reaction order is first order.

Table 11 Reaction Order for α-Amylase-catalyzed Reaction

No.	Log [S]	Log V/(V_{max}-V)
1	-2.602	0.037
2	-2.301	0.254
3	-2.125	0.688
4	-2.000	1.187
5	-1.903	1.275
6	-1.824	1.416
7	-1.757	1.576

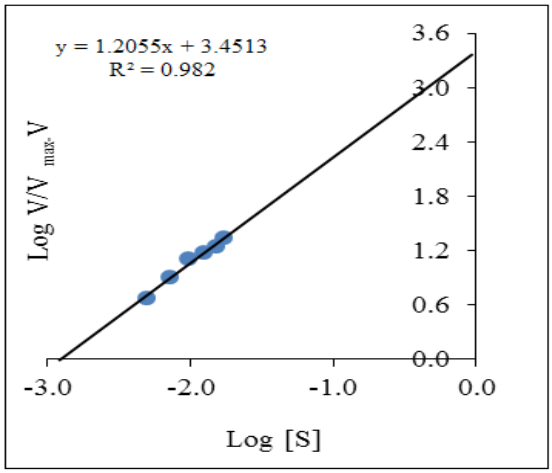

Figure 15 Plot of by V/V $_{max}$-V as a function of log [S] of α-amylase-catalyzed reaction

Conversion of Maltose from Cassava Starch using Maize Grain α-Amylase

Cassava starch is used as a starch source and enzymic hydrolysis of starch was carried out by using crude α-amylase from maize grain. Gelatinized starch solution converted to maltose after heating at 60 °C for 30 min. The maltose content was measured by dinitrosalicylic acid method. The percentage conversion to reducing sugars and maltose was computed with cassava sample having 3.983 %.

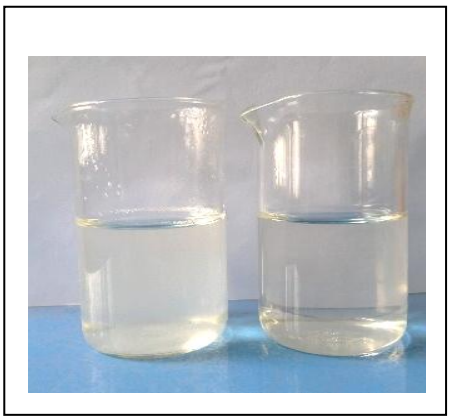

(a) (b)

Figure 16 (a) Gelatinized starch solution without enzyme (control)
(b) Gelatinized starch solution with α-amylase (converted to maltose)

Conclusion

α-Amylase from germinating maize was extracted by using sodium chloride and acetate buffer pH 5.6 solution. α-Amylase activities during germinating of maize grains were studied by determining the daily enzyme activity. α-Amylase activity in plant seeds increases rapidly after germinating the seeds. The maximum α-amylase activity was found at third day of growth. The enzyme unit (EU) of crude α-amylase was found to be 160.01 EU per gram of maize grain. The protein content was observed to be 0.6377 mg mL^{-1}. The specific activity of enzyme solution was calculated to be 12.035 μmol min^{-1} mg^{-1}. The optimum pH of α-amylase was found to be 5.6 in acetate buffer and optimum temperature was found to be 60 °C. The values of K_m and V_{max} treated statistically using the linear regression method were compared with various graphically methods (Michaelis-Menten, Lineweaver-Burk, Eadie-Hofstee and Hanes-Wilkinson). The K_m and V_{max} values of α-amylase were found to be 0.192×10^{-2} g mL^{-1} and 1.978×10^{-3} M min^{-1}, respectively, from Lineweaver-Burk plot. The reaction order (n) for α-amylase was calculated to be 1.203 proving that the reaction order is first order. The activation energy (E_a) of α-amylase-catalyzed reaction was calculated to be 4.977 kcal mol^{-1}. The maltose content was measured by dinitrosalicylic acid method. The percentage conversion to reducing sugars and maltose was computed with cassava sample having 3.983 %. α-Amylase is one of most advantageous because it is stable, inexpensive and widely used in the development of various applications.

Acknowledgements

The authors would like to thank the Myanmar Academy of Art and Science for allowing to present this paper and Professor and Head Dr Ni Ni Than, Department of Chemistry, University of Yangon, for her kind encouragement.

References

Anderson, A. K. (1972). *Essential of Purification Chemistry*. New York: John Wiley and Sons, Inc., pp.191-195

Anto, H., Trivedi, U. and Patel, K. (2006). "Alpha-amylase Production by *Bacillus cereus* MTCC 1305 using Solid-State Fermentation". *Food Technology and Biotechnology,* vol.44(2), pp. 241-245

Atkins, P. W. (1972). *Physical Chemistry*. New York: 5th Edition, Oxford University Press, pp.899-901

Blanchard, P. H. and Katz, F. R. (1995). *Starch Hydrolyzates. Food Polysaccharides and their Applications*. New York: 2nd Edition, Marcel Dekker, Inc., 99-121

Charles, H. H., Larry, C. B. and Norman, W. H. (2007). *A Laboratory for General, Organic, and Biochemistry*. New York: 5th Edition, Mc Graw Hill Co., pp.357-378

Fox, G. and Manley, M. (2009). "Hardness Methods for Testing Maize Kernels". *Journal of Agricultural and Food Chemistry*, vol.57**,** pp.5647-5657

Harper, H. A. (1977). *Review of Physiological Chemistry*. Tokyo: 16rd Edition, Maruzen Co. Ltd ; pp.124-143

Hussain, I., Siddique, F., Mahmood, M. S. and Ahmed, S. I. (2013). "A Review of the Microbiological Aspect of α-Amylase Production". *International Journal of Agriculture and Biology,* vol.15(5), pp.1029-1034

Jessop, W. J. E. (1961). *Pearsons Introduction to Biochemistry*. London: Heinemann Medical Book Ltd., pp.240-251

Kigel, J., Galili, G. and Dekker, G. M. (1995). *Seed Development and Germination*. New York: Marcel Dekker, Inc., pp.507-528

Martin, D. W., Mayer, P. A. and Rodwell, V.W. (1983). *Harpers Review of Biochemistry.* California: Lange Medical Pub., pp.77

Mohamed, S. A., Abdulrahman, L., Malki, A. and Kumosani, T. A. (2009). "Partial Purification and Characterization of Five á-Amylases from a Wheat Local Variety (Balady) During Germination". *Aust. J. Basic & Appl. Sci.*, vol.3(3), pp.1740-1748

Muralikrishna, G. and Nirmala, M. (2005). "Cereal α-Amylases An Overview". *Carbohydrate Polymers*, vol.60, pp.163-173

Nomera, N. (1986). *Inhibition and Activation of Barley Peptide Hydrolyses*. New York: McGraw-Hill Book Company, pp.291-310

Savary, J., Pu, P. H. and Sunderman, F. W. (1969). "A Biuret Method for Determination of Protein in Normal Urine". *Clinical Chemistry*, vol.14(12), pp.1160-1171

Souza, P. M. and Magalhaes, P. O. (2010). "Application of Microbial α-Amylase in Industry". *Braz . J. Microbiol.*, vol.41(4), pp.850–861

Thoma, J. A., Spradlin, J. E. and Dygert, S. (1971). *Plant and Animal Amylases in the Enzymes*. New York: Academic Press., pp.115-123

Walsh, E. O. F. (1968). An Introduction to Biochemistry. London: The English Press Ltd., pp.135-147

MECHANICAL PROPERTIES AND CHARACTERIZATION OF NATURAL RUBBER CHITOSAN COMPOSITES

Mi Myat Su Mon[1], Thinzar Nu [2], Cho Cho[3]

Abstract

The present research work focuses on the preparation and characterization of natural rubber composite by incorporation of chitosan as filler into the rubber matrix. In the preparation of natural rubber chitosan composites, the chitosan powder loading were 0 %, 2.5 %, 5 %, 7.5 % and 10 %. The rubber chitosan composite compounding was prepared by using two roll mills and then molded by compression molding method. The mechanical properties of natural rubber chitosan composites such as specific gravity, tensile modulus (MPa), tensile strength (MPa), elongation at break (%) and tear strength (kN/m) were determined by standard rubber testing methods (ASTM). The result suggested that increasing the chitosan powder loading, specific gravity and tensile modulus of the composites were increased and tensile strength, elongation at break and tear strength of the composites were decreased. The prepared natural rubber chitosan composites were characterized by SEM technique.

Keywords: natural rubber, chitosan, mechanical properties, natural rubber chitosan composites

Introduction

Natural rubber is a naturally occurring elastomeric polymer of isoprene (2-methyl-1, 3-butadiene). Natural rubber is included in at least 40,000 products including food packing materials, medical devices, tires and non-automotive mechanical products. Natural rubber is essential in all these different demanding applications due to its outstanding properties, such as resilience, elasticity, abrasion and impact resistance, efficient heat dispersion and malleable at cold temperatures, which cannot be matched by synthetic rubber (Cornish 2001).

Particulate materials (fillers) have been used for decades for the reinforcement or dilution of natural rubber and other elastomers. The addition of fillers in natural rubber is necessary in order to achieve the mechanical properties required. The efficiency of the fillers depands on parameters that are related to the fillers characteristics, including the particle size, structure and functionality and also parameters related to the rubber and processing conditions. The reinforcing effect of fillers is achieved due to physical and chemical interactions between the rubber and the fillers that allow these two components to produce one material with the inherent properties of both (Ahmadi and Shojaei, 2013).

Natural components are currently being manufacture with carbon black and silica, the former being the most widely used filler in industry. Nevertheless, carbon black is derived from petroleum and so is a non-renewable material. In the last decades some research on alternative filler material has explore bio-based sources (Valodkar and Thakor, 2012).

Chitin is a structural polysaccharide and is the second abundant natural polymer after cellulose. Chitin is found in shells of arthropods (crabs, lobsters, as well as mollusks (eg., squid pens). Chitosan is a linear copolymer d-glucosamine obtained by partial chitin deacetylation normally found in the form of granules, sheets, or powders (Ravi Khumar, 2000). There are currently a variety of applications for chitosan in the biomedical, food, and chemical industries

[1] Assistant Lecturer, Department of Chemistry, Mawlamyine University
[2] Dr, Associate Professor, Department of Chemistry, University of Yangon
[3] Dr, Professor, Department of Chemistry, University of Yangon

owing to its interesting properties, such as biodegradability, biocompatibility, low toxicity, and biological activity (Domard, 2011).

This study focuses on incorporating chitosan to be successful employed as filler is ensuring good interaction with the rubber at a reasonable loading level. Then, the effects of chitosan loading on the mechanical properties, morphology of chitosan-filled natural rubber are reported.

Materials and Methods

All chemicals used in this research were procured from British Drug House (BDH), England. The chemicals were as used as received unless state otherwise. All specific chemicals used were cited detail in each experimental section. The apparatus consist of conventional lab wares, glass wares and modern equipment.

Sampling

Natural rubber sheet was procured from local market, Mawlamyine Township, Mon State. Commercial chitosan purchased from Ever Green Co. Ltd. (Yangon) was used in the present work.

Preparation of Chitosan Sample

The purchased chitosan sample was ground into powder by grinding machine and dried in oven (70 °C, 3 h) prior to use expel moisture.

Preparation of Natural Rubber Chitosan Composites

The vulcanization of natural rubber chitosan composites were carried out for efficient vulcanization system. Composition of the weights of the ingredients used was shown in Table 1.

Natural rubber was first rolled about 7 min by a roller to break out the fibrous bond of rubber polymer chain. This process is called mastication. Stearic acid, zinc oxide and titanium oxide (TiO_2) were added. Simultaneously and continuously rolled about 5 min. Then, mercapto benzadiazole (MBT), zinc diethyl dithiocarbamate (ZDEC) and butylated hydroxytoluene (BHT) and jelly were added in order to make acceleration to prevent oxidized and vulcanite harder. And then, the chitosan powders were added as filler in the compounding. It was then rolled continuously for about 10 min with sulphur to obtain a two millimeter thickness sheet. The total mixing time was approximately 20 min.

Composite A is natural rubber composite by mixing natural rubber (100 g) and other natural rubber chitosan composites were prepared by loading chitosan filler such as 2.5, 5, 7.5 and 10 g.

Table 1 Composition of Ingredients in the Prepared Natural Rubber Chitosan Composites

Ingredients	Composition of ingredients in various natural rubber chitosan composites (g)				
	A_0	$A_{2.5}$	A_5	$A_{7.5}$	A_{10}
Natural Rubber	100	100	100	100	100
Zinc oxide (ZnO)	0.75	0.75	0.75	0.75	0.75
Stearic acid	1.0	1.0	1.0	1.0	1.0
TiO_2	1.0	1.0	1.0	1.0	1.0
ZDEC	1.0	1.0	1.0	1.0	1.0
BHT	0.5	0.5	0.5	0.5	0.5
MBT	2.0	2.0	2.0	2.0	2.0
Jelly	1.0	1.0	1.0	1.0	1.0
Sulphur (S)	1.2	1.2	1.2	1.2	1.2
Chitosan	0	2.5	5	7.5	10

A_0- A_{10} = natural rubber composites with various loading of chitosan 0 to 10 (g)
TiO_2 = titanium oxide
ZDEC = zinc diethyldithiocarbamate

Determination of Mechanical Properties of Natural Rubber Chitosan Composites

Mechanical properties of natural rubber chitosan composites are those physical properties that related to strength, toughness and durability. The properties were determined at Rubber Research and Development Center in Ministry of Agriculture, Livestock and Irrigation Department of Agriculture (Yangon).

Determination of specific gravity

The specific gravity of the composites was measured by Wallace direct reading specific gravity balance. The test piece was suspended on a needle form at one end of the beam which was zeroed by means of quickly adjustable sliding weights. The test piece was then immersed in water contained in a glass beaker locked on a frication-clamped platform. This platform can be raised and lowered easily and remained in position without on additional clamping. When the test piece was immersed, the specific gravity was calculated. The results are shown in Figure 2 and Table 2.

Determination of tensile strength, elongation at break and tensile modulus(M_{300} , M_{400}, M_{500})

The tensile test was done according to H.5000 F tensile testing machine. The test was performed to determine the capability of a material to resist the deformation during stretch. The important data obtained from tensile test were tensile modulus at 300 % (M_{300}), modulus at 400 % (M_{400}), modulus at 500 % (M_{500}), tensile strength and elongation at break. The prepared composites were cut off according to JISK 7127. The both ends of the test pieces were firmly clamped in the jaw of tensile strength testing machine. One jaw was fixed and other was movable. The movable jaw moved at the rate of 10 mm min^{-1}. The resultant data were shown

at the recorder. This procedure was repeated three times for each composite. The results are presented in Figures 3, 4, 5 and Table 2.

Determination of tear strength

The tear strength was measured by tear strength testing machine. The specimen to be tested was cut out by the die from the above sheets. Specimen was cut with a single nick (0.05 mm) at the entire of the inner concave edge by a special cutting device using a razor blade. The clamping of the specimen in the jaw of test machine aligned with travel direction of the grip at the rate of 100 mm min^{-1}. The recorder of the machine showed the highest force to tear from a specimen nicked. The procedure was repeated three times for each result. The results are presented in Figure 6 and Table 2.

Characterization of the Prepared Natural Rubber Chitosan Composites by SEM Modern Technique

The prepared composites were investigated by SEM for surface morphology was performed at West Yangon University, Yangon.

Results and Discussion

This research work focuses on the investigation of the effect of chitosan loading on rubber compounding. There were 5 types of natural rubber chitosan composites prepared as shown in Figure 1. As the result, the changing of the mechanical properties of the prepared composites was observed with increasing filler loading on rubber matrix (Table 2). And then the characterization of the prepared composites by using SEM modern technique was also performed.

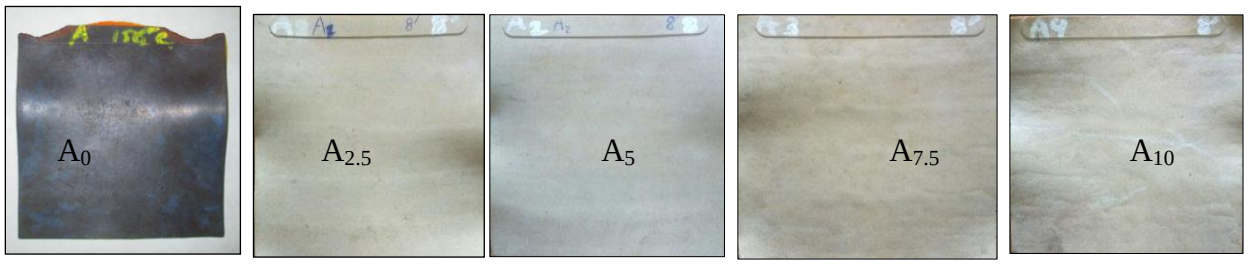

Figure 1 Natural rubber chitosan composites A_0, $A_{2.5}$, A_5, $A_{7.5}$ and A_{10}

Table 2 Mechanical Properties of the Prepared Natural Rubber Chitosan Composites

No.	Test	Resultant data of various natural rubber chitosan composites				
		A_0	**$A_{2.5}$**	**A_5**	**$A_{7.5}$**	**A_{10}**
1.	Specific gravity	0.93	0.95	0.95	0.96	0.96
2.	Tensile Strength (MPa)	5.9	3.9	3.3	1.1	1.1
3.	Elongation at Break (%)	940	883	832	665	667
4.	Tensile modulus at 300% (M_{300})	0.6	0.6	0.7	0.7	0.8
5.	Tensile Modulus at 400% (M_{400})	0.9	0.9	1.0	1.1	1.1
6.	Tensile Modulus at 500% (M_{500})	1.2	1.3	1.3	1.4	1.5
7.	Tear strength (kN/m)	22.9	11.3	8.2	6.1	5.6

Physicomechanical Properties of the Prepared Natural Rubber Chitosan Composites

Specific gravity

From the experiment data, the sample (without filler) had the lowest specific gravity (0.93). As the filler loading increased, the gravity of the composites also increased. In this experiment data, the composite with 10g chitosan filler loading had the highest density as shown in Figure 2 and Table 2.

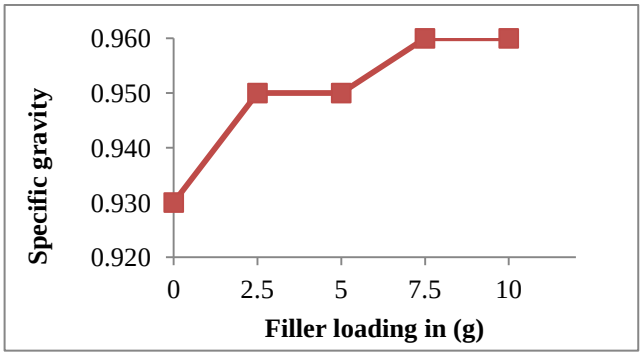

Figure 2 Specific gravity of the prepared natural rubber chitosan composites (A_0-A_{10})

Tensile strength

The tensile strength is the maximum tensile stress reached in stretching a test piece to its breaking point. The effect of chitosan loading on the tensile properties of chitosan filled rubber composites is shown in Figure 3 and Table 2. It can be observed that the tensile strength of the composites decrease with increasing chitosan loading. This may be due to the size and geometrical factor of the filler, whereby irregular shaped fillers tend to decrease the strength of composites due to the inability of the filler to support the stress transferred from the matrix. Large particle size filler provides a smaller surface area, which give rise to a weaker interaction between the filler and rubber matrix.

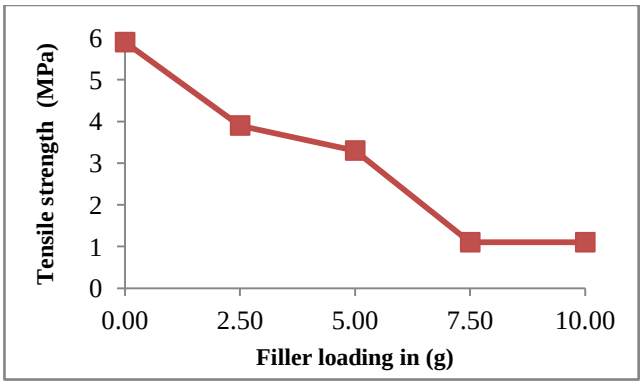

Figure 3 Tensile strength of the prepared natural rubber chitosan composites (A_0-A_{10})

Elongation at break

According to the result data as shown in Figure 4 and Table 2, it revealed that a falling trend of elongation, as the filler loading increased, when the sample (without chitosan filler) had the highest elongation. This is so because rubber is highly elastic and as the filler loading is

increased, there is an adherence of the filler to the polymer phase which results in the reduction of intermolecular bonds between the rubber chains stiffening of the rubber chain and thus leads to resistance to stretching.

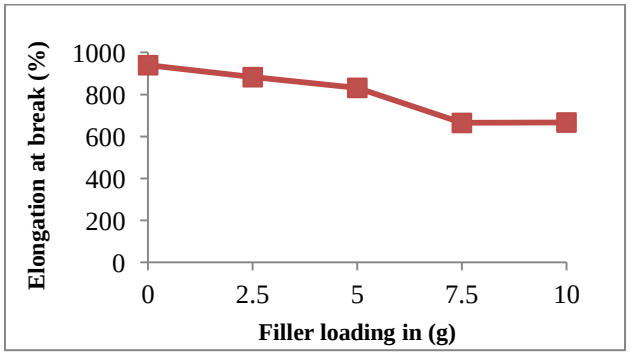

Figure 4 Elongation at break of the prepared natural rubber chitosan composites (A_0-A_{10})

Tensile modulus

Modulus is a measure of the fitness of a material that is its resistance to extension. The higher modulus of a material, the less its extend for a given force. From the result data shown in Figure 5 and Table 2, the modulus (M_{300}, M_{400} and M_{500}) increase as the filler loading increases. This behavior can be by the fact that adhesion occurred between the filler and the rubber which led to increase in stiffness, rigidity and strength.

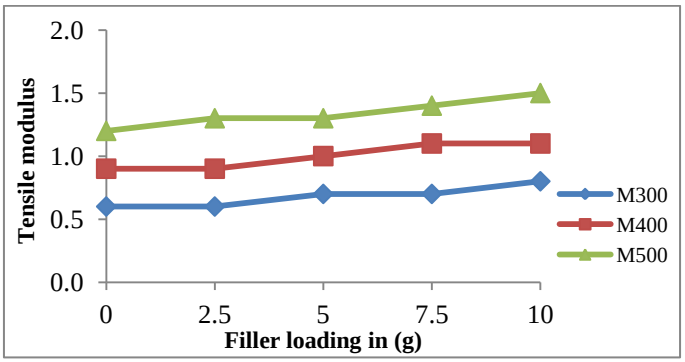

Figure 5 Tensile modulus of the prepared natural rubber chitosan composites (A_0-A_{10})

Tear strength

Tear strength used to characterize the tear resistance is one of the important mechanical parameters of rubber products. The experimental data of the tear strength of rubber (without filler) and rubber chitosan composites ($A_{2.5}$-A_{10}) are shown in Figure 6 and Table 2. With increasing chitosan loading, it can be revealed that the tear strength was decreased due to the poor dispersion of chitosan in rubber matrix.

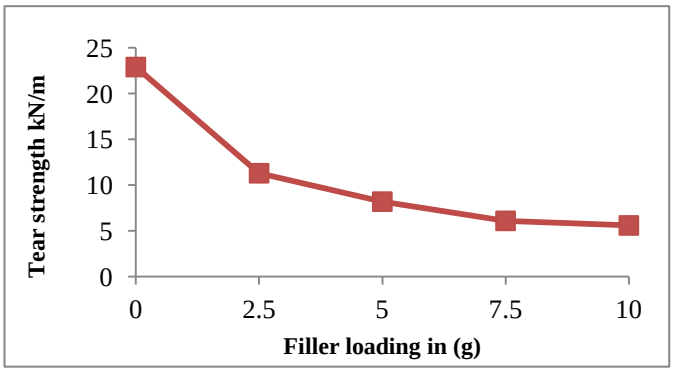

Figure 6 Tear strength of the prepared natural rubber chitosan composites (A_0-A_{10})

Characterization of the Prepared Natural Rubber Chitosan Composites

The SEM micrographs show the fracture surfaces of chitosan filled rubber composites without chitosan (A_0) and with chitosan of $A_{2.5}$, A_5, $A_{7.5}$ and A_{10} as shown in Figure 7. With increasing filler at higher 10 % of chitosan loading, the fructured surfaces show poor dispersion and adhesion of chitosan filler whereby there were aggregations and significant detachment of chitosan from the filled compound, this cause major failure in tensile, elogation at break and tear strength properties of the composites.

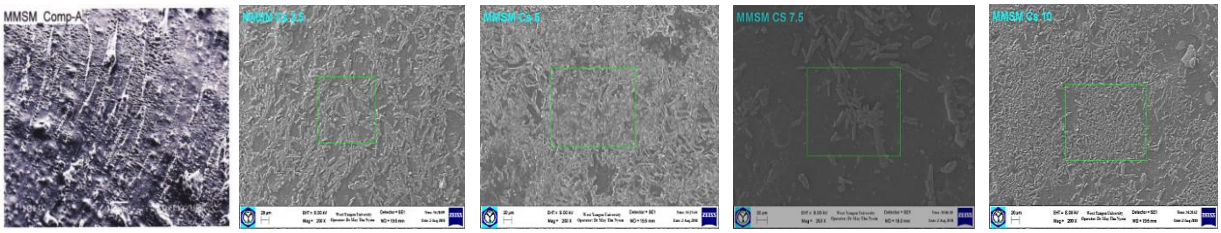

(A_{10}) ($A_{2.5}$) (A_5) ($A_{7.5}$) (A_{10})

Figure 7 Scanning electron micrographs of the prepared natural rubber chitosan composites (A_0-A_{10})

Conclusion

From this study, the following conclusion can be drawn.

The physicochemical properties, such as specific gravity, tensile strength, elongation at break, tensile modulus (M_{300}, M_{400} and M_{500}) and tear strength of composites with various chitosan loading 0 %, 2.5 %, 5 %, 7.5 % and 10 % were examined. As for the mechanical properties result, the tensile strength, elongation at break and tear strength of rubber chitosan composites decreased with increasing chitosan loading whereas modulus (M_{300}, M_{400} and M_{500}) and specific gravity increased. Because of an increase in chitosan loading reduces the elasticity of the prepared composites resulting in more stiff and rigid. The stiffness of the prepared composites increased with increasing chitosan loading due to the ability of chitosan impart greater stiffness to prepared composites. Increase in chitosan loading contributed to an increased in mass of chitosan in the prepared composites, thus the density of the prepared composites increased with increasing chitosan loading. And morphological studies of the tensile fractured surfaces of the vulcanisates indicated that chitosan increased in loading interacts less well. Due to increase of rigid and stiffness of the prepared rubber composites, rubber can be filled with chitosan and can be used for commercial application.

Acknowledgement

The authors would like to express their profound gratitude to the Department of Higher Education (Yangon Office), Ministry of Education, Yangon, Myanmar, for provision of opportunity to do this research and Myanmar Academy of Arts and Science for allowing to present this paper.

References

Ahmadi, M. and Shojae, A. (2013). *Cure Kinetic and Network Structure of NR/SBR Composites Reinforced by Multiwalled Carbon Nanotube and Carbon Blacks*, vol. 566, pp.238-248

Cornish, K. (2001). "Similarities and Differences in Rubber Biochemistry Among Plant Species", *Phytochemistry*, vol. 57, pp. 1123-1134

Domard, A., (2011) "A Perspective on 30 years research on Chitin and Chitosan," *Carbohyhydrate Polymers*, vol.84, pp. 696-703

Ravi Kumar, M. N. V. (2000). "A Review of Chitin and Chitosan Application," *Reactive and Functional Polymers*, vol. 46, pp. 1-2

Valodkar, M. and Thakore, S. I. (2012). "Biopolymers as Effective Fillers in Natural Rubber: versus

EFFECT OF ALKALI TREATMENT ON MECHANICAL PROPERTIES OF BANANA STEM FIBER REINFORCED NATURAL RUBBER COMPOSITES

Nyein Chan Aye[1], Nyo Nyo Myint[2], Thinzar Nu[3]

Abstract

In this present work, composites are made by using untreated banana stem fiber, alkali treated banana stem fiber and natural rubber. A mixture of 4 % NaOH and 2 % Na_2SO_3 were used for modification of banana stem fiber (BSF). The alkali treatment was conducted to reduce the lignin content on the surface of fiber and to improve the adhesion between the rubber and matrix. The natural rubber-banana stem fiber composites were prepared by moulding method with various weight ratio (5%, 10%, 15%, 20%) of untreated and treated banana stem fiber. The untreated and alkali treated banana stem fiber were characterized by modern techniques such as FT IR and SEM. The mechanical properties such as hardness, specific gravity, tensile strength, elongation at break and tear strength of natural rubber- banana stem fiber composites were then determined by standard rubber testing methods.

Keywords: Natural rubber, banana stem fiber, composite, alkali treatment, mechanical properties, FT IR, SEM

Introduction

Banana belongs to Musa family. Banana plant is a large pereminal herb with leaf sheaths that form pseudo stem. Its height can be 0-40 ft (3.0-12.2 m) surrounding with 8-12 large leaves. The leaves are up to 9 ft long and 2 ft wide (2.7m and 0.61m). Its fruits are approximately 4-12 inches (10.2-30.5 cm). Different parts of banana trees serve different needs, including fruits as food sources, leaves as food wrapping and stems for fiber and paper pulp (Sonu, 2014).

Reinforcing efficiency of natural fibers depends upon the nature of cellulose and its crystallinity. Components which are present in natural fibers are cellulose (α cellulose), hemicelluloses, lignin, pectin and waxes (Raghavendra *et al*., 2013).

Use of natural fibers as reinforcements has increased due to their good mechanical properties, low cost and density, their ability to recycle, relatively no abrasion and comparative performance in terms of specific strength. The mechanical properties are determined by the amount of cellulose content and microfibrillar angle. Fibers with high cellulose content and low microfibrillar angle provide higher properties and are preferred for composite preparation (Ezema *et al*., 2014).

Literatures on the use of banana stem fibers are very limited. These fibers from banana are emerging materials for composite manufacture with high conversion rate from agro-waste to high economic value products because banana fibers are available all year round and in every part of the world (Maleque *et al.*,2006).

Surface modifications is performed to increase the number of reactive sites on the surface of fibers, which increases the interfacial bonding between fiber and matrix. Increase in the properties of composites made of chemically treated fibers is attributed to improve interfacial

[1] Assistant Lecturer, Department of Chemistry, Mawlamyine University
[2] Dr, Associate Professor, Department of Engineering Chemistry, Technological University (Mawlamyine)
[3] Dr, Associate Professor, Department of Chemistry, University of Yangon

bonding between fibers and the matrix, decrease in moisture absorption, increase in fiber crystallinity due to variation in treatment time and temperature (Mahesh *et al*., 2014).

Materials and Methods

Materials

Natural rubber (Grade 1) was obtained from Mudon Township, Mon State. The banana stems were collected from Mayangone Quarter, Mawlamyine Township, Mon State. The other compounding ingredients used were zinc oxide, stearic acid, N-cyclohexyl-2-dihydro-benzothiazolesulphonamide (CBS), 2,6-di-tert-butyl-4-hydroxytoluene (BHT) and sulphur, which were supplied by Ministry of Agriculture, Livestock and Irrigation, Department of Agriculture, Rubber Research and Development Centre.

Surface Modification

Banana stem was washed with water several times and extracted by hand to obtain banana stem fiber. These fiber were soaked in the mixture of (4% NaOH and 2% Na_2SO_3) solution for 24 h. Treated fibers were rinsed at least ten times with distilled water till neutral pH value was obtained. Fibers were dried under hot sun and then these dried fiber were ground by grinding machine (Figures 1 and 2).

Figure 1 Alkali treated banana stem fiber

Figure 2 Banana stem powder

Characterization of Banana Stem Fiber by Modern Techniques

Prepared untreated and treated banana stem fiber were characterized by FT IR and SEM techniques. Fourier transfer infrared spectroscopy (FT IR) study was carried out to determine changes in the chemical composition of fibers after alkali treatment. Scanning electron microscopy (SEM) was used to study surface topography of untreated and treated banana stem fiber.

Preparation of the Rubber Composites

The formulation of the rubber is given in Table 1. The mixing of the rubber compounds were carried out by using a laboratory two roll open mixing mill at Rubber Research and Development Centre. The nip gap, mill roll speed ratio, time, temperature of mixing, number of passes and sequence of addition of ingredients during mixing were kept under same conditions for all compounds. The amount of fillers (banana stem fiber) were varied in the range of 5-20 % in each composites.

Table 1 Formulation of Rubber Composites

Ingredients	Composition of Ingredients in Natural Rubber-Banana Stem Fiber composites (g)			
Natural rubber (NR)	100	100	100	100
Zinc oxide (ZnO)	5.0	5.0	5.0	5.0
Stearic acid	1.0	1.0	1.0	1.0
N-cyclohexyl-2-benzothiazayl sulphenamide (CBS)	0.5	0.5	0.5	0.5
Sulphur	2.5	2.5	2.5	2.5
2,6-di-tert-butyl-4-hydroxytoluene (BHT)	1.0	1.0	1.0	1.0
banana stem fiber	5	10	15	20

NR-BSF = untreated banana stem fiber with various weight ratio of 5 to 20 g
NR-TBSF = treated banana stem fiber with various weight ratio of 5 to 20 g

Results and Discussion

Characterization of Banana Stem Fibers

Figure 3 illustrates the FT IR results of untreated and treated fibers. As a result of the alkali treatment, the hydroxy groups of the cellulose react with functional group of the coupling agent, which in turn bond to the polymer matrix and thus establish a good fiber/matrix bonding interaction. Decrease in vibration intensity at 2942 cm^{-1} and 1329 cm^{-1} from C-H of alkyl group and shifting of absorption band from 1254 towards 1109 cm^{-1}(treated BSF) indicate that there is a formation of carboxylic acid or ester which may disappear due to removal of hemicellulose and lignin. Figures 4 (a) and (b) show SEM micrographs of untreated and treated banana stem fibers. In treated banana stem fiber image, some microcracks and degradation of microstructure are seen on the surface of fiber due to the treatment with alkali solution.

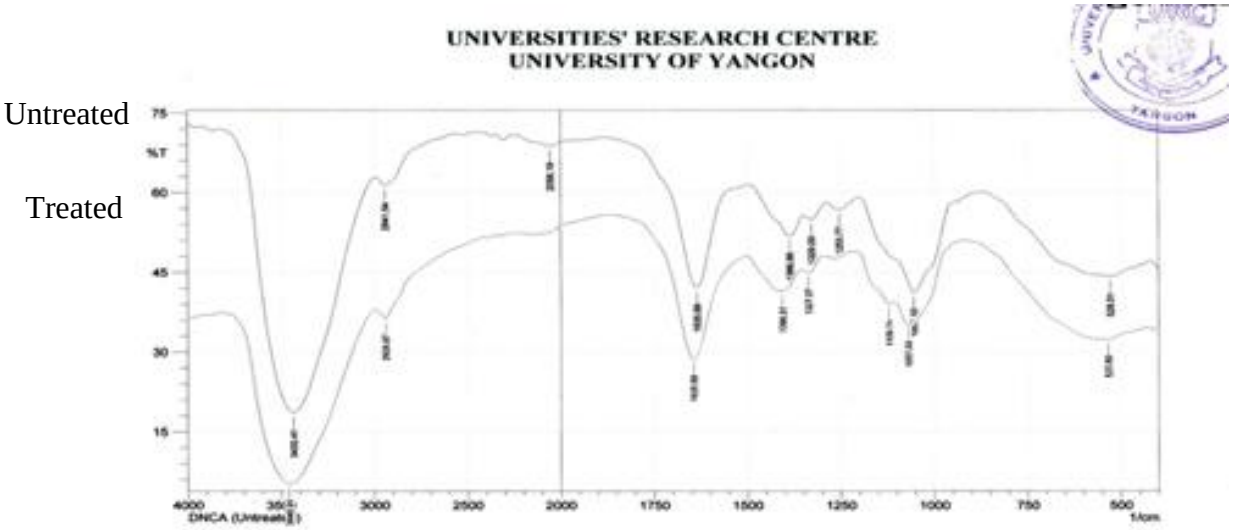

Figure 3 FT IR spectra of untreated banana stem fiber and treated banana stem fiber

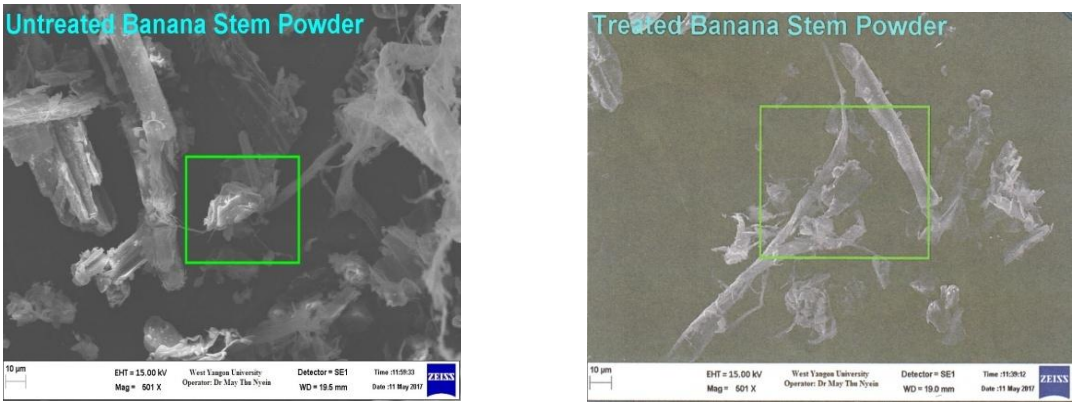

(a) (b)

Figure 4 Scanning electron micrographs of (a) untreated banana stem fiber and (b) treated banana stem fiber (501 × magnification)

Mechanical Properties of Natural Rubber-Banana Stem Fiber Composites

The results of mechanical properties are reported here. These include evaluation of hardness, specific gravity, tear strength, elongation at break and tensile strength that has been studied and discussed. Generally it was observed that the 4% NaOH and 2% Na_2SO_3 treated composites have higher values of hardness, specific gravity and elongation at break for various filler percent than untreated composites.

Hardness

Figure 5 shows that the hardness value of natural rubber-untreated banana stem fiber (NR-BSF) and natural rubber-treated banana stem fiber (NR-TBSF) composites. It can be seen that NR-TBSF composites has the higher hardness value than NR-BSF composites. This is due to the alkali treated fibers could have been the result of finer fibers. Moreover, the reduction in porosity (according to SEM) would then lead to an increase in hardness.

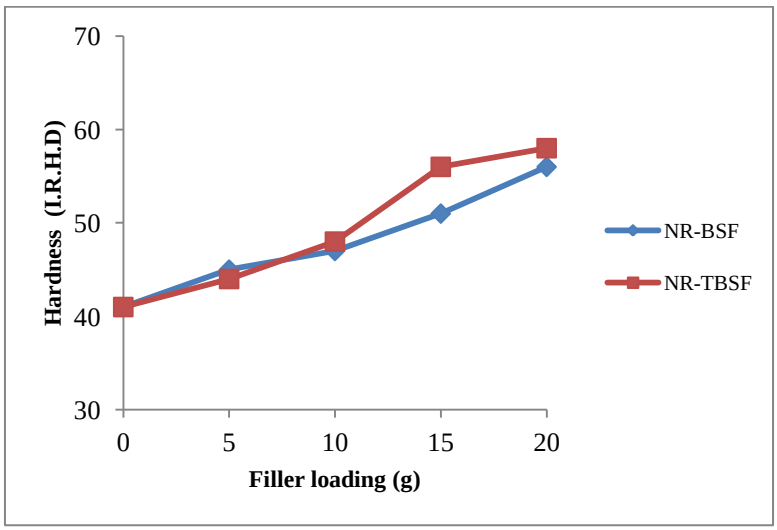

Figure 5 Hardness of the prepared rubber composites Vs various filler (BSF/TBSF) loading

Specific gravity

Figure 6 shows the specific gravity of banana stem fiber reinforced natural rubber composites. When comparing effect of alkali treatment on density of composites made using treated fibers with that of composites made using untreated fibers, an increase in composites density was observed.

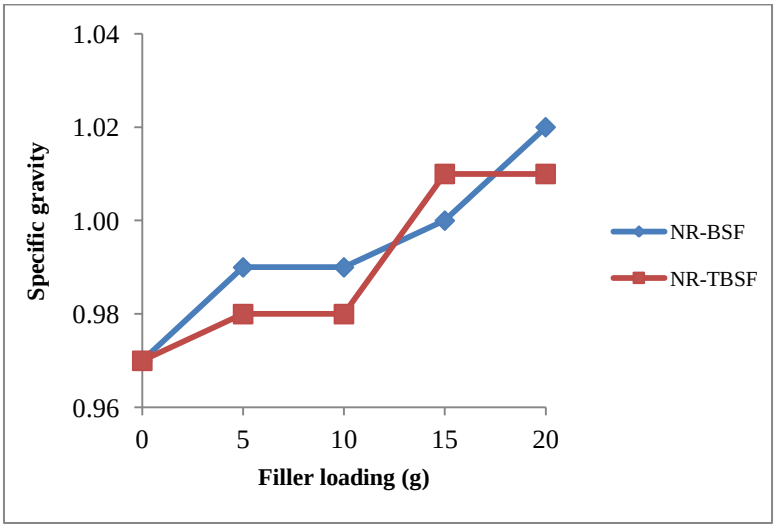

Figure 6 Specific gravity of the prepared rubber composites Vs various filler (BSF/TBSF) loading

Tensile strength

Figure 7 represents the tensile strength of untreated and treated rubber composites. According to Figure 7, ultimate tensile strength at 5 % NR-TBSF composite was 18.30 MPa while that of NR-BSF composite of same filler percent was 18.10 MPa.

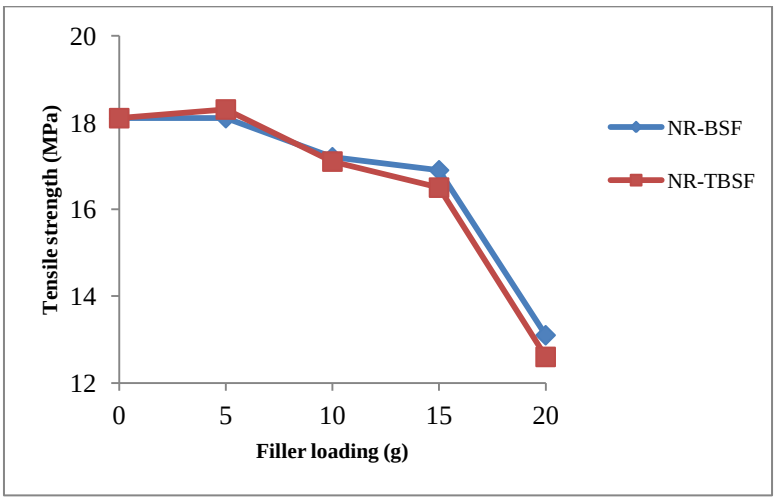

Figure 7 Tensile strength of the prepared rubber composites Vs various filler (BSF/TBSF) loading

Elongation at break

In Figure 8, it could be seen that the elongation at the break of NR-TBSF composites increased with increasing filler loading. Alkali treatment which resulted in removal of hemicellulose and lignin exposed the functional groups present in cellulose in the fibers that would react chemically with the polymer leading to the formation of strong covalent bonds which in turn results in increased mechanical properties.

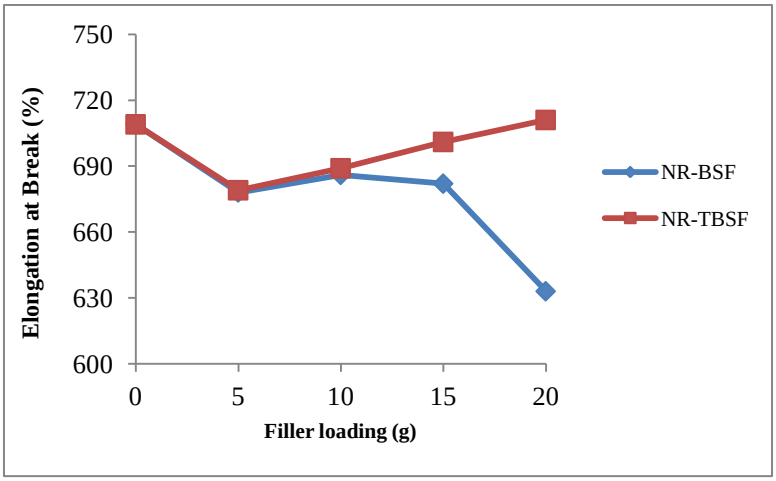

Figure 8 Elongation at break (%) of the prepared rubber composites Vs various filler (BSF/TBSF) loading

Tear strength

According to Figure 9, the tear strength results for NR-TBSF composites decreased with increasing filler loading. On the other hand, the tear strength results for NR-BSF composites were fluctuated.

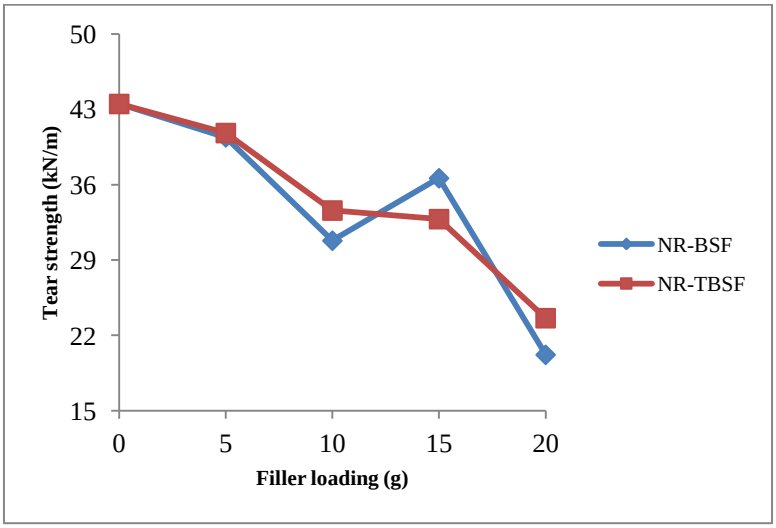

Figure 9 Tear strength of the prepared rubber composites Vs various filler (BSF/TBSF) loading

Conclusion

From the studies reported in this work, SEM micrographs showed removal of unwanted and excess material on the surface of banana fibers, separating the fibers from the fiber bundles. The surface modification by alkali treatment has improved the mechanical properties of treated fiber composites than those of untreated banana stem fiber-natural rubber composites. The alkali treated banana fiber has improved the mechanical properties like hardness, specific gravity and elongation at break. Therefore it is conclusive from the above results that the alkali treatment has provided better mechanical properties. In future various other natural reinforcing materials could be used to mix with banana fiber to form a better hybrid composite which has a better mechanical properties and as well as cost effective.

Acknowledgements

The authors would like to express their profound gratitude to the Department of Higher Education (Yangon Office), Ministry of Education, Yangon, Myanmar, for provision of opportunity to do this research and Myanmar Academy of Arts and Science for allowing to present this paper.

References

Ezema, I. C. and Ravindranatha Mean, A. R. (2014). "Effect of Surface Treatment and Fiber Orientation on the Tensile and Morphological Properties of Banana Stem Fiber Reinforced Natural Rubber Composite". *Journal of Minerals and Materials Characterization and Engineering,* vol.2, pp. 216-222

Mahesh, H., Harika, M. and Shaik, J. (2014). "Comparison of Effects of Alkali Treatment on Flax Reinforced Polyester and Polyester-biopolymer Blend Resins". *Journal of Polymer & Polymer Composites*, vol.23, pp. 229-240

Maleque, M. A., Belal, F. Y. and Sapuan, S. M. (2006). "Mechanical Properties Study of Pseudo-Stem Banana Fiber Resinforced Epoxy Composites". *The Arabian Journal of Science and Engineering*, vol. 32, pp. 359-364

Raghavendra, S., Lingaraju, P.B. and Mukunda, P.G. (2013). "Mechanical Properties of Short Banana Fiber Reinforced Natural Rubber Composites". *International Journal of Innovative Research in Science, Engineering and Technology*, vol. 2(5), pp. 1652-1655

Sonu, E. (2014). "Mechanical and Damping Properties of Rubber Reinforced with Natural Fiber". *The International Journal Engineering and Science*., vol.3(5), pp. 17-24

STUDY ON NUTRITIONAL VALUES, PHYSICOCHEMICAL PROPERTIES, ANTIMICROBIAL ACTIVITY AND CYTOTOXICITY OF PREPARED NUTRACEUTICAL TABLET FROM SELECTED FRUITS

Aye Aye Mar[1] , Aye Chan Nyein[2]

Abstract

In the present work locally grown *T. Chebula* (Phan -kha), *P. emblica* (Zibyu) and *T. bellerica* (Thit-seint) were selected to make nutraceutical tablets. The selected fruit samples were identified at Botany Department University of Yangon. Then the nutritional values, mineral contents, Physicochemical properties, effect of storage time, phytochemical constituents, antimicrobial activity and cytotoxicity of the prepared tablet samples were determined. The water content of 29.94 %, ash content of 4.00 %, protein content of 1.89 %, fiber content of 2.22 %, fat content of 3.04 %, carbohydrate content of 58.91 %, in the tablet sample energy value of 270.56 kcal/100g and vitamin C content of 44.88 mg/100g were observed. The pH of the prepared sample was 4.20 and the total acidity of tablet contained 2.08 mg/100 g . The effect of storage time on water contents, ash contents, vitamin C contents, total acidity contents and pH of prepared tablet samples were also determined. It was found that, the water content slightly decreased from 1 month to 3 month storage time duration. The ash also slightly decreased and the vitamin C content significantly decreased within 3 months duration time. The total acidity slightly decreased and pH values were not changed with the longer storage time. The mineral contents of prepared tablet samples were determined by ED XRF spectrum. It was found that 0.549 % K, 0.138 % Si, 0.118 % Ca, 0.024 % P, 0.021 % S, 0.008 % Fe, 0.003 % Mn, 0.002 % Rb, 0.002 %Cu, 0.002 % Sr and 0.001 % Zn were present in this sample The preliminary phytochemical tests indicated that various types of secondary metabolites such as alkaloids, flavonoids, glycosides, phenolic compounds, reducing sugars, saponins, terpenoids and organic acids together with α -amino acids and starch were present in the sample. The antimicrobial activity of tablet samples from medicinal plant species has been evaluated *in vitro* against microorganisms including five bacterial species (*Bacillus subtilis, Staphylococcus aureus, Pseudomonas aeruginosa, Bacillus pumilus and Escherichia coli*) and one fungus species (*Candida albicans*). In general ethanol and watery extracts of tablet samples exhibited antimicrobial activity. The cytotoxicity of water extracts of nutraceutical tablets was evaluated by brine shrimp cytotoxicity bioassay. The crude watery extract was not cytotoxic to brine shrimp up to maximum dose of 1000 µg/ L. The LD_{50} value of standard $K_2Cr_2O_7$ was <1 µg/L and caffeine was > 1000 µg/L.

Keywords: nutraceutical tablet, the acidity, antimicrobial activity, cytotoxicity

Introduction

Nutraceutical Tablets

The term nutraceutical was coined from nutrition and pharmaceutical in 1989 by Stephen Defelice, founder and Chairman of foundation for innovation in medicine, an American organization which encourages medicinal health. Restated and clarified in press release in 1994, its definition was “any substance that may be considered a food or part of a food and provides medical or health benefits, including the prevention and treatment of disease. About 2000 years ago, Hippocrates emphasized ‘Let food be your medicine and medicine be your food’s. The actual use of Nutraceuticals is to attain desirable therapeutic outcomes with reduced side effects.

[1] Dr, Assistant Lecturer, Department of Chemistry, University of Yangon
[2] MSc, Department of Chemistry, University of Yangon

Such products may range from isolated nutrients, dietary, supplements and diets to genetically engineered 'designer' foods, herbal products and processed foods such as cereals, soups, and beverages (Swaroopa and Srinath, 2017).

(a) **(b)** **(c)**

Figure 1 Fruits of (a) *Terminalia bellerica* (Thit-seint) (b)*Terminalia chebula* (Phan-kha) (c) *Phyllanthus emblica* (Zibyu)

Health benefit and traditional uses of Thit-seint

Fruits are laxative, astringent, althelmintic, and antipyretic; Useful in hepatitis, bronchiyis, asthma, dyspepsia, piles, diarrhoea, coughs, hoarseness of voice, eye diseases and scorpion-sting and hair tonic. Half ripe fruit is used as purgative and kernel of the fruit is narcotic. Plants and plants parts are used in the traditional system of medicines like Ayurveda, Siddha, Unani and Chinese medicine (Anindita *et al*., 2016).

Health benefit and traditional uses of Phan-kha

It exhibit a number of medicinal activities due to the presence of a large number of different types of phytoconstituent. It is used as a traditional medicine for household remedy. It is also extensively used in Ayurveda, Unani and Homoeopathic medicine and become a cynosure of modern medicine. Sometimes it is referred to as 'Mother of all healing' (Anwesa *et al*., 2013).

Health benefit and traditional uses of Zibyu

The fruits are sour, astringent,bitter, acrid, sweet and cooling.It is useful in vitiated conditions of tridosha, diabetes, cough, asthma, bronchitis, cephalalgia, ophthalmopathy, dyspepsia, colic.It is also used to cure skin diseases, leprosy, haematoenesis, inflammations, anemia, emaciation, hepatopathy, jaundice, strangury, diarrhoea, dysentery, emorrhages, leucorrhoea, menorrhagia, cardiac disorders, intermittent fevers and greyness of hair (Rohit *et al*., 2012).

Materials and Methods

Samples

Thit-Seint (*Terminalia bellerica*), Phan-Kha (*Terminalia chebula*) and Zibyu (*Phyllanthus emblica L*.) fruits were collected from Magway region and Kyun Kalay Village, Hlegu Township, Yangon Region.

Materials

Analytical grade reagents were used.

Methods

Nutraceutical tablets were prepared as follows. Mature fresh fruits were washed with water and cut into small slices with the knife. The cut fruits were dried in sunlight and ground with blender. The pure and fine fruits powder was obtained. Next, 10 g of each fruits powder was placed in a beaker and dissolved in 300 mL distilled water. Then 50 g of honey was added in this mixture. This mixture was stirred thoroughy on hot plate until fine paste and tablets were made by hand. Then the nutritional values of prepared tablets were studied. The moisture content of tablet samples was determined by oven drying method. Ash content by Muffle Furnance Method, protein content by Dumas Nitrogen analyzer (NDA 701 analyzer , S -42 Department of Chemistry, UY), fiber content by Acid- based digestion method, carbohydrate and energy content by AOAC (2000) methods, mineral content by EDXRF technique and vitamin C content and total acidity by titration method. The reducing sugar was determined by Fehling's solution test and the preliminary phytochemical investigation was carried out by test tube method. Antimicrobial activity of prepared tablet samples were studied by agar well diffusion method and the cytotoxicity of water extract of prepared tablets was evaluated by brine shrimp cytotoxicity bioassay.

Results and Discussion

Nutraceutical Tablet Samples

In this research, nutraceutical tablet samples were made from three different fruits. The pure and fine nutraceutical tablet samples were prepared by mixing powder of three fruits and honey (Figure 2 and 3).

(a) Zibyu (b) Thit-seint (c) Phan-kha

Figure 2 Pure and Fine fruits Powder

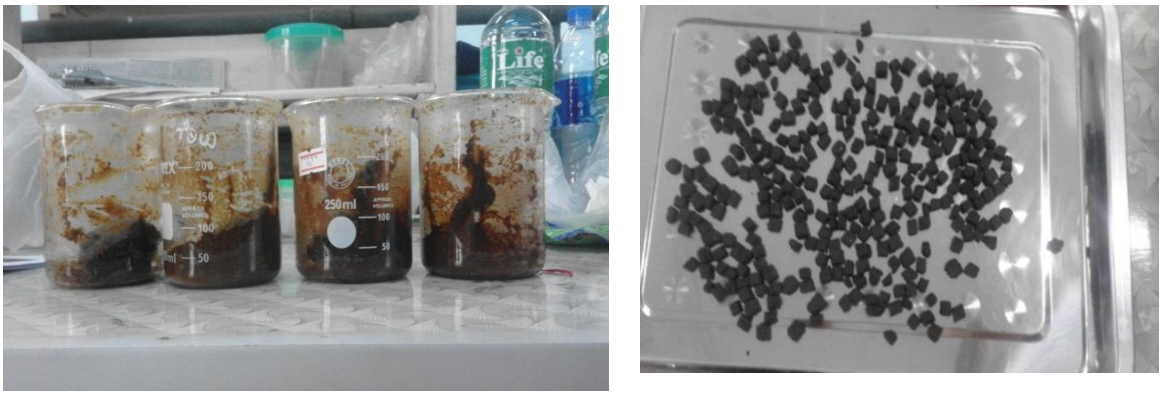

(a) Fine paste sample (b) Tablets

Figure 3 Fine paste sample and Tablets

Nutritional Values of Nutraceutical Tablets

In the present work , water content of nutraceutical tablets were determined by the use of an electric oven at 105 ˚C by drying to obtain constant weight and taking the loss in weight as water. In this study, water content was determined to obtain percentage of water in tablets.

The water content of prepared sample was 29.94 % (Table 1). Water content is one of the most commonly measured properties of food materials. The propensity of microorganisms to grow in foods depends on their water content. For this reason, many foods are dried below some critical moisture content. The texture, taste, appearance and stability of foods depend on the amount of water they contain.

The quantity of ash was determined in order to calculate the carbohydrate content by deduction method. In determining ash, the sample was heated to a high temperature, so that all organic matter is oxidized and volatilized and the mineral are remained. The ash content of prepared nutraceutical tablets was 4.00 % (Table 1).

Various methods have been employed for quantitatively estimation the amount of proteins in biological samples. In this research, NDA 701 Dumas Nitrogen Analyzer was used to determine the protein content of prepared tablet samples and found to be 1.89 % (Table1).

Results from various studies have demonstrated that adequate fiber intake has many additional health benefits and may prevent or decrease an individual's risk of developing coronary disease, stroke, hypertension, diabetes, obesity and colon cancer. In this study, the fiber content of prepared tablet samples was 2.22 %. The result is shown in Table 1.Increase fiber intake may also lower serum cholesterol levels and blood pressure (Anderson *et al*., 2009).

Total fat content was determined by extracting the dried material with petroleum ether (40-60℃) in a continuous extraction apparatus of the Soxhlet type. The fat content of prepared nutraceutical tablet samples was 3.04 % (Table 1). Carbohydrate is one of the main dietary compounds. The carbohydrate content of the diet was calculated by difference.

Carbohydrate % = 100- [protein (%) + water (%) + ash (%) + Fiber(%)]

The carbohydrate contents of the prepared tablet samples was 58.91 %. (Table 1).

Food rich in carbohydrate provide high amount of energy. Carbohydrate can be oxidized to furnish energy and glucose in the blood is a ready source of energy for the human body. The energy content of nutraceutical tablet was 270.56 kcal/ 100 g (Table 1).

Table 1 Nutritional Values of the Prepared Nutraceutical Tablets

No.	Test Parameter	Content
1	water content (%)	29.94
2	Ash (%)	4.00
3	Protein (%)	1.89
4	Crude Fiber (%)	2.22
5	Crude fat (%)	3.04
6	Carbohydrate (%)	58.91
7	Energy value (kcal/100 g)	270.56

Physicochemical Properties of the Prepared Nutraceutical Tablet Samples (pH, Total acidity, Vitamin C content, Reducing sugar content)

pH is one of the important parameters for human diet. Food quality and the stabilization of food colour is mainly due to the pH effect. In this research, the pH content of the prepared tablet samples was 4.2. The result is shown in Table 2. The fluctuations of pH might be due to the variations in titratable acidity.

The organic acids present in foods influence the flavour, colour, prevent the growth of microorganisms or inhibit the germination of spores and providing the proper environment for metal in chelation, an important phenomenon in the minimization of lipid oxidation (Nielsen, 2014). In this study total acidity of 2.08 mg/100 g was observed in prepared nutraceutical tablets. The results are shown in Table 2.

Vitamin C is one of the substances that contribute to the antioxidant capacity in food.. About 30 % of the Vitamin C present in fresh fruit is destroyed during the sample making process, but that which remains in the finish product is stable during storage (Ozkan, 2004). Vitamin C content of nutraceutical tablet samples was determined by iodometric titration and 44.88 mg/100 g vitamin C content was obtained. The result is shown in Table 2.

A reducing sugar is any sugar that is capable of acting as a reducing agent because it has a free aldehyde group or a free ketone group. All monosaccharides are reducing sugars, along with some disaccharides. Reducing sugars react with amino acids in the maillard reaction a series of reactions that occurs while cooking food at high temperature and that is important in determining the flavor of food (William, 1993). The reducing sugar content is determined by Fehling's solution test. It was found that the reducing sugar content of nutraceutical tablet samples was 1.65 % (Table 2).

Table 2 Physicochemical Properties of the Prepared Nutraceutical Tablets

No.	Test Parameter	Content
1	pH	4.20
2	Total acidity (mg/100 g)	2.08
3	Vitamin C (mg/100 g)	44.88
4	Reducing sugar (%)	1.65

Time of Storage

Time of storage is mainly effect on water, ash, pH, acidity and vitamin C content. The high water content in the foods make suspectible to mold damage.

Storage temperature has an important role because this reduces or inhibits the speed of all physicochemical, nutritional and microbiological processes, and thus prolongs, storage period. The storage temperature should be below 2℃ , lower temperature (0.10℃) help maintain taste, colour and water dehydration ratio and also to some extent vitamin C.

The effect of storage time on water content of prepared tablet samples

Water contents of the prepared tablet samples are shown in Table 3 and Figure 3. Storage time effect the water content of prepared tablet samples. There was no changed in the physical quantities of the samples stored at room temperature. The water content ranges from 29.94 % to 28.49 %, 26.59 % and 20.89 % after 1 month, 2 months and 3 months respectively, of storage time.

The lower the water content showed that they would have better keeping quality.

The effect of storage time on ash content of prepared tablet samples

An important determination of the analysis of a food is the estimation of the amount of ash it contains. The ash or inorganic nutrients are the total of non- combustible substances of food.

In this study, the results of the ash content showed that there was gradual decrease in the quality parameters as the storage period increase. The values of the ash contents on the fresh prepared tablet was 4.0 %. After 1 month, 2 months and 3 months of storage time, the values were 3.9 %, 3.1 % and 3.0 %, respectively.

The effect of storage time on pH prepared tablet samples

The effects of storage time on pH of prepared tablet samples are presented in Table 3 and Figure 4. At room temperature, the pH content of tablet sample decreased from 4.2 to 4 and then 3.8 during storage. The pH levels of the tablet samples indicated that they are slightly acidic.

The effect of storage time on total acidity content of prepared tablet samples

The acidity of natural fruit juices is the result of mainly of their content of organic acids. In this study the total acidity of prepared tablet samples were determined monthly by simple direct titration with 0.1 M sodium hydroxide using phenolphthalein as an indicator. The total acidity of in this sample were not significantly changed during the storage time. The result are showed in Table 3 and Figure 5.

The effect of storage time on vitamin C content of prepared tablet samples

Vitamin C is an oxidant and in water, it readily oxidizes first to dehydroascorbic acid. Its content in food can decrease during food preparation and storage. In this research, the vitamin C content of fresh sample was 44.88 mg / 100 g. During the period of 3 months, the vitamin C content was reduced at room temperature conditions. At room temperature, the vitamin C content decreased from 44.88 to 35.90 mg/ 100 g, 26.92 to 26.92 mg / 100 g in tablet samples after 1 month, 2 months, 3 months of storage time, respectively. The results are shown in Table 3 and Figure 4.

Table 3 The Effect of Storage Time of Prepared Nutraceutical Tablets

No.	Month	Water Content (%)	Ash Content (%)	pH	Vitamin C (mg/100 g) Content	Total acidity content (%)
1.	0	29.94	4.0	4.2	44.88	2.08
2.	1	28.49	3.9	4.0	35.90	2.03
3.	2	26.59	3.1	3.8	26.92	1.97
4.	3	20.89	3.0	3.8	26.92	1.87

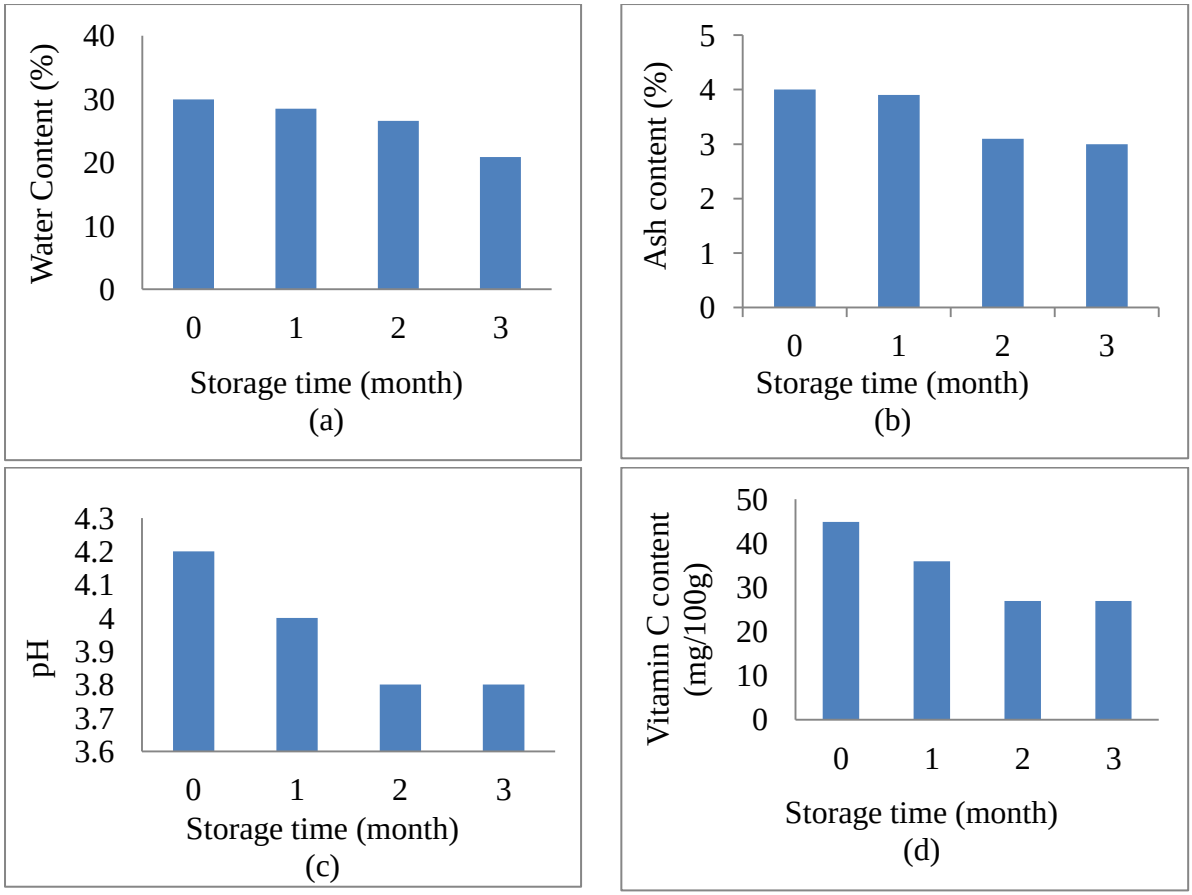

Figure 4 The varation of (a) water content, (b) ash content, (c) pH, (d) vitamin C content of prepared nutraceutical tablets during 3 months storage

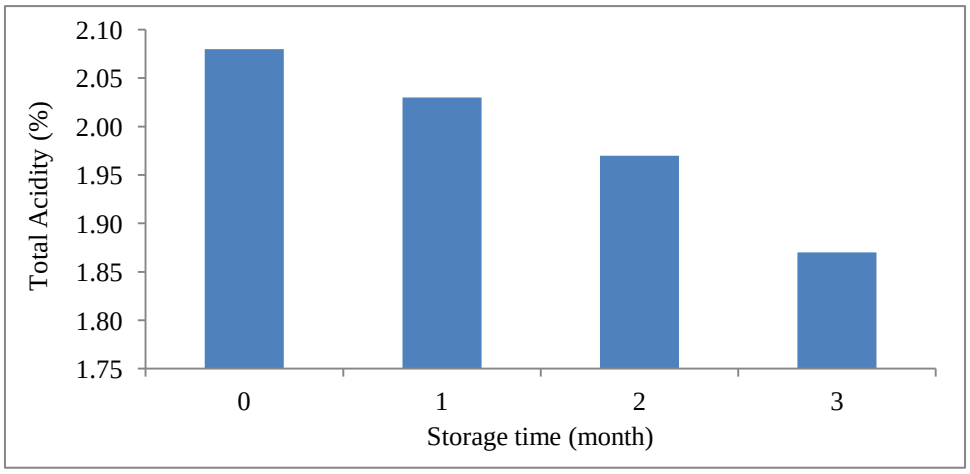

Figure 5 The variation of total acidity contents of prepared nutraceutical tablets during 3 months storage

Mineral Content

Adequate mineral intake is essential throughout the entire life but especially for normal growth and immune function , and to prevent chronic diseases in adulthood (Cabrera-vique *et al.*, 2016).

In the present work the mineral contents found in nutraceutical tablet samples are K, Si, Ca, P, S, Fe, Mn, Rb, Cu, Sr and Zn. From the result the potassium percent was higher than the other metals. The data are shown in Table 4 and Figure 6.

Table 4 Relative Abundance of Elements in the Prepared Nutraceutical Tablets

No	Element	Relative abundance (%)
1.	K	0.549
2.	Si	0.138
3.	Ca	0.118
4.	P	0.024
5.	S	0.021
6.	Fe	0.008
7.	Mn	0.003
8.	Rb	0.002
9.	Cu	0.002
10.	Sr	0.002
11.	Zn	0.001

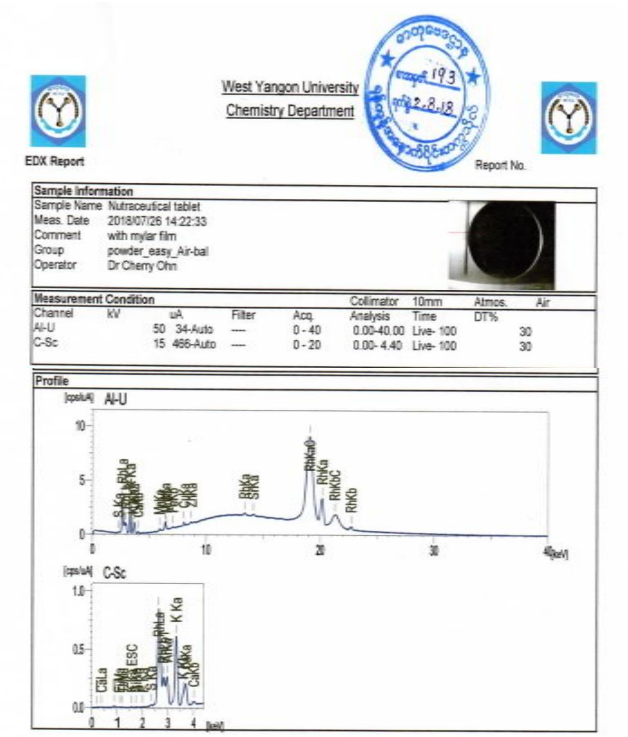

Figure 6 EDXRF spectrum of the prepared nutraceutical tablet

Preliminary Phytochemical Investigations

The phytochemical are naturally occuring substances in medical plants to cure various diseases. The phytochemical screening as qualitative analysis to explore the phytochemicals present in various parts of plants. The medical plants that had been explore are the rich source of natural medicinal agents. The plant leaf, pod and bark of various extracts ethanol, aqueous and ethyl acetate has been identified through phytochemical screening test includes a series of phytochemicals as flavonoids, tannins, polyphenols, reducing sugars, carbohydrates, proteins, saponins, glycosides , steroids terpenoids and α - amino acid (Bhattacharya *et al*., 2015). In the present work it was found that carbohydrates, cyanogenic glycosides, tannins and steroids are absent in the nutraceutical tablet samples. The data are shown in Table 5.

Table 6 Preliminary Phytochemical Investigation of the Prepared Nutraceutical Tablet Samples

No.	Test	Extract	Test Reagents	Observation	Result
1	Alkaloids	1% HCl	Dragendorff's reagent Sodium picrate Wagner's reagent Mayer's reagent	Orange ppt Yellow ppt Brown ppt White ppt	+ + + +
2	Amino-acids	H_2O	Ninhydrin reagent	purple spot on TLC	+
3	Carbohydrates	H_2O	10 % α napthol and H_2SO_4	Red ring	+
4	Cyanogenic Glycosides	H_2O	Sodium picrate solution	No brick red colour ppt	-
5	Flavonoids	EtOH	Mg tunning and conc: HCl	Pink colour solution	+
6	Glycosides	H_2O	10 % lead acetate	White ppt	+
7	Phenolic compounds	EtOH	5 % $FeCl_3$	Dark blue colour solution	+
8	Organic acid	EtOH	Bromocresol green	Yellow colour solution	+
9	Reducing sugars	H_2O	Benedict's Solution	Brick-red colour ppt	+
10	Saponins	H_2O	Distilled water	Forthing	+
11	Starch	H_2O	1 % Iodine	Bluish-black solution	+
12	Steroids	PE	Acetic anhydride & conc: H_2SO_4	No Green colour solution	-
13	Terpenoids	$CHCl_3$	Acetic anhydride & con: H_2SO_4	Pink colour solution	+
14	Tannins	H_2O	1% Gelatin	No Green colour solution	-

(+) = present, (-)= Absent, (ppt) = Precipitate

Antimicrobial Activity

A variety of laboratory methods can be used to evaluate or screen the in vitro antimicrobial activity of an extract or a pure compound. The most known and basic methods are the disk diffusion and broth or agar dilution methods. Other methods are used especially for antifungal testing. In this research, screening of antimicrobial activity of crude extracts has been done by agar well diffusion method, the different extracts from the sample tablets were tested with 6 species of microorganisms (*Bacillus subtilis, S.aureus, Pseudomonas aeruginosa, Bacillus pumilus, Candida albicans and Escherichia coli.*). The measurable zone diameter in (mm) is a measure of the degree of antimicrobial activity. The more active extract shows more remarkable zone of inhibition. In Tables 6 and Figure 7 the mean zone diameters of different extracts were found in the range of 11 to 15 mm. It was observed that ethanol extract and water extract were not significantly different in the treatment of disease caused by 6 microorganism species. But

for *B. subtilis*, the water extract is more effective than ethanol extract according to the mean zone diameter of 15 mm and 13 mm. These microorganisms are found in leprosy, skin lesion, carbuncles, pyemia, furunculosis, diarrhea, pneumonia, suppurative lesion, thrush, leukorrhea disease (Mahajan, 2015).

Table 7 Inhibitiion Zone Diameters (mm) of Antimicrobial Activity for Nutraceutical Tablet

Nutraceutical Tablets Extract	Inhibition zone diameter (mm)					
	Gram-positive bacteria			Gram-negative bacteria		Fungi
	B.subtilis	***S. aureus***	***B. pumilus***	***P. aeruginosa***	***E. coli***	***C. albicans***
Ethanol	13 (+)	12 (+)	13 (+)	12 (+)	13 (+)	13 (+)
Watery	15 (++)	13 (+)	14 (+)	13 (+)	14 (+)	14 (+)

Agar well – 10mm
10 mm ~ 14 mm (+)
15 mm ~ 19 mm (++)
20 mm above (+++)
(-) no activity

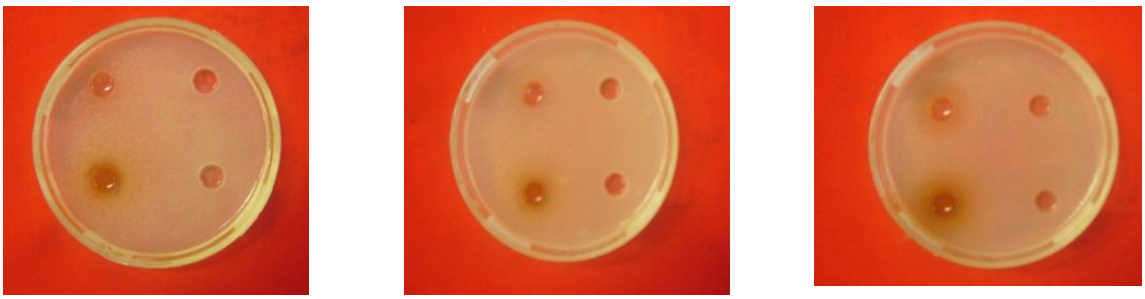

(a) Bacillus subtilis *(b) Staphylococcus aureus* *(c)Pseudomonas aeruginosa*

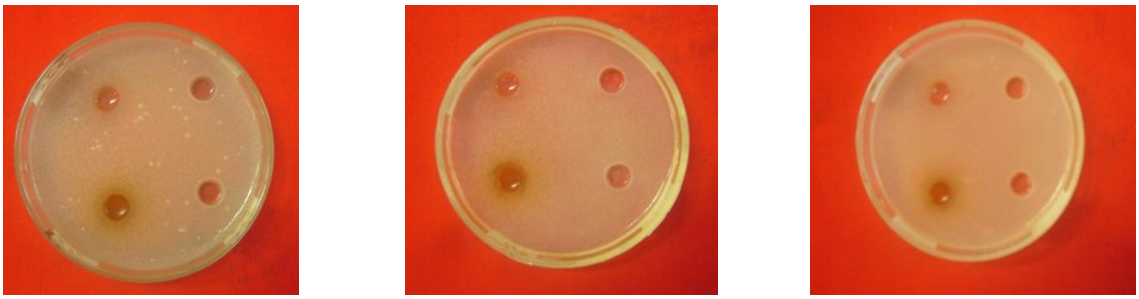

(d) Bacillus pumilus *(e) Candida albicans* *(f) Escherichia coli*

Figure 7 Antimicrobial activity screening of watery and ethanol extracts from prepared nutraceutical tablet samples

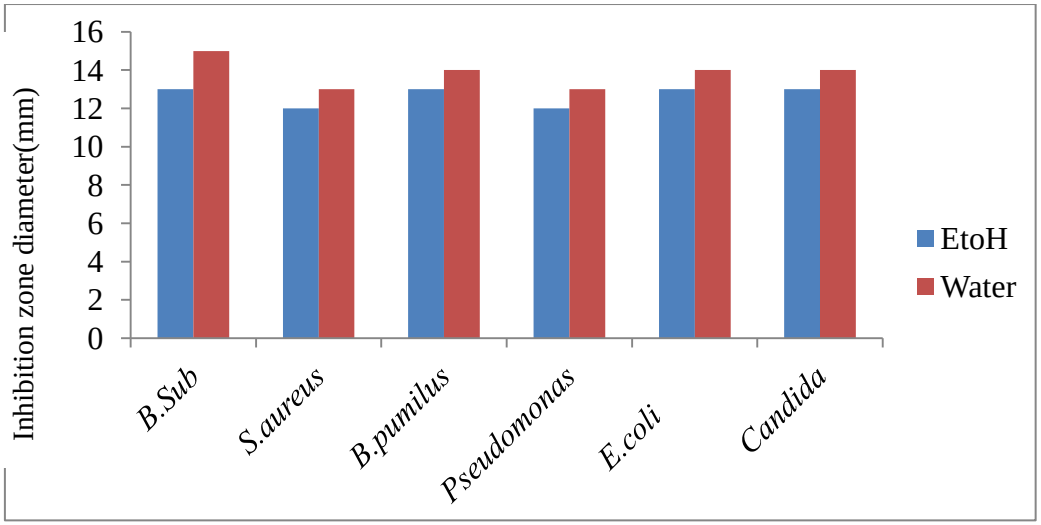

Figure 8 A bar graph of antimicrobial activity of nutraceutical tablet

Cytotoxicity

The cytotoxicity of water extract of nutraceutical tablets was evaluated by brine shrimp cytotoxicity bioassay. This bioassay is general toxicity screening for bioactive plants and their derivatives. A model animal that has been used for this purpose is the brine shrimp, *Artemia salina*. The cytotoxicity of crude watery extract was expressed in term of mean ± SEM (standard error mean) and LD_{50} (50 % Lethality Dose) and the results are shown in Table 8. In this experimental, standard potassium dichromate ($K_2Cr_2O_7$) and caffeine were chosen because $K_2Cr_2O_7$ is well-known toxicity in this assay (Salinas and Fernendez, 2006) and caffeine is a natural product.

As shown in Table 8, the crude watery extract was not cytotoxic to brine shrimp up to maximum dose of 1000 µg / mL. The LD_{50} values of standard $K_2Cr_2O_7$ < 1µg/ mL and caffeine was > 1000 µg / mL.

Table 8 Cytotoxicity Assay of Watery Extract from Nutraceutical Tablet Samples against *Artemia Salina* (Brine Shrimp)

Sample	Dead % of brine shrimp in various contents of sample (µg/L)				LD_{50} (µg/L)
	1	10	100	1000	
$K_2Cr_2O_7$	56.67	83.33	95.00	100	<1
Caffeine	0.00	0.00	10.00	13.33	>1000
Nutraceutical Tablet	13.33	16.67	23.33	43.33	>1000

Conclusion

In this study, from the present preparation of Nutraceutical tablet From selected fruits and study on its nutritional values, mineral contents and their physicochemical properties, the following inferences could be deduced. The nutritional values of the sample were determined by AOAC and Dumas nitrogen analyser. The water content 29.94 %, ash content 4.00 %, protein content 1.89 %, Fiber content 2.22 %, fat content 3.04 %, carbohydrate content 58.91 %, energy value 270.56 kcal/100 g and vitamin C content 44.88 mg / 100 g were observed. The pH of the prepared sample was 4.20 and the total acidity of 2.08 mg /100 g respectively. The reducing sugar content in prepared sample was 1.65 %. The effect of storage time on water content, ash content, vitamin C content, total acidity contents and pH of prepared tablet samples were also determined. From the study work, the water content slightly decreased from 1 month to 3 months storage time duration. The ash content also slightly decreased and the vitamin C content significantly decreased within 3 months duration time. The total acidity were slightly decrease and pH values were not much changed with the longer storage time. The mineral contents of prepared tablet sample were determined by ED XRF spectrum. It was found that 0.549 % K, 0.138 % S, 0.118 % Ca, 0.024 % P, 0.02 % S, 0.008 % Fe, 0.003 % Mn, 0.002 % Rb, 0.002 % Cu, 0.002 % Sr and 0.001 % Zn respectively. Among the presented metals, percent of potassium is higher than other metals. The preliminary phytochemical tests indicated that various types of secondary metabolites such as alkaloids, flavonoids , glycosides , phenolic compounds, reducing sugars, saponins, terpenoids and organic acids together with α-amino acids and starch were present in the sample. The antimicrobial activity of tablet samples from medicinal plant species has been evaluated in vitro against six microorganisms including five bacterial species (*B. subtilis, S. aureus, P. aeruginosa , B.pumilus, E.coli*) and one fungus species (*Candida albicans*). It was observed that, ethanol and watery extracts of tablet samples exhibited antimicrobial activity. The crude watery extract was not cytotoxic to brine shrimp up to maximum dose of 1000 µg / L.

Acknowledgements

The authors would like to thank the Department of Higher Education, Ministry of Education, Yangon, Myanmar, for allowing us to carry out this research programme. Thanks are also extended to the Myanmar Academy of Arts and Science and Professor Dr Ni Ni Than, Head of Department of Chemistry, University of Yangon for allowing to carry out this research programme.

References

Anderson, J. W., Baird, P. and Davis, R. H. (2009). "Health Benefits of Dietary Fiber". *J. of Nutrition*, vol. 67(4), pp. 188- 205

Anindita, D., Sikha, B. and Biswajit, D. (2016). "Pharmacological Activities of Baheda (*Terminalia bellerica*) A review". *J. of Pharmacognosy and Phytochemistry*, vol. 5(1), pp. 194-197

Anwesa, B., Kumar, B.S. and Ranjan, C.R. (2013). "The Development of *Terminalia Chebula Retz*. (Combretaceae) in Clinical Research". *J. of Asian Pacific. Tropikcal Biomedicine*, vol. 3(3), pp. 244-252

AOAC. (2000). *Official Method of Analysis*. Washinton DC: 17th Ed., Association of Official Analytical Chemists , pp. 86-275

Bhattacharya, M., Singh, A. and Khyani, C.R. (2015). "Preliminary Phytochemical Investigation of Various Extracts of Dalbergia sis 00". *J. of Applied Chemistry*, vol. 8 (12), pp. 32-35

Cabrera- Vique, C., Bergillos-Meca, T. and Seiquel, I. (2016). "Mineral content in Fast Foods". *J. of Department of Nutrition and Food Science, university of Granada*, Spain.

Mahajan, D. and Jain, S. (2015) . "Antimicrobial analysis of Triphala and comparison with its individual constituents". *Indian J. Pharm. Biol. Res.*, vol. 3(3), pp. 55-60

Nielsen, S. (2014). *Introduction to Food Analysis*. New York: 4th Ed., Dordrecht Heidelberg, pp. 1-352

Ozkan, M., Kirca, A. and Cemeroglu, B. (2004). "Effects of Hydrogen Peroxide on the Stability of Ascorbic Acid During Storage in Various Fruit Juices". *J. of Food Chemistry*, vol. 88(4), pp. 591-597

Rohit, S., Thakur, G. S., Sanodiyi, S. S., Sanodiyi, A., Savita, A., Pandey, M., Sharmal, A. and Bisen, P. S. (2012). "Therapeutic Potential of Calotropisprocera: A giant milk weed. IOSR". *J. of Pharmacy and Biological Sciences* (IOSR-JPBS) ISSN: 2278-3008, **4** (2), 42-57

Salinas, M. M. G. and Fernandez, S. S. (2006). "A Modified Microplate Cytotoxicity Assay with Brine Shrimp Larvae (*Artemia salina*)". *Pharmacology*, vol. 3, pp. 633-638

Swaroopa, G. and Srinath, D. (2017). "Nutraceuticals and their Health Benefits". *Int.J.Pure App. Biosic*, vol. 5(4), pp. 1151-1155

William, L. (1993). "Protein Fructosylation Fructose and the Maillard Reaction". *The American Journal of Clinical Nutrition American society for Nutrition*, vol. 58 (5), pp.7795-7787

PHYTOCHEMICAL INVESTIGATION AND ANTIMICROBIAL ACTIVITY FROM FRUIT EXTRACT OF *HAPLOPHRAGMA ADENOPHYLLUM* (WALL.) DOP. (PHET-THAM)

Thandar Aung[1], Wint War Htet Naing[2] , Ni Ni Than[3]

Abstract

The present work was conducted to investigate the phytochemical constituents and antimicrobial activity of fruits of *Haplophragma adenophyllum* (Wall.) Dop. (Phet-tham) on different microbial strains. From the phytochemical investigation, fruits of Phet-tham showed positive for alkaloids, α-amino acids, carbohydrates, flavonoids, glycosides, phenolic compounds, reducing sugars, saponins, steroids, tannins, terpenoids and showed negative results for starch and cyanogenic glycoside. Elemental analysis by EDXRF method revealed that fruits of Phet-tham contained K, Ca and Cl as major elements. By silica gel column chromatographic separation, three terpenoid compounds including lupeol (0.033 %, m.pt.=213-214 °C) were isolated from pet-ether extract of fruits of *H. adenophyllum*. Antimicrobial activities of pet-ether, ethyl acetate, 95 % ethanol, methanol and watery extracts from the fruits of *Phet-tham* were investigated against six species of microorganisms such as *Bacillus subtilis*, *Bacillus pumilus*, *Staphylococcus aureus*, *Pseudomonas areuginosa*, *Escherichia coli* and *Candida albicans* by agar well diffusion method at Pharmaceutical Research Department (PRD), Yangon. Among all tested crude extracts EtOAc extract exhibited the highest antimicrobial activity with the inhibition zone diameter in the range of 13~33 mm against all microorganisms tested.

Keywords: antimicrobial activity, *Haplophragma adenophyllum* (Wall.) Dop., lupeol,

Introduction

Haplophragma adenophyllum (Wall.) Dop. (Phet-tham), a member of the Bignoniaceae family, is a deciduous tree grown in tropical and subtropical climates of Southeast Asia and Africa (Jassbi *et al.*, 2004). These trees are commonly known in English as Karen wood. This tree is grown as an ornamental plant in parks and gardens due to the unique magical shape of its pods that distinguishes it amongst other trees of horticultural significance. *Haplophragma adenophyllum* (Wall.) Dop. has been used for various ailments treatment which includes cancer, gastrointestinal disorders, cholera, rheumatoid arthritis, hepatic disorders, leucorrhea and diabetes (Rahmatullah *et al*., 2010). In Myanmar, the plant is distributed in various regions and used as remedy for various medicinal purposes. Hnin Wutt Yee Win reported that the bark of *H. adenophyllum* possesed antimicrobial activity (Hnin Wutt Yee Win, 2013). In this research work, the fruits of *H. adenophyllum* (Phet-tham) were chosen for determination of some phytochemical constituents and evaluation of antimicrobial activity.

1. Dr, Associate Professor, Department of Chemistry, University of Yangon, Myanmar
2. MSc Candidate, Department of Chemistry, Pathein University, Myanmar
3. Dr, Professor and Head, Department of Chemistry, University of Yangon, Myanmar

Botanical Aspect of *Haplophragma adenophyllum* (Wall.) Dop.

Scientific classification

Family : Bignoniaceae
Botanical name : *Haplophragma adenophyllum* (Wall.) Dop.
Myanmar name : Phet-tham
English name : Karen wood
Synonyms : *Fernandoa adenophyllum*
Part used : Fruits

Figure 1 *Haplophragma adenophyllum* (Phet-tham) Fruits

Uses of *Haplophragma adenophyllum* (Wall.) Dop. (Phet-tham)

The fruits of *H. adenophyllum* (Phet-tham) is a traditional medicinal tree used for the prevention and treatment of various diseases. In Thai traditional medicine, the leaves are used for external treatment of skin diseases. As an ingredient in message oils, it is supposed to ease muscular tension sparingly cultivated as an ornamental tree. Folk medicinal uses of *H. adenophyllum* roots are used in piles, constipation and also prescribed as drink in viper bite. *H. adenophyllum* leaves and seeds have been used since centuries in traditional medicinal for the skin, urinary tract infections, antidiarrheal and anti-diabetic agents. It is used for various ailments treatment which includes cancer, gastrointestinal disorders, cholera, rheumatoid arthritis, hepatic disorders, leucorrhea and diabetes (Rahmatullah *et al*., 2010). In Myanmar, the boiled fruits of *H. adenophyllum* are used to eat with fish sauce as diet. In Myanmar, no scientific study was carried out to assess antimicrobial activities of the fruits extracts of *H. adenophyllum*. Therefore, present study was conducted to determine the bioactivities of various crude extract of fruits of *H. adenophyllum*.

Materials and Methods

Collection of *H. adenophyllum* Fruits Sample

The fruits of *H. adenophyllum* (Wall.), Dop., (Phet-tham) belonging to the family Bignoniaceae were collected from Laputta Township, Ayeyarwady Region, Myanmar, during January to February, 2018. The collected fresh fruit sample was washed and peeled. The fruit plups were dried at room temperature for two weeks and dried fruits were ground into powder and then it was stored in air tight container.

Qualitative Screening of the Phytochemicals

In order to classify the types of organic constituents present in fruits samples, preliminary phytochemical tests on samples were carried out according to the series of test tube methods (Trease and Evans, 1980; Marini-Bettole *et al.,* 1981; Shriner *et al.,* 1980; Robinson, 1983; and M-Tin Wa, 1972;).

Qualitative Elemental Analysis of the Fruits of Phet-tham by Energy Dispersive X-ray Fluorescence (EDXRF) Spectrometry

For this measurement, pellets of the powdered sample were first made. X-ray spectrometer permits simultaneous analysis of light element to heavy element. Energy dispersive X-ray fluorescence spectrometer (Shimadzu EDX - 700) can analyze the elements from Na to U under vaccum condition. X-ray fluorescence uses X-rays to excite and unknown sample. The individual elements in the sample are detected by using semiconductor detector [Si-Li] that permits multi-elements, simultaneous analysis. In this way, the elements present in fruits of Phat-tham were measured by EDXRF method using EDX-700 instrument at the Universities' Research Center (URC), Yangon.

Separation and Isolation of some Organic Constituents from the Fruits of Phet-tham
Preparation of crude extracts by successive solvent extraction method

Dried powered sample of fruits of Phet-tham (ca. 200 g) was percolated in 700 mL of 95 % EtOH with occasional shaking for one week and filtered. This procedure was repeated three times. The combined filtrate was concentrated under vacuum evaporator to obtain 95 % EtOH crude extract. The defatted marc was removed. 95 % EtOH crude extract was stirred with 500 mL PE (60-80 °C) and filtered. This procedure was repeated three times. The 95 % EtOH crude extract and PE crude extract were obtained. The 95 % EtOH crude extract was partitioned with EtOAc. After removal of the 95 % EtOH layer, EtOAc soluble extract was obtained. In the same procedure with different solvent, way, PE extract and 95 % EtOH extract from the fruits of Phet-tham were also obtained. These crude extracts were kept for separation of organic constituents and for screening of antimicrobial activities.

Isolation of some organic constituents from pet-ether extract of the fruits of Phet-tham

A glass chromatographic column (50 × 3 cm) with a tap attached was clamped so that it was perfectly vertical. The column was packed by the wet method, using PE:EtOAc (40:1 v/v). The column was plugged by pushing a small piece of cotton wool through the solvent with a glass rod. Care was taken so that no air bubbles were trapped in the cotton wool. Silica gel (ca. 50 g) was measured and placed in a beaker and made into slurry by mixing with pet-ether and the suspension was thoroughly stirred. A portion of the slurry was poured into the column and at the same time the tap was opened so that the solvent flowed at a slow but constant rate. As the column material slowly settled to the bottom, the column was lightly tapped with a rubber tubing around the outside wall so as to achieve an air bubble free, uniform packing. Column materials sticking to the upper walls of the column were washed down with the solvent. When the level of solvent had fallen to a few millimeters above the top of the silica gel column, the tap was closed. PE crude extract (3 g) was dissolved in PE and mixed with a little amount of silica gel. The mixture was allowed to evaporate with continuous agitation so that a free flowing dry silica gel on which the sample was uniformly adsorbed. By careful pouring of the adsorbed gel down the small funnel and adjusting the position of the lower end of the tube, a uniformed layer of adsorbed gel was placed on the top of the column. The top of the layer was wet with solvent. Some adsorbed gel sticking on the inner wall was washed down with the solvent. A piece of cotton wool was placed between the solvent and the column gel. The column was then completely filled with the solvent system and fraction was started; flow rate was adjusted to

about one drop per five seconds. Gradient elution was performed successively with increasing polarity (PE: EtOAc, 40:1, 20:1, 10:1, 5:1, 2:1, 1:1 and 1:2). Successive fractions obtained were combined on the basic of their behavior on TLC. Finally eleven main fractions (F_I to F_{XI}) were collected. Fraction F_I, F_{III}, F_V, F_{VI}, F_{VIII}, F_{IX}, F_X and F_{XI} were found as mixtures. Fraction F_{II} was evaporated and washed with PE and PE: EtOAc (20:1 v/v) and then recrystallized from PE, yield (49.6 mg, 0.033 %) of compound I as colorless needle shaped crystal. Fraction F_{IV} provided the solid material. The solid materials were washed with PE and PE:EtOAc (20:1 v/v) and then purified by recrystallization from PE and EtOAc, to give (110.7 mg, 0.074 %) of compound II as colorless needle shaped crystal. Fraction F_{VII} provided the solid material. The solid materials were washed with PE and PE: EtOAc (10:1 v/v) and then purified by recrystallization from MeOH, to give (6.9 mg, 0.004 %) of compound III as colorless crystal.

Screening of Antimicrobial Activity of Different Crude Extracts

Preparation of crude extracts by direct extraction method

Each dried powdered sample (50 g) was extracted with 150 mL of PE (60-80 °C) for 6 h by using soxhlet extractor. The filtrate was concentrated by removal of the solvent under reduced pressure to give the respective pet-ether crude extract. Preparation of ethyl acetate extract, 95 % ethanol, methanol, and watery extracts were also prepared by similar manner mentioned in above procedure. Each extract was dried at normal pressure on a water bath and stored under refrigerator for screening some bioactivities.

The antimicrobial activities of different crude extracts such as PE, EtOAc, 95% EtOH, MeOH and H_2O extracts from fruits of Phet-tham were determined against six species of microorganisms such as *Bacillus pumilus* (N.C.I.B - 8982), *Bacillus subtilis* (N.C.T.C - 8236), *Candida albicans, Escherichia coli* (N.C.I.B - 8134), *Pseudomonas aeruginosa* (6749) and *Staphylococcus aureus* (N.C.P.C - 6371) by employing agar well diffusion method at the Pharmaceutical Research Department, Ministry of Industry, Yangon, Myanmar.

Results and Discussion

From preliminary phytochemical analysis of the fruits of Phet-tham the results showed that the fruits of Phet-tham contain alkaloids, α-amino acids, carbohydrates, flavonoids, glycosides, phenolic compounds, reducing sugars, saponins, steroids, tannins and terpenoids. But starch and cyanogenic glycosides were found to be absent in the fruits of Phet-tham.

EDXRF elemental analysis revealed that the fruits of Phet-tham contained K, Ca and Cl as major elements. Moreover, S, Br and Mn as minor elements, Cu, Rb, Zn and Br as trace elements were also present in Phet-tham fruits.

By silica gel column chromatographic separation, compound I (lupeol, colourless needle shaped crystals, 0.033 %, m.pt. = 213-214 ^{0}C), compound II (a terpenoid compound, colourless needle shaped crystals, 0.074 %, m.pt. = 121-122 ^{0}C) and compound III (a terpeniod compound, colourless crystals, 0.004 %, m.pt. = 242-243 ^{0}C) were isolated from pet-ether extract of fruits of *H. adenophyllum.* The structure of isolated compounds were classified by chemical reagent tests and identified by applying modern spectroscopic techniques such as UV and FT IR spectrometry (Finar, 1969).

Compound I

Compound I isolated as colourless needle shaped crystals in 0.033 % yield from PE extract of fruits of Phet-tham has the melting point of 213-214 °C. It was soluble in PE, EtOAc, 95 % EtOH, MeOH and $CHCl_3$ but insoluble in H_2O. The R_f value of compound I was found to be 0.53 in PE: EtOAc (10:1 v/v) solvent system and it was UV inactive. It gave violet spot on TLC chromatogram while spraying with anisaldehyde followed by heating, a yellow spot with iodine vapour.

The functional groups present in compound I were studied by UV and FT IR spectroscopy. FT IR spectrum is shown in Figure 4. The FT IR spectrum of compound I showed the bands at 3305 cm^{-1} due to O-H stretching vibration of alcoholic group. Absorption bands at 2921 cm^{-1} and 2849 cm^{-1} were due to asymmetric and symmetric C-H stretching vibration of $–CH_2$ and $–CH_3$ groups and 3067 cm^{-1} was due to =CH stretching vibration of vinylidene $=CH_2$ group. The C=C stretching vibration was observed at 1639 cm^{-1}. The bending vibration of C-H of $–CH_2$ and $–CH_3$ groups were noticed by the medium intense bands at 1450 cm^{-1} and 1379 cm^{-1}, respectively. The C-O stretching vibration of alcohol was shown as intense band at 1190 cm^{-1} and 1037 cm^{-1}. Absorption band at 880 cm^{-1} was due to the –C-H out of plane wagging of CH_2 group. According to the physiochemical properties, spectroscopic data and Co-TLC (Figure 3) with authentic lupeol, compound I was identified as lupeol.

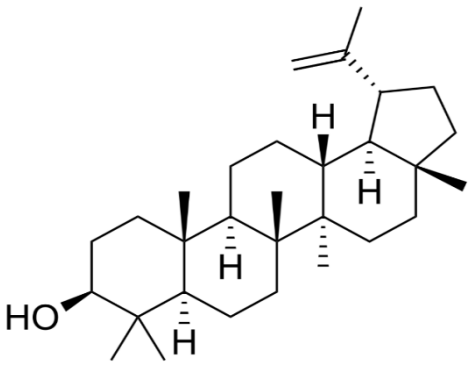

Figure 2 Structure of Lupeol ($C_{30}H_{50}O$)

Compound I
R_f value of compound A : 0.53
R_f value of authentic lupeol : 0.53
Solvent system : PE:EtOAc (10:1 v/v)
Spraing agent : 5 % H_2SO_4, heat

Lupeol **Compound I**

Figure 3 Co-TLC chromatogram of Lupeol and Compound I

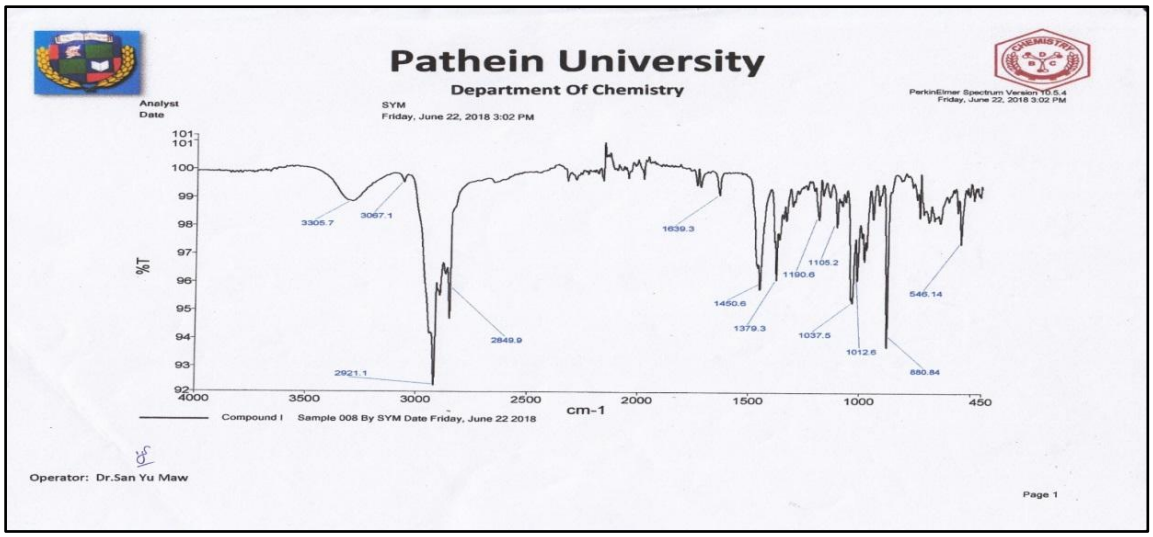

Figure 4 FT IR spectrum of the isolated compound A

Bioactivities

In vitro antimicrobial activity of some crude extracts of fruits of Phet-tham by agar well diffusion method

In vitro antimicrobial activity of various crude extracts such as pet ether, ethyl acetate, 95% ethanol, methanol and watery extracts were investigated by employing agar well diffusion method against six species of microorganisms such as *Bacillus subtilis*, *Staphylococcus aureus*, *Pseudomonas aureginosa*, *Bacillus pumilus*, *Candida albicans* and *Escherichia coli*. The inhibition zone diameter (ID) showed the degree of the antimicrobial activity. The larger the inhibition zone diameters, the higher the antimicrobial activity. The photographs illustrating the inhibition zones provided by crude extracts against six species of microorganisms and the observed data are summarized in Figure 4 and Table 1. Among the tested crude extracts of Phet-tham, ethylacetate extracts showed highest antimicrobial activity against all six microorganism (18 ~33 mm). Pet ether extract of Phet-tham fruits exhibited antimicrobial activity against six tested microorganisms (ID: 14 ~ 18 mm). 95% ethanol extracts of Phet-tham (ID: 15 ~ 19 mm), methanol extract (ID: 16 ~ 20 mm) and watery extract (ID: 11 ~ 15 mm) exhibited activity against all six tested microorganisms, respectively. Therefore, it may be inferred that ethyl acetate extract of fruits of Phet-tham pocesses the highest antimicrobial activity.

Table 1 Results of *in vitro* Antimicrobial Activity Screening of Phet-tham Fruits by Agar Well Diffusion Method (at PRD)

No.	Microorganisms	Inhibition well diameter (mm) of various crude extracts				
		PE	EtOH	EtOAc	H_2O	MeOH
1	*Bacillus subtilis*	18(++)	17(++)	28(+++)	13(+)	18(++)
2	*Staphylococcus aureus*	15(++)	15(++)	18(++)	14(+)	17(++)
3	*Pseudomonus aeruginosa*	15(++)	15(++)	30(+++)	15(++)	17(++)
4	*Baccilus pumilus*	14(+)	19(++)	18(++)	13(+)	16(++)
5	*Candida albicans*	15(++)	17(++)	32(+++)	11(+)	20(+++)
6	*Escherichia coli*	15(++)	15(++)	33(+++)	12(+)	17(++)

Agar well diameter = 10 mm
10mm~14 mm = (+) (low activity)
15mm~19 mm = (++) (medium activity)
20mm and above = (+++) (high activity)
(-) = no zone of inhibition

PE= Pet ether extract
EtOH= Ethyl alcohol extract
EtOAc= Ethyl acetate extract
H_2O= Watery extract
MeOH Methanol extract

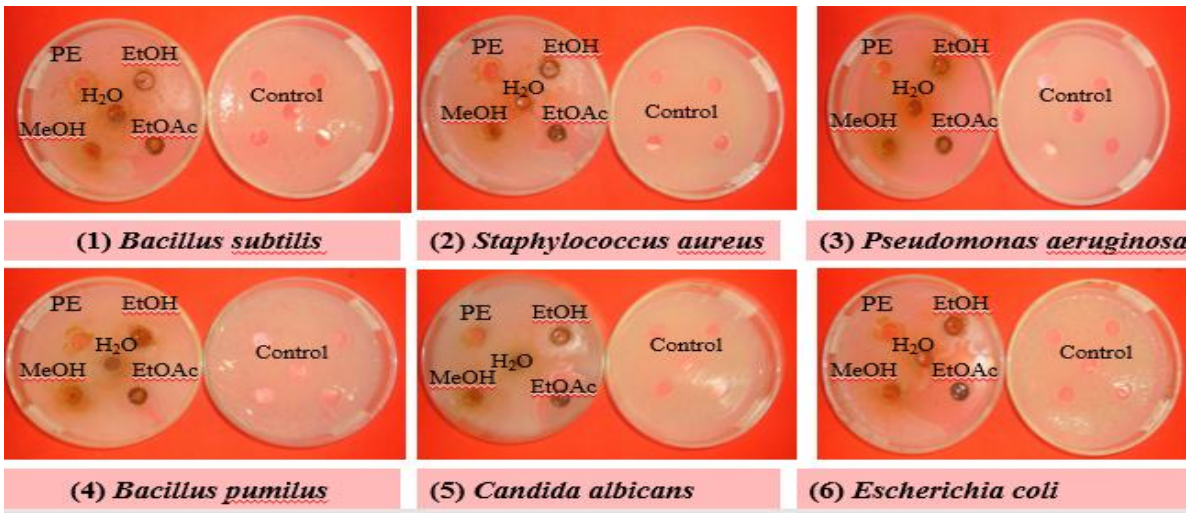

Figure 4. Inhibition wells of crude extracts from Phet -tham fruits against six microorganisms (at PRD)

Conclusion

From the overall assessment of the research work, the following inferences could be deduced. The preliminary phytochemical investigation revealed the presence of alkaloids, α-amino acids, carbohydrates, flavonoids, glycosides, phenolic compounds, reducing sugars, saponins, steroids, tannins and terpenoids in the fruits of Phet-tham. But, starch and cyanogenic glycisides were found to be absent in the fruits of Phet-tham. ED XRF elemental analysis revealed that the fruits of Phet-tham contain K, Ca and Cl as major elements, S, Br and Mn as minor elements and Cu, Rb, Zn and Br as trace elements.

By silica gel column chromatographic separation, compound A (lupeol), colourless needle shaped crystals, 0.033 %, mpt = 213-214 ^{0}C), compound B (a terpenoid compound, colourless needle shaped crystals, 0.074 %, mpt = 121-122 ^{0}C) and compound C (a terpeniod compound, colourless crystals, 0.004 %, mpt = 242-243 ^{0}C) were isolated from pet-ether extract

of fruits of *H. adenophyllum*. The structure of isolated compounds were classified by chemical reagent tests and identified by applying modern spectroscopic techniques such as UV and FT IR spectrometry.

Moreover, the antimicrobial activities of PE, 95 % EtOH, EtOAc, MeOH and H_2O extracts of the fruits of Phet-tham were screened on *Bacillus pumilus, Bacillus subtilis, Candida albicans, Escherichia coli, Pseudomonas aeruginosa* and *Staphylococcus aureus* by agar well diffusion method. From this investigation, EtOAc extract showed highest antimicrobial activity (ID: 18~33 mm) and H_2O extract showed lowest antimicrobial activity (ID: 11~15 mm).

According to the experimental studies, fruits of Phet-tham were found to contain some bioactive compounds and extract may have potent antimicrobial activities. The compound I, Lupeol, a non-toxic, highly potent chemo preventive and chemotherapeutic agent was isolated. From this study, it could be inferred that Phet-tham fruits have valuable medicinal properties.

Acknowledgements

We would like to thank all members of the Myanmar Academy of Arts and Science (MAAS), for inviting us to present research paper. We would like to thank the Department of Higher Education, Ministry of Education in Myanmar, for giving us the opportunity to do this research. Our deepest gratitude is expressed to Dr Si Si Hla Bu, Rector of Pathein University, for her encouragement, kind guidance, and kind help to do this research. We wish to thank Dr Than Tun and Dr Nilar Myint, Pro-Rectors of Pathein University for their invaluable advices and encouragement. Thanks are also extended to Professor Dr Ye Myint Aung (Head of Department) and Dr Than Than Oo (Professor), Department of Chemistry, Pathein University, for their helpful advice, precious suggestions and provision of research facilities at the Department of Chemistry, Pathein University, Myanmar. Our deepest gratitude is also expressed to Dr Pho Kaung, Rector of University of Yangon, for his permission, and kind help to submit this research for paper reading.

References

Finar, I. L. (1969) *Organic Chemistry, Stereochemistry and Chemistry of Natural Product*. London: 4th Edn . Longman Green and Co. Ltd., pp. 308-338

Hnin Wutt Yee Win. (2013). "*Screening on Antimicrobial activity of the Different Extracts From Haplophragma adenophyllum,"* MSc (Thesis), Myanmar: Department of Chemistry, Pathein University

Jassbi A. R., P. Singh, S. Jain, and S. Taharab (2004) "Novel Naphthoquinones from *Hetreophragma adenophyllum*. Helvetica" *Chimica Acta*, vol 87, pp. 820-824

M-Tin Wa. (1972) "*Phytochemical Screening Methods and Procedures*." *Phytochemical Bulletin of Botanical Society of America*, *5*(3), pp. 4-10

Marini-Bettole, G. B., M. Nicolettic, and M. Patamia, (1981) Plant Screening by chemical Chromatographic Procedure Under Field Condition. *J. Chromato*. vol 121, pp. 21-214

Rahmatullah, M., W. Samarrai, R. Jahan, S. Rahman, N. Sharmin, , Z.U.M. Emdad Ullah Miajee, , M.H. Chowdhury, S. Bari, F. Jamal, A.B.M. Anwarul Bashar, A.K. Azad and A. Ahsan, (2010) "An Ethnomedicinal, Pharmacological and Phytochemical Review of Some Bignoneaceae Family Plants and a Description of Bignoniaceae Plants in Folk Medicinal Uses in Bangladesh" *Adv. in Nat. Appl. Sci*. 4 (3): pp.236-253

Robinson, R. L. (1983). *The Organic Constituents of Higher Plants*. North Armberst: 5th Edn., Cordus Press, pp. 285-286

Shriner, R. L., R. C. Fuson, V. Curtin, and T.C. Morrill. (1980) *The Systematic Identification of Organic Compounds A Laboratory Manual*. New York: John Willey and Sons Co., Ltd., pp. 385-425

Trease, G. E. and Evans, W. C. (1980). *Pharmaconosy.* London: 1st Edn., Spottiswoode Ballantyne Ltd., pp.108-529